

AD 663929

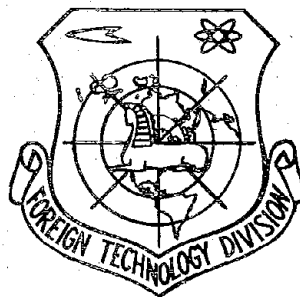
## FOREIGN TECHNOLOGY DIVISION



AIRCRAFT ENGINE DESIGN

By

G. A. Kuz'min



Distribution of this document  
is unlimited. It may be  
released to the Clearinghouse,  
Department of Commerce, for  
sale to the general public.

This document is a machine translation of Russian text which has been processed by the AN/GSQ-16(XW-2) Machine Translator, owned and operated by the United States Air Force. The machine output has been post-edited to correct for major ambiguities of meaning, words missing from the machine's dictionary, and words out of the context of meaning. The sentence word order has been partially rearranged for readability. The content of this translation does not indicate editorial accuracy, nor does it indicate USAF approval or disapproval of the material translated.

# EDITED MACHINE TRANSLATION

AIRCRAFT ENGINE DESIGN

By: G. A. Kuz'min

English Pages: 405

TM7500695

THIS TRANSLATION IS A RENDITION OF THE ORIGINAL FOREIGN TEXT WITHOUT ANY ANALYTICAL OR EDITORIAL COMMENT. STATEMENTS OR THEORIES ADVOCATED OR IMPLIED ARE THOSE OF THE SOURCE AND DO NOT NECESSARILY REFLECT THE POSITION OR OPINION OF THE FOREIGN TECHNOLOGY DIVISION.

PREPARED BY:

TRANSLATION DIVISION  
FOREIGN TECHNOLOGY DIVISION  
WP-AFB, OHIO.



G. A. Kuz'min

KONSTRUKTSIYA AVIATSIONNYKH DVIGATELEY

Dopushchено

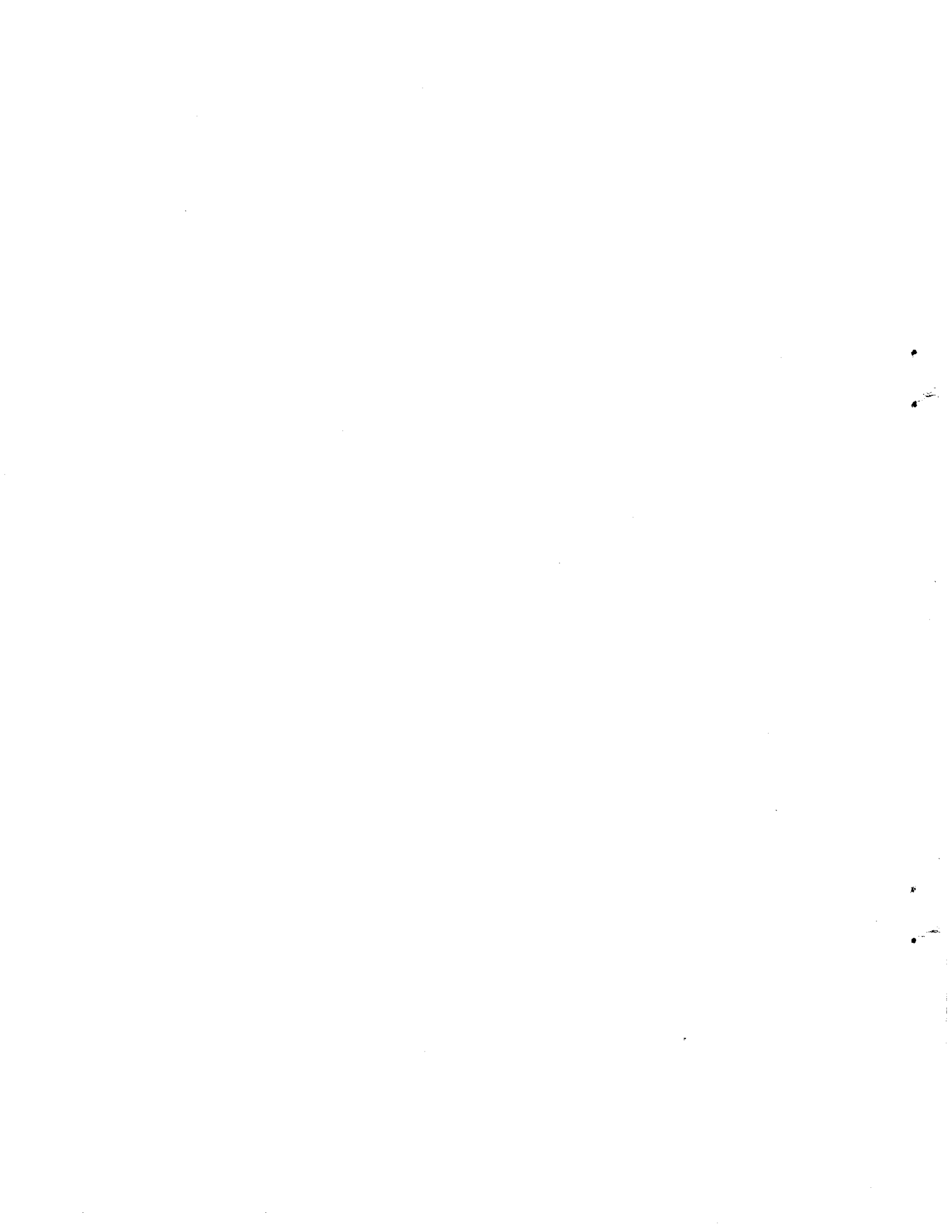
Ministerstvom vysshego i srednego spetsial'nogo obrazovaniya SSSR  
v kachestve uchebnogo posobiya  
dlya aviationsionnykh tekhnikumov

Gosudarstvennoye  
Nauchno-Tekhnicheskoye Izdatel'stvo

Oborongiz

Moskva - 1962

Page 1-443



## ITIS INDEX CONTROL FORM

01 Acc Nr TM7500695	68 Translation Nr MT6400402	65 X Ref Acc Nr AM4007932	76 Reel/Frame Nr 0897 1488				
97 Header Clas UNCL	63 Clas UNCL, O	64 Control Markings O	94 Expansion UR				
02 Ctry UR	03 Ref 0000	04 Yr 62	05 Vol 000	06 Iss 000	07 B. Pg. 0003	45 E. Pg. 0443	10 Date NONE

Transliterated Title

SEE SOURCE

09 English Title  
AIRCRAFT ENGINE DESIGN43 Source  
KONSTRUKTSIYA AVIATSIONNYKH DVIGATELY (RUSSIAN)42 Author  
KUZ'MIN, G. A.16 Co-Author  
NONE16 Co-Author  
NONE16 Co-Author  
NONE16 Co-Author  
NONE

98 Document Location

47 Subject Codes  
01, 11

39 Topic Tags: aircraft engine, gas turbine engine, engine compressor system, aircraft engine manufacture, aircraft material

**ABSTRACT:** This textbook is intended for students in aviation teknikums and may be useful to industrial engineers and technicians interested in aircraft engine design and students studying related subjects at technical institutions of higher learning. The book covers the design of modern aircraft engines and their components. The special design features and typical designs of compressors, turbines, combustion chambers, and crank-gear mechanisms, are described. Methods of computing component strength and means of balancing rotating parts are given. The following metals and alloys are used for the manufacture of various axial compressor assembly components: malleable heat-resistant aluminum alloy AK4; malleable aluminum alloy VD17; aluminum alloy AL5; magnesium alloy ML5; alloy VT1 having good weldability: S20 steel; structural steels 40KhNMA, 30KhGSA, and 38KhA. The RD-500 engine is mentioned. The following metals and alloys are used for the manufacture of various centrifugal compressor components: high-strength [aluminum] alloy AK6; silumin-type aluminum alloys AL4 and AL5; aluminum-magnesium alloy AMg-M; high-strength steels 18KhNVA, 40KhNMA, and 12Kh2N4A. A drawing of the air-cooled turbine bucket of the RD-20 engine is given. The following metals and alloys are used for the manufacture of various turbine components: alloys EI437, EI437A, EI437B, EI617, EI598; nickel-base alloy ZhSZ and cobalt-base alloy LK4; heat-resistant steels EI481, 20Kh3MVF, 25-20, Kh23N18, and 1Kh18N9T. The following metals and alloys are used for the manufacture of rotor shafts and connections: structural alloy steels 40KhNMA, 18KhNVA, and 12Kh2N4A. The following metals and alloys are used for the manufacture of combustion chamber components: heat-resistant nickel-base alloys Kh20N80T and EI602, and heat resistant steel 1Kh18N9T. The following metals and alloys are used for the manufacture of exhaust assemblies and afterburner components: heat-resistant chromium-nickel steels 1Kh18N9T and Kh23N18, and Kh20N80T. The AV-68 propeller is shown. The metals used in the manufacture of reduction gear components are: case-hardened steels 12Kh2N4A and 18KhNVA; nitride-hardened steel 38KhMYuA; steels 40KhNMA and

12Kh2N4A. The metals and alloys used in the manufacture of drives for gas turbine engine assemblies are: case-hardened steels 12Kh2N4A and 12KhN3A; steels 40KhNMA and 18KhNVA; magnesium alloy ML5 and aluminum alloy AL5. The metals and alloys used in the manufacture of lubrication-system components are: case-hardened steels 12KhN3A and 12Kh2N4A; 40KhNMA steel; aluminum alloys AL5 and AL4; magnesium alloy ML5. Drawings of the E348I geared fuel pump, the 7071 booster rotary fuel pump, and the RD-10 single-channel fuel nozzle are given. The metals and alloys used in the manufacture of fuel system components are: aluminum alloys AL5 and AL9; BrAZhN-10-4-4 bronze; steels 12KhN3A, KhVG, ShKh15, 40KhNMA, Kh12, and EI69; nitride-hardened steel 38KhMYuA. The metals and alloys used in the manufacture of cylinder components are 38KhMYuA steel; heat-resistant valve steel EI69; heat-resistant aluminum alloy AL5; BrAZhMts bronze. The metals and alloys used in the manufacture of components of the gas-distribution system are: steels EI69, EI72, EI107, Kh12M, 12KhN3A, 37KhN3A, 30KhGSA, and 40KhNMA; case-hardened steels 13N5A and 12Kh2N4A; wire steel 50KhFA; and BrAZhN10-4-4 bronze. The metals and alloys used in the manufacture of reduction gears and blowers are: case-hardened steels 12Kh2N4A and 18KhNVA; nitride-hardened steel 38KhMyuA; 40KhNMA steel; aluminum alloys D1, AK1, AK6, and AL4; magnesium alloys MA2 and ML4. The metals and alloys used in the manufacture of casings and drives are: aluminum alloys AL4, AL5, and AL6; magnesium alloy ML4; 40KhNMA steel. English Translation: 404 pages.

#### TABLE OF CONTENTS:

- Chapter I. Types and Classification of Gas-Turbine Engines
- Chapter II. Axial Compressors
- Chapter III. Centrifugal Compressors
- Chapter IV. Gas Turbines
- Chapter V. Oscillation of Buckets and Disks
- Chapter VI. Balancing Gas-Turbine Engine Rotors
- Chapter VII. Rotor Shafts and Supports
- Chapter VIII. Critical Number of Rotor Shaft Revolutions
- Chapter IX. Combustion Chambers
- Chapter X. Exhaust Assemblies and Afterburners
- Chapter XI. Turboprop Reduction Gears
- Chapter XII. Drives for Gas-Turbine-Engine Assemblies
- Chapter XIII. System of Load-Bearing Housings of the Gas-Turbine Engine
- Chapter XIV. Lubrication System of the Gas-Turbine Engine
- Chapter XV. Fuel System of the Gas-Turbine Engine and Its Assemblies
- Chapter XVI. Adjusting the Gas-Turbine Engine
- Chapter XVII. Ignition Units of the Gas-Turbine Engine
- Chapter XVIII. The Kinematics and Dynamics of the Crankgear Mechanism
- Chapter XIX. Balancing of Piston Engines

TM7500695

MT6400402

- Chapter XX. Crankshafts
- Chapter XXI. Connecting Rods
- Chapter XXII. Pistons
- Chapter XXIII. Cylinders
- Chapter XXIV. Gas Distribution
- Chapter XXV. Reduction Gears and Blowers
- Chapter XXVI. Casings and Drives for the Lubrication Units  
and Piston Engine Systems
- Chapter XXVII. Piston-Engine Ignition System

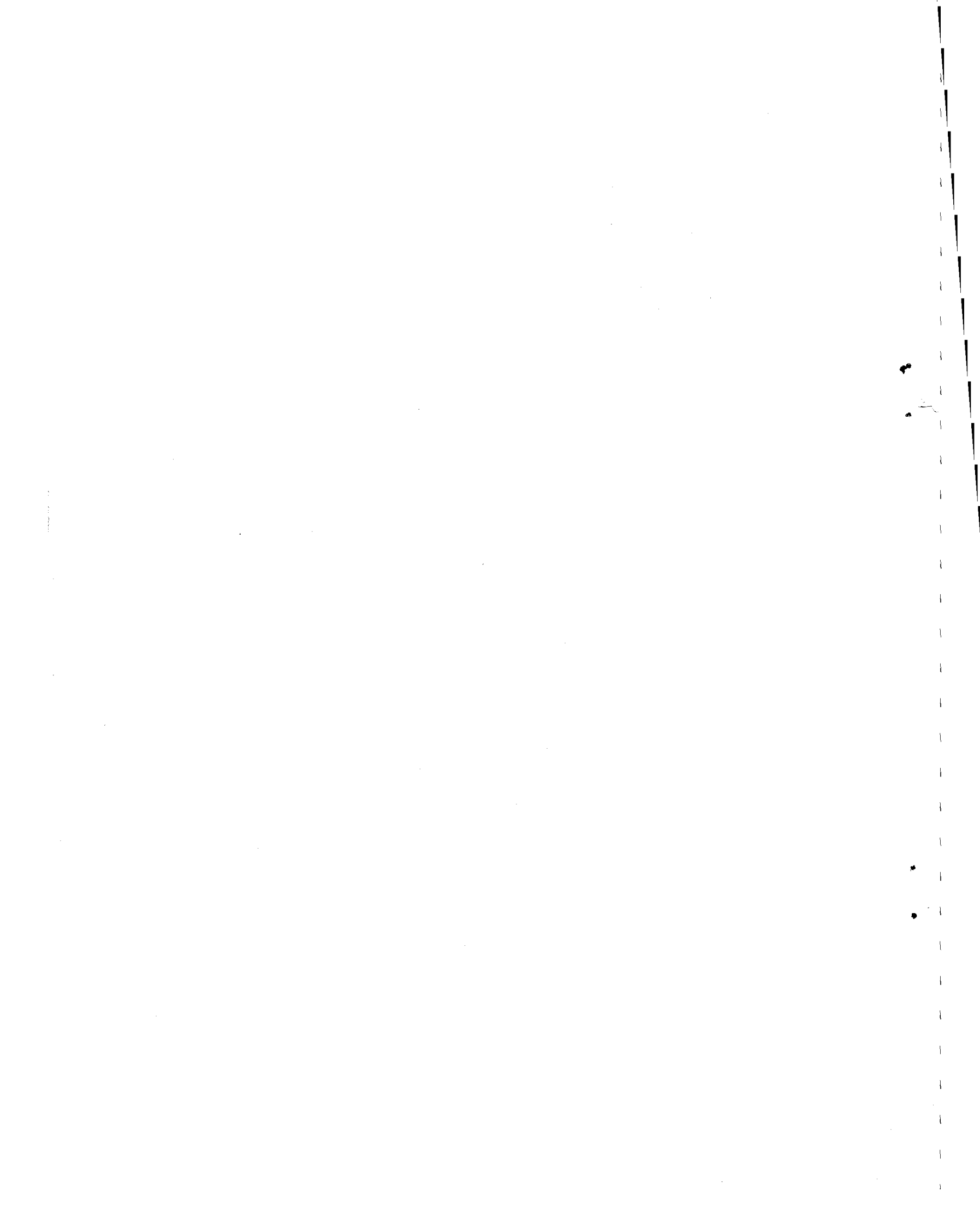


## TABLE OF CONTENTS

U. S. Board on Geographic Names Transliteration System.....	vii
Designations of the Trigonometric Functions.....	viii
Preface.....	1
Introduction.....	5
1. Classification of Engines.....	5
2. Basic Specific Parameters of Aircraft Engines.....	6
3. Brief Survey of Development and Contemporary State of Aircraft Engines.....	7

## FIRST PART

### GAS-TURBINE AIRCRAFT ENGINES

Chapter I. Types of Gas-Turbine Engines and Their Classification.....	13
Chapter II. Axial Compressors.....	19
2.1. General Information.....	19
2.2. Rotor Design.....	27
2.3. Stator Design.....	32
2.4. Clearances and Seals of Compressor Rotor.....	39
2.5. Profiling of Compressor Blades.....	41
2.6. Calculation for Strength.....	42
2.7. Materials.....	67
Chapter III. Centrifugal Compressors.....	68
3.1. General Information.....	68
3.2. Rotor Design.....	70
3.3. Stator Design.....	74
3.4. Clearances Between Stator and Rotor Wheel.....	78
3.5. Calculation of Rotor Wheel Strength.....	78
3.6. Materials.....	91

Chapter IV. Gas Turbines.....	82
4.1. General Information.....	82
4.2. Rotor Design.....	85
4.3. Stator Design.....	90
4.4. Clearances Between Rotor and Stator of Turbine.....	97
4.5. Cooling of Turbines.....	99
4.6. Construction of Blade Profile.....	103
4.7. Strength Calculation.....	105
4.8. Materials.....	121
Chapter V. Vibrations of Blades and Disks.....	122
5.1. General Information.....	122
5.2. Natural Vibrations of Blades.....	123
5.3. Forced Vibrations of Blades.....	126
5.4. Vibrations of Disks.....	129
Chapter VI. Balancing of GTD Rotors.....	130
6.1. General Information.....	130
6.2. Balancing of Revolving Masses.....	132
6.3. Static and Dynamic Balancing of Rotors.....	135
Chapter VII. Shafts and Supports of Rotors.....	138
7.1. General Information.....	138
7.2. Shafts.....	139
7.3. Connection of Rotors.....	140
7.4. GTD Rotor Bearings.....	142
7.5. Axial Fixation of Engine Rotors.....	147
7.6. Design of Bearing Units.....	149
7.7. Loads on Shafts and Bearings.....	152
7.8. Strength Calculation.....	159
7.9. Materials.....	166
Chapter VIII. Critical Speeds of Rotor Shafts.....	168
8.1. General Information.....	168
8.2. Harmonic Motion.....	168
8.3. Natural Bending Vibrations of a Shaft.....	169
8.4. Critical Speed of a Shaft with One Disk.....	171
8.5. Critical Speed of a Shaft with Several Disks.....	175
8.6. Critical Speed of a Shaft Taking Into Account Its Mass.....	176

8.7. Critical Speed of a Shaft of Variable Section with Several Disks.....	177
8.8. Critical Speed of a Shaft in the Case of Its Precessional Motion.....	179
<b>Chapter IX. Combustion Chambers.....</b>	<b>184</b>
9.1. General Information.....	184
9.2. Design of Combustion Chambers.....	190
9.3. Strength Calculation.....	197
9.4. Materials.....	199
<b>Chapter X. Exhaust Units and Afterburners.....</b>	<b>200</b>
10.1. General Information.....	200
10.2. Design of Exhaust Nozzles.....	206
10.3. Strength Calculation.....	208
10.4. Materials.....	211
<b>Chapter XI. Turboprop Reduction Gears.....</b>	<b>212</b>
11.1. General Information.....	212
11.2. Kinematic Patterns and Transmission Ratios of Reduction Gears.....	214
11.3. Elements of Design of Reduction Gears.....	221
11.4. Calculation of Gear Teeth Strength.....	228
11.5. Propeller Hubs.....	233
11.6. Materials.....	240
<b>Chapter XII. Gas-Turbine Engine Assembly Drives.....</b>	<b>241</b>
12.1 General Information.....	241
12.2. Drive Systems and Their Design.....	241
12.3. Materials.....	246
<b>Chapter XIII. GTD Power Unit System.....</b>	<b>247</b>
13.1. General Information.....	247
13.2. Gas Forces.....	248
13.3. Inertial Loads and Mass Forces.....	253
13.4. Mounting of Engine to Aircraft.....	253
13.5. Strength Calculation.....	254
<b>Chapter XIV. GTD Lubrication System.....</b>	<b>257</b>
14.1. General Information.....	257
14.2. Diagrams of GTD Lubrication.....	261
14.3. Design of Oil System Assemblies.....	265
14.4. Materials.....	271

Chapter XV. GTD Fuel System and Its Assemblies.....	272
15.1. General Information.....	272
15.2. Diagrams of GTD Fuel System.....	277
15.3. Design of Fuel System Assemblies.....	279
15.4. Materials.....	288
Chapter XVI. GTD Control.....	289
16.1. General Information.....	289
16.2. Speed Control Units.....	293
16.3. Flow Control Units.....	300
16.4. Natural Stability of GTD.....	301
16.5. GTD Control Systems.....	302
Chapter XVII. GTD Starting Units.....	317
17.1. General Information.....	317
17.2. Types of Starters.....	319
17.3. Igniters.....	322
17.4. Ignition Coil.....	324

## SECOND PART

### AIRCRAFT PISTON ENGINES

Chapter XVIII. Kinematics and Dynamics of the Crankgear.....	327
18.1. Kinematics of a Normal Crankgear.....	330
18.2. Forces of Inertia of a Crankgear.....	332
18.3. Forces of Gas Pressure.....	336
18.4. Total Forces from One Cylinder.....	338
18.5. Firing Sequence.....	339
18.6. Summation of Crank Forces T and Z.....	340
18.7. Force Acting on the Connecting Rod Journal of an Angular Shaft.....	341
18.8. Torque.....	341
18.9. Disturbing Moment.....	342
Chapter XIX. Balancing of Piston Engines.....	344
19.1. General Information.....	344
19.2. Balancing of Single-Row Radial Engines.....	345
19.3. Balancing of Two-Row Radial Engines.....	347
19.4. Pendulum Counterpoises Dampers of Twisting Vibrations.....	349

Chapter XX. Crankshafts.....	354
20.1. General Information.....	354
20.2. Design of Crankshafts.....	354
20.3. Strength Calculation.....	357
20.4. Material and Methods of Increasing the Strength of Crankshafts.....	363
Chapter XXI. Connecting Rods.....	364
21.1. General Information.....	364
21.2. Design of Connecting Rods.....	364
21.3. Strength Calculation.....	366
21.4. Materials and Methods of Increasing the Strength of Connecting Rods.....	369
Chapter XXII. Pistons.....	370
22.1. General Information.....	370
22.2. Piston Design.....	370
22.3. Piston Rings.....	372
22.4. Piston Pins.....	374
22.5. Strength Calculation.....	374
22.6. Materials.....	376
Chapter XXIII. Cylinders.....	377
23.1. General Information.....	377
23.2. Design of Cylinders.....	377
23.3. Strength Calculation.....	379
23.4. Materials.....	379
Chapter XXIV. Gas Distribution.....	381
24.1. General Information.....	381
24.2. Design of Gas Distribution Mechanism.....	384
24.3. Materials.....	387
Chapter XXV. Reduction Gears and Superchargers.....	389
25.1. Reduction Gears.....	389
25.2. Superchargers.....	391
25.3. Materials.....	393
Chapter XXVI. Crankcases, Accessory Drives, and Lubrication System of Piston Engines.....	394
26.1. Engine Crankcases.....	394
26.2. Accessory Drives.....	395

26.3. Lubrication of Piston Engines.....	396
26.4. Materials.....	396
Chapter XXVII. Ignition System of Piston Engines.....	397
27.1. General Information.....	397
27.2. Ignition Plugs.....	397
27.3. Aircraft Magneto.....	398
27.4. Shielding of the Ignition System.....	401
27.5. Starting Ignition.....	402
Literature.....	403

U. S. BOARD ON GEOGRAPHIC NAMES TRANSLITERATION SYSTEM

Block	Italic	Transliteration	Block	Italic	Transliteration
А а	А а	A, a	Р р	Р р	R, r
Б б	Б б	B, b	С с	С с	S, s
В в	В в	V, v	Т т	Т т	T, t
Г г	Г г	G, g	Ү ү	Ү ү	U, u
Д д	Д д	D, d	Ф ф	Ф ф	F, f
Е е	Е е	Ye, ye; E, e*	Х х	Х х	Kh, kh
Ж ж	Ж ж	Zh, zh	Ц ц	Ц ц	Ts, ts
З з	З з	Z, z	Ч ч	Ч ч	Ch, ch
И и	И и	I, i	Ш ш	Ш ш	Sh, sh
Й ѹ	Й ѹ	Y, y	Щ щ	Щ щ	Shch, shch
К к	К к	K, k	Ь ъ	Ь ъ	"
Л л	Л л	L, l	Ы ы	Ы ы	Y, y
М м	М м	M, m	Ь ь	Ь ь	'
Н н	Н н	N, n	Э э	Э э	E, e
О о	О о	O, o	Ю ю	Ю ю	Yu, yu
П п	П п	P, p	Я я	Я я	Ya, ya

\* ye initially, after vowels, and after ъ, ъ; e elsewhere.  
When written as є in Russian, transliterate as yє or є.  
The use of diacritical marks is preferred, but such marks  
may be omitted when expediency dictates.

FOLLOWING ARE THE CORRESPONDING RUSSIAN AND ENGLISH  
 DESIGNATIONS OF THE TRIGONOMETRIC FUNCTIONS

Russian	English
sin	sin
cos	cos
tg	tan
ctg	cot
sec	sec
cosec	csc
sh	sinh
ch	cosh
th	tanh
cth	coth
sch	sech
csch	csch
arc sin	$\sin^{-1}$
arc cos	$\cos^{-1}$
arc tg	$\tan^{-1}$
arc ctg	$\cot^{-1}$
arc sec	$\sec^{-1}$
arc cosec	$\csc^{-1}$
arc sh	$\sinh^{-1}$
arc ch	$\cosh^{-1}$
arc th	$\tanh^{-1}$
arc cth	$\coth^{-1}$
arc sch	$\sech^{-1}$
arc csch	$\csch^{-1}$
rot	curl
lg	log

This book is a course on the design of contemporary aircraft engines (gas-turbine and reciprocating). It briefly describes typical designs of the main units of these engines (compressors, turbines, combustion chambers, crankshafts, and so forth), presents their design features, methods of strength calculation, and also methods for balancing of rotary units.

The book is a training aid for students of technical schools; it will also be useful to engineers and technicians of industry.



## PREFACE

The book acquaints the reader with designs of contemporary aircraft engines and their assemblies.

Basic attention in it is allotted to designs of gas-turbine engines (turbojet and turboprop), widely applied in contemporary high-speed aircraft. Designs of reciprocating engines are not fully presented in the book, inasmuch as in contemporary aviation the application of an engine of this type is limited.

In examining this or that type of engine the author is not limited to the description of the design of its assemblies and considers it expedient to give the conditions of their operation, loads experienced by them, methods of calculation for strength, and materials from which they are made. The entirety of such information gives the possibility to fuller study the engine and evaluate the perfection of its design. Well selected illustrative material in the book, also promotes the best study of engine design.

The author, being extremely concerned with the given contents of the book, was forced in examining the designs of aircraft engines, to limit himself to a minimum quantity of examples. In particular, for this reason the use of examples from Soviet gas-turbine engines is limited. For the same reason the materials on durability of designs are also given with the necessary brevity. Considering the restriction of the contents of the book, the author has tried as much as possible to expound only the basic questions characterizing engine design and methods of calculation of them for durability. In spite of the indicated abbreviations, the material presented in the book is sufficient so that the reader could obtain a clear

presentation on the design and methods of calculation for durability of aircraft engines.

The book consists of two parts. First part is dedicated to gas-turbine engines and the second part to reciprocating engines.

The introduction gives the general characteristics of aircraft engines, presents their specific parameters and briefly outlines the history of development and the contemporary state of aircraft engines.

The first part of the book gives the classification of gas-turbine engines according to their structural criteria, describes designs of their basic units and parts, designs of assemblies of oil and fuel systems, and considers methods of engine regulation. Along with this, it describes vibrations of blades, disks and shafts, appearing during operation of engine, methods of balancing the rotary components, and gives methods of calculation for durability and rigidity of basic elements of engine design with numerical examples. In necessary cases, technological peculiarities of design and peculiarities of processes occurring in different parts of the engine are pointed out.

The second part is less than the first in volume and is dedicated, as already noted above, to reciprocating engines. It explains the kinematics and dynamics of the crankshaft, order of firing and methods of balancing of the engine, and describes the designs of main units and methods of their calculation for durability.

The book is a training aid for students of technical schools and is written in accordance with the program of a course on aircraft engines. The author considers that the book will also be useful for engineers and technicians of industry, interested in the design of aircraft engines, and for students of corresponding speciality in Aviation Schools of Higher Education of a technological nature.

In writing the book the author assumed the readers' acquaintance with the fundamentals of the theory of aircraft engines.

The author expresses his gratitude to colleagues of the department of aircraft engine design of the Kazan Aviation Institute, and Ye. A. Alatskiy and N. M. Nikiforovoy for their help rendered in the preparation of illustrational material and in formulation of the manuscript, and also the critics of the

subject commission of the technical school and engineer V. A. Tyutyunov for his valuable remarks promoting increase of quality of the manuscript.

All remarks on the content of the book the author asks to be directed to this address: Moscow I-51, Petrovka 24, Oborongiz.



## INTRODUCTION

### 1. Classification of Engines

Contemporary flight vehicles use thermal engines which are subdivided into gas-turbine [GTD] (ГТД), reciprocating [PD] (ПД), ram jet [PVRD] (ПВРД), and rocket [RkD] (ЖРД).

Gas-turbine engines in turn are subdivided into simple turbojets (usually they are called simply turbojet engines [TRD] (ТРД)), ducted-fan turbojets [DTRD] (ДТРД), and turboprops [TVD] (ТВД).

Rocket engines, obtaining their name owing to the predominant use of them in rockets, are subdivided into liquid [ZhRD] (ЖРД) and solid propellant [RDTT] (РДТТ).

By method of obtaining thrust, engines of flight vehicles can be divided into jet, prop, and combined (prop and jet).

Jet engines turbojets (TRD and DTRD) ramjets (PVRD), and rockets (ZhRD and RDTT). Thrust of these engines is created by the reaction of the escape of masses of working gases from the exit nozzle.

Turboprop engines (TVD) of normal design pertain to combined engines. Basic thrust is created by their rotary propeller, and additional thrust is created by the reaction of escape of exhaust gas. Additional thrust composes 8-12% of total engine thrust.

Reciprocating engines are prop-driven engines, although their reaction of escape of exhaust gases is also frequently used for obtaining additional thrust. But it is not more than 2-3% of total engine thrust.

PRECEDING  
PAGE BLANK

## 2. Basic Specific Parameters of Aircraft Engines

An aircraft engine should have specific thrust or power, small over-all dimensions, small weight, high economy and reliability, sufficient operation life, and so forth. These requirements are stipulated by its purpose. Furthermore, the design of an engine should be simple and technological.

The quality of an aircraft engine is usually evaluated by the following basic specific parameters: specific thrust or power, specific frontal thrust or power, specific gravity, and specific fuel consumption. These specific parameters are determined by the following relationships:

specific thrust or power

$$P_{yx} = \frac{P}{G_B} \text{ kg thrust/kg } N_{yx} = \frac{N_e}{G_B} \text{ hp/kg,}$$

where  $P$  and  $N_e$  is thrust and power, respectively, obtained during bench tests of engine in standard atmosphere;  $G_B$  is air flow through engine per second; specific frontal thrust of power

$$P_{x06} = \frac{P}{F_{x06}} \text{ kg/m}^2; N_{x06} = \frac{N_e}{F_{x06}} \text{ hp/m}^2$$

where  $F_{x06}$  is the area of frontal surface (middle section) of the engine; specific gravity

$$\gamma_{AB} = \frac{G_{AB}}{P} \text{ kg/kg thrust}; \gamma_{AB} = \frac{G_{AB}}{N_e} \text{ kg/hp,}$$

where  $G_{AB}$  is weight of engine;

specific fuel consumption

$$C_{yx} = \frac{G_m}{P} \text{ kg/kg thrust-hour}; C_s = \frac{G_m}{N_e} \text{ kg/hp hour,}$$

where  $G_m$  is fuel consumption

Specific thrust or specific power characterize the effectiveness of use of air in an engine. Specific frontal thrust or specific frontal power give a comparative appraisal of quality with respect to the over-all dimensions of the engine, i.e., its frontal area. Specific gravity determines the weight qualities of the engine, and specific fuel consumption determines its economy.

The more accomplished engine has more specific thrust and specific frontal thrust or correspondingly more specific power and specific frontal power, and also less specific gravity and specific fuel consumption.

Aircraft engines in their development are continuously improving and their specific parameters are being improved. General improvement of aircraft engines is ensured by increase of parameters of the working process, and also improvement of their design, materials, and technology of production. High thermal and mechanical intensity limits the operation life of aircraft engines until their overhauling by hundreds and sometimes thousands of hours of work.

### 3. Brief Survey of Development and Contemporary State of Aircraft Engines

The first aircraft in the world, built in 1882 by our remarkable compatriot A. F. Mozhayskiy, had two steam engines which revolved the propellers. The power plant with steam engines, owing to its large weight, subsequently did not obtain application in aviation. However, Mozhayskiy for the first time practically proved the possibility of flights on vehicles heavier than air.

Practical development was obtained by aviation in the beginning of the 20th Century on the basis of the gasoline internal-combustion engine invented by then, i.e., the piston (reciprocating) engine (PD). Aircraft with these engines in 1903 in the United States were flown by the Wright brothers. Up to the Second World War the reciprocating engine was the only type of aircraft engine. During that time it received wide development, ensuring continuous growth of speed of flight of aircraft. The development of aviation always was determined by the tendency to fly faster, higher, and farther. In accordance with this, there also proceeded the development of aircraft engines; increase of their absolute and specific power, and also specific frontal power, decrease of specific gravity, and increase of economy.

The first models of reciprocating aircraft engines had a power of several hp and specific gravity from 3 to 4 kg/hp with low specific frontal power and low economy. In the Second World War the power of reciprocating engines reached 2000-3000 hp and above, with specific frontal power from 1200 to 2000  $\text{hp/m}^2$ , specific gravity from 0.4 to 0.6 kg/hp, and specific fuel consumption from 0.24 to 0.32 kg/hp per hour. In the pre-war years and during the years of the Great Patriotic War Soviet aviation was developed on the basis of reciprocating engines

designed by A. A. Mikulin, V. Ya. Klimov and A. D. Shvetsov. With these engines, fighter-aircraft developed a speed of flight of 600-700 km/hr. Further increase of speed of flight required in turn further increase of capacity of power plant of aircraft. Reciprocating engines could not ensure this because of the excessive increase of weight and dimensions. Moreover, with growth of speed of flight the thrust of the propeller sharply drops.

Considerable increase of speed of flight of aircraft was attained with the help of the jet engine, whose thrust is created by reaction of the gas flow, escaping from the engine nozzle with great speed. The founder and creator of contemporary jet engineering is the great Russian scientist K. E. Tsiolkovsky. The first flight in the world in a jet aircraft was accomplished in 1942 by the Soviet pilot G. Ya. Bakhchivandzhi. This aircraft was designed by V. F. Bolkhovitinov and had a liquid-propellant rocket engine.

Turbojet engines started to appear at the end of the Second World War. However, wide practical application of TRD was obtained only after the war and in contemporary high-speed aircraft it became the basic type of engine. At present TRD are constructed with thrust from several hundred to 10,000 kg and above. Their specific thrust reaches 70 kg thrust/kg, and specific frontal thrust from 8000 to 10,000 kg/m<sup>2</sup> with specific gravity from 0.2 to 0.3 kg/kg thrust and specific fuel consumption from 0.75 to 0.9 kg/kg thrust per hour.

At contemporary high speeds of flight the TRD is the most economic engine. However, at low and medium speeds of flight (approximately up to 900 km/hr) TRD with respect to economy yields to engines with a propeller, which in these conditions has high efficiency. Prop-driven engines allow also to obtain large thrust on takeoff, and during landing they create with the prop a negative (brake) thrust, which decreases takeoff run during takeoff and landing run. Therefore, at present in civil aviation along with TRD they are widely using TVD and some PD.

At present TVD are constructed with power from several hundred to 10,000 hp and above. Their specific thrust reaches 250 hp/kg, and specific thrust reaches 250 hp/kg, and specific frontal power from 5000 to 7500 hp/m<sup>2</sup> with specific gravity from 0.15 to 0.3 kg/hp and specific fuel consumption from 0.2 to 0.3 kg/hp per hour and lower. Thus, TVD in comparison with PD can have significantly more power and are higher with respect to basic specific parameters. Ducted-fan jet engines, with respect to their characteristics, occupy the middle position between TVD

and TRD.

Contemporary aircraft have gas-turbine engines (TRD, DTPD, and TWD) and some reciprocating engines. Ramjet engines (PVRD) and rocket engines (RkD) at contemporary speeds of flight have low economy and in the future will probably find wider application.

Gas-turbine (GTD), ramjet (PVRD), and reciprocating (PD) engines have specific limitations with respect to altitude of flight due to the high rarefaction of the atmosphere at high altitudes. Flight at high altitudes can be carried out on vehicles with rocket engines, whose operation does not depend on the earth's atmosphere. Therefore, they are used on spaceships.

The Soviet Union holds many world records in the field of aviation, e.g., for altitude and speed of flight, for flying range, and for high-altitude transport. Thus, for instance in 1961, the Soviet test pilot G. K. Mosolov on the Ye-66 aircraft broke the record flight altitude by more than 34 km, and in 1962, he set a record flight speed of 2678.5 km/hr on the Ye-166. In October 1957, the Soviet Union launched the first artificial earth satellite in the world with a rocket engine, and on 12 April 1961, the whole world witnessed the first flight in the world into outer space on the satellite vehicle "Vostok" by the Soviet pilot-astronaut, Major Yu. A. Gagarin. A second more prolonged flight around the earth was made on 6-7 August of the same year by a Soviet astronaut, Major G. S. Titov on the satellite vehicle "Vostok-2". Finally, on 11-15 August 1962, Soviet astronauts, Major A. G. Nikolayev and Lieutenant Colonel P. R. Popovich, on the satellite vehicles "Vostok-3" and "Vostok-4", made a multiday group flight around the Earth.

Along with aircraft, in aviation we also find helicopters. Drive of the rotor of a helicopter can be mechanical or jet (Fig. 0.1). Mechanical drive is carried out from a reciprocating or gas-turbine engine with transmission of rotation to rotor through a transmission shaft and reduction gear. Figure 0.1a shows the drive of a rotor from a GTD, and Fig. 0.1b shows a jet drive with the use of compressed air. From a turbocompressor fixed in the fuselage of the helicopter, through channels of the shaft and rotor blades, the compressed air moves to the jet nozzles located on the ends of the rotor blades. Figure 0.1c shows a jet drive with turbojet or ramjet engines fixed at the ends of the rotor blades.

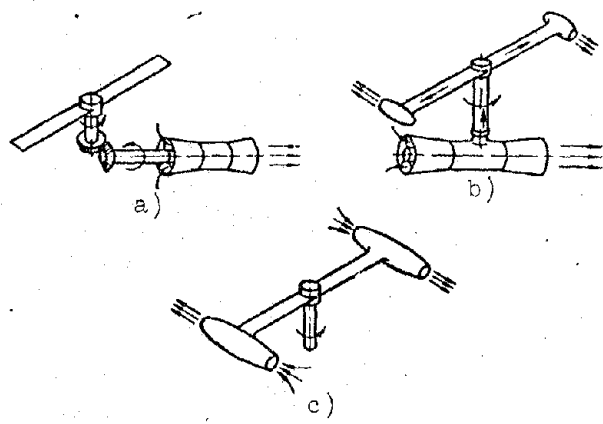


Fig. 0.1. Helicopter rotor drives.

F I R S T   P A R T

GAS-TURBINE AIRCRAFT ENGINES



## C H A P T E R I

### TYPES OF GAS-TURBINE ENGINES AND THEIR CLASSIFICATION

Aircraft gas-turbine engines [GTD] (ГТД) include turbojet [TRD] (ТРД), turboprop [TVD] (ТВД) and ducted-fan turbojet engines ([DTRD] (ДТРД)). Each of these types of engines have inherent peculiarities.

Basic GTD types applied in contemporary aircraft are TRD and TVD, which in turn are distinguished by the design features of specific units.

#### TRD are classified:

- by type of compressor, e.g., with axial or centrifugal compressor,
- by type of exit nozzle, e.g., with variable or fixed-area exhaust nozzle,
- by the presence of boosters, e.g., with afterburner or without it,
- by system of rotors, e.g., single-shaft or double-shaft,
- by system of flow area, e.g., with direct-flow or loop flow area, etc.

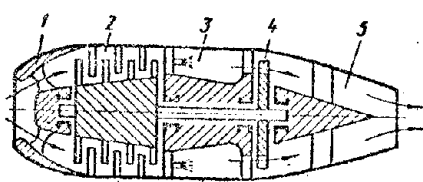


Fig. 1.1. Diagram of a TRD with axial-flow compressor.

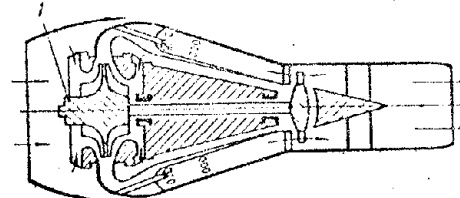


Fig. 1.2. Diagram of a TRD with centrifugal compressor.

Figure 1.1 shows a simple TRD diagram which consists of intake 1, axial-flow compressor 2, combustion chamber 3, turbine 4, and fixed-area exhaust nozzle 5. The diagram of a TRD with centrifugal compressors 1 is shown in Fig. 1.2. Axial-flow compressors are more widely used than centrifugal ones, since they

ensure the best engine economy, and with smaller diametral dimensions they allow large flow rates of air and high degrees of increase of pressure. However, centrifugal compressor designs are more simple and have smaller weight, since in one stage they ensure a greater degree of increase of pressure. They are used for GTD with small thrust. For TRD the field of application of centrifugal compressors is usually limited to thrust of 3000 kilograms.

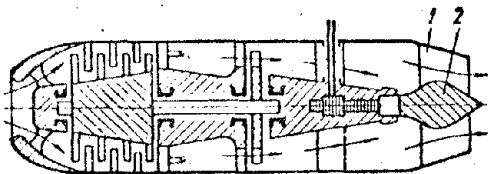


Fig. 1.3. Diagram of a TRD with variable-area exhaust nozzle.

Figure 1.3 shows the diagram of a TRD with variable-area exhaust nozzle. Basic adjustment for the TRD is carried out by change of quantity of fuel passed into the combustion chambers of the engine. The variable-area nozzle gives the possibility of additional adjustment by changing the area of its flow section. In the represented diagram, adjustment is carried out with the help of movement of the central body, i.e., throat bullet 2 fixed in exhaust nozzle 1. For the simple diagram of a TRD adjustment of exhaust nozzle usually gives small advantages, which do not justify the complication of engine design connected with this. Therefore, the majority of TRD, not having boosters are constructed with fixed-area exhaust nozzles.

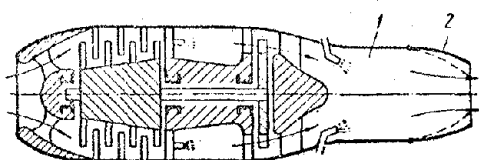


Fig. 1.4. Diagram of a TRD with afterburner.

For forcing of thrust on takeoff and for obtaining maximum speed of flight, behind the turbine there is an afterburner 1 in the TRD (Fig. 1.4). By burning of additional fuel in the afterburner the temperature of gases in front of the exhaust nozzle increases and engine

thrust is increased. During forcing there is required an increase of the area of the flow section of the exhaust nozzle; therefore, for TRD with afterburners they use the variable-area nozzle with variable flow section. Adjustment of nozzle is usually carried out by turning petals 2. The variable-area nozzle in this case is used also for improvement of characteristics and pick-up of engine and in nonboosting conditions.

The diagrams of Figs. 1.1-1.4 show single-shaft TRD, whose turbine rotor in connection with the compressor rotor forms a single rotor of the engine.

Figure 1.5 shows the diagram of a double-shaft TRD having a compressor with two cascades located in series: first cascade is a compressor of low pressure 1 and second cascade is a compressor of high pressure 2. Turbine of engine also

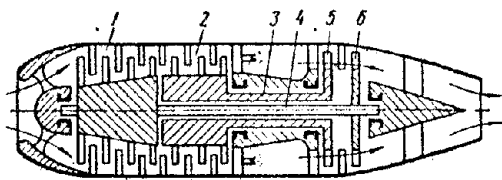


Fig. 1.5. Diagram of a double-shaft TRD.

consists of two separate turbines: a turbine of high pressure 5 and a turbine of low pressure 6.

Turbine and compressor of high pressure are united by a hollow shaft 3 forming one engine rotor, while turbine and compressor of low pressure are joined by a long shaft 4 (passing inside shaft 3) forming another engine rotor. Both of these rotors are not mechanically connected together.

Double-shaft designs are used in TRD with high-pressure compressors for improvement of their performance. Such a design also facilitates starting and acceleration of the engine, since from the starter only one rotor is turned (usually the rotor of high pressure), which requires less power. However, the design of a double-shaft engine is more complicated and heavier than the single-shaft.

The preceding diagrams showed TRD with direct-flow gas duct, in which the direction of motion of gases in the flow area of the engine always remains constant.

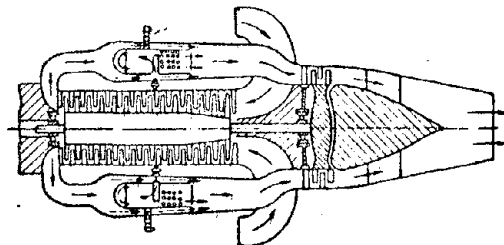


Fig. 1.6. Diagram TRD with loop motion of air.

With the loop gas duct, for instance with location of combustion chambers above compressor (Fig. 1.6), direction of motion of gases changes. With such a duct the length of the engine will be less, and the diametrical dimensions of it and hydraulic losses in the gas-air duct will be significantly more than

in the direct-flow type. Therefore, at present they chiefly use TRD with the direct-flow system of the gas-air duct.

As an example, Fig. 1.7 shows a foreign single-shaft TRD with a 13-stage axial-flow compressor and two-stage turbine. The engine has a direct-flow area and fixed-area exhaust nozzle. The engine does not have afterburners. Figure 1.8 shows a longitudinal section of the single-shaft [TRDVK-1] (ТРДВК-1) with centrifugal compressor and single-stage turbine. The engine does not have an afterburner and its exhaust nozzle has fixed-area. Figure 1.9 shows the over-all view of a foreign TRD with afterburner and variable-area exhaust nozzle.

#### TVD are classified:

- by type of compressor - with axial or centrifugal compressor,

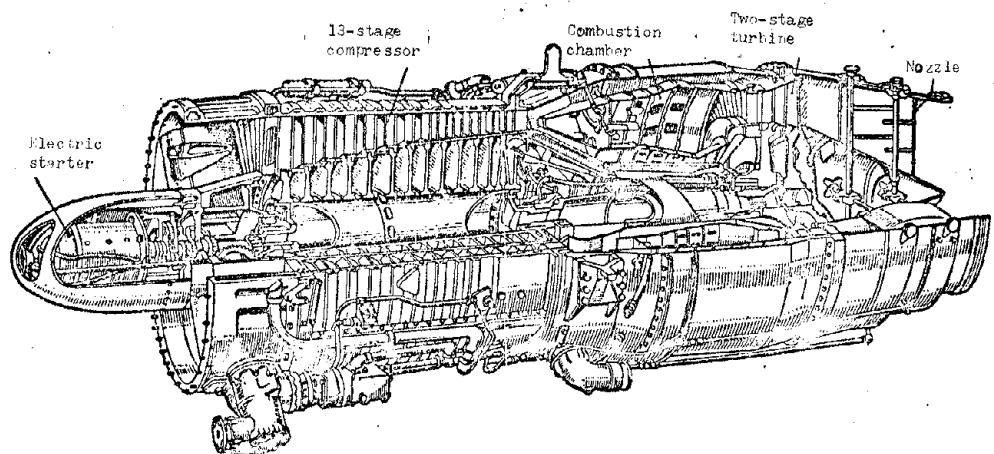


Fig. 1.7. TRD with axial-flow compressor.

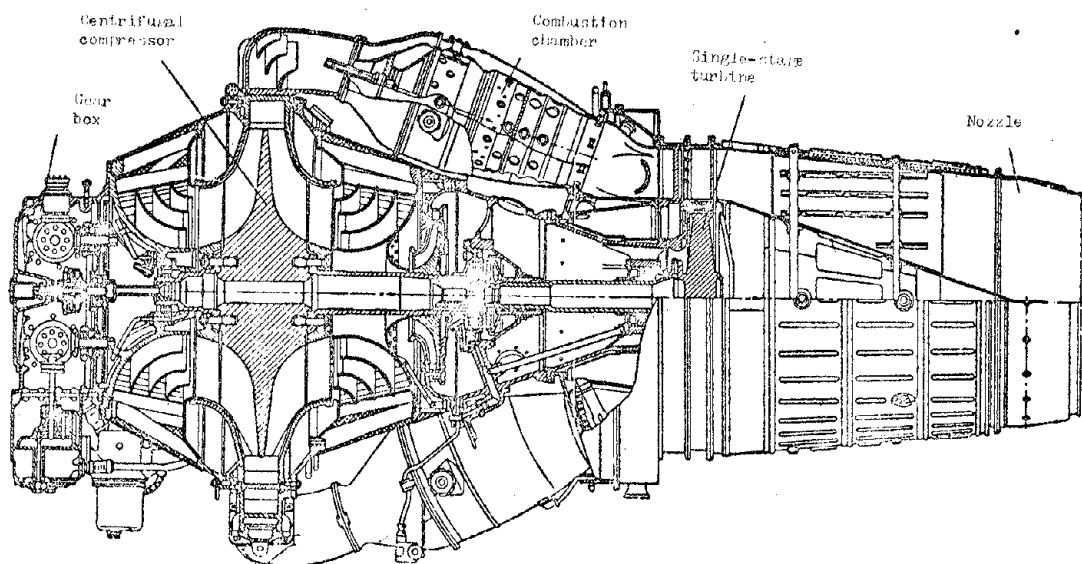


Fig. 1.8. TRD with centrifugal compressor.

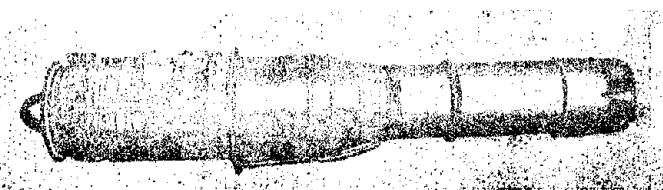


Fig. 1.9. TRD with afterburner.

- by system of rotors - single-shaft and double-shaft,
- by system of flow area - with direct-flow or with loop flow area,
- by number of propellers - with one or two propellers, etc.

Figure 1.10 shows a simple diagram of a single-shaft TVD, consisting of propeller 1, reduction gear 2; intake 3, axial-flow compressor 4, combustion chamber 5, turbine 6, and exhaust 7. In distinction from TRD the TVD turbine uses up almost all the available heat and transmits excess power to the propeller.

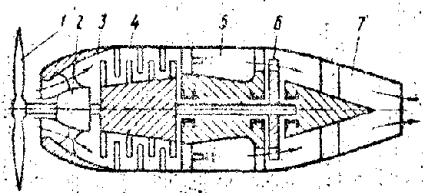


Fig. 1.10. Diagram of single-shaft TVD.

Since the rpm rate of the turbine exceeds the necessary rpm rate of the propeller, its drive is equipped with a reduction gear, lowering the rpm rate. The design of the double-shaft TVD (Fig. 1.11), possessing the same merits as the design of the double-shaft TRD, allows to obtain

the rpm rate in the turbine of low pressure 2 lower than in the turbine of high pressure 1. The design of the reduction gear is simplified. However, the design of the double-shaft TVD is more complicated and heavier than the single shaft. In the TVD high power is established by two coaxial propellers revolving in different directions.

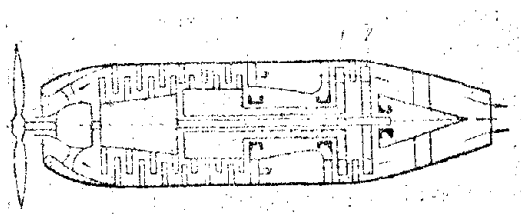


Fig. 1.11. Diagram of a double-shaft TVD.

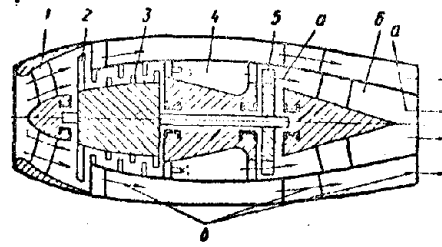


Fig. 1.12. Diagram of single-shaft ducted-fan jet engine.

Figure 1.12 shows a simple diagram of a ducted-fan jet engine, consisting of intake 1, fan 2, axial-flow compressor 3, combustion chambers 4, turbine 5, and exhaust 6. The ducted-fan jet engine has two isolated cycles of the gas-air duct: a) internal and b) external. The turbine with the internal cycle uses up

almost all available heat and transmits its excess power for the drive of fan 2. The ducted-fan jet engine can be single-shaft and double-shaft. In its external cycle there can be fixed an afterburner.

## C H A P T E R   II

### AXIAL COMPRESSORS

#### 2.1. General Information

[ГТД] (ГТД) compressors serve for compression of air. Figure 2.1 shows a structural diagram of a 4-stage axial-flow compressor. The main parts of it are the rotor and stator.

Rotor consists of separate disks 11, head 24, and tail 14, forming a rigid drum. On the circumferences of disks 11 are attached working blades 23. Each annular row of working blades together with their carrier element — the disk or part of the drum is called an impeller. With the help head 24 and tail 14 the rotor is fixed in the stator on rocker bearings 13 and 25.

Stator consists of housing of 21 compressor, housing 5 of front bearing of rotor, and housing 10 of rear bearing of rotor with fixed blades 4, 9, and 22. Blades 4, attached to housing 5, are called guides. An annular row of them will form the inlet guide of the compressor. Blades 9 and 22, attached to housings 10 and 21 are called straighteners. Each annular row of straightening blades with their carrier elements form a straightener.

The impeller with the stator located behind it is collectively called the compressor stage. The inlet guide is located in front of the first stage of the compressor. It is not included in the stage and is absent in certain compressors.

Housing of 5 of front bearing forms in the compressor an annular inlet channel, divided by hollow stands a. They connect the external wall of the housing with its central part, where there are front bearing 25 of rotor and drive transmission of assemblies from rotor of compressor. Drive shafts 3 pass inside hollow

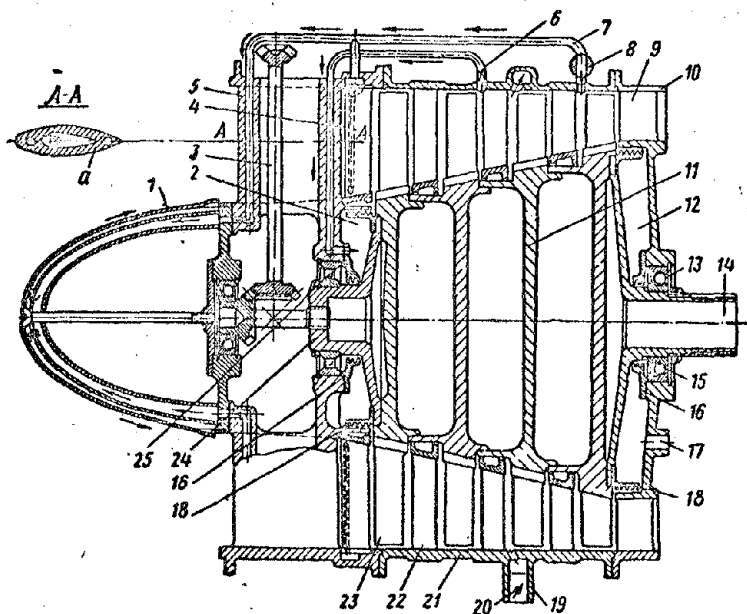


Fig. 2.1. Structural diagram of axial-flow compressor  
 1 — cowl; 2 — front unloading chamber; 3 — drive shaft of assemblies; 4 — inlet guide vane; 5 — housing of front bearing; 6 — channel for feed of air to front unloading chamber; 7 — channel for sampling of air for heating; 8 — valve for sampling of air; 9 and 22 — stator blades; 10 — housing of rear bearing; 11 — disks of rotor; 12 — rear unloading chamber; 13 — rear bearing of rotor; 14 — rotor tail; 15 — regulating ring; 16 and 18 — labyrinth seals; 17 — vent hole; 19 — air bypass; 20 — throttle of air bypass; 21 — housing of compressor; 23 — working blade; 24 — head of rotor; 25 — front bearing of rotor.

stands a. In central part of housing there is attached cowl 1, ensuring smooth feed of air to annular inlet channel of compressor.

Housing 10 of rear bearing of rotor forms the annular outlet channel of the compressor. In the diagram the external wall of the housing is united with its central part with the help of blades 9 of the stator of the last stage. In the central part of the body there is the rear bearing of the rotor.

Flow area of compressor. During passage through compressor air is compressed and its volume decreases. According to this the length of blades from stage to stage also decreases. Flow area of compressor can be made (Fig. 2.2):

with constant external diameter  $D$ ,

with constant middle diameter  $D_{cp}$ ,

with constant internal diameter  $d$ , which is called the hub diameter.

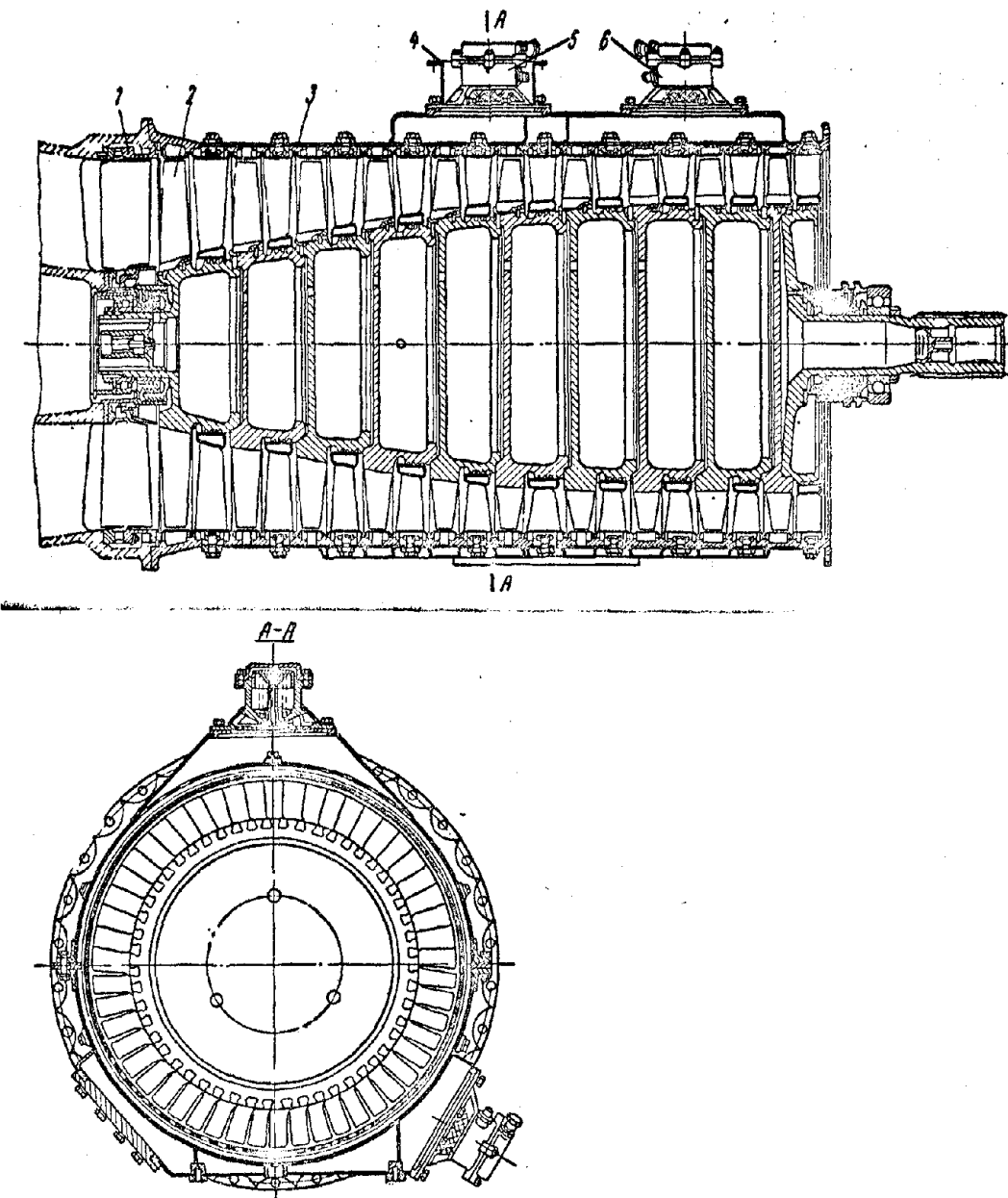


Fig. 2.3. Compressor of AI-20 engine. 1 - intake guide 2 - rotor of compressor, 3 - housing of compressor, 4 - housing for removal of air from bypass valve, 5 and 6 - valves of bypass of air.

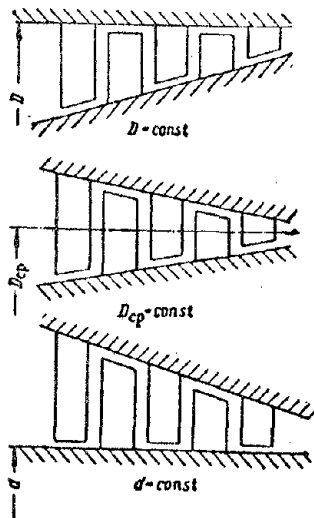


Fig. 2.2. Forms of flow area of compressor.

When  $D = \text{const}$  the pressure state of compressor is somewhat greater because of higher peripheral velocity of working blades of last stages. However, when  $d = \text{const}$  the blades of last stages are longer and therefore, negative influence on efficiency by losses due to overflowing of air through radial clearances is less. At the same number of stages the weight of compressor with flow area made with  $d = \text{const}$ , is also less. Separate sections of flow area of compressor are frequently made in different forms, and in certain compressors all three diameters  $D$ ,  $d$  and  $D_{cp}$  along length of flow areas are variable.

Classification of axial-flow compressors. Axial-flow compressors are distinguished by number of stages, by number of rotors, by airspeed in flow area, and by other criteria.

Number of stages of compressor is determined by degree of increase of pressure and performance of separate stages. In contemporary foreign GTD with high degree of increase of pressure the number of stages of compressor reaches up to 17. As an example, Fig. 2.3 shows the ten-stage compressor of the [AI-20] (AM-20) engine.

By number of rotors (cascades) compressors are divided into single-rotor (single-cascade) and two-rotor (two-cascade). In the last case the first cascade forms the compressor of low pressure 1, and second, the compressor of high pressure 2, whereby both cascades are arranged in series (Fig. 2.4).

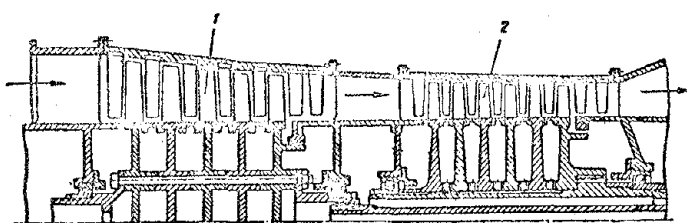


Fig. 2.4. Diagram of two rotor compressor.

By velocity of air we distinguish compressors as subsonic and supersonic. In the first, all stages are subsonic, and in the second, the first or several first stages are supersonic, and others are subsonic. Pressure state of supersonic stages is higher than subsonic; however, their losses are great; therefore, in case of application of supersonic stages the total number of stages in the compressor is less, but its efficiency is lower than in the subsonic compressor.

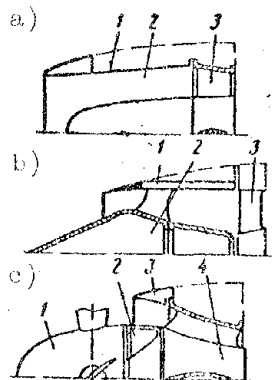


Fig. 2.5. Diagrams of intakes.

Intake constitutes a channel bringing in air to compressor with minimum resistance, uniform field of speeds and pressures. Figure 2.5 shows a model diagram of intakes of [TRD] (ТРД) and [TVD] (ТВД).

Diagram a represents the intake of TRD, designed for medium speeds of flight. The intake consists of air inlet 1 and internal cowl 2 fastened to housing of front bearing 3. Form of intake edge of air inlet and cowl, and also form of channel formed by them, correspond to requirements of aerodynamics of subsonic speeds.

Air inlet is usually included in the aircraft design.

Diagram b represents the intake of TRD, design for high speeds of flight. Here in accordance with aerodynamics of high speeds the intake edge of air inlet 1 is sharp, and internal cowl 2 is in the form of a needle. Transition of supersonic flow to subsonic is ensured by form of channel.

Diagram c represents the intake of TVD. Annular inlet to compressor is above the housing of reduction gear 4, to which are fastened the external 3 and internal 2 annular short cowls. Propeller has cowl 1, ensuring smooth approach of air flow to compressor.

For preventing fall into compressor of outside objects, which can lead to its destruction, intakes are sometimes equipped with suppressor grids or lattices. Diagram a in Fig. 2.6 shows an annular lattice 1 attached at the annular channel of the front bearing housing.

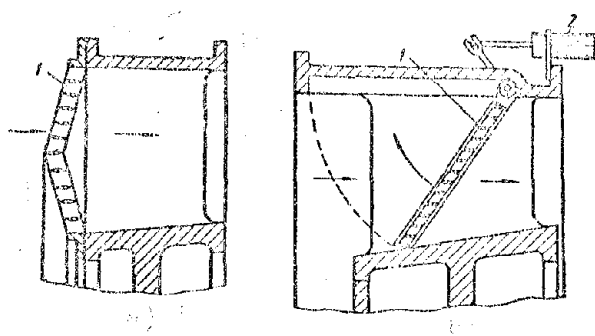


Fig. 2.6. Suppressor grids (lattices) on compressor inlet.

However, suppressor grids and lattices create additional drag on compressor inlet, which lowers engine thrust and increases specific fuel consumption. Furthermore, grids and lattices require heating to counteract icing. Fall of foreign objects into compressor is possible only during work in ground conditions (for instance, during takeoff and landing of aircraft); therefore, safety grids can be made retractable in flight, as was shown in diagram b. In this case grid 1 is made in

-23-

the form of a set of annular sectors, which are hinged to the housing. Ejection of grid and its removal is carried out with the help of hydraulic drive 2.

Deicing system. At a temperature of external air near  $0^{\circ}\text{C}$  and with heightened moisture of it on intake of working compressor there is observed icing of walls, struts and vanes of intake guide. The flow sections on compressor inlet decrease, which leads to decrease of thrust (power) of engine and evokes surging of compressor. During intense icing the engine can die. Finally, detaching pieces of ice may cause damage of vanes and put the compressor out of order.

For protection from icing they apply heating of intake or injection of a deicer into it. Heating of intake is more effective and therefore has obtained wide application. It can be carried out by electrical method, hot gases (products of combustion), or heated air. In TVD heating of struts of housing 5 (see Fig. 2.1) frequently is carried out by used-up hot oil.

In case of electroheating inside separate parts of intake they place heating elements, through which there passes a current. Deficiency of electroheating is large expenditure of electric power.

For heating by gas or air, separate parts of intake are made hollow (double-walled construction). Hot gases can be removed from engine exhaust or from main combustion chambers. For the same purpose it is also possible to apply special combustion chambers fed by air from intermediate stages of compressor. However, heating with hot gases leads to awkward communications and increases fire danger. Therefore, the most widely applied means of heating of the intake is by with moderately heated air which is ejected behind the last compressor stages. This method of heating is represented in a general diagram of a compressor (see Fig. 2.1), and also separately in Fig. 2.7.

Upon opening flap 3, hot air at a temperature of  $200-250^{\circ}\text{C}$  passes through channel 2 for heating the hollow vanes of the intake guide 4, struts of housing of front bearing a, and cowl 1. Flow rate of air is appportioned by flap 3 and calibrated holes in different parts of heating system. The warmed walls are heated to  $20-40^{\circ}\text{C}$ . Upon leaving the heating system, the hot air is mixed with the basic air proceeding to the compressor, or is ejected into the atmosphere.

Heating is included only in case of appearance of danger of icing, since during heating, thrust (power) of engine drops somewhat. On and off switching of heating can be carried out automatically.

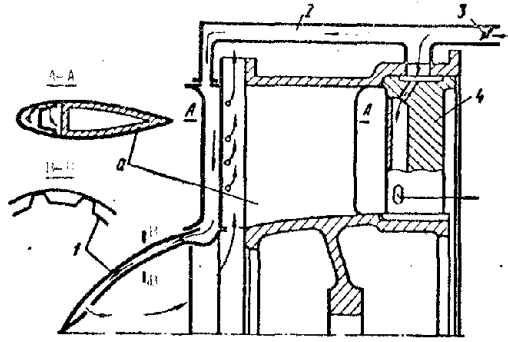


Fig. 2.7. Diagram of heating of intake with hot air.

Anti-surge systems. Upon change of operating conditions of a GTD, in the compressor the flow of air and degree of increase of pressure change. Together with this, the distribution of speeds and pressures along air flow changes. With large deviation from rated conditions the areas of flow sections and angles of setting of vanes cease to correspond to the given operating conditions,

and there appear separations of flow with formation of local vortices. These vortex flows are unstable. Spreading, they fill the intervane channels, they partially stop, and then break off. Compressor starts to operate unstably with pulsating supply of air. This phenomenon is called surging. During surging, engine thrust drops and its economy lowers. There appear strong vibrations which can lead to breaking of vanes and malfunction of engine. Therefore, engine operation during surging is impermissible. Surging appears more intensely the more the given conditions differ from rated and the higher the increase of pressure of compressor.

Surging in conditions lower than rated usually appears in first stages of compressor; surging in this case is removed:

- a) by bypass of 10-20% of the air from one or several middle stages into the atmosphere,
  - b) by turn of vanes of guides and stators of first stages.

During bypass of air, its flow is increased and correspondingly, axial speed at first stages rises. During turn of vanes the cycle of air flow changes. In each case the triangles of speeds of air flow change, becoming similar to calculated ones. The flow around vane profiles of first stages is improved and surging is removed.

Figure 2.8 shows the diagram of devices for bypass of air: a - with throttle flap 1, b - with valve mechanism 2, and c - with steel elastic tape 5, which envelopes the compressor housing and covers the windows located uniformly along its circumference. In Fig. 2.1 bypass of air is carried out by throttle flap 20 through pipe 19.

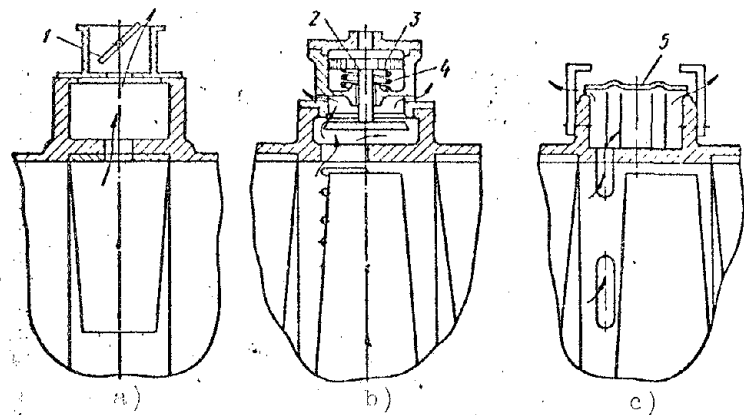


Fig. 2.8. Diagram of air-bypass devices.

Control of bypass devices is executed automatically with the help of hydraulic and pneumatic drives. In diagram b, for instance, opening of valve 2 is carried out by piston 3, to which oil or air is brought in under pressure. After compressor is stable operating conditions, supply of oil or air to piston is disconnected and valve under action of spring 4 is closed.

Rotary blades are fixed in guides and stators on axes, allowing their rotation. Examples of their construction are shown in Fig. 2.25. Angle of rotation of blades depending upon operating conditions of engine is regulated automatically.

Bypass of air and turn of blades of first stages is used also for facilitating engine starting. In the first case the flow rate of air decreases through last stages of compressor, and in the second, admission of air into compressor decreases. Due to this, the required power of actuators for spin-up of rotor is lowered.

Unloading chambers. Air pressure, passing through compressor, increases from stage to stage, owing to which the rotor is loaded by axial force directed towards the intake, i.e., opposite the flow of air. In this case there can be a considerable axial load on radial-thrust bearing 13 (see Fig. 2.1). For decrease of it the compressors frequently have unloading chambers 2 and 12, which in the direction of the flow area of compressor and rotor bearings are insulated by labyrinth seals 16 and 18. Front chamber 2 through channel 6 is connected with one of the intermediate stages of compressor, and rear chamber 12 is connected through hole 17 and channel with atmosphere. Since in chamber 2 pressure will be established higher than in chamber 12, on rotor in the direction of unloading

chambers there will act an axial force, directed towards the compressor outlet. Because of this the resultant axial load on bearing 13 will decrease.

## 2.2. Rotor Design

Figure 2.9 shows the rotor of the compressor of the [AI20] (AN20) engine with ten rows of working blades.

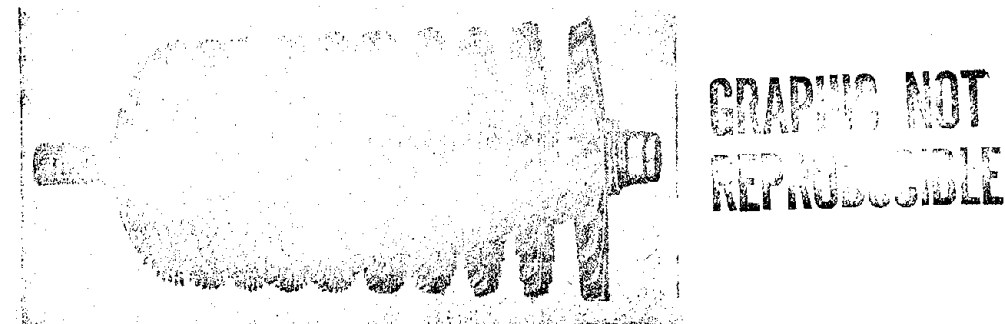


Fig. 2.9. Rotor of compressor of AI-20 engine.

Working blades (Fig. 2.10) pertain to the main working elements of a compressor. Blades have a working (profile) part of fin 1 and leg 2. With the help of the latter the blades are braced to the rim of the disk or to the drum of the rotor. At the impeller the blades form a collar with curvilinear interblade channels. For subsonic speeds these channels are expanded — in form of a diffuser, and for supersonic speeds there are of more complicated form, ensuring transition of supersonic flow to subsonic.

Cross sections of fin of blades have somewhat bent aerodynamic profile. Curvature of profile and angular position of it at the blades are usually made variable from peripheral section to root in accordance with change of triangles of speeds for incident air flow. Fin of blade is as if twirled along its length into a helix. Short blades are not frequently made helical in length.

In designs of compressors the length of blades of first stages reaches 200-250 mm. Length of blades of last stages tend to be limited to a magnitude of not less than 25 to 30 mm, since with short blades the relative losses due to bleeding of air through radial clearances noticeably increase and efficiency drops.

Chord  $b$  profile of blade and stage  $t$  blades of impeller are connected together and are determined by density of cascade of buckets  $b/t$ . Density of cascades is selected on the basis of experimental data of their scavenging.

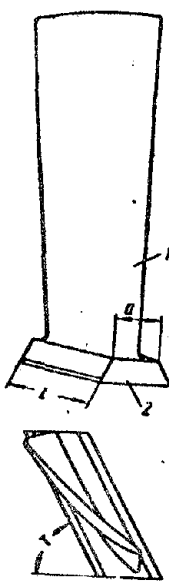


Fig. 2.10.  
Working blade  
of compressor.

During operation, blades are under the action of centrifugal and aerodynamic forces which cause extension, bending and twisting of them. During nonuniform air flow there can also appear vibrations of blades. By conditions of durability, thickness of profile of blades is variable, with increase of it from peripheral to root section.

Blades of compressors operate at moderate temperatures. They are most frequently made from highly durable aluminum alloys and from alloyed steels. Application of aluminum blades is limited to an operating temperature of not more than  $250^{\circ}\text{C}$ . Steel blades can operate at a temperature up to 500 to  $550^{\circ}\text{C}$ . They have higher vibration strength and better resist destruction upon fall of foreign objects into compressor.

The most progressive method of manufacture of blades is their stamping with subsequent caulking of fin. Profile part of blades is made with precision: with respect to linear dimensions  $\pm 0.1$  mm and angular  $\pm 15'$ . High purity of treatment (polishing) increases vibration strength of blades, since presence of small graduation lines can lead to formation of fatigue cracks in them.

For facilitating rotor balancing the working blades are completed according to weight. Small weights for every bucket are allowed within limits of not more than 5 to 6 g.

Retainers of working blades. Working blades are mounted to rotor with the help of retainers.

Figure 2.11 shows certain types of these retainers: a) pin, b) trapezoidal type "swallowtail," c) cylindrical, and d) "herringbone" type.

Compressors widely have utilized retainers of the "swallowtail" type that is distinguished by its relative simplicity of design, small weight, and small geometric dimensions. This retainer has the form of an equilateral trapezoid with angle  $\alpha$  between working surfaces of the order of  $40^{\circ}$ .

Length  $l$  and thickness  $a$  of leg of blade are determined usually by the condition that the root section of the fin circumscribes the leg (see Fig. 2.10). Retainer grooves on disks can be parallel to the axis of rotor or at an angle to

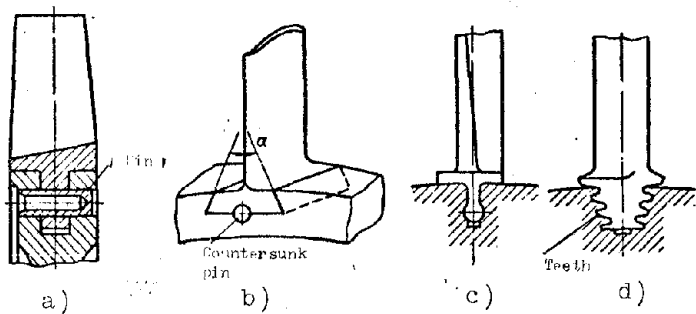


Fig. 2.11. Attachment of working blades.

it in transverse (circumferential) direction (see Fig. 2.12b and a). Location of grooves at angle  $\gamma$  in circumferential direction (slanting grooves) allow the leg of the blade to be thinner and lighter, and also to hold a large number of blades on disk.

With variable diameter of hub  $d$  at flow area of compressor (see Fig. 2.2) grooves are made at an angle also in longitudinal direction. An example of this can be the blades of the first stages of the rotor represented in Fig. 2.12c and 2.17.

Setting of blades in a retainer of the swallowtail type is either tight — with tightness from 0.01 to 0.03 mm, or free — with clearance from 0.01 to 0.03 mm. Free setting facilitates replacement of blades and their selection during

balancing or rotors.

Herringbone retainer has small dimensions and is able to perceive large loads, but in manufacture it is more complicated than the trapezoidal retainer.

Herringbone retainer sometimes finds application in high-loaded blades. Setting of blades in herringbone retainer is usually free.

Fig. 2.12. Fixing of blades in retainer grooves.

Pin and cylindrical retainers are heavier than trapezoidal ones and therefore have limited application.

Working blades in retainer grooves are usually fixed by threaded or smooth pins, laminar stoppers, special stops, and so forth.

Figure 2.12 shows examples of fixing of blades in retainer grooves:

a) fixing of blade with smooth pin 1 which is pressed into a hole located at an angle to the slot in the joint of the blade with disk. After pressing of the pin the hole is caulked;

b) fixing of blade with laminar stopper 2. It is preliminarily placed in a socket made in the slot of disk. After that, into the retainer groove to the stop in the turned end of the stopper, the blades are introduced, and the free end of the stopper is unbended on its leg;

c) fixing of blade with thrust pin 3 and laminar retainer 4. Figure 2.13 shows setting of blade with such fixing on disk.

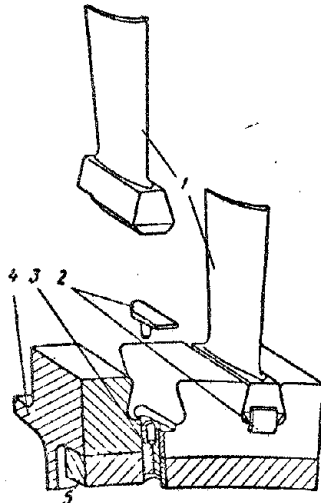


Fig. 2.13. Installation of working blade on rotor of AI-20 engine. 1 — working blade, 2 — retainer 3 — pin, connecting disks, 4 and 5 — disks of rotor.

Fixing with pins (see Fig. 2.12a) is used for a tight fitting of blades in retainer. Laminar stoppers are suitable for free fitting of blades in retainers; they ensure facility of replacement of blades. However, laminar retainers do not allow large loads on the blades. They are under the action of centrifugal force of the blade if the retainer groove is inclined in longitudinal direction (see Fig. 2.12c). In this case stops are used for perceiving the load. Laminar stopper, fixed on the other side of the blade, does not perceive a load.

Rotors of compressors (Fig. 2.14) are of three types: a) drum, b) disk, and c) mixed (disk drum).

Rotor of drum type constitutes a thin-walled drum, whose ends are fitted with support journals. On external surface of drum there are longitudinal or transverse (annular) profiled grooves for attachment of blades. With large number of stages, drums can be sectional. Rotors of drum type possess high bend rigidity and are distinguished by simplicity of construction. However, by conditions of durability they allow peripheral velocities of rotation not more than 180 to 200 m/sec on external surface.

Rotor of disk type constitutes a shaft with disks placed on it. Disks possess greater durability than drums and allow peripheral velocities of the order from 340 to 400 m/sec. However, rotors of disk type possess smaller bend rigidity and therefore their shafts must be massive.

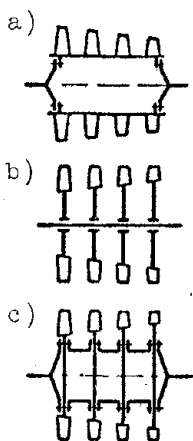


Fig. 2.14.  
Types of  
rotors.

Rotors of mixed type consist of separate disks, united in drum with help of intermediate thin-walled rings, or by means of extended shoulders of disks. They possess the advantages of rotors of drum and disk types and therefore have obtained wide application.

Figure 2.15 shows the forms of disk patterns: a) disk of constant thickness, b) conical disk, and c) disk of composite form. The last two, in comparison with disk of constant thickness, have smaller weight. Diagram d shows a disk with central hole.

The hole weakens the disk. Therefore, for increase of durability of such disk an extension is made. Thickness of disks is determined from conditions of durability. In peripheral part the disks have an extended rim, which has grooves for mounting of blades.

Methods of connecting disks with each other, and also with shafts and support journals in rotors of mixed type are very diverse. These connections must ensure reliable centering of disks and shafts, high durability, sufficient bend rigidity, small weight, and convenience of assembly.

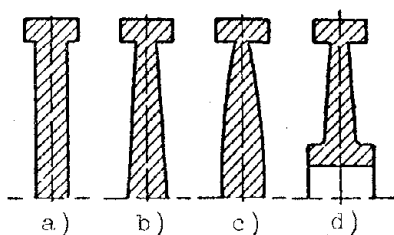


Fig. 2.15. Forms of disk patterns.

Figure 2.16 shows the following examples of connections for compressor rotors: a) with help of triangular butt slits and central tie bolt, b) flanged joint with help of short bolts, and c) flanged joint with help of long tie bolts.

Figure 2.17 shows a rotor of mixed type, whose connection is carried out by radial pins 2 with press fitting of disks on shoulders 1. Pins are pressed in holes located in grooves under blades. This protects pins from falling under action of centrifugal forces.

For equalizing pressure in cavity of rotor the disks have holes 3. Vent holes are also in one band at the wall of the drum.

Rotors of compressors during operation are loaded by considerable inertial and gas forces, turning and bending moments.

Disks of compressors are made from highly durable aluminum and titanium alloys and from alloyed steels.

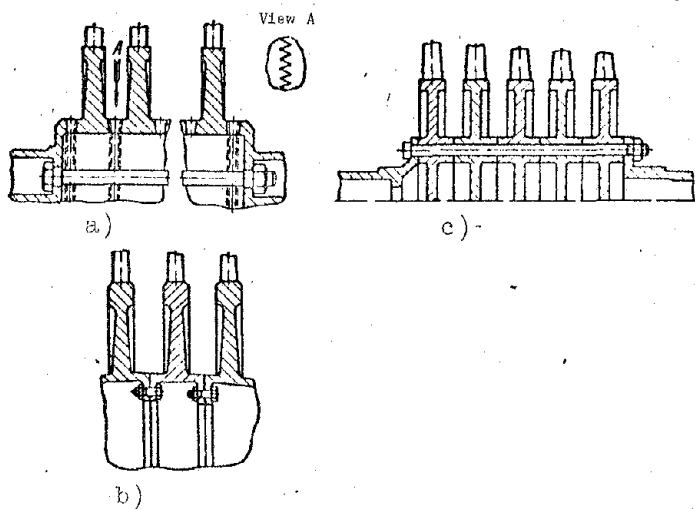


Fig. 2.16. Connection of rotor disks.

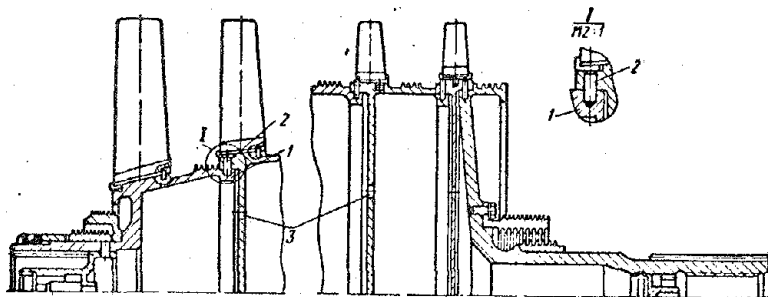


Fig. 2.17. Rotor of compressor of AI-20 engine with disks untied by radial pins.

### 2.3. Stator Design

Figure 2.18 shows a casing with stators.

Guides and stators of compressor are formed by an annular set of stator blades and their carrier elements. They serve as rings in the form of bands or directly the compressor housing itself. For an example, Fig. 2.19 and 2.20 depict intake guides and stators of the AI-20 engine.

Guide and stator blades, as also working blades, are the main working elements of the compressor. In cross section they have a somewhat bent aerodynamic profile. In length the guide and stator blades are frequently constructed with constant thickness of profile.

Length, chord, and curvature of profiled part of blades, and also number of blades are all determined by gas-dynamic calculation. Density cascades is selected

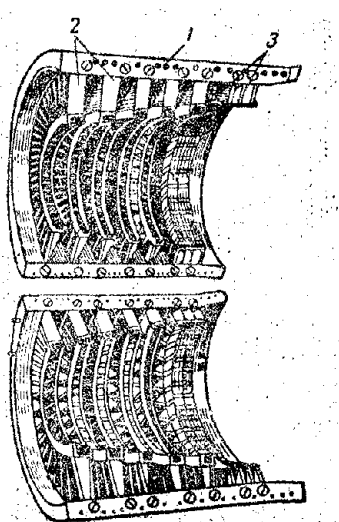


Fig. 2.18. Split housing of compressor  
1 — housing of compressor,  
2 and 3 — stators.

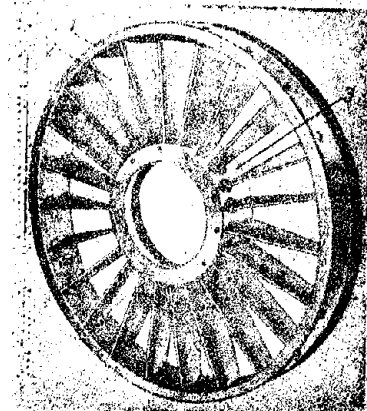


Fig. 2.19. Intake guide of Al-20 engine. 1 — outer ring, 2 — stator blades, 3 — inner ring.

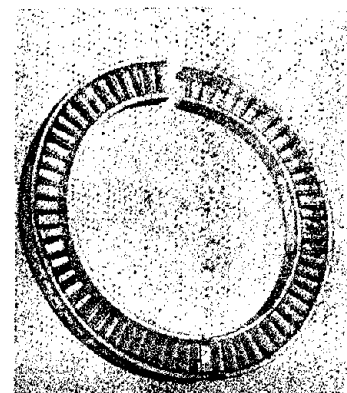


Fig. 2.20. Stator of Al-20 engine.

on the basis of experimental data of scavenging.

During operation, guide and stator blades are subjected to bending and twisting under action of aerodynamic forces. Furthermore, during nonuniform flow there can appear vibrations of blades.

Blades are made from highly durable aluminum alloys or of steel precision stamping, precision casting, or from rolled profiled tape. Profiled part of blades is thoroughly polished. The precision of its manufacture is the same as the working blades.

For heating of blade of intake guide, recesses are made along inlet edge, as shown in Fig. 2.21. Blades a and b have milled recesses with subsequent brazing or welding of edge. Blade c has a hollow inlet edge made from sheet steel and welded by spot welding to steel plugs pressed into the body of aluminum blade.

By design, guides and stators are classified:

- a) with overlapping and double-support attachment of blades;
- b) detachable and nondetachable in axial plane of compressor;
- c) collapsible and noncollapsible;
- d) with rotary and nonrotary blades.

Figure 2.22 shows overlapping attachment of stator blades. Blades are attached in longitudinal profiled grooves of the half-ring with help of swallowtail

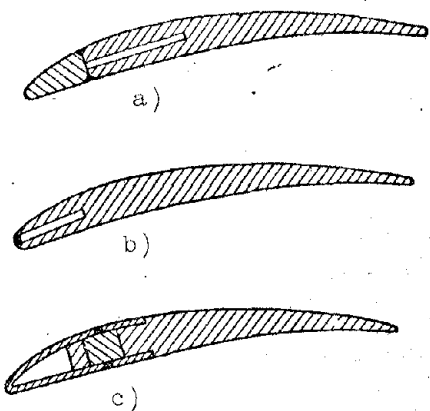


Fig. 2.21. Warmed blades of intake guide.

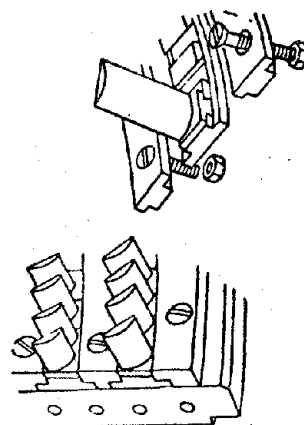


Fig. 2.22. Overlapping attachment stator blades.

type retainers. Half-rings and carrier blades in turn are mounted in the compressor housing with help of superposed intermediate half-rings and bolts having countersunk circular heads. With overlapping attachment of blades the internal support ring of the apparatus is absent and internal contour of flow area will be formed by the wall of the rotor.

Blades with overlapping attachment have a greater inclination to vibrate than double-supported ones and therefore are made thicker.

Figures 2.20 and 2.23 shows a detachable, noncollapsible stator with double-supported nonrotary blades. It is welded and has a disassembly joint in the axial plane of the compressor. Each part of the stator consists of external 2 and internal 4 half-rings of Π-shaped cross section made by rolling from 1.5 mm steel, and steel blades 3 made by method of precision casting with subsequent polishing. Half-rings have profiled screening into which the blades are inserted and they are butt-welded by electric arc. Internal half-ring 4 by electric arc is welded to labyrinth steel half-ring 5, forming an air seal with the rotor lugs. This prevents bleeding of air from outlet side of stator to its inlet. On half-ring 5, by method of metal-plating, a soft layer 7 is applied 0.7 mm thick consisting of aluminum powder and graphite. For best cohesion of layer 7 with labyrinth half-ring 5, the latter is threaded 6.

With the help of drilled holes on the external half-rings the stators are placed in the compressor housing and secured by bolts. Bolts are screwed into bosses 1 welded to external half-rings of stators.

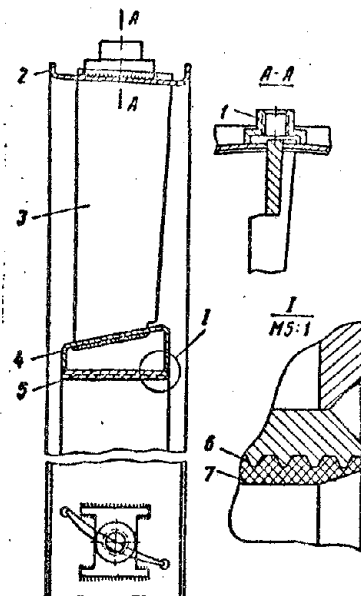


Fig. 2.23. Stator of AI-20 engine.

Figures 2.19 and 2.24 shows an intake guide and stator blade. The guide is nondetachable, collapsible, and has double-supported stator blades.

Blades 1 are steel, made by method of precision casting: on the ends they have journals a and b which are placed in rings of apparatus. Journal b has a flat area for fixing. For heating, the blades have grooves c, which on the leading edge part and upper end are welded by electric arc or argon arc. Upper journal a is hollow and has two drillings made with help of slot d with groove c. Blade slot is made by electro-erosion method.

External ring is made from magnesium alloy and consists of two parts — front 3 and rear 4. In plane of joint there are holes for upper journals a of blades.

Internal ring 6 is made from aluminum alloy and has holes for lower journals b. of blades.

Inlet guide is installed in casing 5 of front bearing. External rings 3 and 4 are centered in flow areas of casing 5, and internal ring 6 is placed around the glass of front bearing 8. They are fixed by dowels 2 and secured by pins.

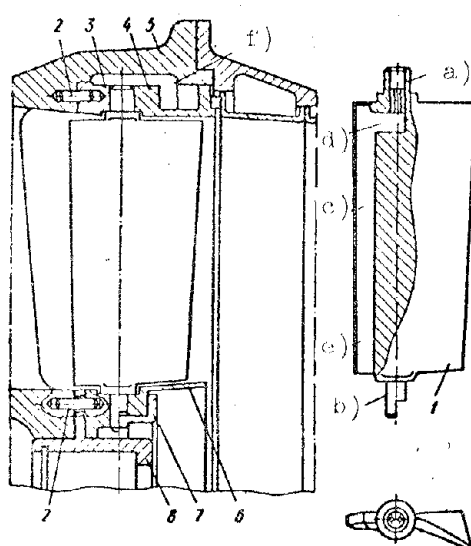


Fig. 2.24. Inlet guide of AI-20 engine.

Angular position of blades is fixed by stopper washer 7. Into annular cavity f of casing 5 from last stage of compressor there is fed hot air which through holes in journals a passes into grooves c, warms the blades and emerges from lower end of blades e, being mixed with general flow of air at compressor inlet.

Figure 2.25 shows arrangement of rotary blades of guides and stators. With their journals the blades are fixed in bushings (bearings). In apparatus a the blades are united with help of toothed sectors 2 with central conical gear 3 fixed inside casing. On

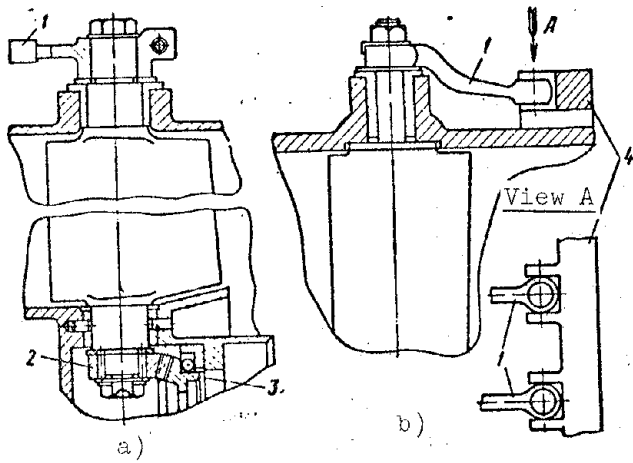


Fig. 2.25. Arrangement of rotary blades of stator and guides.

one of blades there is fixed a lever of control 1 by which it is possible to change angular position of blades of apparatus.

In apparatus b the blades are united with help of levers 1 and ring 4. Ring is fixed on the outside on housing of compressor. Into its grooves enter the heads of levers 1 fixed on all blades. By turning the ring the angular position of blades of apparatus is changed.

Housing of compressor depending upon form of flow area can have the form of a cylinder, frustum of a cone, or more complicated form. From internal side in housing stators are attached (see Fig. 2.18), and from the ends the casings of rotor bearings are attached to it, forming the inlet and outlet of air for the compressor.

Housing of compressor is in the power-distribution system of the engine. It perceives twisting moments from stators and bending moments from forces of weight and inertial forces. From the internal side it is under heightened air pressure. Usually on the compressor housing there are aircraft engine mounting lugs and through it there is transmitted the force of engine thrust.

Compressor housing is made in the form of a thin-walled casting from light alloys or welded construction from sheet steel. For guarantee of durability and rigidity, the walls of the housing have longitudinal and transverse ribs.

Compressor housing can be detachable and nondetachable. The detachable housing has a longitudinal assembly joint as was shown in Fig. 2.18. Nondetachable housing is made in the form of a whole drum. In this case during assembly the rotor is preliminarily put together with stators, and then is placed into the housing from the side of its end. After that the stators are secured in the housing.

Figure 2.26 shows the compressor housing of the AI-20 engine with stators fixed in it. The housing is cylindrical, detachable, steel, welded construction.

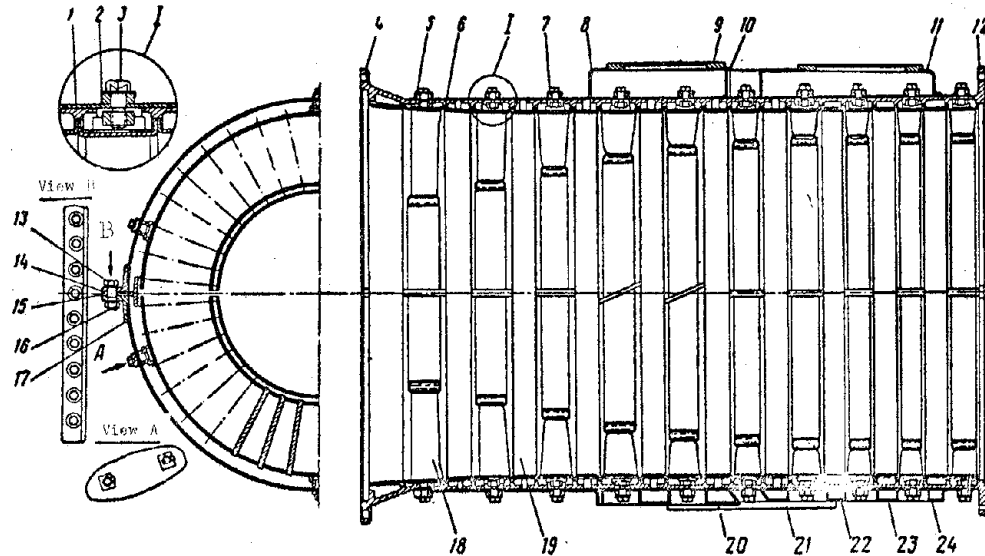


Fig. 2.26. Compressor Housing of AI-20 engine. 1 - half-ring of rigidity; 2 - sunk lock; 3 - bolt for attaching stator; 4 - front flange; 5 and 7 - bosses of stators under bolts 3; 6 - wall of housing; 8 and 11 - receivers; 9 - flange; 10 - glass; 12 - rear flange; 13 - washer; 14 and 17 - longitudinal flanges; 15 - lining; 16 - bolt; 18 - stator; 19 - working ring; 20 and 23 - receivers; 21 - strip; 22 - glass; 24 - half-ring of rigidity.

It is detachable in the horizontal plane. To walls of housing are welded transverse 4 and 12 and longitudinal 14 and 17 flanges. Transverse flanges serve for attachment of casings of rotor bearings, and longitudinal flanges are for connection of parts of the housing. For packing of joint between longitudinal flanges there is an aluminum lining 15.

From internal side to each part of housing are welded 12 T-shaped 1 and three II-shaped 24 half-rings of rigidity. Simultaneously they serve for installation of stators 18. On external surface of housing are welded bosses 5 and 7 for bolts 3 attaching the stators.

Working rings 19 are fixed in housing between adjacent stators and form a radial clearance at the rotor impellers. Figure 2.27 separately shows a working ring. Ring is nondetachable, made of steel and is II-shaped. On its internal surface there is a soft covering, and on its external surface there is a stop 1. During assembly the working rings are placed on working blades or rotor, after which the latter is covered by the housing. From turning the working rings are fixed by their stop with help of lining 15 (see Fig. 2.26).

Bypass of air in AJ-20 compressor is carried out behind the V and VII<sup>th</sup> stages

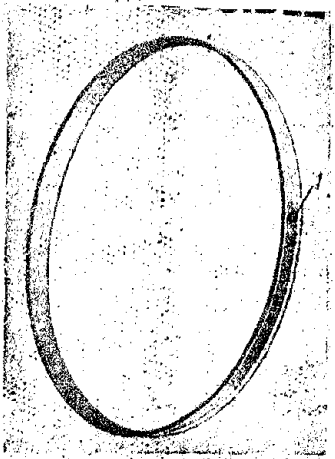


Fig. 2.27. Working ring.

with help of four valves 5 and 6, located two each on upper and lower parts of housing (see Fig. 2.3). For sampling of air from compressor to housing are welded four receivers of box-like form 8 and 11 on upper part and 20 and 23 on lower part of housing (see Fig. 2.26). From compressor air passes into receivers through 64 holes made in walls of housing behind the V and VIIIth stages and proceeds to bypass valves fixed on flange 9 of every receiver. Glasses 10, welded in receivers, serve for access to mounting bolts 3 of stators.

Figure 2.28 shows a bypass valve with hydraulic control. Valve is made according to diagram b in Fig.

2.8 and consists of housing 2, cover 8, valve 1, and piston 7. Housing and cover are cast from magnesium alloy. In central part of housing there is located a directing boss for rod of valve 1, and above it there is a cylinder for piston 7. Connecting pipe 10 serves for drain of oil seeping through piston. In lower

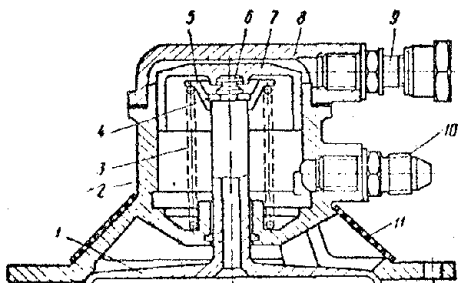
part of lateral walls of housing there are three windows closed by screens 11. Through them air is discharged into the atmosphere.

Valve 1 is steel. In closed position it is held by spring 3 whose upper end is supported on plate 5. Plate is attached to rod of valve with help of cut washers 4 in the flow section of the rod of the valve. Piston 7 is made from aluminum alloy. With help of pivot 6 it rests in valve rod. On cover 8 is fixed connecting pipe 9 for feed of oil to working cavity of hydropiston.

Fig. 2.28. Air bypass valve of AI-20 engine.

Upon inclusion of bypass of air from compressor through connecting pipe 9, oil is brought in under pressure to piston 7. Piston, moving downwards, overcomes elasticity of spring 3 and opens valve 1. For stopping the bypass the hydrocylinder is disconnected from the oil line and the valve, under the action of the spring, is closed. Oil from the cavity of the piston then runs off.

Control of bypass valves is carried out automatically. Upon starting the engine, valves 5 and 6 (see Fig. 2.3) are opened. Upon achievement by rotor of



8600 rpm valves 6 are closed (behind VIIIth stage), and upon achievement of 11,000 rpm, valves 5 (behind Vth stage) are closed. In rated operating conditions of engine the valves are closed.

#### 2.4. Clearances and Seals of Compressor Rotor

For free rotation of rotor without wedging of it in stator due to temperature expansions, elastic deformations, off-axiality, and misalignments in bearings and so forth, between stator and rotor of compressor are created radial  $\delta$  and axial  $\Delta$  clearances (Fig. 2.29). They try to make radial clearances possibly smaller, since through them there occurs overflowing of air, which lowers efficiency of compressor.

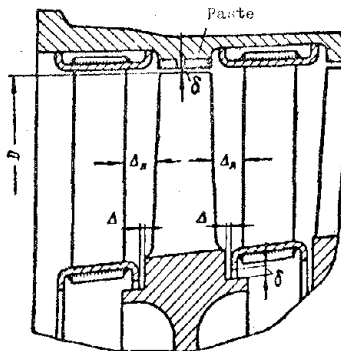


Fig. 2.29. Clearances in impeller.

Radial clearances can be decreased by imposition of a layer of soft plaster made from a special paste on wall of stator. It is up to 2-3 mm thick. For best cohesion of plaster with wall of stator, screw thread 6 (see Fig. 2.23) is sharpened on it. In case rotor touches stator, the paste is easily cleaned off, forming a clearance.

Relative radial clearance in compressors is established within the limits

$$\frac{2\delta}{D} = 0,002 \div 0,005,$$

where  $D$  is the diameter from which the clearance is designated.

Axial clearances  $\Delta$  between rotor and stator are ensured during assembly by special regulating rings 15 fixed in node of radial-thrust bearing (see Fig. 2.1). Axial clearance between working blades and stator blades is established within the limits

$$\Delta_x = (0,15 \div 0,4) b,$$

where  $b$  is chord length of blade.

Increase of clearance  $\Delta_{jl}$  favorably shows up in equalization of speeds of air flow. The danger of vibrations for blades then decreases. However, with increase of  $\Delta_{jl}$  the length dimensions of compressor and its weight are increased.

Labyrinth seal. For decrease of leakage of air through clearances between internal rings of stators and rotor, and also through ends of rotor they use labyrinth seals. They consist of a series of annular grooves — expansion chambers

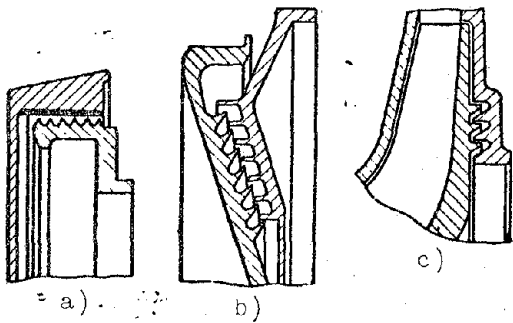


Fig. 2.30. Forms of labyrinth seals.

During flow through labyrinth seal the air in small clearances formed by ridges picks up speed which in the expansion chambers is partially lost with transition of kinetic energy into heat.

This phenomenon in heat engineering is called throttling. Every chamber establishes its own pressure, gradually dropping from first to last chamber. The more ridges the labyrinth seal has the greater its resistance and the less leakage of air through it. With arrangement of ridges of labyrinth seal on conical and vertical walls, the effectiveness of the seal is increased by changing the direction of motion of air.

Magnitude of leakage of air or gases through labyrinth seal can be approximately determined by the Stodoly formula.

$$G_y = kf \sqrt{\frac{g(p_1^2 - p_2^2)}{zp_1v_1}} \text{ kg/sec,} \quad (2.1)$$

where  $p_1$  and  $p_2$  is pressure correspondingly in front of seal and behind it;

$v_1$  is the specific volume of air or gas in front of seal;

$z$  is the number of ridges in the seal;

$g$  is acceleration due to gravity;

$f$  is the flow area of the clearance;

$k$  is the correction factor.

Figure 2.31 gives the values of correction factor  $k$  taking into account construction of labyrinth seal.

Example. Determine leakage of air through labyrinth seal of type a (see Fig. 2.31) of front unloading chamber 2 (see Fig. 2.1).

Given:  $p_1 = 5 \text{ atm. (abs.)}$ ,  $p_2 = 1 \text{ atm (abs.)}$ ;  $v_1 = 0.264 \text{ m}^3/\text{kg}$ ;  $f = 645 \cdot 10^{-6} \text{ m}^2$ ;  $z = 6$ ;  $k = 1.27$ .

<sup>1</sup>Gas-turbine engine.

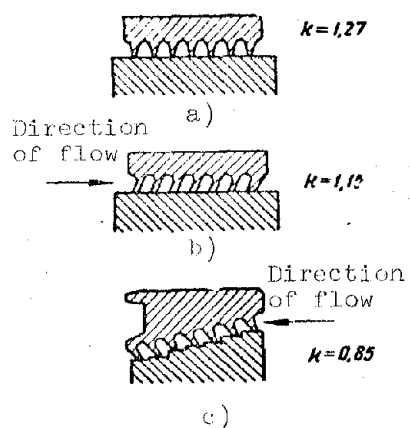


Fig. 2.31. Correction factor  $k$  [see formula (2.1)] in labyrinth.

Leakage of air according to formula (2.1) is equal to :

$$G_{yr} = 1.27 \cdot 645 \cdot 10^{-6} \sqrt{\frac{9.81(50000^2 - 10000^2)}{6 \cdot 50000 \cdot 0.264}} = 0.45 \text{ kg/sec.}$$

## 2.5. Profiling of Compressor Blades

As the original profile in profiling the blades of an axial-flow compressor they most frequently use the symmetric profile, the coordinates of which are shown in Fig. 2.32 in % of chord length  $b$  and greatest thickness of profile  $c$ .

Thickness of profile  $c$  is usually expressed through chord length  $b$ . In working blades the thickness of profile changes along length. For the root section they usually take  $c = (0.1 \text{ to } 0.12)b$ , and for peripheral section  $c = 0.04b$ . In the guides and stator blades the thickness of profile along length of blades is frequently constant.

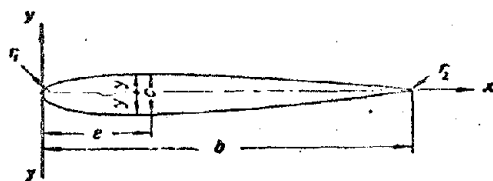


Fig. 2.32. Symmetric compressor profile  $c-b$ .

	$c=0.1b$	$r_1=0.12c$	$r_2=0.06c$	$\epsilon=0.35$					
$x\%b$	0	1,25	2,5	5,0	7,5	10	15	20	30
$y\%c$	0	1,65	22,7	30,8	36,2	40,2	45,5	48,3	50,0
$x\%b$	40	60	60	70	80	90	95	100	
$y\%c$	48,9	45,7	40,5	33,7	25,4	16,0	10,6	0	

Construction of profile is started from its center line ABC (Fig. 2.33). Length of chord  $b$  of bent profile is determined usually in gas-dynamic calculation.

In subsonic stages it is:

at first stages

$$b = (0.22 \div 0.3)L;$$

at last stages

$$b = (0.4 \div 0.55)L,$$

where  $L$  is length of blade.

Length of chord along length of blade is either kept constant, or is changed somewhat.

Curvature of profile  $\theta$  is obtained from gas-dynamic calculation:

$$\theta = \chi_1 + \chi_2,$$

where  $\chi_1$  and  $\chi_2$  are angles of inlet and outlet edges of profile. Angle  $\chi_1$  is usually about 60% of  $\theta$ . Position of point B, i.e., maximum concavity of profile, is given as dimension  $a = (0.4 \text{ to } 0.45)b$ .

Stress of extension in root section of blade

$$\sigma_p = \frac{C_k}{F_k} = \frac{\tau \omega^2}{2g} \left(1 + \frac{F_0}{F_k}\right) L R_u, \quad (2.8)$$

Stress of extension on working blades of first stages of compressor are allowed - for blades made from aluminum alloy, up to  $1300 \text{ kg/cm}^2$ , and for steel blades up to  $3500 \text{ kg/cm}^2$ . On last stages of compressor, for steel blades, stress of extension is allowed up to  $1500 \text{ kg/cm}^2$ .

Example. Determine stress of extension from centrifugal force at root section of working blade of axial-flow compressor.

Given:  $R_u = 50.2 \text{ cm}$ ;  $\tau = 2.85 \cdot 10^{-3} \text{ kg/cm}^3$ ;  
 $F_k = 6.35 \text{ cm}^2$ ;  $\omega = 487 \text{ 1/sec}$ ;  
 $L = 18.85 \text{ cm}$ ;  $F_0 = 2.49 \text{ cm}^2$ .

Stress in root section of blade according to formula (2.8) is equal to:

$$\sigma_p = \frac{2.85 \cdot 10^{-3} \cdot 487^2}{2 \cdot 981} \left(1 + \frac{2.49}{6.35}\right) 18.85 \cdot 50.2 = 455$$

#### Calculation of blades for bending

Moments from gas forces bend the working blade which constitutes the cantilever. Action of gas forces (Fig. 2.35) are considered in plane of rotation (circumferential load) and in axial plane (axial load).

Circumferential force  $P_u$  appears from dynamic impact of flow on blade. Intensity of circumferential load (load per unit of length of blade) is determined by power expended for rotation of impeller or by change of momentum of air flow in circumferential direction during passage of it through buckets:

$$q_u = \frac{71620 N}{n R_{cp} z L}, \quad \left. \begin{aligned} \text{or} \\ q_u = \frac{G_B (c_{1u} - c_{2u})}{g z L} \end{aligned} \right\} \quad (2.9)$$

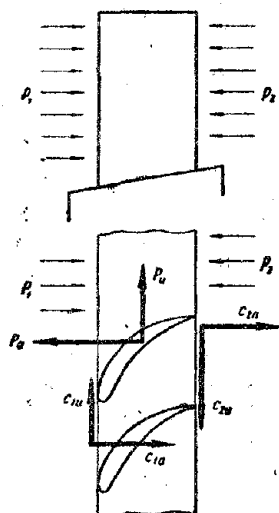


Fig. 2.35. Forces of pressure of gases acting on blades.

where  $N$  is the power consumed by the impeller;  $n$  is the rpm rate;  $R_{cp}$  is mean radius of buckets;  $z$  is number of blades;  $L$  is length of blade;  $G_B$  is expenditure of air per second;  $g$  is acceleration due to gravity;  $c_{1u}$  and  $c_{2u}$

are peripheral velocities of air correspondingly on inlet and on outlet of buckets.

Let us agree to take direction of speed  $c_{1u}$  as positive. Circumferential load

from gas forces on blade of compressor acts in direction opposite rotation of impeller.

Axial force  $P_a$  arises from static and dynamic impact to flow on blade. Intensity of axial load is determined by difference of static pressures  $p_1$  and  $p_2$  acting on both sides of buckets, and by change of momentum of air flow in axial direction, upon passage of it through buckets:

$$q_a = \frac{(p_1 - p_2) 2\pi R_{cp}}{z} + \frac{G_a (c_{1a} - c_{2a})}{gzL}, \quad (2.10)$$

where  $p_1$  and  $p_2$  are static pressures in front of buckets and behind them;  $c_{1a}$  and  $c_{2a}$  are axial airspeeds correspondingly on inlet and outlet of buckets.

In axial-flow compressors  $p_1 < p_2$  and  $c_{1a} \geq c_{2a}$ . The minus sign, which is obtained in  $q_a$  in determination by formula (2.10), indicates that axial load from gas forces acts opposite flow of air, i.e., in the direction of the inlet. Intensity of circumferential and axial loads along length of blades is taken as constant.

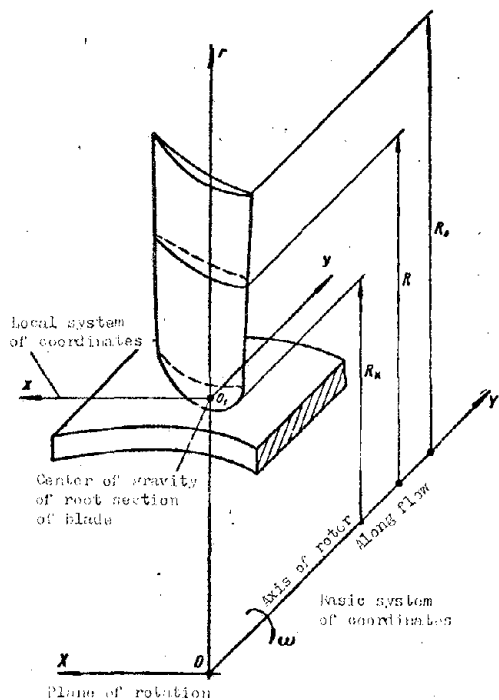


Fig. 2.36. Calculation for strength of blades during bending.

We shall take, in the determination of buckling loads in a blade, the basic system of coordinates XYr (Fig. 2.36) where axis OY coincides with axis of rotation of rotor, axis Or passes through center of gravity of root section of blade, which is calculated in it, and axis OX is in the plane of rotation.

As the positive directions of axes we take:  
for axis OY — with respect to flow of air (gases);

for axis Or — from axis of rotation toward the end of blade;

for axis OX — the direction at which the combination of positive semiaxes OX and Or is attained by turn of semiaxis OX in direction of rotation of rotor at angle  $90^\circ$ .

For the blade we have the case of bending of the cantilever with a uniformly distributed load from gas forces. In the root section of the blade the bending moments have the biggest values. Bending moments

from gas forces in plane of rotation XOr and in axial plane YOr will be:

for current section located on radius R

$$M_y = q_a \frac{(R_0 - R)^2}{2} \text{ and } M_x = q_a \frac{(R_0 - R)^2}{2} \quad (2.11)$$

and for calculated root section of radius  $R_K$

$$M_{yK} = q_a \frac{L^2}{2} \text{ and } M_{xK} = q_a \frac{L^2}{2} \quad (2.12)$$

Example. Determine bending moments from gas forces in the root section of a blade of an axial-flow compressor.

Given:  $G_B = 148 \text{ kg/sec}$ ;  $z = 35$ ;  $c_{1a} - c_{2a} = 10 \text{ m/sec}$ ;  $R_{cp} = 51.57 \text{ cm}$ ;  $c_{1u} - c_{2u} = 121 \text{ m/sec}$ ;  $p_2 - p_1 = 0.206 \text{ kg/cm}^2$ ;  $L = 18.85 \text{ cm}$ .

Intensity of circumferential load according to formula (2.9)

$$q_a = \frac{148 \cdot 12100}{981 \cdot 35 \cdot 18.85} = 2.77 \text{ kg/cm.}$$

Intensity of axial load according to formula (2.10)

$$q_a = \frac{2 \cdot 3 \cdot 14 \cdot 51.57 \cdot 0.206}{35} = \frac{148 \cdot 1000}{981 \cdot 35 \cdot 18.85} = 1.68 \text{ kg/cm.}$$

Circumferential and axial bending moments in root section according to formulas (2.12)

$$M_{yK} = 2.77 \frac{18.85^2}{2} = 492 \text{ kg.cm};$$

$$M_{xK} = 1.68 \frac{18.85^2}{2} = 299 \text{ kg.cm.}$$

Deflections of sections in a blade. Axis of blade passes through centers of gravity of its cross sections. Deviation of axis of blade from axis Or of

basic system of coordinates (Fig. 2.37) is called deflection of sections. Deflections of sections of blade made in plane of rotation of rotor XOr and in axial plane YOr. Usually deflections of sections are given by coordinates of their centers of gravity x and y.

Since in the case of deflections of sections their centers of gravity do not lie

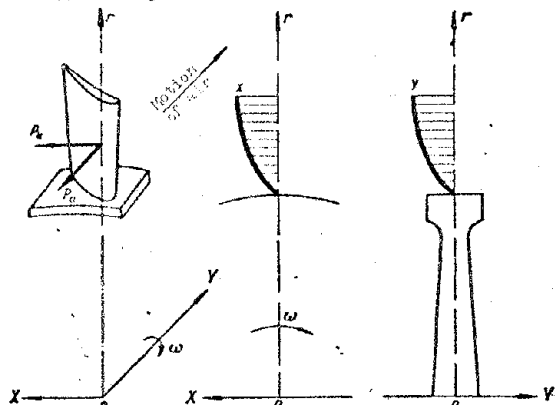


Fig. 2.37. Deflections of sections for a compressor blade.

on axis O<sub>r</sub>, under the action of centrifugal force in planes of deflection XOr and YOr the blade will have bending moments  $m_y$  and  $m_x$ .

Deflections of sections in blades are made for unloading of them from bending by gas forces. Therefore the direction of action of bending moments from centrifugal forces  $m_y$  and  $m_x$  and from gas forces  $M_y$  and  $M_x$  must be opposite. Figure 2.37 shows deflections of sections of blade in planes XOr and YOr, at which there occurs its unloading from bending by gas forces. Direction of rotation of rotor in this case is taken to be clockwise if one were to look along the gas flow.

If one were to take direction of action of moments from gas forces as positive, the total bending moments in plane of rotation  $M_{\Sigma_y}$  and in axial plane  $M_{\Sigma_x}$  for current section of blade located on radius R will be

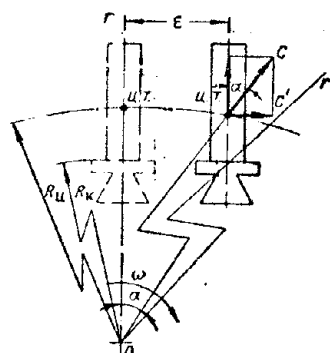
$$M_{\Sigma_y} = M_y - m_y \quad \text{and} \quad M_{\Sigma_x} = M_x - m_x \quad (2.13)$$

and for root section located on radius  $R_K$

$$M_{\Sigma_{yK}} = M_{yK} - m_{yK} \quad \text{and} \quad M_{\Sigma_{xK}} = M_{xK} - m_{xK} \quad (2.14)$$

By deflection of sections of blade they attain its unloading from bending by 50 to 60%. Deflections of sections of blades can be executed according to different laws. The simplest is linear law, at which axis of blade is rectilinear and has inclination to axis O<sub>r</sub> of basic system of coordinates.

Frequently they are limited to deflection of sections of blades of compressors only in plane of rotation XOr. Linear law of deflection in plane XOr can be ensured by parallel displacement of axis of blade on impeller by the progress of its rotation at magnitude  $\epsilon$  (Fig. 2.38). With this displacement the axis of the



blade is inclined to axis O<sub>r</sub> passing through center of gravity of root section and for centrifugal force C there appears a horizontal component

$$C' = C \sin \alpha,$$

which will evoke bending in the blade.

Between angle  $\alpha$  and displacement  $\epsilon$  there exists the following connection:

Fig. 2.38. Displacement of blade on impeller.  
[u.g. = center of gravity]

$$\epsilon = R_u \sin \alpha$$

and bending moment for calculated root section of blade will be:

$$m_{yx} = C(R_a - R_k) \sin \alpha = C \left(1 - \frac{R_k}{R_a}\right) \epsilon, \quad (2.15)$$

where  $R_a$  and  $R_k$  are radii of location of center of gravity of blade quill and its root section.

Example. Determine total bending moment in the blade of a compressor in plane of rotation during displacement of it on impeller (see Fig. 2.38).

Given:

$$\begin{aligned} M_y &= 492 \text{ kg} \cdot \text{cm}; & L &= 18.85 \text{ cm}; & F_x &= 6.35 \text{ cm}^2; \\ F_y &= 2.49 \text{ cm}^2; & R_k &= 42.15 \text{ cm}; & e &= 0.8 \text{ cm}; \\ \gamma &= 2.85 \cdot 10^{-3} \text{ kg/cm}^3; & \omega &= 487 \text{ 1/sec}; & R_a &= 50.2 \text{ cm}. \end{aligned}$$

Centrifugal force at the blade quill according to formula (2.6) is equal to

$$C_k = \frac{2.85 \cdot 10^{-3} \cdot 487^2}{2.981} (6.35 + 2.49) \cdot 18.85 \cdot 50.2 = 2870 \text{ kg}.$$

Bending moment due to centrifugal force in plane of rotation according to formula (2.15)

$$m_{yx} = 2870 \cdot 0.8 \left(1 - \frac{42.15}{50.2}\right) = 367 \text{ kg} \cdot \text{cm}.$$

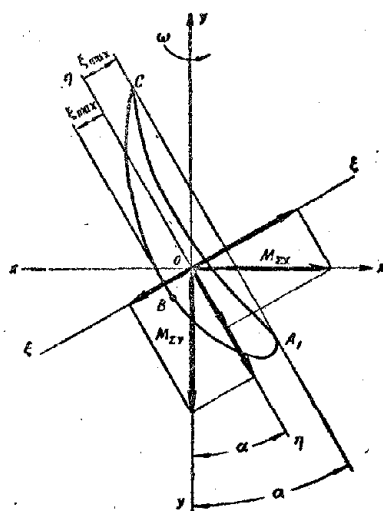
Total bending moment in plane of rotation according to formula (2.14)

$$M_{\Sigma yk} = 492 - 367 = 125 \text{ kg} \cdot \text{cm}$$

Bending of blade relative to main central axis. In examining bending, we will take for the calculated root section of the blade the local system of coordinates

xoy. The origin of coordinates will be in the center of gravity of the section, and axis ox and oy will be directed in parallel to analogous axes of the basic system of coordinates, i.e., axis ox in plane of rotation, and oy parallel to axis of rotor (see Fig. 2.36). Total bending moments  $M_{\Sigma y}$  and  $M_{\Sigma x}$  due to gas and centrifugal forces bend the blade in calculated root section with respect to axes of coordinates oy and ox. Section of blade has main central axes  $\eta-\eta$  and  $\xi-\xi$  with origin of coordinates in center of gravity of section (Fig. 2.39). System of coordinates  $\xi_0\eta$  is turned with respect to local system of coordinates at angle  $\alpha$ . In the calculations we consider angle  $\alpha$

Fig. 2.39. Vectors of bending moments in a compressor blade.



equal to the angle formed by chord  $A_1C$  of blade profile with axis of rotation of impeller  $yy$ .

Since bending moments of blades do not lie in main planes of calculated section, we have here the case of oblique bending of a beam. As is known, oblique bending is usually considered as two flat bends acting in two mutually-perpendicular main planes passing through main central axes of coordinates to perpendicular to the calculated section.

Applying vector representation of moments, the bending moments  $M_{\Sigma_x}$  and  $M_{\Sigma_y}$  should be expanded along principal axes  $\eta-\eta$  and  $\xi-\xi$  of calculated section of blade and then their components should be added taking into account their signs.

Let us remember that vector of moment is perpendicular to plane of its action. Direction of vector of moment is determined according to the following rule; if one were to look from the end of the vector (on the arrow side) at the plane of action of the moment, the moment will tend to turn the system counterclockwise.

For blade profiles the principal moments of inertia of cross sections  $J_{\eta}$  and  $J_{\xi}$  are found in the following relationship:

$$J_{\eta} = (0.01 \div 0.05) J_{\xi}.$$

Therefore, with accuracy sufficient for practice we can limit ourselves to the calculation of blades for bending relative only to one main central axis  $\eta-\eta$  with minimum moment of inertia of section  $J_{\eta}$  (in plane of least rigidity).

Bending moment with respect to axis  $\eta-\eta$  is equal to:

$$M_{\eta} = M_{2x} \sin \alpha + M_{2y} \cos \alpha. \quad (2.16)$$

Sign of moment  $M_{\eta}$  is determined by signs of components of moments  $M_{\Sigma_x}$  and  $M_{\Sigma_y}$ .

Stress of bending in calculated section

$$\sigma_{\eta} = \frac{M_{\eta} \xi}{J_{\eta}}, \quad (2.17)$$

where  $\xi$  is the coordinate of calculated point in calculated section of blade;

$J_{\eta}$  is the main (least) moment of inertia of calculated section of blade (with respect to axis  $\eta-\eta$ ).

The biggest stresses of bending are obtained in points  $A_1$ ,  $B$ , and  $C$  of the section of the blade, as the most remote from axis  $\eta-\eta$ .

Total stresses due to extension and bending. In positive bending moment  $M_\eta$  in points A<sub>1</sub> and C of the profile there will be extension, and at point B there will be compression (see Fig. 2.39).

The biggest total normal stresses in calculated section are obtained in points A<sub>1</sub> and C:

$$\sigma_{\text{max}} = \sigma_p + \sigma_n. \quad (2.18)$$

where  $\sigma_p$  is stress of extension;

$\sigma_n$  is the biggest stress of bending in calculated section (in points A<sub>1</sub> and C).

Allowed total stresses in working blades of first compressor stages due to extension and bending are the following: for blades made from aluminum alloy up to 2000 kg/cm<sup>2</sup>, and for steel blades up to 5000 kg/cm<sup>2</sup>. For steel blades of last compressor stages, total stresses are allowed up to 4000 kg/cm<sup>2</sup>.

Example. Determine stress of bending and maximum total stress in root section of blade of an axial-flow compressor.

Given:  $M_{Z_x} = 299 \text{ kg}\cdot\text{cm}$ ;  $M_{Z_y} = 125 \text{ kg}\cdot\text{cm}$ ;  $\alpha = 25^\circ 22'$ ;  $J_\eta = 0.483 \text{ cm}^4$ ;  $\sigma_p = 467 \text{ kg}/\text{cm}^2$ ;  $\xi = 0.663 \text{ cm}$ .

Bending moment with respect to axis η-η according to formula (2.16):

$$M_\eta = 299 \sin 25^\circ 22' + 125 \cos 25^\circ 22' = 241 \text{ kg}\cdot\text{cm}.$$

The biggest bending stress according to formula (2.17) will be:

$$\sigma_n = \frac{241 \cdot 0.663}{0.483} = 330 \text{ kg}/\text{cm}^2.$$

The biggest total stress in root section according to formula (2.18):

$$\sigma_{\text{max}} = 467 + 330 = 797 \text{ kg}/\text{cm}^2.$$

Determination of area, position of center of gravity, and moment of inertia of section of blades

During calculation for strength in a blade it is necessary to preliminarily determine area of cross section, position of center of gravity, and moment of inertia of section. Area of cross section is usually determined by planimetry with the formula:

$$F = \frac{m_1}{m_2} k \text{ cm}^2,$$

where  $m_1$  is the scale or value of division of planimeter (number of kv.cm per division of meter);

$m_2$  is the scale in which the profile is traced;

$k$  is the reading of the planimeter.

Center of gravity of section can be found by consecutive suspension of a model profile cut from quality drawing paper in two points. Using plumb line from thin thread, on the model we trace vertical lines from points A and B (Fig. 2.40). At point of intersection of these lines we find the center of gravity of the model, and consequently the section of the blade. Model of section of blade is usually made in magnified scale.

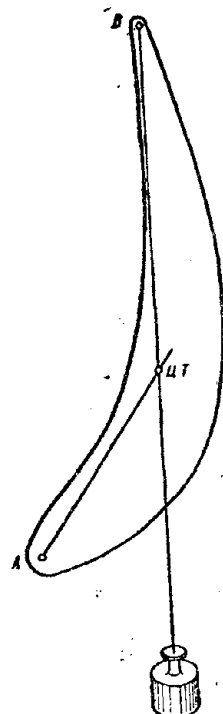


Fig. 2.40.  
Determination  
of center of  
gravity of a  
section by the  
suspension  
method.

For determination of moment of inertia  $J_{\eta}$  of section of blade one should use scale grids which are put on the calculated section of blade (Fig. 2.41). Axis of grid O-O is combined with the main central axis of coordinates  $\eta-\eta$ , with respect to which we determine moment of inertia of section  $J_{\eta}$ . Lengths of segments cut off by profile of blade at lines of grid, with the exception of axial line O-O are measured and then added.

Moment of inertia of section is determined by the formula

$$J_{\eta} = \frac{k}{m^4} \sum l_i$$

where  $k$  is the parameter of grid(indicated on grid);  $m$  is the scale of section of blade;  $\sum l_i$  is the sum of lengths of segments, expressed in cm.

The smaller the parameter  $k$  of the grid, the higher the accuracy of determination of moment of inertia.

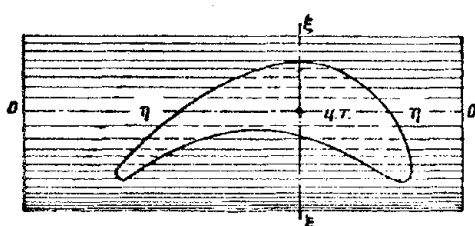


Fig. 2.41. Determination of moment of inertia of a section of blade with the help of grids.

Figure 2.42 shows a combined grid having a series of linear sections with different parameters  $k$ . In this case, in the determination of moment of inertia of section of blade  $J_{\eta}$  the axis of grid O-O is combined with axis of coordinates  $\eta-\eta$  and for every parameter  $k_i$  we determine its total length of segments  $\sum l_i$  cut off by profile. Moment of

inertia of section in this case is determined by the formula:

$$J_1 = \frac{1}{m^4} \left[ k_1 \sum l_1 + k_2 \sum l_2 + k_3 \sum l_3 + \dots \right].$$

Combined grid ensures larger accuracy of determination of  $J_{\eta}$ . Values of ordinates of grid for its construction are given in the table.

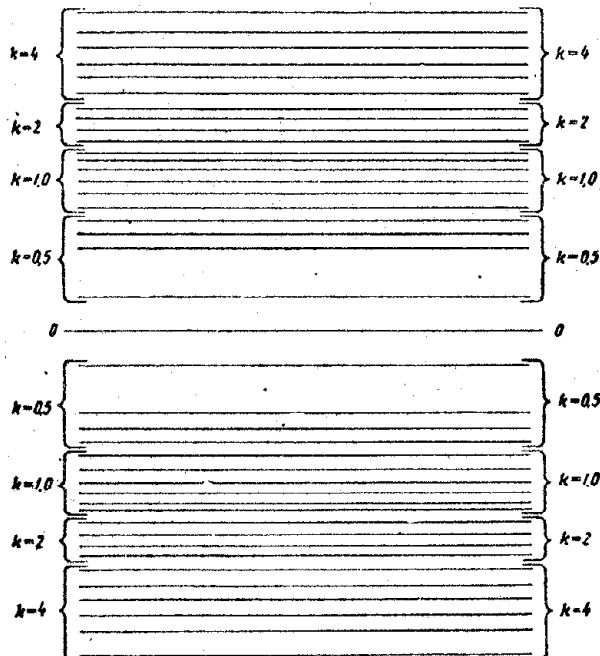


Fig. 2.42. Combined grid for determination of moments of inertia in sections.

For larger accuracy of determination of  $J_{\eta}$  profiles of blade should be traced in magnified scale (5:1 or 10:1). For convenience of use, the grid is usually traced on tracing paper.

Ordinates of Combined Grid

<i>k</i>	0.5					1.0				
Line no.	1	2	3	4	5	6	7	8	9	10
<i>y mm</i>	5,70	12,95	15,50	17,35	19,50	21,85	23,80	25,40	26,90	28,20

Continuation

<i>k</i>	2.0					4.0				
Line no.	11	12	13	14	15	16	17	18	19	20
<i>y mm</i>	30,0	32,0	33,9	35,6	37,8	40,3	42,7	44,8	47,6	50,9

Calculation of Blade Retainer of the "Swallowtail" Type

Blade retainer is loaded by centrifugal force  $C_{JL}$  from mass of entire blade (quill and leg).

Normal component of force  $C_{JL}$  will be equal (Fig. 2.43)

$$N = \frac{C_s}{2 \sin \alpha},$$

where angle  $\alpha$  is usually 15-20°.

Stress of crumpling on lateral surface of retainer will be:

$$\sigma_{cr} = \frac{N}{F} = \frac{C_s}{2 \sin \alpha \cdot F}, \quad (2.19)$$

here  $F = al$  is the area of support surface of retainer (see Fig. 2.43).

Flange of disk, located between two adjacent blades, is calculated for breaking away by force  $Q$  (Fig. 2.44)

$$Q = C + C_B, \quad (2.20)$$

where  $C$  is centrifugal force from two adjacent blades, loading flange of disk.

$$C = 2N \sin\left(\alpha + \frac{\beta}{2}\right) = C_s \frac{\sin\left(\alpha + \frac{\beta}{2}\right)}{\sin \alpha}$$

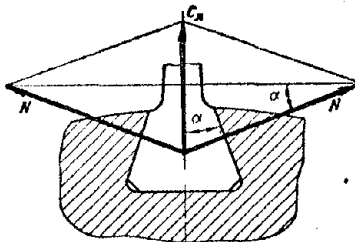
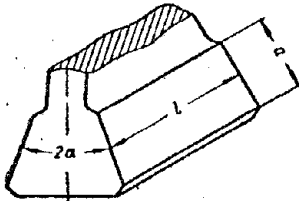


Fig. 2.43. Calculation for strength of blade retainer.

and  $C_B$  is centrifugal force of disk flange

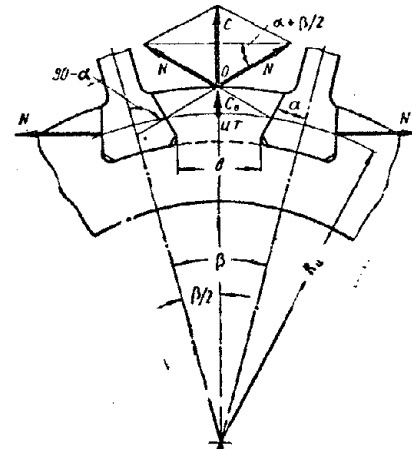


Fig. 2.44. Calculation for strength of a disk flange.

$$C_B = \frac{1}{g} VR_u \omega^2,$$

here  $\beta = \frac{2\pi}{z}$  is the angle between adjacent blades with number of glades  $z$ ;

$\gamma$  is specific gravity of material of disk;

$V$  is volume of disk flange;

$R_{II}$  is radius of location of center of gravity of disk flange.

Stress of extension for disk flange:

$$\sigma_s = \frac{Q}{F}, \quad (2.21)$$

where  $F = bl$  is the area of calculated section of disk flange (see Fig. 2.44).

In blades of compressors made from aluminum alloys

$$\sigma_{CM} \leq 1500 \text{ kg/cm}^2 \text{ and } \sigma_s \leq 1000 \text{ kg/cm}^2,$$

from steel

$$\sigma_{CM} \leq 4500 \text{ kg/cm}^2 \text{ and } \sigma_s \leq 3000 \text{ kg/cm}^2.$$

Calculation of retainer of the "herringbone" type is present in Chapter IV.

In the given designs of compressors the stress of crumpling in a retainer of the "herringbone" type in steel blades is  $\sigma_{CM} = 2500$  to  $3000 \text{ kg/cm}^2$ , and stress of extension in the disk flange is  $\sigma_s \leq 4500 \text{ kg/cm}^2$ .

Example. Determine stress in "swallowtail" retainer.

Given:  $C_{II} = 4000 \text{ kg}$ ;  $C_B = 1715 \text{ kg}$ ;  $z = 35$ ;  $l = 93 \text{ mm}$ ;  $a = 10 \text{ mm}$ ;  $\alpha = 20^\circ$ ;  $b = 31.6 \text{ mm}$ ;  $\beta = 10^\circ 17' 19''$ .

Stress of crumpling at support surface of retainer according to formula (2.19):

$$\sigma_{CM} = \frac{4000}{2 \cdot \sin 20^\circ \cdot 1 \cdot 9,3} = 627 \text{ kg/cm}^2,$$

Pull in the disk flange according to formula (2.20):

$$Q = 4000 \frac{\sin 25^\circ 8' 40''}{\sin 20^\circ} + 1715 = 6685 \text{ kg}$$

Stress of extension in the disk flange according to formula (2.21)

$$\sigma_s = \frac{6685}{3,16 \cdot 9,3} = 228 \text{ kg/cm}^2.$$

#### Calculation of Drum Type Rotor

Drum of rotor during rotation is under action of centrifugal forces from blades fastened to it and from its own mass. Thickness of wall of rotor drum of axial-flow compressor is small as compared to its diameter; therefore during calculation for strength the drum is considered as a thin revolving ring.

Let us consider a drum with annular grooves for blades. For this we will point out in the drum an element restricted by two planes A-A and B-B perpendicular to axis of drum and two radial planes OD and OE (Fig. 2.45). Planes A-A and B-B pass through middles of two adjacent rings of blades, and planes OD and OE form between themselves an infinitesimal angle  $d\phi$ . Centrifugal force of ring of blades is equal to:

$$C_s = \frac{G_s}{g} z R_s \omega^2. \quad (2.22)$$

where  $G_s$  is the weight of blade;  $z$  is number of blades;  $R_s$  is radius of center of gravity of blade;  $\omega$  is angular velocity of rotation of drum;  $g$  is acceleration due to gravity.

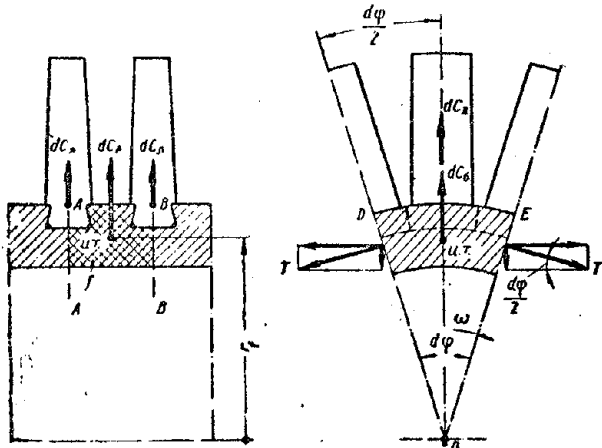


Fig. 2.45. Calculation for strength of drum rotor.

Centrifugal force from ring of blades, loading the isolated element of drum

$$dC_s = \frac{C_s d\phi}{2\pi}. \quad (2.23)$$

Centrifugal force from mass of element of drum

$$dC_b = \frac{\gamma f r_f^2 \omega^2 d\phi}{2}, \quad (2.24)$$

where  $\gamma$  is specific gravity of material

$f$  is area of section of element along generatrix of drum;  $r_f$  is radius of center of gravity of element.

Under action of centrifugal forces  $dC_s$  and  $dC_b$  on lateral faces of element there appear tangential stresses

$$T = \sigma f. \quad (2.25)$$

where  $\sigma$  is normal stress of extension.

From condition of equilibrium of forces acting on element

$$dC_s + dC_b = 2T \sin \frac{d\phi}{2} \approx T d\phi. \quad (2.26)$$

Here for infinitesimal angle  $d\phi$  we take

$$\sin \frac{d\phi}{2} \approx \frac{d\phi}{2}.$$

After substitution of expressions (2.23)-(2.25) in (2.26) and reduction to  $d\phi$  we will obtain the expression for stress of extension in wall of drum

$$\sigma = \frac{1}{g} u_f^2 + \frac{C_s}{2\pi f}. \quad (2.27)$$

where  $u_f = r_f \omega$  is peripheral velocity of center of gravity of element.

For drums made from aluminum alloys we take  $\sigma = 800$  to  $1000 \text{ kg/cm}^2$ , and for steel drums  $\sigma = 2100$  to  $2800 \text{ kg/cm}^2$ .

Example. Determine stress of drum of axial-flow compressor with annular grooves under blades.

Given:  $G_J = 49 \text{ g}$ ;  $R_J = 21.9 \text{ cm}$ ;  $z = 50$ ;  $\omega = 754 \text{ 1/sec}$ ;  $f = 16 \text{ cm}^2$ ;  $r_f = 18.4 \text{ cm}$ ;  $\gamma = 2.8 \cdot 10^{-3} \text{ kg/cm}^3$ ;  $u_f = 138.8 \text{ m/sec}$ .

Full centrifugal force of blade ring according to formula (2.22)

$$C_s = \frac{0.049}{981} 50 \cdot 21.9 \cdot 754^2 = 31100 \text{ kg.}$$

Stress of extension along generatrix of drum according to formula (2.27)

$$\sigma = \frac{2.8 \cdot 10^{-3}}{981} 13880^2 + \frac{31100}{2 \cdot 16} = 860 \text{ kg/cm}^2.$$

#### Calculation of Rotor Disk

Disk of rotor during operation is under action of centrifugal forces of its own mass and mass of working blades. Calculations are conducted on the assumption of elastic state of disk.

Derivation of calculating equations for disk of constant thickness

We shall take a disk with constant thickness  $b$  along radius and isolate in it an infinitesimal element ABCD, restricted by two annular sections taken on radii  $r$  and  $r + dr$ , and two radial sections OA and OB located at angle  $d\phi$  (Fig. 2.46).

During rotation of disk, in element ABCD there appears centrifugal force from its own mass, which can be calculated with respect to its volume  $dV = r d\phi b dr$ :

$$dC = \frac{1}{g} br^2 dr d\phi \omega^2,$$

where  $\gamma$  is specific gravity of material of disk;

$g$  is acceleration due to gravity;

$\omega$  is angular velocity of rotation of disk.

From condition of connection on edges of element ABCD there appear normal stresses:

$\sigma_R$  is radial stress on internal surface  $br d\phi$ ;

$\sigma_R + d\sigma_R$  is radial stress on external surface  $b(r + dr)d\phi$ ;

$\sigma_T$  is circumferential stress on lateral surfaces  $b dr$ .

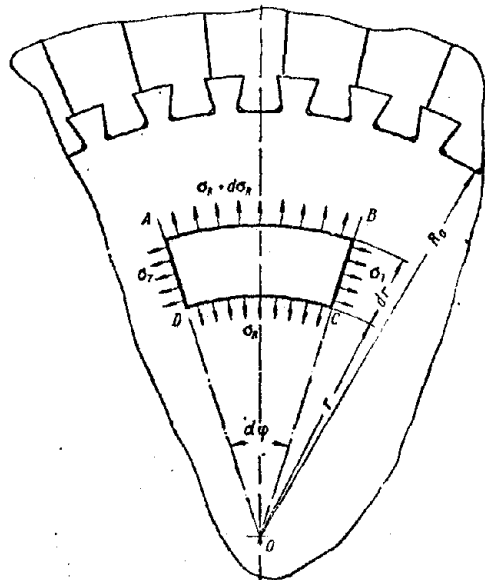


Fig. 2.46. Calculation for disk strength.

Stresses  $\sigma_R$ ,  $\sigma_R + d\sigma_R$  and  $\sigma_T$  with respect to thickness of disk will be considered constant. The forces corresponding to them are equal to

$$dP_1 = \sigma_R br d\varphi;$$

$$dP_2 = (\sigma_R + d\sigma_R) b(r + dr) d\varphi;$$

$$dT = \sigma_T b dr.$$

Under action of forces applied to element ABCD the latter is found in equilibrium, i.e., the sum of projections of these forces on any axis is equal to zero. Projecting the forces applied to element ABCD on bisector of angle  $d\varphi$  (Fig. 2.47) we will obtain:

$$-dP_1 + dP_2 - 2dT \sin \frac{d\varphi}{2} + dC = 0.$$

We shall place in this equation the expressions of forces  $dP_1$ ;  $dP_2$ ;  $dT$  and  $dC$ , and in view of smallness of angle  $d\varphi/2$ , we will replace  $\sin d\varphi/2$  by magnitude  $d\varphi/2$ :

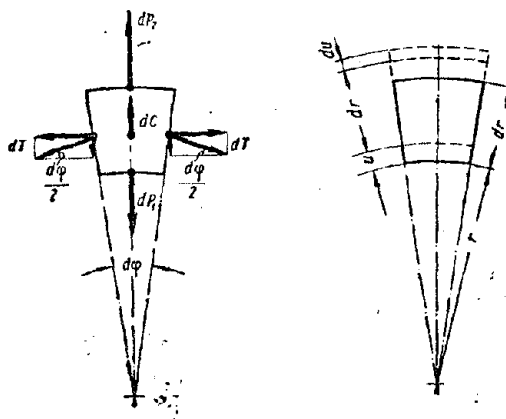


Fig. 2.47. Forces acting on element of disk and elongation of element.

$$-\sigma_R br d\varphi + (\sigma_R + d\sigma_R) b(r + dr) d\varphi -$$

$$-2\sigma_T b dr \frac{d\varphi}{2} + \frac{1}{g} br^2 dr d\varphi u^2 = 0.$$

Reducing the equation to  $b$  and  $d\varphi$ , opening the brackets, rejecting the infinitesimal magnitude of the second order of smallness  $d\sigma_R dr$  and, introducing similar members, we will obtain the following differential equation:

$$r \frac{d\sigma_R}{dr} + \sigma_R - \sigma_T + \frac{\tau \omega^2}{g} r^2 = 0. \quad (2.28)$$

In equation (2.28) there are two unknowns  $\sigma_R$  and  $\sigma_T$ . Therefore, in order to find them, it is required to have a second equation. We shall compose expressions for  $\sigma_R$  and  $\sigma_T$  from consideration of elastic deformations of element ABCD. With absolute elongation of radius  $r$  of disk to magnitude  $u$  (see Fig. 2.47) absolute elongation of circumference  $2\pi r$  will be  $2\pi u$  and aspect ratio in circumferential direction

$$\epsilon_T = \frac{2\pi u}{2\pi r} = \frac{u}{r}.$$

Magnitude  $u$  along disk radius is variable, i.e.,  $u = f(r)$ . At the same time the absolute radial aspect of the element itself ABCD will be  $du$ , and its aspect ratio in radial direction

$$\epsilon_R = \frac{du}{dr}.$$

For elastic state of body, its deformations are expressed through stresses according to the Hook law. For a disk which is in a flat state of strain

$$\epsilon_R = \frac{du}{dr} = \frac{1}{E} (\sigma_R - \mu \sigma_T); \quad (2.29)$$

$$\epsilon_T = \frac{u}{r} = \frac{1}{E} (\sigma_T - \mu \sigma_R), \quad (2.30)$$

where  $E$  is elastic modulus of material of disk;

$\mu$  is Poisson's ratio;

$\sigma_R$  and  $\sigma_T$  are normal stresses in radial and circumferential directions.

Solving these equations with respect to  $\sigma_R$  and  $\sigma_T$ , we find:

$$\left. \begin{aligned} \sigma_R &= \frac{E}{1-\mu^2} \left( \frac{du}{dr} + \mu \frac{u}{r} \right); \\ \sigma_T &= \frac{E}{1-\mu^2} \left( \frac{u}{r} + \mu \frac{du}{dr} \right). \end{aligned} \right\} \quad (2.31)$$

In order to use the obtained expressions (2.31), it is necessary to determine the change of deformation  $u$  of the disk along its radius. For this we will place expressions (2.31) in (2.28):

$$\begin{aligned} r \frac{d}{dr} \left[ \frac{E}{1-\mu^2} \left( \frac{du}{dr} + \mu \frac{u}{r} \right) \right] + \frac{E}{1-\mu^2} \left( \frac{du}{dr} + \mu \frac{u}{r} \right) - \\ - \frac{E}{1-\mu^2} \left( \frac{u}{r} + \mu \frac{du}{dr} \right) + \frac{\gamma \omega^2}{g} r^2 = 0. \end{aligned}$$

Then we will multiply the obtained equation by  $(1 - \mu^2)/E$  and differentiate its first member:

$$\begin{aligned} r \frac{d^2 u}{dr^2} + r \mu \frac{\frac{du}{dr} - u}{r^2} + \frac{du}{dr} + \mu \frac{u}{r} - \frac{u}{r} - \\ - \mu \frac{du}{dr} + \frac{1-\mu^2}{E} \frac{\gamma \omega^2}{g} r^2 = 0. \end{aligned}$$

After reduction of similar members we will obtain

$$\frac{d^2 u}{dr^2} + \frac{1}{r} \frac{du}{dr} - \frac{u}{r^2} + \frac{1-\mu^2}{E} \frac{\gamma \omega^2}{g} r = 0.$$

We shall reduce this equation to a form convenient for integration:

$$\frac{d}{dr} \left[ \frac{1}{r} \frac{d}{dr} (ur) \right] = - \frac{1-\mu^2}{E} \frac{\gamma \omega^2}{g} r$$

or

$$d \left[ \frac{1}{r} \frac{d}{dr} (ur) \right] = -\frac{1-\mu^2}{E} \frac{\gamma \omega^2}{g} r dr.$$

The validity of this equation can be verified by means of its differentiation. Integrating it is the first time, we will obtain

$$\frac{1}{r} \frac{d}{dr} (ur) = -\frac{1-\mu^2}{E} \frac{\gamma \omega^2}{2g} r^2 + C_1,$$

where  $C_1$  is the constant of integration.

The obtained expression is also reduced to a form convenient for second integration:

$$d(ur) = -\frac{1-\mu^2}{E} \frac{\gamma \omega^2}{2g} r^3 dr + C_1 r dr.$$

After secondary integration we will obtain an expression for deformation depending upon radius  $r$ :

$$u = -\frac{1-\mu^2}{E} \frac{\gamma \omega^2}{8g} r^3 + \frac{C_1}{2} r + \frac{C_2}{r}, \quad (2.32)$$

where  $C_2$  is the constant of integration.

Differentiating the obtained expression with respect to  $r$ , we will obtain an expression of relative deformation of the disk in radial direction:

$$\frac{du}{dr} = -3 \frac{1-\mu^2}{E} \frac{\gamma \omega^2}{8g} r^2 + \frac{C_1}{2} - \frac{C_2}{r^2}. \quad (2.33)$$

We shall place the obtained expressions (2.32) and (2.33) in formulas (2.31). After reduction of similar members we will obtain

$$\left. \begin{aligned} \sigma_R &= C'_1 - \frac{C'_2}{r^2} - (3+\mu) \frac{\gamma \omega^2}{8g} r^2, \\ \sigma_T &= C'_1 + \frac{C'_2}{r^2} - (1+3\mu) \frac{\gamma \omega^2}{8g} r^2, \end{aligned} \right\} \quad (2.34)$$

where

$$C'_1 = \frac{E}{1-\mu} \frac{C_1}{2} \quad \text{and} \quad C'_2 = \frac{E}{1-\mu} \frac{C_2}{r}.$$

Values of constants  $C'_1$  and  $C'_2$  are found from boundary conditions. Knowing, for instance, the values of  $\sigma_{R_0}$  and  $\sigma_{T_0}$  in section of disk on radius  $R_0$  and placing them in expressions (2.34), we find:

$$\left. \begin{aligned} C'_1 &= \frac{\sigma_{R_0} + \sigma_{T_0}}{2} + (2-\mu) \frac{\gamma \omega^2}{8g} R_0^2, \\ C'_2 &= \frac{\sigma_{T_0} - \sigma_{R_0}}{2} - (1+2\mu) \frac{\gamma \omega^2}{8g} R_0^2. \end{aligned} \right\} \quad (2.35)$$

We shall place the obtained expressions (2.35) in (2.34). We use Poisson's ratio  $\mu = 0.3$  and designate  $R_0/r = m$ , and then after reduction of similar members we obtain:

$$\left. \begin{aligned} \sigma_R &= \frac{1+m^2}{2} \sigma_{R_0} + \frac{1-m^2}{2} \sigma_{T_0} - \frac{\gamma \omega^2}{8g} r^2 (3.3 - 2.6m^2 - 0.7m^4); \\ \sigma_T &= \frac{1+m^2}{2} \sigma_{T_0} + \frac{1-m^2}{2} \sigma_{R_0} - \frac{\gamma \omega^2}{8g} r^2 (1.9 - 2.6m^2 + 0.7m^4). \end{aligned} \right\} \quad (2.36)$$

For a disk of constant thickness the calculating formulas derived (2.36) express the connection of radial  $\sigma_R$  and circumferential  $\sigma_T$  stresses in a section taken on current radius  $r$ , with radial  $\sigma_{R_0}$  and circumferential  $\sigma_{T_0}$  stresses in a section taken on radius  $R_0$ .

#### Calculation of disks of arbitrary form

For calculation of disk strength it is necessary to trace its profile. A disk of constant thickness is very stressed and heavy in weight. Therefore, disks

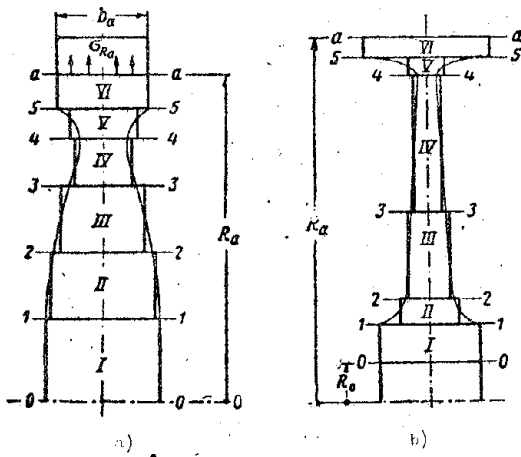


Fig. 2.48. Section of disk.

usually tend to have forms similar to a profile of equal resistance (Fig. 2.48). Transitions to rim and hub as made smooth as possible. Sometimes on separate sections disks are given conical form, and in the central part, a form of constant thickness. During profiling of disks it is possible to use the form of disks of completed compressors. Expediency of selected form of disk is checked by strength calculation.

During calculation of a disk of arbitrary form, it is divided by a series of annular sections into separate portions. Each obtained ring is considered to be of constant thickness, equal to average thickness of disk on this section. Conical rim of disk is reduced to cylindrical form. Thus, the calculating diagram of the disk is in stepped form. Annular sections of disk are arranged in such a manner that the calculating stepped form of the disk as closely as possible approaches its profile. Accuracy of calculation is increased with increase of number of sections. Usually for calculations it is sufficient to take 5-7 sections.

Let us agree to number the sections and annular areas of the disk from center to periphery.

In a solid disk (without central hole) the zero section is plotted on radius  $R = 0$ , i.e., it is drawn to axial line 0-0 (see Fig. 2.48a). In a disk with

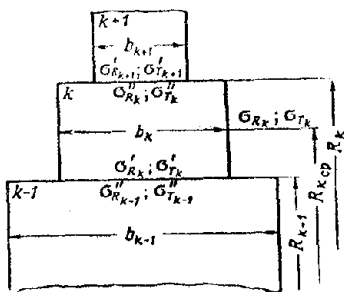


Fig. 2.49. Calculation of disk strength.

central hole the zero section is plotted on radius of hole, i.e., behind zero section we take the surface of the disk around the hole (see Fig. 2.48b). Last annular portion of disk is limited by annular section of radius  $R_a$  of circumference of retainer grooves bases (see Fig. 2.46).

In the calculating diagram of the disk, each annular section has constant thickness and therefore their radial  $\sigma_R$  and circumferential  $\sigma_T$  stresses can be expressed by formulas (2.36).

We shall designate, for an arbitrary annular section  $k$  with constant thickness  $b_k$ , stresses on its external radius  $R_k$  through  $\sigma''_{R_k}$  and  $\sigma''_{T_k}$ , and on its internal radius  $R_{k-1}$  through  $\sigma'_{R_k}$  and  $\sigma'_{T_k}$  (Fig. 2.49). Then formulas (2.36) for the adopted designations will take on the following form:

$$\left. \begin{aligned} \sigma'_{R_k} &= A_k \sigma'_{R_k} + (1 - A_k) \sigma'_{T_k} - (QM)_k \\ \sigma'_{T_k} &= (1 - A_k) \sigma'_{R_k} + A_k \sigma'_{T_k} - (QN)_k \end{aligned} \right\} \quad (2.57)$$

where coefficients  $A_k$ ,  $M_k$  and  $N_k$ :

$$\left. \begin{aligned} A_k &= \frac{1 + m_k^2}{2} \\ M_k &= 3,3 - 2,6m_k^2 - 0,7m_k^4 \\ N_k &= 1,9 - 2,6m_k^2 + 0,7m_k^4 \end{aligned} \right\} \quad (2.58)$$

here  $m_k = \frac{R_{k-1}}{R_k}$ . Values of coefficients  $A$ ,  $M$ , and  $N$  are shown in Fig. 2.50.

Magnitude  $Q$  has the form

$$Q_k = \frac{\tau \omega^2}{2g} R_k^2. \quad (2.59)$$

In stepped form of disk, radius  $R_k$  is simultaneously the external for preceding ring and internal for subsequent ring. On radius  $R_{k-1}$  upon transition from one annular section to another, adjacent to it, thickness of disk varies from  $b_{k-1}$  to  $b_k$  (see Fig. 2.49). In accordance with this the stresses also vary. Radial stresses on radius  $R_{k-1}$  are connected by the expression:

$$\sigma'_{R_k} b_k = \sigma'_{R_{k-1}} b_{k-1}.$$

On the other hand, absolute radial aspect of disk on the boundary of two adjacent annular sections  $k - 1$  and  $k$  can be represented with the help of expression (2.30):

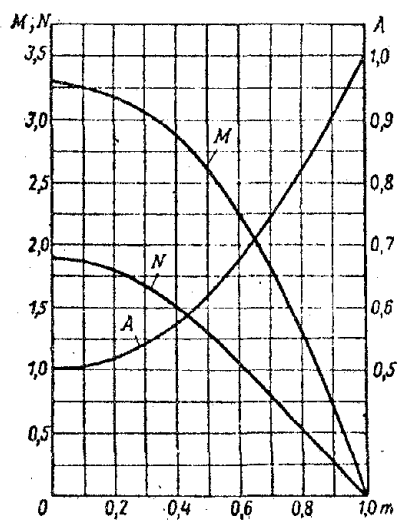


Fig. 2.50. Dependence of coefficients A, M, and N on m.

$$u = \epsilon_T R_{k-1} = \frac{R_{k-1}}{E} \times \\ \times (\sigma'_{T_k} - \mu \sigma'_{R_k}) = \frac{R_{k-1}}{E} \times \\ \times (\sigma'_{T_{k-1}} - \mu \sigma'_{R_{k-1}}).$$

Whence

$$\sigma'_{T_k} - 0.3 \sigma'_{R_k} = \sigma'_{T_{k-1}} - 0.3 \sigma'_{R_{k-1}},$$

where Poisson's ratio  $\mu = 0.3$ .

Thus, stresses  $\sigma'_{R_k}$  and  $\sigma'_{T_k}$  on internal radius of subsequent annular section k are connected with stresses  $\sigma''_{R_{k-1}}$  and  $\sigma''_{T_{k-1}}$  on external radius of preceeding annular section k - 1 (see Fig. 2.49) by the following relationships:

$$\left. \begin{aligned} \sigma'_{R_k} &= \frac{b_{k-1}}{b_k} \sigma'_{R_{k-1}}; \\ \sigma'_{T_k} &= \sigma'_{T_{k-1}} + 0.3 \left( \frac{b_{k-1}}{b_k} - 1 \right) \sigma'_{R_{k-1}}. \end{aligned} \right\} \quad (2.40)$$

The obtained calculating formulas (2.37) and (2.40) give the possibility to calculate a disk of arbitrary profile, passing consecutively from first section to the last one. However, for this, as initial magnitudes it is necessary to know radial  $\sigma_{R_0}$  and circumferential  $\sigma_{T_0}$  stresses in zero section of first portion of disk. In a disk without hole (see Fig. 2.48a) zero section is drawn to axial line 0-0 and therefore  $\sigma_{R_0} = \sigma_{T_0}$ . In a disk with hole (see Fig. 2.48b) for zero section in case of free hole  $\sigma_{R_0} = 0$ , and in case of pressed fittings of disk on shaft  $\sigma_{R_0} = p$ , where  $p$  is specific pressure from the pressed fitting.

It follows from this that for calculation of disk by the formulas (2.37) and (2.40) we will not obtain the following initial data: for solid disk – stresses in center  $\sigma_{R_0} = \sigma_{T_0}$ , for a disk with hole – circumferential stress in zero section  $\sigma_{T_0}$ .

From condition of loading of disk by centrifugal forces from blades and retainer part of rim one can determine radial stress  $\sigma_{R_a}$  for calculated section in a disk on radius  $R_a$  (see Figs. 2.46 and 2.48)

$$\sigma_{R_a} = \frac{C_n + C_s}{2\pi R_a b_a}, \quad (2.41)$$

where  $C_n$  is centrifugal force from profiled part blade ring;  
 $C_s$  is centrifugal force from retainer part of impeller;  
 $R_a$  is external radius of last annular section;  
 $b_a$  is thickness of last annular section.

Centrifugal force from profiled part of blade ring:

$$C_n = Cz, \quad (2.42)$$

where  $C$  is centrifugal force of blade quill (2.6);  
 $z$  is the number of blades.

Centrifugal force from retainer part of impeller

$$C_s = 2\pi \frac{f}{g} R_f^2 \omega^2, \quad (2.43)$$

where  $\gamma$  is specific gravity of material of blade and disk;  
 $f$  is area of cross section of retainer part;  
 $R_f$  is radius of location of center of gravity of area  $f$ ;  
 $g$  is acceleration due to gravity;  
 $\omega$  is angular velocity of rotation.

We shall designate unknown value of stresses in central part of disk (a disk without hole  $\sigma_{T_0} = \sigma_{R_0}$ , and a disk with hole  $\sigma_{T_0}$ ) for community by  $\sigma_{T_0}$ .

Then upon consecutive transition from first calculating section to the last, formulas (2.37) and (2.40) can be reduced to the form:

$$\left. \begin{array}{l} \sigma_{R_k} = \varphi_k \sigma_{T_0} - B_k; \\ \sigma'_{T_k} = t_k \sigma_{T_0} - C_k; \\ \sigma''_{R_k} = \varphi_k \sigma_{T_0} - D_k; \\ \sigma''_{T_k} = \lambda_k \sigma_{T_0} - F_k. \end{array} \right\} \quad (2.44)$$

On external surface of the last (peripheral) annular section, i.e., in section a-a (see Fig. 2.48) stresses will constitute

$$\sigma_{R_a} = \varphi_a \sigma_{T_0} - D_a; \quad (2.45)$$

$$\sigma_{T_a} = \lambda_a \sigma_{T_0} - F_a. \quad (2.46)$$

Here coefficients  $\varphi_a$  and  $\lambda_a$ , and free terms  $D_a$  and  $F_a$  pertain to peripheral annular section disk (in Fig. 2.48 to Section VI).

From expression (2.45) we will obtain the expression for stress

$$\sigma_{T_0} = \frac{\sigma_{R_a} + D_a}{\varphi_a}. \quad (2.47)$$

The coefficients and free terms in these formulas are determined by the following relationships:

$$\left. \begin{aligned} \psi_k &= \frac{b_{k-1}}{b_k} \varphi_{k-1}; \\ \xi_k &= \lambda_{k-1} + 0,3 \left( \frac{b_{k-1}}{b_k} - 1 \right) \varphi_{k-1}; \\ \varphi_k &= \xi_k + A_k (\psi_k - \xi_k); \\ \lambda_k &= \psi_k - A_k (\psi_k - \xi_k). \end{aligned} \right\} \quad (2.48)$$

$$\left. \begin{aligned} B_k &= \frac{b_{k-1}}{b_k} D_{k-1}; \\ C_k &= F_{k-1} + 0,3 \left( \frac{b_{k-1}}{b_k} - 1 \right) D_{k-1}; \\ D_k &= C_k - A_k (C_k - B_k) + M_k Q_k; \\ F_k &= B_k + A_k (C_k - B_k) + N_k Q_k. \end{aligned} \right\} \quad (2.49)$$

Coefficients and free terms are determined consecutively from first (central) section to last one (peripheral). For the first section we take:

a) disk without hole

$$\begin{aligned} \psi_1 &= 1; \xi_1 = 1; \varphi_1 = 1; \lambda_1 = 1; \\ B_1 &= 0; C_1 = 0; D_1 = M_1 Q_1; F_1 = N_1 Q_1. \end{aligned}$$

b) Disk with central hole

$$\begin{aligned} \psi_1 &= 0; \xi_1 = 1; \varphi_1 = 1 - A_1; \lambda_1 = A_1; \\ B_1 &= -\sigma_{R_a}; C_1 = 0; D_1 = M_1 Q_1 - A_1 \sigma_{R_a}; F_1 = N_1 Q_1 - (1 - A_1) \sigma_{R_a}. \end{aligned}$$

Calculated stresses of disk are stresses on mean radius

$$R_{\text{cep}} = \frac{R_k + R_{k-1}}{2} \quad (2.50)$$

of each annular section, which are equal to (see Fig. 2.49):

$$\sigma_{R_k} = \frac{\sigma'_{R_k} + \sigma''_{R_k}}{2} \quad \text{and} \quad \sigma_{T_k} = \frac{\sigma'_{T_k} + \sigma''_{T_k}}{2}$$

and are determined according to the following formulas:

$$\left. \begin{aligned} \sigma_{R_k} &= \frac{\psi_k + \varphi_k}{2} \sigma_{T_0} - \frac{B_k + D_k}{2}; \\ \sigma_{T_k} &= \frac{\xi_k + \lambda_k}{2} \sigma_{T_0} - \frac{C_k + F_k}{2}. \end{aligned} \right\} \quad (2.51)$$

The coefficients and free terms in these formulas are preliminarily determined from expressions (2.48) and (2.49), and stress  $\sigma_{T_0}$  according to formula (2.47).

Radial stresses in  $\sigma_{R_a}$  in formula (2.47) in peripheral section of disk in the presence of blade ring are determined by formula (2.41), and without it are taken as equal to zero. Circumferential stress  $\sigma_{T_a}$  in peripheral section of disk is determined by formula (2.46).

On the basis results of calculation it is possible to construct distribution curves of stresses  $\sigma_{R_k}$  and  $\sigma_{T_k}$  along radius of disk, linking their ends with values of  $\sigma_{R_0}$  and  $\sigma_{T_0}$  in zero in zero section with values of  $\sigma_{R_a}$  and  $\sigma_{T_a}$  in peripheral section of disk. Calculation of disk for convenience is given in the table, as was shown in the example. In finished designs the stresses reach:

in solid disks

from aluminum alloy	1500 to 2500 kg/cm <sup>2</sup>
from titanium alloys	3500 to 5000 kg/cm <sup>2</sup>
from steel	4500 to 6000 kg/cm <sup>2</sup>

in disks with central hole

from aluminum alloy	1000 to 2500 kg/cm <sup>2</sup> ,
from titanium alloys	4000 to 6000 kg/cm <sup>2</sup>
of steel	7000 to 9000 kg/cm <sup>2</sup>

In disks with central hole maximum stresses take place at the hole. In solid disks maximum stresses most frequently are observed in center of disk.

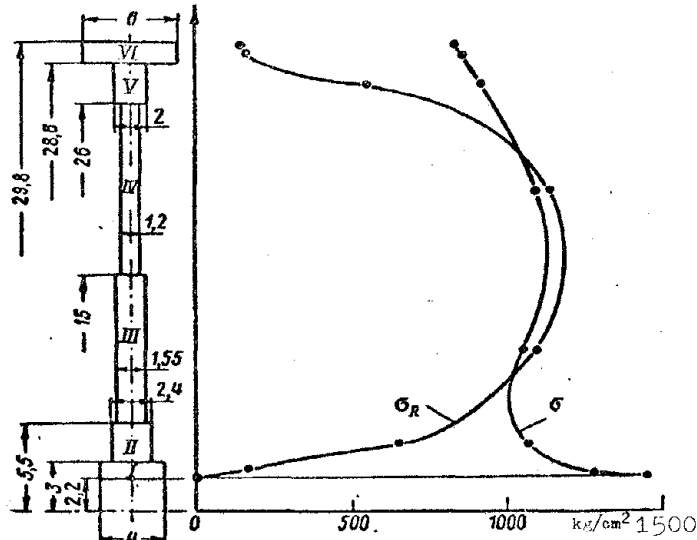


Fig. 2.51. An example of determination of stress in a disk.

Example. Determine stress in a compressor disk with central hole (Fig. 2.51).

Given:  $\omega = 700 \text{ rad/sec}$ ;  $z = 37$ ;  $C_H = 3390 \text{ kg}$ ;  $f = 6 \text{ cm}^2$ ;  $R_f = 30.3 \text{ cm}$ ;  $b_a = 6 \text{ cm}$ ;  $\gamma = 2.77 \cdot 10^{-3} \text{ kg/cm}^3$ ;  $R_a = 29.8 \text{ cm}$ .

Centrifugal force from retainer part of impeller according to formula (2.43)

$$C_s = 2\pi \frac{2.77 \cdot 10^{-3}}{981} 6 \cdot 30.3^2 \cdot 700^2 = 47750 \text{ kg.}$$

Centrifugal force from profile part of blade ring according to formula (2.42)

$$C_s = 37 \cdot 3390 = 125500 \text{ kg.}$$

Radial stress on external calculated diameter of disk according to formula (2.41):

$$\sigma_{R_0} = \frac{125500 + 47750}{2 \cdot 29.8 \cdot 6} = 154 \text{ kg/cm}^2.$$

Coefficients  $A_k$ ,  $M_k$  and  $N_k$  are found on the graphs in Fig. 2.50 or by formulas (2.38).

Value of  $Q_k$  by formula (2.39):

$$Q_k = \frac{2.77 \cdot 10^{-3} \cdot 7002}{8.981} R_k^2 = 0.167 R_k^2.$$

Coefficients  $\psi_k$ ,  $\phi_k$ ,  $\xi_k$  and  $\lambda_k$  are determined by formulas (2.48), and free terms  $B_k$ ,  $C_k$ ,  $D_k$  and  $F_k$ , by formulas (2.49). Disk has a free hole and therefore  $\sigma_{R_0} = 0$ .

Stress  $\sigma_{T_0}$  is found by formula (2.47), and stress  $\sigma_{R_k}$  and  $\sigma_{T_k}$ , by formulas (2.51). Results of calculations are presented in tables. Joining to obtained stresses  $\sigma_{R_k}$  and  $\sigma_{T_k}$  the stresses in zero section of disk  $\sigma_{R_0}$  and  $\sigma_{T_0}$ , and in peripheral section of disk  $\sigma_{R_a}$  and  $\sigma_{T_a}$ , we construct curves of stresses of the disk (see Fig. 2.51). Stress  $\sigma_{T_a}$  is then determined by formula (2.46).

Circumferential stress in zero section by formula (2.47):

$$\sigma_{T_0} = \frac{154 + 164}{0.213} = 1495 \text{ kg/cm}^2.$$

Circumferential stress in peripheral section (2.46):

$$\sigma_{T_a} = 0.621 \cdot 1495 - 173 = 755 \text{ kg/cm}^2.$$

Section number	$R_k$ cm	$b_k$ cm	$m_k$	$A_k$	$M_k$	$N_k$	$Q_k$
I	3	4	0.735	0.77	1.692	0.702	1.55
II	5.5	2.4	0.546	0.65	2.463	1.187	5.23
III	15	1.55	0.367	0.567	2.937	1.563	38.8
IV	26	1.2	0.577	0.666	2.358	1.113	116.5
V	28.6	2	0.908	0.912	0.678	0.232	141
VI	29.8	6	0.96	0.96	0.317	0.103	153

## Continuation

Section number	$M_k Q_k$	$N_k Q_k$	$\frac{b_{k-1}}{b_k}$	$\psi_k$	$\epsilon_k$	$\varphi_k$	$\lambda_k$
I	3	1	—	0	1	0.23	0.77
II	13	6	1.665	0.383	0.815	0.535	0.664
III	114	61	1.55	0.827	0.752	0.795	0.753
IV	275	130	1.29	1.025	0.823	0.956	0.89
V	96	33	0.6	0.573	0.775	0.59	0.756
VI	49	16	0.33	0.196	0.638	0.213	0.621

## Continuation

Section number	$B_k$	$C_k$	$D_k$	$F_k$	$R_{kp}$ cm	$R_k$ kg/cm <sup>2</sup>	$\sigma_k$ kg/cm <sup>2</sup>
I	0	0	3	1	2.6	170	1322
II	5	1.6	17	9	4.25	673	1100
III	26	12	134	73	10.25	633	1085
IV	173	85	419	244	20.5	1185	1118
V	251	188	341	227	27.3	571	937
VI	113	159	164	173	29.2	167	774

## 2.7. Materials

Compressors usually operate at moderate working temperatures. Basic materials for them are light alloys and structural steel. Field of application of those or other materials is limited to their upper limit of working temperatures: for magnesium alloys 200°C, for aluminum alloys 250°C, for titanium alloys 350°C, and for ordinary structural steels 500 to 550°C.

Working and stator blades are usually made from stampings, deformed aluminum alloys AK4 and [VM17] (BД17), stainless steels, structural steel [40KhNMA] (40ХНМА) and [30KhGSA] (30ХГСА), and titanium alloys. For manufacture of hollow blades of inlet guide they frequently apply alloy [VT1] (BT1), possessing good weldability.

Disks are usually made from forgings and stampings of deformed heat-resisting aluminum AK4, structural steel [38KhA] (38ХА), 40KhNMA, stainless steels, and titanium alloys.

Compressor housings are cast from light alloys or welded from steel. For cast housings they use magnesium alloys [MЛ5] (МЛ5) and aluminum alloys [AL5] (АЛ5).

Steel housings of welded design are made from steel [S20] (С20), and their flanges from steel 30KhGSA. For the obtainment of small radial clearances of the rotor, certain places of the stator of the compressor are coated with a paste. The paste is made from potash, talc, graphite, or aluminum powder on a heat-resistant varnish base.

## CHAPTER III

### CENTRIFUGAL COMPRESSORS

#### 3.1. General Information

Figure 3.1 shows the structural diagram of a single-stage centrifugal compressor with one-way entry. Rotor consists of rotor wheel (impeller) 1 and shaft 2. Stator consists of inlet duct 5, compressor housing with vane diffuser 3 and outlet ducts 4.

Impeller together with the diffuser located behind it form the compressor stage.

Figure 3.2 shows the single-stage centrifugal compressor [VK-1] (BK-1) with two-way entry. Impeller 3, set on shaft 2, has working blades 6 on both sides of disk. According to this, from every side of the impeller the compressor has inlet ducts. Inlet ducts are of annular form. On the outside they have safety grids 8, and inside there are fixed guides 7. The housing carries vane diffuser 1 from which air heads in 9 outlet ducts 4. Inside them are fixed stator blades 5. Figure 3.3 shows a longitudinal section of the same compressor.

Single-stage centrifugal compressor can ensure a compression ratio  $\pi_K$  of not more than 4 to 4.5. For higher compression they use two and three-stage compressors (Fig. 3.4). However, the application of several stages leads to noticeable decrease of efficiency of centrifugal

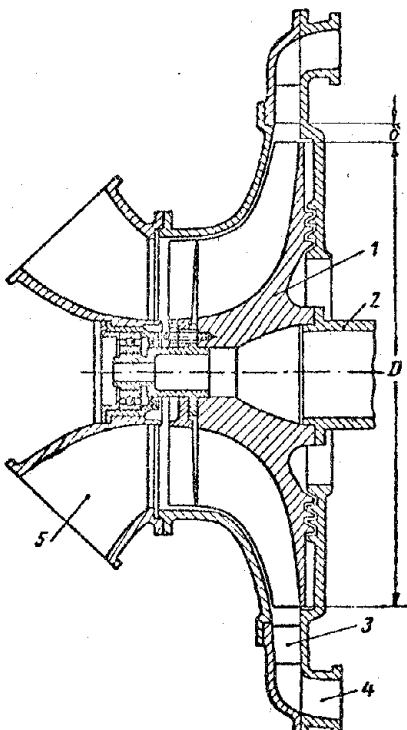


Fig. 3.1. Structural diagram of a single-stage centrifugal compressor.

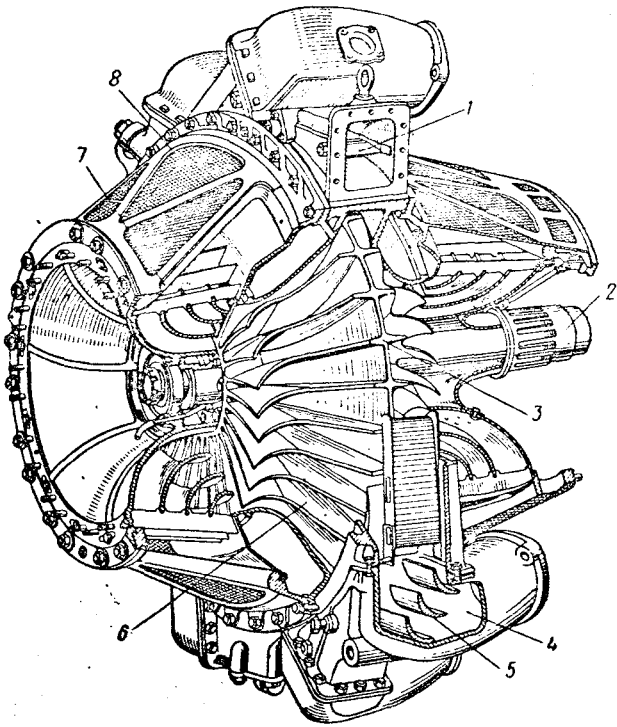


Fig. 3.2. Compressor of VK-1 engine.

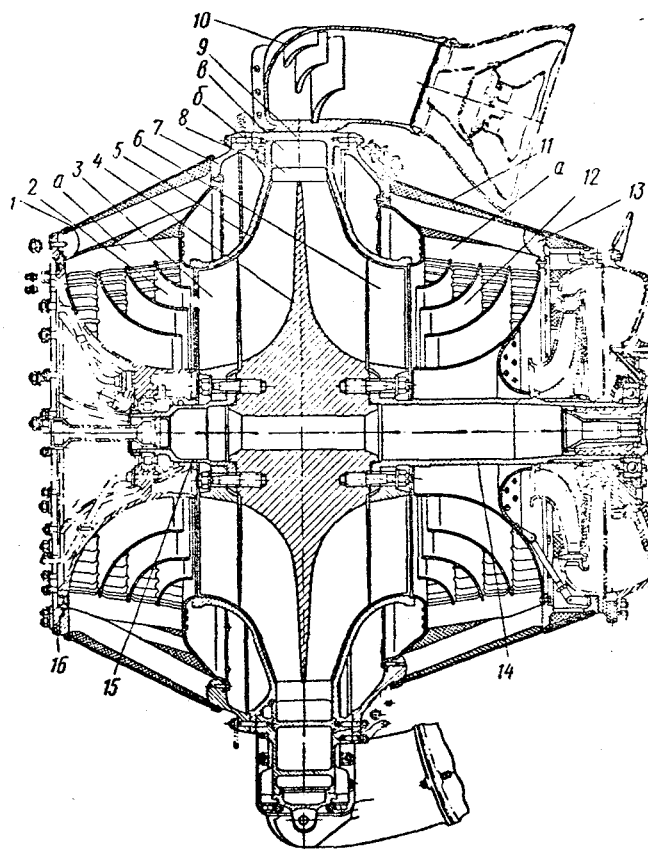


Fig. 3.3. Longitudinal section of compressor of VK-1 engine. 1 and 11 – grids of front and rear ducts, 2 and 12 – front and rear inlet ducts, 3 and 6 – front and rear revolving guide, 4 – impeller, 5 – cover of housing, 7 and 13 – front and rear girder, 8 – sealing ring, 9 – housing of compressor, 10 – outlet duct, 14 – shaft of compressor, 15 – front journal, 16 – front bearing casing, a) fixed guide vane, b) radial clearance between impeller and vaned diffuser, c) blade of diffuser.

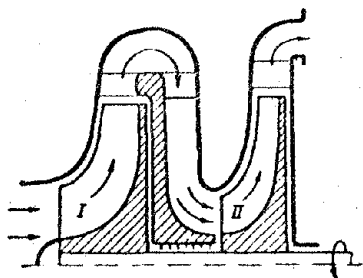


Fig. 3.4. Diagram of two-stage compressor.

compressor, and in the two-way entry design it is considerably complicated.

In [GTD] (ГТД)<sup>1</sup> we find the application of the combined axial-centrifugal compressor, the diagram of which is shown in Fig. 3.5. Its first stages are axial, and the last one is centrifugal. Application of axial stages allows us to increase the compression ratio of the compressor with preservation of high values of efficiency. Application of centrifugal stage allows us to limit ourselves to a smaller number of axial stages, i.e., to decrease length and weight of compressor.

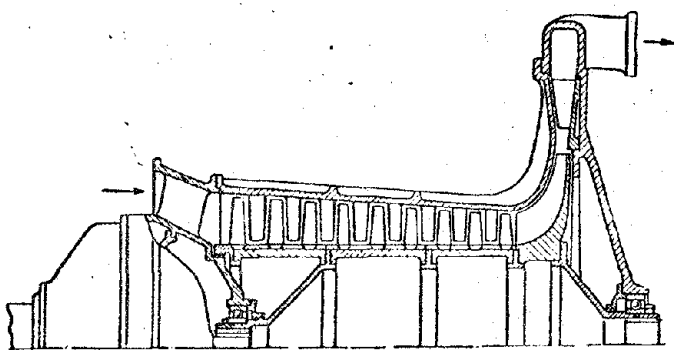


Fig. 3.5. Structural diagram of combined axial-centrifugal compressor.

entry, and one-way impeller, and compressors with two-way entry and two-way impeller;

3 - type of wheels, i.e., compressors with open, closed, and half-closed wheel;

4 - design of wheel blades, i.e., compressors with radial blades and with blades turned toward rotation or opposite rotation of wheel;

5 - type of entry, i.e., compressors with axial, lateral, and annular inlets;

6 - type of diffuser, i.e., compressors with vaneless and slotted (vaneless) diffuser.

### 3.2. Rotor Design

Figure 3.6 shows the rotor of a centrifugal compressor with two-way impeller and with one-way fan impeller 2, and Fig. 3.7 shows impeller 1 and housing wall.

<sup>1</sup>Gas-turbine engines.

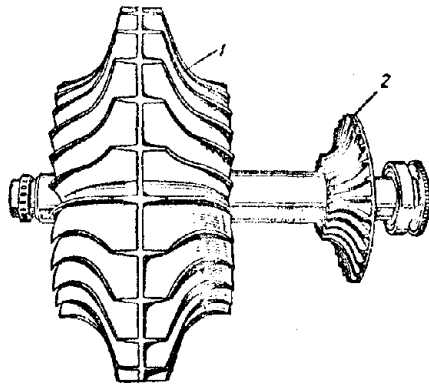


Fig. 3.6. Rotor of centrifugal compressor TRD RD-500.

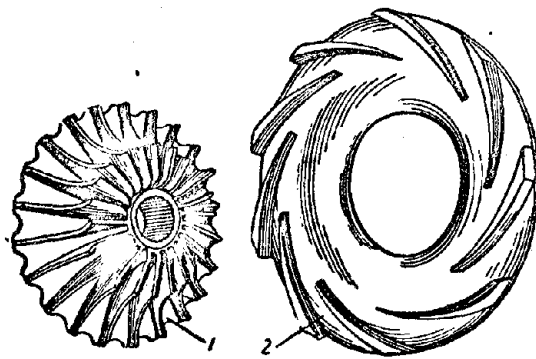


Fig. 3.7. Rotor wheel and diffuser.

with vanes of diffuser 2.

Rotor wheel (impeller) transmits to the air the energy necessary for its compression in the compressor. Figure 3.8 shows types of wheels: a) open wheel, b) closed wheel, c) half-closed one-way wheel, and d) half-closed two-way wheel. Open wheel consists of a bushing with straight radial blades. Its interblade channels are open from both sides. Closed wheel has two walls in the form of

disks with blades located between them. Front disk has entry to wheel, and rear disk passes into the hub.

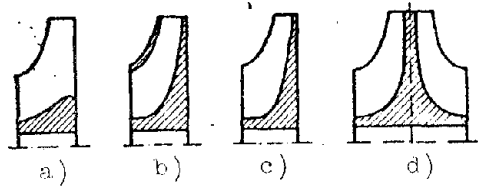


Fig. 3.8. Types of wheels.

The half-closed wheel constitutes a disk with extended hub, on which from one or two sides are located working blades. In the first case the wheel is one-way, and in the second it is two-way. Interblade channels of the wheel do not have one wall; therefore these wheels are called half-closed or half-open. The open wheel creates heightened losses (has lower efficiency), and the closed wheel is complicated in manufacture and with respect to durability yields to other types of wheels. Therefore, compressors of GTD predominantly use the wheel of the half-closed type. They are simple in manufacture and possess high durability, allowing peripheral velocities up to 450-580 m/sec. Two-way wheels find application for large air consumption. In this case, calculation of each side of the wheel is conducted on half of the air consumption, and inlet diameter of such wheel is less. In accordance with this the external diameter of the wheel can also be less.

The main operating elements of the wheel are its blades which are arranged uniformly along its circumference. Number of blades is limited to their possible distribution around the wheel hub and is usually from 15 to 30. With increase of number of blades the thrust ratio of the wheel somewhat increases. Figure 3.9 schematically shows the possible forms of blades: a) radial blades, b) blades, turned towards rotation, and c) blades turned opposite rotation of wheel. At the same peripheral velocity of rotation the biggest thrust ratio is ensured by

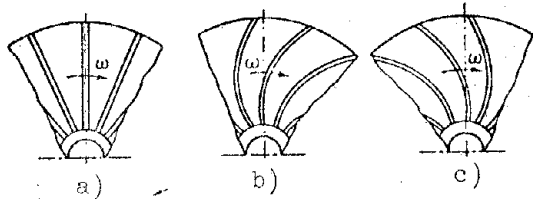


Fig. 3.9. Forms of rotor wheel blades.

thickening in the direction of the disk. Blades have the form either an isosceles or nonisosceles trapezoid (Fig. 3.10). In the last case the angle of inclination

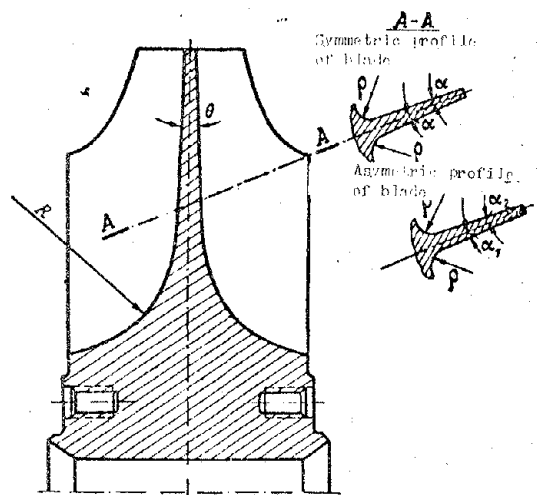


Fig. 3.10. Rotor wheel.

blades turned in the direction of rotation. However, under conditions of durability in GTD compressors, wheels with radial blades have obtained predominant application.

From the condition of durability and rigidity, blades are usually made with

thickening in the direction of the disk. Blades have the form either an isosceles or nonisosceles trapezoid (Fig. 3.10). In the last case the angle of inclination  $\alpha_2$  of the blade from the nonworking side is made larger than angle  $\alpha_1$ . Linkage of blade with disk is done with radius  $\rho = 6$  to 10 mm.

From the condition of durability the disk of the wheel is made slightly conical in form with angle of conicity  $\theta = 2$  to  $6^\circ$ . For guarantee of smooth turn of air flow from axial direction on inlet to radial on outlet the wheel hub is made prominently extended in axial direction with smooth transition of it to the disk.

Rotor wheels are usually fabricated from stamped aluminum highly durable alloy. Their interblade channels by means of polishing are made with high purity of processing. For increase of resistivity of corrosion, wheels are subjected to anode oxidizing.

Revolving guide (intake) the [VNA] (BHA)<sup>1</sup> is a component part of the rotor wheel. VNA are most frequently made in the form of a separate part (Fig. 3.11)

<sup>1</sup>Revolving guide.

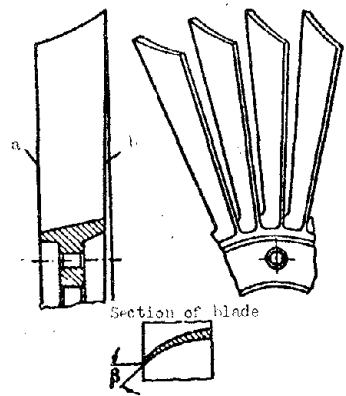


Fig. 3.11. Revolving guide (VNA).

and are attached at the inlet to the rotor wheel. VNA constitutes a hub with radial blades. Inlet edges  $a$  of VNA blades are turned in the direction of rotation of the wheel, which ensures shock-proof entry of air into rotor wheel. Angle  $\beta$  of bend of VNA blades is increased from hub to periphery in accordance with change of relative airspeed on wheel inlet. Rear edges  $b$  of VNA blade adjoin the blades of the rotor wheel, forming with them channels for passage of air.

VNA are manufactured from highly durable aluminum alloys and less often from steel. Their blades by means of polishing are made with high purity of treatment. VNA made from aluminum alloys are anodized. For small wheels they sometimes make VNA simultaneously with the rotor wheel. In this case the VNA will be formed by the bend of the inlet edges of wheel blades (see Fig. 3.7).

Rotor of compressor. Figure 3.12 shows the rotor of the compressor of the VK-1 engine. It consists of a one-sided half-closed wheel 5 with radial blades, two VNA 4 and 6, front journal 1, shaft 7, and impeller of fan 8.

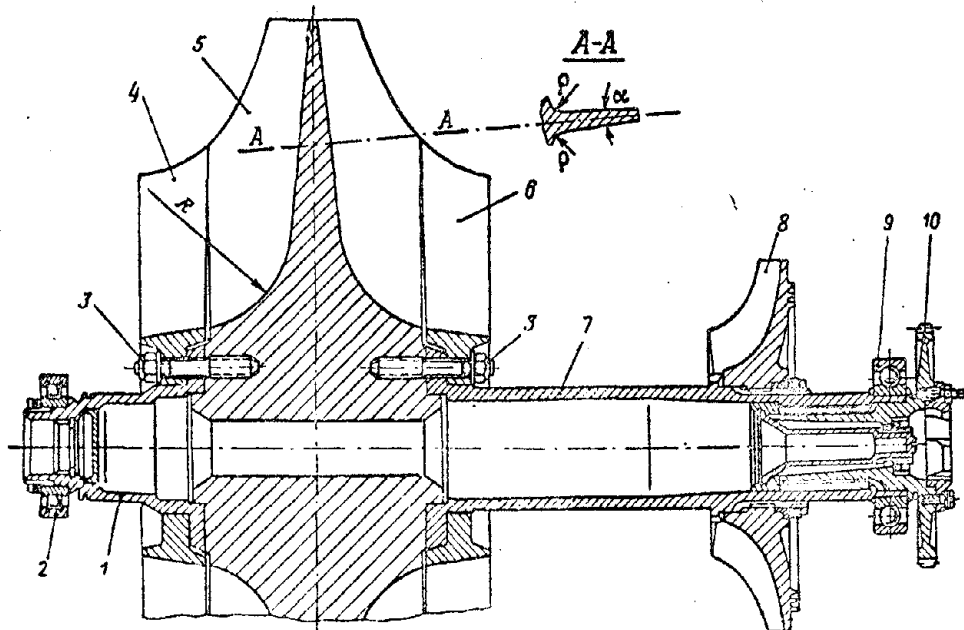


Fig. 3.12. Rotor of compressor of VK-1 engine.

Wheel and VNA are made in the form of separate parts from stamped aluminum alloy. They each have 29 radial blades. Rear ends 6 of VNA blades are drilled onto a cone (see Fig. 3.11) and in connection with wheel blades they form a tightness from 0.35 to 0.53 mm (at the expense of deformation of VNA blades). This decreases vibrations of blades of VNA during work. Mountings of wheel and VNA with shaft and journal are flanged and are made with the help of pins 3 (see Fig. 3.12), screwed into the wheel hub. Centering of wheel is carried out along its cylindrical beads, and the VNA is centered along the pilots of the shaft and journal. Pins are screwed into blind threaded holes of the wheel hub with small diametrical tightness and with a stop at the bottom of the hole. This attains a more uniform loading of all turns of the thread during tightening of pins. Torque in connections of shaft and journal with wheel and with VNA is transmitted by friction at the flanges, appearing when tightening the pins.

To front journal 1 is attached support roller bearing 2. Through internal slits of journal the assemblies are drawn and fixed in the front part of the engine. To shaft 7 are attached impeller of fan 8, radial-thrust ball bearing 9, and splined bushing 10. Impeller of fan serves for supply of air coolant to turbine and bearing casings. The splined bushing serves for connection with shaft of turbine.

### 3.3 Stator Design

Inlet device of compressor ensures feed of air to rotor wheel with minimum losses. It constitutes a discharge pipe which frequently contains a fixed guide.

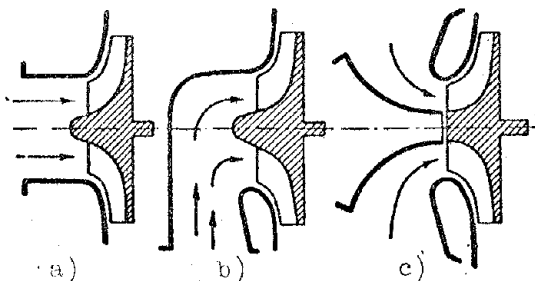


Fig. 3.13. Form of discharge pipes.

Figure 3.13 shows a diagram of inlet ducts which form: a) axial inlet, b) lateral inlet, and c) annular inlet. Axial inlet ensures least losses; however it is not always possible to use it with respect to design considerations. Most frequently in GTD we find the application of the annular inlet which ensures uniform feed of air around circumference of wheel. Inlet channel of compressor is usually made with small contraction, which ensures the best uniformity of air flow at inlet to rotor wheel. In powerful GTD air consumption is great; therefore, their centrifugal

compressors are made with one-sided entrance (see Fig. 3.2).

At the annular inlet device there is a fixed guide [NNA] (HHA) which consists of an annular set of blades 1 and guide cones 2 (Fig. 3.14). Blades 1 create preliminary twisting of air in direction of rotation of wheel and thereby decrease its relative velocity at wheel inlet to subsonic values. NNA blades have constant profile, their external edges are directed radially, and internal edges are turned in the direction of rotation of the wheel at an angle of about  $20^{\circ}$ . Guide cones 2 divide flow area of inlet duct into a series of annular channels. They level the field of velocities during turn of air flow on its approach to the rotor wheel. The guide cones are mounted on blades 1.

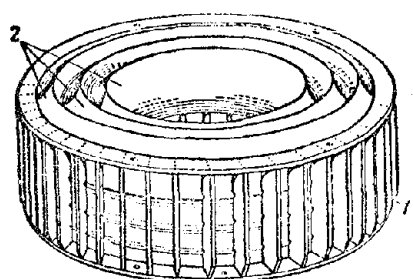


Fig. 3.14. Fixed guide.

As example, Fig. 3.15 shows the rear inlet duct of centrifugal compressor of engine VK-1 which consists of walls 1 and 4, 48 stator blades 2, and three guide cones 3. On ends of blades 2 there are three pins each, and on outlet edge there are three slits each.

Corresponding slits are also made on periphery of guide cones 3. During assembly of discharge pipe the blades are grouped in the slits of cones and with rear pins are drawn into the beds of the walls. After that, the projecting ends of pins are unriveted.

Components of inlet devices are made from sheet aluminum-magnesium alloy, while the guide cones and walls are produced by drawing, and blades by stamping.

Diffuser is arranged in housing of compressor at rotor wheel outlet. In it there occurs transformation of kinetic energy of air into pressure. We distinguish diffusers as vaneless and slotted (vaneless). Vaned diffuser is formed by vanes 2 (see Fig. 3.7) which are arranged in annular cavity of compressor housing. Slotted diffuser constitutes an annular cavity without vanes.

Vaned diffuser has higher efficiency and smaller diametrical dimensions than the slotted diffuser. The vanes form its channels, gradually expanding in direction of motion of air. Number of vanes of the diffuser, which is from 9 to 30, is not recommended to be equal to or multiple to the number of vanes of the wheel, since pulsation of air flow is intensified in this instance.

As an example, Fig. 3.16 shows a diffuser, and Fig. 3.17 shows the housing of

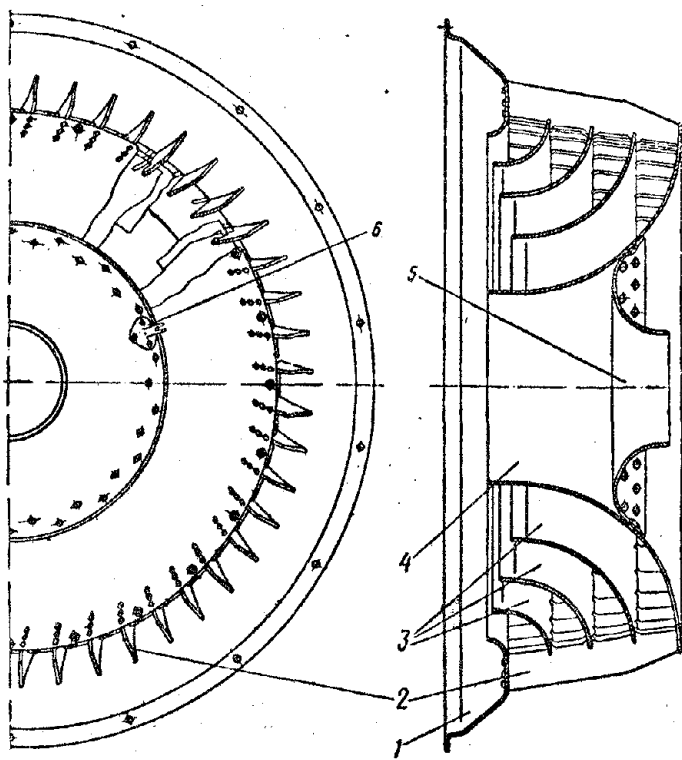


Fig. 3.15. Rear inlet duct of centrifugal compressor of VK-1 engine.

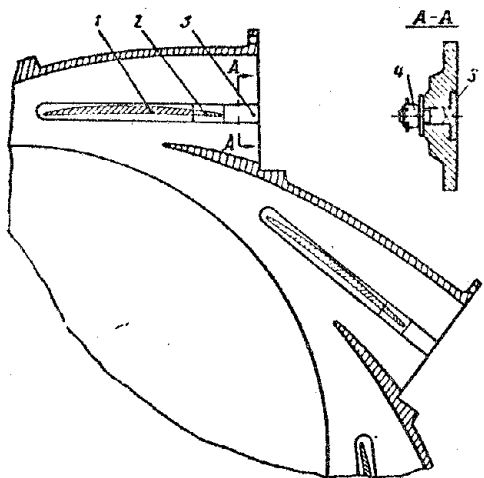


Fig. 3.16. Vaned diffuser of compressor of VK-1 engine.

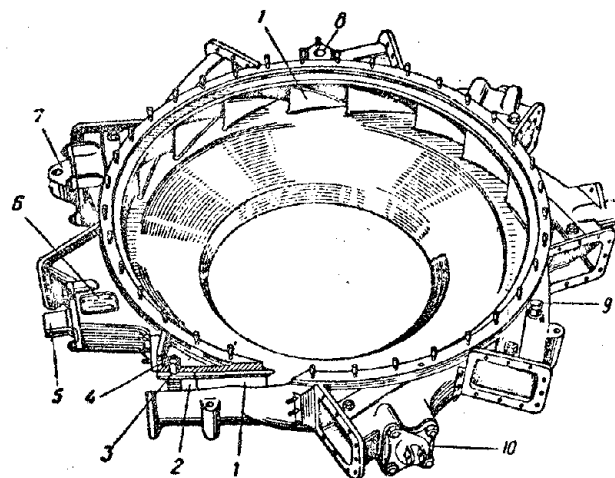


Fig. 3.17. Compressor housing of VK-1 engine. 1 - diffuser vane, 2 - vane tip of diffuser, 3 - vane stop of diffuser, 4 - bracing nut of stops, 5 - journal support, 6 - engine plate, 7 - suspension bracket, 8 - air sampler for needs of aircraft, 9 - stub pipe for discharge of air to labyrinth seal of front bearing, 10 - lower support.

centrifugal compressor of engine VK-1. For decrease of diametrical dimensions the vaned diffuser is combined with outlet ducts. Diffuser has 18 vanes. Of them 9 are cast together with housing and pass into walls of ducts. The other 9 vanes are insertable. They are fixed in rectangular grooves made inside the ducts, and consist of two parts: aluminum vane 1 and steel tip 2. The vane and tip are steadied from axial shifts by two steel stops 3 which with the help of their shanks are braced to the housing by nuts 4.

Outlet device of a centrifugal compressor with individual combustion chambers is usually made in the form of outlet pipes.

In the VK-1 engine (see Fig. 3.2) elbow outlet pipes 4 are fastened to pipe flanges of housing. Through these pipes air from compressor is fed to nine combustion chambers. For decrease of hydraulic losses during turn of air flow the outlet pipes each have three stator blades 5. Outlet pipes are cast from aluminum alloy.

The compressor housing is the main support component of the engine. From condition of assembly the housing is sectional with disassembly in the plane perpendicular to axis of rotor. In the centrifugal compressor of the VK-1 engine (see Fig. 3.3) the housing consists of two parts — its own housing 9 and housing cover 5 cast from aluminum alloy. Cover is centered by the bead in the housing boring and attached to it with pins. The housing (see Fig. 3.17) has a rear wall and 9 outlet pipes which house the vaned diffuser. For mounting of engine to aircraft on two pipes there are basic support journals 5 of the engine, and on three other pipes there are auxiliary supports 7 and 10.

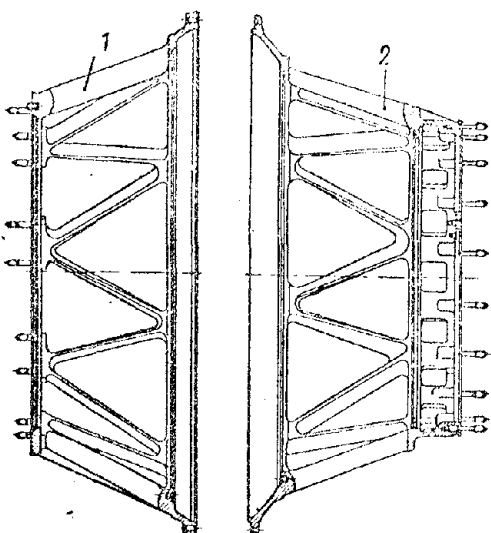


Fig. 3.18. Front and rear support frames of compressor of VK-1 engine.

Support frames. In the presence of annular inlet the compressor stator has support frames of the girder type. Figure 3.18 shows the front 1 and rear 2 support frames of compressor of the VK-1 engine, having a two-way entrance. Support frames are cast from aluminum alloy and consist of two annular flanges united by 18 rods, i.e., ribs.

With large flanges the frames are connected with the compressor housing, and with smaller ones, correspondingly: front —

with accessory box, and rear - with bearing casing (see Fig. 1.8). Air passes into compressor between rods of frames. Inside frames there are inlet annular devices. On the outside they are closed by wire screens 8, protecting from fall of foreign objects (see Fig. 3.2). At the small flange of the rear girder on the circumference there are 18 apertures for passage of air to fan.

#### 3.4. Clearances Between Stator and Rotor Wheel

Between stator and rotor wheel of compressor there are created radial and axial clearances ensuring free rotation of rotor (see Fig. 3.1). Radial clearance between wheel and diffuser vanes is usually equal to  $\delta = 12$  to 30 mm. This radial clearance is an element of the slotted diffuser. It ensures, at entrance to vane diffuser, levelling of velocities of air flow, and at supersonic velocity it provides for transformation of it into subsonic with least losses.

In axial direction the compressor rotor is fixed in the housing by radial-thrust ball bearing 9 (see Fig. 3.12). In the installation of axial clearances the different thermal expansions for rotor and stator are considered.

#### 3.5. Calculation of Rotor Wheel Strength

Wheel of centrifugal compressor is calculated on load by centrifugal forces from mass of disk and blades. During calculation the rotor wheel is divided into a series of annular sections and for each section its mass is determined. Thus, for a two-sided wheel the mass  $m$  of one of the annular sections having average radius  $R_{cp}$  (Fig. 3.19) is equal to

$$m = \frac{1}{g} 2\pi R_{cp} b \Delta R + 2 \frac{1}{g} \delta b_1 z \Delta R = \\ = \left( 1 + \frac{\delta b_1 z}{\pi R_{cp} b} \right) \frac{1}{g} 2\pi R_{cp} b \Delta R, \quad (3.1)$$

where  $\gamma$  is specific gravity of material of rotor wheel;

$g$  is acceleration due to gravity;

$b$  is average thickness of annular section of disk;

$b = \frac{b_1 + b_2}{2}$  is average thickness of section of blades in annular section;

$b_1$  is average width of blade in annular section;

$z$  is the number of blades.

Usually for convenience of calculations they introduce the idea of given specific gravity  $\gamma_{np}$  of annular sections of disk, considering

$$\gamma_{np} = \gamma \left(1 + \frac{\delta b_1 z}{2\pi R_{cp} b}\right). \quad (3.2)$$

Each annual section of disk will have its own given specific gravity. For a one-sided wheel the given specific gravity will be

$$\gamma_{np} = \gamma \left(1 + \frac{\delta b_1 z}{2\pi R_{cp} b}\right). \quad (3.3)$$

Calculation of disk of wheel of centrifugal compressor is done by the same method as calculation of disks of axial-flow compressor, but in the first case the radial stresses on external radius of disk will be equal to zero,  $\sigma_{R_a} = 0$ .

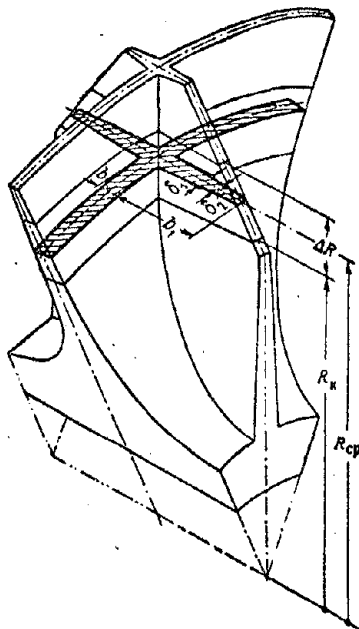


Fig. 3.19. Calculation of compressor wheel strength.

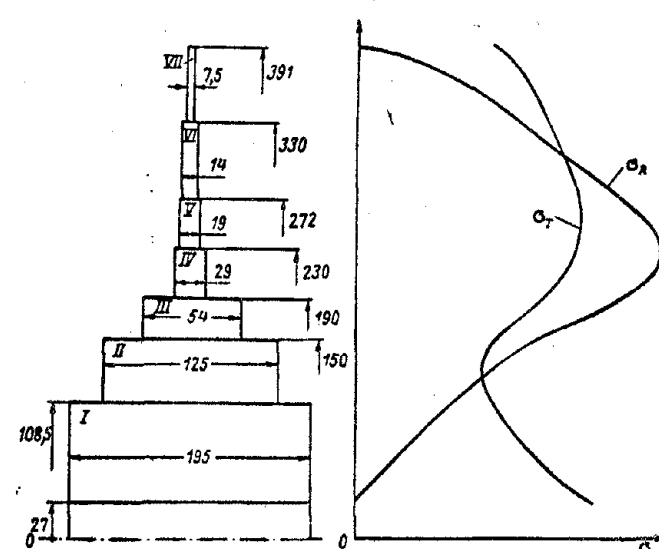


Fig. 3.20. An example of calculation of the wheel.

Stresses on disks of wheels made from aluminum alloys are allowed to 2800 kg/cm<sup>2</sup>.

Example. Determine the stresses in the disk of a two-sided wheel of a centrifugal compressor (Fig. 3.20).

Given:  $\omega = 1210 \text{ rad/sec}$ ;  $\gamma = 2.75 \text{ g/cm}^3$ .

We divide the disk into seven calculating sections and for each of them we find: given specific gravity by formula (3.2), coefficients A, M and N on the graph of Fig. 2.50, and value of Q by formula (2.39).

$$Q_k = \frac{\gamma_{np}}{8.981} 1210^2 R_k^2 = 0.187 \gamma_{np} R_k^2.$$

Values of given specific gravity  $\gamma_{np}$  and magnitudes necessary for its determination are given in Table 3.1, and values of coefficients A, M, N and magnitudes Q, MQ, and NQ are presented in Table 3.2. Disk has free hole and therefore  $\sigma_{R_0} = 0$ . Calculations of stresses  $\sigma_R$  and  $\sigma_T$  in disk are given in Table 3.3. Joining to the obtained tabulated data on  $\sigma_R$  and  $\sigma_T$  the stresses in zero and peripheral sections of the disk, we construct curves of stresses in disk (see Fig. 3.20).

Table 3.1

Section No.	$R_{cp}$ mm	$b$ mm	$b_1$ mm	$\delta$ mm	$\gamma_{np}$ g/cm <sup>3</sup>
I	67,7	195	—	—	2,75
II	129	125	35	9,6	3,28
III	170	54	70,5	10,9	4,88
IV	210	29	82,5	10	6,2
V	251	19	88	8,4	6,7
VI	301	14	65	7,5	5,7
VII	360,5	7,5	48	6,5	5,7

Table 3.2

Section No.	$R_k$ cm	$b_k$ cm	$m_k$	$A_k$	$M_k$	$N_k$	$Q_k$	$M_k Q_k$	$N_k Q_k$
I	10,85	19,5	0,249	0,53	2,14	1,74	60,5	130	105
II	15	12,5	0,725	0,76	1,74	0,73	138	240	101
III	19	5,4	0,79	0,81	1,4	0,55	330	462	182
IV	23	2,9	0,825	0,84	1,21	0,46	612	740	282
V	27,2	1,9	0,845	0,86	1,685	0,4	927	1005	370
VI	33	1,4	0,825	0,84	1,21	0,46	1160	1405	533
VII	39,1	0,75	0,845	0,86	1,085	0,4	1730	1770	652

Table 3.3

Section No.	$\frac{b_{k-1}}{b_k}$	$\psi_k$	$\xi_k$	$\varphi_k$	$\lambda_k$	$B_k$
I	—	0	1	0,47	0,53	0
II	1,56	0,733	0,609	0,703	0,639	203
III	2,32	1,63	0,893	1,49	1,034	987
IV	1,86	2,77	1,42	2,55	1,64	2490
V	1,525	3,89	2,06	3,635	2,315	4575
VI	1,36	4,95	2,708	4,588	3,07	7100
VII	1,865	8,56	4,26	7,96	4,86	14750

Table 3.3 (cont'd)

Section No.	$C_k$	$D_k$	$F_k$	$R_{k_{cp}}$ cm	$\sigma_{R_k}$ kg/cm <sup>2</sup>	$\sigma_{T_k}$ kg/cm <sup>2</sup>
I	0	130	105	6,77	386	1416
II	127	425	246	12,9	1065	1011
III	414	1340	705	17	1831	1290
IV	1049	3000	1562	21	2365	1635
V	2035	5220	2765	25,1	2317	1800
VI	3327	7902	4463	30,1	1650	1650
VII	6503	15270	8402	36,05	835	1275

Circumferential stress in zero section by formula (2.47):

$$\sigma_{T_0} = \frac{0 + 15270}{7,96} = 1920 \text{ kg/cm}^2.$$

Circumferential stress in peripheral section by formula (2.46):

$$\sigma_{T_a} = 4,86 \cdot 1920 - 8402 = 930 \text{ kg/cm}^2.$$

### 3.6. Materials

Single-stage centrifugal compressors operate at moderate temperatures.

Wheels and VNA are usually made from stamped highly durable alloy [AK6] (AK6). Housings, covers, and support frames are cast from aluminum alloys of the type Silumin [AL4] (АЛ4) or [AL5] (АЛ5). NNA components are stamped from sheet aluminum-magnesium alloy [AMg-M] (AMг-М). For prevention of corrosion all aluminum components are anodized. Shafts are manufactured from highly durable steel [18KhNVA] (18ХНВА), [40KhNMA] (40ХНМА), or [12Kh2N4A] (12Х2Н4А).

## C H A P T E R IV

### GAS TURBINES

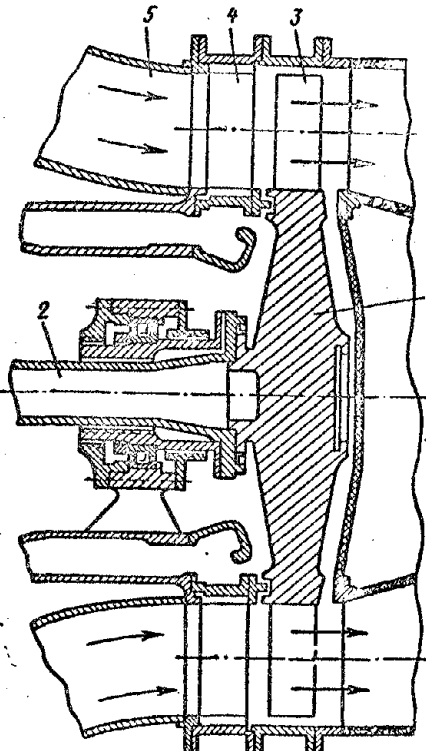
#### 4.1. General Information

Gas turbines of [TRD] (ТРД)<sup>1</sup> are the drives for the compressor and accessories, and in [TVD] (ТВД)<sup>2</sup> they are also the drive for the propeller. Axial reactive

turbines with pressure stages are predominantly used because of their small dimensions, small weight of construction, and high efficiency. In small auxiliary gas turbine installations along with axial turbines sometimes radial turbines are used.

Figure 4.1 shows the structural diagram of a single-stage axial gas turbine. Disk of turbine 1 with working blades 3 form the rotor wheel, and jointly with shaft 2, the rotor of the turbine. Blades of nozzle apparatus 4 with housings and inlet part (gas collector) 5 form the stator of the turbine. The turbine stage consists of nozzle apparatus and the rotor wheel located behind it. Number of stages is determined by magnitude of heat ratio in the turbine. The diagram shows the support roller bearing of the

Fig. 4.1. Structural diagram of a single-stage axial gas turbine.



<sup>1</sup>Turbojet engines.

<sup>2</sup>Turboprop engines.

turbine attached in the housing. Working gases from the combustion chamber proceed to the inlet device of the turbine, pass through its flow area, and through outlet device go into the atmosphere.

Figure 4.2 shows a low capacity gas turbine installation consisting of radial gas turbine 1 and centrifugal compressor 2. Rotor wheels of turbine and compressor are mounted on shaft 3.

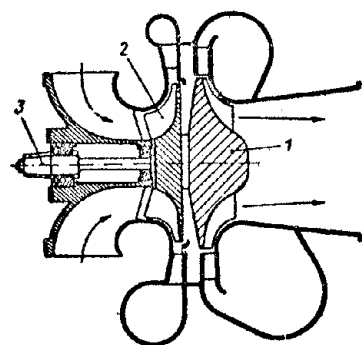


Fig. 4.2. Low capacity gas turbine installation with radial turbine.

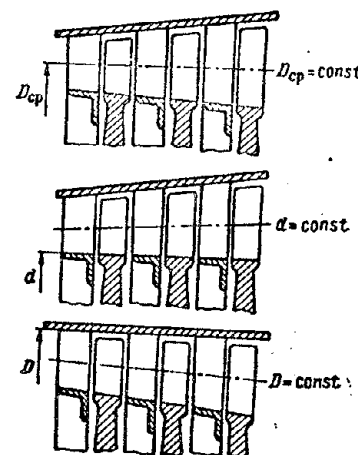


Fig. 4.3. Forms of turbine flow area.

Gas turbines operate in conditions of high temperatures and loads.

Reliability of their operation is ensured by limitation of temperature of working gases, the use of special fire-proof and heat-resistant materials for their manufacture, and cooling of the most heated parts.

Flow area of turbines. Upon passage through turbine the working gases are expanded and increase in volume. Therefore its blades from stage to stage along gas duct gradually extend. Flow area of turbines can be (Fig. 4.3):

with constant middle diameter  $D_{cp}$ ;

with constant diameter of bushing  $d$ ;

with constant external diameter  $D$ ;

Sometimes the flow area of turbines is made with variable  $D_{cp}$ ,  $d$ , and  $D$ .

Classification of gas turbines. Aircraft axial gas turbines:

1) single-, double-, and multi-stage (Figs. 4.4 and 4.5);

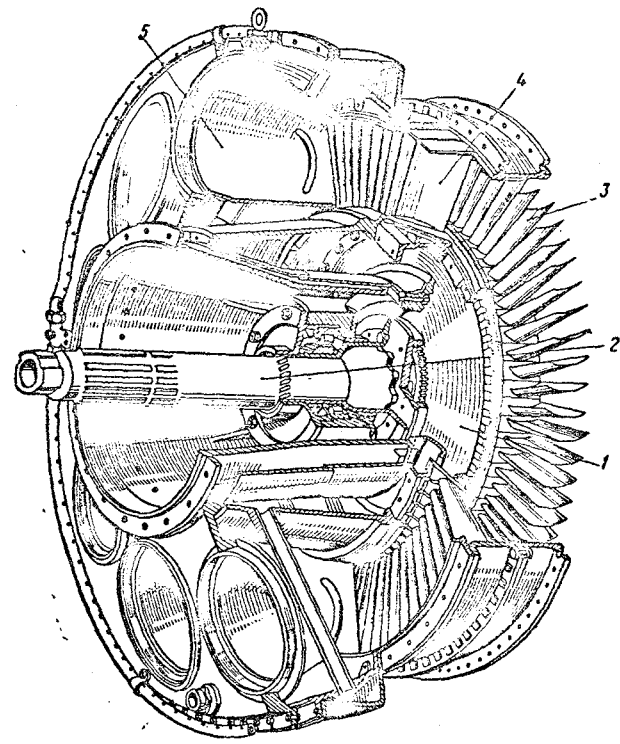


Fig. 4.4. Single-stage axial turbine of VK-1 engine. 1 - turbine disk, 2 - shaft, 3 - moving blades, 4 - nozzle blades, 5 - gas collector duct.

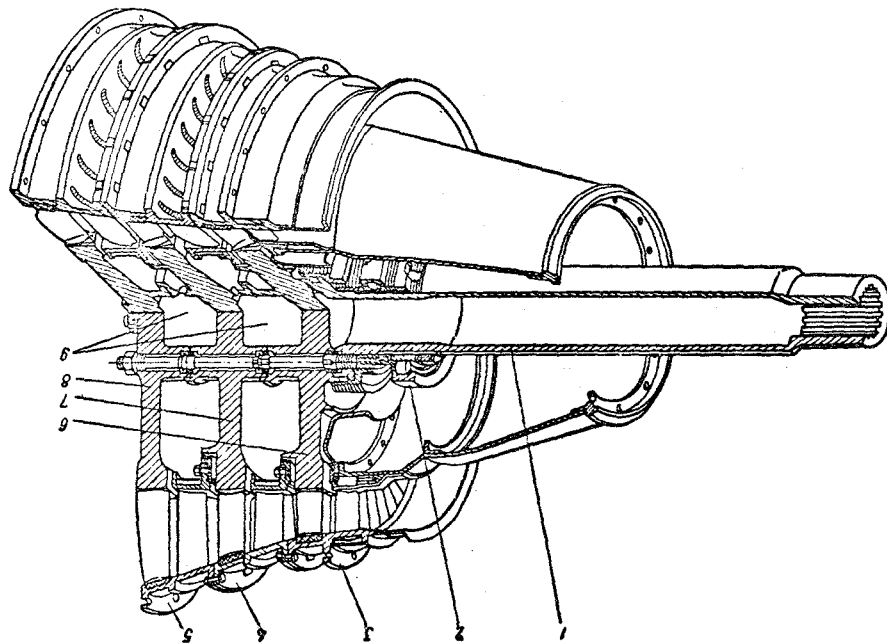


Fig. 4.5. Triple-stage axial turbine of AI-20 engine. 1 - turbine shaft, 2 - roller bearing, 3, 4 and 5 - nozzle apparatuses of 1st, 2nd, and 3rd stages, 6, 7 and 8 - rotor wheels of 1st, 2nd, and 3rd stages, 9 - rotor cavity.

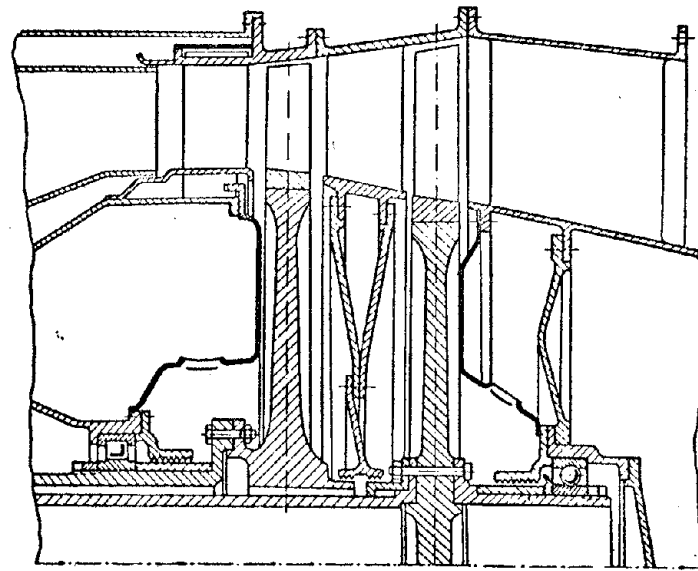


Fig. 4.6. Diagram of double-shaft turbine.

- 2) single-rotor (single-shaft, Figs. 4.4-4.5) and double-rotor (double-shaft, Fig. 4.6);
- 3) with uncooled and with cooled blades.

#### 4.2. Rotor Design

Figure 4.7 shows the rotor of the axial single-shaft, single-stage turbine [VK-1] (BK-1) with uncooled blades.

Moving blades (Fig. 4.8) pertain to the main moving elements of the turbine. They distinguish a profile part or scroll and leg (shank). With the help of the latter the blades are attached to rim of rotor disk.

Blades form at the rotor wheel a blade ring with curved channels. Blade channels of reactive turbines have contracted form, with which the gas flow is accelerated. Turbine blades differ from compressor blades by the fact that their profiles are thicker and more bended. Leg of turbine blades is more extended.

In connection with change of velocity triangles of incident gas flow, the curvature of the profile and its angular position along the length of the blade are variable. Thus, the blade scroll's length is as if twisted into a helix. Short blades are not frequently twisted.

In the existing designs of turbines the length of blades reaches 170 mm. Length of chord  $b$  and pitch  $t$  of blades of rotor wheels are connected together and are determined by density of cascade of blades  $b/t$ , which selected on the basis of

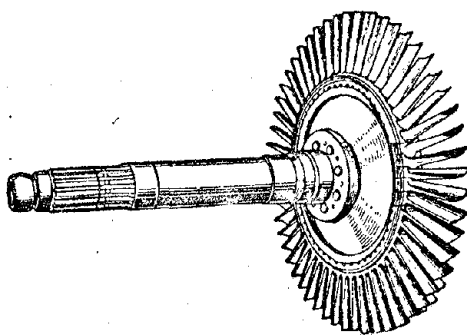


Fig. 4.7. Turbine rotor of VK-1 engine.

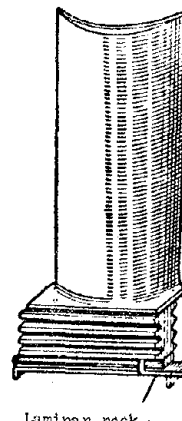


Fig. 4.8.  
Moving blade  
of turbine of  
VK-1 engine.

experimental purging data.

Moving blades of turbines, as also of compressors, are under the action of centrifugal and aerodynamic forces which evoke their extension, bending, and twisting. With irregularity of gas flow there can appear vibrations of blades. According to conditions of durability the thickness of profile along length of blades is made variable by increasing it according to a definite law from peripheral to root section.

Moving blades operate at a temperature from 650 to 750°C and above. With such temperature, under the action of centrifugal forces there is observed the phenomenon of creep of moving blades, i.e., their continuous, although slow, plastic flow. This flow limits the operation life of moving blades.

Moving blades of turbines are made from fire-proof and heat-resistant alloys by stamping or precision casting with subsequent machining. Profile part of blades is usually made with high precision, allowing deviations in linear dimensions no more than 0.1 mm, and in angular dimensions, no more than 15'. High purity of treatment by polishing increases vibration durability of blades, since the presence of small grooves can lead to formation of fatigue cracks. For the purpose of facilitating rotor balancing the moving blades are completed with respect to weight.

Moving blades according to design:

- a) cooled and uncooled;
- b) banded and unbanded.

Cooled blades are hollow for internal cooling. Possible diagrams of cooling of blades are given in paragraph 4.5 "Cooling of turbines".

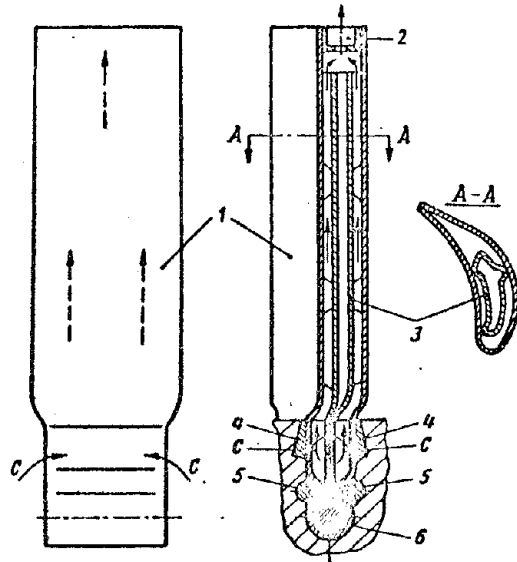


Fig. 4.9. Moving blade with air cooling of turbine of RD-20 engine.

Blade is attached to disk of rotor wheel with help of pins 5 and wedges 4. Air coolant proceeds inside blade through lateral holes in its lock part as shown by arrows C, and emerges through hole in header 2. Deflector directs air along hot walls of blade and improves its cooling. Flow of air through blade is determined by dimension of hole in header 2.

Cooling of blades allows us to increase operating temperature of gases of turbine or to use less scarce materials for manufacture of blades. However, because of the complexity of their manufacture at moderate operating temperatures we prefer to use uncooled blades. Figure 4.8 shows an uncooled moving blade of turbine of the VK-1 engine.

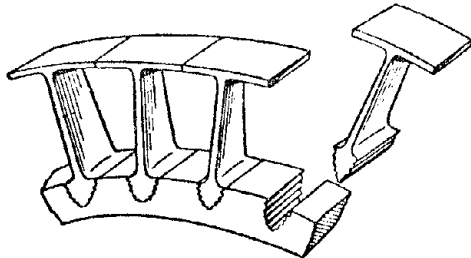


Fig. 4.10. Banded moving blades.

Figure 4.10 shows banded moving blades with shelves on their ends. Losses due to leakage of gases through radial clearances of a turbine with such shelves are less and efficiency of turbine somewhat increases. However, shelves increase loading of blades from centrifugal forces.

Locks of moving blades. Moving blades are attached to disks with locks. Figure 4.11 shows some types of attachment of moving blades: a) pin lock, b) cylindrical lock, c) by means of welding, and d) lock of the "herring bone" type.

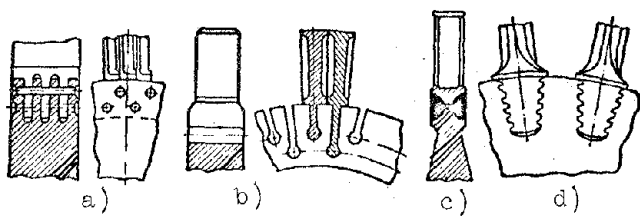


Fig. 4.11. Attachment of moving blades. replacement of blades during maintenance. Wide application has been obtained by a demountable lock of the "herringbone" type, having small weight and small over-all dimensions.

Connection with a lock of the "herringbone" type is carried out by means of teeth on the tapered leg of the blade in the corresponding groove of the disk. Depending upon load, the number of teeth of a lock varies from 2 to 6 from each side of the wedge. For guarantee of equal distribution of load on teeth, the lock of the "herringbone" type requires high precision of manufacture.

Lock grooves of the disk are either straight, parallel to axis of rotation, or slanting at an angle to the axis in transverse (circumferential) direction. Slanting grooves allow installation of a large number of blades on the disk. Fitting of blades in the lock is free, and it ensures thermal expansion of connected parts and self-adjustment of blade in lock under the action of centrifugal force. Free setting of blade in lock is controlled during assembly by rocking it in a plane perpendicular to the groove. In the turbine of the VK-1 engine the deviation of free end of blade during rocking varies from 0.8 to 1.5 mm. From axial shift in grooves, the blades are fixed by stops and laminar plugs. The latter ensure easy replacement of blades.

Figure 4.8 shows the VK-1 blade, on whose leg there is a lip and transverse slot for a laminar stopper. During assembly the turned end of the stopper is preliminarily started in the leg slot and the blade is inserted into the groove of the disk until stopped by the lip. After that the free end of the stopper is unbended on the face of the disk.

In the [AI-20] (AM-20) turbine the moving blades (Fig. 4.12) are fixed by laminar stopper 3. On leg of blade 1 there is a transverse slot a. During assembly, the stopper by its own lip is preliminarily started into the leg slot and the blade is inserted into the herringbone groove of disk 2. After that the

Pin and cylindrical locks of [GTD] (ГТД) blades at present are not used, since they increase the weight of construction. Attachment of blades by means of welding also is not used, since it does not allow for

. . . . .

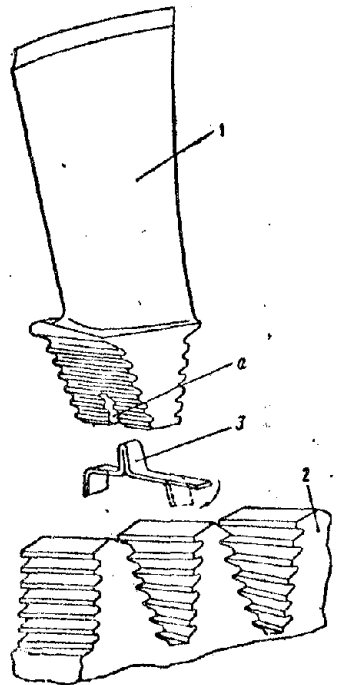


Fig. 4.12. Installation of moving blade on disk of turbine of AI-20 engine.

of torque by friction due to tie of bolts, and d) flanged joint on additional slit connection 6 for transmission of torque.

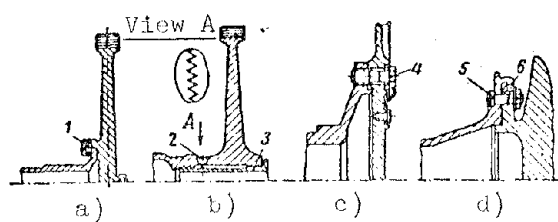


Fig. 4.13. Types of connection of disks with shaft.

annular beads for labyrinth seals, and disk 4 (3rd stage) has in its center a mushroom-like flange utilized during dismantling of turbine. Moving blades are attached by means of herringbone locks and fixed by laminar stoppers.

Disk are united together and with shaft by flanges, forming a rotor of the disk-drum type. They are centered on the fitting beads of the hubs. Disks are secured by eight pins 7 tightly screwed into flange of shaft 1. Tie is controlled by extraction of pins to 0.1 mm. Nuts 8 are locked by laminar locks.

ends of the stopper are unbended on the disk.

Turbine disks in distinction from compressors are more loaded and therefore they are made thicker. Their profile usually has a conical or more complicated form (see Fig. 2.15).

Multistage turbines chiefly use rotors of the disk drum type (see diagram c in Fig. 2.14). Connections of disks with shaft, and the multistage turbines also connections of disks to one another, are different. These connections are presented with the same requirements as are the connections of compressor rotors. Figure 4.13 shows some types of connections of turbine disks with shaft, which are also used for connection of disks together: a) connection by radial pins 1 with pressed setting of disk on shaft, b) connection by triangular end slits 2 and central tie bolt 3, c) flanged joint on bolts 4 screwed into flange of shaft with transmission of torque by friction due to tie of bolts, and d) flanged joint on bolts 5 and additional slit connection 6 for transmission of torque.

Figure 4.14 shows the rotor of the AI-20 three-stage turbine which consists of rotor wheels 2, 3, and 4, attached at an angle to shaft 1. Profile of disks has conical form which passes to periphery into rim, and in the central part, into the hub. Disks 2 and 3 (1st and 2nd stages) have

laminar locks and fixed by laminar stoppers.

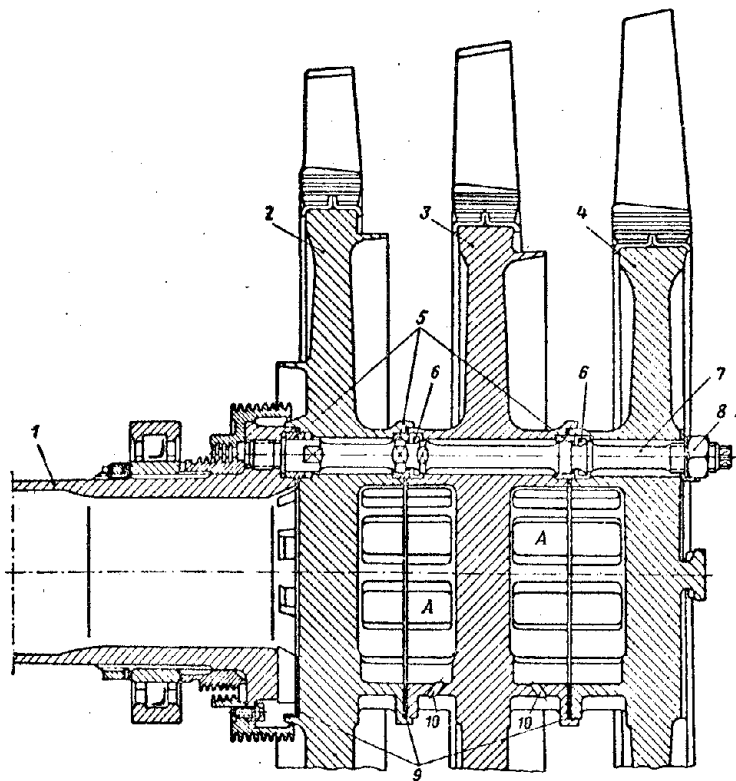


Fig. 4.14. Turbine rotor of AI-20 engine.

In places of joint of disks there are prison bushings 5 and steel linings 9. Bushings serve for transmission of torque. With the aid of linings the axial clearances between stator and rotor of turbine are selected. Drillings 10 ensure breathing of cavity A disk hubs.

For guarantee of consecutive dismantling of disks, the annular apertures of pins 7 are filled with slotted blocks 6 consisting of two halves which serve for axial fixation of disks 3 and 2 on pins 7. The removal of disks 3 and 2 requires preliminary removal of the blocks.

Disks of turbines operate in conditions of high temperatures; therefore, they are made from special heat-resisting steel and alloys.

#### 4.3. Stator Design

Turbine stator consists of housings with nozzles secured in them.

Nozzles are formed by the annular set of stator blades and their carrier elements. They are rings in the form of bands or directly the turbine housing. Figure 4.15 shows nozzles of the 2nd and 3rd stages of the turbine of the AI-20 engine.

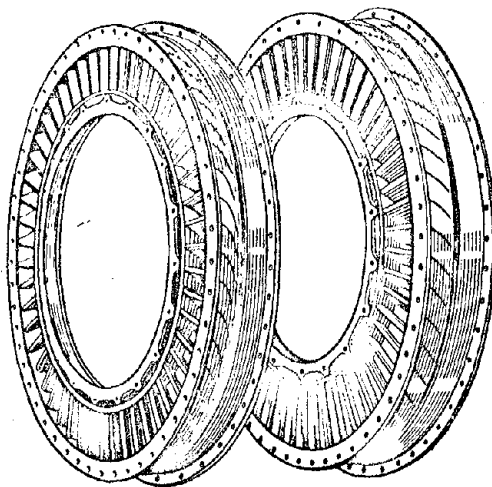


Fig. 4.15. Nozzle apparatuses of turbine of the AI-20 engine.

Nozzle blades, as also moving blades, pertain to the basic moving elements of the turbine. Cross sections of blades have bent profile with small resistance in gas flow, which is obtained by construction similar to moving blades.

During operation, nozzle blades are loaded by aerodynamic forces which cause them to bend and twist. Furthermore, during nonuniform gas flow there can appear oscillations of blades.

Nozzle blades operate at a temperature of 800-900°C and above. They are made from heat-resistant alloys by precision casting or stamping. For decrease of weight and increase of resistance to thermal shocks which appear during fast heating or cooling, cast blades frequently are made hollow (Fig. 4.16).

Nozzle blades are made with the same precision as moving blades. Their profile part is polished.

Nozzle blades are cooled and uncooled. Cooled blades are hollow for internal air cooling. Figure 4.17 shows a cooled blade of the [RD-10] (РД-10) engine.

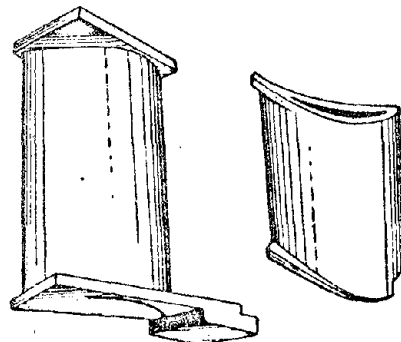


Fig. 4.16. Hollow nozzle blades.

Blade is a hollow, welded construction, and is made from heat-resistant sheet steel. On peripheral end of blade there is welded a plate 3, and at the outlet edges there are welded tapered plates 1 forming outlet slits 7. Inside blade there is a deflector 5 which is welded to internal end of blade. Blade is welded to internal band of nozzle apparatus. Air coolant proceeds inside the deflector and through holes 6 in it heads for the leading edge of the blade, which is the most heated. Then

air passes through the cavity between deflector and blade, cools the blade and emerges through slots 7 at the outlet edge of the blade, being mixed with the operating gases.

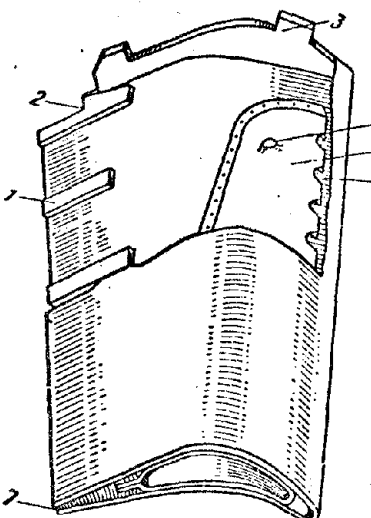


Fig. 4.17. Nozzle blade of turbine of the RD-10 engine with air cooling. 1 - plates, 2 - notch on outlet edge of blade, 3 - plate, 4 - flange on deflector, 5 - deflector, 6 - apertures in deflector, 7 - slot on outlet edge between plates 1.

Connection of nozzle blades with their carrier elements must ensure free thermal expansion of blades. Figure 4.18 shows types of these connections:

- free (floating) setting of blades in recesses of external and internal carrier rings;
- stiffening of blades of internal ring and free setting of them on external ring;
- stiffening of blades of external ring and free setting on internal ring.

The variety of the third type of connections is the cut internal ring, the separate parts of which are rigidly secured to internal end of blades or are made in the form of shelves forming one unit with the blade.

Connections a and b are usually applied on first stages of turbines whose external and internal rings of the nozzle apparatus are rigidly secured to the turbine intake.

Connection c is used in subsequent stages of turbines whose external carrier rings of nozzle apparatuses are rigidly joined with the turbine housing, and internal rings are fixed to the free ends of blades and form labyrinth seals with the turbine disks preventing leakage of gases (see Fig. 4.5).

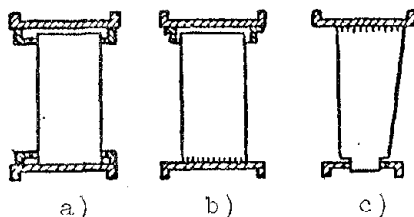


Fig. 4.18. Types of nozzle blade attachment.

Nozzle apparatuses in existing turbine designs are various. There are collapsible and noncollapsible nozzle apparatuses. Figure 4.19 shows a collapsible nozzle apparatus which consists of a set of uncooled blades 2, internal 6 and external 1 rings. The rings are correspondingly secured to internal drum 5 and gas collector casing 3. Connection of blades with rings 6 and 1 is free and is carried out by means of slanting grooves on the rings and shelves 8 and 9 corresponding to them on ends of blades 2. Shelves 9 have a tooth 10 for fixing the blades.

During assembly the nozzle blades are placed in grooves of internal ring 6 which are then secured to drum 5. Blades are fixed by their own teeth 10 with bead

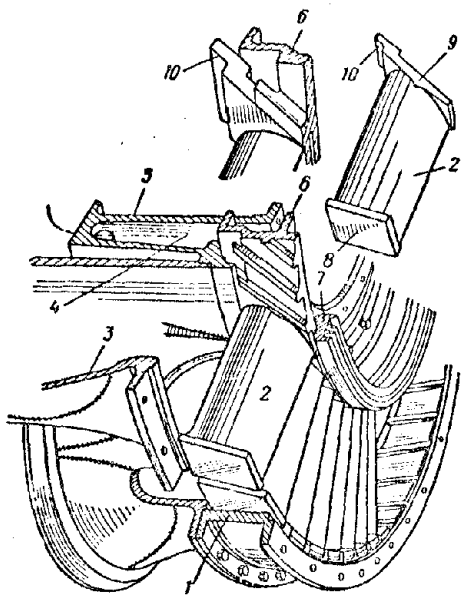


Fig. 4.19. Collapsible nozzle apparatus. 1 — external ring, 2 — nozzle blades, 3 — gas collector casing, 4 — drum cavity, 5 — drum, 6 — internal ring, 7 — labyrinth ring, 8 and 9 — shelves on ends of blades, 10 — tooth for fixation.

of drum 5. Then on shelves 8 of blades, external ring 1 is placed freely and is secured to housing 3. Since grooves of ring 1 and shelves 8 of blades are inclined, the ring is turned a bit when it is put on (as if screwed on the shelves of blades). Free setting of blades in grooves ensures them thermal expansion during operation.

Figure 4.20 shows the noncollapsible nozzle apparatus of the 1st stage of the turbine of the AI-20 engine with free setting of blades. Apparatus consists of external ring 1, internal body 9, and blades 3. External ring 1 is part of turbine housing. With front flange the ring is attached to external housing of combustion chamber, and with rear flange, to nozzle apparatus of 2nd stage. In middle

part on circumference of rings there are notches under blades 3. Cermet inserts 2 form a radial clearance between rotor wheel and housing.

Internal body 9 is a welded construction. By its flanges 7 it is attached to the rotor bearing casing, and with cone 8 forms the internal wall of combustion chamber. From rear side to cone 8 there are welded a duct ring 10 and adjusting ring 11. Duct ring forms the internal contour of gas duct. For installation of blades 3 on it there are corresponding notches, and the adjusting ring 11 has welded cuffs, forming recesses for blades.

Blades 3 are made by method of precision casting. They are freely inserted in notches of external 1 and duct 10 rings until they rest in recesses of adjusting ring 11. Then blades are fixed from radial shift by annular stopper lock 4. The lock with its annular flange enters the notches of blades and with bolts 6 is attached to flange of adjusting ring 11. After that, ring-tape 12 is placed on the housing; the ends of the tape are welded with a cover plate. Ring-tape 12 prevents leakage of air from combustion chamber into gas duct through clearances between blades 3 and notches for them in the housing.

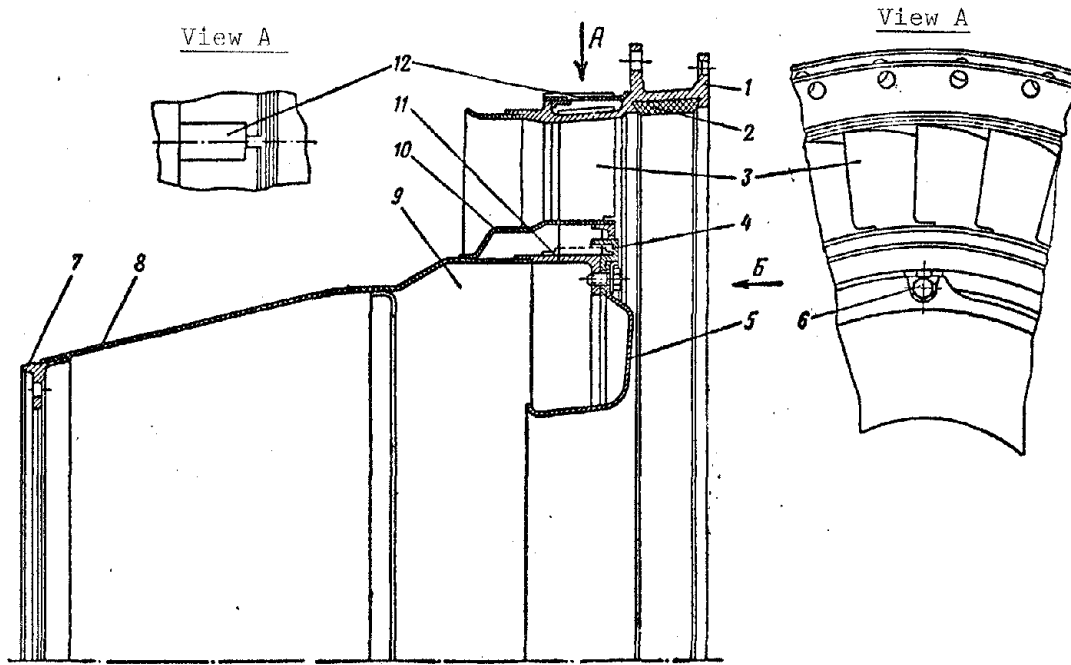


Fig. 4.20. Noncollapsible nozzle apparatus of 1st stage of turbine of AI-20 engine. 1 - external ring, 2 - insert, 3 - blade, 4 - stopper lock, 5 - deflector, 6 - bolt, 7 - flange, 8 - cone, 9 - internal housing, 10 - duct ring, 11 - adjusting ring, 12 - ring.

Figures 4.15 and 4.21 show the noncollapsible nozzle apparatus of the 2nd stage of the turbine of the AI-20 engine with blades rigidly attached to external

ring. Apparatus consists of external ring 1, internal ring 4, and blades 3. External ring 1 is part of turbine housing. With its front flange it is secured to nozzle apparatus of 1st stage, and with rear flange, to nozzle apparatus of 3rd stage. In its middle part on external surface there is an annular rib of rigidity. On the circumference between front flange and rib of rigidity the external rings have notches under blades 3. Cermet inserts 2 form radial clearance between rotor wheel and housing.

Internal ring has notches under blades 3 and two beads which annular rim 5 is welded to. The latter eliminates the possibility of leakage of working gases through clearances between blades 3 and grooves for them on ring 4.

Fig. 4.21. Noncollapsible nozzle apparatus of 2nd stage of turbine of AI-20 engine. 1 - external ring, 2 - insert, 3 - blade, 4 - internal ring, 5 - annular rim, 6 - labyrinth ring, 7 - remote ring.

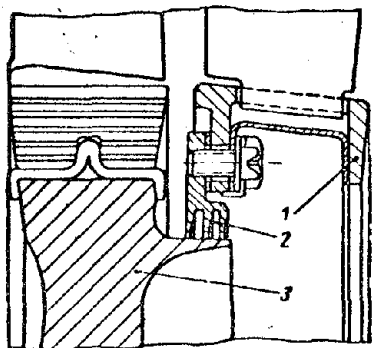


Fig. 4.22. Labyrinth seal of turbine of AI-20 engine.  
1 - nozzle apparatus, 2 - labyrinth ring, 3 - turbine wheel.

Blades 3 are made by method of precision casting. They are inserted in notches of external and internal rings and then welded to external ring. To front bead of internal ring 4 is secured ring of labyrinth seal 6. The latter forms a seal from leakage of working gases with annular flange of rotor wheel of 1st stage (Fig. 4.22).

Turbine housings hold nozzle apparatuses and are in the structural system of the engine just as compressor housings. They perceive twisting moments in the nozzle apparatus area and bending moments

from forces of weight and forces of inertia. In the gas duct area the housings are under heightened pressure of gases and operate at high temperatures. They are manufactured by forging, centrifugal casting, or welding from heat-resistant steel and alloys. For guarantee of assembly of turbines the housing are split along planes perpendicular to axis of rotor, in the form of narrow rings with flanges for connection. From external side they frequently have annular ribs. Ribs and flanges give housings necessary rigidity. In the area of the turbine inlet its housings are connected with combustion chambers, and in the outlet area, with outlet devices. In case of individual (tubular) or tubular-annular combustion chambers, turbines have intakes in the form of gas collectors which ensure uniform feed of working gases to nozzle apparatus of 1st stage. Annular chambers of special devices for this purpose are not required.

Figure 4.23 shows the flow area of the single-stage turbine of the VK-1 engine. Stator of turbine consists of gas collector, nozzle apparatus, and housing covering the rotor wheel.

Gas collector is a split design and consists of housing 1, cover 4, and drum 13. In connection these components form a rigid support box. By flange a the gas collector is attached to casing of rotor bearings.

In wall of housing 1, uniformly along the circumference there are nine cylindrical windows with bronze bushings 2, forming recesses for installation of individual combustion chambers. From internal side to housing 1 by means of flanges, nine transfer pipes 5 are attached.

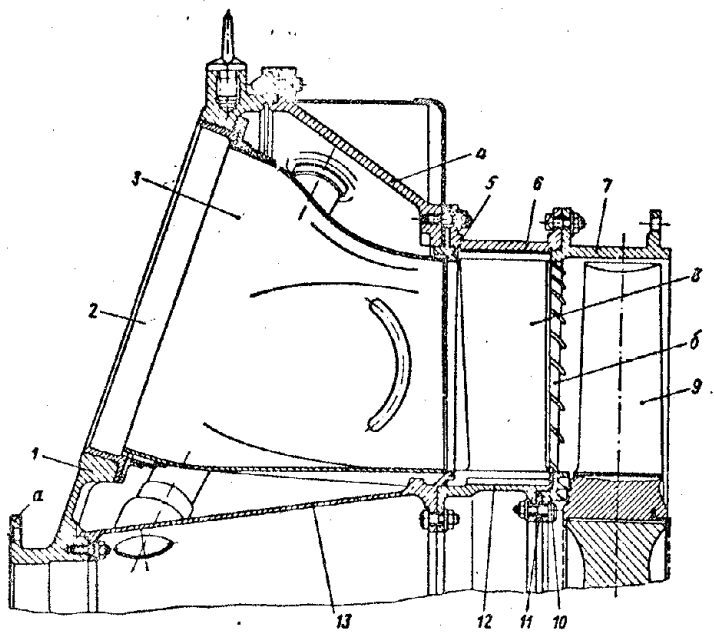


Fig. 4.23. Flow area of turbine of VK-1 engine. 1 - gas collector housing, 2 - bushing, 3 - transfer pipes, 4 - cover, 5 - centering ring, 6 - external ring of nozzle apparatus, 7 - housing, 8 - nozzle blade, 9 - rotor wheel, 10 - labyrinth ring, 11 - regulating ring, 12 - internal ring of nozzle apparatus, 13 - drum.

shelf by bead of drum 13. To rear flange of internal ring 12 there is attached labyrinth ring 10 which forms a seal with rotor wheel 9. With help of regulating ring 11 during assembly an axial clearance is made between labyrinth ring 10 and rotor wheel 9. To rear flange of external ring 6 nozzle apparatus is secured to housing 7 forming radial clearance with rotor wheel 9. The front bead of housing 7 has 62 grooves 6 (according to number of moving blades of wheel). For decrease of leakage of gases through radial clearance of the moving blades, boring of bead is smaller than diameter of rotor wheel. Grooves 6 give the possibility during assembling of freely supporting housing 7 above rotor wheel. To rear flange of housing 7 there is attached the exit nozzle. Figure 4.25 shows the housing of three-stage turbine of AI-20 engine, which consists of three parts: 2, 3, and 4, connected in series with help of flanged joints. Each of the housings carries its own nozzle apparatus. In housings, above moving blades there are holes which are filled by inserts 5 made from soft heat-resistant material ensuring minimum radial clearances between stator and rotor wheel and not

Figure 4.24 shows a transfer pipe separately. The pipe is a welded construction and has a round cross-section on its inlet, and on outlet it has the form of an annular sector. Behind the gas collector there is the nozzle apparatus (see Fig. 4.23). Its internal ring 12 is secured to drum 13, and external ring 6 through centering ring 5 to cover 4. Nozzle apparatus is similar to the one shown in Fig. 4.19. Nozzle blades 8 are freely placed in slanting grooves of rings 12 and 6 and are fixed with their flange on lower

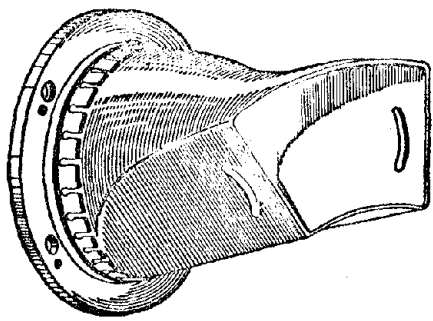


Fig. 4.24. Transfer pipe.

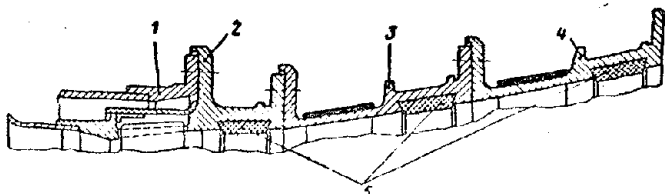


Fig. 4.25. Housing of three-stage turbine of Al-20 engine.

damaging moving blades when grazing around them. Housing joints allow assembly and disassembly of turbine in consecutive order from stage to stage (see Fig. 4.5). With front flange, housing of 1st stage is attached to external housing of combustion chamber 1, and to rear flange of housing of 3rd stage the exhaust pipe is attached.

#### 4.4. Clearances Between Rotor and Stator of Turbine

Between rotor and stator of turbine, just as in axial-flow compressors (see Fig. 2.29) there are radial  $\delta$  and axial  $\Delta$  clearances ensuring free rotation of rotor. Maximum magnitude of radial clearances is limited by growth of losses due to gas leakage, i.e., decrease of turbine efficiency, and their minimum magnitude, by grazing of rotor against stator during operation.

Turbine clearances vary considerably with change of operating conditions of engine. This is explained by distinction of operating temperatures and coefficients of linear expansion of separate parts of rotor and stator. In transitional operating conditions the clearances change also due to different speed of heating or cooling of the comparatively massive rotor and thin-walled bodies of stator. Character of change of clearances in transitional modes of turbine is seen from Table 4.1.

Table 4.1

Operating conditions	Radial clearance	Axial clearance of rotor wheel in the area of the thrust bearing
Starting of engine	increases	decreases
Transition to constant operating conditions	decreases	increases
Transition to idling and stop of engine	decreases	increases

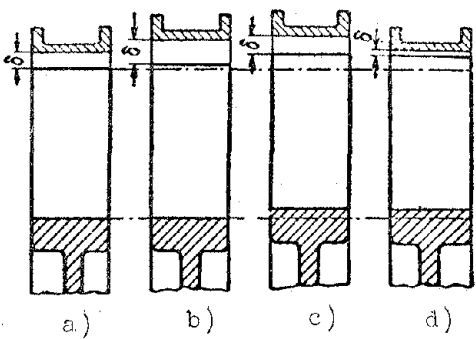


Fig. 4.26. Change of radial clearances in a turbine under various conditions.

Figure 4.26 shows the change of radial clearances of turbine: a) clearance of cold engine, b) clearance during starting, c) clearance during steady performance, and d) clearance upon stop of engine.

In case of small radial clearances during stop of engine the moving blades can be welded in the housing. Therefore it is sometimes recommended after stop of engine, several times with interruptions, to turn its rotor from the starter in order to expel cold air through engine and to accelerate cooling of rotor.

Cooling of turbine decreases thermal expansion of its separate parts and the clearance are then changed in a smaller degree.

In process of prolonged operation, radial clearances in turbine decrease. Due to creep of material of the moving blades and disks, under action of centrifugal forces there occurs their continuous lengthening in radial direction. In turbine housings there has been observed a reverse phenomenon, i.e., their shrinkage and warping. This decrease of clearances usually limits the operation life of engines. Thus, in the turbine of the VK-1 engine (see Fig. 4.23) initial radial clearance between rotor wheel 9 and body 7 is established from 2.3 to 2.6 mm. Its decrease in the process of operation is allowed up to 1.3 mm, after which the clearance is restored by boring the housing 7.

In the turbine of the Al-20 engine (see Fig. 4.25) in the housing above moving blades are mounted soft cermet inserts 5 made from nickel, graphite and silicon, which eliminate the possibility of serious damages in case the blades happen to graze them.

Radial clearances  $\delta$  between moving blades and housing in a nonoperating (cold) engine are usually no less than  $\delta = (0.003 \text{ to } 0.004)D$ , where D is the external diameter of the rotor wheel.

Axial clearances  $\Delta$  (see Fig. 2.29) between rotor and stator are usually ensured by regulating rings. For instance, in the turbine of the VK-1 engine (see Fig. 4.23) axial clearance between labyrinth ring 10 and rotor wheel 9 is established during assembly from 2.7 to 2.9 mm by selection of regulating ring 11.

In the turbine of the Al-20 engine the axial clearances between nozzle apparatuses and rotor wheels are established by selection of regulating rings 9 (see Fig. 4.14).

Axial clearances  $\Delta_{JI}$  (see Fig. 2.29) between nozzle and moving blades are established within the limits of  $\Delta_{JI} = (0.1 \text{ to } 0.4)b$ , where  $b$  is the length of chord of profile of blades. The large value of clearance  $\Delta_{JI}$  favorably indicates equalization of gas flow.

#### 4.5. Cooling of Turbines

Aircraft gas turbines operate in conditions of high temperatures and therefore their most heated and responsible parts are usually cooled by air. Cooling

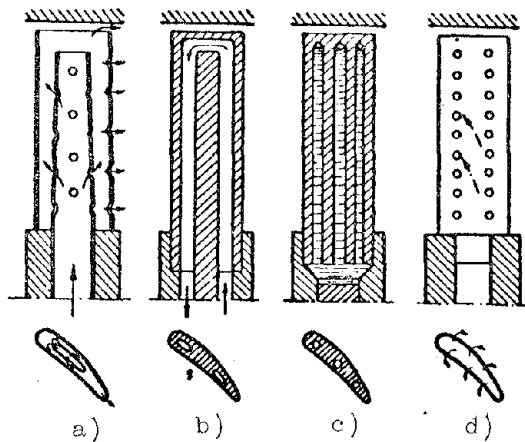


Fig. 4.27. Diagrams of blade cooling.

increases reliability of work of turbines and allows to increase temperature of working gases or to use less scarce materials for their manufacture.

The most heat is received by the nozzle and moving blades of turbines, located directly in the flow of hot gases. Since the coefficient of thermal conduction of fire-proof and heat-resistant materials is comparatively low, cooling of moving blades with heat removal in disks, and nozzle blades in their carrier housings is not very effective.

Figure 4.27 shows possible diagrams of blade cooling: a) blade with air cooling, b) blade with closed circulatory system of cooling, c) blade with thermosyphon circulation, and d) blade with film cooling.

Blades with air cooling are the simplest and therefore are used in certain engine designs. They are made from light-gage sheet. Inside blades there is a deflector insert. Air coolant is brought in through leg of blade into cavity of deflector, and then through holes in it passes into the clearance between deflector and blade. Cooling the blade, air emerges into the flow area of turbine through holes in end of blade and through slots at its outlet edge. Deflector ensures feed of air coolant to the most heated parts of blade and decreases flow areas. Owing to the latter, the speed of air coolant increases and heat-transfer

coefficient considerably increases.

We also know of experimental designs of blades made by method of powder metallurgy, with large quantity of channels of small diameter passing along the blade. Air is brought into them in the area of the leg and, cooling the blade, emerges through its face.

Blades with closed circulatory system can be cooled by air or liquid. The system of cooling includes a compressor or pump, and radiator. The first ensure circulation of air or liquid in the system, and the radiator cools them. This system of cooling was not used in aircraft GTD because of its complexity.

Blades with thermosyphon cooling can be used only as moving blades. These blades have closed channels filled by liquid. During rotation of rotor due to centrifugal forces the colder and heavy particles of liquid will move to peripheral part of blade, and the hotter and lighter ones will move to the root part. The hotter liquid will then emit heat to the less heated turbine disk. There can also be transmission of heat to air coolant through special ribbings at the blade leg.

The liquid coolant can be a light liquid metal, for instance, sodium, which has specific gravity  $\gamma = 0.97 \text{ g/cm}^3$ , melting temperature  $97^\circ\text{C}$ , and boiling point  $880^\circ\text{C}$ . With such cooling, blades can operate at temperature of gases on turbine inlet up to  $1100\text{-}1200^\circ\text{C}$ .

Blades with film cooling have special holes or a porous wall (in manufacture by method of powder metallurgy). Air coolant from internal cavity of blade through holes or pores in wall joins its surface. On surface of blade there will be formed an air boundary layer in the form of a film. Instead of air it is possible to use the liquid boiling on the surface of the blade. The main difficulty of film cooling consists in guarantee of stability of film from erosion by its stream of gas.

Internal cooling of blades is quite effective, but it is connected with considerable complications of their design and manufacture. It is especially complicated to carry out internal cooling of moving blades attached to a revolving wheel.

Internal air cooling is frequently used in nozzle and less often in moving blades of first stages of turbines. At moderate operating temperatures, moving blades are made without internal cooling with the application of external blowing

by air coolant of disks of moving wheels and with blowing through clearances in locks of blade shanks. Figure 4.28 shows a diagram of blowing of moving wheels of a two-stage turbine. Motion of air coolant is shown by arrows. Air for cooling is rejected from main airduct of engine - behind one of the stages of the axial-flow compressor or from combustion chambers (in the last case, secondary air). Place of sampling of air is determined by necessary pressure for its passage through cooling system and its lower temperature is possible. Furthermore, design considerations are also taken into account.

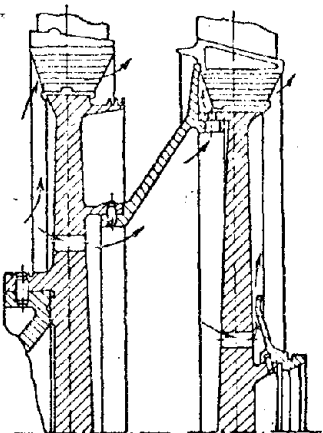


Fig. 4.28. Diagram of blowing of turbine rotor wheels.

In GTD with centrifugal compressor for cooling there is frequently used a special fan.

Consumption of air coolant usually composes 2-4% of total flow of air through engine. Large air flow through cooling system leads to noticeable lowering of thrust (power) and economy of engine.

For external cooling of bodies atmospheric air is usually used. With the impact pressure obtained in flight the air is expelled through an annular cavity formed around the housing as a

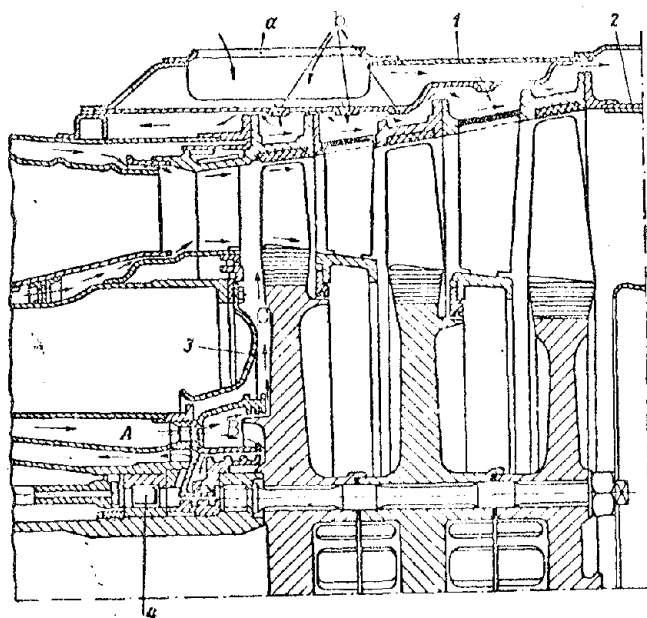


Fig. 4.29. Diagram of turbine cooling of the AI-20 engine.

light outer skin. Figure 4.29 shows a diagram of cooling of the turbine of the AI-20 engine. Nozzle apparatus and disk of wheel of 1st stage are cooled by air which is rejected from combustion chamber (secondary air). For cooling of nozzle apparatus, air is brought in through radial clearances between walls of flame chamber and housing of nozzle apparatus. Heading along walls of the latter (as shown by arrows), air coolant forms a protective film around them and simultaneously cools ends of nozzle

blades. Then, this air, partially cooling the root and peripheral parts of moving

blades of 1st stage, is mixed with working gasses.

For cooling of rotor disk of 1st stage, secondary air from combustion chamber through annular channel A is brought into annular cavity B and through clearances in labyrinth seal enters cavity C. Directed by deflector 3 along disk, air cools it and the locks of the moving blades, after which it passes into gas duct and is mixed with working gasses. Disks of rotors of 2nd and 3rd stages, which are less heated, are not cooled. Passing through annular channel A, located around roller bearing casing 4 of rotor, secondary air protects it from unnecessary heating in the area of the combustion chamber.

Turbine housing from external side is cooled by atmospheric air. For this purpose the engine has a welded annular air collector 1. In its internal wall is a large number of holes 6 located uniformly on its circumference. Atmospheric air under impact pressure enters air collector through throat a, and through holes 6 cools the turbine housing; it then cools exhaust pipe 2 and is ejected into the atmosphere. Motion of air coolant is shown by arrows.

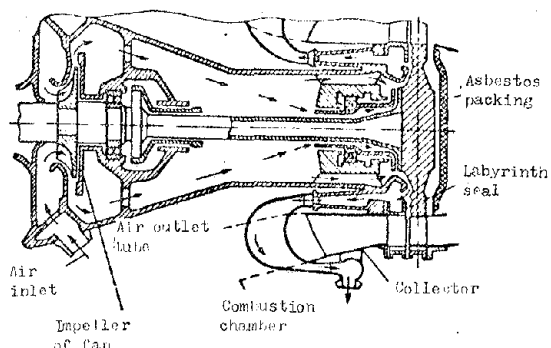


Fig. 4.30. Diagram of cooling of a TRD with centrifugal compressor.

Figure 4.30 shows the diagram of cooling a TRD with centrifugal compressor in which on the rotor shaft inside the housing there is a centrifugal fan. Cavity of housing serves for passage of air coolant; therefore rotor bearings inside housing are insulated and have seals. Rear bearing is fixed on intermediate bushing which is attached to shaft of turbine and forms with it a radial clearance for passage of air coolant. With help of labyrinth face seal on rim of turbine disk, the system of air cooling is isolated from the flow area.

Atmospheric air is expelled by fan, cooling the bearing nodes on the way, the disk of the rotor wheel, and gas collector housing. Part of air passes through radial clearance between shaft and bushing of rear bearing, cooling the latter. Air through tubes collects in ring header, from where it is ejected into the atmosphere. Motion of air in the diagram is shown by arrows.

#### 4.6. Construction of Blade Profile

The profile of turbine blades are constructed. Initial data for this include: velocity triangles, pitch  $t$  of blades in cascade, width of blade  $s$ , and radii of rounding of edges  $r_1$  and  $r_2$ . Velocity triangles and pitch of blades in cascade are taken from gas-dynamic calculation. Width of blade  $s$  and radii of rounding of inlet  $r_1$  and outlet  $r_2$  edges of blades are selected within the following limits:

$$s = 30 \div 60 \text{ mm}; r_1 = 1 \div 3 \text{ mm} \text{ and } r_2 = 0.4 \div 1 \text{ mm.}$$

Order of construction of blade profile is the following (Fig. 4.31). At distance  $s$  draw parallel lines A-A and B-B, and parallel to vector of mean velocity

$\bar{w}_{cp}$  (at angle  $\gamma_{yct} = 90 - \beta_{cp}$ ) draw line 1-1 which intersects lines A-A and B-B.

Radii  $r_1$  and  $r_2$  are described by the circumferences of inlet and outlet edges correspondingly touching lines A-A and B-B, and their centers  $O_1$  and  $O_2$  lie on line 1-1.

From center  $O_2$  draw half-line  $O_2-2$  parallel to velocity vector  $\bar{w}_2$ , and to circumference  $r_2$  at an angle of  $2-3^{\circ}$  to half-line  $O_2-2$  draw two tangents 3-3 and 4-4. These tangents form a vertex angle at the outlet edge of the blade  $\delta = 4$  to 6. Point of tangency of tangent 4-4 with circumference  $r_2$  will be designated H.

Fig. 4.31. Construction of profile of moving blade.

After that, from center  $O_2$  at an angle of  $90^{\circ}$  to tangent 3-3 draw half-line  $O_2-5$  and with radius  $R_K$  circumscribe the blade profile. The arc of circumference  $R_K$  is connected to circumferences of edges  $r_1$  and  $r_2$ , and its center is arranged on half-line  $O_2-5$ .

By approximate formula we determine dimension of cascade throat:

$$a_2 = (1.02 \div 1.06) t \sin \beta_2$$

At distance of cascade pitch  $t$  we find center  $O_2$  of circumference  $r_2$  of outlet edge of adjacent blade, from which we describe an arc of circumference with radius of  $R = a_2 + r_2$ .

From center  $O_1$  of inlet edge of blade we draw half-line  $O_1-6$  parallel to velocity vector  $\bar{w}_1$ , and through point of connection of circumference  $r_1$  with arc of circumference  $R_K$  we draw tangent 7-7 common to them.

Then from point D of intersection of tangent 7-7 with half-line  $O_1-6$  to circumference of inlet edge  $r_1$  we draw a second tangent 8-8 until intersection with line 4-4 at point E. Point F is the point of tangency of tangent 8-8 with circumference  $r_1$ .

Tangents 7-7 and 8-8 form vertex angle at inlet edge of blade. If this angle is too large (greater than  $30^\circ$ ), for its decrease the blade trough is circumscribed by arcs of two circumferences  $R_{K1}$  and  $R_{K2}$ , as was shown separately in Fig. 4.31.

Back of blade can be outlined by arcs of circumferences, parabola, or limniscate. The curves must be joined with tangent 4-4 and 8-8 in points F and H of their tangency with circumferences  $r_1$  and  $r_2$  and, furthermore, they must be tangent to circumference R. Point of tangency of back with circumference R is recommended to be selected so that the tangent forms angle  $\delta$  not more than  $15^\circ$ .

Figure 4.31 gives construction of blade back with respect to a parabola. For this, segments of lines H-E and F-E are divided into an equal number of parts and points of division are subsequently connected with each other by lines. The parabola is the envelope of these lines.

In order to ensure contact of parabola with circumference R it is usually necessary to repeatedly construct the profile, changing each time angle  $\gamma_{yct}$  of line 1-1. In this case, line 1-1 will not be parallel to vector  $\bar{w}_{cp}$ .

After construction of blade profile we check the form of interblade channel.

Interblade channel from inlet to outlet should have a smoothly narrowed form (contracting) which is attained by selection of curves outlining back of blade. Small contraction is allowed sometimes only in front part of channel (in the inlet area).

Blade thickness is determined from conditions of its durability; it should decrease from root section of blade to peripheral section. The greatest thickness

of blade profile on middle radius usually composes  $(0.1 \text{ to } 0.16)b$  (length of its chord). Profiling of nozzle blades can be carried out by the same method.

#### 4.7. Strength Calculation

Creep and tensile strength. In ordinary temperature conditions the strength of materials under constant loads is estimated by tensile strength or yield point. At high temperatures under action of constant loads in ordinary structural materials there appears the phenomenon of creep, which occurs in the form of slowly and continuously developing plastic deformation. In these conditions the strength of materials is determined by the tensile strength.

Figure 4.32 shows curves of creep of alloy [EI437A] (3И437А) at constant temperature  $t = 700^{\circ}\text{C}$  and at different constant loads. They are characterized by tensile stresses in samples from 16 to  $32 \text{ kg/mm}^2$ . These curves are the dependence of aspect ratio  $\Delta l$  of samples on duration of test. From them it follows that at a temperature of  $700^{\circ}\text{C}$  in alloy EI437A the phenomenon of creep is observed at stress  $\sigma > 16 \text{ kg/mm}^2$  and in even greater degree the higher the stress. Process of creep is terminated by destruction of sample. The higher the temperature the more quickly proceeds the process of creep.

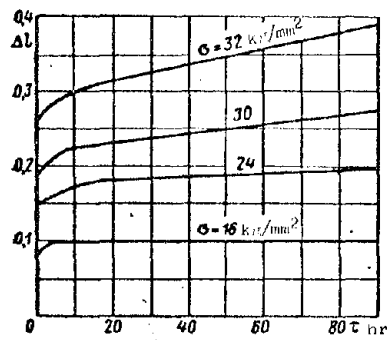


Fig. 4.32. Curves of creep of alloy EI437A (KhN77ТYu).

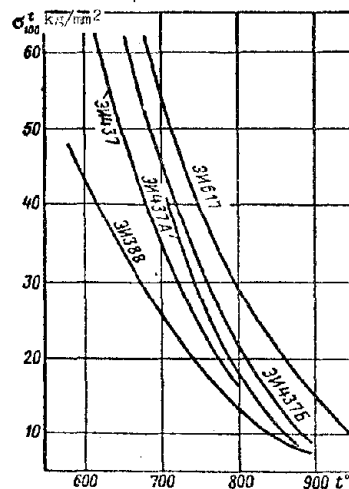


Fig. 4.33. Approximate change of tensile strength of certain materials depending upon temperature.

Gas turbines operate in conditions of high temperatures and therefore in such stressed components as moving blades and disks there appears the phenomenon

of creep.

Ultimate tensile stress is the stress which at operating temperature  $t^{\circ}\text{C}$  upon the expiration of  $\tau$  hours of work leads to destruction of test sample or component.

It is designated by the letter  $\sigma$  with indices: upper is the working temperature and lower are the hours of work. For instance,  $\sigma_{300}^{700}$  designates ultimate tensile strength at a temperature of  $700^{\circ}\text{C}$  in 300 hours of work. Figure 4.33 shows the change of ultimate tensile strength  $\sigma_{100}^t$  for certain blade materials.

Reserve of ultimate strength is determined by the formula:

$$n = \frac{\sigma_t}{\sigma}. \quad (4.1)$$

where  $\sigma$  is working stress of a component.

#### Calculation of Moving Blades

In distinction from blades of axial-flow compressors, moving blades of turbines work in conditions of high temperatures. Owing to heat removal in disk, blade temperature decreases towards the root part. Ultimate tensile strength  $\sigma_t^t$  of blades increases towards the root section in a stronger decree than stress  $\sigma$  and minimum safety factor by formula (4.1) is obtained in blades usually not in the root, but in the intermediate section, i.e., at distance  $(\frac{1}{4} \text{ to } \frac{1}{2})L$  from root section. Therefore, for determination of minimum reserve of strength, calculation of blade strength of a turbine must be conducted in a number of sections.

#### Calculation of blade tension

For lowering of stresses the thickness of moving blades is decreased from root section to periphery. Area of section of blade frequently varies according to root law with index  $m < 1$ :

$$F = F_K - (F_K - F_0) \left( \frac{r - R_k}{L} \right)^m. \quad (4.2)$$

where  $F_K$ ;  $F_0$  and  $F$  are the areas of root, peripheral and current sections;

$R_k$  and  $r$  are the radii of location of root and current sections,

$L$  is the length of blade.

During strength calculation blades are divide with respect to length into a number of calculating sections in which they then determine the stresses. With increase of number of sections the accuracy of calculation is increased. It is

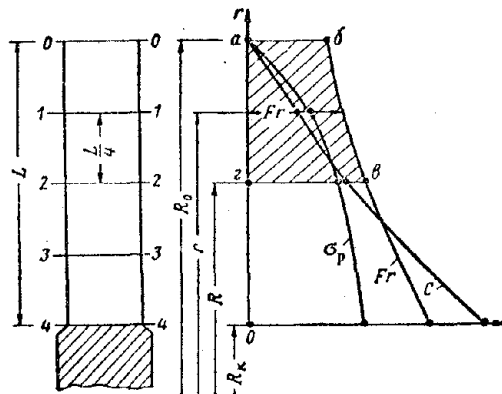


Fig. 4.34. Calculation of turbine blade strength.

practically possible to be limited to 4-6 sections. Sections are numbered from peripheral end of blade to its base, considering the peripheral section to be zero (Fig. 4.34).

For an arbitrary element of blade  $i$ , located between two adjacent calculating sections  $i-1$  and  $i$  the centrifugal force by formula (2.2) will be equal to:

$$\Delta C_i = \frac{\gamma \omega^2}{g} \int_{R_{i-1}}^{R_i} F_r dr. \quad (4.3)$$

Considering

$$F_r = \frac{F_{i-1} + F_i}{2} = \text{const},$$

we obtain

$$\Delta C_i = \frac{\gamma \omega^2}{4g} (F_{i-1} + F_i)(R_{i-1}^2 - R_i^2), \quad (4.4)$$

where  $F_{i-1}$  and  $F_i$  are areas of sections;

$R_{i-1}$  and  $R_i$  are radii of location of sections.

Usually the calculating sections of a blade are divided into  $k$  equal parts.

In this case

$$R_{i-1} - R_i = \frac{L}{k},$$

where  $L$  is length of blade.

In this case formula (4.4) can be represented in the following form:

$$\Delta C_i = \frac{\gamma \omega^2}{4g} \frac{L}{k} (F_{i-1} + F_i)(R_{i-1} + R_i). \quad (4.5)$$

Centrifugal force of part of the blade located above the current calculating section  $n-n$ , will be equal to:

$$C_n = \sum_{i=1}^{n-1} \Delta C_i \quad (4.6)$$

and tensile stress in current calculating section will be equal to:

$$\sigma = \frac{C_n}{F_n}, \quad (4.7)$$

where  $F_n$  is the area of current calculating section.

Centrifugal forces loading separate sections of blade can be determined also by graphic method. For a number of sections of the blade they preliminarily calculate the product  $F_r$ , where  $F$  is the area of the section, and  $r$  is the radius of its location. After that, they construct a curve of  $F_r$  (see Fig. 4.34).

Product  $F_r$  is the integrand in formula (2.2), and area under the curve of  $F_r$  is the integral. Selecting a number of values of  $R$  for the lower bound of the integral, we find the area abcd corresponding to them under the curve. Multiplying then the value of these areas by  $\gamma\omega^2/g$ , we obtain the values of centrifugal forces  $C$ , according to which it is possible to construct their curve. Stress  $\sigma$  is found by formula (4.7).

#### Bend calculation of blades

Intensity of circumferential and axial loads of moving blades of turbines from gas forces is determined by formulas (2.9) and (2.10). In formula (2.9)  $N$  designates the power developed by the rotor wheel of the turbine.

Circumferential load from gas forces of turbine acts in direction of rotation of wheel, and axial acts toward the flow of gases in the outlet area [in formula (2.10) for the given case  $p_1 > p_2$ ]. Bending moments from gas forces for current calculating section are found by formulas (2.11).

For unloading from bending by gas forces, sections of blades are displaced (deviated) both in the plane of rotation  $x\omega r$  and also in axial plane  $y\omega r$ . Deviations in plane of rotation are in the direction of the back of the blade, and in axial plane they are toward the motion of gases (Fig. 4.35).

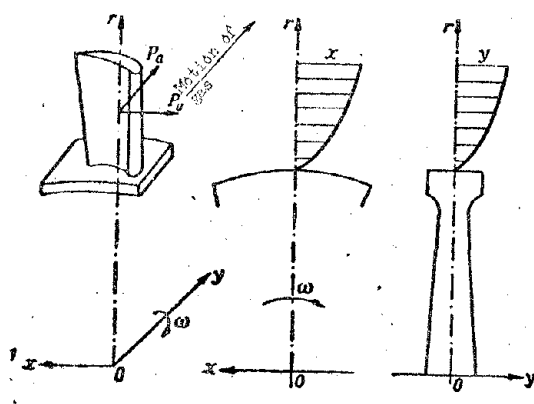


Fig. 4.35. Deviations of sections of turbine blade.

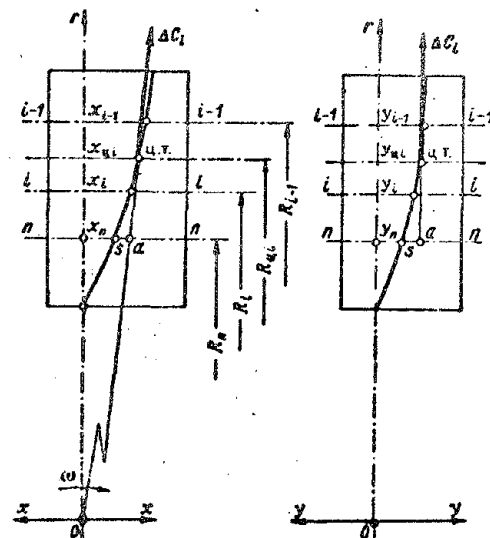


Fig. 4.36. Bend calculation of blades.

In Fig. 4.36 a blade is depicted in blades xor and yor. In an arbitrary element of blade  $i$ , limited by sections  $i-1$  and  $i$ , during rotation there appears centrifugal force  $\Delta C_i$ . In plane xor its component acts along the radius, and in plane yor it is parallel to axis or. Force  $\Delta C_i$  is applied in the center of gravity of element  $i$ , the coordinates of which are assumed to be equal to

$$x_{ui} = \frac{x_{i-1} + x_i}{2}; \quad y_{ui} = \frac{y_{i-1} + y_i}{2}; \quad R_{ui} = \frac{R_{i-1} + R_i}{2},$$

where  $x_{i-1}$ ;  $y_{i-1}$ ;  $R_{i-1}$ ;  $x_i$ ;  $y_i$  and  $R_i$  are coordinates of center of gravity in sections  $i-1$  and  $i$ ;

We transfer force  $\Delta C_i$  to the current calculating section n-n (point a). Coordinates of point a are equal to (see Fig. 4.36):

$$x_a = R_n \frac{x_{ui}}{R_{ui}} = R_n \frac{x_{i-1} + x_i}{R_{i-1} + R_i} \quad \text{and} \quad y_a = y_{ui} = \frac{y_{i-1} + y_i}{2},$$

where  $R_n$  is the radius of location of current calculating section n-n.

Bending moments from force  $\Delta C_i$  are assumed to be:  
in plane of rotation xor

$$\Delta m_y = \Delta C_i (x_a - x_n) = \Delta C_i \left( R_n \frac{x_{i-1} + x_i}{R_{i-1} + R_i} - x_n \right)$$

and in axial plane yor

$$\Delta m_x = \Delta C_i (y_a - y_n) = \Delta C_i \left( \frac{y_{i-1} + y_i}{2} - y_n \right),$$

where  $x_n$  and  $y_n$  are coordinates of center of gravity of current calculating section n-n.

Bending moment acting on current calculating section n-n from all elements lying above this section will be equal to:

in plane of rotation

$$m_y = R_n \sum_{i=1}^{n-1} \Delta C_i \frac{x_{i-1} + x_i}{R_{i-1} + R_i} - C_n x_n \quad (4.8)$$

and in axial plane

$$m_x = \sum_{i=1}^{n-1} \Delta C_i \frac{y_{i-1} + y_i}{2} - C_n y_n. \quad (4.9)$$

Bending moments from centrifugal forces  $m_y$  and  $m_x$  are directed to the side opposite the action of corresponding moments from gas forces  $M_y$  and  $M_x$ .

By deviator of blade sections we usually attain its unloading from bending by 10-60%. Deviation of sections of blades can be carried out by various laws.

The simplest one is the law in which the axis of blade is rectilinear and is inclined to axis or of the basic system of coordinates.

Deviations of sections according to linear law in plane of rotation can be carried out by parallel displacement of axis of blade on rotor wheel against its rotation by magnitude  $\epsilon$  (Fig. 4.37). Bending moment for current calculating section n-n in this case will be equal to:

$$m_{yn} = C_n \epsilon \left(1 - \frac{R}{R_{nn}}\right), \quad (4.10)$$

where  $\epsilon$  is displacement of blade,

$R_{nn}$  is the radius of location of center of gravity of the part of the blade lying above section n-n.

$$R_{nn} = \frac{\sum_{i=1}^{l-n} \Delta C_i R_{ni}}{C_n}.$$

Total bending moments  $M_{\Sigma_y}$  and  $M_{\Sigma_x}$  (Fig. 4.38) are found by formulas (2.13), and moment  $M_\eta$  by formula (2.16).

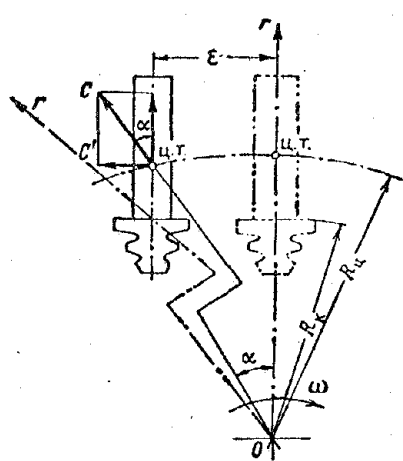


Fig. 4.37. Displacement of blade on rotor wheel.

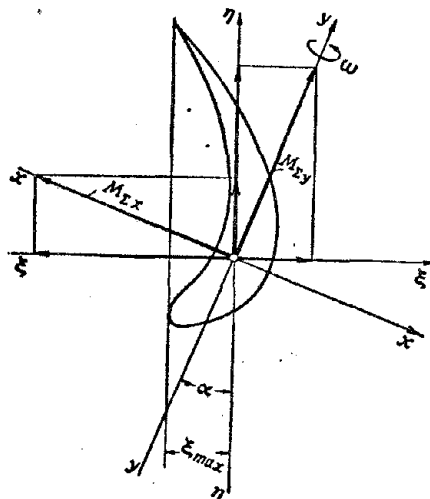


Fig. 4.38. Determination of bending moments of blade.

Bending stress in characteristic points is determined by formula (2.17), and total stresses from tension and bending are found by formula (2.18).

#### Safety factor

For moving blades the formula of safety factor (4.1) takes on the following form:

$$n = \frac{\sigma_t}{\sigma_{\Sigma_{\max}}}, \quad (4.11)$$

where  $\sigma_{\Sigma_{\max}}$  is total maximum stress in calculating sections of a blade from tension and bending [formula (2.18)];

$\sigma_t$  is the optimum tensile strength of the blade material.

Depending upon operation life the safety factor of a blade can be determined by its optimum tensile strength  $\sigma_{100}^t$ ,  $\sigma_{200}^t$ ,  $\sigma_{300}^t$ , and others. However, more frequently the calculation is made with  $\sigma_{100}^t$ . Actual operation life of a blade will be more than 100 hours, since in maximum rated conditions an engine usually operates for a limited time.

For finding  $\sigma_{100}^t$  it is possible to use Fig. 4.33, but it is then necessary to know the temperature of heating in the calculating sections of the blade. Due to nonuniform temperature of gas flow and heat transfer in turbine disk the temperature along blade will be variable. In the absence of experimental data it is possible approximately to take the following law of change of blade temperature:

$$t_s = t_w^* - 100 \left( \frac{R_0 - r}{L} \right)^4, \quad (4.12)$$

where  $t_w^*$  is the mean, braked in relative motion, temperature of gas in front of the blade;

$R_0$  and  $r$  are the external and current radii of the blade ring;

$L$  is the length of the blade.

Temperature  $t_w^*$  can be determined by the expression

$$t_w^* = t_r + \left( \frac{w_1}{50} \right)^2,$$

where  $t_r$  is average temperature of gas in front of the blade;

$w_1$  is relative velocity of gas at inlet of blades of rotor wheel.

Results of calculations of blade are usually depicted graphically in the form of curves: distribution of temperature  $t_s$  along blade, maximum stresses  $\sigma_{\Sigma_{\max}}$ , change of ultimate tensile strength  $\sigma_t^t$ , and safety factor  $n$  (Fig. 4.39).

Usually  $n_{\min}$  is at distance  $\left(\frac{1}{4} \text{ to } \frac{1}{2}\right)L$  from root section of blade and in existing GPD designs composes 1.3 to 2.5.

From Fig. 4.39 it follows that from the point of view of strength it is desirable to have smaller temperature at root part of blade. This is possible to carry out by assigning the distributive law of temperature of gas flow, and also by more intense cooling of root part of blade.

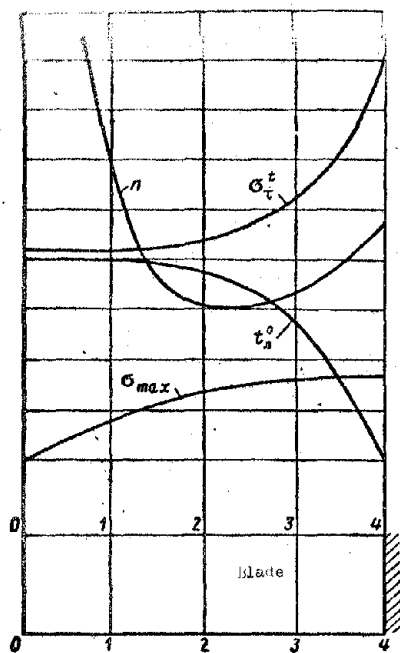


Fig. 4.39. Change of safety factor of blade on its section.

Example. Determine stresses and safety factor of the blade of a gas turbine.

Given:  $n = 12300 \text{ rpm}$ ;  $z = 54$ ;  $31.15 \text{ cm}$ ;  
 $R_K = 19.75 \text{ cm}$ ;  $R_{cp} = 25.45 \text{ cm}$ ;  $L = 11.4 \text{ cm}$ ;  
 $N = 11250 \text{ hp.}$ ;  $G_p = 41.17 \text{ kg/sec}$ ;  $\gamma = 8.1 \cdot 10^{-3} \text{ g/cm}^3$ ;  
 $p_1 - p_2 = 0.816 \text{ kg/cm}^2$ ;  $c_{1a} - c_{2a} = -79 \text{ m/sec}$ .

Remaining data and all calculations are presented in the tables.

We shall select five sections of the blade (see Fig. 4.34) and determine tensile stress [formulas (4.5), (4.6), and (4.7)]:

Intensity of circumferential load from gas forces by formula (2.9)

$$q_u = \frac{71620 \cdot 11250}{12300 \cdot 25.45 \cdot 11.4 \cdot 54} = 4.2 \text{ kg/cm.}$$

Intensity of axial load from gas forces by formula (2.10)

$$q_a = \frac{2 \cdot 3.14 \cdot 25.45 \cdot 0.816}{54} + \frac{41.17(-79)}{9.81 \cdot 54 \cdot 11.4} = 2 \text{ kg/cm.}$$

Table 4.2.

Section No.	$R \text{ cm}$	$F \text{ cm}^2$	$\Delta C_I \text{ kg}$	$C_n \text{ kg}$	$\sigma_p \text{ kg/cm}^2$
0	31.15	1.03	—	—	—
1	28.3	1.32	1550	1550	1175
2	25.45	1.8	1620	3170	1760
3	22.6	2.52	2040	5210	2070
4	19.75	3.54	2480	7690	2170

Determination of circumferential bending moments:  $M_y$  — from gas forces by formula (2.11),  $m_y$  — from centrifugal forces by formula (4.8), and  $M_{\Sigma y}$  — total bending moment by formula (2.13). All data are presented in Table 4.3.

Determination of axial bending moments:  $M_x$  — from gas forces by formula (2.11),  $m_x$  — from centrifugal forces by formula (4.9), and  $M_{\Sigma x}$  — total bending moment by formula (2.13). All data are presented in Table 4.4.

Table 4.3

Section No.	$R$ cm	$M_y$ kg·cm	$x$ cm	$R_{l-1} + R_l$	$x_{l-1} + x_l$	$\Delta C_l \frac{x_{l-1} + x_l}{R_{l-1} + R_l}$	$\sum_{l=1}^n \Delta C_l \frac{x_{l-1} + x_l}{R_{l-1} + R_l}$	$C_n X_s$	$m_y$ kg·cm	$M_{z,y}$ kg·cm
0 31,15	—	0,054	—	—	—	—	—	—	—	—
1 28,3	17	0,070	59,45	0,124	3,225	3,225	91,3	108,5	-17	34
2 25,45	68,3	0,033	53,75	0,103	3,11	6,335	161,5	104,5	57	11,3
3 22,6	153	0,0075	48,05	0,0465	1,72	8,055	182	39	143	10
4 19,75	273	0,0	42,35	0,0075	0,438	8,493	168	0	168	105

We define:  $M_{\eta}$  — the resultant bending moment by formula (2.16);  $\sigma_u$  — bending stresses on a blade by formula (2.17);  $\sigma_{\Sigma}$  — total stress due to tension and bending by formula (2.18);  $t_{\eta}$  — temperature in sections of blade by formula (4.12);  $\sigma_{100}^t$  — optimum tensile strength according to Fig. 4.33, and  $n$  — safety factor by formula (4.11). All calculations are presented in Table 4.5.

Table 4.4

Section No.	$R$ cm	$M_x$ kg·cm	$y$ cm	$\frac{y_{l-1} + y_l}{2}$	$\Delta C_l \frac{y_{l-1} + y_l}{2}$	$\sum_{l=1}^n \Delta C_l \frac{y_{l-1} + y_l}{2}$	$C_n y_n$	$m_x$ kg·cm	$M_{z,x}$ kg·cm
0 31,15	—	0,19	—	—	—	—	—	—	—
1 28,3	8,1	0,047	0,1185	183,5	183,5	73	110,5	-102,4	
2 25,45	32,5	0,042	0,0445	72	255,5	133	122,5	-90	
3 22,6	73	0,014	0,028	57	312,5	73	240	-168	
4 19,75	130	0,0	0,007	17,35	330	0	330	-200	

Calculations are made for point  $A_1$  of the blade profile in Fig. 2.39.

From the table it follows that the obtained safety factor  $n > 1.5$  and therefore it is sufficient.

Table 4.5

Section No.	$a^o$	$M_{x,y} \sin a$ kg·cm	$M_{x,y} \cos a$ kg·cm	$M_y$ kg·cm	$J_A$ cm <sup>4</sup>	$\epsilon_A$ cm	$\sigma_u A$ kg/cm <sup>2</sup>	$\sigma_B$ kg/cm <sup>2</sup>	$t_A$ °C	$\sigma_{100}^t$ kg/cm <sup>2</sup>	$n$
1 17°12'	-30,2	32,4	2,2	0,105	0,57	11,9	1187	735	2600	2,19	
2 12°24'	-19,3	11	-8,3	0,16	0,62	-32	1728	729	2800	1,62	
3 9°24'	-27,4	9,8	-17,6	0,28	0,79	-49,7	2020	703	3380	1,67	
4 5°8'	-18	104,5	86,5	0,53	0,83	135,5	2305	635	5280	2,29	

### Calculation of "Herringbone" Lock

Centrifugal force of blade is perceived by support surfaces of lock teeth which are arranged at an angle of  $90^\circ - \alpha^\circ$  to the axis of the blade, where angle  $\alpha$  is usually  $15^\circ$  (Fig. 4.40). Spreading the centrifugal force of the blade  $C_s$  to the direction of normals to support surfaces, we obtain

$$N = \frac{C_s}{2 \cos \alpha}.$$

Full centrifugal force of blade

$$C_s = C_u + C_b,$$

where  $C_u$  and  $C_b$  are centrifugal forces of profile and lock part of blade.

We take equal distribution of load along all teeth.

Crumpling stress will be equal to (see Fig. 4.40):

$$\sigma_{cu} = \frac{N}{a \sum l} = \frac{C_s}{2 \cos \alpha \cdot a \sum l}, \quad (4.13)$$

where  $a$  is the width of support surface of teeth;

$\sum l$  is total length of all teeth of one side of the blade

$$\sum l = l_1 + l_2 + l_3 + \dots$$

Number of pairs of teeth in blades are usually  $n = 3$  to  $6$ . At constant thickness of rim  $\Sigma l = nl$ . In existing turbine designs  $\sigma_{CM} \approx 2200 \text{ kg/cm}^2$ .

Leg of blade and lock flanges of disk experience tension from centrifugal force. Figure 4.40 shows distribution of stresses along lock of blade and flanges of disk. The most stressed in the blade is its first section, and in flanges of disk the last section.

Section I-I of blade is loaded by centrifugal force

$$C_i = C_s - C'_b,$$

Fig. 4.40. Strength calculation of herringbone lock.

where  $C'_b$  is centrifugal force of lock part of blade, lying below first section.

Tensile stress will be equal to:

$$\sigma_p' = \frac{C_1}{F_1}, \quad (4.14)$$

where  $F_1$  is the area of a calculated section of blade shank. In existing turbine designs  $\sigma_p \leq 2000 \text{ kg/cm}^2$ .

The calculated section of the lock flange of the disk is loaded by centrifugal force of the blade and the flange itself

$$Q = C_{\pi} + C_{\Delta}, \quad (4.15)$$

where  $C_{\Delta}$  is centrifugal force of disk flange.

Tensile stress will be equal to

$$\sigma_p = \frac{Q}{F_2}, \quad (4.16)$$

where  $F_2$  is the area of calculating section of disk flange. In existing turbine designs  $\sigma_p \leq 2200 \text{ kg/cm}^2$ .

Example. Determine the stresses in a "herringbone" lock of a gas turbine blade.

Given:  $C_{\pi} = 1300 \text{ kg}$ ;  $C_1 = 10670 \text{ kg}$ ;  $C_{\Delta} = 2550 \text{ kg}$ ;  $n = 6$ ;  $\alpha = 15^\circ$ ;  $F_1 = F_2 = 7.25 \text{ cm}^2$ ;  $l = 49 \text{ mm}$ ;  $a = 1.4 \text{ mm}$ .

Tensile stresses in dangerous section of blade by formula (4.14):

$$\sigma_p = \frac{10670}{7.25} = 1475 \text{ kg/cm}^2.$$

Force loading the calculating section of lock flange of disk by formula (4.15)

$$Q = 13000 + 2550 = 15550 \text{ kg}.$$

Tensile stress in dangerous section of disk flange by formula (4.16):

$$\sigma_p = \frac{15550}{7.25} = 2150 \text{ kg/cm}^2.$$

Crumpling stresses of teeth by formula (4.13):

$$\sigma_{cw} = \frac{13000}{2 \cdot 0.966 \cdot 0.14 \cdot 6 \cdot 4.9} = 1635 \text{ kg/cm}^2.$$

#### Calculation of Gas Turbine Disks

Disks of turbines in distinction from disks of compressors operate at heightened temperatures with nonuniform heating. Heat-resisting materials from which they are made possess low thermal conduction. Peripheral part of disks obtains influx of heat from moving blades and directly from working gases, the

disks have more or less intense cooling by air, and in central part the heat is ejected into the turbine shaft and other components connected with it. Thus, temperature of turbine disks decreases from periphery to center. The less heated central part of disk prevents its more heated peripheral part to be freely expanded and in the latter there appear circumferential compression stresses (negative stresses).

Calculation of disk strength of a gas turbine is conducted on the assumption of its elastic state, taking into account thermal stresses.

Distribution of temperature along radius of disk is selected from experimental data or with great enough accuracy it is determined by calculation with equations of heat transfer. Temperature of disk on periphery reaches 450 to 700°C, and in its center 150 to 600°C. Distribution of temperature of disk along its radius is possible to take according to the law of square parabola:

$$t = t_0 + (t_a - t_0) \left( \frac{r}{R_a} \right)^2, \quad (4.17)$$

where  $t_a$  and  $t_0$  are temperatures on periphery and in center of disk;

$R_a$  and  $r$  are the external and current radii of disk.

Thermal stresses are considered in the following manner.

Absolute radial elongation of disk on current radius  $r$  taking into account the temperature of its expansion during operation is equal to:

$$u' = u + u_t, \quad (4.18)$$

where  $u$  is the absolute radial elongation of disk under action of dynamic loads by formula (2.30);

$u_t$  is its absolute radial elongation during thermal expansions.

During uniform heating of disk

$$u_t = \alpha r t, \quad (4.19)$$

where  $\alpha$  is the coefficient of linear expansion of disk material;

$r$  is the current radius,

$t$  is the temperature of the disk.

After substitution of expressions (2.30) and (4.19) in formulas (4.18) for current radius  $r$  we obtain:

$$u' = \frac{r}{E} (\sigma_T - \mu \sigma_R) + \alpha r t. \quad (4.20)$$

If during calculation of a nonuniformly heated disk its temperature within the limits of each annular section is assumed constant and equal to its value for average radius of section  $R_{k \text{ cp}} = \frac{R_k + R_{k-1}}{2}$ , absolute radial elongation of disk on radius  $R_{k-1}$ , taken on boundary of two adjacent annular sections  $k - 1$  and  $k$  (see Fig. 2.49), can be expressed, using formula (4.20), thus:

$$\begin{aligned} u'_{k-1} &= \frac{R_{k-1}}{E_k} (\sigma'_{T_k} - \mu \sigma'_{R_k}) + \alpha R_{k-1} t_k = \\ &= \frac{R_{k-1}}{E_{k-1}} (\sigma'_{T_{k-1}} - \mu \sigma'_{R_{k-1}}) + \alpha R_{k-1} t_{k-1}. \end{aligned}$$

Considering Poisson's ratio  $\mu = 0.3$  and  $\Delta t_k = t_k - t_{k-1}$ , we obtain the following expression for circumferential stress:

$$\sigma'_{T_k} = \frac{E_k}{E_{k-1}} \sigma'_{T_{k-1}} + 0.3 \left( \frac{b_{k-1}}{b_k} - \frac{E_k}{E_{k-1}} \right) \sigma'_{R_{k-1}} - \alpha E_k \Delta t_k. \quad (4.21)$$

Instead of the earlier obtained expressions (2.40) we obtain for the turbine disk

$$\left. \begin{aligned} \sigma'_{R_k} &= \frac{b_{k-1}}{b_k} \sigma'_{R_{k-1}}; \\ \sigma'_{T_k} &= \frac{E_k}{E_{k-1}} \sigma'_{T_{k-1}} + 0.3 \left( \frac{b_{k-1}}{b_k} - \frac{E_k}{E_{k-1}} \right) \sigma'_{R_{k-1}} - \alpha E_k \Delta t_k. \end{aligned} \right\} \quad (4.22)$$

Calculation of turbine disk is done by the same method as the compressor disk. The given form of the disk is replaced by a step calculating diagram with a series of annular sections of constant thickness. Average stresses of annular sections are determined by formulas (2.51), coefficients  $\psi_k$ ,  $\varphi_k$  and  $\lambda_k$ , by formulas (2.48), and free terms  $B_k$ ,  $D_k$  and  $F_k$ , by formulas (2.49).

Coefficient  $\xi_k$  and free term  $C_k$  are determined by the formulas

$$\xi_k = \frac{E_k}{E_{k-1}} \lambda_{k-1} + 0.3 \left( \frac{b_{k-1}}{b_k} - \frac{E_k}{E_{k-1}} \right) \varphi_{k-1}; \quad (4.23)$$

$$C_k = \frac{E_k}{E_{k-1}} F_{k-1} + 0.3 \left( \frac{b_{k-1}}{b_k} - \frac{E_k}{E_{k-1}} \right) D_{k-1} + \alpha E_k \Delta t_k. \quad (4.24)$$

The value of  $E$  — the elastic modulus of disk material — is determined on graphs of the type in Fig. 4.41 depending upon temperature of annular sections.

Coefficient of linear expansion  $\alpha$  of disk material is equal to: for steel [20KhZMVF] (20X3MBФ),  $\alpha = 14 \cdot 10^{-6}$ ; for steel [EI481] (ЭИ481) ([4Kh12N8G8MFB] (4Х12Н8Г8МФБ))  $\alpha = 21 \cdot 10^{-6}$ .

Calculations are presented in tables as shown below, and then the curve of stresses is constructed.

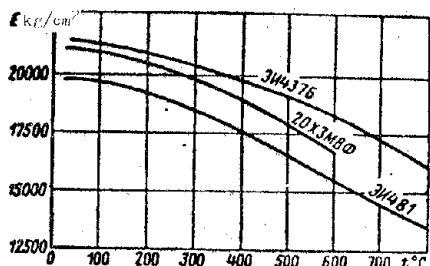


Fig. 4.41. Change of elastic modulus  $E$  of steel and alloys depending upon temperature.

In the existing designs of turbine disks the stresses reach: in solid disks 4500 to 6000  $\text{kg}/\text{cm}^2$  and in disks with central hole 7000 to 9000  $\text{kg}/\text{cm}^2$ .

Example. Determine stress in the disk of a gas turbine.

Given:  $\omega = 1290 \text{ 1/sec}$ ;  $\gamma = 8.1 \cdot 10^{-3} \text{ kg}/\text{cm}^3$ ;  $\alpha = 14 \cdot 10^{-6}$ ;  $t_a = 550^\circ\text{C}$ ;  $t_0 = 200^\circ\text{C}$ ;  $C = 7690 \text{ kg}$ ;  $z = 54$ ;  $f = 10.55 \text{ cm}^2$ ;  $R_f = 18.2 \text{ cm}$ ;  $R_a = 17.4 \text{ cm}$ ;  $b_a = 4.2 \text{ cm}$ .

Profile of disk is given in Fig. 4.42. Disk is divided into 6 annular sections.

Centrifugal force of profile part of blades by formula (2.42):

$$C_n = 7690 \cdot 54 = 415000 \text{ kg.}$$

Centrifugal force from lock part of rotor wheel by formula (2.43)

$$C_s = 2\pi \frac{8.1 \cdot 10^{-3}}{981} \cdot 10.55 \cdot 18.2^2 \cdot 1290^2 = 302000 \text{ kg.}$$

Radial stress on external calculating diameter of disk by formula (2.41)

$$\sigma_{R_a} = \frac{415000 + 302000}{2\pi \cdot 17.4 \cdot 4.2} = 1565 \text{ kg}/\text{cm}^2.$$

Coefficients  $\Lambda$ ,  $M$  and  $N$  are found on the graphs of Fig. 2.50 or by formulas (2.38).

The value of  $Q$  is determined by formula (2.39):

$$Q_k = \frac{8.1 \cdot 10^{-3} \cdot 1290^2}{8.981} R_k^2 = 1.72 R_k^2.$$

Distribution of temperature along annular sections of disk is determined by formula (4.17), considering then the temperature for each annular section of disk as constant.

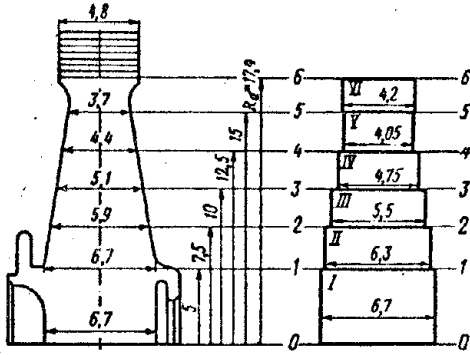


Fig. 4.42. Determination of stresses in the disk of a gas turbine.

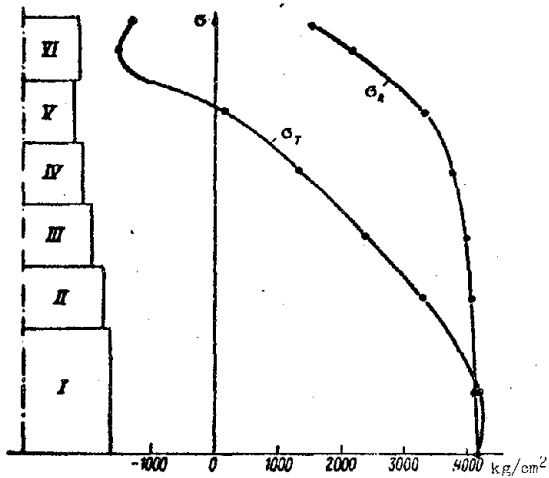


Fig. 4.43. Distribution of stresses in a turbine disk.

Disk is solid without hole and therefore  $\sigma_{R_0} = \sigma_{T_0}$ . Calculations are presented in Table 4.6. Adding to obtained  $\sigma_{R_k}$  and  $\sigma_{T_k}$  the stresses in zero  $\sigma_{R_0}$  and  $\sigma_{T_0}$  and in the last  $\sigma_{R_a}$  and  $\sigma_{T_a}$  sections of the disk, we construct curves of disk stresses (Fig. 4.43).

Table 4.6

Section No.	$R_k$ cm	$b_k$ cm	$m_k$	$A_k$	$M_k$	$N_k$	$Q_k$	$M_k Q_k$	$N_k Q_k$
I	5	6.7	0	0.5	3.3	1.9	43	141	82
II	7.5	6.3	0.667	0.722	2.01	0.885	96	194	85
III	10	5.5	0.75	0.781	1.62	0.66	172	279	114
IV	12.5	4.75	0.8	0.82	1.35	0.522	268	362	140
V	15	4.05	0.823	0.847	1.157	0.433	286	447	167
VI	17.4	4.2	0.863	0.872	0.977	0.353	520	508	184

Continuation

Section No.	$t_k$ C	$\Delta t_k$	$E_k$ kg/cm²	$\alpha E_k \Delta t_k$	$\frac{b_{k-1}}{b_k}$	$\frac{E_k}{E_{k-1}}$	$\psi_k$	$\xi_k$
I	229	—	$2.03 \cdot 10^6$	—	1	—	1	1
II	265	36	$2 \cdot 10^6$	1010	1.063	0.985	1.063	1.008
III	315	50	$1.95 \cdot 10^6$	1365	1.145	0.975	1.20	1.073
IV	380	65	$1.9 \cdot 10^6$	1730	1.157	0.975	1.357	1.132
V	460	80	$1.83 \cdot 10^6$	2060	1.173	0.965	1.555	1.203
VI	550	90	$1.74 \cdot 10^6$	2200	0.965	0.95	1.45	1.198

Table 4.6 continued

Section No.	$\varphi_k$	$\lambda_k$	$B_k$	$C_k$	$D_k$	$F_k$	$R_{k \text{ cp}}$ cm	$\sigma_{R_k}$ kg/cm <sup>2</sup>	$\sigma_{T_k}$ kg/cm <sup>2</sup>
I	1	1	0	0	141	82	2.5	4180	4209
II	1.048	1.023	150	1094	6'6	917	6.25	4102	3314
III	1.172	1.101	695	2288	1325	2051	8.75	4020	2450
IV	1.325	1.164	1535	3802	2304	3535	11.25	3780	1211
V	1.50	1.257	2700	5610	3592	5332	13.75	3334	-241
VI	1.418	1.23	3460	7248	4456	6944	16.2	2142	-1980

Stress in center of disk by formula (2.47):

$$\sigma_{T_0} = \frac{1565 + 4456}{1.418} = 4250 \text{ kg/cm}^2.$$

Circumferential stress in peripheral section of disk by formula (2.46):

$$\sigma_{T_a} = 1.23 \cdot 4250 - 6944 = 1717 \text{ kg/cm}^2.$$

Elastic-plastic state of disk. In certain cases, in the central part of the disk, stresses are permitted above the limit of proportionality of its material. In this region a plastic ring is formed and the disk will be in an elastic-plastic state.

In this ring there will appear plastic deformations and the initial stresses in it will drop because of this. Subsequent peripheral annular sections, being in elastic state, will obtain additional loading and their initial stresses will be somewhat increased. Thus, initial distribution of stresses in the disk can be considerably changed.

If for a disk in an elastic-plastic state we increase the rpm rate above the calculated  $n_p$ , the region of its plastic state along the radius will be increased and at a certain limiting rpm rate  $n_{up}$  will reach the peripheral part of the disk. Such a state of the disk can be considered as limiting. A criterion of strength of a disk operating under conditions of an elastic-plastic state can be the safety factor

$$k = \frac{n_{up}}{n_p}.$$

In existing designs of disks  $k = 1.5$  to  $2.0$ .

Elastic-plastic state can be allowed in disks with central hole, for which, in the zero section (around the hole) with a slightly extended hub, there appear high circumferential stresses  $\sigma_{T_0}$ . These high stresses usually have a local

character and are sharply lowered along the radius.

#### 4.8. Materials

A basic requirement of materials for turbines is high-temperature strength and thermal stability. High-temperature strength is the ability of material to sustain a load at high temperatures. It is determined by the optimum tensile strength. Thermal stability (heat resistance) is the ability of material to resist corrosion (oxidation) in an oxidizing medium of hot gases.

Blades of turbines operate in the heaviest conditions and for their manufacture we use metallic high-heat and heat-resistant alloys on a nickel or cobalt base. These alloys have additives of chrome, nickel, tungsten, molybdenum, titanium, aluminum, iron, and so forth. Moving blades are subjected to considerable loads and therefore they are made most frequently by the method of forging and stamping from deformed nickel alloys. Blades of nozzle apparatuses of first stages are usually made by the method of precision casting from more heat-resistant nickel or cobalt foundry alloys. Nozzle blades of last stages, just as moving blades, are made by the method of forging and stamping from deformed nickel alloys.

Depending upon conditions of operation, stamped blades are made from alloys of brands [EI437A] (ДИ437А), [EI437B] (ДИ437Б), EI617, EI598, and so forth. Blades are made by precision casting from alloys of the following brands: on a nickel base [ZhsZ] (ХСЗ) and on a cobalt base [LK4] (ЛК4).

Turbine disks operate in more favorable temperature conditions than blades. They are made from forged heat-proof steel EI481, 20KhZMVF, and others, or from heat-proof alloy EI457. Turbine housings are either cast or made from sheet material by welding. The material for them is heat-resistant steel 25-20, [Kh23N18] (Х23Н18), [1Kh18N9T] (1Х18Н9Т) and so forth.

## CHAPTER V

### VIBRATIONS OF BLADES AND DISKS

#### 5.1. General Information

Blades of compressors and turbines during operation of a [GTD] (ГТД)<sup>1</sup> frequently are subjected to vibrations which sometimes lead to their break-down. Vibrations are distinguished by mode and form.

Vibration modes for blades can be bending, twisting and combined – bending and twisting.

Vibration nodes. In a vibrating blade certain sections are in a state of rest. These sections are called the vibration nodes.

Vibration form is characterized by the number vibration nodes of a blade. There are one-node, two-node, three-node, etc. vibration forms which are also called vibration forms of first tone, second tone, third tone, etc. Figure 5.1 shows four forms of bending vibrations of a rod, and Fig. 5.2 shows a one-node form of torsional vibrations of a blade.

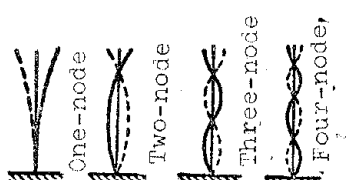


Fig. 5.1. Forms of bending vibrations of a rod.

Different modes and forms of vibrations of blades can be obtained by experimental means with the help of different external impulses. If on a horizontally set blade we apply a thin layer of powder, and then with some impulse we vibrate the blade, the powder will fall from all vibrating sections of the blade except the nodal sections.

Figure 5.3 depicts three different forms of bending vibrations of a blade of

<sup>1</sup>Gas-turbine engine.

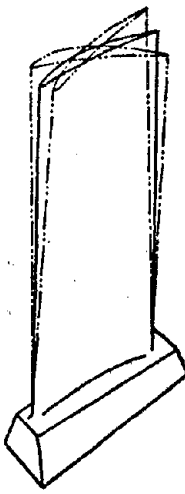


Fig. 5.2.  
One-node form  
of torsional  
vibrations  
of a blade.

a centrifugal compressor obtained in this manner. The first a has one vibration node at the place of fitting the blade into the disk, the second b has two vibrating sections and two nodes, and the third c has three vibrating sections and three nodes. Vibrating sections of blades are separated from each other by fixed sections, i.e., vibration nodes.

Figure 5.4 shows obtained in this way different forms of bending, torsional, and combined (bending-torsional) vibrations of a blade of a turbine or axial-flow compressor: a, b and c depict the one-node, and three-node forms of bending vibrations; d and e are the one-node and two-node forms of torsional vibrations; f shows the combined bending-torsional vibrations (two-node bending and one-node torsional forms of vibrations).

Vibrations are characterized by frequency and amplitude.

Frequency of vibrations of a blade is the number of its full vibrations in a unit of time (usually per second).

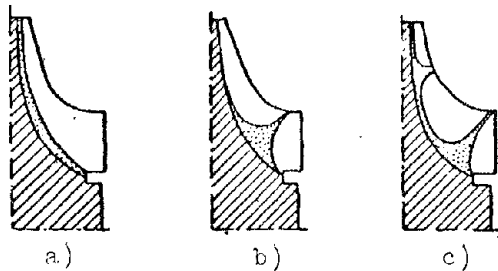


Fig. 5.3. Forms of vibrations of blades of a centrifugal compressor.

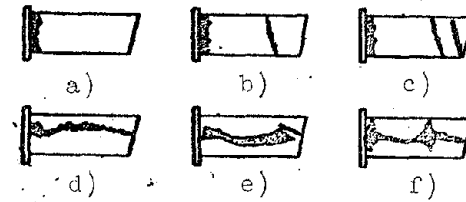


Fig. 5.4. Forms of vibrations of blades of a turbine and axial-flow compressor.

Amplitude of vibrations of a blade is the magnitude of its biggest deviation from the average position which it occupied in a state of rest, i.e., maximum elastic deformation which the blade is subjected to during vibrations. Consequently, amplitude of vibrations characterizes the magnitude of stresses appearing in the blade during vibrations.

There are natural and forced vibrations.

#### 5.2. Natural Vibrations of Blades

Natural or free vibrations are accomplished by the blade under the action of

natural elastic forces and inertia of its mass, if preliminarily with the help of a brief external impulse (for instance, an impact) the blade removed from the state of rest.

Frequency of natural vibrations of the blade depends on dimensions and form of the blade, elastic properties of its material, character of attachment of the blade, mode and form of vibrations.

The lowest frequency of vibrations corresponds to the one-node form. With transition to higher forms of vibrations, their frequency increases. Thus, for instance, frequency of vibrations of second tone is 1.5-3 times more than the frequency of vibrations of first tone, etc. Usually, of practical interest are vibrations of first tone (one-node form) and less often vibrations of second tone, since amplitude of vibrations, and consequently also stresses in these cases are the biggest.

For blades of an axial-flow compressor or turbine, whose area of cross section with respect to length varies according to linear law, frequency of one-node form of natural bending vibrations can approximately be expressed by the formula:

$$f_c = \frac{8}{\pi} \sqrt{\frac{(6-c)EJ_k}{(1.25-c)\gamma F_k}}, \quad (5.1)$$

where  $l$  is length of blade;

$E$  is the elastic modulus of material of blade;

$J_k$  is the minimum moment of inertia of root section of blade;

$\gamma$  is the specific gravity of material of blade;

$F_k$  is the area of root section;

$$c = \frac{F_p - F_k}{F_k}$$

here  $F_p$  is the area of peripheral section of blade.

Bending vibrations of blades are usually considered with respect to the axis, for which there is obtained a minimum moment of inertia of the section (with respect to axis  $\eta-\eta$  in Fig. 2.39), i.e., in the plane of least rigidity of blade. In this plane the frequency of vibrations is the lowest.

Example. Determine the frequency of natural bending vibrations of a moving blade of an axial-flow compressor.

Given:  $\eta = 18.85 \text{ cm}$ ;  $F_k = 6.35 \text{ cm}^2$ ;  $J_k = 0.483 \text{ cm}^4$ ;  $E = 0.72 \cdot 10^6 \text{ kg/cm}^2$ ;

$$c = 0.6; \gamma = 2.85 \cdot 10^3 \text{ kg/cm}^3.$$

Frequency of natural bending vibrations by formula (5.1):

$$f_1 = \frac{\delta}{18.85^2} \sqrt{\frac{(6 - 0.6) \cdot 0.72 \cdot 10^6 \cdot 0.483}{(1.25 - 0.6) \cdot 2.85 \cdot 10^3 \cdot 6.35}} = 285 \text{ vib/sec.}$$

The frequency of natural vibrations of one-node form in a blade of a centrifugal compressor can be approximately determined by the formula:

$$f_c = 1.8 A \frac{\delta_1}{l^2} \sqrt{\frac{E}{\gamma}} \text{ vib/sec} \quad (5.2)$$

Here  $\delta_1$  and  $\delta_2$  is the thickness of blade at its base and tip. Coefficient A depends on the relation  $c = \frac{\delta_2}{\delta_1}$  and is determined on the graph of Fig. 5.5. The dimensions

of the blade  $\delta_1$  and  $\delta_2$ , and also  $l$  are determined in section B-B, where length  $l$  is the longest.

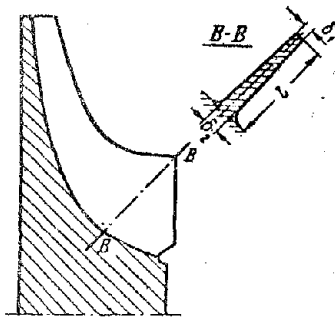
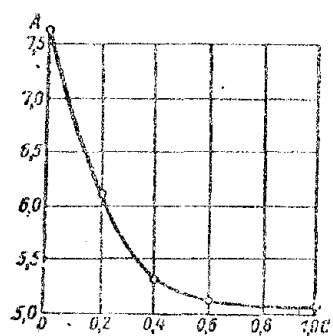


Fig. 5.5. Determination of frequency of natural vibrations of an impeller blade.

Example. Determine frequency of natural bending vibrations of blades of the rotor wheel of a centrifugal compressor.

Given:  $\delta_1 = 3.6 \text{ mm}$ ;  
 $\delta_2 = 1.25 \text{ mm}$ ;  $l = 60 \text{ mm}$ ;  $E = 0.735 \cdot 10^6 \text{ kg/cm}^2$ ;  $\gamma = 2.85 \cdot 10^3 \text{ kg/cm}^3$ .

Frequency of natural vibrations of first (one-node) form by formula (5.2) is equal to:

$$f_c = 1.8 \cdot 5.4 \frac{0.36}{6^2} \sqrt{\frac{0.735 \cdot 10^6}{2.85 \cdot 10^3}} = 1580 \text{ vib/sec.}$$

Influence of material of blade on frequency of natural vibrations in formulas (5.1) and (5.2) is expressed through relation  $E/\gamma$ . For different materials which blades are made from, this relation varies insignificantly. Nonetheless, in axial-flow compressors the blades of first stages are frequently made of steel, since they possess greater fatigue durability than aluminum.

With increase of operating temperature the elastic modulus  $E$  of materials decreases, which leads to decrease of frequency of natural vibrations of blades. Thus, for instance, natural frequency of vibrations of blades decreases by

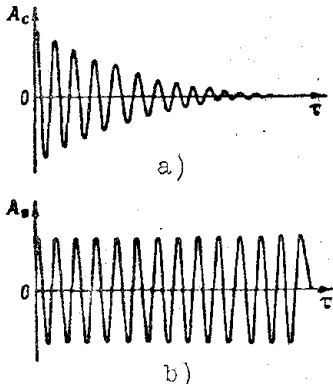


Fig. 5.6. Vibrations of a blade.

approximately 10% upon heating aluminum blades to  $240^{\circ}\text{C}$  and blades made from alloys  $750^{\circ}\text{C}$ .

With increase of thickness of blades their rigidity is increased and frequency of natural vibrations increases. During rotation of rotor under action of centrifugal forces, blades are stretched and their rigidity is increased. There is also an increase of frequency of their natural vibrations, which in this case is called dynamic frequency of natural vibrations and can be expressed by the formula:

$$f_d = \sqrt{f_c^2 + Bn_c^2}, \quad (5.3)$$

where  $f_c$  is the frequency of natural vibrations of blade in static conditions (without its rotation);

$B$  is the proportionality factor;

$n_c$  is the number of turns of rotor per second.

Character of setting of blades in locks (tight or free) in an operating engine does not render essential influence on frequency of natural vibrations of blades, since under action of centrifugal forces the blades are rigidly secured in the disks. Furthermore, clearances in locks during operation of engine are also selected due to the large thermal expansions of the blade shank in comparison with the disk groove.

Amplitude of natural vibrations  $A_c$  depends on magnitude of external impulse exciting the vibrations of the blade, and on time  $t$ . Natural vibrations in time comparatively quickly attenuate owing to resistance of environment and internal friction in material of blade (Fig. 5.6a).

### 5.3. Forced Vibrations of Blades

Forced vibrations occur under action of external disturbing forces periodically applied to blade. Frequency of forced vibrations  $f_B$  is equal to the frequency of application of disturbing force.

Forced vibrations do not attenuate while their disturbing forces are acting (see Fig. 5.6b). The greater the resistance to vibrations, the lower the amplitude of forced vibrations. Resistance to vibrations (resistance of environment and internal friction in material of blade) is usually characterized

by the damping coefficient  $\mu$ . In this case, the greater the resistance, the larger the coefficient  $\mu$ .

Amplitude of forced vibrations  $A$  of a blade can be significantly larger than static deformation  $\delta$  which is obtained during static application of the same disturbine force to the blade.

Figure 5.7 shows curves of dependence of relation of amplitude of forced vibrations to static deformation  $A/\delta$  on the relation of frequency of forced

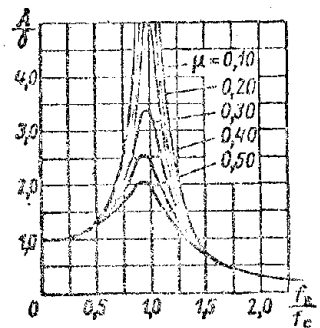


Fig. 5.7. Change of relation of amplitude of forced vibrations of a blade to its static deflection depending upon relation of frequency of disturbing force to frequency of natural vibrations.

(with respect to speed and pressure) of flow appears usually owing to its disturbing action in the area of the struts, blades, separate combustion chambers, and so forth. Frequency of disturbing forces is proportional to the number of sources  $z$  of disturbance of flow on the circumference in some section of the flow area (number of struts, number of combustion chambers, number of blades of nozzle apparatus, guide or diffuser, and so forth) and number of revolutions of rotor  $n$  rpm:

$$f_s = \frac{zn}{60}. \quad (5.4)$$

With constant number of sources of disturbance  $z$  of gas flow, the frequency of disturbing forces depends on the number of rotor revolutions. Number of revolutions  $n_p$  at which there appears the phenomenon of resonance is called the resonance number of revolutions. Figure 5.8 shows the change of amplitude of

vibrations (frequency of disturbing force) to frequency of natural vibrations for a number of values of the damping factor. Curves show that in the case of resonance, when frequency of forced and natural vibrations become equal ( $f_p = f_c$ ), amplitude of vibrations sharply increases.

Appearing during vibrations, the stresses in the blades carry a sign-alternating character and in magnitude are proportional to amplitude of vibrations. Upon the appearance of resonance, the stresses in blades increase and can exceed the fatigue limit of their material, as a result of which there will occur break-down of blades.

The cause of the appearance of forced vibrations of blades of compressor and turbine is the nonuniformity of gas flow on the blades during operation. Nonuniformity

(with respect to speed and pressure) of flow appears usually owing to its disturbing action in the area of the struts, blades, separate combustion chambers, and so forth. Frequency of disturbing forces is proportional to the number of sources  $z$  of disturbance of flow on the circumference in some section of the flow area (number of struts, number of combustion chambers, number of blades of nozzle apparatus, guide or diffuser, and so forth) and number of revolutions of rotor  $n$  rpm:

$$f_s = \frac{zn}{60}. \quad (5.4)$$

With constant number of sources of disturbance  $z$  of gas flow, the frequency of disturbing forces depends on the number of rotor revolutions. Number of revolutions  $n_p$  at which there appears the phenomenon of resonance is called the resonance number of revolutions. Figure 5.8 shows the change of amplitude of

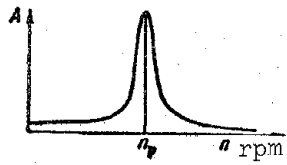


Fig. 5.8. Change of amplitude of vibrations of a blade of an axial-flow compressor depending upon engine revolutions.

vibrations of a compressor blade depending upon number of revolutions of rotor. With resonance number of revolutions  $n_p$ , the amplitude of vibrations of blade increases to 2.7 mm.

Resonance number of revolutions  $n_p$  can be determined from formula (5.4), considering in it  $f_B = f_c$ :

$$n_p = \frac{60f_c}{z}.$$

Resonance number of revolutions can also be determined graphically, plotting along the axis of abscissas the number of rotor revolutions, and along the axis of ordinates, the frequency of blade vibrations (Fig. 5.9).

In this case the frequency of forced vibrations  $f_B$  will be expressed by the line extending from the origin coordinates, and the frequency of natural vibrations  $f_c$ , by the line parallel to the axis of abscissas.

Point of intersection of these lines also gives the resonance number of revolutions  $n_p$ .

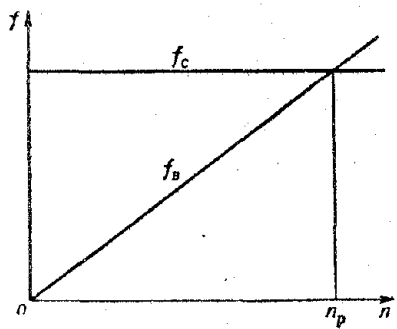


Fig. 5.9. Determination of resonance number of revolutions of compressor.

From Figs. 5.7 and 5.8 it follows that amplitude of forced blade vibrations reaches its dangerous values not only at the resonance number of revolutions, but also in its nearest zone. Therefore, for guarantee of reliability of operation, it is desirable that resonance engine revolutions  $n_p$  differ somewhat from operating revolutions  $n$ . It is possible, for instance, to recommend that  $n_p$  be 30% more or less than  $n$ .

If resonance number of revolutions  $n_p$  is in the range of operating revolutions  $n$  of the engine, one should adjust the blades to other resonance conditions. This is produced either by change of frequency of natural vibrations of blades, or by change of frequency of the disturbing force (frequency of forced vibrations). The first is carried out by change of profile of blades (thickness of blades), and the second by change of number of sources of disturbance of flow along the circumference (number of struts, individual combustion chambers, blades in blade rings, and so forth).

#### 5.4. Vibrations of Disks

During operation there can also appear vibrations of disks of compressors and turbines. Their basic cause are the variable gas forces acting on the blade rings of disks, and also bending vibrations of shafts.

Their two vibration modes of disks: with nodes located on the circumference (Fig. 5.10a), and with nodes located on the diameters (practically - with nodes extending to external circumference of disk in diametrically-opposite points, Fig. 5.10b). The first of them, which are usually called umbellate, in GTD practice are rarely encountered and therefore are of no special interest.

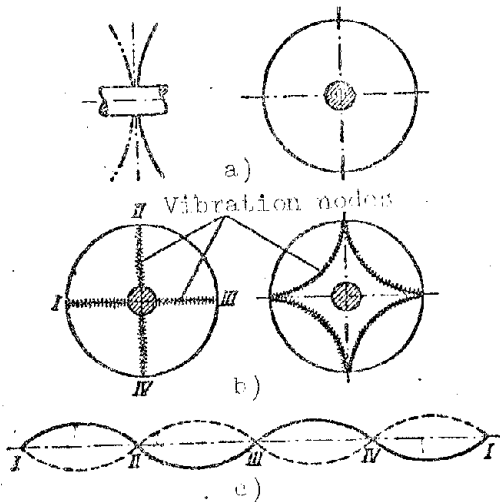


Fig. 5.10. Forms of vibrations of disks.

presence of struts unfavorably located in flow of gases), and speed of rotation at which there appears resonance, and are called critical vibrations,

Just as in blades, the frequency of natural vibrations of a disk depends on speed of rotation. The dynamic frequency of natural vibrations  $f_d$  can be expressed by formula (5.3). Heating of disk and its character also affect the frequency of natural vibrations of disk.

During vibrations with nodes located on diameters, the vibration nodes can be fixed and moving along the circumference. In the first case, the waves (antinodes) forming between nodes (Fig. 5.10c) will be standing waves, and in the second case they will be traveling along circumference of disk.

In GTD practice the most dangerous are vibrations in which the waves, traveling against the rotation of disk, are propagated with the angular velocity of the latter. These vibrations are excited by constant sources of excitation (for instance, in the

## CHAPTER VI

### BALANCING OF GTD ROTORS

#### 6.1. General Information

Variable in magnitude and direction, the forces and their moments which appear during operation of an engine and are transmitted through mounting lugs to an aircraft are called unbalanced. These forces and their moments have a dynamic (vibration) character. They create additional loads on shafts, bearings, engine housings, and on elements of construction of the aircraft. Therefore, there appears the question concerning methods of balancing these forces and moments.

Balancing of [GTD] (ГТД) rotors reduces to balancing their revolving masses. There is static and dynamic unbalance.

In a statically unbalanced disk (Fig. 6.1a), having mass  $m$ , the center of gravity  $s$  does not lie on the axis of rotation, but is displaced from it at distance  $e$ . During rotation of disk with angular velocity  $\omega$  it experiences centrifugal force

$$C = m e \omega^2. \quad (6.1)$$

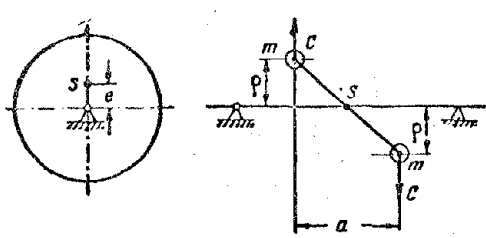


Fig. 6.1. Static and dynamic unbalance.

This force is constant in magnitude, but variable in direction. Static balancing reduces to matching the center of gravity of mass with axis of rotation. Static unbalance can be determined and eliminated in static conditions.

Figure 6.1b shows an example of a dynamically unbalanced system, consisting

of two masses  $m$ , located in one plane at distance  $\rho$  from axis of rotation. Center of gravity of system lies on axis of rotation; therefore it is statically balanced. However, during rotation the system experiences an unbalanced pair of centrifugal forces with moment

$$M = m\rho\omega^2a, \quad (6.2)$$

where  $a$  is the arm of masses  $m$ .

This moment is constant in magnitude, but variable in direction. Dynamic unbalance can be detected only during rotation.

Since centrifugal force  $C$  and moment of centrifugal forces  $M$ , unbalanced in the system, appear simultaneously dynamic balancing is essentially full balancing of the system. In a dynamically balanced system the axis of rotation is its main central axis of inertia. As it is known, any body has three mutually perpendicular main central axes of inertia, which in symmetric bodies are the axes of symmetry.

From unbalanced forces  $C$  and moment  $M$  on supports of rotor there appear additional loads. Balancing of rotors consists of such distribution of its mass at which the centrifugal forces and their moments appearing during rotation are balanced in the system of the rotor and on the supports of the rotor there are no loads due to them. Gas-turbine engines (GTD) are high-speed machines in which the centrifugal forces are very considerable; therefore, balancing of their rotors has an especially important value. Let us illustrate this with examples.

Example. Determine unbalanced centrifugal force in the rotor of a compressor, having weight  $Q = 71$  kg, and angular velocity of rotation  $\omega = 1287$  1/sec if its center of gravity is displaced with respect to the axis of rotation at magnitude  $e = 0.1$  mm.

Unbalanced centrifugal force by formula (6.1) is equal to

$$C = \frac{75}{981} 0.01 \cdot 1287^2 = 1270 \text{ kg.}$$

Example. One moving blade of a turbine is set with a weight 10 g greater than the others. Center of gravity of blade is located on radius 286 mm. Angular velocity of rotation of rotor  $\omega = 1210$  1/sec. Determine value of unbalanced force.

Unbalanced centrifugal force

$$C = \frac{0.01}{981} 28.6 \cdot 1210^2 = 427 \text{ kg.}$$

Example. Determine unbalanced force of the rotor of an axial-flow compressor, appearing upon break of scroll in one blade. Weight of blade scroll is 68.5 g. Radius of location of center of gravity of blade scroll is 560 mm. Angular velocity of rotation is  $\omega = 487 \text{ 1/sec.}$

Unbalanced centrifugal force

$$C = \frac{0.0685}{981} 56.487^2 = 930^3 \text{ kg.}$$

Unbalance of rotors is usually eliminated by balancing them.

### 6.2. Balancing of Revolving Masses

Rotor instability is usually characterized by its unbalance

$$D = Qe, \quad (6.3)$$

where  $Q$  is the weight of rotor;

$e$  is eccentricity (displacement of center of gravity of rotor with respect to axis of rotation).

Unstable centrifugal force of a rotor can be expressed through its unbalance:

$$C = \frac{Q}{g} e \omega^2 = \frac{D}{g} \omega^2 \quad (6.4)$$

or by expressing unbalance in g·cm, we obtain:

$$C = \frac{D \cdot 10^{-3}}{981} \omega^2 \approx D \left( \frac{\omega}{1000} \right)^2. \quad (6.5)$$

Example. Determine unstable centrifugal force of the rotor of a turbine.

Given:  $D = 30 \text{ g} \cdot \text{cm}$ ;  $\omega = 702 \text{ 1/sec.}$

Unstable centrifugal force is equal to

$$C = 30 \left( \frac{702}{1000} \right)^2 = 14.7 \text{ kg.}$$

Let us take a rotor, whose disk is set on the shaft with eccentricity  $e$ .

During its rotation there will appear an unstable centrifugal force  $C$  in the plane of rotation of the rotor. Force  $C$  can be balanced by setting in the plane of rotation of the disk a balancing load - counterweight (Fig. 6.2a) or by removal of part of the material in a disk with diametrically opposite side (Fig. 6.2b).

Between these two methods of balancing there is no fundamental difference.

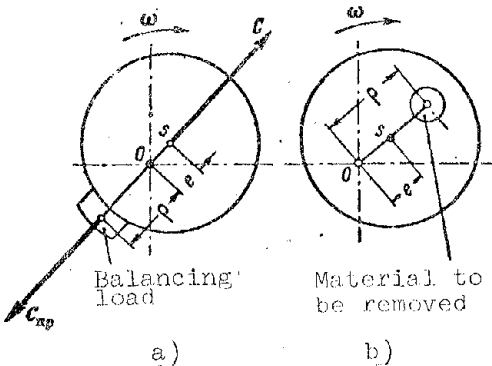


Fig. 6.2. Balancing of a disk.  
a) counterweight; b) removal of material.

Therefore, we subsequently will consider balancing only with counterweights.

Centrifugal force created by counterweight is equal to:

$$C_{qp} = \frac{q}{\rho} \rho \omega^2, \quad (6.6)$$

where  $q$  is the weight of the counterweight;

$\rho$  is the radius of location of center of gravity of counterweight.

The condition of balancing will be

$$C = C_{qp}$$

or, considering expressions (6.4) and (6.6),

$$D = Qe = qp.$$

Hence the weight of the balancing load

$$q = Q \frac{e}{\rho} = \frac{D}{\rho}. \quad (6.7)$$

Thus, the weight of the counterweight is inversely proportional to the radius of location of the counterweight  $\rho$  and does not depend on speed  $\omega$  of rotation of rotor.

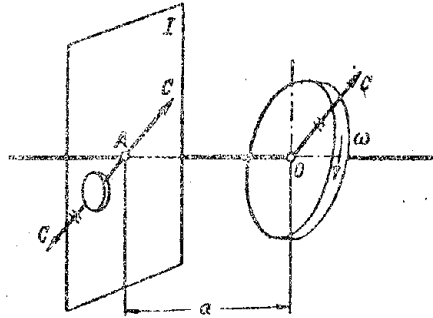


Fig. 6.3. Balancing of rotor by one counterweight.

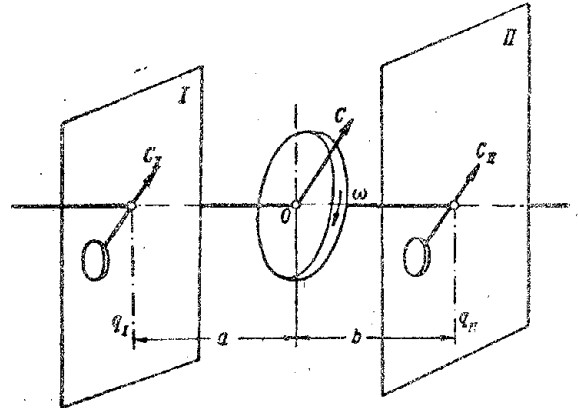


Fig. 6.4. Balancing of rotor in two planes.

Let us consider balancing of rotor by counterweight, if plane of balancing does not coincide with plane of its rotation and is parallel to it at a certain distance  $a$  (Fig. 6.3).

We transfer force  $C$  to the plane of balancing. Then we obtain: force  $C$ , located in plane of balancing, and moment from pair of forces  $M = Ca$ . Force  $C$  in plane of balancing can be balanced by counterweight, but pair of forces remains unbalanced in this case. Complete balancing of rotor is possible by means of a system of two counterweights located in two arbitrarily taken planes I and II parallel to the plane of rotation of rotor (Fig. 6.4). For this we divide centrifugal force  $C$  into two parallel components located in these planes:

$$C_I = C \frac{b}{a+b} \text{ and } C_{II} = C \frac{a}{a+b}.$$

Forces  $C_I$  and  $C_{II}$  can be balanced by counterweights  $q_I$  and  $q_{II}$  located on radii  $\rho_I$  and  $\rho_{II}$ . The weight of the counterweights will then be equal to:

$$q_I = \frac{D}{\rho_I} \frac{b}{a+b} \text{ and } q_{II} = \frac{D}{\rho_{II}} \frac{a}{a+b},$$

where  $D$  is unbalance of rotor.

Let us consider balancing of a rotor consisting of three disks placed on a common shaft (Fig. 6.5). Unbalanced centrifugal forces of disks will be designated by  $C'$ ,  $C''$ , and  $C'''$ . In the system of the rotor we single out two planes I and II parallel to planes of rotation and suitable for attachment of counterweights. Let us divide forces  $C'$ ,  $C''$ , and  $C'''$  into two components located in planes I and II. Returning to Fig. 6.5, we find:

$$\begin{aligned} C'_I &= C' \frac{l_2 + l_3 + l_4}{l}; & C'_{II} &= C' \frac{l_1}{l}; \\ C''_I &= C'' \frac{l_3 + l_4}{l}; & C''_{II} &= C'' \frac{l_1 + l_2}{l}; \\ C'''_I &= C''' \frac{l_4}{l}; & C'''_{II} &= C''' \frac{l_1 + l_2 + l_3}{l}. \end{aligned}$$

In planes of balancing I and II we obtain vector bunches of forces  $C'_I$ ;  $C''_I$ ;  $C'''_I$  and  $C'_II$ ;  $C''_II$ ;  $C'''_II$ , extending from points A and B. Using the rule of geometric addition of vectors, we find the resultant forces  $C_I$  and  $C_{II}$  which can be balanced by counterweights  $q_I$  and  $q_{II}$ .

In case of mutual balancing of disks  $C_I = 0$  and  $C_{II} = 0$ .

Considering a system with arbitrary number of disks, it is possible to prove that any system of the rotor can be completely balanced with the help of two counterweights placed in two planes of balancing parallel to the plane of rotation.

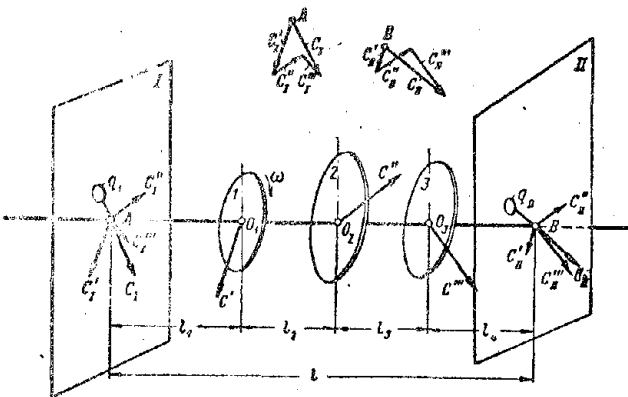


Fig. 6.5. Balancing of a rotor consisting of three disks in two planes.

#### 6.7. Static and Dynamic Balancing of Rotors

Instability of rotors is eliminated by balancing them. In static balancing the rotor is placed on prisms (Fig. 6.6) or on rollers. Under action of moment

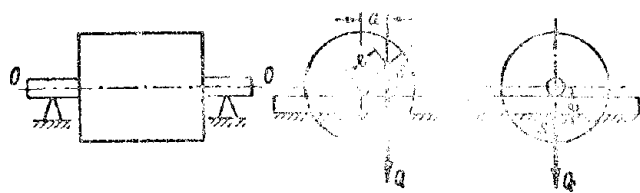


Fig. 6.6. Static balancing of rotor.

of gravity of rotor. Adding then to the rotor a balancing load or, conversely, removing its superfluous material, we obtain a neutral position of rotor on prisms at arbitrary a quite deviations of it from initial equilibrium position. With help of static balancing we attain static equilibration at which the center of gravity of the rotor will be on the axis of rotation.

Static balancing does not possess high accuracy. Furthermore, it does not attain full equilibrium of the rotor, since the free pair of forces (see Fig. 6.1b) is not revealed in this instance. Full of dynamic equilibrium is attained by dynamic balancing of the rotor, which is produced on special balancing machines with a revolving rotor. Figure 6.7 shows a fundamental diagram of a balancing machine of the frame type. The machine has a pendular frame (cradle) 1, which, leaning on spring 2, can oscillate with respect to the horizontal swinging axis 3. The rotor 4 to be balanced is placed on bearings of the pendular frame and rotated by a special electric motor not shown in the diagram.

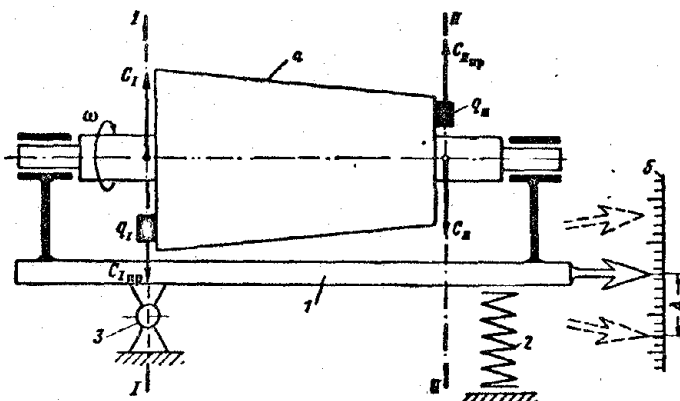


Fig. 6.7. Fundamental diagram of a balancing machine of the frame type.

Rotor is placed on frame of machine in such a manner so that the plane of balancing I passes through axis 3 of frame. Thus the unbalanced centrifugal force  $C_I$ , presented to plane I, does not evoke oscillations of the frame. Unbalanced centrifugal force  $C_{II}$ , presented to plane of balancing II, creates a moment variable in magnitude and direction with respect to axis 3 of the frame. Owing to this moment, in the frame there appear forced vibrations, the amplitude of which is measured on scale 5. Selecting balancing load  $q_{II}$ , it is possible to eliminate the frame vibrations and balance the given centrifugal force  $C_{II}$ . Then the rotor is transposed on supports in such a manner so that the plane of

I balancing II now passes through axis 3 of the frame, and the given centrifugal force  $C$  is balanced by load  $q_I$ .

In practice we find the application of different types of balancing machines, which in detail are considered in special courses.

Balancing is produced by means of attaching balancing weights (Fig. 6.8), by selection of blades with respect to weight, or by removal of some of the rotor material. Places intended for attachment of the balancing weights and for removal of material are usually indicated in drawings. Rotor is balanced with a definite accuracy which is indicated in drawings in the form of permissible unbalance D.g.cm.

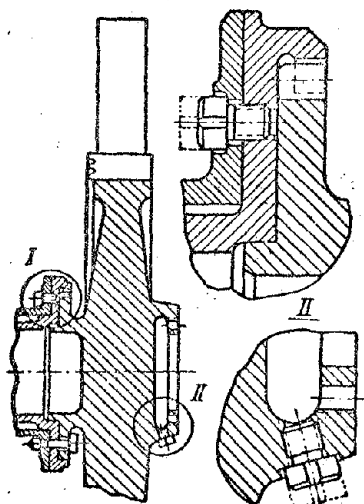


Fig. 6.8. Application of balancing weight-screws in a turbine for balancing the rotor.

Permissible unbalance for a rotor of a GFD turbine and compressor is from 15 to 40 g·cm.

Upon setting radial roller bearings on the rotor, its balancing can be disturbed due to the eccentricity of internal rings of bearings, since the center of gravity of the rotor will then be displaced from the axis of rotation. Therefore, balancing of rotors is usually recommended to be produced on its moving bearings or, more exactly, on the inner rings of moving bearings. In the replacement of moving blades and moving bearings or at least in their transposition to the rotor into a new position it is necessary to again produce balancing.

## C H A P T E R VII

### SHAFTS AND SUPPORTS OF ROTORS

#### 7.1. General Information

Turbine and compressor rotors together form the engine rotor. Figure 7.1 shows the [TRD] (ТРД) [VK-1] (ВК-1) rotor. The rotor of its compressor consists of a two-sided impeller 1, shaft 2, and short nose 7. On shaft 2 sits impeller of fan 6. Turbine rotor consists of rotor wheel 3 and shaft 4. With help of slit coupling 5 rotors of compressor and turbine are united into a single rotor of the engine.

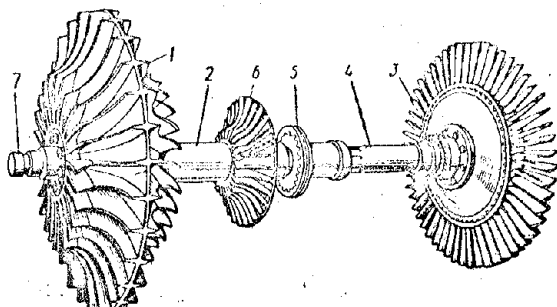


Fig. 7.1. Rotor of engine VK-1.

As supports of [GTD] (ГТД) rotors they usually use roller bearings. With respect to number of supports there are four, three, and two-support rotors of engines (Fig. 7.2). Diagram a shows a four-support rotor of an engine, whose compressor rotor and turbine rotor have two bearings each.

In the three-support engine rotor (diagram b) the rotor of the compressor has two, and the rotor of the turbine has two, and the rotor of the turbine has one bearing. By its front end the turbine shaft, through the rotor connector, is supported on the compressor shaft. The rotor wheel of the turbine is located at an angle. In contemporary GTD three-support rotors have obtained wide application. In comparison with the four-support type, the three-support rotor is simpler in design, and weight of engine is less. Furthermore, because of the

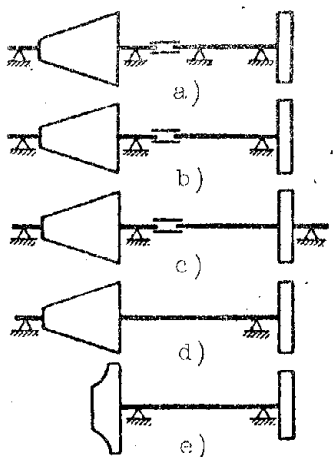


Fig. 7.2. Diagrams of location of rotor supports.

smaller number of bearings, total heat radiation in oil and its circulatory consumption in the engine is less. An example of three-support rotors made according to diagram b could be the TRD VK-1 (see Fig. 1.8) and the [TVD] (TBII) [AI-20] (AM-20).

Diagram c shows a three-support rotor with bearing located behind the turbine. Such location of support is used in the case of multistage turbines having a solid rotor, and for two-shaft engines.

Diagram d shows a double-support rotor. Since in this case the distance between supports is considerable, the shafts and housings of the engine must be made more rigid and heavier than in the case of a three-support rotor. Diagram e shows a double-support rotor of a low-capacity GTD.

Two-shaft engines (see Fig. 1.5 and 1.11) have two systems of rotors with total number of bearings from 6 to 8. Weight of the two-shaft engine, in comparison with the single-shaft ones, is greater by 10 to 20%. Because of the large number of bearings, heat radiation in oil and its circulatory consumption in two-shaft engines is also greater.

## 7.2. Shafts

Shafts of GTD rotors are made from highly durable structural steel and for lightness are hollow. Besides strength, shafts must have sufficient bend rigidity, which is checked in them by critical revolutions. Frequently GTD shafts are made in the form of short noses and shanks (journals) secured to the

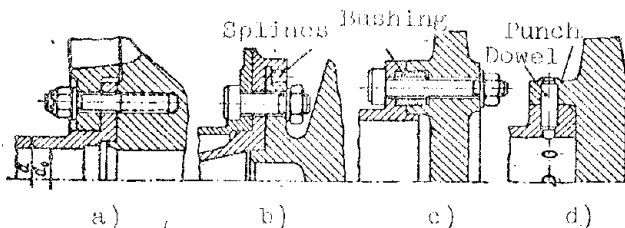


Fig. 7.3. Diagrams of flanged and dowel connections of shafts with rotor wheels.

ends of drums and on disks of rotors, or made simultaneously with rotor disks (see Fig. 2.17).

Connections of shafts with drums and disks are very diverse; they were considered above in Chapters II, III and IV. Figure 7.3 shows diagrams of flanged and dowel connections of shafts with rotor wheels. Diagram a depicts a flanged joint with transmission of torque by friction of joint due to corresponding

tightening of pins. An example of such connection could be the compressor rotor of engine VK-1 (see Fig. 3.12). During transmission of large torques, such connection is heavy, since it requires considerable tightening.

Flanged joints shown in diagrams b and c require less tightening, since transmission of torque in them is accomplished or with splines (diagram b), or with bushings (diagram c). An example of the first is the connection of shaft with disk of turbine of engine VK-1 (see Fig. 4.4), and the second is the connection of shaft with disks of the turbine of the AI-20 engine (see Fig. 4.14).

In the dowel connection (diagram d) the disk is pressed on the shaft. Radial location of dowels allows free thermal expansion of disk without disturbance of centering. So that the dowels under the action of centrifugal forces do not drop, they are frequently punched. An example of a dowel connection is the rotor of the compressor of the AI-20 engine (see Fig. 2.17).

### 7.3. Connection of Rotors

Transmission of torque from turbine to compressor, both in TVD and also the reduction gear of the propeller is carried out usually through spline connections of rotors. Rotor shafts are connected by splines directly or with the help of spline connectors. Splines are rectangular or evolvent.

Rotors of compressor and turbine carry axial loads. Axial fixation of them together allows the use in the system of engine rotor, instead of two, one radial-thrust bearing unit. Axial fixation of rotors is carried out by thread, ball and socket joint connections and other forms of connections.

Figure 7.4 shows the connection of rotors of compressor and turbine of the TVD AI-20. Turbine shaft 6 with the help of splines is directly connected with shank 1 of compressor rotor. Through this spline connection torque is transmitted from turbine to compressor and further to the propeller.

Axial fixation of rotors is carried out by bolt 8 which is screwed into shank 1 of compressor rotor until it stops in washer 7. The washer is on the face of shank 1 of compressor rotor and its bead does not allow movement of turbine shaft to the right - in the direction of action of axial force in turbine rotor. In tightening of bolt 8 thrust washer 7 is fixed from turning by its splines which enter the spline grooves of turbine shaft 6. Bolt 8 is locked by a spring-spline lock which consists of spline bushing 5, adjusting dowel 3, and

spring 4. Dowel 5 is expanded in shank 1 and serves as a stop for the spring. Spline bushing 5 sits on splines of shank 1, and under the action of spring 4 enters the splines of bolt 8, carrying out its locking. Upon release of spline bushing 5 to the left, bolt 8 is liberated from locking. Selection of distance sleeve 2 establishes axial clearance  $A = 0.3$  to  $0.5$  mm. Free setting through splines and axial clearance  $A$  allows for some misalignments of rotor axes.

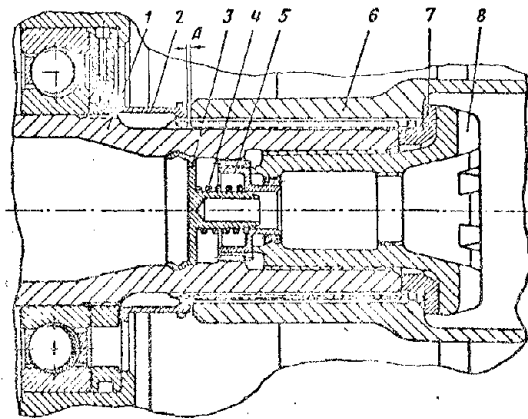


Fig. 7.4. Connection of rotors of compressor and turbine of the TVD Al-20.

shaft splines of turbine 1. From axial shift the sleeve is retained by fixing ring 2. The ring has on its internal side two rows of splines. With front splines the ring 2 enters the annular orifice of sleeve 3, and with rear splines, the orifice splines of shaft 1. Axial fixation of sleeve 3 is carried out by face stop of ring splines 2 in orifices of sleeve 3 and shaft 1. In such position, ring 2 is stopped by spring retainer 4. Driven sleeve 7 sits on internal splines of compressor shaft 11 and is secured by coupling figure bolt 12.

Ball and socket joint connection, carrying out axial fixation of turbine rotor, consists of spherical shank of turbine shaft 1 and spherical recess formed by driven sleeve 7 and cover 16. Shank of shaft and cover have three grooves a piece carried out at an angle of  $120^\circ$  which ensure assembly and disassembly of connection. Axial fixation is carried out by stop of flanges of shaft shank in cover flange. In such position the turbine shaft is fixed by three retainers 6, which enter the holes of driving sleeve 3. Retainers 6 are used also for attaching cover 16 to driven sleeve 7 along with other bolts.

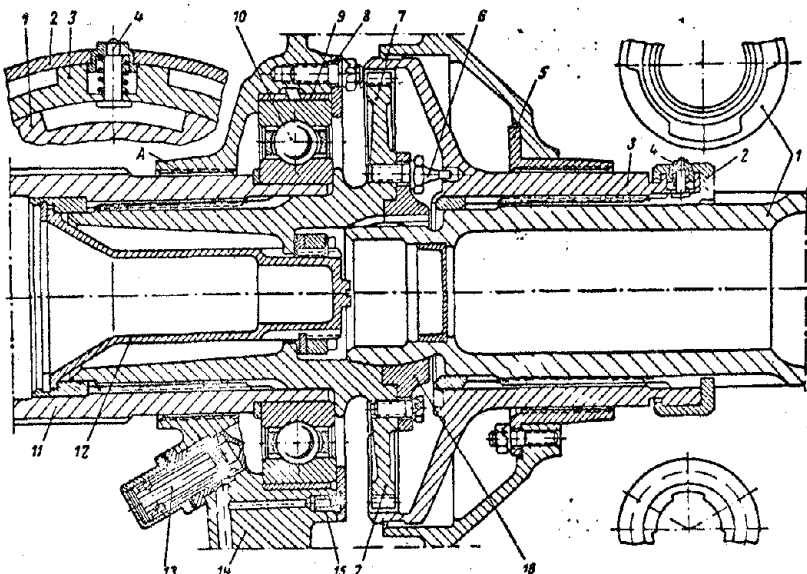


Fig. 7.5. Connection of rotors of turbine and compressor of the VK-1 engine. 1 and 11 - shafts of turbine and compressor, 2 - fixing ring, 3 and 7 - driving and driven sleeves of coupling, 4 - spring retainer, 5 - packing sleeve, 6 - retainer bolts, 8 - washer, 9 - bushing, 10 - radial-thrust ball bearing, 12 - tie bolt, 13 - burner, 14 - bearing casing, 15 - jet, 16 - cover of ball support. A - oil-elimination thread.

During disassembly it is necessary to sink stopper 4 into its recess and turn ring 2 until its rear splines match the grooves of the turbine shaft splines. After that, the driving sleeve 3 is displaced along the splines in the direction of the turbine and is disengaged from driven sleeve 7. The retainers 6 are then removed from holes of sleeve 3. Then by turning the turbine rotor to angle 60° the flanges of the spherical shank of shaft 1 match the grooves on cover 16 and turbine rotor is freely removed.

#### 7.4. GTD Rotor Bearings

GTD rotors usually have antifriction bearings which in comparison with sliding bearings are shorter and have smaller coefficient of friction. They are less sensitive to brief interruptions in supply of lubricant to them and can work on less viscous grades of oil. The last circumstance facilitates starting of engine at low temperature, since it does not require preliminary preheating of oil with decrease of temperature to -30 to -40°C. A certain deficiency of antifriction bearings in comparison with sliding bearings is their greater weight and greater diametrical dimensions.

The rpm rate of GTD rotors is from 5000 to 15,000 rpm. Therefore, for their supports special high-speed ball and roller bearings of light series are used: extra-precision [SA] (GA) and super-precision [S] (C) classes of precision. Bearings located in hot zone of engine operate in conditions of heightened temperatures.

Types of bearings. Figure 7.6 shows types of bearings applied for GTD rotors. Single-row radial-thrust ball bearings a and b perceive radial and axial loads. Bearing b has a detachable outer ring. Sometimes the inner ring is detachable. Bearings with detachable ring can have a large number of balls, and the track can have special pattern and be deeper. There can be obtained three or four points of contact in balls with angle  $26^\circ$ , instead of the usual  $12^\circ$ . Owing

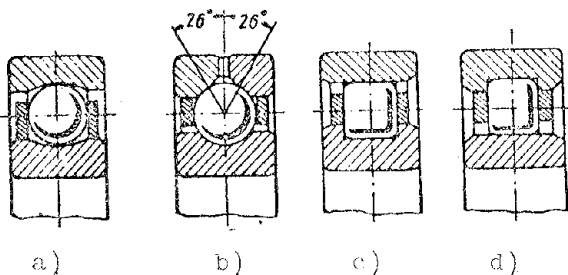


Fig. 7.6. Types of bearings used for GTD rotors.

to this, the bearings with cut ring are able to perceive a larger load.

Roller bearings c and d perceive only radial loading. Rollers are short (usually their length is equal to their diameter), cylindrical, or barrel-shaped. One of the rings has beads for retention of rollers in axial direction, and the other is smooth, without beads. The latter provides the rotor with free thermal expansion in axial direction. The width of the smooth ring is made larger than

the length of rollers so that during movement of ring there would be no one-sided hanging of rollers from it.

Balls, rollers, and rings of bearings are made from high-alloy steels, allowing operation of bearings at the heightened temperatures and at high speeds of rotation.

Radial clearance between balls (rollers) and rings of GTD bearings is larger than usual. Thus, for instance, in bearings of the rotor of the VK-1 engine the radial clearance is from 0.07 to 0.1 mm. Increased clearance ensures normal work of bearings at

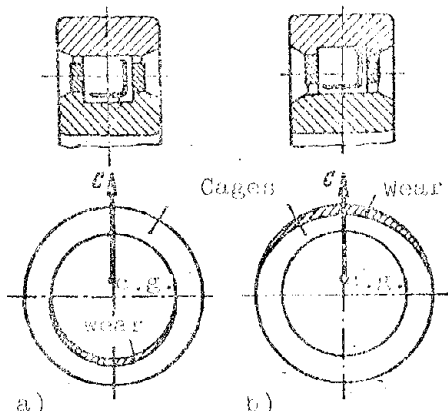


Fig. 7.7. Wear of bearing cages.

heightened temperatures and high speeds of rotation.

Cages of bearings are solid, well balanced, and made from forged bronze or duralumin. Light stamped cages usually do not endure large turns.

Centering of cages is produced on the inner (Fig. 7.7a) or outer (Fig. 7.7b) bearing rings. Centering of a cage on the outer ring has the advantage that in the process of wear its balancing is improved, and with centering on the inner ring it worsens. With centering of case on outer ring, the clearance between it and the ring should be sufficient in order to avoid jamming during thermal expansion of the cage.

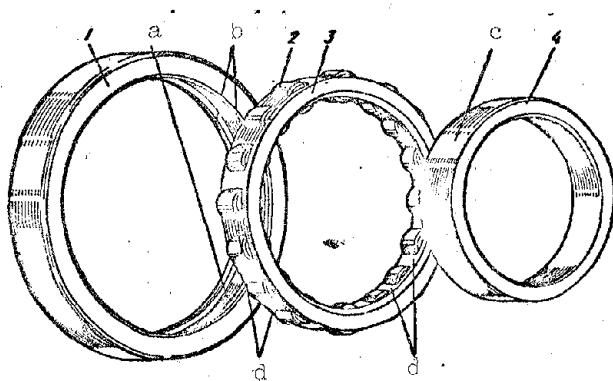


Fig. 7.8. Roller bearing of front support of the VK-1. 1 and 4 - outer and inner ring, 2 - roller, 3 - cage, a and c) tracks of outer and inner rings, b) annular beads, d) calking.

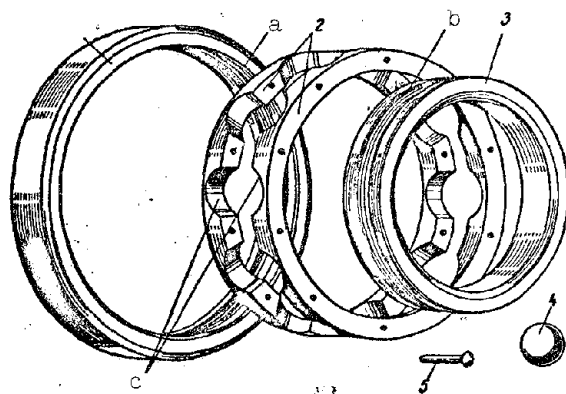


Fig. 7.9. Ball bearing of the VK-1 engine. 1 and 3 - outer and inner ring, 2 - cage halves, 4 - ball, 5 - rivet, a and b) tracks of outer and inner rings, c) ball recesses.

Figures 7.8 and 7.9 show bearings of the TRD VK-1 in dismantled form. The cage of the roller bearing is forged duralumin and nondetachable; the ball bearing cage is forged bronze and detachable, in the form of two halves united by rivets. Cages are centered on outer rings of bearings. The clearance is from 0.6 to 0.9 mm.

Selection of bearings is produced proceeding from their operation life in hours, which is determined by the empirical formula

$$h = \frac{1}{n} \left( \frac{C}{Q} \right)^{3.33} \text{ hours} \quad (7.1)$$

where n is the rpm rate;

C is the efficiency factor;

Q is the reduced conditional load in kilograms.

The efficiency factor is usually given in the catalogs of the bearings. It can be determined also by the following formulas: for single-row radial-thrust ball bearings

$$\left. \begin{aligned} C &= 65z^{0.7}d_0^2 \frac{\cos \beta}{1 + 0.2d_0} \\ C &= 80z^{0.7}d_0 l, \end{aligned} \right\} \quad (7.2)$$

and for roller bearings:

where  $z$  is the number of balls or rollers of the bearing;

$d_0$  is the diameter of the ball or roller in mm;

$l$  is the length of the roller in mm;

$\beta$  is the angle of pressure. Usually  $\beta = 26^\circ$  (see Fig. 7.6).

Reduced conditional load in common form is expressed by the following formula:

$$Q = (R + mA)K_R K_b K_T, \quad (7.3)$$

where  $R$  and  $A$  is the radial and axial load on bearings in kg;

$m$  is the coefficient of reduction of axial load to radial (depends on type of bearing);

$K_R$  is the coefficient considering the character of work. With a revolving inner ring of bearing  $K_R = 1$ , and with revolving outer ring  $K_R = 1.35$ ;

$K_b$  is the coefficient considering the character of load. For GTD rotor bearings it is possible to take  $K_b = 1$ , and for reduction gear  $K_b = 1.5$  to 1.5;

$K_T$  is the coefficient considering the temperature conditions of operation. Its values are:

$t^{\circ}\text{C}$  ..... 125; 150; 200; 250

$K_T$  ..... 1.05; 1.1; 1.25; 1.4

High-speed of bearings is characterized by the product  $dn$ , where  $d$  is the diameter of the setting neck of the shaft in mm, and  $n$  is the rpm rate. For GTD bearings  $dn = (0.5 \text{ to } 1.5) \cdot 10^6$ , which characterizes their high speed.

#### Temperature conditions of operation of bearings and their lubrication.

During work, bearings are heated by the heat given off as a result of the work of resulting forces in the bearing itself, and by external preheating from adjacent hot parts of the engine.

Figure 7.10 gives the results of investigation of work of a roller bearing

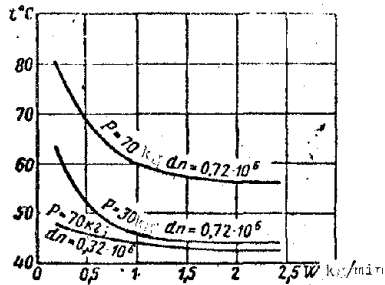


Fig. 7.10. Change of temperature of bearing depending upon quantity of feed oil.

after which it remains almost constant. Optimum quantity of fed oil depends on dimensions of bearing, load, and value of parameter dn.

Intensity of external preheating depends on place of location of bearing and on heat release rate of engine. Approximate values of operating temperatures GTD bearings are given in the table.

Bearing unit	During work of engine °C	After stop of engine °C
TVD propeller shaft bearing	80 to 110	80 to 110
Front rotor bearing	50 to 80	50 to 80
Central rotor bearing	100 to 125	125 to 150
Rear (turbine) rotor bearing	125 to 150	240 to 260

Central and rear bearings of rotor are located in hot part of engine. Increase of their temperature after stop of engine is explained by ceasing of pumping of oil through them, whereupon the engine still remains hot for a certain time.

At high operating temperature, the lubrication of bearings worsens and there occurs tempering of bearing steel. Therefore for decreasing external preheating the casings of bearings located in the hot zone are frequently heat-insulated and cooled by air. Simultaneously for guarantee of reliable lubrication and cooling, the bearings are usually fed an excess quantity of oil, which depending upon conditions of operation is within the limits of 1.5 to 6 l/min and

<sup>1</sup>G. A. Kuz'min and V. M. Demidovich. Investigation of the work of high-speed GTD roller bearings during supply of large quantities of oil, Proceedings of Kazan' Aviation Institute, Nos. 33 and 34, 1958.

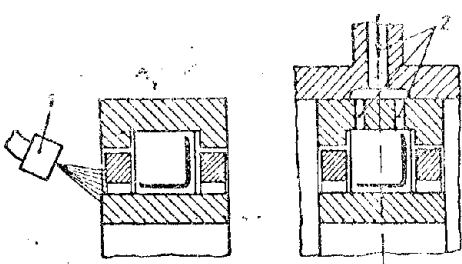


Fig. 7.11. Feed of lubricant to bearings.

above.

Oil is fed to bearings through one or several nozzles 1 fixed in casing on the side, or through drillings 2 in casing and outer ring of bearing (Fig. 7.11). In the first case the stream of oil heads into the clearance between the inner ring of the bearing and its cage. In the second case the oil moves directly to the working substances of the bearing.

In order to prevent the possibility of penetration of oil into the gas-air duct of the engine, the bearings of the rotor have sealer devices in the form of labyrinth seals, sealing rings, and packings with oil-elimination thread.

#### 7.5. Axial Fixation of Engine Rotors

For guarantee of free thermal expansion of rotor and stator, axial fixation of rotor is carried out in one point -- by one radial-thrust bearing unit. The other supports usually have support roller bearings. For guarantee of free rotation of rotor, between it and the stator there are axial clearances which consider the distinction in thermal expansions of rotor and stator during

operation.

Figure 7.12 gives the diagram of determination of axial assembly clearances for the rotor wheel of a centrifugal compressor, all parts of whose stator are made from aluminum alloy.

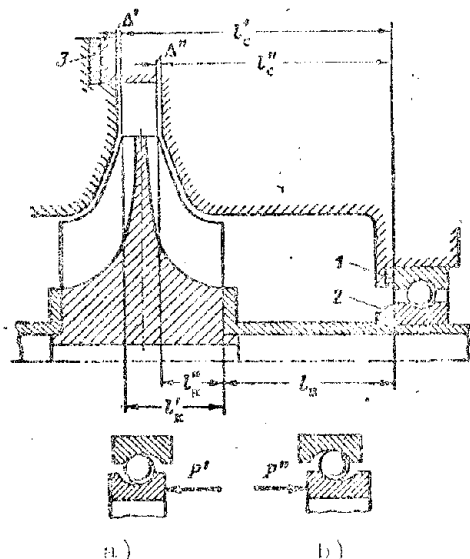
Its expansion due to heating during work can be determined by the formula:

$$\Delta_c = l_c \alpha_c (t_c - t_0).$$

Rotor of compressor has steel shaft and rotor wheel of aluminum alloy. Its expansion due to heating during operation is determined by the formula:

$$\Delta_p = l_b \alpha_b (t_b - t_0) + l_k \alpha_k (t_k - t_0),$$

Fig. 7.12. Determination of axial assembly clearances for the wheel of a centrifugal compressor.



where  $l_c$ ,  $l_B$ , and  $l_K$  are the length dimensions of stator, shaft, and rotor wheel (see Fig. 7.12);

$\alpha_c$ ,  $\alpha_B$ , and  $\alpha_K$  are coefficients of linear expansion of materials of stator, shaft, and rotor wheel;

$t_c$ ,  $t_B$ , and  $t_K$  are operating temperatures of stator, shaft, and rotor wheel;

$t_0$  is the temperature of stator, shaft, and wheel during assembly.

Assembly axial clearances between rotor and stator are determined by the formulas:

from front side -

$$\Delta' = \Delta_r - \Delta_c + \Delta_p,$$

from rear side -

$$\Delta'' = \Delta_r + \Delta_c - \Delta_p.$$

here  $\Delta_r$  is the guaranteed (minimum) axial clearance in an operating (hot) engine.

Necessary axial clearances between rotor and stator are selected during assembly with help of regulating rings and linings. Thus, for instance, in the diagram of Fig. 7.12 the clearance  $\Delta''$  can be selected with help of regulating rings 1 or 2, and clearance  $\Delta'$  with help of lining 3 or ensured by the precision of manufacture of the components.

Since a ball bearing usually has an axial gap, during measurement of assembly clearances this gap is preliminarily selected by release of rotor in axial direction. Thus, during measurement of clearance  $\Delta'$  the rotor is released by stress  $P'$  to the left (diagram a), and during measurement of clearance  $\Delta''$  by stress  $P''$  to the right (diagram b).

Axial gap of GTD ball bearings is usually from 0.35 to 0.65 mm. In the VK-1 engine the guaranteed (minimum) clearance of the rotor wheel is  $\Delta_r = 1.3$  mm, and assembly clearances:  $\Delta' = 0.5$  to 0.7 mm and  $\Delta'' = 1.5$  to 1.7 mm.

Changes of axial clearances between rotor and stator depend on location of radial thrust bearing unit of engine. The radial-thrust bearing unit, the most loaded, is usually placed in the colder part of the engine, i.e., either in its front part at point A (at entrance to compressor), or in its middle part at point B (Fig. 7.15). Since in the last case the radial-thrust bearing unit is nearer to the turbine ( $l_2 < l_1$ ), the changes of its axial clearances  $\Delta'$  and  $\Delta''$  are less.

Distribution of load between radial-thrust bearings in the unit. Depending upon axial loads, the radial-thrust bearing unit is constructed from one to three

single-row ball bearings. For equal distribution of axial load between bearings there are distance rings or washers of definite size.

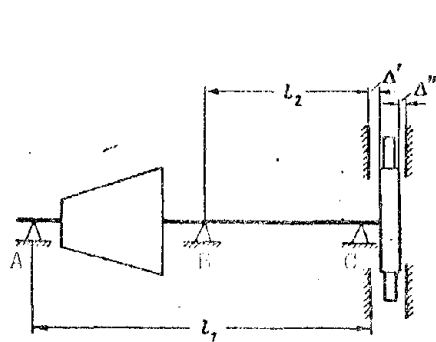


Fig. 7.13. Determination of axial clearances of a turbine.

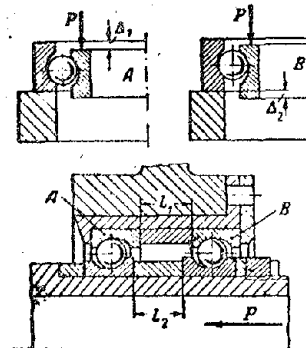


Fig. 7.14. Selection of regulating rings.

Dimensions of rings are determined in the following way. Bearings are preliminarily loaded with design axial load  $P$  (Fig. 7.14), selecting their axial gaps. After that we measure, in bearing A, the magnitude of sinking  $\Delta_1$ , and in bearing B, the magnitude of projection  $\Delta_2$  of internal rings with respect to external. At equal distribution of axial load and its given direction (in this case to the left) dimensions of distance rings must be connected together by the following equality:

$$l_2 = l_1 + \Delta_1 - \Delta_2. \quad (7.5)$$

#### 7.6. Design of Bearing Units

Figure 7.15 shows the central support of the Al-20 turboprop engine (TVD), having radial-thrust ball bearing 5 which perceives radial and axial loads and fixes engine rotor in axial direction with respect to stator. With its internal ring the bearing together with labyrinth bushing 12, regulating ring 11, and oil deflector 10 is secured to rear journal of rotor of compressor 9 by nut 8. With its external ring the bearing is fixed in the socket of casing of rotor bearings 4 and is secured jointly with injector ring 7 and labyrinth bushings 3 and 2 by nut 1.

Axial clearances between rotor and stator of compressor are established during assembly by selection of regulating ring 11. In the compressor area the central support has a three-row labyrinth seal and oil deflector 10. Borings of

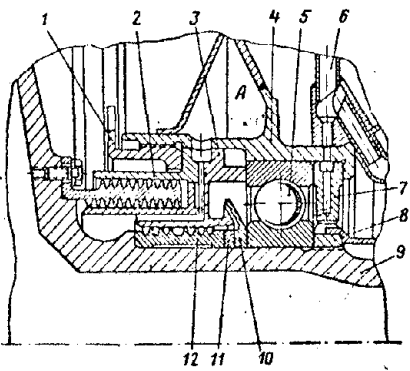


Fig. 7.15. Selection of regulating rings.

labyrinth bushings above ridges have a soft covering that allows decrease of radial clearances in seal to 0.06 to 0.15 mm. For the best seal the cavity between first and second rows of the seal is connected with cavity A of the bearing casing which is evacuated. Compressed air, seeping in Two rows of sealings, is removed through a system of evacuation into the atmosphere and does not go into the cavity of the bearing. Oil deflector 10 in turn rejects oil on the periphery and prevents it from falling into the labyrinth seal.

Oil for lubrication and cooling of bearing moves from main oil line 6 through three holes of ejector ring 7.

Figure 7.5 shows the radial-thrust ball bearing 10 of the central rotor support of TRD VK-1. By its internal ring the bearing is secured to the journal of the compressor rotor, and by its external ring is fixed in steel bushing 9 which is pressed into the socket of aluminum casing 14. From axial shifts the bearing is fixed by washer 8 attached to the casing with the help of pins. Oil cavity of bearing and connector has seals in the form of an oil-rejection thread A, in casing 14 and in bushing 5. Oil for lubrication and cooling is fed to bearing through injector 13, and to spline sleeve through jet 15. On the outside the bearing casing is air cooled.

Figure 7.16 shows the rear support of the TVD AI-20 with roller bearing 4 which perceives a radial load in the rotor area. External ring of bearing has beads fixing the rollers in axial direction. Its internal ring is smooth, owing to which there is ensured the possibility of axial shift of turbine rotor during operation. By its external ring the bearing is fixed in the socket of bearing casing 3 and together with ejector ring 2 is secured by nut 5. Internal ring of bearing is placed on rotor shaft of turbine 7 and jointly with labyrinth bushing 6 is secured by nut 8.

In the turbine area the bearing has a three-row labyrinth seal. Borings in labyrinth bushings above ridges have a soft covering which allows small radial clearances in the seal. Cavity A in front of the labyrinth seal is under pressure

of secondary air proceeding from combustion chamber. For the best sealing the cavity between the second and third rows of seals through drillings is connected with cavity B of the bearing casing, which is evacuated. Compressed air, seeping through one row of sealing, is removed through the system of evacuation into the atmosphere and does not go into the cavity of the bearing. Oil for lubrication and cooling of bearing moves from main oil line 1 through several holes in ejector ring 2, as this is carried out in the central bearing (see Fig. 7.15).

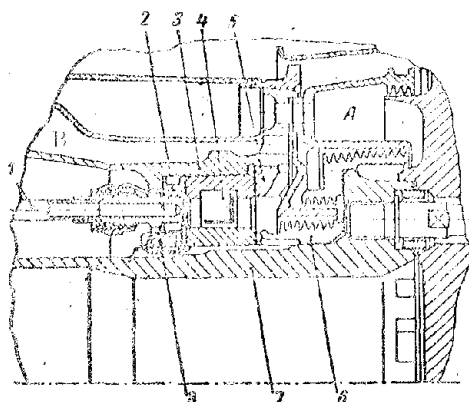


Fig. 7.16. Rear rotor support of AI-20 engine.

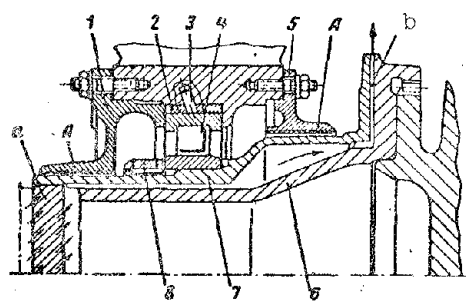


Fig. 7.17. Rear rotor support of VK-1 engine.

Figure 7.17 shows the rear rotor support of the TRD VK-1 with roller bearing 4. By external ring the bearing is attached to steel bushing 2 which is pressed into the socket of the aluminum casing and is fixed by pin 3. Internal ring of bearing is placed on intermediate bushing 7 and is secured by nut 8. Bushing 7 is attached to shaft and forms with it a radial clearance for passage of air coolant. It is centered on the shaft by two setting bands. For passage of air they have spiral grooves a on the front, and at the rear and on the flange of bushing 7 there are grooves b.

Oil cavity of bearing from both sides is closed by covers 1 and 5 which have with bushing 7 a seal in the form of an oil-rejection thread A cut in holes of covers. Front cover 1, furthermore, by its bead fixes the bearing in the casing. On the outside, the bearing socket is air cooled. Owing to the pump action of spiral grooves a on shaft 6 and radial grooves b on flange of bushing, air coolant also passes through the clearance between bushing 7 and shaft 6.

### 7.7. Loads on Shafts and Bearings

During work, engine rotors are under the action of pressure forces of gases, forces of inertia and gravity.

Forces of gas pressure create torque and axial stresses in rotors. Inertial loads include: centrifugal force of unbalanced masses of rotor, centrifugal force of weight overload and gyroscopic moment. Centrifugal force of weight overload and gyroscopic moment are brief loads appearing during evolutions of aircraft.

Axial stresses in rotors appear due to the static pressure of gases and due to the dynamic impact of gas flow. Stress from static pressure of gases is equal to

$$P = pF, \quad (7.6)$$

where  $p$  is the static pressure of gases,

$F$  is the area of projection of wall or blade ring, which participate in creation of axial stress from pressure of gases, on a plane perpendicular to the axis of the rotor.

In general form

$$F = \frac{\pi}{4} (D^2 - d^2), \quad (7.7)$$

where  $D$  and  $d$  are the larger and smaller diameters limiting area  $F$ .

Stresses from dynamic impact of moving gas appear in blade rings and are determined by change of momentum:

$$P_x = \frac{G}{g} (c_{1a} - c_{2a}), \quad (7.8)$$

where  $G$  is expenditure of gas per second;

$c_{1a}$  and  $c_{2a}$  are axial speeds on inlet and outlet of blade rings;

$g$  is acceleration due to gravity.

Stress from dynamic impact of gases during their delayed motion ( $c_{1a} > c_{2a}$ ) is directed towards the flow gases, and during accelerated motion ( $c_{1a} < c_{2a}$ ), against the flow of gases. In the first case stress  $P_x$  by formula (7.7) is obtained with plus sign, and in the second case with negative sign. In accordance with this we take the direction of axial forces in rotors in the flow of gas as positive.

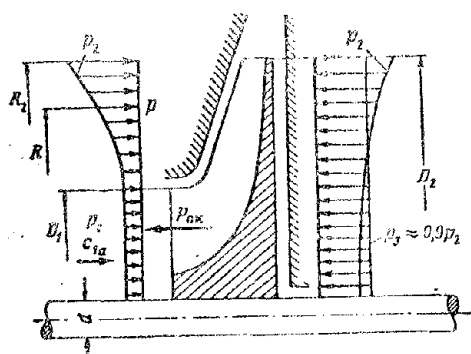


Fig. 7.18. Determination of axial force of rotor of centrifugal compressor.

Figure 7.18 depicts the diagram of a one-sided half-closed wheel of centrifugal compressor with diagrams of pressures acting from both sides of wheel. Here  $p_1$  and  $p_2$  are wheel inlet and outlet pressures, and  $p_3$  is pressure behind the wheel.

On the section from  $D_1$  to  $D_2$  in the wheel inlet area there acts axial stress

$$P_1 = p_1 F_1 + P_R.$$

Area  $F_1$  is determined by formula (7.7), and stress from dynamic impact of air flow  $P_R$  by formula (7.8). In the last case one should consider that axial speed  $c_{2a} = 0$ .

Air pressure in rotor wheel increases along radius  $R$  according to the law

$$p = p_2 \left( \frac{R}{R_2} \right)^2,$$

where  $R_2$  is external radius of wheel.

Then on the section from  $D_1$  to  $D_2$  on the disk of the wheel there will act an axial stress

$$P_2 = \int_{R_1}^{R_2} p 2\pi R dR = 2\pi \frac{p_2}{R_2^2} \int_{R_1}^{R_2} R^3 dR = \frac{\pi}{2} p_2 \left[ R_2^2 - R_1^2 \left( \frac{R_1}{R_2} \right)^2 \right].$$

From rear side on wheel there acts stress

$$P_3 = p_3 F_3,$$

where  $p_3 \approx 0.9 p_2$ .

Total axial stress acting on the one-sided half-closed wheel will be

$$P_{o,R} = P_1 + P_2 - P_3. \quad (7.9)$$

It is obtained with negative sign, i.e., it is directed towards the inlet area.

Absolute value of this stress can be determined also by empirical formula:

$$P_{o,R} = 0.011 (D_2^2 - d^2) u_2^2, \quad (7.10)$$

where  $u_2$  is peripheral velocity of wheel on diameter  $D_2$  m/sec,  $D_2$  and  $d$  are diameters of wheel, m (see Fig. 7.18).

At identical inlet conditions of double-sided axial stress  $P_{o,R} = 0$ . Different inlet conditions lead to the fact that from every side of the wheel the pressure and expenditure of air are different, and consequently the axial stresses

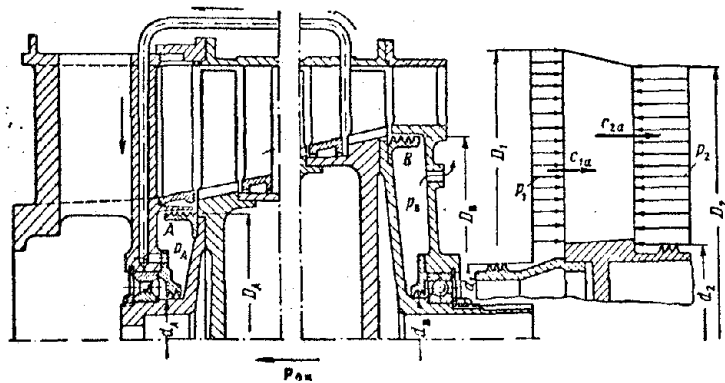


Fig. 7.19. Determination of axial force of the rotor of an axial-flow compressor.

on both sides of the wheel will also be different. Total axial stress of the wheel is determined by the difference of these stresses.

On each rotor wheel of an axial-flow compressor (Fig. 7.19) in the flow area there act axial stresses

$$\Delta P_o = p_1 F_1 - p_2 F_2 + P_{\alpha}$$

In the determination of areas  $F_1$  and  $F_2$  by formula (7.7) one should take  $D = \frac{D_1 + D_2}{2}$  (see Fig. 7.19).

From the face side on the rotor there act pressures  $p_A$  and  $p_B$  which are established in the compressor in chambers A and B. Axial stress in the rotor of an axial-flow compressor is equal to

$$P_{o.K} = \sum_i \Delta P_o + p_A F_A - p_B F_B, \quad (7.11)$$

where  $z$  is the number of compressor stages;

$F_A$  and  $F_B$  are the areas of projections of corresponding sections of rotor faces on a plane perpendicular to its axis, by formula (7.7).

In the rotor of an axial-flow compressor the axial stress  $P_{o.K}$  by formula (7.11) is obtained with negative sign, i.e., it is directed against the flow of air in the inlet area.

On the rotor wheel of the turbine shown in Fig. 7.20, from the front side there acts pressure of working gases on wheel inlet  $p_1$  and pressure of air coolant  $p_3$ , and from rear side, the pressure of working gases on wheel outlet  $p_2$  and pressure of gases in clearance between wheel and cone of exit nozzle  $p_4$ . Axial stress in rotor of turbine is equal to:

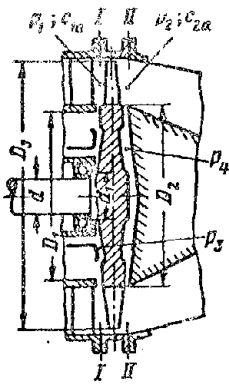


Fig. 7.20.  
Determination of  
axial force of  
rotor wheel of  
turbine.

$$P_{o.z} = p_1 F_1 + p_3 F_3 - p_2 F_2 - p_4 F_4 + P_R \quad (7.12)$$

where  $F_1$ ,  $F_2$ ,  $F_3$ , and  $F_4$  are areas of projections of corresponding sections of rotor wheel on plane perpendicular to axis of rotor, taken by formula (7.7).

In the absence of feed of air coolant to rear side of disk it is possible to consider  $p_4 = p_2$ .

In rotor of turbine, axial stress  $P_{o.T}$  by formula (7.12) is obtained with plus sign, i.e., it is directed toward flow of gases → toward outlet. Expansion of working gases in TRD turbines is incomplete, and in TVD complete. Therefore  $P_{o.T} < P_{o.K}$  in TRD and  $P_{o.T} \approx P_{o.K}$  in TVD.

Usually axial stresses in rotors of turbine and compressor attain considerable values and act in opposite directions. For unloading of bearings they apply axial fixation of rotors. In this case the resultant axial stress will be equal to:

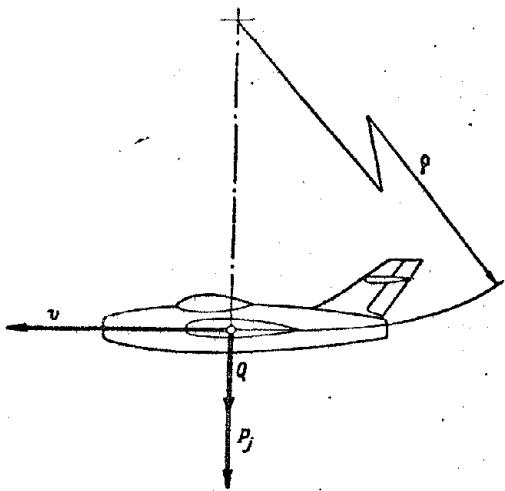
$$P_o = P_{o.K} - P_{o.z} \quad (7.13)$$

In addition to this, TRD have special unloading chambers. Thus for instance, in the diagram of the axial-flow compressor (see Fig. 7.19) there are front A and rear B unloading chambers formed by stator and face walls of rotor. Unloading of rotors is carried out by varying the pressure in chambers. For this, the front unloading chamber A with the help of a channel is connected with one of the compressor stages and heightened pressure  $p_A$  is created in it. Rear unloading chamber B through a hole is connected with the atmosphere or with the system of cooling of turbine and lowered pressure  $p_B$  is created in it. Unloading chambers have sealings in the flow-area of compressor and in the bearing unit area.

Unbalanced centrifugal force of rotor is determined by formula (6.5). This force is a constant revolving vector, periodically coinciding with direction of action of force of weight  $Q$ .

Centrifugal force of weight overload appears in the rotor during curvilinear flight of an aircraft. In calculations we take case of exit of an aircraft from diving (Fig. 7.21)

$$\rho_j = \frac{Q}{g} \frac{v^2}{r},$$



where  $Q$  is the weight of the rotor wheel;  
 $g$  is acceleration due to gravity;  
 $v$  is speed of the aircraft;  
 $\rho$  is the radius of curvature of trajectory.

Force  $P_j$  is directed normal to trajectory and at exit of aircraft from diving coincides with action of force of weight  $Q$ .

Force  $P_j$  is usually expressed through weight:

$$P_j = kQ, \quad (7.14)$$

Fig. 7.21. Determination of centrifugal force of weight over-load.

where  $k$  is the dynamic factor:

$$k = \frac{v^2}{\rho g} = \frac{\Omega v}{g}; \quad (7.15)$$

here  $\Omega = v/\rho$  is the angular velocity of the aircraft.

Dynamic factor  $k$  depends on type of aircraft and character of evolution.

In calculations for fighter aircraft they usually take  $k = 8$  to 10.

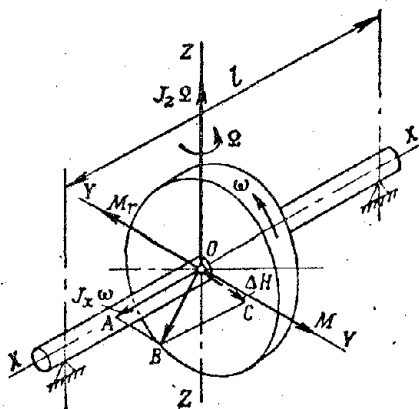


Fig. 7.22. Determination of gyroscopic moment of rotor.

Gyroscopic moment appears in the revolving rotor during curvilinear flight of an aircraft. In this case the GTD rotor obtains complicated rotation, i.e., with respect to its axis of rotation and with respect to the axis of rotation of the aircraft. Figure 7.22 depicts a rotor in the form of a disk placed on the shaft and revolving in supports with angular velocity  $\omega$  with respect to axis X-X. We shall impart to the rotor additional rotation with respect to vertical axis Z-Z with angular velocity  $\Omega$ . We obtain a system with two rotations with respect to intersecting axes X-X and Z-Z. Rotation with respect to axis X-X will be relative, and with respect to an axis Z-Z, transposed.

Momenta with respect to axes X-X and Z-Z correspondingly will be  $J_x \omega$  and  $J_z \Omega$ , where  $J_x$  and  $J_z$  are moments of inertia of rotor with respect to axes X-X and Z-Z. Vectors of momenta are plotted just as vectors of angular velocities on axis

of rotation. Direction of vector of angular momentum is determined by the following rule: if one were to look from the end of the vector (towards the arrow) on its base (on plane of rotation), one may see rotation of disk counterclockwise.

From mechanics it is known that the moment of external forces acting on a revolving body with respect to its axis of rotation is equal to the change of momenta referred to a unit of time:

$$M = \frac{\Delta H}{\Delta t},$$

where  $\Delta H$  is the change of angular momentum during the time  $\Delta t$ . When  $\Omega = \text{const}$ , angular momentum  $J_z \Omega$  is constant in magnitude and direction. Therefore it does not render influences on rotor.

Momentum  $J_x \omega$  when  $\omega = \text{const}$  is also constant in magnitude, but its vector continuously changes its direction, accomplishing uniform rotation with respect to axis Z-Z together with the rotor system in its transfer motion with angular velocity  $\Omega$ .

After an element of time  $\Delta t$  vector OA =  $J_x \omega$  will turn at angle  $\Omega \Delta t$ , and its end will shift to point B (see Fig. 7.22). We shall unite points A and B and complement the obtained vector triangle OAB to parallelogram OABC. Vector OB is the geometric sum of vectors OA and OC. Designating component vector OC through  $\Delta H$ , we obtain:

$$\Delta H = J_x \omega \Omega \Delta t.$$

Component vector  $\Delta H$  is the change of angular momentum  $J_x \omega$  during the time  $\Delta t$  during transfer motion of rotor. It appears as a result of action of external moment applied in the area of the aircraft to the rotor through its supports.

External moment M is equal to:

$$M = \frac{\Delta H}{\Delta t} = J_x \omega \Omega,$$

Vector of moment M will be located on axis Y-Y and in the direction of vector  $\Delta H$ .

In accordance with Newton's third law in the area of the rotor, on its supports there will act an oppositely directed moment of inertial forces. This moment is called gyroscopic

$$M_r = -M,$$

Figure 7.22 depicts gyroscopic moment  $M_g$  by the vector located on axis Y-Y. It is directed opposite the vector of external moment M.

For axes of rotation of rotor X-X and Z-Z, intersecting at a right angle, gyroscopic moment will be expressed by the formula:

$$M_g = J_x \omega \Omega. \quad (7.16)$$

If axes X-X and Z-Z intersect at angle  $\alpha$ , gyroscopic moment will be expressed by the formula:

$$M_g = J_x \omega \Omega \sin \alpha. \quad (7.17)$$

Under action of gyroscopic moment the rotor attempts to turn with respect to axis Y-Y in such a manner that its axis of relative rotation X-X becomes parallel to the axis of transposed rotation Z-Z (or is combined with it) and that the directions of relative and transposed rotations coincide.

In the calculations we shall take the case of exit of an aircraft from diving at  $\alpha = 90^\circ$ . In this case gyroscopic moment has maximum value and acts on rotor in horizontal plane.

Value of angular velocity of aircraft  $\Omega$  depends on its type and character of evolution. For fighters during pullout it is possible to take  $\Omega = 0.2$  to 0.5

1/sec.

Example. Determine the inertial loads of a turbine rotor.

Given: unbalance of rotor D = 15 g·cm; Q = 96 kg; k = 8;  $J_x = 34.25 \text{ kg} \cdot \text{cm} \cdot \text{sec}^2$ ;  $\omega = 1210 \text{ 1/sec}$ ;  $\Omega = 0.314 \text{ 1/sec}$ .

Unbalanced centrifugal force in the rotor by formula (6.5) is equal to:

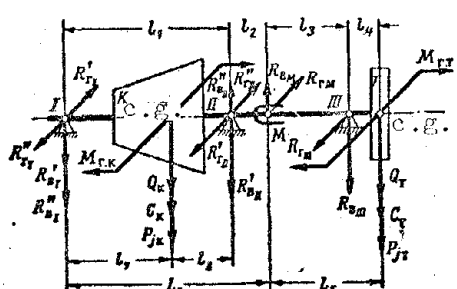


Fig. 7.23. Determination of loads on GTD rotor bearings.

$$C = 15 \left( \frac{1210}{1000} \right)^2 = 22 \text{ kg.}$$

Centrifugal force of weight overload by formula (7.14) is equal to:

$$P_J = 8 \cdot 96 = 768 \text{ kg.}$$

Gyroscopic moment by formula (7.16) is equal to:

$$M_g = 34.25 \cdot 1210 \cdot 0.314 = 13000 \text{ kg} \cdot \text{cm.}$$

Loads acting on bearings of GTD rotors. Axial resultant stress in the rotor

of an engine [see formula (7.13)] is perceived by one radial-thrust bearing unit.

Radial loads are perceived by all bearings. Maximum load of bearings by radial loadings correspond to moment of pullout of aircraft.

Figure 7.23 depicts the forces and moments acting on a three-support rotor.

Forces  $Q$ ,  $C$  and  $P_j$  are applied to centers of gravity of rotors of compressor and turbine and in calculations act in the vertical plane coinciding in direction. Gyroscopic moment acts in horizontal plane.

Using the known laws of mechanics, we break down the acting forces and moments into forces applied to supports. In support III and connector M there will act these forces: in vertical plane

$$R_{vIII} = (Q_r + C_r + P_{j,r}) \frac{l_5}{l_3} \text{ and } R_{vM} = (Q_r + C_r + P_{j,r}) \frac{l_4}{l_3}$$

and in horizontal plane

$$R_{rIII} = R_{rM} = \frac{M_{r,r}}{l_3}.$$

In supports I and II there will act these forces: in vertical plane

$$R_{vI} = (Q_k + C_k + P_{j,k}) \frac{l_3}{l_1} + R_{vM} \frac{l_2}{l_1}$$

and

$$R_{vII} = (Q_k + C_k + P_{j,k}) \frac{l_7}{l_1} - R_{vM} \frac{l_6}{l_1},$$

or

$$R_{vI} = R'_{vI} + R''_{vI} \text{ and } R_{vII} = R'_{vII} - R''_{vII};$$

in horizontal plane

$$R_{rI} = \frac{M_{r,k}}{l_1} - R_{rM} \frac{l_3}{l_1} \text{ and } R_{rII} = \frac{M_{r,k}}{l_1} - R_{rM} \frac{l_7}{l_1},$$

or

$$R_{rI} = R'_{rI} - R''_{rI} \text{ and } R_{rII} = R'_{rII} - R''_{rII}.$$

Resultant radial loadings on bearings are found from the expression

$$R = \sqrt{R_v^2 + R_r^2}.$$

According to the obtained loads we select the bearings.

#### 7.8. Strength Calculation

Calculation of shafts. Shafts of GTD rotors during operation are subjected

to torsion, bending, and extension.

Shafts of rotors are twisted by torque

$$M_{sp} = 71620 \frac{N}{n}, \quad (7.18)$$

where N is the power transmitted through shaft;

n is the rpm rate of the shaft.

Torsional stress

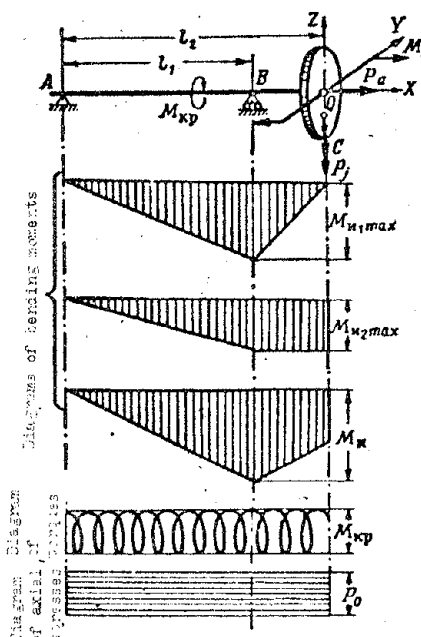
$$\tau = \frac{M_{kp}}{W_{kp}}, \quad (7.19)$$

where moment of resistance to torsion

$$W_{kp} = \frac{\pi}{16} \frac{d^4 - d_0^4}{d}; \quad (7.20)$$

here d and  $d_0$  are the external and internal diameters of shaft (see Fig. 7.3a).

During calculation of shaft for bending we take into account both the constant and brief loads. The latter appear during evolutions of the aircraft.



Loads bending the shaft:

- 1 - force of weight of rotor wheel  $Q$  kg;
- 2 - unbalanced centrifugal force of rotor  $C$ ;
- 3 - centrifugal force of weight overload  $P_j$ ;
- 4 - gyroscopic moment  $M_r$ .

Shaft of rotor bends in two planes: in vertical under the action of forces  $Q$ ,  $C$ , and  $P_j$ , and in horizontal under the action of gyroscopic moment  $M_r$ . Diagrams of bending moments of turbine shaft with slanted location of disk are shown in Fig. 7.24: in vertical plane  $M_{u1}$  and in horizontal  $M_{u2}$ .

At point B bending moments are equal to

$$M_{u1, max} = (Q + C + P_j)(l_2 - l_1); \quad (7.21)$$

$$M_{u2, max} = M_r = J_x \omega \Omega. \quad (7.22)$$

Fig. 7.24. Strength calculation of turbine shaft.

Total bending moment is equal to

$$M_u = \sqrt{M_{u1}^2 + M_r^2}. \quad (7.23)$$

Bending stress of shaft is equal to

$$\sigma_u = \frac{M_u}{W_u}, \quad (7.24)$$

where moment of resistance to bending

$$W_u = \frac{\pi}{32} \frac{d^3 - d_0^3}{d}. \quad (7.25)$$

Here  $d$  and  $d_0$  are the external and internal diameters of shaft (see Fig. 7.3a).

Axial stress  $P_0$  acting on rotor stretches the shaft. Tensile stress of shaft from axial stress is equal to

$$\sigma_p = \frac{P_0}{F}, \quad (7.26)$$

where area of section of shaft

$$F = \frac{\pi}{4} (d^2 - d_0^2). \quad (7.27)$$

Total normal stress of shaft

$$\sigma = \sigma_u + \sigma_p. \quad (7.28)$$

Combined stress is found by third theory of strength:

$$\sigma_{cs} = \sqrt{\sigma^2 + 4\tau^2}; \quad (7.29)$$

for GPD  $\sigma_{cs} \leq 4000 \text{ kg/cm}^2$ .

Example. Determine stresses of turbine shaft (see Fig. 7.24).

Given:  $N = 13,800 \text{ hp}$ ;  $n = 11,560 \text{ rpm}$ ;  $Q = 96 \text{ kg}$ ;  $C = 22 \text{ kg}$ ;  $P_j = 768 \text{ kg}$ ;  $M_T = 13000 \text{ kg}\cdot\text{cm}$ ;  $P_0 = 1500 \text{ kg}$ ;  $d = 76 \text{ mm}$ ;  $d_0 = 62 \text{ mm}$ ;  $l_1 = 374 \text{ mm}$ ;  $l_2 = 513 \text{ mm}$ .

Torque by formula (7.18)

$$M_{kp} = 71620 \frac{13850}{11560} = 86000 \text{ kg}\cdot\text{cm}.$$

Moment of resistance to torsion by formula (7.20)

$$W_{kp} = \frac{3.14}{16} \cdot \frac{7.6^4 - 6.2^4}{7.6} = 48 \text{ cm}^3.$$

Torsional stress by formula (7.19)

$$\tau = \frac{86000}{48} = 1795 \text{ kg/cm}^2.$$

Maximum bending moment in vertical plane by formula (7.21)

$$M_{u1max} = (96 + 22 + 768) \cdot (51.3 - 37.4) = 12300 \text{ kg}\cdot\text{cm}.$$

Total bending moment on support B by formula (7.23)

$$M_B = \sqrt{12300^2 + 13000^2} = 17900 \text{ kg}\cdot\text{cm}.$$

Moment of resistance to bending by formula (7.25)

$$W_s = \frac{W_{sp}}{2} = 24 \text{ cm}^3.$$

Bending stress by formula (7.24)

$$\sigma_s = \frac{17900}{24} = 747 \text{ kg/cm}^2.$$

Area of section of shaft by formula (7.27)

$$F = \frac{3.14}{4} (7.6^2 - 6.2^2) = 15.2 \text{ cm}^2.$$

Tensile stress by formula (7.26)

$$\sigma_p = \frac{1500}{15.2} = 99 \text{ kg/cm}^2.$$

Total normal stress by formula (7.28)

$$\sigma = 747 + 99 = 846 \text{ kg/cm}^2.$$

Combined stress by formula (7.29)

$$\sigma_{ct} = \sqrt{846^2 + 4 \cdot 1795^2} = 3700 \text{ kg/cm}^2.$$

Obtained stress is in permissible limits.

Calculation of slit connections is produced for crumpling and shearing:

$$\sigma_{cm} = \frac{8M_{kp}}{(D^2 - d^2) z l k} \quad \dots \quad (7.30)$$

$$\tau_{cp} = \frac{4M_{kp}}{(D + d) z l b k} \quad \dots \quad (7.31)$$

where  $M_{kp}$  is the torque transmitted through slits;  $D$  and  $d$  are the external and internal diameters of working surfaces of slits (Fig. 7.25a);  $z$  is the number of slits;  $l$  is the length of working surface of slits;  $b$  is the thickness of slits;  $k$  is the variation factor of distribution of load on slits.

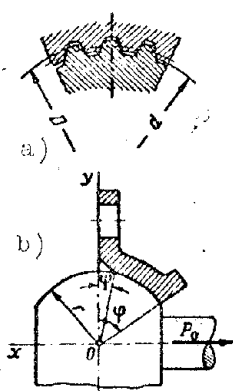


Fig. 7.25. Strength calculation of slit and ball and socket joints of shafts.

In gas-turbine engines  $\sigma_{cm} = 500$  to  $2000 \text{ kg/cm}^2$  and  $\tau_{cp} = 400$  to  $1500 \text{ kg/cm}^2$ .

Upper limit pertains to fixed connections to motionless, precision made, and lower refers to mobile connections, having misalignments and impact load during operation.

Example. Determine crumpling stress of the slit connection of the driving bushing with the turbine shaft.

Given:  $M_{kp} = 86,000 \text{ kg}\cdot\text{cm}$ ;  $D = 74.6 \text{ mm}$ ;  $d = 68.2 \text{ mm}$ ;

$a = 15$ ;  $b = 7 \text{ mm}$ ;  $l = 72 \text{ mm}$ ;  $k = 0.75$ .

Crumpling stress in slits by formula (7.30)

$$\sigma_{\text{cm}} = \frac{8.86000}{(7.46^2 - 6.82^2) \cdot 15 \cdot 7.2 \cdot 0.75} = 923 \text{ kg/cm}^2.$$

Shear stress in slits by formula (7.31)

$$\tau_{\text{cp}} = \frac{4.86000}{(7.46 + 6.82) \cdot 15 \cdot 7.2 \cdot 0.75} = 425 \text{ kg/cm}^2.$$

Calculation of hinged ball and socket joint of rotor shafts is produced with respect to axial stress of turbine rotor (see Fig. 7.25b). Maximum normal specific pressure on support surface of ball and socket joint is found by the formula

$$p_{\text{max}} = 1.5 \frac{P_0 \sin \varphi}{k \pi r^2 (\sin^3 \varphi - \sin^3 \psi)}, \quad (7.32)$$

where  $P_0$  is the axial stress of turbine rotor;

$k$  is the utilization factor of support surface;

$r$  is the radius of the sphere;

$\varphi$  and  $\psi$  are angles limiting the support surface of the sphere.

Coefficient  $k$  considers grooves for assembly of the ball and socket joint (see Fig. 7.5), which decrease support surface. With grooves  $k = 0.5$ , and without them  $k = 1$ .

In existing GPD  $p_{\text{max}} \approx 800 \text{ kp/cm}^2$ .

Example. Determine maximum specific pressure on the ball and socket joint of rotors of turbine and compressor.

Given:  $P_0 = 1185 \text{ kg}$ ;  $\varphi = 30^\circ$ ;  $\psi = 0^\circ$ ;  $r = 30 \text{ mm}$ ;  $k = 0.5$ .

Maximum specific pressure by formula (7.32)

$$p_{\text{max}} = \frac{1.5 \cdot 1185 \cdot 0.5}{0.5 \cdot 3.14 \cdot 3^2 \cdot 0.5^3} = 504 \text{ kg/cm}^2.$$

Calculation of bolts (pins) of flanged joints. During transmission of torque  $M_{\text{fl}}$  through a flanged joint by friction (see Fig. 7.3a) the necessary compression force of the joint  $T$  is found from the expression;

$$T = \frac{\epsilon M_{\text{fl}}}{R_{\text{cp}} \mu^2}, \quad (7.33)$$

where  $\alpha = 1.25$  to  $1.5$  is the tightening factor;

$R_{cp}$  is the mean radius of surface of friction;

$\mu = 0.15$  to  $0.2$  is the coefficient of friction of the flanges;

$z$  is the number of bolts (pins);

$$R_{cp} \approx \frac{R_2 + R_1}{2},$$

here  $R_2$  and  $R_1$  are the external and internal radii of the flanged joint (see Fig. 7.26).

In case of loading of the flanged joint by bending moment  $M_M$  and axial force  $P_0$  the resultant axial load arriving on the bolt (Fig. 7.26) can be found by the formula:

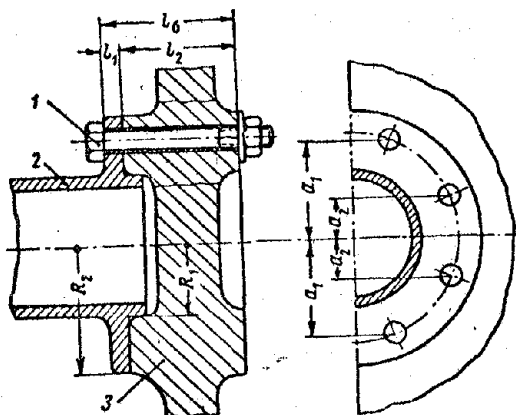


Fig. 7.26. Strength calculation of bolts of a flanged joint.

$$P = \frac{M_M a_1}{4 \sum_1^n a_l^2} + \frac{P_0}{z}, \quad (7.34)$$

where  $\sum a_l^2 = a_1^2 + a_2^2 + \dots$  (see Fig. 7.26);  $n$  is the number of pairs of bolts.

In the presence of a rigid flanged joint (without elastic linings of flanges) we frequently are limited to the calculation of bolts (pins) with respect to force of preliminary tightening

$$T = \alpha P. \quad (7.35)$$

In this case the tensile stress will be equal to

$$\sigma = \frac{T}{f}, \quad (7.36)$$

where  $f$  is the calculated section of the bolt.

In GVD bolts (pins) usually operating under conditions close to static loading. Their safety factor

$$n = \frac{\sigma_T}{\sigma}, \quad (7.37)$$

where  $\sigma_T$  is the yield point of bolt material at operating temperature.

Usually under normal temperature conditions we take  $n \geq 1.5$ . At heightened operating temperatures we take  $n > 2.5$ . In this case we consider the possibility of weakening of the tightening of the joint due to the phenomenon of creep of materials; therefore, larger stresses in bolts (pins) are not permitted.

Example. Determine the safety factor of pins of the flanged joint of the wheel of a centrifugal compressor with shaft transmitting torque by friction at the

surface of the joint (see Fig. 7.3a).

Given:  $M_{kp} = 70,000 \text{ kg}\cdot\text{cm}$ ;  $z = 8$ ;  $\mu = 0.2$ ;  $\alpha = 1.25$ ;  $f = 1.52 \text{ cm}^2$ ;  $R_{cp} = 70 \text{ mm}$ ;  $\sigma_T = 9500 \text{ kg/cm}^2$ .

Necessary tightening stress by formula (7.33) is equal to

$$T = \frac{1.25 \cdot 70000}{7 \cdot 0.2 \cdot 8} = 7800 \text{ kg.}$$

Tensile stress of pin on thread by formula (7.36) is equal to

$$\sigma_p = \frac{7800}{1.52} = 5130 \text{ kg/cm}^2$$

Safety factor of pin by formula (7.37) is equal to:

$$n = \frac{9500}{5130} = 1.85.$$

Example. Determine the stress and safety factor of bolts of the flanged joint of a turbine disk with shaft during a load by bending moment and axial force.

Given:  $M_B = 13,900 \text{ kg}\cdot\text{cm}$ ;  $P_{0,T} = 1250 \text{ kg}$ ;  $z = 8$ ;  $a_1 = 64$ ;  $a_2 = 27 \text{ mm}$ ;  $\alpha = 1.5$ ;  $f = 63.5 \text{ mm}^2$ ;  $\sigma_T = 9000 \text{ kg}\cdot\text{cm}^2$ .

Basic load of bolts by formula (7.34) is equal to

$$P = \frac{13900 \cdot 6.4}{4(6.4^2 + 2.7^2)} + \frac{1250}{8} = 616 \text{ kg.}$$

Preliminary tightening of bolt by formula (7.35) is equal to

$$T = 1.5 \cdot 616 = 925 \text{ kg.}$$

Tensile stress by formula (7.36) is equal to

$$\sigma_p = \frac{925}{0.635} = 1455 \text{ kg/cm}^2.$$

Safety factor of bolt by formula (7.37)

$$n = \frac{9000}{1455} = 6.2.$$

Thermal stresses of bolts of a flanged joint (see Fig. 7.26) appear at heightened operating temperatures, if coefficients of linear expansion in connective components 2 and 3 are greater than for bolts 1.

Usually the operating temperature of bolts and flanges is identical and their difference in thermal expansions is:

$$\Delta l = \left( \sum_{i=1}^k x_i l_{x,i} - \alpha_p l_0 \right) \Delta t,$$

where  $\alpha_{\Delta i}$  and  $\alpha_6$  are the coefficients of linear expansion of individual connective components and the bolt;

$l_{\Delta i}$  and  $l_6$  is the thickness of flanges of components and length of bolt;

$\Delta t$  is the increase of temperature during work;

$k$  is the number of connective components.

With sufficient accuracy for practice it is possible to disregard elasticity of flanges. Then under the influence of thermal loads the bolt obtains the aspect ratio

$$\lambda_i = \frac{\Delta t}{l_6}.$$

Hence we obtain the expression of thermal stress of bolts:

$$\sigma_t = \lambda_i E_6 = \frac{\sum_{i=1}^k \alpha_{\Delta i} l_{\Delta i} - \alpha_6 l_6}{l_6} \Delta t E_6, \quad (7.38)$$

where  $E_6$  is the elastic modulus of bolt material at operating temperature.

Example. Determine the thermal stresses of bolts of the preceding example.

Given:  $\alpha_6 = \alpha_{\Delta 1} = 12 \cdot 10^{-6}$ ;  $\alpha_{\Delta 2} = 21 \cdot 10^{-6}$ ;  $l_{\Delta 1} = 16 \text{ mm}$ ;  $l_{\Delta 2} = 10 \text{ mm}$ ;  $l_6 = 26 \text{ mm}$ ;  $\Delta t = 300^\circ\text{C}$ ;  $E_6 = 1.75 \cdot 10^6 \text{ kg/cm}^2$ ;  $\sigma_T = 9000 \text{ kg/cm}^2$ ,

Additional thermal stresses of bolt by formula (7.38) are equal to:

$$\sigma_t = \frac{12 \cdot 10^{-6} \cdot 1.6 + 21 \cdot 10^{-6} \cdot 1 - 12 \cdot 10^{-6} \cdot 2.6}{2.6} \cdot 300 \cdot 1.75 \cdot 10^6 = \\ = 1820 \text{ kg/cm}^2.$$

Total stress

$$\sigma_s = \sigma + \sigma_t = 1455 + 1820 = 3275 \text{ kg/cm}^2.$$

Safety factor of bolt

$$n = \frac{9000}{3275} = 2.75.$$

Thermal stresses considerably lower the safety factor.

### 7.9. Materials

Shafts are manufactured from structural alloyed steel [4KhNMA] (40XHMA), [18KhNVA] (18XHBA), and [12Kh2N4A] (12X2H4A), and connecting sleeves from steel 18KhNVA and 12Kh2N4A. The components forming the ball and socket joint connection of shafts have cemented working surfaces.

The material for the roller and ball bearings is usually high-carbon chrome-magnagese steel. For bearings working at heightened temperatures they use steel of the instrument type containing tungsten, vanadium, and others additives. Bearing cells are made from bronze, aluminum, or other durable antifriction alloys.

## C H A P T E R VIII

### CRITICAL SPEEDS OF ROTOR SHAFTS

#### 8.1. General Information

Besides the basic strength calculation, rotor shafts are checked for bending vibrations. This check reduces to the determination of critical speeds and selection of such dimensions of shaft at which the period of its natural bending vibrations does not coincide with the period of change of external forces, i.e., the phenomenon of resonance does not take place. In case of resonance the amplitude of vibrations of shaft increases and can attain such values at which the shaft can be destroyed. Speed of rotor at which resonance occurs is called critical.

#### 8.2. Harmonic Motion

If one were to consider rotation of a point A on the circumference of radius R with constant angular velocity  $\rho$ , the projections of it  $A_x$  and  $A_y$  on axes of coordinates will accomplish harmonic motions (Fig. 8.1). We designate by  $A_0$  the position of point A in initial moment of time  $t = 0$  which is determined by angle  $\beta_0$ . Then the current position of point A in turn will be determined by angle  $\rho t + \beta_0$  and motion of its projections on axes of coordinates can be expressed in analytic form. Thus, for instance, for projection  $A_y$  we obtain the following expression:

$$y = R \sin(\rho t + \beta_0). \quad (8.1)$$

This expression represents a function periodic in time  $t$  with period of change  $2\pi$ . It expresses harmonic motion of point  $A_y$  with respect to its middle

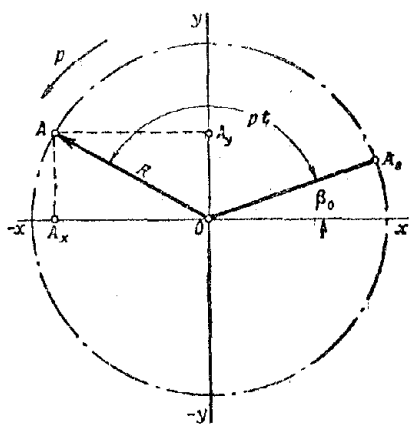


Fig. 8.1. Geometric presentation of harmonic motion.

position, i.e., the origin of coordinates.

In expression (8.1) the magnitude  $R$  is called the amplitude of function. It is the magnitude of maximum deviation of point  $A_y$  from the origin of coordinates during harmonic motion. Magnitude  $p$  is called the circular frequency of harmonic motion,  $p t + \beta_0$  is the phase, and  $\beta_0$  is the initial phase. Harmonic motion constitutes simple vibrational motion:

### 8.3. Natural Bending Vibrations of a Shaft

Figure 8.2 depicts a double-support shaft with a disk on it. Shaft possesses elasticity; therefore, upon giving it a shock in the plane of the disk it will start to vibrate. These are called bending vibrations since they are accompanied by bending

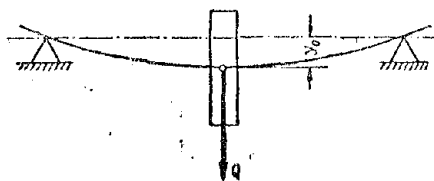


Fig. 8.2. Deflection of a shaft under the action of a static load.

of the shaft. These vibrations are also called natural or free, since the shaft, initially removed by the shock from the state of rest, accomplishes its own vibrations freely without the influence of external forces, and only due to its elasticity and inertia of the disk mass (mass of shaft will be disregarded). Force of elasticity of the double-support shaft is expressed by the following formula;

$$P_{y0} = \frac{48EIy}{l^3} = K_0 y, \quad (8.2)$$

where  $y$  is deflection of shaft;

$E$  is the elastic modulus of the shaft material;

$J$  is the moment of inertia of a section of the shaft;

$l$  is the length of the shaft;

$K = \frac{48EI}{l^3}$  is the stiffness coefficient of shaft during bending.

Stiffness coefficient of shaft during bending is the force which evokes deflection of shaft in 1 cm. If under the action of force  $Q$  the shaft has deflection  $y_0$  (see Fig. 8.2), then

$$K = \frac{Q}{y_0} \quad (8.3)$$

Force of inertia  $P_j$  appears because of the motion of the disk during vibrations with variable speed,

$$P_j = -m \frac{d^2y}{dt^2} = -my'' \quad (8.4)$$

where  $y$  is shift of disk during its vibrations;

$m = \frac{Q}{g}$  is mass of disk by weight  $Q$  kg;

$y'' = \frac{d^2y}{dt^2}$  is acceleration of disk in its vibrational motion.

According to D'Alembert's principle, during natural vibrations of a shaft the forces of its elasticity are equal to the forces of inertia of the disk:

$$P_{\text{in}} = P_j$$

or, putting expressions (8.2) and (8.4), we obtain:

$$Ky = -my''$$

Whence

$$y'' + \frac{K}{m} y = 0 \quad (8.5)$$

Here we obtain a differential equation of the second order. The solution of this equation will be a periodic function in time  $t$  with period of change  $2\pi$ :

$$y = y_A \sin\left(\sqrt{\frac{K}{m}} t + \beta_0\right) \quad (8.6)$$

Differentiating it twice, we obtain:

$$y'' = \frac{d^2y}{dt^2} = -y_A \frac{K}{m} \sin\left(\sqrt{\frac{K}{m}} t + \beta_0\right) \quad (8.7)$$

Placing expressions (8.6) and (8.7) in equation (8.5), we obtain an identity that proves the correctness of solution (8.6). Comparing expression (8.6) with (8.1), we conclude that bending vibrations of shaft with disk have the character of harmonic motion with amplitude  $y_A$ , circular frequency  $\rho = \sqrt{\frac{K}{m}}$  and initial phase  $\beta_0$ . The period of natural vibrations of the shaft

$$T = \frac{2\pi}{\rho} = 2\pi \sqrt{\frac{m}{K}} \text{ sec.} \quad (8.8)$$

and frequency of natural vibrations of shaft

$$f_c = \frac{1}{T} = \frac{1}{2\pi} \sqrt{\frac{K}{m}} \text{ vib/sec.} \quad (8.9)$$

#### 8.4. Critical Speed of a Shaft with One Disk

Figure 8.3a depicts a double-support shaft with a disk on it. The center of gravity of the disk  $s$  does not coincide with axis of rotation of shaft A-B,

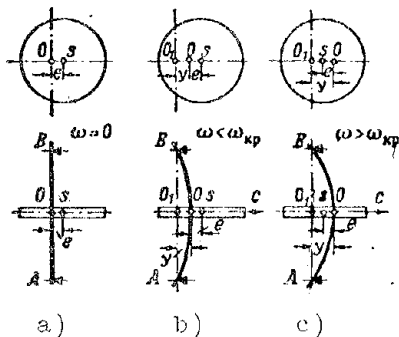


Fig. 8.3. Double-support shaft with eccentrically fitted disk.

forming eccentricity  $e$ . So that we subsequently may exclude from consideration the deflection of shaft from the force of weight of the disk, in the figure the shaft is located vertically.

During rotation of rotor the disk experiences centrifugal force  $C$ , which is called deflection of shaft  $y$  (see Fig. 8.3b). Rotation of rotor will occur with respect to vertical axis  $A_1O_1B$ , center of shaft  $O$  in plane of disk will describe a circumference with radius of  $y$ , and center of gravity of disk  $s$ , a circumference with radius of  $y + e$ . With angular velocity of rotation  $\omega$  centrifugal force of disk will be equal to:

$$C = m(y+e)\omega^2,$$

where  $m$  is the mass of the disk.

This force is balanced by elasticity of the shaft

$$C = P_{y_{\text{up}}}$$

or

$$m(y+e)\omega^2 = Ky;$$

whence, deflection of shaft is equal to:

$$y = \frac{e}{\frac{K}{m\omega^2} - 1}. \quad (8.10)$$

With increase of angular velocity of rotation  $\omega$  the denominator in formula (8.10) will decrease, i.e., deflection of shaft will increase. With  $\omega$  equal to

$$\omega_{\text{kp}} = \sqrt{\frac{K}{m}}, \quad (8.11)$$

the denominator of expression (8.10) becomes equal to zero, and deflection of shaft  $y$  is infinite. Angular velocity of rotation  $\omega_{\text{kp}}$  is called critical.

Critical speed of shaft per minute will be equal to:

$$n_{\text{kp}} = \frac{30\omega}{\pi} = \frac{30}{\pi} \sqrt{\frac{K}{m}} \text{ rpm.} \quad (8.12)$$

Placing under the radical, instead of mass of disk, its weight  $Q = mg$ , we obtain:

$$\omega_{kp} = \frac{30}{\pi} \sqrt{\frac{9\pi K}{Q}} \approx 300 \sqrt{\frac{K}{Q}} \text{ rpm.} \quad (8.13)$$

Critical speed of shaft per second will be equal to:

$$\omega_{kp, cek} = \frac{\omega_{kp}}{60} = \frac{1}{2\pi} \sqrt{\frac{K}{m}}. \quad (8.14)$$

From comparison of obtained expression (8.14) with expression (8.9) it is clear that critical speed of shaft is equal to the frequency of its natural vibrations:

$$\omega_{kp, cek} = f_c.$$

This corresponds to the phenomenon of resonance at which the shaft becomes dynamically unstable. It experiences vibrations passing into large beats. Operation at critical speeds is not allowed, since there is possible destruction of shaft and the engine may go out of order. Speeds of shaft below critical are called subcritical, and above critical are called supercritical.

With increase of angular velocity of rotation of shaft, when  $\omega > \omega_{kp}$  (in the region of supercritical speeds), the denominator of expression (8.10) becomes negative and increases with respect to its absolute value. As shown by experience, deflection of shaft  $y$  quickly decreases and the shaft again becomes dynamically stable. The negative sign obtained in the right part of expression (8.10) indicates the fact that eccentricity  $e$  is opposite deflection of shaft  $y$  (see

Fig. 8.3c).

When  $\omega \rightarrow \infty$ ,  $y$  in turn tends to  $-e$ . Thus, at high speeds of rotation the rotor tends to revolve around its own center of gravity  $s$  (see Fig. 8.3c). Figure 8.3 also shows the mutual location of the center of rotation of disk  $O_1$ , center of shaft  $O$ , and center of gravity of disk  $s$  in the plane of rotation of the disk at various speeds of rotation.

Figure 8.4 shows the graph of  $y = f(\omega)$ , built by formula 8.10. The right branch of the

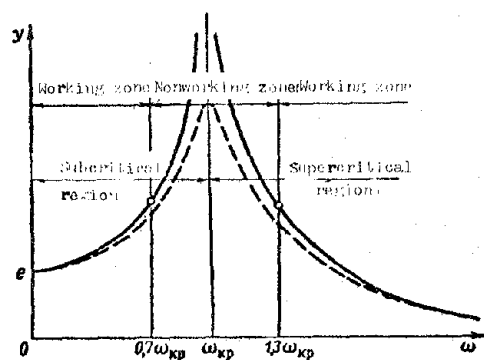


Fig. 8.4. Dependence of deflection of shaft on the speed of its rotation.

graph is built taking into account the simultaneous change of sign in the denominator and numerator (in eccentricity of disk e). Deflection of shaft y preserves the plus sign and in case  $\omega > \omega_{kp}$ .

When  $\omega + \omega_{kp}$  deflection shaft becomes equal to infinity. However, due to resistances in the rotor system deflection of shaft y in this case practically preserves a finite value, as is depicted by the dotted curve in Fig. 8.4. Nonetheless, deflection of shaft can then be considerable and impermissible for the strength of the shaft.

Working speed of rotation of rotor can be less or greater than critical speed. If operating conditions are subcritical ( $\omega < \omega_{kp}$ ), the shaft is called rigid. If, however, operating conditions are supercritical ( $\omega > \omega_{kp}$ ), the shaft is called flexible. In process of spin-up (from small speeds to working speeds) flexible shafts pass through the zone of critical speed. This is not dangerous when transition is accomplished without delay at critical speeds, since in this case the shaft does not receive large deflections.

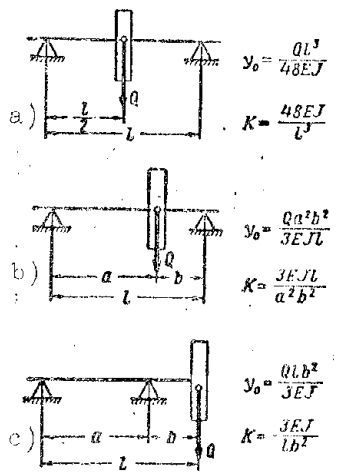


Fig. 8.5. Values of deflections and stiffness coefficients of shaft during bending.

Critical speed of shaft  $n_{kp}$  can also be expressed through static deflection of shaft  $y_0$  from the action of force of weight of disk Q. For this, in formula (8.13) we place expression (8.3) of the stiffness coefficient K. After reduction we obtain:

$$n_{kp} \approx \frac{30}{\sqrt{y_0}} \text{ rpm.} \quad (8.15)$$

Static deflection of shaft of rotor  $y_0$  is determined by the known formulas of resistance of materials depending upon power structure of the shaft. Figure 8.5 gives expressions of static deflections and stiffness coefficients of a shaft during bending.

From Fig. 8.4 it follows that deflection of shaft y attains its dangerous values not only at critical (resonance) speeds, but also in the zone nearest to them. Therefore, for guarantee of reliability it is desirable that critical speeds  $n_{kp}$  of the engine be somewhat further from working speeds n. It is possible, for instance, to recommend that  $n_{kp}$  be 30% more or less than n.

Since critical speeds of shaft  $n_{kp}$  [see formulas (8.15) and (8.13)] depend on its static deflection  $y_0$  or on the relation of the stiffness coefficient  $K$  to weight of disk  $Q$ , then, changing the latter, it is possible also to change the critical speed of the shaft. In practice, during coincidence of critical speeds of shaft with working speeds, critical speeds are usually displaced to one side of the zone of operating conditions by the change of stiffness coefficient  $K$  of the shaft. This is done by changing the diameters of the shaft. Addition of a support for the shaft also leads to an increase of its stiffness coefficient.

Rigid shafts frequently are thick, and consequently also heavy. Therefore, [GTD] (ГДЛ) shafts are sometimes flexible. In order to obtain their critical speeds lower than working speeds and not to weaken the shaft, the shaft system sometimes contains certain elastic elements lowering the rigidity of the system on the whole. An example of this could be the elastic bushing  $\gamma$  between the shaft and bearing of the [TRD] (ТРД) [VK-1] (ВК-1) (see Fig. 7.17). If deflections of flexible shaft upon transition through critical speeds exceed permissible, it is necessary to apply deflection limiters or damping devices. A deficiency of the flexible shaft is its increased deflection which takes place during aircraft evolutions under action of the force of weight overload  $P_j$  and gyroscopic moment  $M_F$ . Here, so that the rotor does not graze around the stator, the clearances between them must be increased.

Example. Determine the critical speed of the shaft of a centrifugal compressor made according to the diagram (Fig. 8.5b).

Given:  $Q = 120 \text{ kg}$ ;  $d = 103 \text{ mm}$ ;  $d_0 = 88 \text{ mm}$ ;  $a = 13 \text{ cm}$ ;  $b = 26.4 \text{ cm}$ ;  $l = 39.4 \text{ cm}$ ;  $E = 2.1 \cdot 10^6 \text{ kg/cm}^2$ .

Moment of inertia of a section of the shaft:

$$J = \frac{3.14}{64} (10.3^4 - 8.8^4) = 256 \text{ cm}^4$$

Stiffness coefficient of shaft (see Fig. 8.5b):

$$K = \frac{3 \cdot 2 \cdot 1 \cdot 10^6 \cdot 2 \cdot 6 \cdot 39.4}{13^2 \cdot 26.4^2} = 0.538 \cdot 10^6 \text{ kg/cm}.$$

Critical speed of rotor shaft by formula (8.13) is equal to

$$n_{kp} = 300 \sqrt{\frac{0.538 \cdot 10^6}{120}} = 20000 \text{ rpm.}$$

Example. Determine critical speed of the shaft of a turbine made according to the diagram (Fig. 8.5c).

Given:  $Q = 96 \text{ kg}$ ;  $d = 76 \text{ mm}$ ;  $d_0 = 62 \text{ mm}$ ;  $a = 37.4 \text{ cm}$ ;  $b = 13.7 \text{ cm}$ ;  $l = 51.1 \text{ cm}$ ;  $E = 2.1 \cdot 10^6 \text{ kg/cm}^2$ .

Moment of inertia of a section of the shaft

$$J = \frac{3.14}{64} (7.6^4 - 6.2^4) = 91.5 \text{ cm}^4$$

Static deflection of shaft from weight of turbine wheel (see Fig. 8.5c);

$$y = \frac{96 \cdot 51.1 \cdot 13.7^2}{3 \cdot 2.1 \cdot 10^6 \cdot 91.5} = 0.0016 \text{ cm}$$

Critical speed of rotor shaft by formula (8.15) is equal to

$$n_{kp} = \frac{300}{\sqrt{0.0016}} = 7500 \text{ rpm.}$$

### 8.5. Critical Speed of a Shaft with Several Disks

If a combined system of shaft with  $z$  disks is divided into simple systems with one disk (Fig. 8.6) and we determine for each of them critical speed  $n_{kp1}$ ,  $n_{kp2}$ , ...,  $n_{kpz}$ , the critical speed of this system can be found with sufficient accuracy for practice by the following formula:

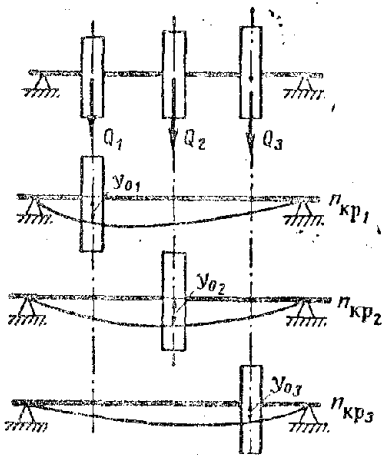


Fig. 8.6. System of shaft with three disks.

$$\frac{1}{n_{kp}^2} = \frac{1}{n_{kp1}^2} + \frac{1}{n_{kp2}^2} + \dots + \frac{1}{n_{kpz}^2} \quad (8.16)$$

or expressing critical speeds by static deflections of shaft by formula (8.15):

$$\frac{1}{n_{kp}^2} = \frac{y_{01} + y_{02} + \dots + y_{0z}}{300^2}$$

Whence

$$n_{kp} = \frac{300}{\sqrt{y_{01} + y_{02} + \dots + y_{0z}}}, \quad (8.16)$$

where  $y_{02}$ ,  $y_{03}$ , ...,  $y_{0z}$  are static deflections of shaft during loading by one disk at the place of attachment of the disk.

Example. Determine critical speed of the rotor shaft of a turbocompressor (Fig. 8.7).

Given:  $Q_{tp} = 4.4 \text{ kg}$ ;  $Q_R = 4.5 \text{ kg}$ ;  $a = 3.3 \text{ cm}$ ;  $b = 16.8 \text{ cm}$ ;  $c = 4 \text{ cm}$ ;  $d = 30 \text{ mm}$ ;  $d_0 = 0 \text{ mm}$ ;  $E = 2.1 \cdot 10^6 \text{ kg/cm}^2$ .

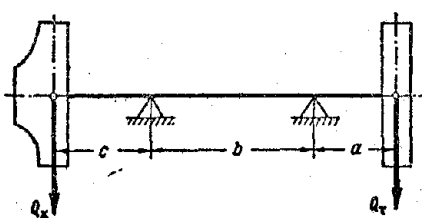


Fig. 8.7. Calculation of critical speeds of the rotor shaft of a turbocompressor.

Moment of inertia of a section of the shaft

$$J = \frac{3.14}{64} (3^4 - 0.94) = 3.94 \text{ cm}^4.$$

Deflections of shaft from weight of turbine and compressor will be determined on the diagram of Fig. 8.5c:

$$y_{0r} = \frac{4.5(3.3 + 16.8)3.3^2}{3 \cdot 2.1 \cdot 10^6 \cdot 3.94} = 39.8 \cdot 10^{-6} \text{ cm};$$

$$y_{0k} = \frac{1.5(4 + 16.8)4^2}{3 \cdot 2.1 \cdot 10^6 \cdot 3.94} = 20.1 \cdot 10^{-6} \text{ cm}.$$

Critical speed of rotor shaft by formula (8.17) is equal to

$$n_{kp} = \frac{300}{\sqrt{39.8 \cdot 10^{-6} + 20.1 \cdot 10^{-6}}} = 38700 \text{ rpm.}$$

### 8.6. Critical Speed of a Shaft Taking Into Account Its Mass

In preceding derivations we did not consider the natural mass of the shaft.

In most cases, in the determination of critical speeds the natural mass of the shaft can be disregarded, and the rotor wheel may be considered as a thin disk set on the shaft. In the calculation of natural mass of the shaft its critical speed can be determined by the formula:

$$n'_{kp} = \frac{n_{kp} n_{kp,s}}{\sqrt{n_{kp}^2 + n_{kp,s}^2}}, \quad (8.18)$$

where  $n_{kp,s}$  is the critical speed of a shaft without a disk;

$n_{kp}$  is the critical speed of a shaft with a disk, but without considering its mass.

Critical speed of a steel shaft on constant section, lying on two supports (see Fig. 8.2), without a disk can be determined by the formula:

$$n_{kp,s} = 13.9 \cdot 10^6 \frac{d}{l^2} \sqrt{1 + \left(\frac{d_0}{d}\right)^2} \text{ rpm.} \quad (8.19)$$

where  $d$  and  $d_0$  are correspondingly the external and internal diameters of the shaft;

$l$  is the distance between supports.

Example. Determine critical speed of the rotor shaft of a compressor (see first example) taking into account mass of shaft.

Given:  $n_{kp} = 20,000 \text{ rpm}$ ;  $d = 103 \text{ mm}$ ;  $d_0 = 88 \text{ mm}$ ;  $l = 39.4 \text{ cm}$ .

Critical speed of shaft without rotor wheel of compressor by formula (8.19) is equal to

$$n_{kp,s} = 13.9 \cdot 10^6 \frac{10.3}{39.4} \sqrt{1 + \left(\frac{8.8}{10.3}\right)^2} = 121500 \text{ rpm},$$

Critical speed of rotor shaft taking into account its mass by formula (8.18) is equal to

$$n_{kp} = \frac{20000 \cdot 121500}{\sqrt{20000^2 + 121500^2}} = 19700 \text{ rpm.}$$

### 8.7. Critical Speed of a Shaft of Variable Section with Several Disks

For a shaft of variable section with several disks the critical speed can be determined with accuracy sufficient for practice by the following formula:

$$n_{kp} = 300 \sqrt{\frac{Q_1 y_{01} + Q_2 y_{02} + \dots + Q_z y_{0z}}{Q_1 y_{01}^2 + Q_2 y_{02}^2 + \dots + Q_z y_{0z}^2}}, \quad (8.20)$$

where  $Q_1, Q_2 \dots Q_z$  is the weight of concentrated loads (disks),

$y_{01}, y_{02} \dots y_{0z}$  are static deflections of shaft in places of location of loads.

Considering the natural weight of the shaft, it is divided into separate sections and the weight of each one is taken as a concentrated load  $Q$  applied to the center of gravity of the section. For determination of static deflections of shaft it is convenient to apply the graphic method which is expounded in the course on resistance of materials. The shown method is applied in the following example.

Example. Determine critical speed of the turbine rotor depicted in Fig. 8.8.

Given:  $Q_3 = 96 \text{ kg}$ ;  $a = 37.4 \text{ cm}$ ;  $b = 7.4 \text{ cm}$ ;  $c = 6.3 \text{ cm}$ ;  $D_1 = 7.6 \text{ cm}$ ;  $d = 6.2 \text{ cm}$ ;  $D_2 = 10 \text{ cm}$ ;  $d_2 = 8.7 \text{ cm}$ .

Elastic modulus of shaft material  $E = 2.1 \cdot 10^6 \text{ kg/cm}^2$  and its specific gravity  $\gamma = 7.85 \cdot 10^{-3} \text{ kg/cm}^3$ .

We divide the shaft into two sections. Weight and moments of inertia of sections of shaft are equal to: for section a between supports  $- Q_1 = 4.45 \text{ kg}$  and  $J_1 = 91.3 \text{ cm}^4$  and for the inclined section b  $- Q_2 = 11 \text{ kg}$  and  $J_2 = 209 \text{ cm}^4$ .

We trace the calculating diagram of the shaft, taking the scale of its length  $m_l = 5 \text{ cm}$  in 1 cm and scale of forces  $m_Q = 10 \text{ kg}$  in 1 cm. Vectors of forces presenting loads are directed according to the direction of deflections of sections of the shaft: vector  $Q_1$  upwards, and vectors  $Q_2$  and  $Q_3$  downwards (see Fig. 8.8a).

We shall construct diagrams of bending moments. Selecting pole  $O_1$  and polar distance  $h_1 = 7 \text{ cm}$ , we construct a polygon of forces  $Q_1, Q_2$ , and  $Q_3$  (see Fig. 8.8c). With this polygon we construct a funicular polygon which we close with line  $nm$  (see Fig. 8.8b). The funicular polygon is a diagram of bending moments. Magnitude of this moment for separate sections of the shaft is:

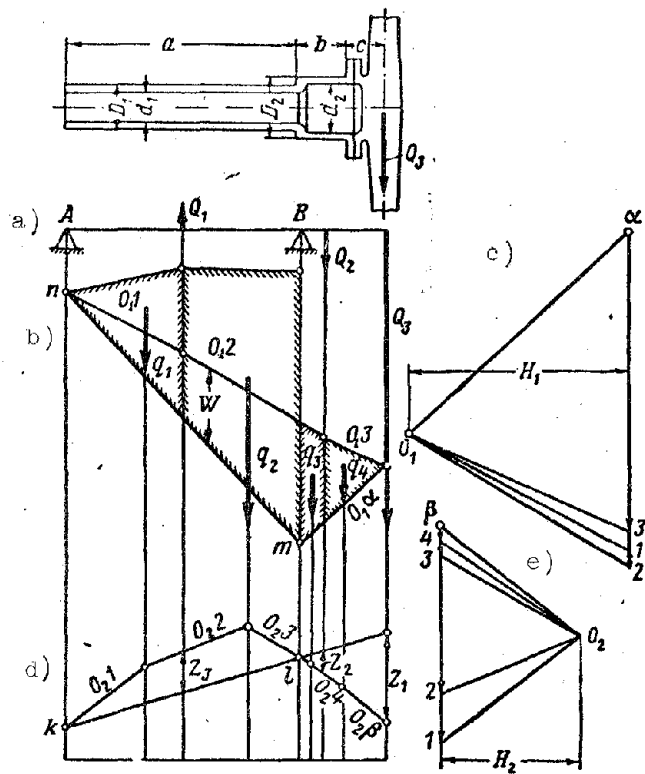


Fig. 8.8. Graphic method for the determination of critical speeds.

$$M = m_t m_q H_1 W = 5 \cdot 10 \cdot 7 W = 350 W \text{ kg} \cdot \text{cm},$$

where  $W$  is the ordinate of the diagram in cm.

A variable section of the shaft is considered as a "reduction" of the diagram of bending moments to a shaft of constant section. For this, ordinates  $W$  of separate sections of the diagram are multiplied by the ratio  $J_0/J$ , where  $J_0$  is the moment of inertia of the section to which the shaft is reduced, and  $J$  is the moment of inertia of the section of a given portion of the shaft. The shaft usually leads to its biggest section. In our case the biggest section is section  $b$ . Therefore, diagrams of moments are reduced by multiplication of its ordinates  $W$  on the section  $a$  and the shaft by the ratio  $J_0/J_1 = 209/91.3 = 2.29$ . The reduced diagram of moments in Fig. 8.8b is separated by shading.

After that, we shall construct a diagram of deflections of the shaft, for which the diagram of moments will be taken as a fictitious load. Dividing the diagram of moments into separate sections in the form of triangles and trapezoids, we measure the area  $f \text{ cm}^2$  of each one and determine the values of fictitious forces:  $q = m_t^2 m_q H_1 f = 5^2 \cdot 10 \cdot 7 f = 1750 f \text{ kg} \cdot \text{cm}^2$ .

Table 8.1

Section No.	$J_{cm^2}$	$q$ $kg \cdot cm^2$
1	8.62	15 100
2	25.3	44 300
3	2.44	4 270
4	2.63	4 600

In our case the diagram moments is divided into four sections. Their areas and the values of fictitious forces have been placed in Table 8.1.

We select the scale of fictitious forces —  $m_q = 10^4$   $kg \cdot cm^2$  in 1 cm and place their vectors in the centers of gravity of corresponding sections of the diagram (see Fig. 8.8b). Selecting pole  $O_2$  and polar distance

$H_2 = 4.5$  cm, we construct at first a polygon of fictitious forces  $q_1, q_2, q_3$ , and  $q_4$  (see Fig. 8.8e), and then a second funicular polygon (see Fig. 8.8d), which we close by line  $kl$ .

The second funicular polygon is the diagram of deflections of the shaft. Deflection of separate sections of the shaft is equal to

$$y = \frac{m_1 m_4 H_2}{E \cdot J_2} Z = \frac{5 \cdot 10^4 \cdot 4.5}{2.1 \cdot 10^6 \cdot 209} Z = 0.000517 Z \text{ cm},$$

where  $Z$  is the ordinate of the deflector diagram in cm.

Determining deflections of shaft  $y_1, y_2$ , and  $y_3$  in places of application of loads  $Q_1, Q_2$ , and  $Q_3$ , we introduce the intermediate calculations in Table 8.2.

Table 8.2

$Q$ $kg$	$y$ $cm$	$Q_i y_i$	$Q_i y_i^2$
4.45	$0.67 \cdot 10^{-3}$	$2.98 \cdot 10^{-3}$	$2 \cdot 10^{-6}$
11	$0.36 \cdot 10^{-3}$	$3.96 \cdot 10^{-3}$	$1.43 \cdot 10^{-6}$
96	$1.4 \cdot 10^{-3}$	$134.5 \cdot 10^{-3}$	$188 \cdot 10^{-6}$

$$\sum_i^3 Q_i y_i = 141.44 \cdot 10^{-3};$$

$$\sum_i^3 Q_i y_i^2 = 191.43 \cdot 10^{-6}$$

and determine critical speed of rotor by formula (8.20)

$$n_{kp} = 300 \sqrt{\frac{141.44 \cdot 10^{-3}}{191.43 \cdot 10^{-6}}} = 8150 \text{ rpm.}$$

### 8.8. Critical Speed of a Shaft in the Case of Its Precessional Motion

Figure 8.9 depicts elastic lines of rotor shafts due to the action of weight of disks. In usual conditions rotation occurs around a bent elastic line of the shaft, which in space will occupy a constant position. However, in certain cases

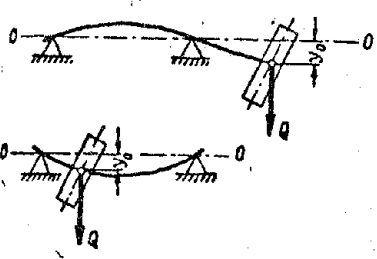


Fig. 8.9. Deflection of a shaft.

there can appear rotation and the most elastic line of the shaft around axis O-O, on which are located the supports of the rotor. Rotation around the elastic line will then be relative, and around axis O-O it will be transportation. Absolute velocity of rotation of shaft remains constant. Such resultant motion is called precessional.

Upon the appearance of precession, the disk located on the shaft at an angle (Fig. 8.10) will revolve around axis O<sub>1</sub>-A (tangent to elastic line of shaft at point of its fastening) with relative angular velocity  $\omega_0$  and around axis O-O with angular velocity of transportation  $\Omega$ .

The axis of disk O<sub>1</sub>-A will describe around axis O-O a conical surface with summit at point A. Absolute angular velocity of rotation

$$\omega = \omega_0 \pm \Omega. \quad (8.21)$$

The sign in expression (8.21) is determined by the direction of precessional motion. If it coincides with rotation of rotor, the precession is called direct and takes the sign "+". If, however, it is opposite the rotation of the rotor, the precession is called reverse and takes the sign "-".

Fig. 8.10. Determination of gyroscopic moments of a turbine disk.

In the case of precessional motion in the disk there appears centrifugal force C, moment of centrifugal forces  $M_C$ , and gyroscopic moment  $M_T$  (see Fig. 8.10).

Centrifugal force appears due to noncoincidence of center of gravity of disk with axis of rotation O-O; it is equal to:

$$C = m y_0 \Omega, \quad (8.22)$$

where m is mass of disk;

$y_0$  is the distance of center of gravity of disk from axis of rotation O-O.

Moment from centrifugal forces appears due to the slanted location of the disk with respect to axis of rotation O-O under the action of centrifugal force AC in elementary  $\Delta m$  of the disk.

Moment reduces to the form

$$M_c = \frac{1}{2} J_0 \Omega^2 z_0. \quad (8.23)$$

where  $J_0$  is the polar moment of inertia of disk;

$\alpha_0$  is the angle of inclination of axis of disk to axis of rotation O-O.

Deflection of shaft  $y_0$  and its angle of inclination  $\alpha_0$  under the action of force C increases, and under the action of moment  $M_c$  decreases.

Gyroscopic moment is found in the following way. Angular momentum L of the disk in its relative rotation is equal to:

$$L = J_0 \omega_0.$$

Based on the accepted rule of mapping of vectors of moments (see Chapter VII, 7.7) we place the origin of vector L at point A. Then its end, depicted in Fig. 8.10 by point B, during precessional motion will describe a circumference with radius  $R = O_2 B$ . After the final element of time  $\Delta t$  at the end of vector L will shift from point B to point  $B_1$ . Connecting them, we obtain the vector triangle  $ABB_1$ . Vector  $AB_1$  is the geometric sum of vectors  $AB$  and  $BB_1$ . Designating the latter by  $\Delta H$ , we obtain:

$$\Delta H = R \Omega \Delta t = J_0 \omega_0 \Omega \Delta t \sin \alpha_0,$$

where

$$R = L \sin \alpha_0 = J_0 \omega_0 \sin \alpha_0$$

and gyroscopic moment (see Chapter VII, 7.7)

$$M_r = \frac{\Delta H}{\Delta t} = J_0 \omega_0 \Omega \sin \alpha_0. \quad (8.24)$$

In view of the smallness of angle  $\alpha_0$  we assume  $\sin \alpha_0 = \alpha_0$ . Taking into account expression (8.21), we obtain:

in direct precession

$$\left. \begin{aligned} M_r &= J_0 (\omega - \Omega) \Omega z_0 \\ \text{and in reverse precession} \quad M_r &= J (\omega + \Omega) \Omega z_0. \end{aligned} \right\} \quad (8.25)$$

Above, in the determination of gyroscopic moment (see Chapter VII, 7.7) it was established that vector  $M_r$  lies on one line with vector  $\Delta H$ , but is opposite to it in direction. For element of time  $\Delta t \rightarrow 0$  vectors  $\Delta H$  and  $M_r$  will occupy a position tangent to circumference R at point B. It follows from this that gyroscopic moment acts in the plane of location of the bent elastic line of the

shaft. Under its action, deflection of shaft  $y_0$  and angle of inclination  $\alpha_0$  in case of direct precession will decrease, and in case of reverse precession it will increase. Figure 8.10 shows the case of direct precession.

Total bending moment of shaft will be equal to:

$$M_B = M_T \pm M_C \quad (8.26)$$

here the sign "+" is taken in the case of direct, and sign "-" in the case of reverse precession.

Of special interest is the case of synchronous precession, when  $\Omega = \omega$ .

During direct synchronous precession  $M_B = 0$  [see formula (8.25)] and

$$M_B = \frac{1}{2} J_0 \omega^2 z_0 = J_s \omega^2 \alpha_0, \quad \left. \right\} \quad (8.27)$$

and during reverse synchronous precession

$$M_B = \frac{3}{2} J_0 \omega^2 z_0 = 3 J_s \omega^2 \alpha_0, \quad \left. \right\} \quad (8.27)$$

where  $J_0 = \frac{1}{2} J_0$   $J_0$  is the equatorial moment of inertia of the disk (with its small thickness).

Deflection  $y_0$  and angle of inclination of elastic line  $\alpha_0$  of the shaft at point of fastening of disk can be represented by the following equations:

$$\begin{aligned} y_0 &= C \delta_c \mp M_S \delta_M; \\ \alpha_0 &= C \varphi_c \mp M_S \varphi_M, \end{aligned} \quad \left. \right\} \quad (8.28)$$

where  $\delta_c$  and  $\delta_M$  are deflections of shaft at point of fastening of disk under the action of force  $C = 1$  kg and moment  $M_S = 1$  kg·cm;  $\varphi_c$  and  $\varphi_M$  are angles of inclination of elastic line of shaft at point of fastening of disk under the action of force  $C = 1$  kg and moment  $M_S = 1$  kg·cm.

In these expressions the sign "-" pertains to direct, and sign "+" to reverse precessions.

In the case of direct synchronous precession, equations (8.28) reduce to the form:

$$\begin{aligned} y_0 &= m y_0 \omega^2 \delta_c - J_s \omega^2 z_0 \delta_M, \\ \alpha_0 &= m y_0 \omega^2 \varphi_c - J_s \omega^2 z_0 \varphi_M. \end{aligned} \quad \left. \right\} \quad (8.29)$$

Excluding angle  $\alpha_0$  from these equations, we obtain

$$y_0 \left[ 1 - m \delta_c \omega^2 + \frac{J_s m k M^2 \delta_c \omega^4}{1 - J_s^2 \delta_M^2} \right] = 0. \quad (8.30)$$

At critical speed of rotation, deflection of shaft  $y_0$  takes finite values,

different from zero, and therefore equation (8.30) can be satisfied only if the expression in the bracket is equal to zero, i.e.,

$$J_s m (\delta_C \varphi_M - \delta_M \varphi_C) \omega^4 - (J_s \varphi_M - m \delta_C) \omega^2 - 1 = 0. \quad (8.31)$$

Since the free term of this biquadratic equation has the sign "-", of the four roots of the equation one will be positive, one negative, and two imaginary. In this case the physical meaning corresponds only to the positive root. Thus for a rotor with one disk during direct precession there exists one critical velocity  $\omega'_{kp}$  and critical speed  $n'_{kp}$  corresponding it. The cause of the appearance of the appearance of direct synchronous precession is usually the unbalanced centrifugal force of the rotor,

Proceeding analogously to the preceding, we find a biquadratic equation for reverse precession

$$3J_s m (\delta_C \varphi_M - \delta_M \varphi_C) \omega^4 - (3J_s \varphi_M + m \delta_C) \omega^2 + 1 = 0. \quad (8.32)$$

Since the free term of the equation here has the sign "+", of the four roots of the equation two will be positive and two negative. Thus, during reverse precession there exist two critical velocities  $\omega''_{kp 1}$  and  $\omega''_{kp 2}$  and critical speeds  $n''_{kp 1}$  and  $n''_{kp 2}$  corresponding to them.

For the appearance of reverse precession there is required the existence of variable forces exciting bending vibrations of the shaft with a definite frequency. Similar conditions for GTD are encountered comparatively less often and therefore of practical interest are: critical speeds without precession  $n_{kp}$  [see formula (8.15)] and critical speeds with direct precession  $n_{kp}$ . With this,  $n'_{kp} > n_{kp}$ .

## C H A P T E R    IX

### COMBUSTION CHAMBERS

#### 9.1. General Information

[GTD] (ГТД) combustion chambers serve for burning of fuel and preheating with this of working gases before they enter the turbine. Combustion chambers must ensure:

1. Stable burning of fuel in all operating conditions of engine and in all conditions of its use.
2. High completeness of fuel combustion.
3. Small flow friction of gas flow.
4. Uniform (or with defined character of nonuniformity) temperature field at combustion chamber exit.
5. Reliable starting of engine under all conditions of use.
6. Small dimensions and small weight.
7. Reliability and sufficient operation life.

Coefficient of heat emission of GTD combustion chambers  $\xi = 0.95$  to  $0.98$ , coefficient of total pressure loss  $\sigma_{K.C} = 0.92$  to  $0.96$ , and coefficient of volume heat rate  $q = (20 \text{ to } 40) \times 10^6 \text{ kcal/m}^3 \cdot \text{hr} \cdot \text{atm}(\text{abs.})$ .

Organization of burning process. The quantity of burned fuel in GTD combustion chambers is limited by temperature of gases  $T_3$  at entry to turbine. In contemporary GTD under maximum operating conditions it is  $T_3 = 800$  to  $900^\circ\text{C}$ , which corresponds to the coefficient of air surplus  $\alpha = 4.5$  to  $3.8$ . Under lowered operating conditions fuel feed to combustion chamber decreases, due to which the temperature  $T_3$  drops, and coefficient  $\alpha$  considerably increases. Burning

of fuel should occur in a flow of air, the speed of which is very considerable and at compressor exit is from 100 to 150 m/sec. Organization of the process of burning in these conditions encounters considerable difficulties and is usually carried out with the help of a special arrangement of combustion chambers, which has two zones: zone of burning and zone of mixing.

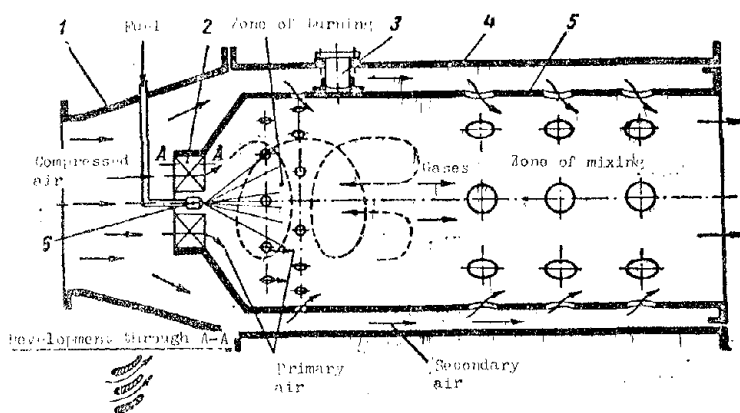


Fig. 9.1. Fundamental diagram of combustion chamber.

of the tube there is an annular series of holes. In the front part of the flame tube, where through the burner moves the fuel, there will be formed the zone of burning, and in its rear part, the zone of mixing.

In the intake device the speed of air flow is lowered to 40 to 60 m/sec; air is divided into two parts — into primary and secondary. Primary air through swirl vane and first two rows of holes passes into the front (head) part of the flame tube, i.e., into the zone of burning. Secondary air passes through an annular cavity between casing 4 and flame tube 5 to the rear rows of holes and through them enters the zone of mixing.

The quantity of primary air is usually 25-35% of the total expenditure of air, which ensures in the zone of burning the formation of a fuel-air mixture with coefficient of air surplus  $\alpha = 1$  to 1.5. Temperature of burning due to this reaches 1500 to 2000°C. This ensures favorable conditions for burning. Carburetion in the chamber is carried out by a fine fuel spray by burner 6 and intense mixing of it with air due to the turbulence of the latter.

(stable burning in the flow of air (burning without pulsations, breakdowns, and damping of flame, and also without ejection of it beyond the limits of chamber))

Figure 9.1 depicts the fundamental diagram of a GTD combustion consisting of an intake device in the form of a diffuser 1, casing 4, and flame tube 5. The flame tube has a frontal device in the form of a conical head with an air swirl vane 2. In the center of the latter there is a fuel spray nozzle 6. Along the length

is ensured by lowering the forward velocity of gases in the zone of burning 15-25 m/sec and the formation in it of reverse vertical currents of hot gases continuously igniting the fuel proceeding to the chamber. Formation of reverse vertical currents is carried out by flame holders. Flame holders are included in the forward devices of the flame tubes. They are usually made in the form of shields, swirl vanes, or in combinations of them.

Shields are walls (partitions) or conical inserts in the flow of air at the entry to the zone of burning. Figure 9.2 shows the stabilizing action of a plate

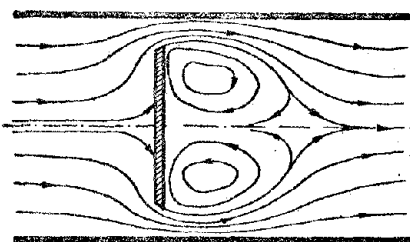


Fig. 9.2. Diagram of the stabilizing action of a plate in a flow of air.

(wall). Stabilizing action of swirl vane 2 (see Fig. 9.1) consists in the following. Passing through it into the zone of burning, the air swirls, decreasing its forward velocity. Due to the centrifugal effect from twirling, the air is rejected to the periphery and is mixed with the fuel. In the central part of the tube there will form a rarefaction, where in the form of reverse vertical currents rush hot gases. They then

continuously ignite the fuel proceeding to the chamber through the burner.

From the zone of burning, the products of combustion pass into the zone of mixing, where there proceeds the secondary air. As a result, of their mixing, the temperature of gases at the entry to the turbine drops, composing in maximum operating conditions of engine 800 to 900°C. The velocity of gases at the combustion chamber exit is increased to 100-150 m/sec. In the zone of mixing there also occurs reburning of products of incomplete burning.

During starting of engine, initial ignition of fuel in the combustion chambers (starting of chambers) is carried out with the help of igniters, whose description is given in Chapter XVII.

Length of flame tube, and also quantity, dimensions, and location of holes for passage of air are selected by experimental means, proceeding from conditions of guarantee of fuel combustion and obtaining the desirable temperature field of gas flow at the turbine inlet. Holes for passage of air at the flame tubes are frequently in the form of slots. For best mixing of combustion products with secondary air the latter is sometimes directed to the central part of the flame

space of the tube through special mixing tubes 7 (see Fig. 9.12).

Operating conditions. Combustion chambers operate in conditions of high temperature of gases, at their heightened pressure. Due to the presence of free oxygen, the working gases also possess high chemical activity. In especially heavy conditions are the flame tubes, whose temperature reaches 800 to 900°C. Most cases of their overheating and burnout are connected either with incorrect location of flame jet in tube, or with insufficient cooling and protection of tubes from heating. Scale formation in tubes is a result of unsatisfactory process of combustion,

Heating of flame tubes is nonuniform both along the circumference, and also along the length. This leads to the appearance of local thermal stresses with formation of warping and cracks. Pressure in chambers frequently has a pulsating character that evokes vibrations which can lead to formation of fatigue cracks. Cracks in flame tubes most frequently appear around the holes, which are a source of concentration of stresses. Casings of chambers operate in more favorable conditions: their operating temperature is about 300°C.

Reliability of work of combustion chambers is ensured by correct organization of the process of combustion, application of special heat-resistant alloys for the flame tubes, and their cooling. In the manufacture of flame tubes attention is given to the quality of their welding. Walls of flame tubes are polished and sometimes coated by special heat-resistant enamels. Holes in the tubes after drilling are thoroughly processed.

Cooling. Secondary air, passing through the cavity formed by the flame tube and casing (see Fig. 9.1), cools the tube from the outside and creates a protective layer around the casing. Certain designs of chambers have flame tubes for best cooling, which are ribbed on the outside (see Fig. 9.14). On the inside the flame tubes are cooled and are protected from unnecessary heating by a protective layer. Thus the air, proceeding to the zone of burning through holes in the wall of the flame tube and having a speed from 40 to 60 m/sec, drives away the flame to the center and, being mixed with the gases, forms a protective shell around the walls with lowered temperature.

The most effective protection of walls of the flame tube is the so-called film cooling. Examples of it are shown in Fig. 9.3. In diagram a the tube has a

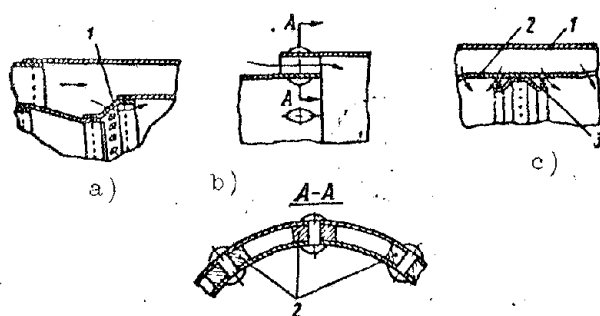


Fig. 9.3. Film cooling of flame tubes.

through small holes or slots, obtains direction along the wall, forming, a protective film around it.

Thermal expansions of flame tubes attain considerable magnitudes. In order to ensure free expansion in axial direction, the tubes are fixed in one band; the other supports of tubes are of the sliding type. In order to ensure tubes free expansion also in radial direction, their retainers are made in the form of radial pins 3 (see Fig. 9.1).

Types of combustion chambers. With respect to design, GTD combustion chambers are of three types: a) can-type (individual), b) annular, and c) tubo-annular (block). In Fig. 9.4 these types of combustion chambers are shown

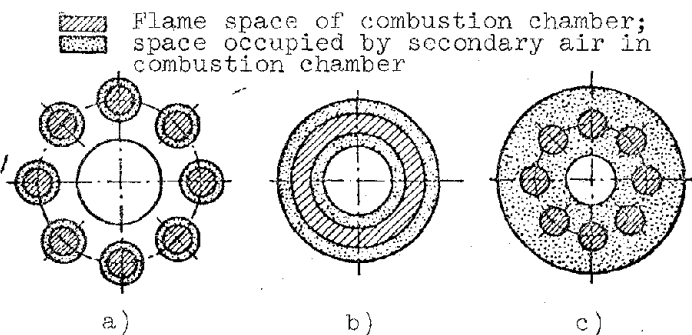


Fig. 9.4. Diagram of combustion chambers in cross section of engine.

the volume of each can-type chamber is small. This facilitates their finishing in laboratory conditions, since this requires relatively small expenditure of air.

During replacement of can-type combustion chambers it is not required to disassemble the engine. They well are composed with the centrifugal compressor,

local annular strip 1 with a row of small holes. Diagram b shows a riveted connection of the tube. By means of local stands 2 slots are formed in the connection. Diagram c shows casing 1 and flame tube 2. Tube has two annular rows of small holes, and between them is welded a guide ring 3. In all these devices, the air coolant, passing

schematically in cross section.

The can-type combustion chamber consists of one flame tube located inside the casing. The number of can-type chambers in an engine is usually from 6 to 10 and above. They are uniformly arranged around the central housing of the engine. Owing to their large quantity on the engine

not increasing the engine's diameter. However, for an engine with an axial-flow compressor, can-type combustion chambers lead to increase of diameters. Another deficiency of can-type chambers is their large weight in comparison with other types of chambers,

The annular combustion chamber consists of outer and inner flame jackets and outer and inner casings. They are arranged around the central engine housing concentrically to each other. In connection the flame jackets form an annular flame chamber, and the casings form around it two annular cavities for passage of secondary air.

Annular combustion chambers are distinguished by compactness, small weight, and small overall diameter. Their outer and inner casings are usually included in the support system of the engine, which leads to lowering of weight of the latter. However, inspection and replacement of annular chambers includes disassembly of the engine.

The tubo-annular combustion chamber consists of several flame tubes located uniformly in the annular space between the outer and inner casings. They are arranged around the central engine housing concentrically to each other. As also in the annular chamber, the outer and inner casings of the tubo-annular combustion chamber are usually included in the support system of the engine. With respect to weight and dimensions the tubo-annular chamber occupies the middle position between can-type and annular chambers,

The tubo-annular and annular combustion chambers are well composed for engines with an axial-flow compressor, in which they have also obtained wide application.

By direction of motion of gases, combustion chambers are divided into direct-flow, i.e., without change of direction of motion of gases, and loop (see Fig. 1.6), in which there occurs revolution of gases at  $180^{\circ}$ . Contemporary GTP combustion chambers usually are the direct-flow type, since they possess smaller flow frictions and ensure less overall diameter of engine.

By method of carburetion, the chambers are classified: with atomization of fuel and vaporizing. In contemporary engines predominant application has been found by combustion chambers with atomization of fuel by burners under high pressure.

## 9.2. Design of Combustion Chambers

Can-type combustion chambers. Figure 9.5 shows a can-type combustion chamber of the [VK-1] (BK-1) engine. The engine has nine such chambers. The chamber consists of a casing throat and flame tube. In Fig. 9.6 these components are shown separately.

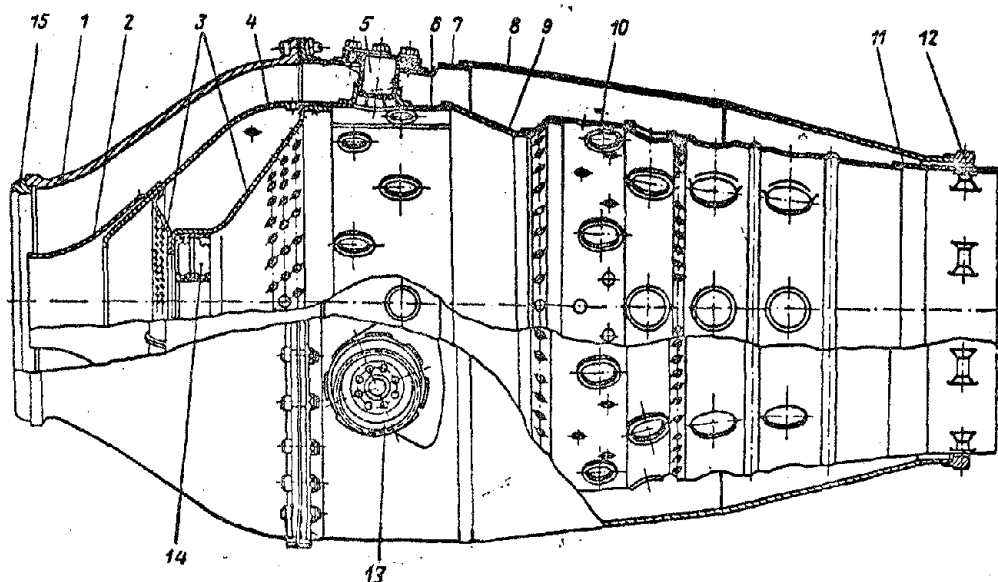


Fig. 9.5. Can-type (individual) combustion chamber of the VK-1 engine. 1 — throat, 2 — inlet cone, 3 — perforated partition, 4 — cap of flame tube, 5 — flame tube suspension pin, 6 and 9 — cylindrical and conical section of flame chamber, 7 and 8 — cylindrical and conical section of combustion chamber casing, 10 — conical section of flame tube, 11 — cylindrical baffle, 12 — adjusting ring, 13 — connecting branch, 14 — swirl vane, 15 — spherical insert.

Throat 1 (see Fig. 9.5) is cast from aluminum alloy and has the form of a diffuser. By a small flange it is attached to the outlet branch of the compressor, and by a large flange with the help of bolts it is attached to the casing.

The combustion chamber casing is welded, made from low-carbon sheet steel 1.5 mm thick with subsequent calorizing. Casing II, shown in Fig. 9.6, consists of three parts welded together by electric roller welding. Their slanted seam increases the durability of the welding connection. In subsequent modifications the casing was made from two parts: cylindrical 7 and conical 8. Each one is made from a whole sheet by means of deep drawing (see Fig. 9.5). To front end of casing is welded a steel flange for connection with the throat, and to rear, an adjusting (sealing) ring 12 with a spherical support surface for placing chamber

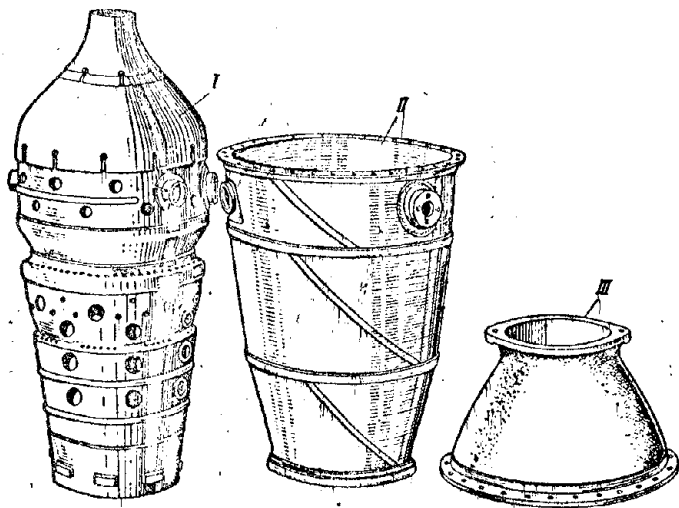


Fig. 9.6. Components of the combustion chamber of the VK-1 engine. I - flame tube, II - casing, III - throat,

central and rear parts of the tube form the zones of burning and mixing.

The forward section of the tube consists of inlet cone (snout) 2 and cap 4. On the inside, to the cap is welded a double-walled perforated (with rows of holes) partition 3, in the center of which is welded a swirl vane 14 with central orifice for the burner. Cap 4 is welded to cylindrical section 6 of central part of tube. From the rear side of inlet cone 2 and cap 4 in places of their welding there are small longitudinal slits (see Figs. 9.6 and 9.7). These slits, decreasing rigidity,

thereby decrease the stresses appearing in the tube due to its nonuniform heating. Furthermore, they facilitate trimming of components before welding. For decrease of concentration of stresses and removal of possible formation of cracks the ends of the slits are bored,

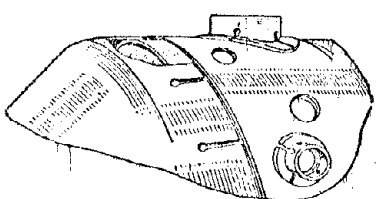


Fig. 9.7. Longitudinal slits in places of welding,

A swirl vane is shown separately in Fig. 9.8.

It consists of bushing 1 forming the orifice for the burner, ring 2, and vanes 3.

By means of folded tabs 4 the vanes are welded by electric spot welding to the ring and bushing. In existing chambers the swirl vanes usually have 5-10 vanes with outlet angle  $\varphi = 30$  to  $30^\circ$ . The greater angle  $\varphi$ , the greater the

in socket of gas collector. To cylindrical part of casing 7 are welded three flanges, one of which serves as a retainer 5, and the two others are connecting branches 13.

Flame tube (see Figs. 9.5 and 9.6) consists of separate parts (sections) united together by electric welding. The material for its manufacture is sheet heat-resistant alloy 1.3 to 2 mm thick. Front part of flame tube is the forward section. The

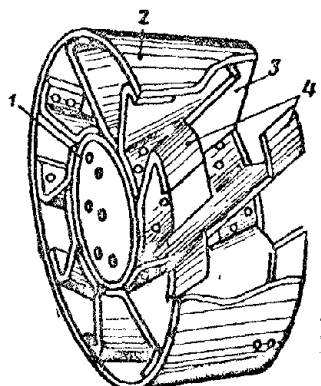


Fig. 9.8. Swirl vane.

swirl of air passing through it, but simultaneously with this there is also an increase of flow friction of the swirl vane. In chambers of the VK-1 engine the swirl vane has 10 vanes with angle  $\phi = 42^\circ$ . Through holes in partition 3 and swirl vane 14 (see Fig. 9.5) the air, proceeding to inlet cone 2, passes into the zone of burning.

Central part of flame tube consists of a cylindrical section 6, conical section 9, and perforated ring, forming an annular band (see Fig. 9.5) around the tube.

On the outside, to the cylindrical sections are welded three bushings: one for a retainer 5 and two for connecting branches 13.

Rear part of flame tube consists of conical section 10 and cylindrical baffle 11. For increase of rigidity the conical section has three ridges. On baffle 11 there are 8 stamped flanges for centering the tube in the chamber casing. To eliminate wear, the flanges on the outside are fused by stellite.

For passage of air the flame tubes have 6 annular rows of large holes, two of which are in cylindrical section 6 and four in conical section 10.

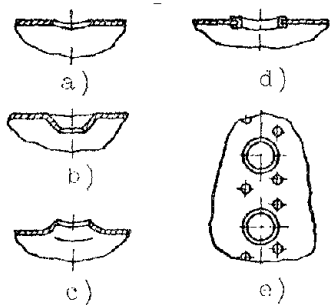


Fig. 9.9. Forms of holes in flame tubes.

Figure 9.9 shows the forms of air holes of flame tubes of different designs: a) simple hole; b) and c) holes that are flanged inside and outside the tube for reinforcement; d) holes reinforced by edging with a special piston; and e) small holes located between large holes.

Small holes decrease nonuniformity of heating of wall, which is usually observed on sections between large and remotely located holes.

In flame tube of the VK-1 engine, some of the large holes are flanged inside the tube, and some are edged. On the conical section of the tube in the band of the first row of large holes there are two annular rows of small holes, but around the strip and first ridge there is formed film cooling.

Igniters of the [fRD] (TPD) VK-1 are mounted on two combustion chambers located approximately in diametrically opposite parts of the engine (in 3rd and 8th chambers). For transfer of flame to all remaining chambers, and also for

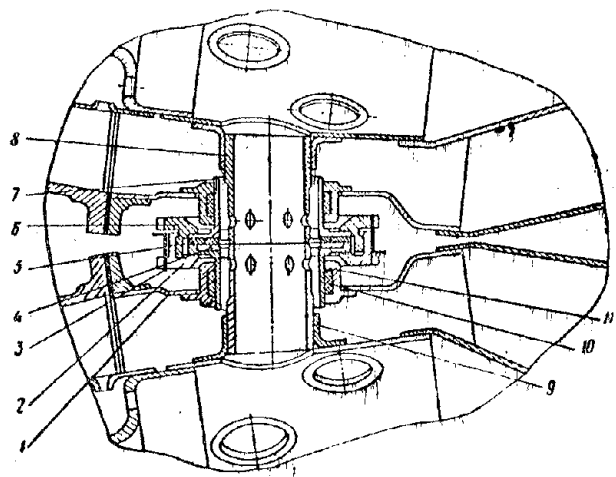


Fig. 9.10, Connecting pipe of combustion chambers of the VK-1 engine.

equalizing pressure in them the combustion chambers are connected together by pipes (Fig. 9.10).

The flame tubes are united by internal pipes 4 and 8, whose ends are inserted in bushings 9 welded to flame tubes. Casings of chambers 1 are connected by means of external pipes 7. The ends of these pipes enter flanges 11 of casings. Connecting pipes of two adjacent chambers are attached by means of a threaded flange

6 and sleeve nut 2. Locking is carried out by folding the tabs of retaining ring 3. Between flanges of pipes there is a copper and asbestos lining 5. Sealing of flanges 11 is ensured by a filling 10 made from asbestos graphitized cord. Connecting pipes allow for some movement of adjacent chambers on the perimeter of their location on the engine without disturbance of the seal,

Flame tube is attached to the chamber casing in the following way. Its rear end freely enters adjusting ring 12 of the casing, and in the center is fixed in three points located in one band; by radial retainer 5 and two connecting pipes 13 (see Fig. 9.5). Such retention ensures the pipe free thermal expansion both in axial and also in radial directions. Figure 9.11b separately shows centering of tube in adjusting ring 12 of the casing, and Fig. 9.11a shows its retention by retainer 5. The tube is centered in the adjusting ring by means of stamped flanges, between which passes the air coolant. Retainer 5 is made in the form of a glass. It freely enters the bushing of the tube and is mounted on the casing by screws,

During installation on the engine each combustion chamber with its rear end is inserted into the socket of the gas collector, and the throat is attached by two bolts to outlet branch of compressor (see Fig. 1.8). Figure 9.11b shows centering of chamber by adjusting ring 12 in orifice of gas collector 16, and Fig. 9.11c shows its attachment to the compressor branch. Between flanges of branch 17 and throat 1 there is a spherical insert 15, allowing for some misalignment without disturbance of airtightness of the connection, which can appear during

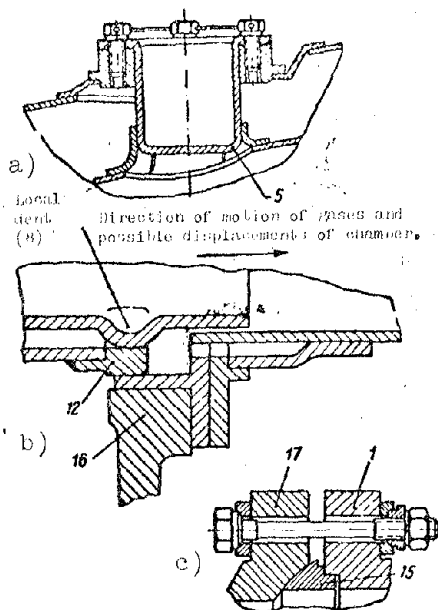


Fig. 9.11. Fittings of combustion chamber of the VK-1 engine. a) retention of flame tube, b) centering flame tube in gas collector, c) attachment of combustion chamber to outlet branch of compressor.

combustion chamber and nozzle apparatus II of the first stage of the turbine are attached, which is shown separately in Fig. 4.20. Inside the annular space formed by the bearing housing I, casing 8 and inner cone 19 of nozzle apparatus II, there is an annular flame tube III, shown separately in Fig. 9.13.

Flame tube is made from heat-resistant sheet material. Its forward section is welded and consists of ten conical heads 2 welded by spot welding to tabs of two concentrically located rings 5 and 20. For compensation of thermal expansions the joints of the heads have clearances. In the walls of the heads there are holes for passage of air. At each head on inlet there is welded a swirl vane 1 with central orifice for burner 26. Inside heads there is welded diffuser 21 consisting of two parts. Rear part of diffuser has two rows of holes and by means of vanes is welded by spot welding to its front part. Through the holes and clearance between front and rear parts of diffuser the air passes.

To outer 5 and inner 20 rings of head block by means of rivets the outer 10 and inner 18 flame jackets are attached. In the band of rivet connections of the jackets there are longitudinal slits, decreasing rigidity and facilitating

operation due to different thermal expansions of compressor and turbine, and also during assembly.

Annular combustion chamber. Figure 9.12 shows the annular combustion chamber of the [TVD] (ТВД) [AI-20] (АИ-20), which is manufactured in one unit with the rotor bearing housing.

The bearing housing I is welded from heat-resistant sheet steel. It consists of outer 4 and inner 22 concentrically located cones which are rigidly joined together by ten hollow struts 25 and form the inlet of the combustion chamber in the form of an annular diffuser.

The central part of the housings contain sockets of the central 23 and rear 17 rotor bearings. By front flange 24 the bearing housing is attached to the compressor housing, and to the rear by its flanges the outer casing 8 of the

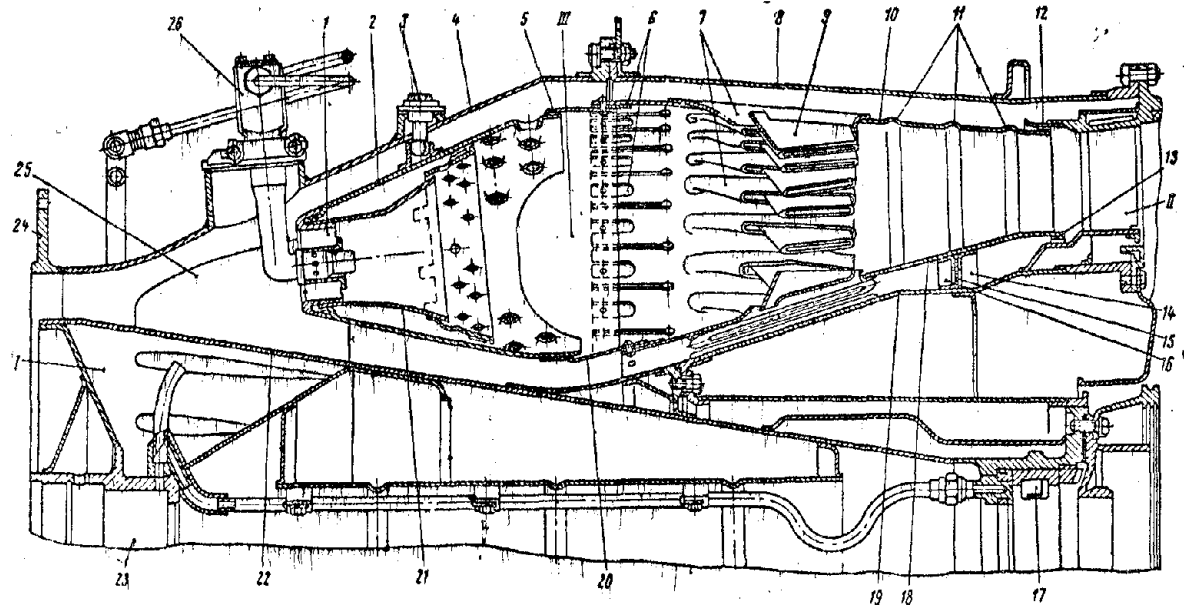


Fig. 9.12. Annular combustion chamber of the TVD AI-20. I - bearing housing, II - turbine nozzle apparatus, III - flame tube. 1 - swirl vane, 2 - conical head, 3 - radial pins, 4 and 22 - outer and inner cones of housing, 5 and 20 - outer and inner rings of head block, 6 - plates, 7 - mixing pipes, 8 - outer casing, 9 - inserts of pipes, 10 and 18 - outer and inner flame jackets, 11 - ridges, 12 and 13 - rings of rigidity of outer and inner jackets, 14 and 16 - rings of rigidity, 15 - sealing ring, 17 - roller bearing of rotor, 19 - cone of nozzle apparatus, 21 - diffuser, 23 - socket of central rotor bearing, 24 - front flange of bearing housing, 25 - hollow struts, 26 - burners.

trimming during riveting. In rivet connections there are plates 6 forming slots for passage of air. Air goes through slots along walls and cools them. For passage of secondary air the jackets 10 and 18 have mixing pipes 7, welded by roller welding. To mixing pipes are welded inserts 9, which direct secondary air

to the central part of gas flow. Secondary air through pipes also goes along front wall of insert, cooling it from the outside.

On outer jacket for rigidity there are three ridges 11. To inner jacket there are welded two rings of rigidity 14 and 16, between which there is freely installed sealing ring 15. The ring rests on the cone of nozzle apparatus 19. For passage of air coolant the rings have 50 holes with diameter 4 mm. To outlet edges of outer and inner flame jackets there are welded rings of rigidity 12 and 13 and a set of plates forming together a slot for passage of air coolant.

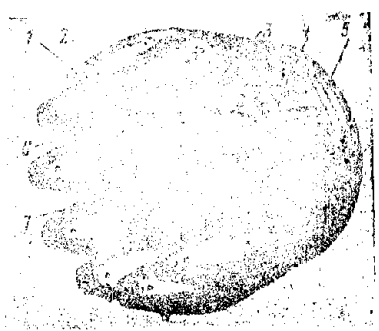


Fig. 9.13. Flame tube of the TVD AI-20. 1 - swirl vane, 2 - conical head, 3 and 6 - outer and inner rings of head block, 4 - mixing pipes, 5 and 7 - outer and inner flame jackets.

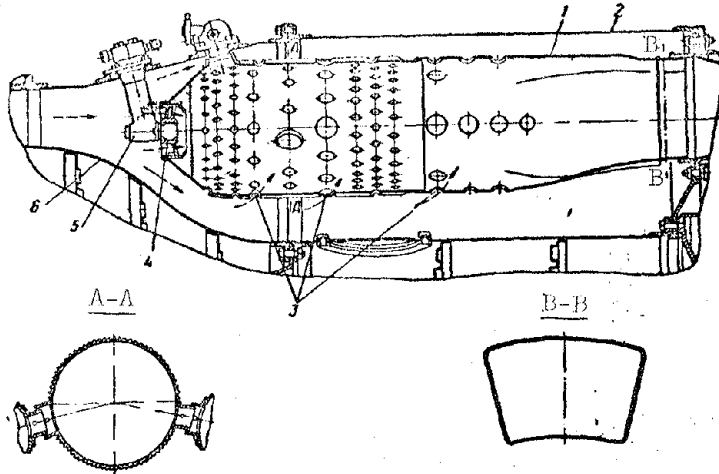


Fig. 9.14. Tubo-annular combustion chamber. 1 — flame tube, 2 and 6 — outer and inner casings of combustion chamber, 3 — holes for passage of secondary air, 4 — swirl vane, 5 — burner.

rigidity 12 and 13 the secondary air passes for cooling of nozzle apparatus.

In combustion chamber there are 10 working burners 26, two igniters, and two additional starting burners.

Tubo-annular combustion chambers. Shown in Fig. 9.14, the tubo-annular combustion chamber consists of several flame tubes 1, located in the annular space between outer 2 and inner 6 casings of chamber. Casings are welded and each one consists of two parts united by means of flanges. Casing at chamber inlet form an annular diffuser, in which the air proceeding from the compressor lowers its speed.

Flame tubes consist of a conical head, central part, and rear part, welded together. To conical head is welded swirl vane 4, in center of which is located burner 5.

Central part of tube has the form of a cylinder, on the external surface of which there are small longitudinal ribs. The ribs improve cooling of the most heated part of the tube and increase its longitudinal rigidity. For passage of air inside the tube, in its wall there are annular rows of holes 3 of different diameter. In upper part of tube there is an igniter which ensures initial ignition of fuel during starting of engine (see Chapter XVII "GTD starting assemblies").

In section A-A of the tube there are welded two pipes of various diameter,

Flame tube is located with its heads between struts 25 of bearing housing I. It is attached to wall of housing with its heads by means of eight radial pins 3 fixed in one transverse plane. By its rear part the flame tube freely enters its socket at nozzle apparatus II. Such connection ensures free thermal expansion of flame tube. Through slots between plates of rings of

which telescopically enter similar pipes of adjacent flame tubes. These pipes connect all flame tubes. These connections are made for transfer of flame during starting of engine from one flame tube to another, since igniters are usually installed only in part of them. In rear part of flame tube there is a smooth transition from round to trapezoidal form of section B-B,

Each flame tube by its rear end telescopically enters the socket of the inlet device of the turbine, and by its front end rests on the burner attached to the outer casing of the combustion chamber. In axial direction the flame tubes are fixed by the igniter case and special retainers.

Thus, in a working state the flame tubes have the possibility of free thermal expansion in the direction of the turbine. Location of rear flange of outer casing  $\Sigma$  allows to shift it back and obtain an access to the flame tubes for their inspection and replacement without disassembly of the engine.

### 9.3. Strength Calculation

The housings of combustion chambers and flame tubes are calculated as thin-walled shells. Under the action of a tensile or compressional axial load  $P_0$  (Fig. 9.15a and b), in the cross sections of a shell there appear stresses of tension or compression which can be determined by the formulas:

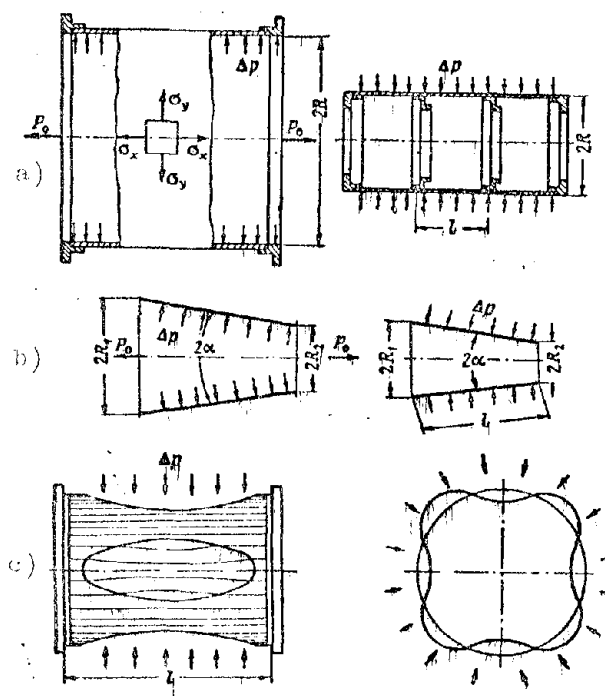


Fig. 9.15. Strength calculation of a combustion chamber

for a cylindrical shell -

$$\sigma_x = \frac{P_0}{2\pi R\delta}$$

and for a conical shell - } (9.1)

$$\sigma_x = \frac{P_0}{2\pi R\delta \cos \alpha},$$

where  $R$  is the radius of the shell;

$\delta$  is thickness of wall;

$\alpha$  is the generating angle of cone with its axis (see Fig. 9.15b).

Under the action of internal or external excess pressure of gases  $\Delta p$  (see Fig. 9.15a and b), in the longitudinal sections of the shell there appear tangential stresses of tension or compression. The latter can be determined by the formulas:

for a cylindrical shell -

$$\left. \begin{aligned} \sigma_x &= \frac{\Delta p R}{t} \\ \sigma_y &= \frac{\Delta p R}{t \cos \alpha} \end{aligned} \right\} \quad (9.2)$$

and for a conical shell

Figure 9.15a depicts the direction of action of stresses  $\sigma_x$  and  $\sigma_y$ , appearing on the edges of an element separated in the shell by transverse and longitudinal sections.

Shells having complicated form of rotation can be reduced in some of their sections to cylindrical or conical form.

In housings of combustion chambers stress  $\sigma_x$  usually does not exceed 200 to 250 kg/cm<sup>2</sup>. Their basic load is the excess pressure of gases, under the action of which stress  $\sigma_y$  reaches 1400 kg/cm<sup>2</sup> and higher. Safety factor of shells can be determined by yield point (see Chapter XIII).

Shells under the action of external pressure are also checked for stability. If excess pressure exceeds its critical value  $\Delta p_{kp}$ , the shell loses its stability and is deformed, as for instance is shown in Fig. 9.15c. Value of critical pressure can be determined by the formula:

$$\Delta p_{kp} = 0.92 E \frac{t}{l} \left( \frac{\delta}{R} \right)^{3/2} \quad (9.3)$$

where  $E$  is the elastic modulus of shell material at operating temperature;

$t$  is the calculated length of the shell.

For guarantee of stability the shell is frequently reinforced by rigid rings (bands). In this case the calculated length of the shell is taken as the distance between rings (see Fig. 9.15a). For a conical shell in formula (9.3) we take:

$t$  is the length of the generatrix and  $R = \frac{R_1 + R_2}{2 \cos \alpha}$  (see Fig. 9.15b).

Stability margin of shell

$$K = \frac{\Delta p_{kp}}{\Delta p_{th}} \quad (9.4)$$

Stability margin of GTD housings is allowed not less than 1.8.

Example. Determine tangential stress in the outer housing of a combustion chamber.

Given:  $\Delta p = 7.5$  kg/cm<sup>2</sup>;  $R = 31$  cm;  $t = 2$  mm.

Tensile stress by formula (9.2)

$$\sigma_y = \frac{7,5 \cdot 31}{0,2} = 1160 \text{ kg/cm}^2,$$

Example. Determine tangential stress in the inner housing of an annular combustion chamber and its safety factor,

Given:  $\Delta p = 7,5 \text{ kg/cm}^2$ ;  $R = 12,6 \text{ cm}$ ;  $\delta = 1,5 \text{ mm}$ ;  $E = 1,76 \cdot 10^6 \text{ kg/cm}^2$ ;  
 $t = 21,6 \text{ cm}$ .

Compressional stresses by formula (9.2)

$$\sigma_y = \frac{7,5 \cdot 12,6}{0,15} = 630 \text{ kg/cm}^2.$$

Critical pressure by formula (9.3);

$$\Delta p_{kp} = 0,92 \cdot 1,76 \cdot 10^6 \cdot \frac{0,15}{21,6} \left( \frac{0,15}{12,6} \right)^{3/2} = 14,7 \text{ kg/cm}^2,$$

Stability margin by formula (9.4);

$$K = \frac{14,7}{7,5} = 1,96,$$

Thus, the accepted thickness of the wall is determined basically by stability,

#### 9.4. Materials

Flame tubes operate in conditions of high temperatures; therefore, the basic requirements of materials for their manufacture are heat resistance and high-temperature stability. Furthermore, materials for combustion chambers must possess good plasticity, permit large drawing during cold stamping and be welded well. For flame tubes of contemporary engines they apply heat-resistant alloys on a nickel base [Kh20N80T] (Х20Н80Т), [EI602] (ЕИ602), and others.

Outer and inner casings of combustion chambers operate at considerably smaller temperatures. For their manufacture heat-resistant steel [1Kh18N9T] (1Х18Н9Т), carbon steel with carburizing of surface, and so forth are used.

## C H A P T E R X

### EXHAUST UNITS AND AFTERBURNERS

#### 10.1. General Information

Exhaust units serve for exit from the engine of working gases used in the turbine and the creation jet thrust.

Part of the head of working gases in [TRD] (TPII) is used up in the turbine, and part in the exhaust unit 5 (see Fig. 1.1). The exhaust unit of a TRD constitutes an exhaust pipe 1 and nozzle caps 2 (Fig. 10.1), which together is called exhaust (propulsion) nozzle.

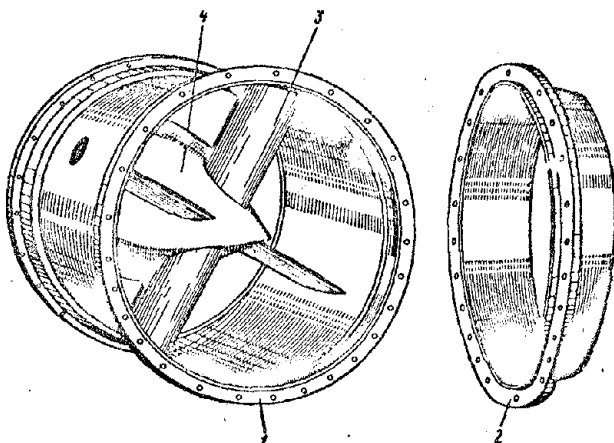


Fig. 10.1. Exhaust nozzle.

Exhaust pipe is attached to turbine housing. Inside it by means of radial struts 3 is mounted the bullet 4 of the turbine disk, which ensures smooth transition of gas flow from annular section at turbine exit to circular section of exhaust pipe. Exhaust pipe is in the form of the frustum of a cone, forming for the gases a channel with fixed or somewhat divergent passage sections.

For outlet of gases beyond the limits of the aircraft the exhaust pipe is frequent enlarged by means of installation of an additional, so-called extension pipe. In this case exhaust pipes are usually somewhat expanded. Speed of gases decreases, which leads to decrease of hydraulic losses in extension pipe.

The nozzle cap is the main working part of the exhaust nozzle. In it there occurs expansion of working gases and available head is converted in to kinetic energy of gases. Since speed of gas flow on outlet from nozzle reaches 450 to 600 m/sec, for decrease of hydraulic losses the nozzle cap is placed on the end of the exhaust pipe, and with an extension pipe, on the end of it. Nozzle caps usually have the form of a convergent channel (see Fig. 10.1). However, at large pressure drops they have the form of a laval nozzle (Fig. 10.2).

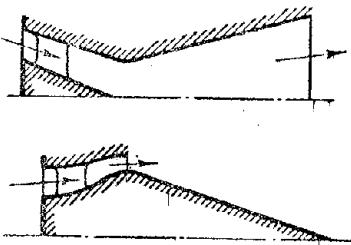


Fig. 10.2, Forms of supersonic nozzles,

Exhaust nozzles operate in conditions of high temperature, which in gases at nozzle, outlet is from 550 to 650 °C. Exhaust nozzles are made from heat-resistant sheet steel of welded construction. In order to protect aircraft components located near the exhaust nozzle from heating, and to decrease losses of heat in the environment, the walls of

the exhaust and extension pipes from the outside are frequently covered by thermal insulation material. Sometimes for cooling on the outside of the exhaust pipe there is a special casing, forming with it a radial clearance. Through this clearance under impact pressure atmospheric air is blown.

Types of nozzles. TRD exhaust nozzles are nonadjustable and adjustable, fixed-area exhaust nozzles have constant outlet sections. In variable-area nozzles the outlet sections can be changed by means of regulating devices depending upon operating conditions of engine and conditions of flight. Figure 10.1 shows a fixed-area exhaust nozzle, and Fig. 1.7 and 1.8 shows TRD with fixed-area exhaust nozzles,

Figure 10.3 depicts the diagram of variable-area nozzles. In diagram a adjustment of outlet section is carried out by axial shift of central housing, i.e., bullet 1, which is fixed in the central bullet housing. In diagram b adjustment is carried out by means of two flaps 2, hinged to the exhaust nozzle. When closing of the flaps, initially the circular section of the nozzle obtains an elliptic form. In diagram c adjustment is carried out by means of an annular set of flaps 3, hinged to the exhaust nozzle. Because of the large number of flaps the circular form at the nozzle exit is kept also when flaps are closed. Diagram d depicts a nozzle with aerodynamic adjustment.

Annular cavity 4 from one stage of the compressor receives compressed air which on the nozzle section heads perpendicular to the flow of gases, compressing it and decreasing its effective cross section. Figure 1.3 shows the diagram of a TRD with variable-area propulsion nozzle, made according to diagram a.

Adjustable nozzles make it possible to regulate engine operation. Thus, with increase of area of passage section of the exhaust nozzle the pressure of gases behind the turbine decreases, in consequence of which the pressure drop in the turbine increases. With decrease of area of passage section the pressure of gases behind the turbine increases, in consequence of which the pressure drop in the turbine decreases. During constant fuel consumption in the first case there occurs increase of capacity of turbine, and consequently also engine revolutions, and in the second case they are decreased.

Simultaneous adjustment of area of passage section of exhaust nozzle and fuel feed can improve TRD performance, facilitate starting and, improve pick-up of engine. However, in TRD, intended for a comparatively narrow speed range of flight, adjustment by the exhaust nozzle is not very effective. Therefore, for the purpose of simplification of construction of the exhaust nozzle, TRD frequently have fixed-area nozzles. Variable-area nozzles are widely used in TRD with afterburners, in which under non-boosted and boosted operating conditions by the change of passage section of nozzle the parameters of gases in front of the turbine are kept constant. Of special interest for the case of large pressure drops are adjustable nozzles of the Laval type.

Afterburners. TRD augmentation by increasing fuel feed to the main combustion chambers is limited by the temperature rise of working gases in front of the turbine. Along with this, the presence of free oxygen in the working gases allows additional burning of fuel in afterburners, attached behind the turbine. Due to increase of temperature there is an increase of exhaust velocity of gases from the nozzle attached to the end of the afterburner, and consequently thrust of the TRD. Temperature of working gases in afterburners can be increased to  $1300\text{-}1700^{\circ}\text{C}$ . Engine thrust will then increase by 25 to 50% and above. Figure 1.4 shows the diagram of a TRD, and Fig. 1.9 gives the overall view of a TRD with afterburners.

Figure 10.4 depicts the diagram of an afterburner. In distinction from from the main combustion chambers (see Fig. 9.1) the afterburners do not have

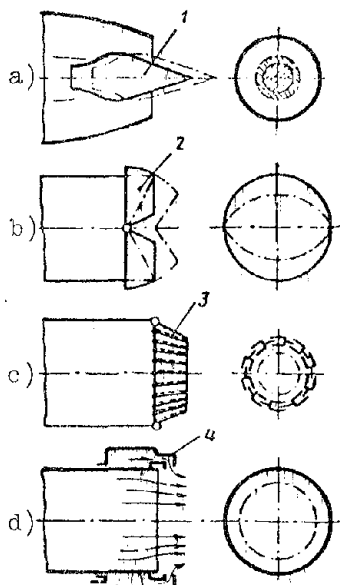


Fig. 10.3. Diagram of adjustable nozzles,

flame tubes and stable process of burning is ensured in them due to the high temperature of gases, leaving the turbine, and the flame holders,

Intake of chamber is made in the form of an annular diffuser which is formed by tube 1 and cowl of turbine disk 2. The cowl is attached to the tube by struts 3. In diffuser there occurs lowering of speed of gas flow, which by means of a large number of burners 4 receives the fuel.

Flame holders are usually made in the form of rings 5 of corner section (annular holder), behind the edges of which there appears breakdown of gas flow with formation of reverse vertical currents. Cowl 2 of the turbine is frequent made in the form of the frustum of a cone. Its rear wall forms the central flame holder; behind it there are also reverse vertical currents. In the zone flame holders the front of the flame is also stabilized,

The starter consists of electric igniter 6 and starting burners 7. Basic fuel is ignited from starting flame jet,

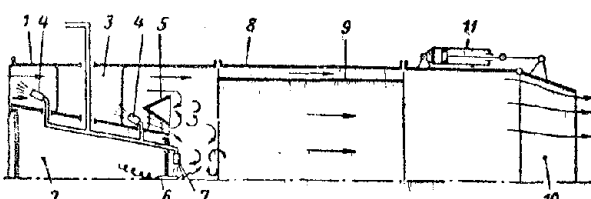


Fig. 10.4. Diagram of afterburner.

Burning occurs in center of chamber which is made in the form of a cylindrical or slightly conical pipe 8. For decrease of heating it frequently has inside a shielding pipe 9. Through the radial clearance between them pass the less heated gases not participating in burning.

At the afterburner exit there is an adjustable nozzle 10 (in the diagram it is the flap type). It is controlled by means of hydraulic cylinders 11. Adjustable nozzle allows for a maximum outlet section of nozzle in augmentation conditions and minimum outlet section with afterburner off. This ensures support in front of the turbine of constant basic parameters of working gases, both in augmented, and also in non-augmented operating conditions. Furthermore, in certain conditions it is possible to establish intermediate positions of opening of nozzle.

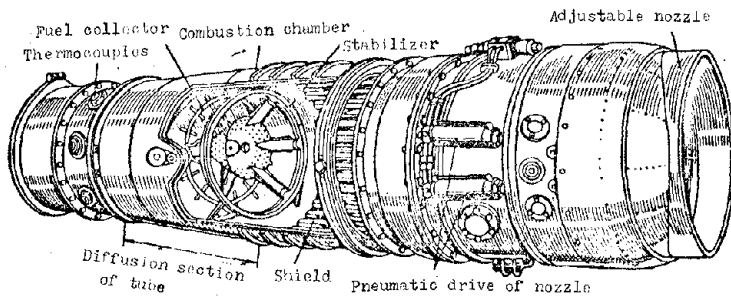


Fig. 10.5. Afterburner.

Figure 10.5 shows the afterburner of a foreign engine. In the beginning it has a diffusion section, at the end of which there is a stabilizer. The stabilizer consists of a ring and central perforated cone united by radial struts. Ring and struts have a corner profile. In center of cone there is an electric igniter ensuring initial fuel ignition during starting of chamber. In front of the stabilizer there is an annular fuel collector with a large number of burners. Behind the stabilizer in the zone of burning inside the afterburner there is a corrugated shield that protects the walls of the chamber from excessive heating. At the afterburner exit there is an adjustable nozzle which is controlled by means of a pneumatic drive.

Afterburners operate at high temperatures. They are welded from heat-resistant alloys and steel.

Thrust reversal. One of the most effective means of decreasing the landing distance of an aircraft with TRD during landing are the special reversal units called thrust reversal. With the help of reversal the gas flow behind the turbine turns, and at a certain angle emerges toward the motion of the aircraft. Negative thrust is created, which brakes the motion of the aircraft during landing. Due to this the run of the aircraft can be reduced approximately in half. Furthermore, thrust reversal in flight can perform the role of an air brake, facilitating diving and increasing maneuverability of the aircraft.

Reversal units are classified:

- 1) by place of turn of gas flow - with turn in exhaust nozzle or behind it.
- 2) by method of deflection of gas flow - with mechanical or gas-dynamic deflection.

Figure 10.6 gives some typical diagrams of thrust reversals. Motion of gases is shown by arrows.

In diagrams a and b thrust reversal is in the exhaust nozzle. In diagram a deflection of gas flow is carried out mechanically by shutting flat 1 with

simultaneous movement into working position of carriage 2 with a screen. In diagram b deflection of gas flow is carried out by gas-dynamic method. Simultaneously with shift of carriage 2 working position through channels of hollow strut 1 at an angle to main flow there heads the flow of air with great speed. This also deflects the main flow of gases towards the screen. Air for thrust reversal is ejected from the main compressor of the engine at about 2 to 3% of the flow rate. In diagrams c and d the thrust reversal devices are behind the exhaust nozzle. Deflection of gas flow is carried out by mechanical method: in diagram c by means of two folding doors 1, and in diagram d with flap 1,

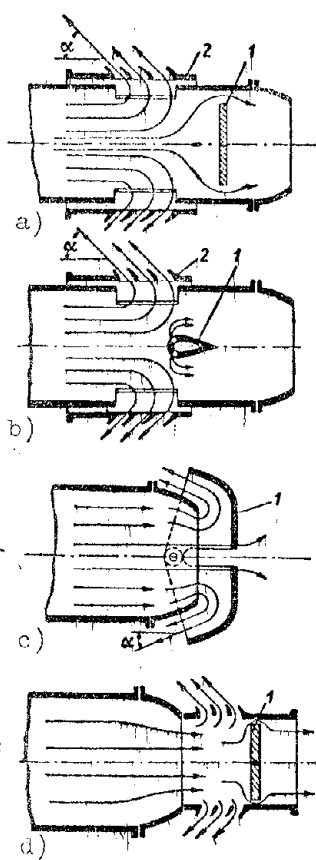


Fig. 10.6. Diagrams of thrust reversal devices.

Negative thrust is even greater the smaller the outlet angle  $\alpha$  of flow. However, its minimum value is limited by the possibility of contact of gas flow with parts of the aircraft and fall of gases into engine inlet; therefore, usually  $\alpha > 45^\circ$ . Reversal devices should ensure symmetric outlet of flow of gases, in order to avoid appearance of moments disturbing aircraft balancing.

Thrust reversal is usually characterized by the value of the thrust reversal coefficient  $K$ , which is equal to the ratio of negative thrust  $P_r$  developed by an engine during flight of an aircraft to positive thrust in static ground conditions  $P_0$ :

$$K = \frac{P_r}{P_0},$$

The reversal coefficient depends on speed of flight of aircraft and varies in rather wide limits.

Noise silencers. The main source of noise in a TRD is the flow of exhaust gases which with a speed of the order 600 m/sec emerges from the exhaust nozzle and, being mixed with atmospheric air, causes strong turbulization in it. Intensity of noise varies in proportion to the eighth degree of speed of gas flow and first degree of area of its section.

For reduction of noise of the exhaust nozzle TRD are sometimes supplemented by special devices — noise silencers — with the help of which there occurs admixing of atmospheric air to the flow of exhaust gases at their outlet from

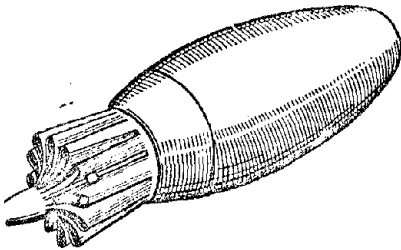


Fig. 10.7. Noise silencer.

the nozzle. Speed of gases drops and intensity of noise decreases. Admixing of air to gases is carried out by installation of an ejector pipe around the exhaust nozzle, by given the nozzle of a corrugated form or, finally, by replacement of one large nozzle by a group of smaller nozzles.

Figure 10.7 shows an exhaust nozzle with corrugated outlet form.

Noise silencers noticeably lower performance, increase drag and weight of TRD. Therefore, they have limited application.

[TVD] (TRD) exhaust devices. The total head of working gases of TVD is usually exhausted in the turbine. Therefore, their exhaust device does not have a nozzle cap and is made in the form of a simple exhaust pipe 7 (see Fig. 1.10). The pipe is attached to the turbine housing and serves for ejection of gases out of the aircraft without their essential expansion. Sometimes, according to the conditions of installation of TVD on an aircraft the ejection of exhaust gas is done at a small angle downwards or aside with respect to flight. This is ensured by the corresponding form of exhaust pipe.

#### 10.2. Design of Exhaust Nozzles.

Fixed-area exhaust nozzle. Figure 10.8 shows the detachable fixed-area exhaust nozzle of the TRD [VK-1] (BK-1) which consists of exhaust pipe 4, bullet 6, four streamlined bars 11, tie rods 9, and nozzle cap 15.

Exhaust pipe 4 has small taper in the direction of the nozzle cap. By its front flange 3 the pipe is attached to the turbine housing, and to rear flange 12 are attached nozzle caps 15 or an extension pipe. On external surface of pipe 4 there are out five annular bands 7. Pipe has thermal insulation in the form of a layer of asbestos fabric and several layers of aluminum foil. Foil on the pipe held by a screen made from spiral wire. From above the pipe is covered by aluminum casing 8 split along its axis. The casing is mounted on bands and held by four collars 10. The strip of pipe located between first and second bands does not have thermal insulation. It is covered by casing 5 and forms an annular cavity which preheats the air proceeding for heating of the cockpit. On exhaust pipe there are four receivers for measurement of temperature of gases.

Cone 6 consists of three parts welded together. For protection of turbine disk from heating in the area of the exhaust nozzle, to flange 2 of the cone is fastened a thermal insulation screen that has a double bottom 1 with asbestos lining. Cone 6 is attached to exhaust pipe by two pairs of tie rods 9 closed in the flow area by four streamlined bars 11. Rods are located cross-like in strips and pass through guide sleeves. Welded to the cone and exhaust pipe. To ensure free thermal expansion, rods 9 are attached on one end, and their other end remains free. Figure 10.9 shows bolt attachment of rod 9 to exhaust pipe 4. Streamlined bars 11 (Fig. 10.10) are made from sheet heat-resistant steel. Inside each one there are three reinforcing shelves and guide sleeves for rods 9.

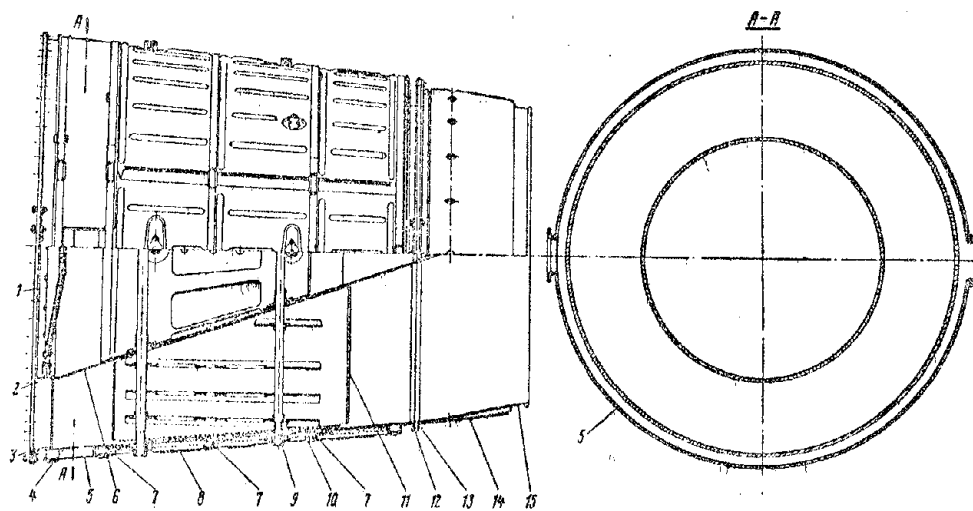


Fig. 10.8. Exhaust nozzle of the VK-1 engine.

Nozzle cap 15 (see Fig. 10.8) has flange 13 and deflector 14 with holes. By mean of flange 13 the cap is attached to the exhaust or extension pipes. Deflector with cap forms an annular slot. By the ejectional action of the stream of gases, leaving the cap, there is ensured blowing of the annular slot by cold air which enters it through holes in the front part of deflectors.

Figure 10.11 represents the exhaust nozzle of the VK-1 in dismantled form.

Variable-area exhaust nozzle. Figure 10.12 shows the variable-area exhaust nozzle of the [RJ-10] (PJ-10) engine with throat bullet. Throat bullet 1 of welded construction is movable on roller supports 2 and 4 central part of internal cone 3.

Control of bullet movement is carried out by automatically by hydraulic drive and mechanical transmission. The automatic device and hydraulic drive

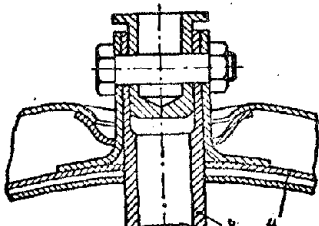


Fig. 10.9. Attachment of rod to exhaust pipe.

are not shown in the figure. Mechanical transmission consists of a pair of conical gears 6, vertical shaft 5, and cylindrical gear 8 with toothed rod 7. Conical gears 6 are placed above exhaust nozzle in its upper part and are brought into motion through the horizontal shaft from the hydraulic drive. Cylindrical gear 8 is placed in central part of internal cone 3 and is linked with toothed rod 7 which is connected to throat bullet 1. Vertical shaft 5 passes through hollow strut of nozzle and transmits motion to cylindrical gear 8. Depending upon conditions and performance of engine, by moving the throat bullet is possible to change the area of outlet section of the exhaust nozzle from 0.1 to  $0.165 \text{ m}^2$ .

Guide sleeve for tie rod.

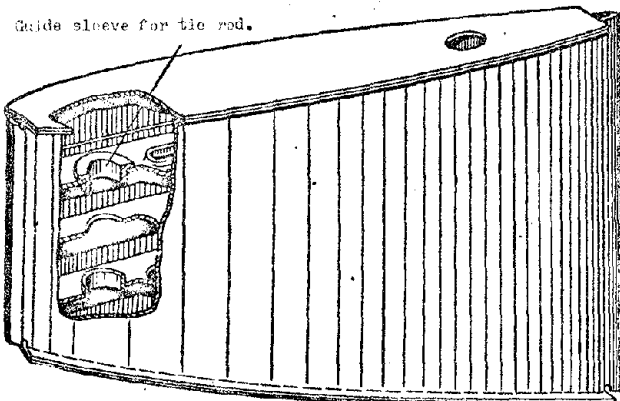


Fig. 10.10. Rod fairing.

Exhaust nozzle is cooled by air which is ejected behind the 4th stage of the compressor and is feed into the radial clearance b between external wall of nozzle and casing. Hence, air through hollow struts passes for cooling of internal cone and throat bullet. Air cooling the bullet emerges through clearance a between bullet and internal cone

to flow area of nozzle. At outlet end of nozzle there is welded a deflector. By the ejectional action of the ensuing stream of gases the air is blown from environment through clearance c at the deflector and cools the outlet part of nozzle.

### 10.3. Strength Calculation

Exhaust nozzle, extension pipe, and afterburner are calculated as thin-walled shells. Appearing in them under the action of an axial load and internal excess pressure, stresses  $\sigma_x$  and  $\sigma_y$  are determined by formulas (9.1) and (9.2). In [GTD] (ГТД) devices stress  $\sigma_x$  does not exceed  $250 \text{ kg/cm}^2$ , and  $\sigma_y$  reaches  $1000 \text{ kg/cm}^2$ .

Upon turning off engines in flight (for instance during diving) in the engine nacelle there appears excess air pressure which can reach  $\Delta p = 0.3 \text{ kg/cm}^2$  and higher. Under the action of this pressure the shells of the exhaust devices

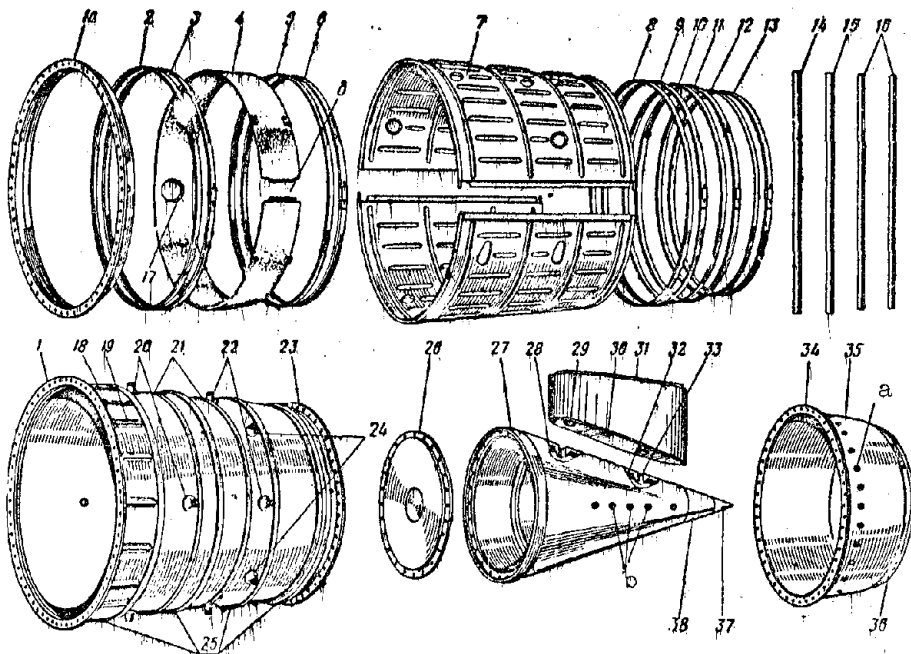


Fig. 10.11. Exhaust nozzle of VK-1 engine in dismantled form, 1 and 23) front and rear flanges of exhaust pipe; 1a) support ring; 2, 5, 8, 10 and 12) lining of collars; 3, 6, 9, 11 and 13) collars; 4) front casing; 7) casing; 14, 15 and 16) tie rods; 17) outlet throat of casing; 18) exhaust pipe; 19) stripping; 20 and 22) guide sleeves of tie rods; 21 and 25) bands; 24) bushing for thermocouples; 26) bottom of cone; 27) flange of cone; 28) cone; 29) fairing of tie rods; 30 and 31) cover of fairing; 32) bushing holder; 33) bushing of tie rods; 34) flange; 35) deflector; 36) nozzle caps; 37) tip of cone; 38) vertex of cone; a) inlets of deflector, b) holes for equalizing pressure around cone, d) inlet slit of casing 4,

will be compressed. Therefore, they are checked for stability by formulas (9.3) and (9.4). Reserve of stability is usually greater than 2.

Axial force, applied to the nozzle can be determined by the following formula

$$P_0 = \frac{\pi}{4} (D_1^2 p_1 - D_2^2 p_2) + \frac{G}{g} (c_{1a} - c_{2a}) \quad (10.1)$$

where  $G$  is the flow rate of gases through nozzle, kg/sec;  $p_1$  and  $p_2$  are the pressures of gases on inlet and outlet of nozzle, kg/cm<sup>2</sup>;  $c_{1a}$  and  $c_{2a}$  is the speed of gases on inlet and outlet of nozzle, m/sec;  $D_1$  and  $D_2$  are the diameters of sections at inlet and outlet of nozzle,

Force  $P_0$  is directed towards the flow of gases (Fig. 10.13). Flange for attaching exhaust nozzle to turbine housing is calculated for bending from axial force  $P_0$

$$\sigma_y = \frac{P_0 d}{W_u}, \quad (10.2)$$

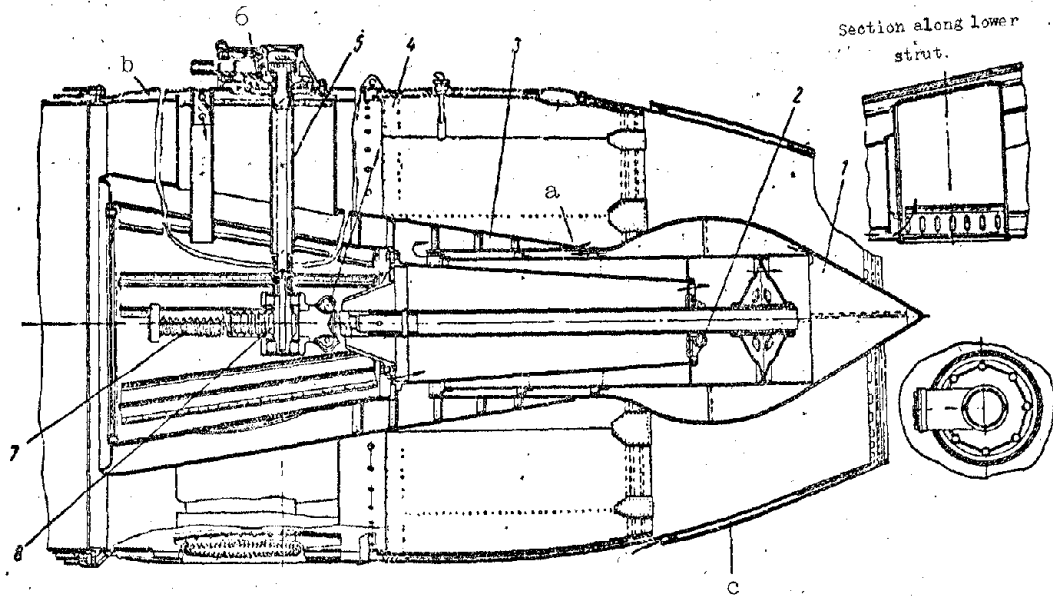


Fig. 10.12. Exhaust nozzle of RD-10 engine.

where moment of drag

$$W_d = \frac{\pi D_3 a^2}{6}. \quad (10.3)$$

For flanges of steel GTD housings,  $\sigma_u < 1500 \text{ kg/cm}^2$ .

Example: Determine stresses and reserve of stability of exhaust nozzle.

Given:  $p_1 = 1.48 \text{ kg/cm}^2$ ;  $p_2 = 1.033 \text{ kg/cm}^2$ ;  $G = 48 \text{ kg/sec}$ ;  $c_{1a} = 395 \text{ m/sec}$ ;  $c_{2a} = 556 \text{ m/sec}$ ;  $D_1 = 74 \text{ cm}$ ;  $D_2 = 54 \text{ cm}$ ;  $D_3 = 76 \text{ cm}$ ;  $b = 10 \text{ mm}$ ;  $a = 3 \text{ mm}$ ;  $\delta = 1 \text{ mm}$ ;  $E = 1.4 \cdot 10^6 \text{ kg/cm}^2$ ;  $l = 25 \text{ cm}$ .

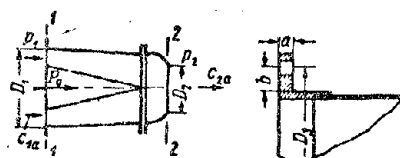


Fig. 10.13. Calculation of exhaust nozzle strength.

Axial force by formula (10.1):

$$P_o = \frac{\pi}{4} (74^2 \cdot 1.48 - 54^2 \cdot 1.033) + \frac{48}{9.81} (395 - 556) = 4250 \text{ kg}.$$

Tensile stress in cross section by formula (9.1):

$$\sigma_x = \frac{4250}{2 \cdot 3.14 \cdot 37 \cdot 0.1} = 183 \text{ kg/cm}^2$$

and in longitudinal section by formula (9.2):

$$\sigma_y = \frac{(1.48 - 1.033) \cdot 37}{0.1} = 167 \text{ kg/cm}^2.$$

Critical pressure by formula (9.3):

$$\Delta p_{kp} = 0.92 \cdot 1.4 \cdot 10^6 \frac{0.1}{25} \left( \frac{0.1}{37} \right)^{3/2} = 0.724 \text{ kg/cm}^2.$$

Reserve of stability by formula (9.4):

$$K = \frac{0.724}{0.3} = 2.41.$$

Thus, thickness of wall is determined by condition of stability moment of drag of flange by formula (10.3):

$$W_s = \frac{3,14 \cdot 76 \cdot 0,32}{6} = 3,58 \text{ cm}^3$$

Bending stress on flange by formula (10.2):

$$\sigma_s = \frac{4250 \cdot 1}{3,58} = 1190 \text{ kg/cm}^2$$

#### 10.4. Materials

Exhaust nozzle and afterburner operate in conditions of high temperatures. The basic requirements for materials are heat resistance and high-temperature stability. Furthermore, material should possess good plasticity, allow large drawing during cold stamping, and be welded easily.

In contemporary engines, for the exhaust pipe, outlet cap, and extension pipes, heat-resistant chrome-nickel steel [1Kh18N9T] (1X18H9T) is used. Certain elements of afterburners, operating in conditions of heightened temperatures, are made from nickel-chrome alloy [Kh20N8OT] (X20H8OT) and chrome-nickel steel [Kh23N18] (X23H18).

## C H A P T E R XI

### TURBOPROP REDUCTION GEARS

#### 11.1. General Information

Propellers are selected considering [TVD] (ТВД) power and aerodynamic properties of the aircraft. Optimum speed of prop, corresponding to its highest efficiency, is usually from 800 to 1200 rpm, and speed of TVD turbine is from 6000 to 18,000 rpm. For lowering the propeller speed, TVD has a reduction gear with transmission ratio from 0.05 to 0.15.

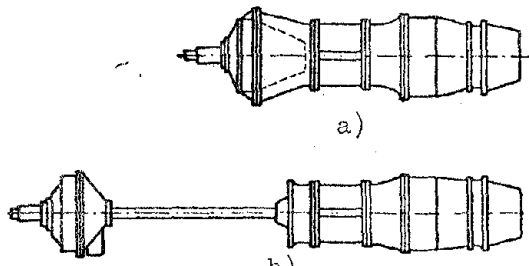


Fig. 11.1. Diagrams of location of TVD reduction gears.

The reduction gear can be included in the engine design, as shown in Fig. 11.1a, or be made in the form of a separate unit which receives engine power through an intermediate transmission shaft (Fig. 11.1b).

The efficiency of a reduction gear is  $\eta = 0.98$  to  $0.99$ , i.e., 1-2% of the transmitted power is lost due to friction in the teeth of the gears and in the bearings. However, the obtained gain in propeller efficiency considerably exceeds these losses and justifies the application of a reduction gear. Work of friction in reduction gear is turned into heat, which is equal to:

$$Q = 632 (1 - \eta) N \text{ kcal/hr}, \quad (11.1)$$

where 632 is the thermal equivalent of work;

$N$  is power of engine fed to reduction gear.

This heat is drawn off by oil, proceeding for lubrication of the reduction gear and is partially transmitted through walls of housing into the environment.

Types of reduction gears, TVD reduction gears can be classified in the following way;

- 1) by relative location of shafts of propeller and engine – coaxial and displaced,
- 2) by number of propellers – with transmission to one and two propellers,
- 3) by number of stages – two and three-stage,
- 4) by kinematic pattern – with simple, planet, differential, and compound transmissions. Compound systems of transmissions are obtained as a result of combining the three preceding systems.

To ensure free access of air to compressor with uniform field of speeds, reduction gears are made chiefly with coaxial location of shafts of engine and propeller. Diameters of reduction gears should be as small as possible.

Reduction gears with displaced axes of shafts can find application in the form of independent units with transmission of rotation through an intermediate transmission shaft (see Fig. 11.1b) from one or two engines,

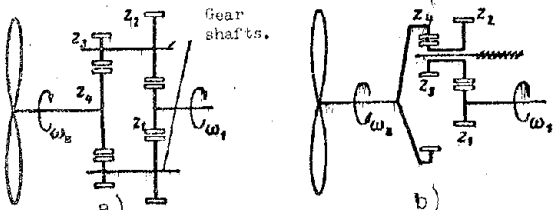


Fig. 11.2. Diagrams of TVD reduction gears with simple transmission. a) with external engagement, b) with internal engagement of second stage.

In powerful TVD the propellers are large and heavy. Therefore, they have two propellers located coaxially and revolving in different directions. Application of two coaxial propellers gives the following advantages:

- 1) decrease of diameter of propellers;
- 2) some increase in propeller efficiency;
- 3) balancing of jet and gyroscopic moments of propellers;
- 4) decrease of air swirling behind propellers.

Along with this, the kinematic pattern and design of the reduction gear for two coaxial propellers are more complicated and heavier. Therefore, in TVD of low and medium power they chiefly apply one propeller.

Number of stages of reduction gear is determined by transmission ratio and its kinematic pattern. With increase of number of stages the diameters of reduction gears decrease, but its design is more complicated.

For decrease of load on gear teeth in case of simple transmission they apply

several intermediate gear shafts, parallel connected to transmission (Fig. 11.2a), and in case of planet and differential transmissions, several satellites are used. Intermediate shafts and satellites are uniformly arranged along the circumference to unload the radial bearings of the drive shaft and propeller shaft from tangential forces. Equal distribution of load between intermediate shafts or satellites is attained by high precision of manufacture.

### 11.2. Kinematic Patterns and Transmission Ratios of Reduction Gears

Reduction gears with simple transmission. Figure 11.2 shows diagrams of reduction gears with two-stage simple transmission. Application of internal engagement on the second stage ensures smaller gear diameters. Transmission ratio of reduction gear is equal to

$$i_g = \frac{z_1 z_3}{z_2 z_4}. \quad (11.2)$$

Planet reduction gears. Figure 11.3 depicts diagrams of planet reduction gears with single and double satellites. Planet reduction gear consists of driving  $z_1$ , fixed  $z_3$ , and satellite gears:  $z_2$  in the case of single satellites,  $z_2'$  and  $z_2''$  in the case of double satellites. Satellites are mounted on axles attached to pinion carrier (satellitecarrier). During rotation of gear  $z_1$  satellites  $z_2$  run around fixed gear  $z_3$  and rotate the pinion carrier, and together with it the propeller shaft. Satellites  $z_2$  or  $z_2'$  and  $z_2''$  accomplish resultant motion which consists of two simple motions: relative rotation with angular velocity  $\omega_2$  around its own axis and transportation with angular velocity  $\omega_B$  jointly with the pinion carrier and propeller shaft around the axis of the latter.

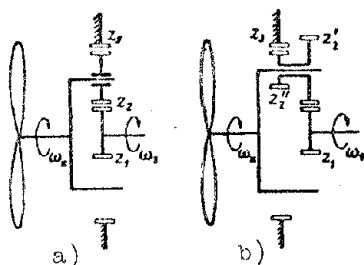


Fig. 11.3. Diagrams of TVD reduction gears with planet transmission. a) with single satellites, b) with double satellites.

To determine transmission ratio of planet reduction gear, we reduce it to simple transmission. For this we mentally revolve the whole reduction gear with angular velocity  $\omega_B$  in direction opposite the rotation of the pinion carrier with respect to the axis of the latter. Then the pinion carrier stops and the satellites revolve only with respect to their axes with angular velocity  $\omega_2$  as idle

gears. At the same time pinion gear  $z_1$  will revolve with angular velocity  $\omega_1 - \omega_B$ , and fixed gear  $z_3$  with angular velocity  $\omega_B$ . This is how we obtain simple transmission ratio will be equal to:

$$i = \frac{\omega_2}{\omega_1 - \omega_3} . \quad (11.3)$$

This transmission ratio, expressed by ratios of number of teeth, will be equal to:

$$\left. \begin{array}{l} \text{with single satellites } i = \frac{z_1}{z_3}, \\ \text{with double satellites } i = \frac{z_1 z_2}{z_3 z_2}, \end{array} \right\} \quad (11.4)$$

From expressions (11.3) and (11.4) we obtain the transmission ratios of the planet reduction gear:

with single satellites

$$i_p = \frac{\omega_2}{\omega_1} = \frac{1}{\frac{z_3}{z_1} + 1}, \quad (11.5)$$

with double satellites

$$i_p = \frac{\omega_2}{\omega_1} = \frac{1}{\frac{z_3 z_2}{z_1 z_2} + 1}, \quad (11.6)$$

From consideration of Fig. 11.3 and the obtained expression it is not difficult to arrive at the conclusion that at a given transmission ratio the double satellites of a planet reduction gear ensure smaller diameters than single satellites.

At the low transmission ratio which are used for TVD, reduction gears with simple and planet transmission do not have any significant advantages over one another. As an example, Fig. 11.4 shows a planet reduction gear with double satellites. Its undercarriage consists of drive shaft 1 (constructed simultaneously with pinion gear), double satellites 2 and 3, satellitecarrier 4 and fixed gear ring 5.

Differential reduction gear. Figure 11.5 depicts diagrams of a differential reduction gear driving two coaxial propellers. Front propeller obtains rotation from pinion and rear from gear  $z_3$ . Differential mechanism of reduction gear divides rotation into two coaxial propellers in opposite directions. Differential reduction gear has small dimensions, minimum number of stages, and high efficiency. At the same time, it has two degrees of freedom and transmission ratios for the front and rear propellers are established depending upon characteristics of loads of propellers.

For finding the transmission ratios of the differential reduction gear we use the method of pinion stop. For this we shall revolve the whole reduction gear with respect to its axis with angular velocity  $\omega_B$  in a direction opposite

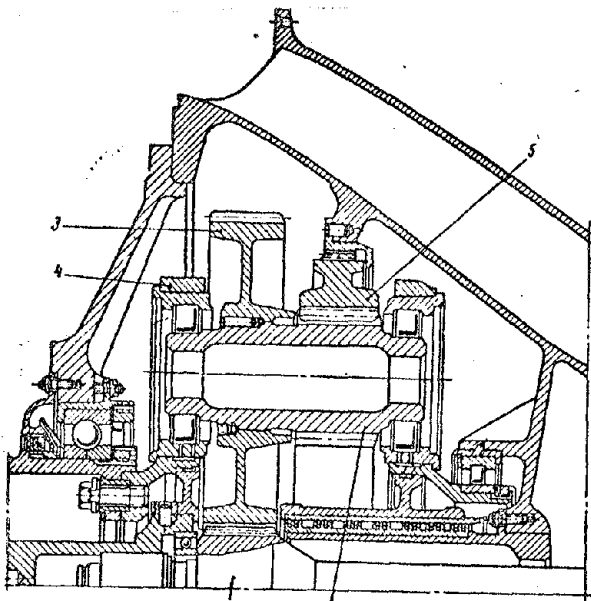


Fig. 11.4. TVD planet reduction gear with double satellites.

the rotation of the pinion. Then the pinion is stopped and we obtain simple transmission in which gear  $z_1$  will revolve with angular velocity  $\omega_A - \omega_B$ , and gear  $z_3$  with angular velocity  $\omega_C + \omega_B$ . Transmission ratio in this case will be equal to:

$$i = \frac{\omega_C + \omega_B}{\omega_A - \omega_B}. \quad (11.7)$$

This transmission ratio, expressed through ratios of number of teeth, will be equal to:

with single satellites (see Fig. 11.5a))

$$i = \frac{z_1}{z_3},$$

with double satellites (see Fig. 11.5b))

$$i = \frac{z_1 z_3}{z_2 z_4}.$$

} (11.8)

From expression (11.7) we obtain

$$\omega_A - (1+i) \omega_B - \omega_C = 0, \quad (11.9)$$

or

$$i_C + (1+i) i_B - i = 0, \quad (11.10)$$

where

$$i_C = \frac{\omega_C}{\omega_A} \text{ and } i_B = \frac{\omega_B}{\omega_A} \quad (11.11)$$

express transmission ratios between driving link A and driver links B and C. Obtained expression (11.10) connects transmission ratios of front B and rear C propellers. It constitutes one equation with two unknowns and therefore does not give a definite solution. This is explained by the fact that the differential mechanism has two degrees of freedom. Second equation is composed from the characteristics of loads of propellers. Thus, moments of resistance to rotation of front B and rear C propellers can be represented in the form

$$\left. \begin{aligned} M_B &= K_B \omega_B^2; \\ M_C &= K_C \omega_C^2, \end{aligned} \right\} \quad (11.12)$$

where  $K_B$  and  $K_C$  are proportionality factors which will be called the parameters

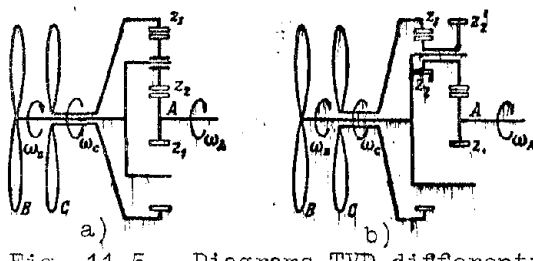


Fig. 11.5. Diagrams TVD differential reduction gears, a) with single satellites, b) with double satellites.

of the propellers,

If one does not consider losses due to friction in the reduction gear, it is possible to compose an equation of operations for the driving and driven links of the mechanism in the following form:

$$M_A \omega_A - M_B \omega_B - M_C \omega_C = 0, \quad (11.13)$$

From comparison of equations 11.13 and 11.9, we obtain;

$$\left. \begin{aligned} M_A &= \alpha \\ M_B &= \alpha(1+\delta) \\ M_C &= \alpha \end{aligned} \right\} \quad (11.14)$$

where  $\alpha$  is the proportionality factor,

Using expressions (11.14) and (11.12), obtain

$$\frac{M_B}{M_C} = 1 + i = \frac{K_B}{K_C} \left( \frac{\omega_B}{\omega_C} \right)^2, \quad (11.15)$$

whence

$$\omega_B^2 = (1+i) \frac{K_C}{K_B} \omega_C^2, \quad (11.16)$$

Dividing this expression term, by term by  $\omega_A^2$  and considering expressions (11.11), we obtain a second equation for transmission ratios;

$$i_s = i_q \sqrt{(1+i) \frac{K_C}{K_B}}, \quad (11.17)$$

The root here is taken as arithmetical (positive).

As a result of joint solution of equations (11.10) and (11.17) we obtain expressions of transmission ratios for front and rear propellers of differential reduction gear depending upon transmission ratio of simple transmission  $i$  [ratio of number of teeth according to expression (11.8)] and on the ratio of propeller parameters  $K_C$  and  $K_B$ :

$$i_s = \frac{i \sqrt{(1+i) \frac{K_C}{K_B}}}{1 + (1+i) \sqrt{(1+i) \frac{K_C}{K_B}}}, \quad (11.18)$$

and

$$i_c = \frac{i}{1 + (1+i) \sqrt{(1+i) \frac{K_C}{K_B}}},$$

Roots here are taken as arithmetical (positive).

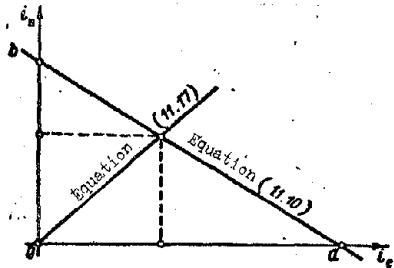


Fig. 11.6. Graphic solution of equations (11.10) and (11.17).

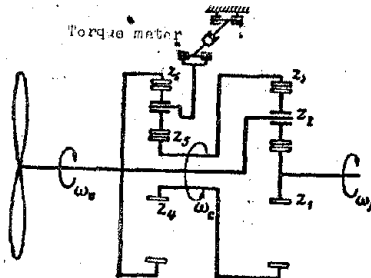


Fig. 11.7. Diagram of closed TVD differential reduction gear.

Graphic solution of the system of two equations (11.10) and (11.17) is shown in Fig. 11.6. With the selected number of teeth of the mechanism of the reduction gear by means of selection of propellers (parameters  $K_B$  and  $K_C$ ) transmission ratios  $i_B$  and  $i_C$  can vary from zero to values, limited by points a and b. Point O corresponds to stop of propeller at which  $K = \infty$ . Thus, for instance, upon stop of rear propeller the differential reduction gear becomes a planet gear. In this case  $K_C = \infty$ , and  $i_C = 0$ , and the expression for  $i_B$  after preliminary division of numerator and denominator by  $\sqrt{\frac{K_C}{K_B}}$  (for the purpose removal of uncertainty) can be reduced to the form

$$i_B = \frac{1}{i+1}, \quad (11.19)$$

identical to formulas (11.5) and (11.6).

Distribution of power for the differential reduction gear between front and rear propellers can be obtained by using expressions (11.15) and (11.16):

$$\frac{N_B}{N_C} = \frac{M_B \omega_B}{M_C \omega_C} = \sqrt{(1+i)^3 \frac{K_C}{K_B}}. \quad (11.20)$$

Closed differential reduction gear. Figure 11.7 shows the diagram of a closed differential reduction gear, which pertains to a group of compound kinematic diagrams. In this case the first stage of the reduction gear is differential with transmission of rotation from the pinion directly to the propeller. Second stage is simple. It transmits rotation from gear  $z_3$  also to the propeller shaft. Stage of differential transmission in the beginning divides rotation into two branches to the pinion and to movable gear ring  $z_3$  and then these two branches are closed by the propeller shaft. This reduction gear only has one degree of freedom with a definite transmission ratio. The ratio is found in the following way. Equation (11.10) gives the connection

of transmission ratios of differential stage of reduction gear for the pinion (satellitecarrier)  $i_B$  and for the large movable gear  $z_3 - i_C$ .

$$i_C + \left(1 + \frac{z_1}{z_3}\right) i_B - \frac{z_1}{z_3} = 0 \quad (11.21)$$

The condition of connection gives us a second equation

$$i_B = \frac{z_1}{z_3} i_C \quad (11.22)$$

Solving jointly equations (11.21) and (11.22), we obtain transmission ratio

$$i_B = \frac{1}{1 + \frac{z_3}{z_1} + \frac{z_3 \cdot z_6}{z_1 \cdot z_4}} \quad (11.23)$$

The ratio of transmitted moments  $M_B$  of the pinion and  $M_C$  of the large movable gear  $z_3$  by formula (11.14) is equal to;

$$\frac{M_B}{M_C} = 1 + \frac{z_1}{z_3},$$

Ratio of transmitted powers is equal to

$$\frac{N_B}{N_C} = \frac{M_B \cdot \omega_B}{M_C \cdot \omega_C} = \left(1 + \frac{z_1}{z_3}\right) \frac{z_4}{z_6}. \quad (11.24)$$

Figure 11.8 shows the closed differential reduction gear of the TVD [AI-20] (AM-20). Undercarriage of reduction gear consists of drive shaft 2, pinion gear 3, six single satellites 6, satellitecarrier 5, movable gear ring 7, central gear of transmission 1, six intermediate gears 15, gear ring 10, and propeller shaft 14. On flange of the propeller shaft there are face slits for attaching the propeller hub. Pinion gear 3, stellites 6 with satellitecarrier 5 and movable gear ring 7 form the differential stage of the reduction gear, and central gear 1, intermediate gears 15 and gear ring 10 form the simple stage.

Pinion gear 3 obtains rotation from drive shaft 2, which is united with rotor of compressor. Satellitecarrier 5 with help of slits on its nose is united with propeller shaft 14. Gear ring 10 with slits is united with support disk 11 which is secured to propeller shaft 14. Transmission ratio of reduction gear is  $i = 0.0873$ , and ratio of transmitted powers  $N_B/N_C = 0.49$ ,

Selection of number of gear teeth. The compactness of the reduction gear depends on the modulus and number of gear teeth. With decrease of number of teeth the coefficient of covering drops, and also the thickness of the tooth in its base, i.e., strength of tooth. Furthermore, with decrease of number of

teeth below the determined value there appears cutting of teeth at which the tooth is clearly weakened. Proceeding from these considerations, usually the number of teeth of pinions of the reduction gear of a TVD is selected from 25 to 35. Number of teeth for other gears is determined by transmission ratios.

Number of gear teeth of reduction gear must also satisfy the conditions of coaxiality, proximity, and assembly.

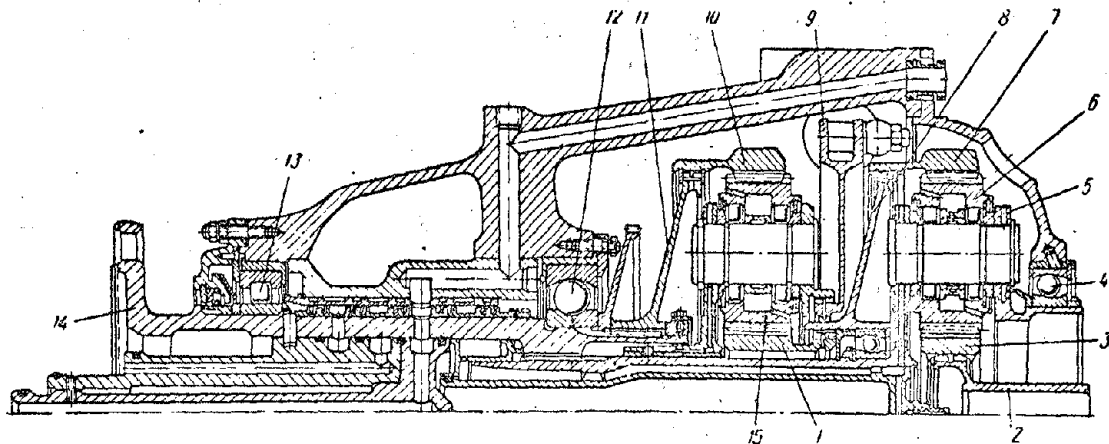


Fig. 11.8. Closed differential reductor of the TVD AI-20.

1) central gear, 2) drive shaft, 3) pinion gear, 4) ball bearing, 5) satellite carrier, 6) satellite, 7) gear ring, 8) support disk, 9) disk of torque meter, 10) gear ring, 11) support disk, 12) ball bearing, 13) roller bearing, 14) propeller shaft, 15) intermediate gear.

The condition of coaxiality ensures matching of axes of driving and driven shafts of reduction gear. For a two-stage simple transmission (see Fig. 11.2) the condition of coaxiality will be expressed thus:

$$(z_1 + z_2)m_I = (z_4 \pm z_3)m_{II}, \quad (11.25)$$

where  $m_I$  and  $m_{II}$  are moduli of engagement of corresponding pairs of gears.

Sign «+» is taken from external, and «—» — for internal engagement in transmission.

Conditions of coaxiality for a planet reduction gear (see Fig. 11.3):

with single satellites

$$z_1 + 2z_2 = z_3$$

and with double satellites

$$(z_1 + z_2)m_I = (z_3 - z_2)m_{II} \quad | \quad (11.26)$$

Condition of proximity ensures distribution of satellites or transmission gears around small central gear of transmission without their mutual engagement (Fig. 11.9). It is express by the following inequality:

$$\sin \frac{180}{k} > \frac{z_2 + 2}{z_1 + z_2}, \quad (11.27)$$

where  $k$  is the number of satellites or transmission gears. Check of proximity

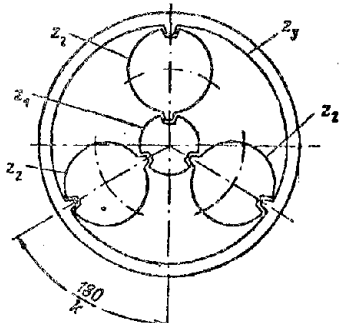


Fig. 11.9. Schematic representation of conditions of proximity and assembly of a planet reduction gear.

is conveniently conducted graphically.

Condition of assembly determines the possibility of simultaneous engagement of several satellites or transmission gears with central gears. Figure 11.9 shows the diagram of planet transmission with single satellites (Fig. 11.3a and 11.9) is ensured, if

$$N = \frac{z_1 + z_2}{k} \quad (11.28)$$

is an integer. Here  $k$  is the number of satellites. For transmission with double satellites (Fig. 11.3b) the integer should be

$$N = \frac{z_1 z'_1 + z_2 z'_2}{z_3 k} \quad (11.29)$$

### 11.3. Elements of Design of Reduction Gears.

Gears. Gear transmissions of TVD reduction gears operate under large loads. Their first stages have high speeds of rotation which frequently exceed 70 m/sec.

Gear transmissions can have evolvent engagement and engagement with circular profile of teeth, developed by M. L. Novikov. The latter possesses higher load ability than evolvent engagement. Figure 11.10 shows gear engagements: a) evolvent and b) Novikov's. In Novikov's engagement one gear has convex, and the other has concave teeth.

Reduction gears are usually cylindrical. Transmissions with evolvent engagement can have straight, slanting, or double-helical teeth, but with Novikov's engagement only slanting or double-helical teeth. With evolvent engagement straight gears have predominant application, since they do not cause axial forces, are simpler in manufacture, and can be made with great precision. Slanting gears, in comparison with straight gears, have higher load ability, and their coefficient of covering and smoothness of engagement are higher. At the same time slanting gears have axial forces which require the setting thrust bearing in the gear. Gears with double-helical teeth are free from axial forces, but are more complicated to manufacture.

For the purpose of increasing load ability of evolvent engagement they widely apply corrugated teeth. In certain cases they apply also a nonstandard original contour with contact angle  $\alpha > 20^\circ$ . Height of teeth of original evolvent contour can be made with coefficient of height of head  $f_0 = 0.8, 0.9, 1$  and

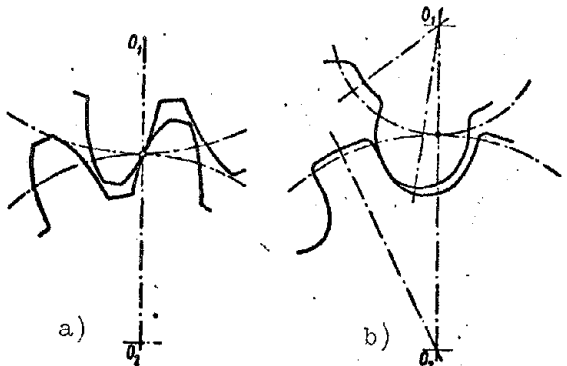


Fig. 11.10. Types of gearings.

and 1.25. Shortened teeth with  $f_0 = 0.8$  to 0.9 possess increased bend resistance. Normal teeth with  $f_0 = 1$  and high teeth with  $f_0 = 1.25$  in comparison with shortened ones ensure a large coefficient of covering and greater smoothness of engagement. Their load ability is higher.

Under a load teeth in engagement are deformed and their pitch is changed — in the pinion gear it decreases to  $\Delta t_1$ , and in the driven gear it increases to  $\Delta t_2$  (Fig. 11.11). To ensure entry of teeth into engagement, flanking, is applied. For this the theoretical profile of the tooth is somewhat pointed at the vertex, as shown in Fig. 11.11. Flanking is made on the evolvent at height of tooth  $H = 0.45$  m with smooth transition to theoretical profile. Magnitude A-B depends on value of elastic deformation of teeth under working load; it is selected by experimental means. Usually  $A-B = 0.01$  to 0.05 mm.

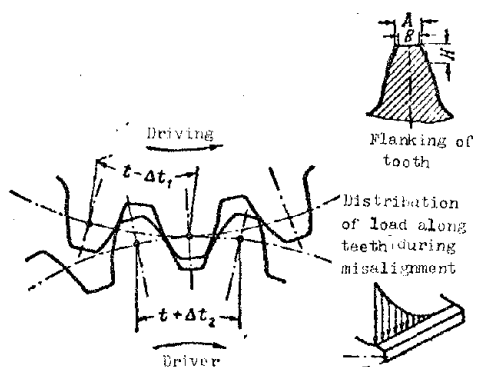


Fig. 11.11. Diagram of deformation of teeth and flanking of tooth.

Modulus  $m$  of original contour is selected according to a standard, usually  $m = 2.5$  to 7 mm. Along with the conditions of strength they also take into account the gear diameters.

According to conditions of strength, gear rings of TVD reduction gears usually have a great width which frequently exceeds 20 m. In case of misalignments the load on the length of the teeth will be distributed nonuniformly, as shown in Fig. 11.11. Longer teeth will be

overloaded correspondingly to a larger degree. Misalignments in engagement of gears appear due to inaccuracies of manufacture, and also because of deformation of shafts, and carrier gears. For decrease of deformation, shafts are made rigid, and supports are placed in direct proximity to gears and symmetrically around them. To remove the harmful effect of misalignments, the connection of gears with their carrier elements (with shafts and support disks) is done with free setting through slits, i.e., floating.

Figure 11.12 shows the differential stage of the reduction gear of the TVD AI-20, in which satellite 1 is linked to the driving 2 and driven 3 gears.

Central gears 2 and 3 are made in the form of gear rings and are united by means of slits: the first with drive shaft 5, and the second with support disk 7. Slit connections have a clearance of the order 0.1 mm, and axial retention of gears is carried out by notched spring rings 4 and 8. Drillings 6 ensure supply of lubricant to slits. By means of floating fitting gears 2 and 3 during operation under a load are self-adjusted on the teeth of satellite 1. This ensures more uniform distribution of load on length of teeth. Since the reduction gears usually have several satellites or intermediate gears, floating fitting also ensures more uniform distribution of load between individual satellites or intermediate gears of transmissions.

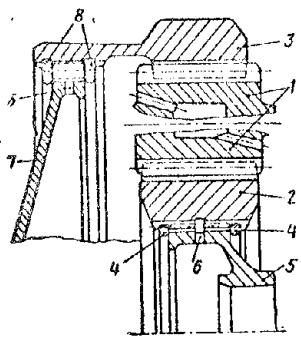


Fig. 11.12. Floating fitting of gears.

Double satellites, during grinding of teeth, frequently are made in the form of two gears with subsequent rigid connection. For guarantee of simultaneous engagement of several satellites with central gears 1 and 5, mutual location of teeth of gears 2 and 3 of satellites should be exact (see Fig. 11.4).

Satellitecarriers are made in the form of a rigid annular housing connected with the shaft. They are nondetachable and detachable. Figure 11.13 shows the nondetachable satellitecarrier of the TVD AI-20, which is made from one forging with shaft and rear support journal. Uniformly along circumference of satellitecarrier there are 6 apertures 1 for satellites, and in lateral walls there are holes 2 for their shafts. Holes 3 in crosspieces between apertures serve for lightening.

Figure 11.14 shows a satellite 2 of the TVD AI-20, placed in nondetachable satellitecarrier 3 on fixed shaft 4 by means of rollers 1. During assembly the satellite is placed in the aperture of the satellitecarrier, and its shaft is inserted in holes of lateral walls of the latter until it is stopped by bead a. In holes of satellitecarrier the shaft has a tight fitting and for facilitation of assembly it is stepped around its external diameter. Axial retention of shaft is carried out by spring ring 11.

Figure 11.15 shows a detachable satellitecarrier which is made from two parts 1 and 2. The parts are connect by crosspieces between three apertures for satellites by means of triangular face slits 3 and bolts 4. Centering is carried out by slits. Figure 11.4 shows a double satellite in a detachable satellitecarrier. Its roller bearings are located in sockets of the satellitecarrier.

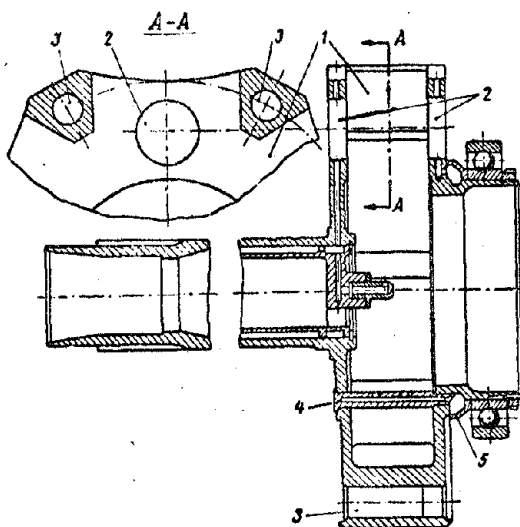


Fig. 11.13. Nondetachable satellitecarrier of the TVD AI-20. 1) apertures for satellites, 2) holes for shafts, 3) holes for lightening, 4) oil tube, 5) ring.

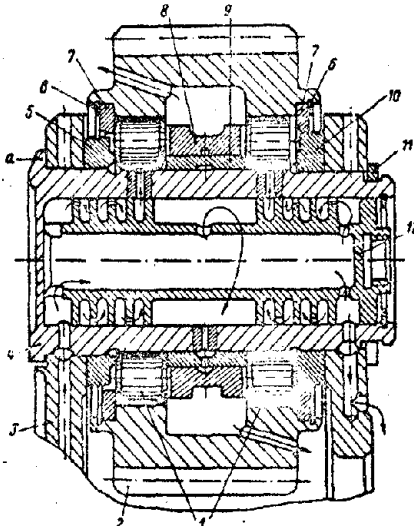


Fig. 11.14. Satellite of the TVD AI-20. 1) rollers, 2) satellite, 3) satellitecarrier, 4) shaft, 5) ring, 6) spring ring, 7) thrust ring, 8) cage, 9) hub, 10) ring, 11) spring ring, 12) hub.

Satellitecarriers and shafts are made from structural steel. For lightness the shafts are hollow, and inside them are oil-lines for lubrication and propeller control.

Bearings. For supports of shafts and satellitecarriers of TVD reduction gears they usually apply antifriction bearings. Axial retention of shafts and satellitecarrier in the housing is carried out by means of radial-thrust ball bearings; they perceive the propeller thrust.

Satellites and intermediate gears are also mounted on antifriction bearings. For decrease of their diameters and weight the bearings frequently do not have rings (casings).

Propeller shaft of the TVD AI-20 (see Fig. 11.8) is placed in the housing on two bearings, one of which, the front 13 is a roller bearing, and rear 12, is a radial-thrust ball bearing. By means of the latter, propeller thrust is transmitted to the reduction gear housing. Satellitecarrier by its shank rest on ball bearing 4, placed in rear cover of housing, and it is retained in axial direction. By its nose the satellitecarrier rests on a support attached inside the propeller shaft, and is connected with the shaft by slits. The satellite of the TVD AI-20 (see Fig. 11.14) is placed on the shaft by means of two rows of rollers 1. Rollers do not have external and internal rings and their

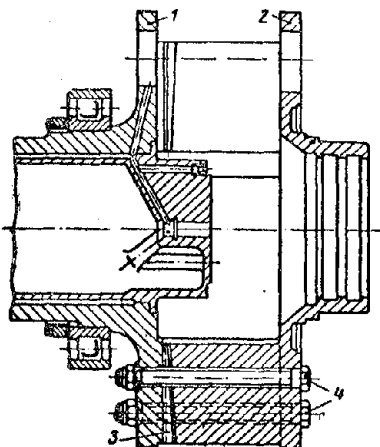


Fig. 11.15. Detachable satellitecarrier. 1 and 2) front and rear parts of satellitecarrier, 3) face slits, 4) bolts.

tracks are made directly in the satellite orifice and on the shaft. Cage 8 for two rows of rollers is made in the form of one component. Axial shifts of rollers are limited by hub 9 and rings 5 and 10 attached to the shaft, and axial shifts of satellite, through rollers 1 by means of thrust rings 7. The rings are placed in hollows of the satellite orifices and retainer by notched spring rings 6.

In the reduction gear shown in Fig. 11.4 the bearings of the satellites do not have internal rings and tracks for rollers are made on support journals of the satellite. Axial shifts of satellites are limited by rollers.

Lubrication system of lubricant of reduction gear. Gears and bearings of reduction gear are lubricated by oil which moves along channels through calibrated jets and holes. Figure 11.16 shows a tube with calibrated holes for supply of oil to gear teeth. Oil moves usually to the area of entry of teeth into engagement. However, under the action of oil pressed by the teeth, in high-speed gears there is observed wedging of teeth. To avoid it, oil is fed sometimes to the area of outlet of teeth from engagement or the clearances in engagement of teeth are increased from 0.5 to 0.6 mm.

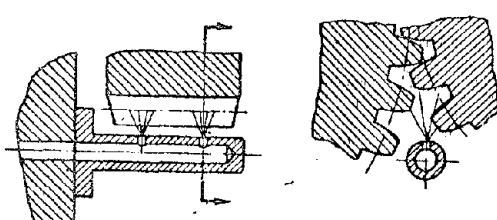


Fig. 11.16. Oil feeder-tube.

For lubrication of bearings of satellites the oil is fed through drillings in the satellitecarrier. Thus, for instance, in the satellite of the TVD AI-20, shown in Fig. 11.14, oil is fed into the cavity of the satellite shaft through a drilling in the front wall of

satellitecarrier 3 and lubricates roller supports and cage through drillings in shaft 4. Bushing 12 inside shaft 4, ensures purification of oil. Thus, during rotation of satellitecarrier, the dirty oil, which is heavier, under the action of centrifugal forces will be collected in the upper part of the internal cavity of the shaft, and the clean oil, which is lighter, will be collected in its lower part. Bushing 12 has a row of ridges dividing the internal cavity of shaft 4 into a row of annular sections connected together either in the upper, or in the

lower part of the cavity. With their help the oil fed to the rollers is repeatedly cleansed (Fig. 11.14 motion of oil is indicated by arrows).

From cavity of satellite shaft the oil through a drilling in the rear wall of the satellitecarrier (see Fig. 11.13) passes into the annular cavity formed by ring 5, and then proceeds to tubes 4. Through the drillings in tubes 4 the oil lubricates the gears.

In the variable pitch prop-control unit [VISH] ( BMIII ) the oil serves as the working fluid. Feed and drain of oil in the VISH is carried out through channels, in the reduction gear housing and in the cavity of the propeller shaft. Channels in the reduction gear housing are connected to channels in revolving shaft by means of a special oil-sealer. Such a device is shown in Fig. 11.17. It consists of bushing 1 and ring holder 2, in the annular grooves of which there are notched spring oil-sealing rings 3. Steel nitrated bushing 1 is pressed into the reduction gear housing and serves as a support for oil-sealing rings 3, and ring holder 2 is set on propeller shaft 4. Bushing 1 and ring holder 2 form between themselves a radial clearance which by sealing rings 3 is divided into two annular channels. These channels, through holes in bushing 1 and in ring holder 2, are connected with similar channels a and b of the reduction gear housing and propeller shaft.

In the TVD AI-20 supply and drainage of oil in the VISH is carried out through a similar system of channels. Figure 11.8 shows one of these channels in the reduction gear housing, and the annular oil-sealer of the propeller shaft. Inside the shaft the channels are formed by means of inserts made from magnesium

alloy.

Sealing of nose of propeller shaft. At outlet of propeller shaft from reduction gear housing there is a seal that eliminates oil leakage. Figure 11.18 shows a) cup and b) annular sealing of propeller shaft.

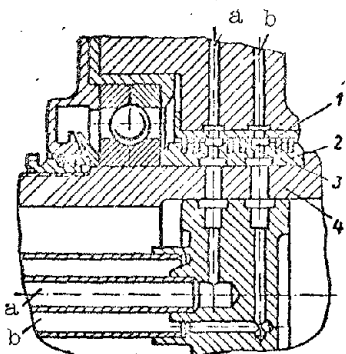


Fig. 11.17. Oil-sealer.  
1) bushing, 2) ring holder, 3) oil sealing ring, 4) propeller shaft, a and b) channels for oil.

Cup seal consists of cup 1 pressed into boring of cover 4 and reinforced additionally by spring ring 3. The cup is made from special rubber having good antifriction properties. It encircles bushing 6, mounted on propeller shaft 2, which ensures sealing of shaft. Spiral spring 7 presses cup to shaft.

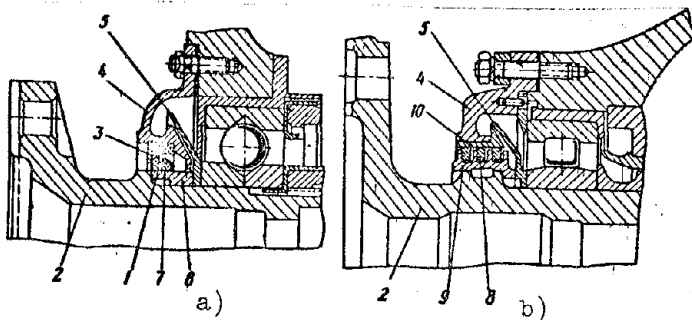


Fig. 11.18. Sealing of nose of propeller shaft.  
a) cup, b) annular.

Annular sealing consists of oil sealing rings 8, placed in grooves of ring holder 9 which is secured to propeller shaft 2. By their elasticity the rings are pressed to the support surface of bushing 10 pressed into boring of cover 4, which ensures sealing of the shaft.

In front of the seals there are usually oil-deflector rings 5. Oil leaving the bearing goes to the oil-deflector ring and centrifugal forces is ejected to the wall of the cover. Flowing oil leaks through a hole in the lower part of bearing unit in the reduction gear housing.

Torque meters. Upon change of external conditions (altitude or speed of flight) TVD power changes in wide limits. To control engine operation, and in particular, not to allow excessive overload of reduction gears, frequently torque meters [IKM] (*ИКМ*) are installed in TVD reduction gears. Torque transmitted through reduction gear to propeller is measured by IKM usually by magnitude of tangential force acting on one of the fixed elements of the reduction gear, or by magnitude of twisting (deformation) of the long drive shaft.

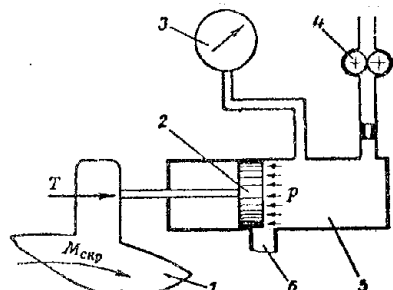


Fig. 11.19. Fundamental diagram of torque meter.

Figure 11.19 shows a fundamental diagram of an IKM with measurement of torque by magnitude of tangential force. The IKM consists of reduction gear element 1, piston 2, cylinder 5 with port 6, oil pump 4 and manometer 3.

Oil pump 4 of high pressure continuously feeds oil to cylinder 5, from where it flows through port 6 into the reduction gear housing. Element 1 (for instance, fixed gear of planet transmission) in the area of the movable parts of the reduction gear receives twisting moment  $M_{CKP}$ , which in the form of tangential force  $T$  will act on piston 2. Piston 2, under the action of tangential force  $T$ , moves and partially covers port 6. Due to this, in cylinder 5 there is established

such pressure of oil  $p$ , at which tangential force  $T$  balanced. Pressure of oil  $p$  in cylinder is measured by manometer. Its magnitude is proportional to torque, transmitted through reduction gear to propeller. Power of engine is determined by the following formula:

$$N = kp \cdot n,$$

where  $p$  is the pressure of oil in the cylinder,  $\text{kg/cm}^2$ ,

$n$  is the rpm rate.

$k$  is a constant coefficient which depends on dimensions of components of reduction gear and IKM.

Figure 11.20 shown IKM element of the reduction gear of the TVD AI-20, which operates on principle of measurement of tangential force. The IKM consists of disk 5 and six cylinders 1 with piston 2. By means of shafts the 4 cylinders are hinged to the disk uniformly on its circumference, and piston in this way are attached to the reduction gear housing 3. Disk 5 by its hub with the help of slits is united with the housing of the second stage of the reduction gear (see Fig. 11.7 and pos. 9, Fig. 11.8) and perceives from it the twisting moment shown in fig. 11.20 by the arrow.

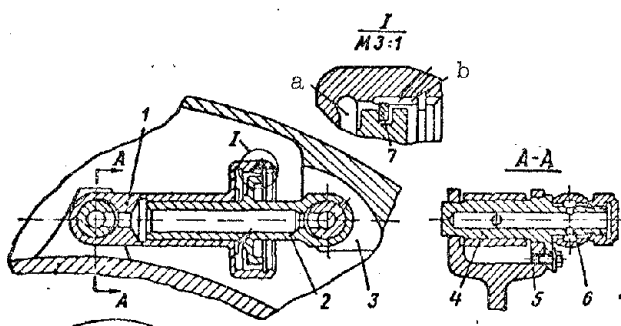


Fig. 11.20. Torque meter of the TVD AI-20. 1) cylinder, 2) piston, 3) reduction gear housing, 4) shaft, 5) intermediate drive housing, 6) oil collector, 7) piston ring.

The working cavities  $a$  of cylinders are united together through drillings in rods of pistons 2 and shafts 4 by annular oil collector 6. Oil in IKM system is fed by a special oil pump under a pressure of the order  $90 \text{ kg/cm}^2$  through a channel in the reduction gear housing and drillings in the shaft and rod of one of the pistons.

The cylinders have grooves 6 with holes, through which is carried out drainage of oil from cylinders to reduction gear housing. Sealing between pistons and cylinders is carried out by piston rings 7 which, depending upon magnitude of torque, in some degree cover the drainage grooves of the cylinders. The principle of work of the IKM was described above.

#### 11.4. Calculation of Gear Teeth Strength.

Gear teeth are calculated for contact strength on working surfaces and for bending on base of teeth. A simplified strength calculation of cylindrical gears with evolvent teeth is described below.

Specific rated load applied normally to profile of tooth is equal to

$$p_p = \frac{2M}{kd_1 b \cos \alpha} K_{np} K_k \frac{k\epsilon/c\mu}{}, \quad (11.30)$$

where  $M$  is torque acting on pinion gear;

$k$  is the number of satellites or intermediate shafts (layshafts);

$d_1$  is the diameter of initial circumference of pinion gear;

$b$  is the working width of the gear (length of tooth) on diameter of initial circumference;

$\alpha$  is the contact angle;

$K_{np}$  is the variation factor of distribution of load between satellites or intermediate shafts.  $K_{np} = 1.1$  to  $1.2$ ;

$K_k$  is the load factor with which we consider dynamic load in transmission and nonuniformity of distribution of load on length of tooth.  $K_k = 1.15$  to  $1.35$ .

Smaller values of coefficients  $K_{np}$  and  $K_k$  pertain to drives of reduction gears of high precision of manufacture and assembly. Furthermore, smaller values of coefficient  $K_{np}$  pertain to drives with smaller number of satellites or intermediate shafts ( $k = 3$ ), and smaller values of coefficient  $K_k$  pertain to drives having rigid shafts, symmetric location of supports with respect to gears, and floating fitting of gears. High speeds of rotation of gears correspond to large dynamic loads, and consequently also to large values of coefficient  $K_k$ .

Calculation of teeth for contact strength. For determination of contact stresses we use the following formula of Hertz:

$$\sigma_k = 0.418 \sqrt{\frac{p_p E}{r_{np}}}, \quad (11.31)$$

where  $p_p$  is the specific rated load;

$E$  is the elastic modulus of material of reduction gears;

$r_{np}$  is the given radius of curvature of profiles of teeth at point of contact.

For steels from which reduction gears are made, it is possible to take  $E = 2.15 \cdot 10^6$  kg/cm<sup>2</sup>.

If one were to agree, for a pair of gears, in contact, to call the larger one the wheel (index  $k$ ), and the smaller the gear (index  $m$ ), the given radius of curvature in the pole of contact would be expressed thus:

$$r_{np} = \frac{d_k \sin \alpha}{2(i \pm 1)}, \quad (11.32)$$

where  $d_k$  is the diameter of initial circumference of the wheel;

$i = \frac{d_k}{d_m} = \frac{z_k}{z_m} \geq 1$  is the transmission ratio in contact.

In parentheses the plus pertains to external, and the minus to internal contact.

Placing in initial formula (11.31) the expression (11.32) and the accepted value of elastic modulus E, we obtain the following calculating formula for contact stresses:

$$\sigma_c = 867 \sqrt{\frac{P_p(i \pm 1)}{d_k \sin \alpha}} \text{ kg/cm}^2. \quad (11.33)$$

For gears made from steel [12Kh2N4A] (12X2H4A) and [18KhNVA] (18XHBA) with hardness of core of tooth HRC > 35, allowed contact stress can be presented in the form

$$|\sigma_c| = 185 HRC \sqrt{\frac{25 \cdot 10^7}{N_{eq}}} \text{ kg/cm}^2, \quad (11.34)$$

where HRC is the hardness of the cemented working surface of the tooth;

$N_{eq}$  is the equivalent number of cycles of variation of stresses in the full operation life of the gear taking into account variable conditions.

Under constant operating conditions the number of cycles of variation of stresses is equal to

$$N_a = 60 a n T. \quad (11.35)$$

Under variable operating conditions we determine equivalent number of cycles of variation of stresses

$$N_{eq} = 60 a \sum \left( \frac{M_i}{M} \right)^3 n_i T_i. \quad (11.36)$$

where  $a$  is the number of contacts of each tooth in one turn of the gear;

$n$  and  $n_i$  is the design rpm rate and the rpm rate in different operating conditions, respectively;

$T$  and  $T_i$  is the period of operation in hours in full operation life and in different operating conditions, respectively;

$M$  and  $M_i$  is the rated torque and torque in different operating conditions, respectively.

For satellites and idle gears we take  $a = 1$ , since upon their contact with two central gears their teeth work with various sides, in one case driver, and in the other, driving.

For central gears, number  $a$  is equal to the number of satellites or intermediate shafts. Since in them  $a > 1$ , then  $N_a$  is also larger than in the gears linked with them.

In case of planet or differential drive the rates  $n$  and  $n_1$  are taken to be relative (with stopped pinion).

Dividing expression (11.36) by (11.35), we obtain

$$N_{\text{max}} = K_p N_a, \quad (11.37)$$

where  $K_p = \sum \left( \frac{M_t}{M} \right)^3 \frac{n_t}{n} \frac{T_t}{T}$  is the condition factor.

During calculation of gear strength in nominal operating conditions of engine it is possible to approximately take  $K_p = 0.75$  to  $0.85$ . When  $N_{\text{max}} \geq 25 \cdot 10^7$  the value of the square root in formula (11.34) is taken equal to 1. In this case  $|\sigma_k| = 185$  HRC takes the value of the endurance limit, at which the teeth sustain an unlimited large number of changes of stresses, i.e., operation life of gears is not limited by time. When  $N_{\text{max}} < 25 \cdot 10^7$  the operation life of gears is limited by time and therefore  $|\sigma_k|$  can be greater than the endurance limit.

Calculation of teeth for bending. If a load is applied to the vertex of a tooth, the bending stress is determined by the following formula:

$$\sigma_b = \frac{Pb}{my} \frac{b}{b'} \text{ kg/cm}^3, \quad (11.38)$$

where  $m$  is the modulus in cm;

$y$  is the form factor of the tooth;

$b$  и  $b'$  is the length of tooth on initial circumference and on root calculated section, respectively.

For the driving gear, with a threaded rack tool ( $\alpha_0 = 20^\circ$ ;  $f_0 = 1$  and  $c_0 = 0.25$ ), the form factor of the tooth can be determined depending upon number of teeth  $z$  and coefficient of displacement  $\xi$  according to Fig. 11.21. (With correction of teeth  $\xi \neq 0$ ). For the driver gear the value of the form factor of the tooth is taken according to the same figure with coefficient 1.145. This considers the different effect of forces of friction in the contact of driving and driven gears.

Load to tooth is applied periodically (at every other entry of tooth into contact). In the usual gears it varies from zero to maximum (pulsating cycle of load), and in satellites and idle gears, from maximum to minimum (symmetric cycle of load). In accordance with the form of loads the safety factor of teeth undergoing bending is determined by fatigue limit:

$$n = \frac{\sigma_0}{K_s \sigma_b} \quad \text{and} \quad n = \frac{\sigma_{-1}}{K_s \sigma_b}, \quad (11.39)$$

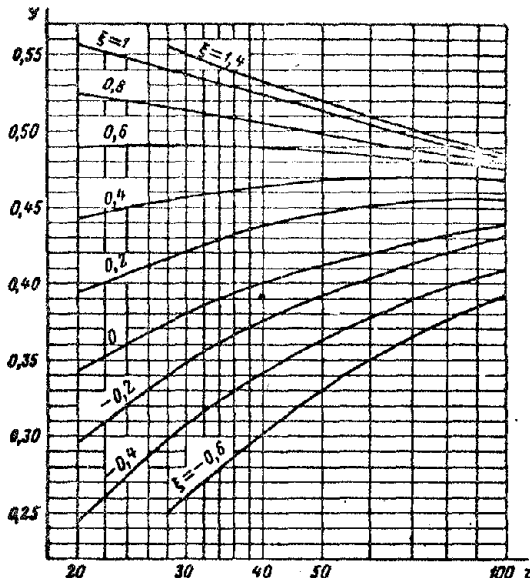


Fig. 11.21. Calculation of teeth for bending.

where  $\sigma_0$  and  $\sigma_{-1}$  are fatigue limits correspondingly during pulsating and symmetric cycles of load. For steel 12Kh2N4A, 18KhNVA and [38KhMYuA] (38XM10A) it is possible to take  $\sigma_0 = 8000 \text{ kg/cm}^2$  and  $\sigma_{-1} = 5000 \text{ kg/cm}^2$ ;

$K_\sigma$  is the effective coefficient of concentration of stresses on fillets of teeth. With a cemented or nitrated fillet it is possible to take  $K_\sigma = 1.2$ .

Safety factor during bending of teeth is recommended  $n \geq 2$ . Safety factor of satellites and idle gears is less than that of central gears ( $\sigma_{-1} < \sigma_0$ ).

Example. Calculate the strength of the teeth of central wheel  $z_K$  and idle gear  $z_{III}$  of intermediate drive of reduction gear.

Given:  $M_{kp} = 50000 \text{ kg}\cdot\text{cm}$ ;  $k = 6$ ;  $z_K = 35$ ;  $z_{III} = 31$ ;  $d_K = 135.76 \text{ mm}$ ;  $d_{III} = 120.24 \text{ mm}$ ;  $i = 1.129$ ;  $f_0 = 1$ ;  $m = 3.75 \text{ mm}$ ;  $b = 46 \text{ mm}$ ;  $b' = 50 \text{ mm}$ ;  $\alpha = 24^\circ 42'$ ;  $\epsilon = 0.6$ ; HRC = 60;  $\sigma_{-1} = 5000 \text{ kg/cm}^2$ ;  $K_\sigma = 1.2$ ;  $T = 200 \text{ hrs.}$ ;  $n_K = 2975 \text{ rpm}$ .

The coupling drive is wheel  $z_K$  which is in external contact with idle gear  $z_{III}$ . We select the values of coefficients:  $K_{sp} = 1.15$  and  $K_a = 1.25$ .

Specific rated load by formula (11.30) is equal to:

$$P_p = \frac{2 \cdot 50000}{6 \cdot 13,576 \cdot 4,6 \cdot 0,908} \cdot 1,15 \cdot 1,25 = 423 \text{ kg/cm}.$$

Contact stress by formula (11.33) is equal to:

$$\sigma_k = 867 \sqrt{\frac{423(1,129+1)}{13,576 \cdot 0,418}} = 10900 \text{ kg/cm}^2.$$

Equivalent number of cycles of change of stresses is determined with respect to wheel  $z_K$  by formula (11.37), taking  $K_p = 0.8$ :

$$N_{eq,k} = 0.8 \cdot 6 \cdot 2975 \cdot 200 = 17,1 \cdot 10^7.$$

Allowed contact stress in contact by formula (11.34) is equal to:

$$|\sigma_k| = 185 \cdot 60 \sqrt{\frac{25 \cdot 10^7}{17,1 \cdot 10^7}} = 11800 \text{ kg/cm}^2.$$

Thus  $\sigma_K < |\sigma_k|$ . At the same time

$$\sigma_k < 185 \text{ HRC} = 11100 \text{ kg/cm}^2.$$

i.e., less than endurance limit. Therefore, the operation life of gear drive is not limited by contact durability.

Bending stress is determined for gear  $z_{\text{III}}$  by formula (11.38):

$$\sigma_k = \frac{423}{0.375 \cdot 0.56} \cdot \frac{4.6}{5} = 1900 \text{ kg/cm}^2.$$

Value of form factor of tooth  $y = 0.56$  is taken according to Fig. 11.21 with coefficient 1.145.

Safety factor during bending by formula (11.39)

$$n = \frac{5000}{1.2 \cdot 1900} = 2.2.$$

### 11.5. Propeller Hubs

Propeller creates thrust. Power consumed by propeller is equal to:

$$N_s = \beta \rho n_B^3 D^5. \quad (11.40)$$

where  $\beta$  is the load factor, depending on geometric form of propeller and blade angle  $\phi$  (Fig. 11.22);

$\rho$  is air density;

$n_B$  is propeller speed;

$D$  is the diameter of the propeller.

Types of propellers. Propellers are fixed-pitch [VFSH] (B $\Phi$ III) and variable-pitch [VISh] (B $\Psi$ III). In VFSH the blades are rigidly joined with the hub and blade angle  $\phi$ , which determines propeller pitch, is constant (see Fig. 11.22). In VISh load factor  $\beta = \text{const}$ .

Blades of VISh can turn and angle  $\phi$  can be changed. Load factor of VISh varies. With increase of angle  $\phi$  propeller pitch is increased, the propeller becomes heavier and engine speed decreases; with decrease of angle  $\phi$  propeller pitch decreases, the propeller becomes lighter and engine speed is increased. For different conditions of flight with VISh each time optimum propeller pitch is set and thereby the greatest efficiency of the propeller-driven installation is ensured. In operating conditions angle  $\phi$  usually varies from 20 to 30°.

Classification of VISh. By design VISh are classified as simple, feathering, and reversible (braking).

The feathering propeller allows setting of blades with respect to the incident flow of air in the position of least drag. This eliminates rotation of the propeller as a windmill (windmilling) with engine off. Reversible (braking) propeller allows setting of blades at negative angle  $\phi$  with formation

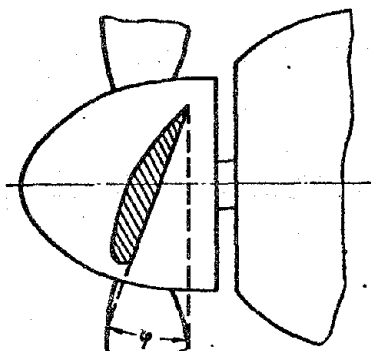


Fig. 11.22. Blade angle of propeller.

pump through the propeller shaft to the VISh servo-piston. In electric VISh turn of blades is carried out by a special electric motor.

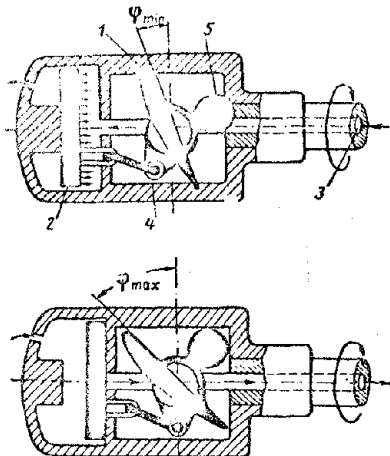


Fig. 11.23. Diagram of VISh hub of direct action.

accomplished through guide 4 by servo-piston 2 which is fed oil under pressure for this purpose through channel 3.

In the reverse diagram of action (Fig. 11.24) the blades 1 do not have counterpoises and therefore try to stay in the low-pitch position. They are turned at high-pitch through guide 3 by servo-piston 2 which is fed oil under pressure through channel 4 for this purpose.

In the bilateral diagram of action (Fig. 11.25) the blades 1 also do not have counterpoises. They are turned at low and high pitch through guide 5 by servo-piston 2. Supply and drain of oil are produced through channels 3 and 4. Since turn at low pitch is promoted by centrifugal forces of blades, the oil through channel 3 sometimes moves under lowered pressure directly from the engine oil system (under a pressure from 5 to 8 kg/cm<sup>2</sup>).

of reverse thrust. The reversible propeller is used for decreasing run of an aircraft during its landing. Simple VISh does not allow setting of blades in feathering and braking position.

Depending upon blade-turning mechanism, VISh can be hydraulic and electric. Hydraulic propellers have obtained the biggest application. Turn of blade is carried out by oil which is fed under a pressure from 20 to 40 kg/cm<sup>2</sup> from a special oil

Fig. 11.24. Diagram of VISh hub of reverse action.

Diagrams of action of hydraulic VISh. During rotation of propeller its blades under the action of centrifugal forces try to stay in low-pitch position. In the diagram of action, hydraulic propellers are distinguished by direct reverse, and bilateral diagram.

In case of direct diagram of action (Fig. 11.23) the butt of the blades 1 of the propeller has counterpoises 5 which overcome the centrifugal forces of the blades and try to set the blades in the high-pitch position. Turn of blades at low-pitch is

accomplished through guide 4 by servo-piston 2 which is fed oil under pressure

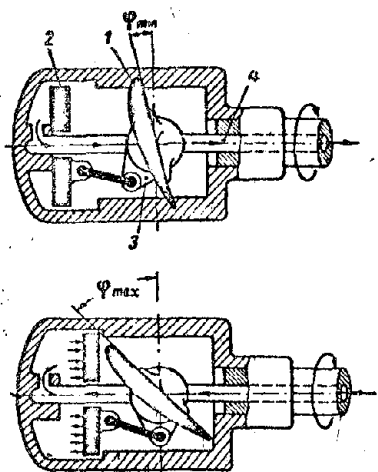


Fig. 11.24. Diagram of VISH hub of reverse action.

VISH of direct diagram require installation of heavy counterpoises and therefore find limited application. In VISH with reverse and bilateral diagrams, upon failure of the oil system the blades under the action of centrifugal forces inadvertently try to set themselves to low pitch. This can lead to a sharp increase of engine speed, i.e., to racing. To eliminate this defect the propellers are equipped with special hydraulic locks in the form of valves. They automatically close up the oil outlet from the servo-piston cavitation upon drop of pressure in the oil system and lock the blades of the propeller in the specified position.

The speed-control unit automatically maintains the specified engine speed with change of conditions of flight by variation of propeller blade angle  $\varphi$ . Speed-control units are of the centrifugal type.

Figure 11.26 shows the operational diagram of a control unit of a VISH of bilateral pattern. The unit has valve 5, which controls supply and drain of oil of the servo-mechanism of the VISH hub. From a special pump under high pressure to the valve is fed oil through channel 1. Channels 3 and 4 are connected to the servo-mechanism of the VISH hub (see Fig. 11.25), and channel 2 serves for drainage of oil.

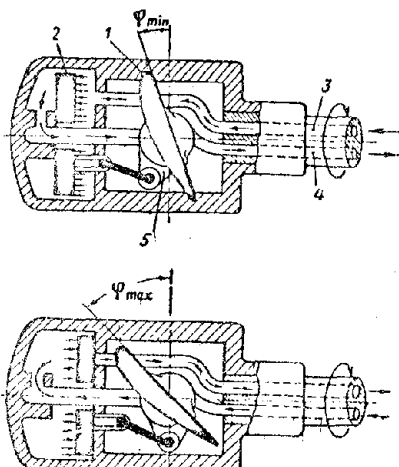


Fig. 11.25. Diagram of hub of VISH of bilateral action.

The valve is simultaneously under the action of calibrated spring 7 and weights of control unit 6. Weights sit on shafts and revolve from the engine around the valve shaft through a special drive not shown in the diagram. During rotation of weights there appear centrifugal forces  $C$  which in overcoming the elasticity of the spring try to turn the weights with respect to their axes. The weights move the valve into such position at which their centrifugal forces are balanced by the elasticity of the spring. Adjustment of the control unit to a certain engine speed  $n_0$  is carried out

by change of tension of spring 7. Turn of flywheel 8 and gear 9 connected to it

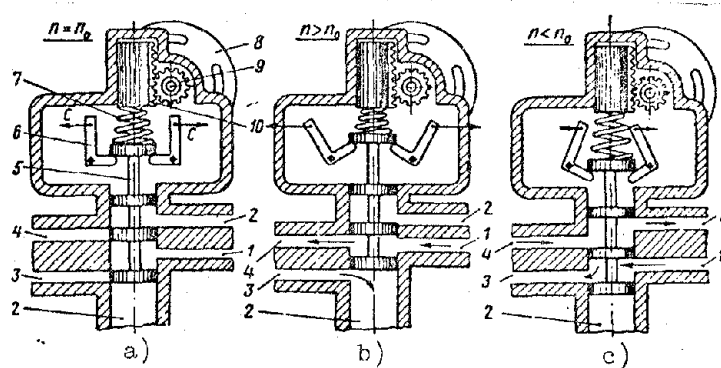


Fig. 11.26. Diagram of action of speed-control unit.

moves rack 10 and thus changes the tension of spring 7.

Diagram a shows the neutral position of the valve when channels 3 and 4 are covered and engine speed  $n$  corresponds to adjustment of control units,  $n = n_0$ .

Diagram b shows  $n > n_0$ . Under the action of increasing centrifugal forces of weights 6, valve 5 moves upwards and opens channel 3 of the servo-mechanism of the VISH hub to drain the oil, and channel 4 to supply the oil. Owing to this the propeller increases in weight and the engine decreases its speed to  $n_0$ , after which the control unit arrives at position a.

Diagram c shows  $n < n_0$ . In this case the centrifugal forces of weights 6 decrease and valve 5 under the action of the spring moves downwards. Channel 4 of the servo-mechanism of the VISH hub opens for drain of oil, and channel 3 for supply of oil. Owing to this the propeller becomes lighter and the engine increases its speed to  $n_0$ , after which the control unit again goes into position a.

Engine speed is controlled by the pilot of a special automatic device connected with the gas sector.

VISH [AV-68] (AB-68) hub. Figure 11.27 shows the design of the VISH AV-68 installed on the TVD AI-20. The VISH AV-68 is four-blade, hydraulic, and has bilateral action with setting of blades in feathering position.

The propeller consists of hub 6, four blades 1, servo-piston 15, lock valve 12, and centrifugal lock 16. Propeller and hub 6 are attached to flange of shaft 3. Torque from shaft to propeller hub is transmitted by face slits a. Blades 1 are set in propeller hub 6 on ball bearings 2 placed in four rows in the annular tracks at the butt of the blade and propeller hub, which allows blades to turn around their own axis. Centrifugal forces from them through balls 2 are taken by the propeller hub. On end of butt part of blade there are eccentrically located pins 4.

In cylinder 14 moves servo-piston 15, connected with crossarm 18. The crossarm by means of connecting rods 7 is connected with pins 4 of the blade butt. Since pins are located with respect to axis of blade eccentrically,

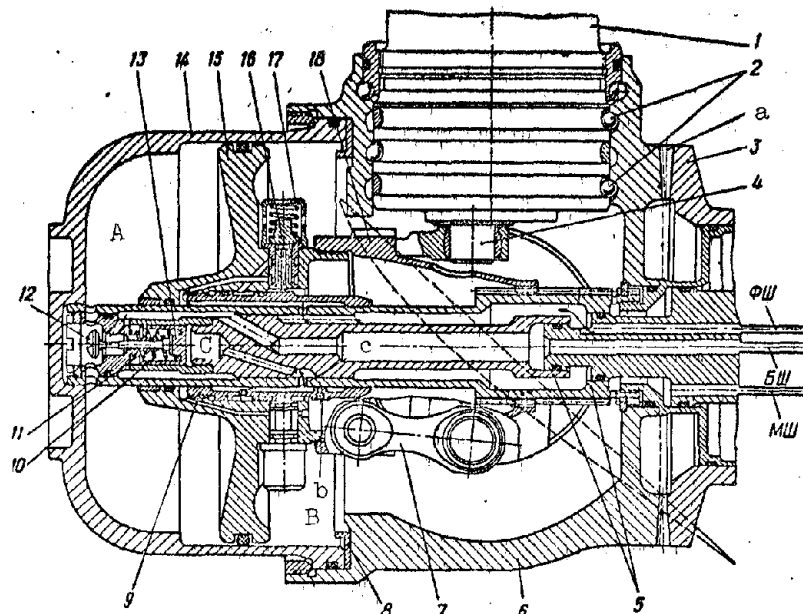


Fig. 11.27. Diagram of propeller AV-68. 1) blade, 2) ball bearings, 3) propeller shaft, 4) butt pin, 5) oil-line, 6) propeller hub, 7) connecting rod, 8) thrust ring, 9) piston bush, 10 and 11) springs, 12) lock valve, 13) plunger, 14) cylinder, 15) servo-piston, 16) centrifugal lock, 17) spring of centrifugal lock, 18) crossarm BII—high-pitch channel, MII low-pitch channel, OMII—fixed-pitch channel, A and B cavities of servo-piston, C—cavity of lock, a) slits, b and c) holes.

during shift of piston 15 to one side there occurs turn of propeller blades 1 with respect to their axes. Thus is carried out by change of propeller pitch, i.e., blade angle  $\phi$  (see Fig. 11.22).

The operating principle of the blade-turning mechanism is hydrocentrifugal and bilateral. Working fluid is oil. Control of propeller is carried out by means of three channels in oil-line 5: high-pitch channel BII united with cavity A, low-pitch channel MII united with cavity B, and fixed-pitch channel OMII united with cavity C of valve 12 of pitch lock.

In steady running conditions lock valve 12 is in open position. Cavity A is connected to the BII channel, and cavity B with the MII channel. The transverse components of centrifugal forces of blades, and also pressure of oil on piston in the area of cavity B are balanced by the oil pressure on the piston in the area of cavity A.

With increase of engine speed the speed-control unit through the BII channel turns on supply of oil under pressure to cavity A, and cavity B through the MII channel is connected with the drain. Then servo-piston 15 begins to move to the right and through crossarm 18 and connecting rods 7

begins to turn the propeller blades 1 towards increase of pitch. Power consumed by the propeller will then be increased and engine speed begins to decrease.

With decrease of engine speed the speed-control unit through the  $B_{III}$  channel turns on supply of oil under pressure to cavity A, and cavity B through the  $M_{III}$  channel is connected with the drain. Then servo-piston 15 begins to move to the right and through crossarm 18 and connecting rods 7 begins to turn propeller blades 1 towards increase of pitch. Power consumed by the propeller will then be increased and engine speed begins to decrease.

With decrease of engine speed the speed-control unit connects cavity A through the  $B_{III}$  channel with the drain. Then under the action of transverse components of centrifugal forces of blades and pressure of oil in cavity B the piston begins to move to the left and through crossarm and connecting rods 7 the blades begin to turn toward decrease of propeller-pitch. Power consumed by propeller will decrease and engine speed will begin to increase. In first and second case turn of blades will occur until the specified engine speed is restored.

Lock valve 12 serves for disconnection of  $B_{III}$  channel from cavity A. Valve is connected to plunger 13 which under the action of spring 10 is released to the right. Valve 12 under the action of its spring 11 sits on its seat and covers the  $B_{III}$  channel. Working cavity C for plunger 13 is connected with the  $\Phi_{II}$  channel. During supply of oil from  $\Phi_{II}$  channel to cavity C under pressure, plunger 13 moves to the left and opens lock valve 12; connecting the  $B_{III}$  channel to cavity A.

Centrifugal lock 16 is a maximum-speed control unit and is for emergency. Centrifugal lock constitutes a valve with a weight which is under the action of calibrated spring 17. It is placed in the system of oil supply from  $\Phi_{II}$  channel to cavity C of the lock valve and controls the latter.

In case of disturbance of normal operation of the propeller control system (upon malfunction of speed-control unit), when propeller begins to arbitrarily lose weight, the engine increases its speed. However, upon its achievement of maximum permissible speed the centrifugal lock 16, moving, separates the  $\Phi_{II}$  channel from cavity C of the lock and connects it to the drain in cavity B. Owing to this the lock valve 12 under the action of springs 10 and 11 closes and drain of oil from cavity A through the  $B_{III}$  channel stops. At the same time the decrease of propeller pitch will stop, since cavity A will be locked and the oil

in it will form a hydraulic stop for servo-piston 15.

Unfixing of pitch is produced with decrease of engine speed (by throttling it), when centrifugal force acting on the valve decreases and under the action of elasticity of spring 17 it returns to its initial position. Valve separates cavity C of lock from cavity B and connects it to the  $\Phi$ II channel. Then lock valve 12 under the action of oil pressure opens and connects cavity A to the BII channel. For limitation of negative propeller thrust during landing of an aircraft there is foreseen fixing of propeller pitch at intermediate blade angle. This lightening of the propeller is limited by the position servo-piston 15 at which channel 6 of piston bush 9 is matched with hole c and lock cavity C, which is disconnected from the  $\Phi$ II channel, and is connected to the drain to cavity B. Lock valve 12 closes and oil to cavity A is cut off, creating for servo-piston 15 a hydraulic rest. In the AV-68 propeller the blade angle on intermediate stop is  $\varphi = 12^\circ$ .

Removal from stop is produced by supply of oil to cavity B from the speed-control unit pump under heightened pressure. Owing to this the pressure in cavity C increases and the lock valve opens, connecting cavity A through the BII channel to the drain. Piston 15 then moves to the left and the propeller blades turn towards decrease of angle.

In case of stop of engine in flight (for instance, in case the pilot turns off part of the engine in a multi-engine aircraft), when engines do not transmit power to the propeller, the latter will revolve as a windmill, creating additional drag for the aircraft. In this case the AV-68 propeller allows blade setting in feathering position, i.e., in position of least propeller drag. In the AV-68 propeller the angle of blade feathering position is  $\varphi_{\text{fe}}=83^\circ$ .

Introduction of propeller blades into feathering position and withdrawal of them from feathering position is forced by means of a special feathering oil pump. This pump leads from an electric motor which is fed from the power-supply network of the aircraft.

Propeller feathering is produced by connection of feathering pump to BII channel. Oil will move to propeller cavity A, and cavity B will be connected to the drain. Owing to this, piston 15 moves to the right until it stops at thrust ring 8, turning the propeller blades in feathering position.

Removal of propeller from feathering position is accomplished by connecting propeller cavity A through the BII channel to the drain with simultaneous supply

of oil from feathering oil pump to cavity B.

#### 11.6. Materials

Gears are usually made from cemented steel 12Kh2N4A or 18KhVA and nitrated steel 38KhMYuA. In conformity with this, gear teeth are cemented or nitrated. Propeller shaft and satellitecarrier are made from steel [40KhNMA] ( 40XHMA ) Satellite shafts are made from steel 12Kh2N4A with cemented tracks for bearing rollers.

## C H A P T E R XII

### GAS-TURBINE ENGINE ASSEMBLY DRIVES

#### 12.1. General Information

[GTD<sup>1</sup>] (ГТД) have many different types of assemblies which require drive. These assemblies are divided into two basic groups: assemblies servicing the engine, and assemblies servicing the aircraft. The engine assemblies include fuel and oil pumps, air separators, centrifugal vents, electric tachometers, starting assemblies, and so forth. The aircraft assemblies include electric generators, hydraulic pumps, vacuum pumps, high-pressure air compressor, and so forth.

Assemblies are installed on parts of engines with lowered temperature in places convenient for access to them during servicing, adjustment and possible replacement. They attempt to reduce communications (pipelines) connected with the operation of assemblies. For improvement of operating conditions of the lubrication system the oil pumps are usually arranged in the lower part of the engine.

Operating speeds of assemblies are quite diverse, and are ensured by gear transmissions. Supports in drives are ball and roller bearings. Long shafts of transmissions are usually called springs. For the drive of GTD assemblies there is expended about 1% of the power developed by the engine turbine.

#### 12.2. Drive Systems and Their Design.

Drives for GTD assemblies with axial-flow compressor. GTD with axial-flow

<sup>1</sup>Gas-turbine engines.

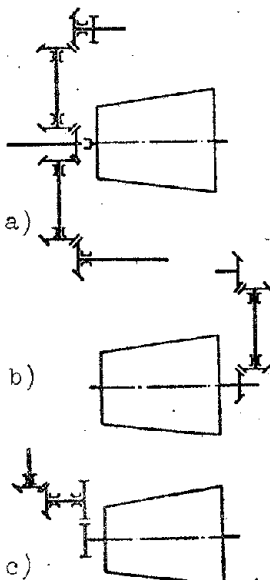


Fig. 12.1.  
Diagrams of drive  
transmissions of  
GTD assemblies  
with axial-flow  
compressor.

Fig. 12.1.  
Transmission includes another pair of cylindrical gears, as shown in diagram of c

In order not to increase dimensions of engine, and also for decrease of transmission load, assemblies are usually divided into groups and each one is placed in its own gear box. Sometimes each gear box of engine assemblies and gear box of aircraft assemblies are separated. Each gear box obtains drive through its own spring shaft. Drive of engine assemblies is carried out by means of two or three shafts, as shown in diagram a of Fig. 12.1.

Figure 12.2 shows a kinematic diagram of drives for TVD assemblies of the [AI-20] (AM-20), having, a axial-flow compressor. Central transmission unit consists of a pinion 2, and two drive 3 and 4 bevel gears. Pinion gear obtains rotation from engine rotor through spring shaft 1 of reduction gear and transmits it through driven gears 3 and 4 to upper and lower spring shafts.

From upper spring shaft by means of gear transmissions the following assemblies located on upper part of front bearing casing of rotor obtain:  
 I - propeller speed control unit, II - centrifugal vent, and III - two starters-generators. Drive IV is united with parking brake.

<sup>1</sup>Turbojet engine.

<sup>2</sup>Turboprop engines.

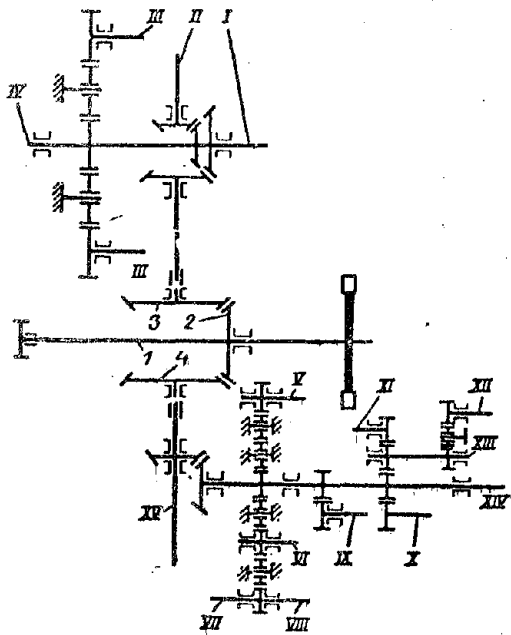


Fig. 12.2. Kinematic diagram of assembly drives of the TVD AI-20.

shanks are mounted on ball bearings. By means of slits the pinion gear is united with drive shaft 9 of propeller reduction gear, and driven gear 5 with spring shaft 2. The spring shaft passes through hollow strut of casing 4 of front rotor bearing and drives the assemblies located in the upper part of the casing. For lowering of speed the driven gear is made larger than the pinion gear. Clearance in engagement of gears is established during assembly by selection of regulating rings 6 and 8. Housing 1 is cast from aluminum alloy and in the sockets of its bearings are pressed steel bushings 3 and 10.

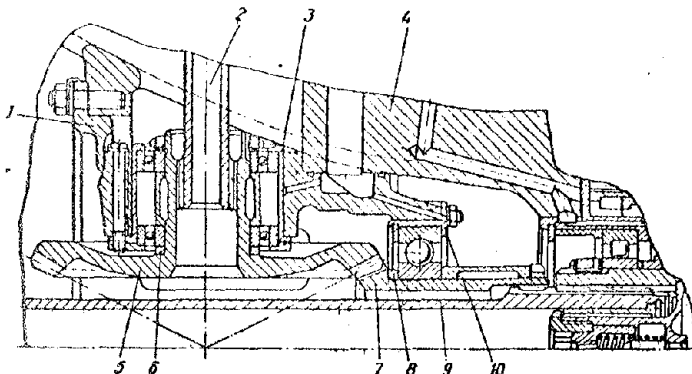


Fig. 12.3. Central transmission unit for drives of assemblies of the TVD AI-20.

scavenger pump is carried out through intermediate gear 4 and gear 5, and to air separator and oil booster pump through intermediate gear 7 and gear 8.

From lower spring shaft through gear transmissions the following obtain rotation: V - ac electric generator, VI - oil delivery pumps from central and rear rotor bearings, VII - air separator, VIII - oil delivery pump, IX - main fuel pump, X - fuel delivery pump, XI - oil delivery pump from assembly gear box, XII - transducer of tachometer, XIII - hydraulic pump, XIV - fuel control unit, and XV - main oil pump.

Figure 12.3 shows the central unit of transmission for drives of assemblies of the TVD AI-20, located in housing 1. Pinion 7 driven 5 bevel gears of transmission by their

Figure 12.4 depicts a cross section made through the box of lower drives of the following assemblies of the TVD AI-20: ac electric generator, oil scavenger pumps, air separator, and oil booster pump. Drive to electric generator is carried out through two intermediate gears 3 and gear 2. Drive to

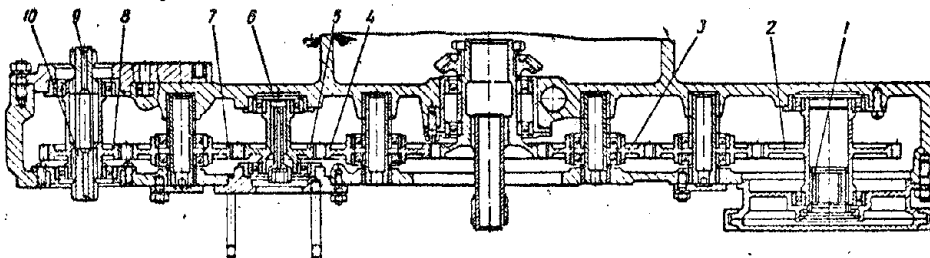


Fig. 12.4. Lower-gear box of lower assemblies of the TVD Al-20. 1 and 2 - coupling and drive gears of generator, 3, 4, and 7 - intermediate gears, 5 and 6 - gears and drive shaft of oil scavenger pump, 8 - gears, 9 - drive shaft of oil booster pump, 10 - drive shaft of air separator.

Drives for TRD assemblies with centrifugal compressor. TRD with centrifugal compressor have their assemblies on gear box 1 located in the front part of the engine (see Fig. 1.8).

Figure 12.5 depicts a kinematic diagram of the gear box of assemblies of the [VK-1] (BK-1) engine. Through spring shaft 9 and spur gear 10 rotation from engine is transmitted by two cylindrical gears 8 which sit on the stocks of bevel gears 6 and 12. Through bevel gears 3 there are set into rotation two fuel pumps of high pressure. Upper bevel gear 3, furthermore, transmits rotation to bevel gear 7 of drive of aircraft assembly box, and through spring shaft 5 to generator of tachometer. Lower bevel gear 3 through gear 1 transmits rotation to vertical shaft which through a pair of bevel gears 2 and 13 sets into rotation the air separator, and through a pair of spur gears the oil pump is rotated.

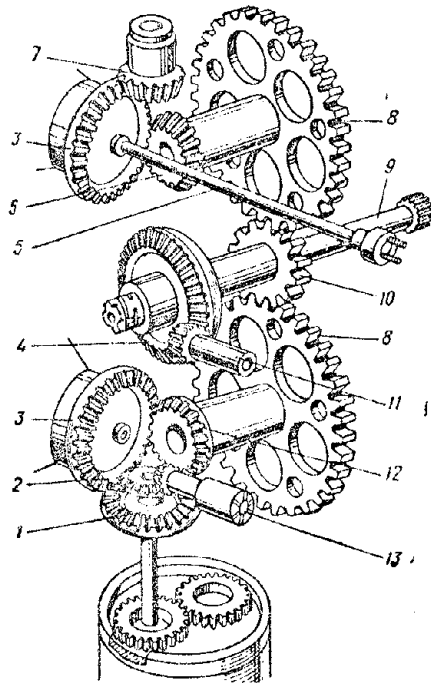


Fig. 12.5. Kinematic diagram of gear box of TRD VK-1.

Through a pair of bevel gears 11 and 4, shaft of pinion gear 10 and spring 9 rotation is transmitted from electric starter to engine rotor. Drive from electric starter is turned on only when starting the engine by means of the pawl clutch connecting gear 4 with gear shaft 10. Description of pawl clutch is given in Chapter XVII "GTD Starting."

Figure 12.6 shows the gear box of TRD assemblies with centrifugal compressor. The kinematic diagram of these drives is similar to the diagram shown in Fig. 12.5.

**GRAPHIC NOT  
REPRODUCIBLE**

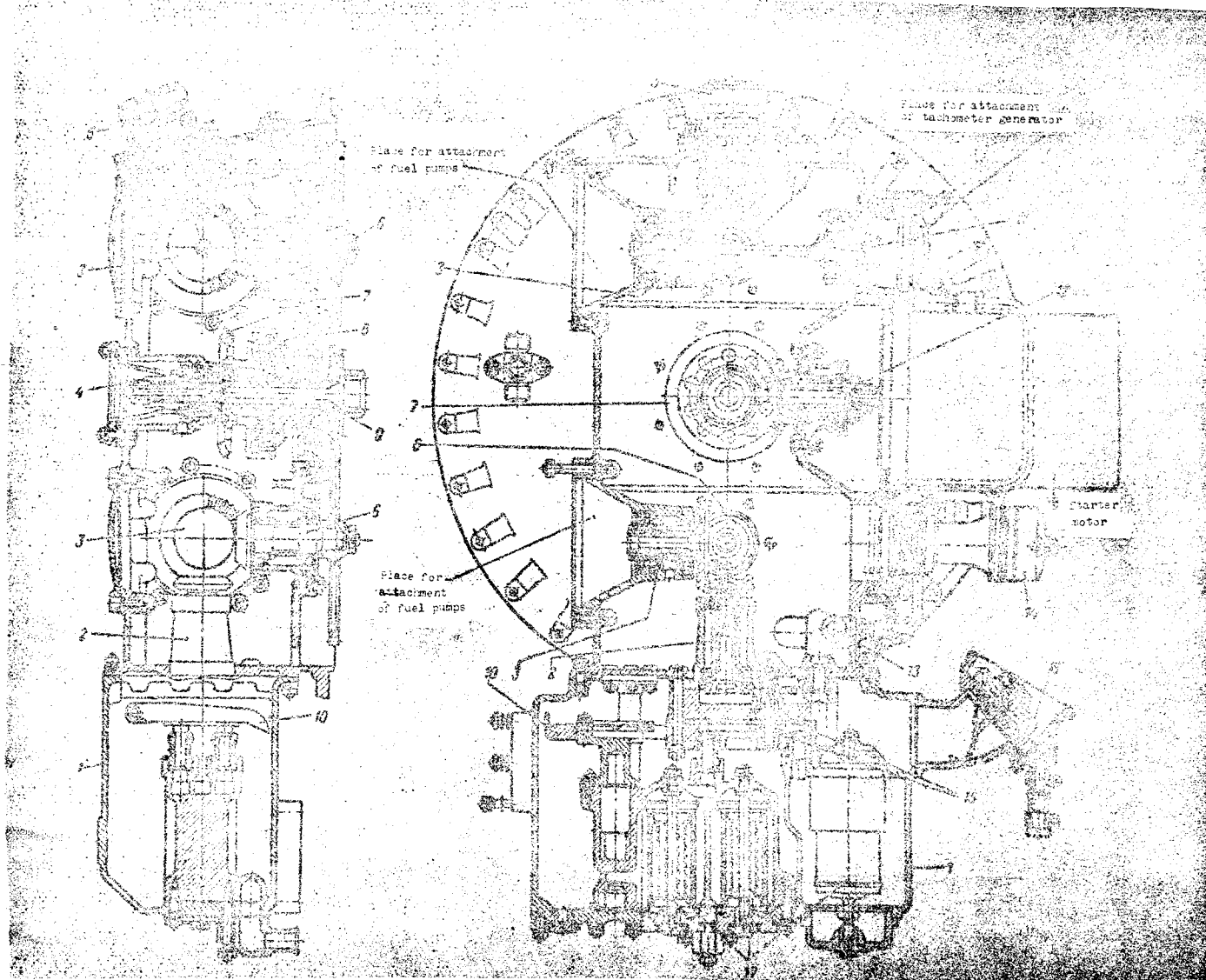


Fig. 12.6. Gear box of assemblies of a TRD with centrifugal compressor. 1 - oil pan, 2 - drive of oil pump, 3 - drives of fuel pumps, 4 - vent, 5 - drive of aircraft assembly box, 6 - intermediate drives, 7 - drive gears of starter, 8 - pawl clutch, 9 - main drive shaft, 10 - oil tray, 11 - drive of tachometer generator, 12 - drive of starter, 13 - reducer valve, 14 - transducer of oil pressure gauge, 15 - oil pumps, 16 - throat for filling of oil, 17 - oil filters.

### 12.3. Materials

Drive gears are usually made from cemented steels [12Kh2N4A] (12X2H4A) or [12KhN3A] (12XH3A). For decrease of wear, gear teeth are cemented. Shafts and spring shafts are made from steel [40KhNMA] (40XHMA), [18KhNVA] (18XHBA), and [12Kh2N4A] (12X2H4A). The gear box is cast from magnesium alloy [ML5] (M15) or aluminum alloy [AL5] (Al5).

## C H A P T E R XIII

### GTD POWER UNIT SYSTEM

#### 13.1. General Information

The power system of a [GTD] (ГТД) is formed by a system of power units which in [TRD] (ТРД) includes the casings of compressor, turbine, rotor bearings, and housing of combustion chambers. To them are attached inlet and outlet devices and accesso<sup>r</sup> boxes. The power-distribution system of [TVD] (ТВД) units also includes the reduction gear housing. Power units have mounting lugs for attachment of engine to aircraft.

Power units are perceive the weight of parts of the engine, forces of gases, forces of inertia, and moments from these forces. Some of these forces and moments in the housing system are mutually balanced and are closed or internal. Others remain free and are transmitted through mounting lugs to aircraft. Certain loads have a cyclical character and cause vibration of the housings. Since individual parts of the engine operate at different temperature conditions, in the housings there appear thermal stresses. Design of housings should respond to conditions of strength, rigidity, minimum weight, and simplicity of assembly.

Power-distribution systems of GTD housing are basically distinguished by type of connection of housings of compressor, turbine, and rear rotor bearing. Figure 13.1 gives four typical diagrams of TRD housings with axial-flow compressor and three-support rotor. Housing 1 of compressor is directly connected to housings 3 of front and 4 central rotor bearings. In diagram a the turbine housing 2 is connected to housing 4 of central rotor bearing through housing 5 of rear

rotor bearing and housing 7 of gas collector. In diagram b the rear rotor bearing is located behind the turbine and its housing 5 through housing 2, of turbine and casing 6 of combustion chamber is connected to housing 4 of central rotor bearing. Diagram c depicts branched connection of housings, in which to housing 4 of central rotor bearing is independently attached housing 5 of rear rotor bearing, and through casing 6 of combustion chamber, housing 2 of turbine. Diagram d depicts a closed (double) connection of housing 2 of turbine with housing 4 of central rotor bearing through housing 5 of rear rotor bearing and casing 6 of combustion chamber.

Diagram a applies when there are individual (can-type) combustion chambers, which usually are not included in the power-distribution system of the engine. Diagrams b, c, and d find application in annular and tubular-annular combustion chambers. Diagram d ensures more rigid connection of housings of turbine and compressor, but with various heating of housing 5 and casing 6 in them there can appear additional thermal stresses.

In TRD with centrifugal compressor they apply usually the can-type combustion chamber and power-distribution system of housings is according to diagram a. In

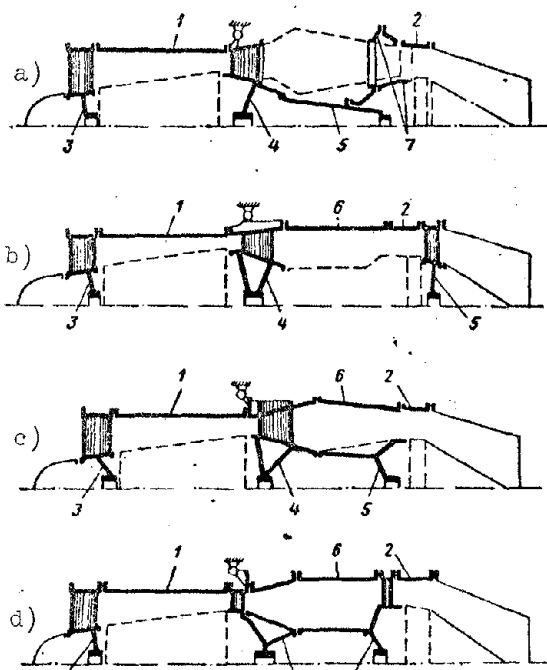


Fig. 13.1. Power diagrams of TRD housings.

TVD the power diagrams of housing are similar to those shown in Fig. 13.1. Reduction gear housing can enter engine design or can be made in the form of a separate unit, as shown in Fig. 11.1. In the first case the reduction gear housing is connected with the front rotor bearing housing.

### 13.2. Gas Forces

Forces of gases create effective operation in the engine system. These forces cause radial, tangential, and axial loads in the housings.

Radial loads appear in housings due to the static pressures of gases. Radial forces are internal, closed forces.

Tangential loads in housings appear due to the dynamic effect of gas flow during change of its tangential speed component in nozzle, guides, and stators,

and also in struts straightening the flow. Magnitude of twisting moments applied to GTD housings is determined by change of angular moment  $\alpha$  of gas flow:

$$M_{\text{exp}} = \frac{G}{g} (c_{1u} - c_{2u}) R, \quad (13.1)$$

where  $G$  is the gas expenditure per second;

$g$  is acceleration due to gravity;

$R$  is the mean radius of location of channel;

$c_{1u}$  and  $c_{2u}$  are the tangential speed components of gases at inlet and outlet of channel taking into account their sign.

Direction of twisting moments is determined by character of change of tangential speed component of flow.

Torque of TRD turbine is transmitted to rotation of compressor:

$$M_t = M_k, \quad (13.2)$$

where  $M_t$  is torque on turbine shaft;

$M_k$  is moment of resistance to rotation of compressor rotor.

Torque  $M_t$  is directed towards rotation of rotor, and moment of resistance  $M_k$ , against its rotation.

According to the third law of mechanics — equality of action and counter-action of forces — housings perceiving tangential loads of turbine are twisted by reactive moment

$$M'_t = M'_k, \quad (13.3)$$

and housing perceiving tangential loads of compressor, and twisted by moment

$$M'_k = M'_t. \quad (13.4)$$

Direction of action of twisting  $M'_t$  and  $M'_k$  is correspondingly opposite the direction of moments  $M_t$  and  $M_k$ .

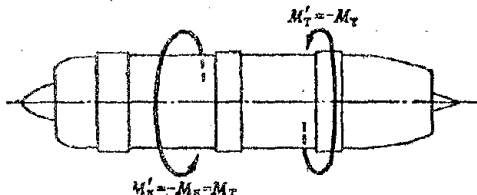


Fig. 13.2. Twisting moments of TRD housings.

Taking into account expression (13.2), we arrive at the conclusion that TRD power units during operation are twisted by moments  $M'_k$  and  $M'_t$ , equal in magnitude and inverse in direction, which in the engine system are mutually balanced (Fig. 13.2).

For the rotor of TVD turbine the tangential loads create useful torque which is transmitted to rotation of compressor and propeller:

$$M_t = M_k + I_p M_n, \quad (13.5)$$

where  $M_b$  is the moment of resistance to rotation of propeller;  
 $i_p < 1$  is the transmission ratio of the reduction gear;  
 $i_p M_b$  is the moment of resistance to rotation of propeller, applied to turbine shaft.

Moments of resistance  $M_k$  and  $i_p M_b$  are directed opposite rotation of rotor.

Housings perceiving tangential loads of turbine are twisted by reactive moment

$$M'_r = M_r, \quad (13.6)$$

directed opposite rotation of rotor. If one considers that moment of resistance to rotation of compressor rotor

$$M_k' = M_k - i_p M_b$$

is directed opposite rotation of rotor, then housings perceiving tangential loads of compressor would be twisted by moment

$$M'_k = M_k' = M_k - i_p M_b, \quad (13.7)$$

directed towards rotation of rotor. Reduction gear housing perceives twisting moment in the area of the gear drive. Thus, for instance, in a planet reduction gear with transmission of rotation to one propeller (see Fig. 11.3a) toward fixed gear  $z_3$  the housing will receive twisting moment  $M_p$  (Fig. 13.3),

$$M_p = P_1 R_3, \quad (13.8)$$

where  $P_1$  is the tangential stress on pinion gear;

$R_3$  is the radius of the fixed gear.

Moment  $M_p$  is directed opposite the rotation of the turbine rotor. Transmission ratio  $i_p$  of planet reduction gear is:

$$i_p = \frac{1}{\frac{z_3}{z_1} + 1} = \frac{1}{\frac{R_3}{R_1} + 1},$$

whence

$$R_3 = R_1 \left( \frac{1}{i_p} - 1 \right).$$

Placing in expression (13.8) the obtained value of  $R_3$ , we find:

$$M_p = P_1 R_1 \left( \frac{1}{i_p} - 1 \right) = i_p M_b \left( \frac{1}{i_p} - 1 \right) = M_b (1 - i_p), \quad (13.9)$$

where magnitude  $P_1 R_1 = i_p M_b$  is the moment of resistance of rotation of the propeller applied to turbine shaft.

Summarizing twisting moments  $M'_r$ ,  $M'_k$ , and  $M_p$ , applied to TVD power units taking into account the direction of their action (see Fig. 13.3) and considering expressions (13.7) and (13.9), we obtain:

$$M_z = -M'_r + M'_k - M_p = -M_p \quad (13.10)$$

Here the plus is taken as the direction of rotation of the rotor, with which in this case coincides the direction of rotation of the propeller.

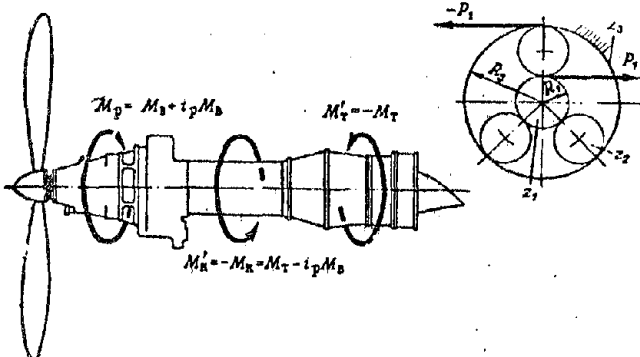


Fig. 13.3. Twisting moments of TVD housings.

It follows from this that in the system of TVD power units, total twisting moment remains free and is transmitted to the aircraft through the engine mounting lugs. It is called disturbing moment. With respect to magnitude the disturbing moment of TVD is equal to the moment of resistance to propeller rotation

and is directed opposite propeller rotation.

Disturbing moment of TVD with two propellers revolving in different directions is equal to the difference of moments of resistance to propeller rotation, and with equality of the latter will be equal to zero.

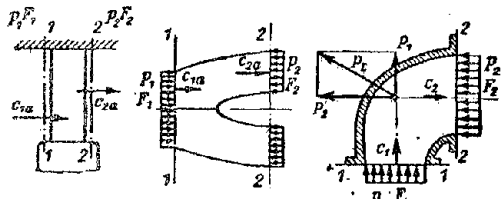


Fig. 13.4. Determination of axial force of blade rim of inlet channel of axial-flow compressor and branch of centrifugal compressor.

In case of a differential reduction gear on two coaxial propellers, for which  $M_p = 0$ , disturbing moment is equal to the difference of moments of resistance to propeller rotation and is directed opposite the rotation of the engine rotor.

Axial stresses appear due to the static pressure of gases and due to dynamic impact in the area of gas flow. Axial stress due to static pressure is determined by the product of static pressure of gases  $p$  on a corresponding area of cross section of channel or wall  $F$ . Axial stress due to dynamic impact is determined by the change of quantity of motions of gas flow in axial direction.

For any section of the engine gas duct, separated by parallel sections 1-1 and 2-2 (Fig. 13.4), axial stresses  $P_o$  will be expressed by the formula:

$$P_o = p_1 F_1 - p_2 F_2 + \frac{G}{g} (c_{1a} - c_{2a}), \quad (13.11)$$

or

$$P_o = \left( p_1 F_1 + \frac{G}{g} c_{1a} \right) - \left( p_2 F_2 + \frac{G}{g} c_{2a} \right), \quad (13.12)$$

where  $p_1$  and  $p_2$  are pressure of gases in sections 1-1 and 2-2;

$F_1$  and  $F_2$  are areas of cross sections;

$c_{1a}$  and  $c_{2a}$  are axial speeds of gas in sections 1-1 and 2-2;

$G$  is the expenditure of gases per second;

$g$  is acceleration due to gravity.

Sign of force  $P_0$  determines its direction. With the plus sign stress is directed from section 1-1 to section 2-2 (toward the flow), and with the negative sign, from section 2-2 to section 1-1 (opposite the flow).

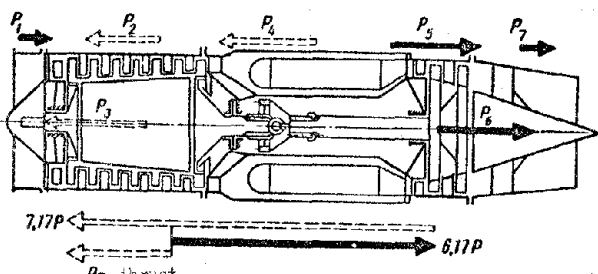


Fig. 13.5. Axial stresses of individual TRD units.

In case of a curvilinear channel, for instance in the outlet branch of a centrifugal compressor, the resultant force towards air flow will be directed at a certain angle and will be determined as the geometric sum of forces:

$$P_1 = p_1 F_1 + \frac{G}{g} c_{1a} \quad \text{and} \quad P_2 = p_2 F_2 + \frac{G}{g} c_{2a}.$$

In the engine system the axial stresses are applied to different parts of it. Some of them are directed towards flight, and others opposite flight. All resultant axial forces are free and form engine thrust. It is directed in the engine opposite gas flow, i.e., in the direction of flight of the aircraft.

Figure 13.5 depicts vectors of axial forces acting during operation on certain TRD units with axial-flow compressor. In this case their magnitude expressed through thrust  $P$  is:

for intake  $- P_1 = 0.12P$ ;

for compressor stator  $- P_2 = 1.07P$ ;

for compressor rotor  $- P_3 = 3.09P$ ;

for combustion chamber  $- P_4 = 2.2P$ ;

for turbine stator  $- P_5 = 1.75P$ ;

for turbine rotor  $- P_6 = 3.87P$ ;

for exhaust nozzle  $- P_7 = 0.43P$ .

The resultant of these forces is engine thrust. From consideration of Fig. 13.5 it follows that individual GTD units during operation carry very considerable axial loads which must be considered in strength calculations.

The propeller of a TVD converts the power developed on the engine shaft into thrust:

$$P = 75 \frac{N\eta}{V}, \quad (13.13)$$

where  $N$  is engine power;

$\eta$  is propeller efficiency;

$V$  is the speed of flight of the aircraft.

During operation on ground (at moment of starting aircraft during takeoff) the propeller develops maximum thrust which composes:

$$P_{\max} = (1.3 \div 1.5) N_{\text{ts}},$$

where  $N_{\text{ts}}$  is the takeoff power.

### 13.3. Inertial Loads and Mass Forces

Inertial forces and moments appearing in GTD are unbalanced, free, and are transmitted through mounting lugs to the aircraft. They include: unbalanced centrifugal forces of rotors [formula (6.5)], gyroscopic moments of rotors [formula (7.16)] and inertial force of mass overload [(see Fig. 7.21)]; the latter is expressed by the following formula:

$$P_j = KQ, \quad (13.14)$$

where  $K$  is the coefficient of mass overload;

$Q$  is the weight of the engine.

Gyroscopic moment and inertial mass overload appear during evolution of aircraft and are brief. Coefficient of mass overload depends on type of aircraft and character of evolution. In the designs of fighters they usually take  $K = 8$  to 10.

Mass forces are free and are transmitted through mounting lugs to aircraft. Total weight of engine is applied to its center of gravity.

### 13.4. Mounting of Engine to Aircraft

Mounting lugs of GTD to aircraft are placed on power units. Since during operation certain GTD parts are considerably heated, the mounting lugs must ensure free thermal expansion of engine.

Figure 13.6 shows a typical diagram of mounting a TRD with axial-flow compressor to an aircraft at three points. Compressor housing at points A and B, located near the center of gravity of the engine, has two journals with spherical supports. The supports allow for misalignments in the joint. Journal A is locked in the mounting lug, and journal B, resting freely on a spherical insert, ensures the engine transverse thermal expansion.

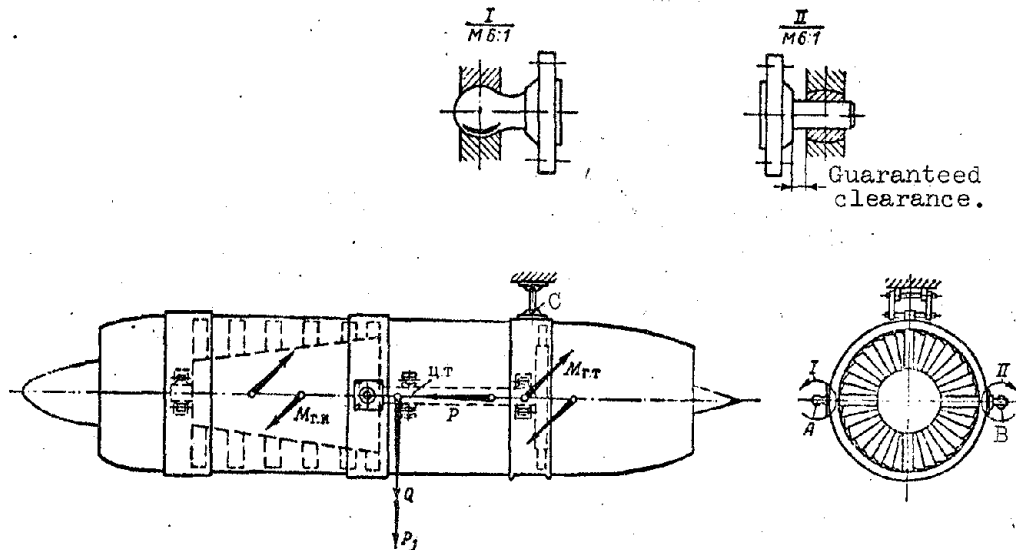


Fig. 13.6. Diagram of mounting a TRD with axial-flow compressor to an aircraft.

An additional mounting lug is located on the turbine housing at point C. It is made in the form of a hinged suspension which perceives only vertical loads. Hinged suspension ensures free expansion of engine in axial direction.

The diagram gives the following forces and moments of forces transmitted through mounting lugs to aircraft:

P is the thrust acting along the engine axis;

Q is the weight of the engine;

$P_j$  is the inertial centrifugal force of mass overload, applied to center of gravity of engine;

$M_{rk}$  and  $M_{rt}$  are the gyroscopic moments of rotors of compressor and turbine.

### 13.5. Strength Calculation

Housings of compressor, turbine, combustion chambers, exhaust nozzle, and afterburner are calculated as thin-walled shells. Calculation of shells for axial and radial loads was presented in Chapters IX and X.

Under the action of lateral loads shells experience bending. Bending stresses are determined by the following formula:

$$\sigma_b = \frac{M_b}{W_b} = \frac{M_b}{\pi R^2 \delta}, \quad (13.15)$$

where  $M_b$  is the bending moment in the calculated section;

$W_b = \pi R^2 \delta$  is the moment of bending strength of a thin-walled shell;

R is radius of shell;

$\delta$  is thickness of wall.

Figure 13.7a shows a cantilever shell. Its bending occurs under the action of an external load in the form of the moment of a pair of forces  $M_B$  and lateral force  $Q_B$  applied to its flange, and also under the action of the natural weight  $Q$  of the shell and its inertial force of mass overload  $P_j$  applied in a section to the center of gravity of the shell. Maximum bending moment will act in the fitting; it is equal to:

$$M_{B \max} = M_B + Q_B l + (Q + P_j) l_1.$$

Bending stresses in GTD housings usually do not exceed 100 to 150 kg/cm<sup>2</sup>.

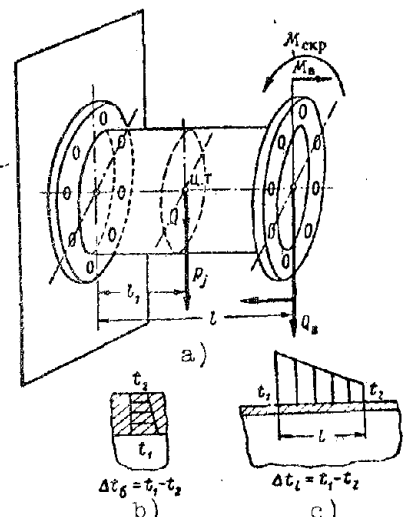


Fig. 13.7. Strength calculation of shells.

Under the action of twisting moment  $M_{ckp}$  (see Fig. 13.7a) the shells experience tangential stresses which are determined by the formula

$$\tau = \frac{M_{ckp}}{W_{kp}} = \frac{M_{ckp}}{2\pi R^2 b}, \quad (13.16)$$

where  $W_{kp} = 2\pi R^2 b$  is the moment of torsional strength of the thin-walled shell.

Tangential stresses in GTD housings usually do not exceed 100 kg/cm<sup>2</sup>.

During nonuniform heating of shells there appear thermal stresses which for cylindrical shells can be determined by the formulas:

during nonuniform heating along thickness of wall (see Fig. 13.7b)

$$\sigma_{tx} = \sigma_{ty} = 0.715 E \alpha \Delta t_b \quad (13.17)$$

and during nonuniform heating along generatrix (in case of linear law, Fig. 13.7c)

$$\sigma_{tx} = 0.353 E \alpha \frac{\Delta t_l}{l} \sqrt{R^2}, \quad (13.18)$$

where

$E$  is the elastic modulus of shell material;

$\alpha$  is the coefficient of linear expansion of shell material;

$\Delta t_b$  and  $\Delta t_l$  are temperature drops along thickness of wall and on length  $l$  of shell.

Stresses  $\sigma_{tx}$  act in lateral sections, and  $\sigma_{ty}$  in longitudinal sections of the shell (see Fig. 9.15a).

Combined stress in shells can be determined by the third theory of strength:

$$\sigma_{eq} = \sqrt{\sigma_{eqs}^2 + 4\tau^2}, \quad (13.19)$$

where  $\sigma_{eqs}$  is the equivalent normal stress;

$$\sigma_{\text{eqs}} = \sqrt{\sigma_{xx}^2 + \sigma_{yy}^2 - \sigma_{xx}\sigma_{yy}}, \quad (13.20)$$

here  $\sigma_{xx}$  and  $\sigma_{yy}$  are total normal stresses in lateral and in longitudinal sections of shell.

Safety factor

$$k = \frac{\sigma_y}{\sigma}, \quad (13.21)$$

where  $\sigma_y$  is the yield point of shell material at operating temperature.

Safety factor of GTD housings is usually no less than 1.8.

## C H A P T E R XIV

### GTD LUBRICATION SYSTEM

#### 14.1. General Information

In [GTD] (ГТД) are lubricated bearings, gears and partially slit connections of shafts. Lubrication decreases their friction, wear, and hardening, carries solid particles, between working surfaces, and draws off heat.

For [TRD] (ТРД) they basically use petroleum oils MK-8 or transformer oil. For engines operating at high temperatures, we find the application of synthetic oils. High-loaded drive transmissions of reduction gears require oil with viscosity. Therefore, in TVD they use either a mixture of MK-8 (or transformer oil) and MK-22 oils (or [MS-20] (MC-10)) or turbine oil.

Oil is supplied under a pressure from 3 to 6 kg/cm<sup>2</sup>. Through injectors and jets the oil is directed in the form of a stream on the working surfaces of contact components. Low-loaded transmissions of the accessory drive box are partially lubricated by flushing.

GTD usually have a circulatory (closed) system of lubrication, in which oil by means of pumps continuously circulates in a closed circle: oil tank -- engine -- radiator -- oil tank. TRD with small heat radiation in oil the radiator is sometimes omitted, and the oil tank serves as the oil pan of the engine. Cooling of oil occurs through walls of oil pan, which on the outside is blown by flow of air.

Certain GTD have a short-circuited circulatory system of lubrication in which the oil circulates in a closed circle: engine -- radiator -- engine. Oil tank is turned off from main circulation system and serves only for augmentation of

of decrease of oil in the main system.

In TRD designed for a small period of action we find the application of the so-called open (unclosed) system of lubrication, which supplies an oil-air emulsion contact components of the engine through injectors. Through an ejection system this emulsion is then expelled into the atmosphere. The shortcoming of this system is the great expenditure of oil.

Oil tank contains necessary supply of oil for normal engine operation. Oil is fed to the engine at a temperature from 50 to 80°C and is pumped from it at a temperature reaching up to 110 to 120°C. Radiator serves for cooling of oil leaving the engine. Radiators can be oil-air and oil-fuel. In the first case the coolant is the incident flow of atmospheric air, and in the second it is the fuel. Application oil-fuel radiators usually is limited by the permissible temperature of heating of fuel, which should be lower than the temperature of its boiling at the design altitude of flight.

Circulation of oil is carried out by means of pressure and scavenge oil pumps. Pressure pumps feed oil under pressure to the engine, and scavenge pumps evacuate it. The oil is pumped out completely, i.e., the system operates on the principle of "dry bodies."

Usually there is one main pressure pump. Furthermore, the engine can have low-pressure oil pumps (booster or makeup pumps) feeding oil to the main pump, and also high-pressure pumps ensuring supply of oil in the form of working fluid to certain engine assemblies. The number of scavenge oil pumps usually is determined by the number of evacuation places.

The engine oil system also includes oil filters and centrifugal air-separators. Oil filters serve for purification of oil from dirt, coke, metallic particles, and dust. Filters are classified as fine and coarse purification. Since fine filters have increased resistance to passage of oil, then there are installed as a rule on the pressure line, i.e., behind the pressure oil pump at the engine inlet. Coarse filters are sometimes placed on the suction line of pumps. They protect these pumps from fall into them of bigger objects (nuts, splint pins, shavings, and so forth).

Passing through the GTD the oil is saturated by air and gas. Scavenge oil pumps, having usually excess productivity, together with oil, pump a considerable quantity of air in the form of an air-oil emulsion and air bubbles.

In the oil the air occupies a specific volume in it, promoting burst of the oil film on the contact working surfaces, decreases the coefficient of thermal conduction of the oil, and gives it elastic properties. For this reason the productivity of pressure oil pumps and the height of the oil system is lowered, while lubrication of contact components, effectiveness work of oil cooler and work of many automatic devices (for which the oil serves as the working fluid) decreases in quality.

Centrifugal air-separators constitute centrifuges for separation of air from oil. They are usually placed at the engine outlet behind the scavenge oil pumps.

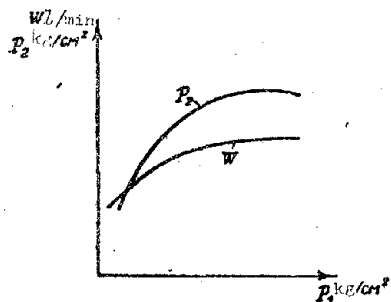


Fig. 14.1. Cavitational characteristic of a pump.

Breather system. Normal work of oil-system requires breathing of engine and oil tank, i.e., maintaining atmospheric pressure in them. For this purpose, by means of a system of channels and pipelines the oil cavities of the engine and oil tank are connected through a vent with the atmosphere.

Vents serve for separation of suspended drops of oil from the air exiting through them. This oil is bled back into the engine. Frequently GTD have centrifugal breathers, i.e., centrifuges with mechanical drive.

Height of oil system. With rise to a height the pressure in the oil tank, and consequently also at the pressure oil pump inlet, drops, increases, and separation of gases dissolved in the oil and saturated vapors is increased. Furthermore, the oil has a large quantity of small suspended bubbles of air that expand at lowered pressures, which leads to intensive foaming and disturbance of continuity of oil flow at pump inlet. This phenomenon is called cavitation. The quantity of oil proceeding to the pump with cavitation decreases, which evokes lowering of performance of the pump. Figure 14.1 shows the cavitational characteristic of an oil pump in the form of the dependence of pressure of oil  $p_2$  at the pump outlet and its performance  $W$  on absolute pressure of oil  $p_1$  at the pump inlet.

The height at which pump performance and pressure of oil attain their minimum permissible value for reliable work of the engine is called the height of the oil system. Height of the oil system is ensured in the first place by the performance reserve of the pumps. Furthermore, suction pipe make as large a section

as possible and with small flow friction, while the oil tank is placed above the oil pumps, thus ensuring a certain pressure at the pressure oil pump inlet. For the same purpose in the oil tanks there sometimes is created heightened pressure, etc.

The short-circuited system of lubrication possesses larger height, since the suction line of the pressure oil pump is under a head which is created by the scavenge pump.

Circulatory expenditure of oil is called the quantity of oil which is pumped through the engine in a unit of time. Circulatory expenditure of engine oil (flow rate of oil) is determined by the reliable operation of its bearings and gear drives. Furthermore, the flow rate also considers the oil proceeding as the working fluid in systems of control and regulation of the engine.

The necessary quantity of oil for each rotor bearing is determined by its location on the engine. Thus, to the front rotor bearing located in the cold zone of the engine, the oil is usually supplied in a quantity of 1-2 l/min, and to the central and rear bearings located in the hot zone of the engine, in a quantity of 2-6 l/min and above. Oil, going for lubrication of accessory drives and for control and regulation systems usually composes 20-50% of its total flow rate through the engine. In TVD oil is supplied in addition for lubrication of the reduction gear, to the system of propeller control, and to the torque meter.

In the existing GTD designs the specific heat radiation  $Q$  in oil and its specific flow rate  $W$  through the engine, referred to 1000 kg of thrust for TRD and to 1000 hp for TVD, are:

	$Q$ kcal/min	$W$ l/min
ТРД	30÷60	3÷5
ТВД	140÷200	12÷30

Increased heat radiation and oil flow rate of TVD are explained by the presence of the reduction gear and the system of propeller control.

Expenditure of oil is called loss of oil in the process of engine operation. This loss occurs because part of the oil penetrates the flow area of the engine, and is also carried through a vent into the environment. Expenditure of oil in GTD is from 0.3 to 1.5 l/hour.

Performance of oil pump. For guarantee of normal engine operation under all conditions and at all altitudes of flight, the pressure oil pump is usually oversized, i.e., with a performance reserve 150-200% greater than circulatory expenditure. This reserve is maintained by bypass of excess quantity of oil through a reduction valve back to the suction side of the pressure pump (see Fig. 14.5).

Since from the engine there emerges foamed oil, the volume of which exceeds the volume of oil proceeding to the engine, then for guarantee of its full evacuation the scavenging pumps with respect to total performance are also oversized, i.e., with reserve 2-4 times more than the performance of the pressure oil pump.

#### 14.2. Diagrams of GTD Lubrication

Typical diagram of TRD lubrication (Fig. 14.2) consists of oil tank 2, pressure oil pump 4, fine filter 6, distribution column 9, scavenging oil pumps 3, 15, and 16, air separator 17, oil pan 13, oil cooler 1, and vent 10.

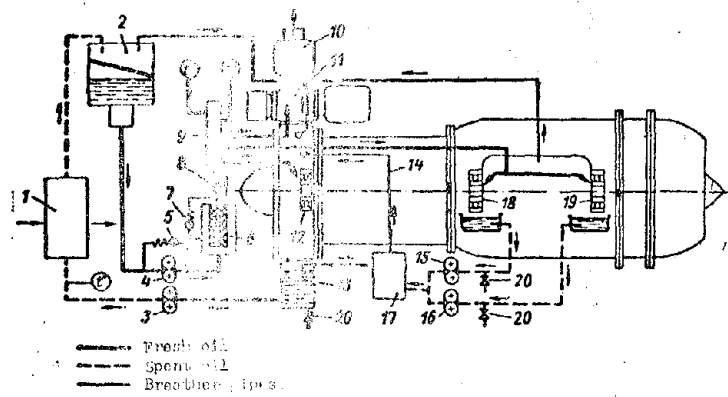


Fig. 14.2. Typical diagram of TRD lubrication.  
 1 - oil cooler, 2 - oil tank, 3 - scavenging oil pump,  
 4 - pressure oil pump, 5 - reduction valve, 6 -  
 filter, 7 - bypass valve, 8 - check valve, 9 -  
 distribution column, 10 - vent, 11 - accessory  
 gearbox, 12, 13 and 14 - rotor bearings, 13 - oil  
 pan, 14 - overboard breather pipe, 15 and 16 -  
 pressure oil pumps, 17 - air separator, 20 -  
 blow-off valves, 11) manometer, 12) thermometer.

The pressure oil pump supplied oil from oil tank to engine. Reduction valve 5 on pump 4 maintains constant pressure of oil, bypassing its surplus back to the suction side of the pump.

From the pressure pump the oil enters thin oil filter 6. Bypass valve 7 serves for bypass of unpurified oil to engine near the filter. This necessary when there is contamination of the filter or when starting the engine in the cold season when the oil in the engine thickens. Behind the filter there is check valve 8 which ensures passage of oil only to engine.

From the distribution column the oil is tapped by its individual consumers, i.e., to rotor bearings 12, 18, 19 and to accessory gearbox 11. Quantity of oil passed to them is apportioned by means of jets and injectors.

Spent oil from central 18 and rear 19 rotor bearings is collected in their oil pans, from which it is pumped out by pumps 15 and 16 and moves to centrifugal air separator 17. In air separator there occurs separation of air and oil vapors, which through pipe 14 are directed to the front bearing housing of the compressor. Purified oil enters the main oil pan 13, where by gravity there also flows the oil from the front rotor bearing and from the accessory gearboxes. In the oil pan there are screens and partitions which divide the solid stream of oil into separate streams and promote separation of air from it. Main pump 3 pumps out oil from the oil pan and through radiator 1 passes it to oil tank 2. Blow-off valves 20 serve for drain of oil from engine after it stops.

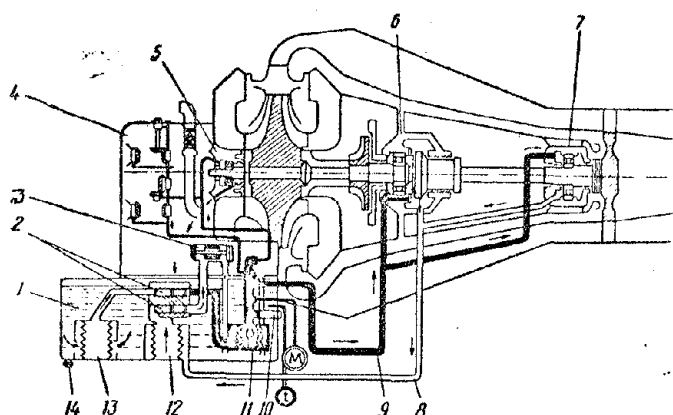


Fig. 14.3. Diagram of TRD VK-1 lubrication.

Operation of oil system is controlled by metering the pressure and temperature of oil at the engine inlet and metering temperature at its outlet. In the diagram manometer is designated M, and thermometers  $t^{\circ}$ .

In the engine the working cavities of the central and rear rotor bearings front rotor bearing

housing, accessory gearbox, and oil tank are vented. By means of tubes these working cavities, housings, and oil tank are connected with centrifugal vent 10, in which there occurs separation of drops of oil from air and gases. The drops are ejected into the atmosphere, and oil flows into the front rotor bearing housing.

Diagram of TRD [VK-1] (BK-1) lubrication (Fig. 14.3) does not have an oil cooler. The reservoir for oil is the oil pump housing 1 fastened to the lower part of the accessory gearbox 4, where there is flooded 6 l of oil. The lubrication system is circulatory. Housing 1 contains two gear oil pumps 2, three filters 11, 12 and 13, and reduction valve 10. Through coarse filter 13 oil passes to pressure section of oil pump 2 and passing then through fine filter 11 passes into the vertical pressure channel which serves as a distribution column. Reduction

valve 10 maintains constant oil pressure at the pump outlet, bypassing the oil surplus back to housing 1.

From the vertical pressure channel the oil moves to the injector of the front rotor bearing 5 for lubrication of accessory drives and through tube 9 to injectors of the central 6 and rear 7 rotor bearings, and also for lubrication of the shaft joint. In the gearbox the oil is supplied to all bearings and, being sprayed, lubricates the drive gears.

From front rotor roller bearing 5 and from the accessory gearbox 4 the spent oil flows into the oil pump housing 1 by gravity.

From the central 6 and rear 7 rotor bearings the oil through tube 8 is pumped through coarse oil filter 17 by the scavenged oil pump and moves into air separator 3.

In it there occurs separation of air from oil. Oil from air separator 3 drains into oil pump housing 1, and air goes into the accessory box 4. The box through a vent is connected with the atmosphere. Oil is drained from engine through valve 14.

Diagram of lubrication of the TVD [AI-20] (AM-20) (Fig. 14.4) is short-circuited. It consists of oil tank 33, main oil pumps — pressure 2 and scavenged 4 — makeup pump 1, scavenged oil pumps 3, 5 and 6, fine oil filters 15 and 20, coarse oil filters 7, centrifugal air separator 9, air-oil cooler 8, oil-lines, and injectors. Circulation of oil is carried out in a short-circuited cycle: main pressure oil pump — engine — main scavenged oil pump — air separator — oil cooler — main pressure oil pump.

At the exit of pressure oil pump 2 the oil is divided into two flows. One heads to the reduction gear, and the other to the main part of the engine. On the way the oil passes through fine oil filters 15 and 20, where it is cleaned. Oil pressure gauge 21 behind filter 20 meters the pressure of the oil, which by means of reduction valve 19 is maintained at nominal conditions from 4 to 4.5 kg/cm<sup>2</sup>. Temperature of oil is measured at engine inlet and at its outlet.

Oil proceeding to reduction gear ensures its lubrication and feeds oil pump 22 of the torque meter. Oil proceeding to engine moves for lubrication of rotor bearings 26, 27, and 28, central drive transmission, accessory gearbox 14 and the accessories themselves. In addition, the oil, as the working fluid, moves to the speed regulator 25 and the fuel-control unit 11.

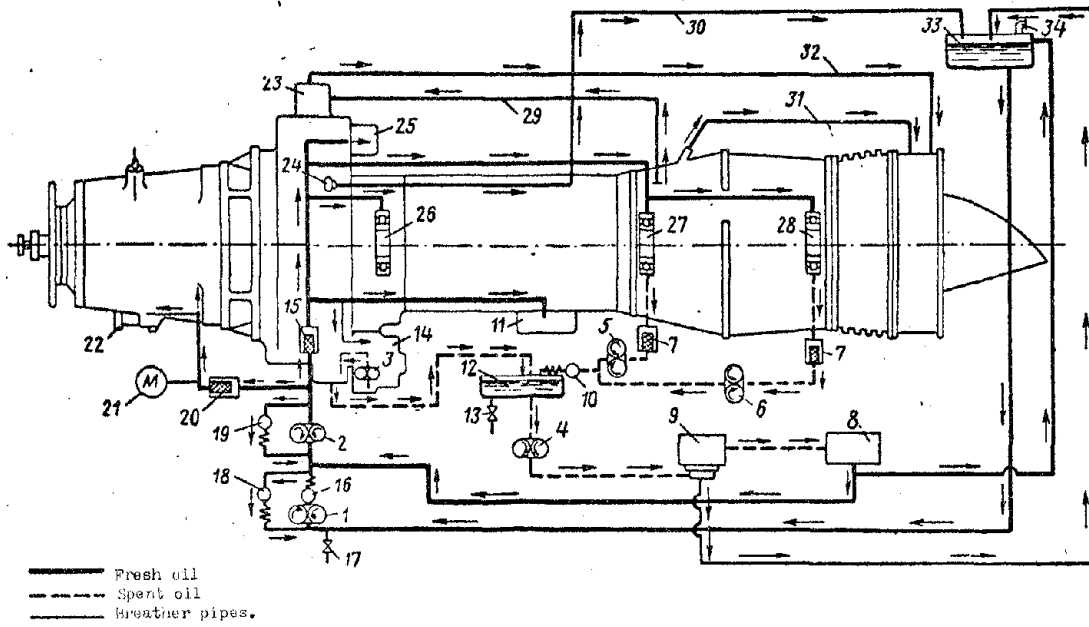


Fig. 14.4. Lubrication system of the TVD AI-20. 1 - makeup pump, 2 - pressure oil pump, 3, 5, 6 - scavenge oil pumps, 4 - scavenge oil pump, 7 - coarse oil filters, 8 - air-oil cooler, 9 - air separator, 10 and 16 - check valves, 11 - fuel-control unit, 12 - oil pan, 13 and 17 - relief valves, 14 - accessory gearbox, 15 and 20 - fine oil filters, 18 - reduction valve, 19 - reduction valve, 21 - oil pressure gauge, 22 - oil pump of torque meter, 23 - centrifugal breather, 24 - central drive breather, 25 - speed-control unit, 26, 27 and 28 - rotor bearings, 29, 30, 31 and 32 - breather pipes, 33 - oil tank, 34 - oil tank vent.

Lower cavity of front bearing housing of compressor forms oil pan 12. Here the oil is drained by gravity from the cavity of the central drive transmission, from the front rotor bearing, and from the reduction gear. Here oil is pumped out by auxiliary scavenge oil pumps 3, 5 and 6: from accessory gearbox 14, and from cavities of central 27 and rear 28 rotor bearings.

From oil pan 12 oil is pumped out by main scavenge oil pump 4 and heads to air separator 9. In air separator 9 there occurs separation of air from oil. Air heads to oil tank 33 and from there through vent 34 on it, into the atmosphere. Purified from air the oil enters air-oil cooler 8, where occurs it is cooled, and then to the entry to the main pressure oil pump 2. Furthermore, at the exit of the radiator the oil in a quantity from 5 to 8 l/min is drained into the oil tank for removal of the possibility of the oil freezing in it.

Makeup oil pump 1 supplements from oil tank 33 the decrease of circulating oil through the engine. With its help at the entry to the main pressure oil pump 2 there is maintained pressure of oil from 0.6 to 0.8 kg/cm<sup>2</sup>, and excess oil is passed through reduction valve 18 of makeup pump to its suction side. Check valves 10 and 16 in the system ensure supply of oil only in one direction.

Oil is drained from oil system through drain valves 13 and 17, on oil pan 12 and on main line of makeup pump 1.

In the AI-20 engine the following are vented: Cavity of central transmission, front bearing housing of compressor, cavity of central and rear rotor bearings and their labyrinth seals.

Cavity of central transmission through vent 24 is connected by pipe 30 with oil tank, which in turn is connected with the atmosphere through vent 34.

Air in cavity of bearings 27 and 28 is intensely saturated by oil. For purification the air heads through tube 29 to centrifugal breather 23. From this breather the air is tapped through pipe 32 to the exhaust pipe of the engine, and the oil is drained into the cavity of the central transmission.

Venting of labyrinth seals of bearings 27 and 28 is produced with the help of pipe 31 with ejection of air into exhaust pipe of engine.

#### 14.3. Design of Oil System Assemblies

Oil pumps usually are of the gear type, and in rare cases, the revolving type. The pumping unit of the gear pump consists of two coupled gears, upon rotation of which the oil from suction cavity A is fed to pressure cavity B (Fig. 14.5).

The pumping unit of the revolving pump consists of two plates inserted in a slot of the shaft and released by a spring. The shaft is eccentrically located in the housing and during its rotation the oil from the suction cavity A is fed the pressure cavity B (Fig. 14.6).

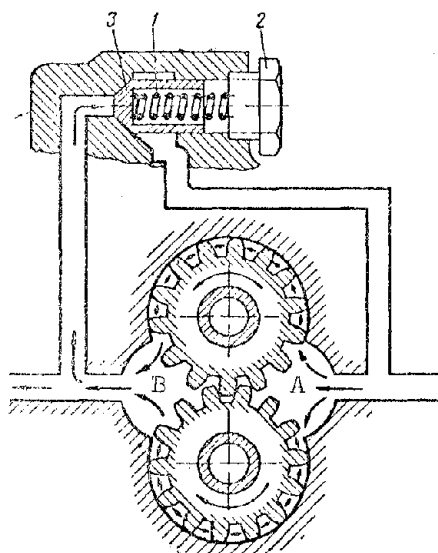


Fig. 14.5. Diagram of gear pump.

For maintaining the necessary pressure the pressure oil pumps have a reduction valve 3 which passes the excess quantity of oil back to the suction side of the pump. Reduction valve is pressed to its seat by spring 1 and is regulated at a determined pressure with the help of regulating screw 2. Scavenge pumps do not have a reduction valve.

Delivery of the gear oil pump  $W$  depends on size of gears, speed, and supply factor:

$$W = 2Fb\eta \cdot 10^{-6} \text{ l/min}, \quad (14.1)$$

where  $F$  is the area of cavities of teeth for one gear in  $\text{mm}^2$ ;

$b$  is the length of a tooth in mm;

$n$  is the rpm rate;

$\eta$  is the volume supply factor which in calculations is equal to 0.8 to 0.9.

Area of cavities is equal to

$$F = \frac{\pi}{8} (d_r^2 - d_h^2),$$

where  $d_r$  and  $d_h$  are the diameters of circumferences of head and legs of gear teeth.

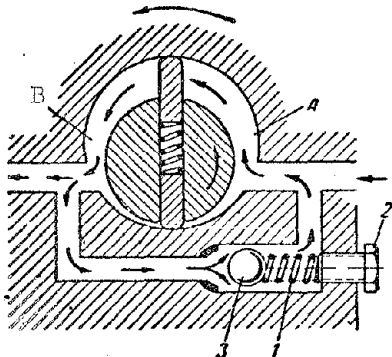


Fig. 14.6. Diagram of revolving pump.

For obtaining small diameters the number of gear teeth is small -- from  $z = 7$  to 12 -- and modulus  $m = 2$  to 4. To avoid large a notch on the base of the teeth, the teeth are corrugated. The driving and driven gears of the pump are usually made with identical number of teeth. Gears of pumps are made from structural steels, while the housing is cast from aluminum or magnesium alloys.

Upon entry of teeth into engagement the oil from their cavities is extracted. In case of small clearances in engagement of teeth there is formed a closed space in which there maybe created a high pressure, wedging the gears and overloading the bearings of the pump. For removal of this phenomenon, frequently the face surfaces of the housings have grooves connecting the region of high pressures in the engagement of teeth with the discharge chamber (Fig. 14.7).

Speed of pumps is selected from the condition of obtaining peripheral velocity on the external diameter of gears within the limits of  $V = 5$  to 8 m/sec. At higher speed there starts to show up a negative action of centrifugal forces on the oil filling of teeth cavities and supply factor  $\eta$  noticeably drops. The supply factor also depends on the resistance to suction of the pump, on the viscosity of oil, and on the clearances in gears. With their increase,  $\eta$  drops.

For decreasing the number of drives the oil pumps are usually grouped into separate oil-units. Figure 14.8 shows the two-section oil pump [VK-1] (BK-1), consisting of pressure 3 and scavenge 4 sections. Pinion gear sit on shaft 1, and driven gears on axis 5 secured to housing. Drive of oil pumps is carried out through a pair of spur gears -- driving 2 and driven -- made simultaneously with shaft 1. For guarantee of assembly the oil pump housing is sectional.

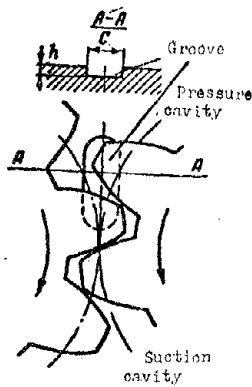


Fig. 14.7. Relief groove.

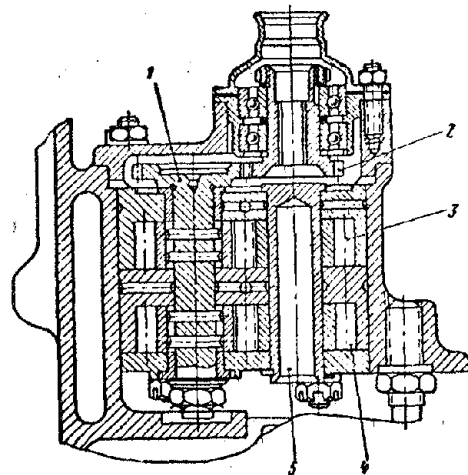


Fig. 14.8. Two-section oil pump of the VK-1 engine.

Valves. Figure 14.9 shows a reduction valve of the disk type - a, and a check valve of the ball type - b.

The reduction valve maintains constant pressure in the main oil line by means of bypass from it of the excess amount of oil. It consists of housing 1, the disk valve itself 2, calibrated spring 3, and regulating screw 4. Rod of regulating screw is a guide disk. Adjustment of valve to some pressure is done by change of tension of spring by turning the regulating screw. The screw is turned with the help of collar 6 which enters with its tetrahedral shank the tetrahedral hole of washer 5 attached to the hole of the regulating screw. Washer 5 allows some non-coaxiality of the collar and regulating screw. The collar is secured by tightening sleeve nut 7. Sealing is ensured by a rubber ring 8.

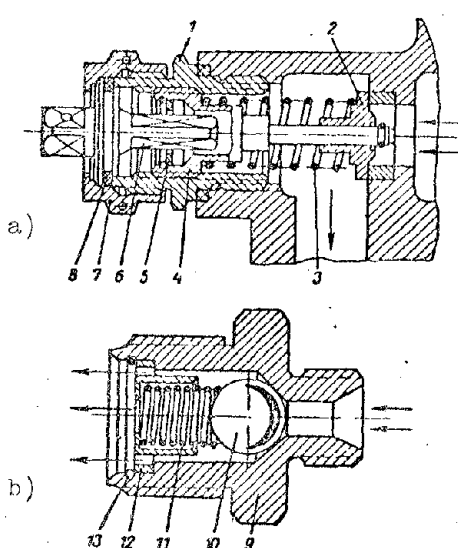


Fig. 14.9. Valves.

Check valve ensures oil passage only in one direction. It consists of housing 9, ball 10, and spring 11. Bushing 12 has a drilling for passage of oil. It is secured to housing with the help of spring ring 13. Oil, proceeding in the direction of the arrows, by its pressure opens the valve and passes freely through it. With ceasing of oil supply the valve is closed and the oil-line is disconnected.

Oil filters serve for purification of oil entering the engine from coke, metallic particles, dust, sand, and so forth. Their filtering element

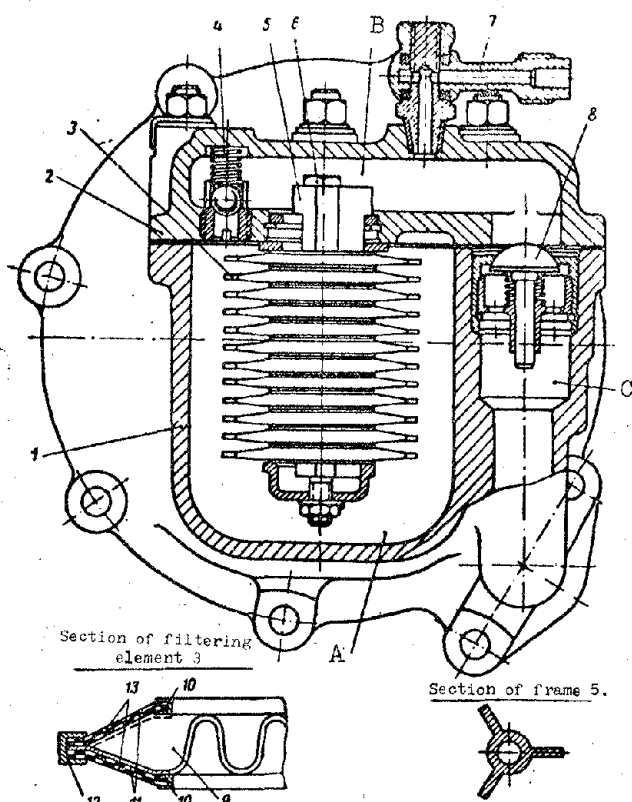


Fig. 14.10. Fine oil filter.

is most frequently a screen. Usually oil filters have a screen with number of sections from 400 to 5000 per  $1\text{ cm}^2$  of its surface. Figure 14.10 shows a fine oil filter. It consists of housing 1, cover 2, and 12 sections 3 of the filtering element, put on frame 5 and tightened by bolt 6. Each section consists of a corrugated diaphragm 9, two coarse frame screens 11, two fine screens 13, external 12 and internal 10 casings.

Oil through a connecting pipe (not shown in figure) enters cavity A, passes through filtering sections 3 and goes into cavity of pure oil B. Through check valve 8 and channel C the purified oil emerges from the filter. Filter has a safety bypass valve 4 of the ball type. In case of increase of resistance upon contamination of filter or upon thickening of oil (starting engine in the cold season) under the action of heightened pressure valve 4 is opened and

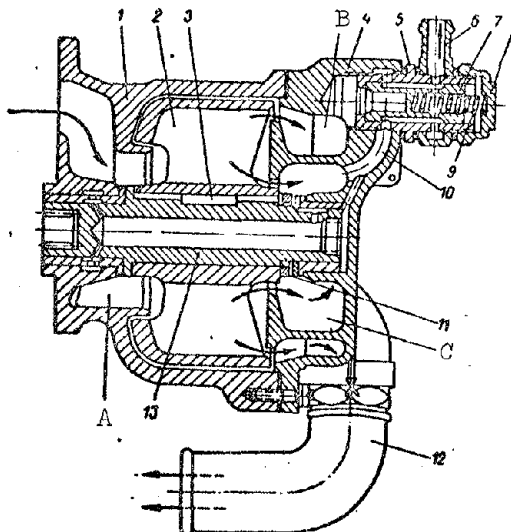


Fig. 14.11. Air separator.

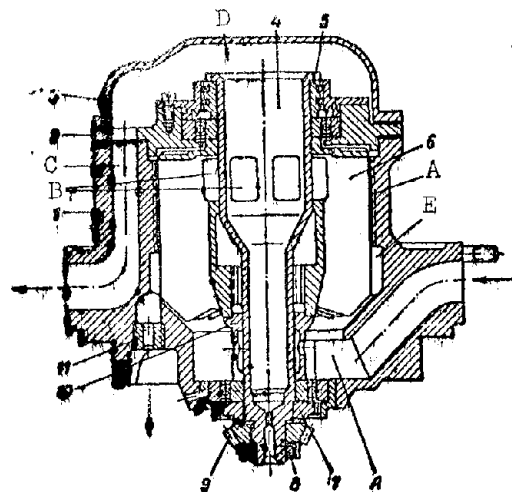


Fig. 14.12. Centrifugal breather, located the rotor. The rotor consists of drum 2, cast from magnesium alloy, and shaft 13.

Drum has radial blades. It is attached with its hub to the shaft by cotter 3 and is secured by nut 11. Rotor is lead in rotation with help of internal slits, carried out on shaft 13.

Scavenge pump feeds spent oil to annular cavity A of air separator and enters cavity of drum 2, where it is set into rotation. Under the action of centrifugal forces the oil, being heavier, is rejected to the periphery and passes into annular cavity B, from where through pipe 12 it is removed from the air separator. The air, being lighter, is driven to the center of the drum. It then passes into annular cavity C and through channel 10, bypass valve 7, and turning nipple 6 is removed from the air separator.

Bypass valve does not allow outlet of oil through air channels of air separator. It consists of a bronze housing 5, steel valve 7, and spiral spring 9. Turning nipple 6 is secured by cap 8 and is sealed by linings. Valve 7 has an external duct. Its end with the help of spring 9 is pressed housing 5. Air from channel 10 through drillings in housing 5 and duct in the valve passes into nipple 6. With increase of pressure of oil, valve 7 compresses spring 9 and covers air channel 10.

For lubrication of rotor bearings the oil from cavity A through drillings and ducts proceeds to left bearing bushing, and then through drillings in shaft moves to right bushing.

Centrifugal breather is a centrifuge and serves for separation of oil from air, leaving the breather cavities of the engine.

Figure 14.12 shows the centrifugal breather of the AI-20 engine, which consists of housing 1 and covers 2 and 3, cast from magnesium alloy. Inside them on ball bearings is located the rotor. The rotor consists of shaft 4, to which are attached: impeller 6, bushings 5, 7 and 10, ball bearings, and drive gear 9. All these components are secured to the shaft by nut 8.

Air saturated by oil enters annular cavity A and passes then to the impeller, where it is set into rotation. Under the action of centrifugal forces the oil is rejected to the periphery. On the wall of housing 1 there is a 10-setting left-handed square thread a, guiding the oil into annular groove E. From groove E the oil through jet 11 is drained into the engine housing. Air, purified from oil, through apertures B in impeller hub and shaft passes inside shaft 4 and into cavity D of cover 3. The air through channel C then is ejected into the atmosphere. Rotor bearings have seals, i.e., in the air of air cavity D in the form of two bronze sealing rings in the grooves of bushing 5, and in the area of drive gear 9 in the form of a labyrinth seal of bushing 7.

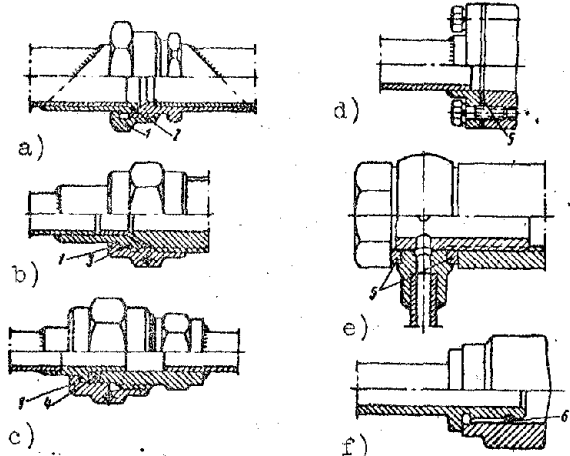


Fig. 14.13. Types of connections of pipelines.

(30 to 40) d, where d is the diameter of the pipes. For compensation of the difference of thermal expansions of the housings and pipes, the latter have bends and elbows.

Connections of pipelines must ensure airtightness. Some of them are shown in Fig. 14.13. Tightening of nipple connection a, b, and c is carried out by sleeve nut 1. and seals: a) on the spherical surface of nipple 2, b) by a special insert 3 made from soft metal, c) by rubber ring 4. Sealing of flanged joint d and turning bracket e is carried out by linings 5, and connections f) by rubber ring 6.

#### 14.4. Materials

For gears of oil pumps and drive shafts the following structural steels are used: [12KhN3A] (12XH3A), [12Kh2N4A] (12X2H4A), or [40KhNMA] (40XHMA). First two brands of steel are cemented. Housings of oil assemblies are usually cast from aluminum alloys [AL5] (Al5) and [AL4] (Al4) or from magnesium alloy [Mg5] (Mg5).

## C H A P T E R XV

### GTD FUEL SYSTEM AND ITS ASSEMBLIES

#### 15.1. General Information

The fuel system ensures supply to combustion chambers of well atomized fuel in the quantity necessary for normal engine operation. Since gas-turbine engines in the process of utilization operate in different modes and under different external conditions (altitude, speed of flight), supplying them with fuel requires constant regulation. Fuel feed is carried out by pumps, atomization by injectors, and metering of fuel to engine by regulators. [GTD] (ГТД) regulation is considered in Chapter XVI.

We distinguish main and priming GTD fuel systems. The first ensures constant engine operation, and second, its starting.

The main GTD fuel system consists of fuel tanks, fire cock, low pressure booster pumps and high pressure main pumps, filters, control system, throttling cock, working burners, control valve, shutoff valve, pipelines, and so forth.

Fuel tanks are included in the aircraft system and are connected to the engine fuel system through the fire cock. The fire cock also serves for cutoff of aircraft fuel tanks from engine system in the event of fire. This is how it got its name.

Booster fuel pumps under a pressure from 1.5 to 3 kg/cm<sup>2</sup> feed fuel to the main pumps. This ensures more favorable operating conditions the main pumps, i.e., their cavitation is removed. Booster pumps are usually installed on fuel tanks, and frequently a second booster pump is installed on the engine itself. Booster pumps can be revolving, centrifugal, or gear.

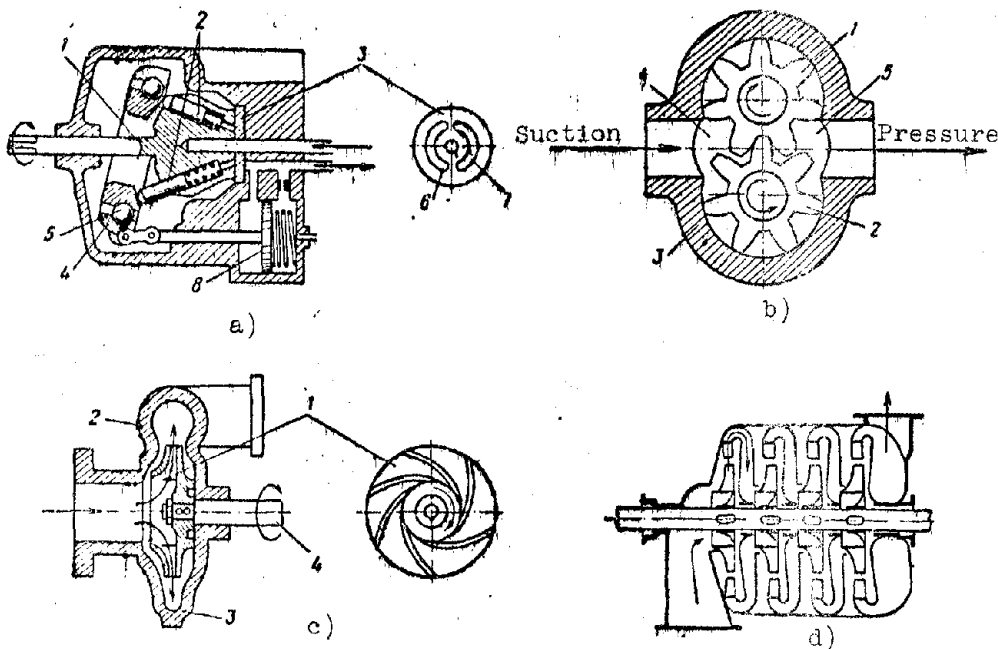


Fig. 15.1. Diagrams of fuel pumps.

Main fuel pump under a pressure from 60 to 80 kg/cm<sup>2</sup> and above feeds fuel to working burners. High pressure ensures good atomization of fuel by burners. For large fuel feed the engines frequently have two main fuel pumps operating with parallel connection.

Main fuel pumps usually applied are the plunger or gear types. For feeding of [TRD] (TPU) afterburners sometimes centrifugal pumps of high pressure are used. Figure 15.1 shows diagrams of a) plunger, b) gear, c and d) centrifugal fuel pumps.

The pumping unit of the plunger pump consists of rotor 1 with plunger 2, distribution valve 3, and slanted washer mounted on bearing 5 in casing 4. Plungers 2 are located uniformly along circumference in holes of rotor at a certain angle to its axis. With the help of springs attached in the holes under plungers 2, the latter are pressed to the slanted washer. Casing 4 with slanted washer is attached to pump housing on horizontal journals and its slant can be changed by moving the servo-piston 8 connected to it. The servo-piston is under action of a spring and the pressure of fuel in its working cavities. Movement of servo-piston is carried out as a result of the difference of fuel pressures in its working cavities, which is established by adjustment of fuel drainage from the right cavity where the spring is. Distribution valve 3 has two kidney-shaped ports, one of which, port 6, is connected to the suction channel, and port 7 with the pressure channel of the pump.

Upon rotation of the rotor, due to the slanted position of the washer, plungers 2 accomplish a reciprocating motion corresponding to the movement of suction and pressure. In the course of suction, into the cavity of the plungers through intake port 6 of distribution valve from the suction channel there proceeds fuel which then in the pressure course through pressure port 7 it is displaced in the pressure channel of the pump.

Delivery of the plunger pump depends on the speed and position of the slanted washer. With its position at an angle of  $90^{\circ}$  to the axis of the rotor the pump delivery is equal to zero. Maximum slant of washer corresponds to peak output of pump. During control of engine operation the pump delivery is changed automatically by change of position of the slanted washer.

Gear pump consists of a pair of spur gears 1 and 2 attached to housing 3. During their rotation the fuel in the area of suction cavity 4 fills the teeth cavity and is transferred to the pressure cavity 5. Delivery of the gear pump depends only on speed. Therefore, control of fuel feed to the engine with this pump is carried out by bypass of fuel to the suction side. This leads to expenditure of excess power for the pump and lowers its cavitation characteristics.

Centrifugal pump consists of rotor wheel 1 mounted on shaft 4 in housing 2. Blades of wheels turn opposite rotation. On outlet the pump has a collection chamber 3 which leads to the discharge nozzle. During rotation of wheel the fuel under the action of centrifugal force is rejected to the periphery and enters the collection chamber 3 from which it emerges through the discharge nozzle.

Centrifugal pumps can ensure very large flow rates of fuel with relatively small dimensions and weight. But since the pressure of their spent fuel varies in proportion to the speed squared, when the engine is idling the pressure of the fuel in front of the burners is low, which does not ensure normal feeding of engine.

High pressure in centrifugal pumps can be obtained by the application of several stages (diagram d) or high speeds of rotation. Thus, in pumps used for feeding afterburners the speed reaches 25,000 to 35,000 rpm. In this case they are driven from an air-driven turbine; for which the air is taken from the TRD compressor.

Plunger pumps frequently are united with regulators in unit, i.e., "automatic pump." In gear pumps the regulators are usually united in a separate unit, which is called the fuel-control unit.

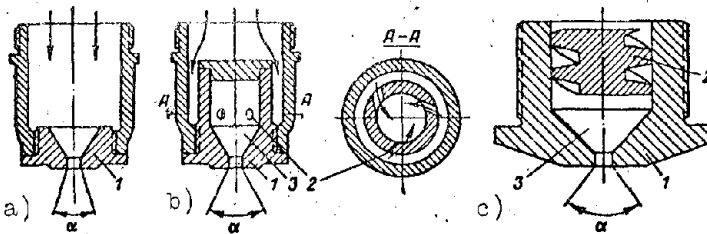


Fig. 15.2. Fuel burner with mechanical spraying.

Working burners spray the fuel to be fed to the combustion chamber. Stability and effectiveness of burning of fuel in a considerable degree depends on the quality of spraying, i.e., the size of the drops and uniformity of distribution in the zone of burning.

By method of spraying the fuel we distinguish burners with mechanical and with air spraying. Mechanical spraying occurs by means of the high pressure of fuel, under the action of which there is accomplished expiration and disintegration of the stream into small drops. During air spraying the burners received compressed air, under the action of which the fuel is sprayed. GTD have received predominant application of burners with mechanical spraying, since air spraying requires bulky air compressors of high pressure.

Burners with mechanical spraying are divided into jet and centrifugal (Fig. 15.2). The jet burner a consists of nozzle 1, through which there occurs expiration of fuel and its disintegration into small drops. In centrifugal burners b and c in front of the nozzle hole are swirl vane 2 and swirl chamber 3. In diagram b the swirl vane has three tangential holes. Passing through these holes, the fuel is twisted, and under the action of the centrifugal forces at the nozzle outlet the stream is broken up into small drops. Diagram c shows a screw swirl vane.

In GTD predominant application has been obtained by centrifugal burners. They ensure a larger angle  $\alpha$  of the sprayer and finer spraying than jet burners.

For guarantee of good fuel spraying when the GTD is idling they usually apply a system of two parallel connected burners, i.e., main and auxiliary (idle). The principle of their operation is shown in Fig. 15.3.

The main 1 and auxiliary 2 burners received fuel from a common fuel line 7 separately through two channels, i.e., main 3 and auxiliary 4. In idle conditions control valve 5 under the action of spring 6 covers channel 3 of the main burner, only auxiliary burner 2 will operate. Starting from the nominal engine rating the fuel pressure in main line 7 will increase so much that control valve 5 will open

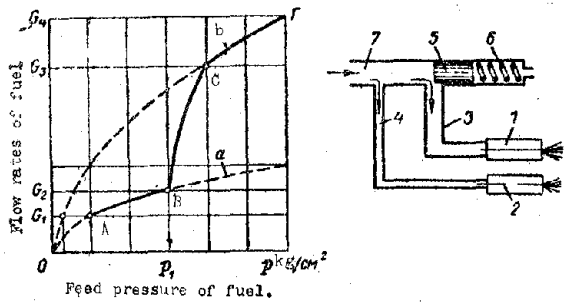


Fig. 15.3. Diagram of operation of two-channel burner.

the total flow rate of fuel through the auxiliary and main burner. Fuel feed to main burner occurs at pressures of fuel in main line 7 greater than  $p_1$ , when flow rate fuel is greater than  $G_2$ . At flow rates less than  $G_2$ , there operates one auxiliary burner, in the region of flow rates  $G_2-G_3$  there occurs connection of the main burner, and in region  $G_3-G_4$  both burners operate. From the curve of Figure 15.3 it is clear that in the region of small flow rates (less than  $G_2$ ) by turning off the main burner the pressure of the fuel in the auxiliary burner is increased, which ensures good fuel spraying.

The main and auxiliary burner are usually united by one housing. Such burners are called two channel (two-section, two-stage or two-cascade).

Throttle valve serves for manual control of fuel feed to working burners. With it the pilot controls engine operation, i.e., he changes its rating and adjusts the main automatic devices. Throttle valve is mounted on outlet line of main fuel pump. Frequently it is part of the pump itself of the fuel-control unit. A sample throttle valve is shown in Fig. 15.14.

Shutoff valve serves for turning off fuel feed to working burners, owing to which the engine stops. Shutoff valve is mounted behind the throttle valve and is usually part of the pump, control valve, or the fuel-control unit. A sample shutoff valve is shown in Fig. 15.15.

Filters serve for purification of fuel. They protect fuel apparatus from wear and obstruction. Filters are usually placed between the booster and main pumps.

Pipelines. Assemblies of the fuel system are connected by pipelines. There are pipelines of low and high pressure. The first form the fuel line from the fuel tank to the high pressure pumps and the second from the high pressure pumps to the working burners.

Starting fuel system and consists of low pressure pump having electric drive with supply from the power-supply network of the aircraft, and igniters which consist of a starting burner and electric plug. The last two will be considered in Chapter XVII.

### 15.2. Diagrams of GTD Fuel System

Diagram of fuel system of the [VK-1] (BK-1) engine (Fig. 15.4) consists of fuel tank 1 with centrifugal booster pump 2, fire cock 3, filter 4, two plunger pumps of high pressure 5, barostatic regulator 8, throttle valve 14, control valve 11 with shutoff valve 12, and two-channel working burners 10. Starting system consists of rotary starting pump 7 and igniters 9.

Fuel from tank 1 is fed by booster pump 2 through fire cock 3 and filter 4 through low pressure main line 16 to two pumps of high pressure 5, which operate in parallel. From pumps 5 fuel through high pressure main line 17 moves through throttle valve 14 and shutoff valve 12 to control valve 11, and then through main 22 and auxiliary 21 pipelines (collectors) proceeds to two-channel working burners 10.

Shutoff valve of the VK-1 engine is manufactured in one unit with control valve and is controlled by lever 13. During engine operation the shutoff valve

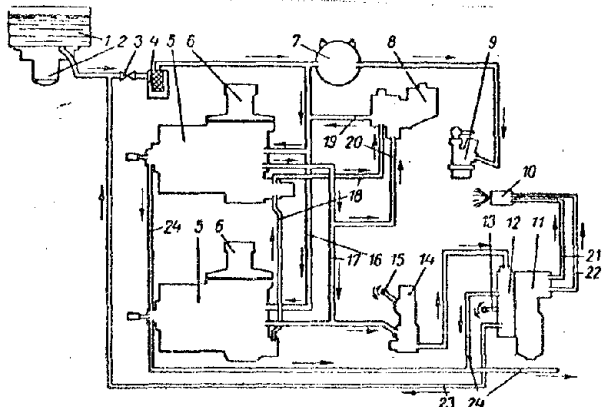


Fig. 15.4. Diagram of fuel system of the TRD VK-1. 1 - fuel tank, 2 - booster pump, 3 - fire cock, 4 - filter, 5 - high pressure pumps, 6 - speed governor, 7 - starting pump, 8 - barostatic regulator, 9 - igniter, 10 - working burners, 11 - control valve, 12 - shutoff valve, 13 and 15 - levers, 14 - throttle valve, 16 - low pressure line, 17 - high pressure line, 18 and 19 - tube of bypass of fuel from servomechanism, 20 - tube of feed of fuel to barostatic regulator, 22 and 21 - basic and auxiliary fuel collectors of burners, 23 - fuel bypass tube, 24 - drain tube.

is open and fuel has free access to control valve and working burners. When engine is off the shutoff valve closed and access of fuel to working burners is ceased. Simultaneously with this the shutoff valve connects high pressure main line 17 through pipeline 23 with low pressure main line 16, while the control valve and fuel collectors 22 and 21 are connected with drain 24, through which the fuel remaining in them is ejected into the atmosphere. Drain tube 24 also ejects fuel leaking through the stuffing boxes of drive shafts of pumps 5.

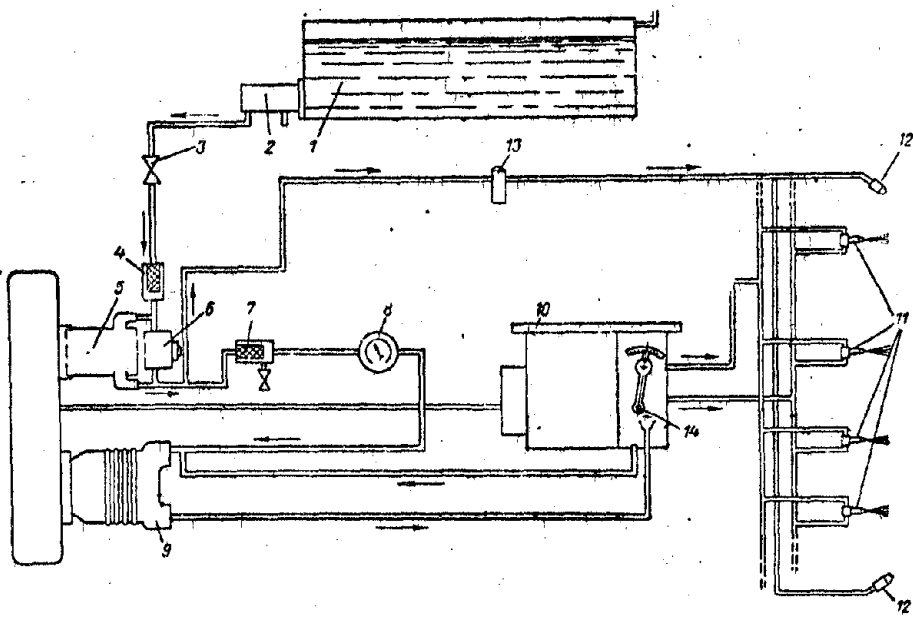


Fig. 15.5. Diagram of the fuel system of the TVD AI-20.

With lever 15 of throttle valve 14 the pilot changes fuel feed to burners 10 and establishes the engine rating. Barostatic regulator 8 automatically regulates delivery of pumps 5. It is connected by tube 20 with high pressure line 17, and through tubes 18 and 19 passes fuel from servomechanisms of pumps 5 to low pressure line 16. Each pump 5 also has maximum speed governors 6. Operation of the governors is described in Chapter XVI.

Igniters 9 consist of starting burner and electric plug. During starting of engine the starting pump 7, driven by an electric motor, feeds fuel to the starting burners, which with the help of the electric plug is ignited. The torch igniter ignites the fuel proceeding from the main working burners 10.

Diagram of the fuel system of TVD AI-20 (Fig. 15.5) consists of fuel tank 1 with centrifugal booster pump of low pressure 2, fire cock 3, coarse filter 4, revolving booster pump 5 with bypass reduction valve 6, fine filter 7, flow-control meter 8, high pressure gear pump 9, fuel-control unit 10, and working burners 11. Throttle valve 14, shutoff valve, and control valve are part of fuel-control unit. The last two are joined in a group of regulators, regulating fuel feed to engine.

From fuel tank 1 the booster pump 2 feed the fuel through a fine mesh filter 4 to low pressure fuel booster pump 5 mounted on engine. Under a pressure from 2.5 to 3 kg/cm<sup>2</sup> the fuel passes through the fine filter 7 and flow-control meter 8 to high pressure pump 9. The pump feeds the fuel under high pressure

to the fuel-control unit 10, regulating fuel feed to engine through two-channel burners depending upon conditions and engine rating. Excess quantity of fuel is then passed to the suction line of the main fuel pump. Starting burners 12 receive fuel during starting by booster pump 5 through electromagnetic valve 13.

### 15.3. Design of Fuel System Assemblies

Plunger pump. Figure 15.6 shows the plunger pump of the VK-1 engine. It consists of the pumping unit, servo-piston, and limiter (regulator) of maximum speed. The pump housing, cast from aluminum alloy, has channels of suction 5 and pressure 6. At the pump inlet there is a mesh filter 2.

Rotor 1 of the pump revolves on two bearings: one of them is a roller 15, and the other is copper-graphite 3. Rotation is transmitted to rotor from the engine through shaft-spring 16 having in the housing cover a cup packing 17. In the rotor at an angle of  $15^{\circ}$  to its axis uniformly along the circumference there are seven holes (cylinders), which contain plunger 12 with springs 19. Odd number of cylinders of the pump ensures more uniform fuel feed. For decrease of wear the rotor is made from antifriction bronze, and the plungers from steel. The plungers are nitrated. High pressure of fuel at the pump outlet is ensured by small clearances between plungers and cylinders, which are equal to 0.015 to 0.025 mm.

Between plungers of rotor there are drilled seven channels 18 connecting suction channel 5 with cavity E of the pumping unit through the central hole of distribution valve 4. During rotation of the rotor the fuel in channels 18 is under the action of centrifugal forces and therefore in cavity E of the pumping unit there is established heightened pressure. By its end rotor 1 is pressed to distribution valve 4 by depressing spring 19 and by heightened pressure in the cavity of the pumping unit. For decrease of wear and improvement of running in, the face of the rotor is coated with a layer of indium.

Steel distribution valve 4 has two kidney-shaped ports a and b. One port is connection with the suction channel 5, and the other with the pressure channel 6.

Slanted washer 13 is placed in casing 14 on roller and thrust ball bearings. Casing in turn is placed in the housing on two pins 11. In holes under pins in casing there are pressed bronze bearing bushings. Maximum angle of inclination of washer is limited by stop 20.

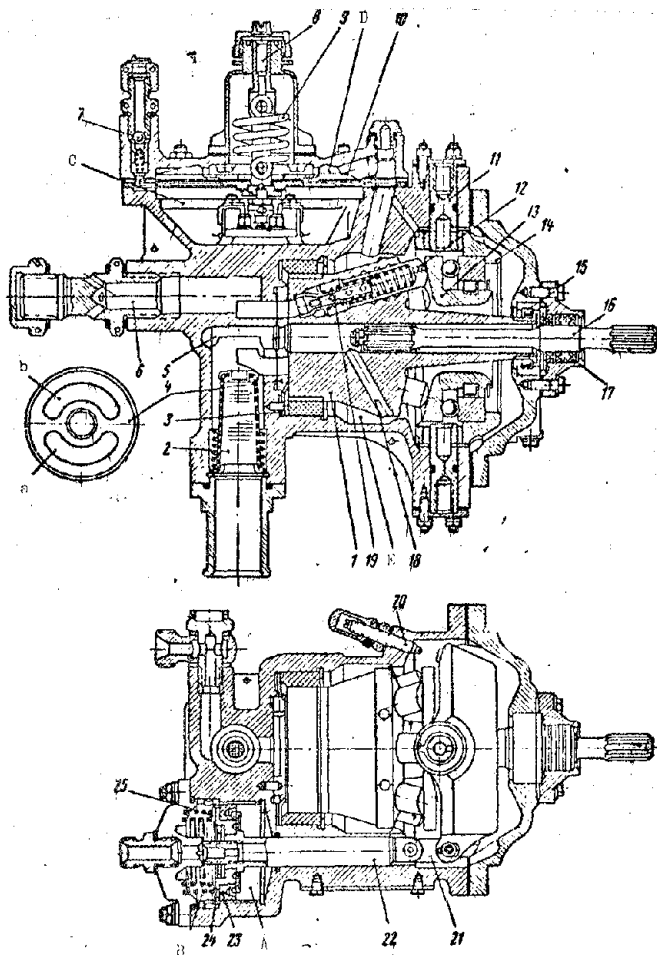


Fig. 15.6. Plunger pump of the TRD VK-1.  
1 - rotor, 2 - coarse net filter, 3 and 15 - rotor bearings, 4 - valve, 5 and 6 - suction and pressure channels, 7 - ball valve, 8 - adjustment screw, 9 - spring, 10 - diaphragm, 11 - pins, 12 - plunger, 13 - slanted washer, 14 - casing, 16 - spring shaft, 17 - cup packing, 18 - channels, 19 - spring, 20 - stop, 21 - link, 22 - rod, 23 - cup, 24 - servo-piston, 25 - spring, A and B) cavities for servo-piston, C, D and E) cavities for speed governor and pump. a and b) suction and pressure ports for valve.

the pump. In the area of chamber D is the diaphragm is loaded by spring 9, operated by extension. Tension of spring is regulated by screw 8. In chamber C there is a bypass valve. Using this valve, the diaphragm controls bypass of fuel from cavity B of the servo-piston. Description of the work of the maximum speed governor is given in Chapter XVI. Ball valve 7 serves for removal of air from chambers of pump during their filling with fuel. It is opened by depressing the ball through the sleeve hole.

For determination of delivery of the plunger pump Fig. 15.7 depicts its diagram.

Servo-piston 24 is mounted on rod 22, which by its other end with the help of link 21 is hinged to casing 14. Sealing of the servo-piston is carried out by a rubber cup 23, and the rod by a rubber ring. In cavity B of the servo-piston there are two springs 25 which release it in the position of peak output of pump. Operation of plunger pump was described above. Movement of servo-pump controls the barostatic regulator and maximum speed governor. Barostatic regulator is made in the form of a separate unit. It is described in Chapter XVI.

Maximum speed governor of diaphragm type is attached directly in pump. Diaphragm 10 is made from fiberglass laminate is attached to the housing by a cover. The upper chamber of diaphragm D is connected to cavity E of the pumping unit, where heightened pressure has been established, and lower chamber C is connected to the suction channel of

Lines  $M_0M_0$  and MN represent the slanted washer in its two positions, i.e., neutral (at zero delivery) and operating. Point  $O_1$  is the center of turn of the slanted washer and is determined by angle  $\alpha = 90^\circ$ . Operating position of slanted washer is determined by angle of inclination  $\gamma$ . Axes of plungers are uniformly distributed along the circumference at angle  $\beta$  to axis of rotor. Points M and N characterize extreme positions of plunger during its movement. Full movement of plunger is equal to:

$$s = MM_0 + NN_0 = 2l \sin \beta \cdot \operatorname{tg} \gamma. \quad (15.1)$$

where  $MM_0 = NN_0 = l \sin \beta \cdot \operatorname{tg} \gamma$ .

Pump delivery will be equal to:

$$W = \frac{\pi d^2}{4} s z n \eta \cdot 10^{-6} \text{ l/min.} \quad (15.2)$$

where d and s is the diameter and movement of plunger, mm;

z is the number of plungers;

n is the speed, rpm;

$\eta = 0.94$  to  $0.96$  is the supply factor.

Example. Determine the delivery of a plunger pump.

Given:  $l = 115.5$  mm;  $\beta = 15^\circ$ ;  $d = 13$  mm;  $z = 7$ ;  $n = 2850$  rpm;  $\eta = 0.94$

Full stroke of plunger by formula (15.1) is equal to:

$$s = 2 \cdot 115.5 \cdot \sin 15^\circ \cdot \operatorname{tg} 15^\circ = 16 \text{ mm.}$$

Pump delivery by formula (15.2) is equal to:

$$W = \frac{3.14 \cdot 13^2}{4} \cdot 16 \cdot 7 \cdot 2850 \cdot 0.94 \cdot 10^{-6} = 40 \text{ l/min.}$$

Gear pumps are distinguished by simplicity of design and small dimensions.

These pumps are of high and low pressure.

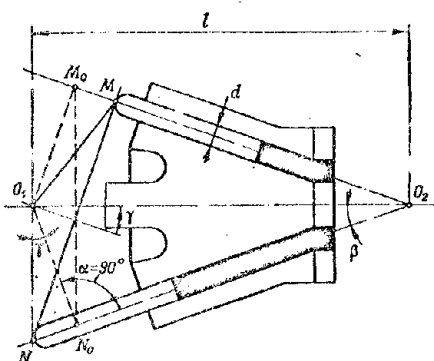


Fig. 15.7. Calculation of delivery of a plunger pump.

In distinction from the oil pumps considered in Chapter XIV, the contact parts of fuel gear pumps operate in less favorable conditions, since they are not lubricated by oil. Their working surfaces are moistened by fuel. Gears of fuel pumps for decrease of their wear are usually made from nitrated steels with hardness of working surfaces HRC 62 to 64. For this purpose the gears of the pumps are mounted on antifriction bearings — roller or needle.

Leakage of fuel from pressure side to suction side through clearances between gear and housing lowers pump delivery. Since viscosity of fuel is lower than viscosity of oil, the fuel pumps are more sensitive to the magnitude of clearances than oil pumps. An especially large value is obtained by these clearances in high pressure fuel pumps which operate at a pressure from 60 to 80 kg/cm<sup>2</sup> and above. Delivery of gear fuel pumps is determined by formula 14.1.

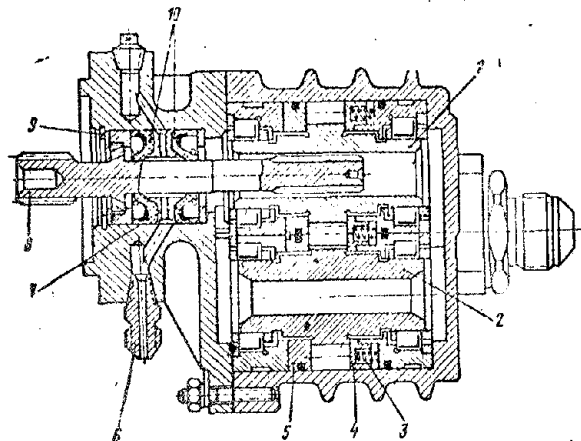


Fig. 15.8. Gear fuel pump E348I.

Figure 15.8 shows a high pressure fuel pump of the gear type [348I] (348N) in the TVD AI-20.

The pumping unit of the pump consists of driving 1 and driven 2 spur gears attached to the housing on roller bearings. On their faces the gears have bronze step bearings 4 and 5. Step bearings 4 are the floating type, i.e., with free setting in housing. With the help of

springs 3, and also fuel pressure in the area of the bearings, step bearings 4 are pressed to the face surfaces of the gears and their face clearance is selected.

Drive of pump is carried out from the spring shaft 8 which through slits is connected to pinion gear 1. The spring is fixed by its flange by spring ring 9 from axial shift in the pump housing. Spring has sealing in the form of two rubber cups 10 pressed in the pump housing. Front cup prevents penetrating of oil into pump in the area of the drive, and rear cup prevents penetration of fuel into drive from the pump. Between distance bushing 7 and spring 8 there is a small annular cavity, from which the oil and fuel seeping through cup packings 10 are drained through scavange port 6.

Rotary pumps are usually in the form of booster pumps of low pressure. Figure 15.9 shows the rotary booster pump 707I in the TVD AI-20. Its pumping unit consists of rotor 10 eccentrically located in bucket 14. In slots of rotor there are four plates 15 which rest on one side in floating pin 11, and on the other - on the internal surface of bucket 14. All components of pumping unit are made of steel and are nitrated for decrease of their wear. The rotor by its journals rests on bearing bushings 9 and 12 made from stannous-lead bronze. The bushings close bucket 14 from the faces and are secured together with it in the housing.

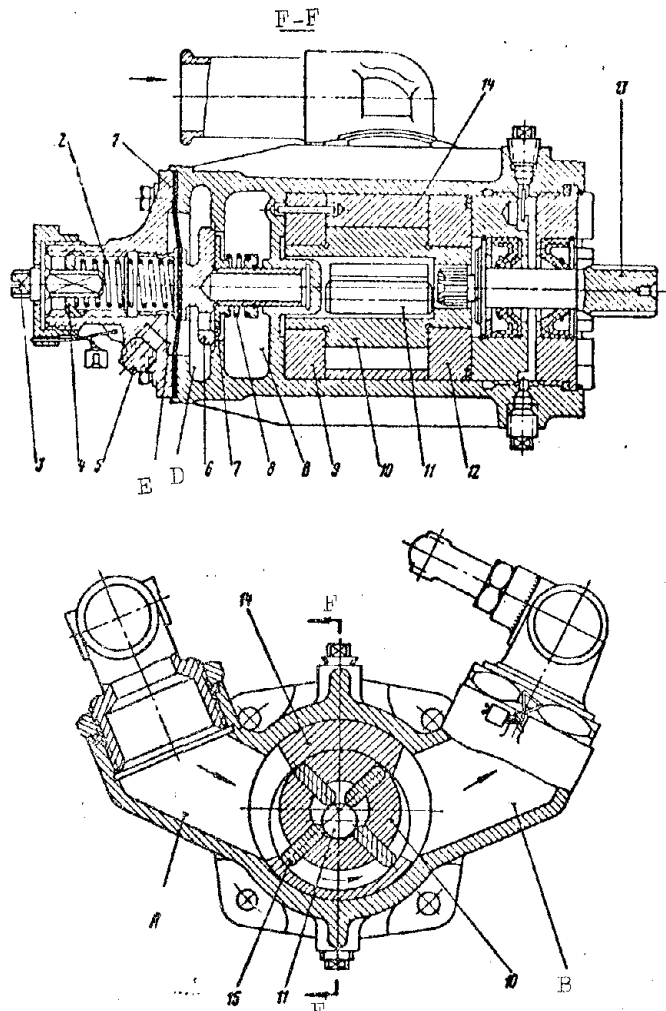


Fig. 15.9. Rotary fuel pump 707I.

C and D. Without diaphragm 1 the valve would maintain this difference of pressures by constant bypass of excess fuel to the suction side of the pump. With decrease of pressure for suction (for instance, with decrease of fuel level in tanks) there would also decrease pressure of fuel at pump outlet. Diaphragm 1 removes this deficiency. Cavity E in front of the diaphragm through jet 5 is connected with the atmosphere and the diaphragm is under the action of the difference of pressure in the suction side of the pump and the atmospheric side. With decrease of pressure for suction the diaphragm creates additional pressure on reduction valve and, covering it, maintains constant pressure of fuel at pump outlet.

The reduction valve unit includes filling valve 7 which freely sits on the shank of reduction valve 6 and with the help of spring 8 covers the holes, on the head of the reduction valve. Filling valve 7 serves for filling the system

Rotor is driven from splined shaft 13. Shaft has a stuffing box similar to the gear pump 348I. During rotation of rotor the plates 15 take fuel from suction cavity A and transfer it to pressure cavity B.

Pump ensures fuel feed under constant pressure of  $2.5 \text{ kg/cm}^2$  which it maintains by reduction valve 6. Reduction valve is pressed to its seat by spring 2 and by the force in the area of diaphragm 1. The diaphragm is made from rubberized lined and is pressed between the housing and cover of the pump. The reduction valve is regulated with the help of collar 3 and nut 4.

Cavity C of the valve is connected to the pressure side, and cavity D with the suction side of the pump. Reduction valve 6 is under the action of the pressure difference in cavities

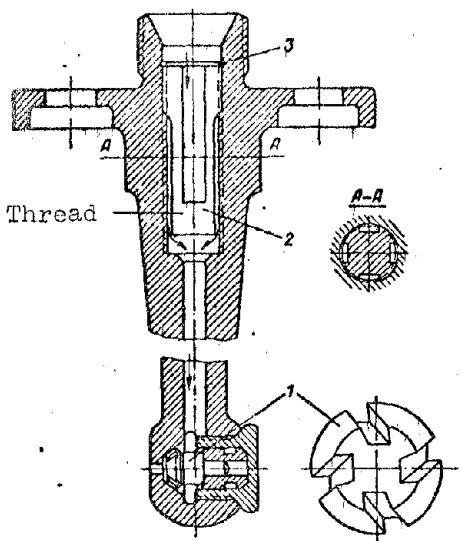


Fig. 15.10. Single-channel burner RD-10.

fuel emerges from the filter. Filtration of fuel occurs by its passage through clearances in the thread between slots. Filter is locked by stopper ring 3. Burner is attached by flange to housing of combustion chamber.

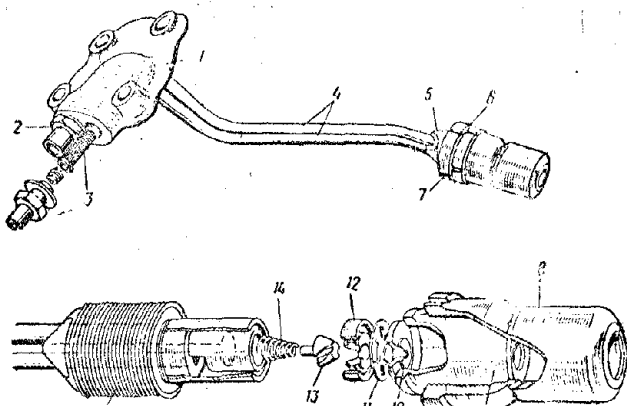


Fig. 15.11. Two-channel burner.

main and auxiliary — each of which is own pipe 4. In the channels of the flange there are filters 3 which with the help of spring are tightened by inlet sleeves

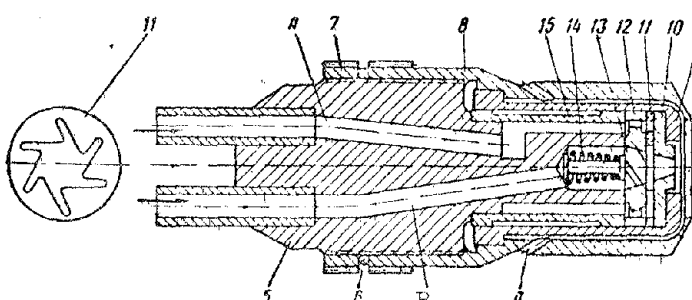


Fig. 15.12. Atomizing device of burner.

with fuel before starting the engine. Fuel moves to the suction side of the pump (into cavity D) and, releasing valve 7, passes into cavity C and further into the fuel line of the engine.

Burners. Figure 15.10 shows a single-channel centrifugal burner having a conical atomizer 1 with four helical slots. Burner housing is steel. Its inlet has a slot filter 2 which is a threaded rod with four longitudinal slots. Two slots emerge on the upper face of the rod and into them proceeds the fuel. The other two slots are on the lower face of the rod and through them the

GTD have received wide application of two-channel centrifugal burners, the principle of operation of which was described above. Figures 15.11 and 15.12 show a two-channel centrifugal burner, whose flange 1 and housing 5 are united by two pipes 4, soldered on the ends. Flange serves for mounting the burner on the combustion chamber housing and has two inlet channels 2 —

screwed into the flange on a thread.

Housing 5 (see Fig. 15.12) also has two-channels — main A and auxiliary B — which receive fuel through pipes 4. The housing has a bushing 15, and with the help of contained 9 and shroud 8

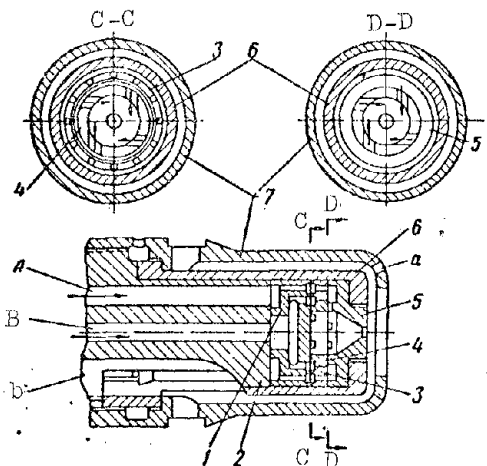


Fig. 15.13. Atomizing device of the burner of the TVD AI-20.

on it there are attached the atomizing components of the burner. The latter consist of a screw-on conical swirl plug 13 with spring 14, socket 12 of swirl plug, tangential swirl plate 11, and nozzle 10. The shroud is turned on the thread of housing 5 and locked by locknut 7 and tab washer 6. Faces of atomizing components are manufactured with high surface purity for prevention of fuel leakage.

Fuel passed through auxiliary channel B is twisted by conical swirl plug 13 and passes through nozzle 10. Fuel passed through main channel A passes through the annular channel between bushing 15 and housing 5 and through drillings in socket 12 of swirl plug proceeds to tangential swirl plate 11. The plate twists the fuel in the swirl chamber and passes it through nozzle 10.

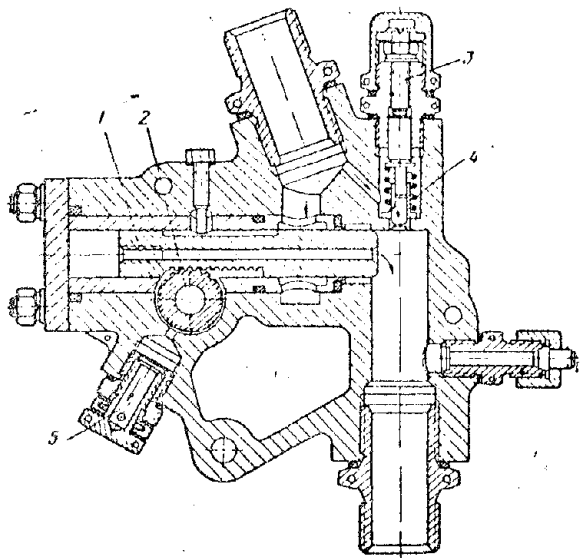


Fig. 15.14. Throttle valve of the VK-1 engine.

Swirl plate 11 and plug 13 twist the fuel in one direction. During joint operation of both systems the fuel upon entering nozzle 10 is mixed, and when leaving it forms a spray burner in the form of a hollow cone.

For cooling of burner and preventing of scale formation on its outlet end the shroud 8 around its circumference has drillings a. Through them the air passes into the radial clearance between the shroud and container 9, cools them and at outlet heads to the face of the burner.

Figure 15.13 shows the atomizing device of the two-channel centrifugal burner of the AI-20 engine, which consists of adapter 1, swirl plate 4 of the auxiliary system with pressed ring 3 and nozzle 5 which holds the swirl plate of the main system. All these components are contained in barrel 6 and are secured with the help of shroud 7 to burner housing 2. Swirl plates of main and auxiliary systems are carried out in the form of four tangential grooves. Swirl chambers in them

are formed by borings of swirl plate 4 and nozzle 5.

From auxiliary channel B the fuel moves to the central cavity of adapter 1 and through its drilling goes into the annular boring of swirl plate 4. From here the fuel passes with great speed through the four tangential grooves in the swirl chamber, where it is twisted and then passes through nozzle 5.

From main channel A the fuel moves into the annular boring of the adapter 1 and passes through holes in it and in ring 3 into the annular boring of nozzle 5. From here the fuel through four tangential grooves enters the swirl chamber, where it is twisted and passes through nozzle 5. Direction of twisting of both swirl plates is identical. With the main system on the flows are mixed in the nozzle chamber. At the nozzle outlet there will form a hollow cone of finely-atomized fuel.

For cooling of the burner and preventing of scale formation on its output end the housing 2 and container 6 have three channels b (millings). Air passes through these channels into the radial clearance between container 6 and shroud 7 and emerges to the face of nozzle 5, and through drillings a on the face of shroud 7.

Throttle valve. Figure 15.14 shows the throttle valve of the VK-1 engine. Metering needle 1 with profiled end moves through a sleeve. With the help of a rack gear clutch the needle is connected to the control shaft 2 that has a manual control lever attached to it. By turning the lever the needle 1 moves, which changes the passage section for the fuel.

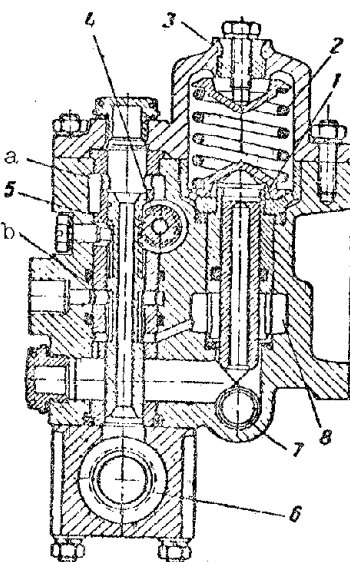


Fig. 15.15. Fuel distributor of the TRD VK-1.

Idling valve 4 ensures fuel feed to burners while engine is idling, when throttle valve is covered. Valve 4 is pressed to regulating screw 3 by a spring, and with its cylindrical end is placed in a socket having a longitudinal slot. Regulating screw 3 regulates flow rate of fuel through idling valve 4 by change of the passage section. Sleeve 5 serves for drain of seeping fuel to the line of suction.

Distribution valve and shutoff cock. The distribution valve is placed by the two-channel burners. Figure 15.15 shows the distribution valve of the VK-1 engine, manufactured jointly with the shutoff cock.

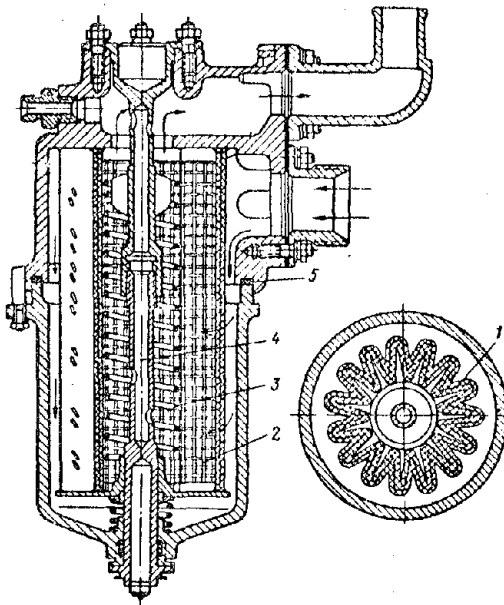


Fig. 15.16. Fuel filter of the TRD VK-1.

Distributor consists of needle 1, moving in the sleeve, and spring 2 with regulating screw 3. The housing has two channels — auxiliary 7 and main 8. The auxiliary channel receives fuel during operation of engine without hindrance, and the main channel is covered by needle 1. Spring of needle is regulated by connection of main channel at fuel pressure of about  $10 \text{ kg/cm}^2$ . Needle 1 is released and opens passage to fuel in main channel.

Shutoff cock turns off fuel feed to working burners when engine stops. It consists of valve 5, which moves in sleeve.

With the help of a rack gear clutch the valve is united with control shaft 4, which has a lever of manual control attached to it. By turning the lever the shutoff cock opens or closes.

The valve is hollow, and in the upper part of its sleeve there are holes a. With closed shutoff cock, through these holes the fuel pressure line 6 of the pumps is connected with the suction line. In the middle of the valve there is an annular boring which connects through hole b the fuel lines of the burners with the system of drainage in closed position of the shutoff cock. Figure 15.15 shows the shutoff cock in closed position.

Fuel filters serve for purification of fuel from external impurities, dust, sand, metal filings, shavings, and so forth. Filters create some resistance for passage of fuel; therefore, in fuel systems they are usually placed behind the booster pump in front of the main fuel pump inlet. Filters are easily detachable for periodic inspection and washing. Their filtering element is usually a screen (mesh filters) or felt (felt filters).

Figure 15.16 shows the fuel filter of the VK-1 engine with filtering element 1 made from felt. For increase of surface the filtering element has longitudinal corrugations. Frame 2 is made from a large screen. Internally, the frame by its corrugations rests on spiral spring 3. Filter housing consists of two parts united with the help of bolt 4. Sealing around the joint is ensured by rubber ring 5.

Fuel manifolds can be rigid and flexible. The first type are made from steel pipes, and the second - from reinforced rubber hoses. The latter are convenient during assembly and permit considerable misalignments and displacements. Moreover they are insensitive to vibrations. The deficiency of hoses is their large weight and large diameter. At heightened temperatures they are less stable than steel pipes. Types of manifold connections are shown in Fig. 14.13.

#### 15.4. Materials

Materials for the housings of fuel pumps, filters, and so forth are usually aluminum foundry alloys of brands [AL5] (АЛ5) and [AL9] (АЛ9).

Rotor of plunger pumps is manufactured from bronze [BrAZhN-10-4-4] (БрАЗН-10-4-4), plungers from steel [12KhNZA] (12ХНЗА) or [KhVG] (ХВГ), slanted washer from steel [ShKh15] (ШХ15), and diaphragm of maximum speed governor from fiberglass laminate.

Gears of pumps are made from cemented steels 12KhNZA or from nitrated steels [38KhMYuA] (38ХМЮА). Housings of fuel burner are manufactured from steel [40KhNMA] (40ХНМА), swirl plate and nozzle from steel KhVG or [Kh12] (Х12), and shroud from steel [EI69] (ЭИ69).

## C H A P T E R XVI

### GTD CONTROL

#### 16.1. General Information

[GTD] (ГТД) operate at maximum, nominal, and cruise ratings, and idling. The ratings are characterized by thrust (for [TRD] (ТРД)) or power (for [TVD] (ТВД)) and specific flow rate of fuel. When idling the engine should run stably at minimum thrust (or power).

Aircraft engines work under variable external conditions (altitude of flight) and therefore their ratings in flight can be arbitrarily changed. For maintaining the rating constant or for varying it by specified law it is necessary to continuously control the work of the engine and in good time regulate its parameters. These functions for GTD are usually carried out by automatic regulators. Engine control, i.e., transfer from one rating to another, is carried out by the pilot.

GTD rating is determined by many interconnected parameters. Basic parameters are those, the change of which the most effectively affects the change of the engine rating. Such parameters in GTD are speed  $n$  and temperature of gases in front of turbine  $T_3$ .

Figures 16.1 and 16.2 show the TRD characteristic, i.e., the dependence of thrust  $P$  and specific flow rate of fuel  $C_{уд}$  on speed  $n$  and on temperature of gases in front of turbine  $T_3$ .

Elements control system. In control systems we distinguish the control object, the controlling member, and the automatic regulator.

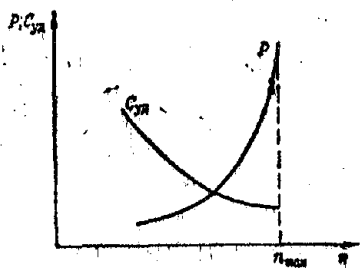


Fig. 16.1. Dependence of thrust and specific flow rate of fuel of a TRD on speed.

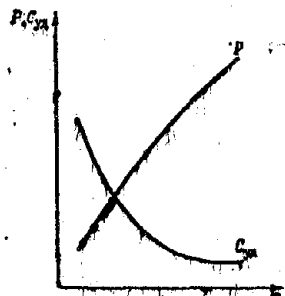


Fig. 16.2. Dependence of thrust and specific flow rate of fuel of a TRD on temperature of gases in front of turbine.

Control can be carried out by means of change of flow rate fuel (in TRD and TVD), area of passage section of exhaust nozzle (in TRD) and propeller pitch (in TVD). In accordance with this, for GTD the control objects can be the fuel pumps, exhaust nozzle, and propellers.

The controlling member controls the control object. The control member of a plunger fuel pump is usually the swash plate 4 (see Fig. 15.1a), and in the gear pump it is the bypass bullet (valve) 2 (see Fig. 16.10). They vary fuel feed to the engine.

The controlling member of the exhaust nozzle may be the central mobile body (bullet) 2 (see Fig. 1.3) or folding doors 2 (see Fig. 1.4). They change the area of the outlet section of the exhaust nozzle and the pressure drop, which is actuated in the engine turbine.

The control unit of the propeller are its blades. With turn of blades in the hub with respect to their axes the propeller pitch and moment of its resistance to rotation change (Fig. 11.22).

Regulators have a sensitive meter element (transducer), which continuously measures the value of the control parameter and in accordance with this, either directly, or through an intermediate servo-mechanism, controls the position of the control unit.

Classification of regulators. Depending upon control parameter we distinguish speed regulators, gas, temperature regulators, pressure regulators, and fuel regulators. The sensory elements (meters) speed regulators are tachometers, gas temperature regulators — thermometers, pressure regulators — manometers, and so forth.

According to the character of work, regulators can be continuous and intermittent. For regulators of the first group with continuous change of the control parameter, the control unit is also reset continuously. These regulators usually carry out the main GTD regulation. For regulators of the second group, with continuous change of the control parameter, the control unit is intermittently reset. They include governors (for instance, engine speed governors), which are frequently installed in GTD control systems in addition to the main regulators. The control unit governors is reset only upon achievement by the control parameters of maximum values. This ensures reliability of engine operation.

Regulators are distinguished by direct and indirect action. In regulators of direct action the sensory element is directly connected to the control unit and the latter moves in the process of regulation by means of the energy of the sensory element itself.

Regulators of indirect action have a special servo-mechanism which obtains signals from the sensory element and then resets the control unit from the external source of energy. Usually the servo-mechanism serves as the slave mechanism.

Direct and indirect control. Control of GTD parameters can be accomplished directly and indirectly.

In the case of direct control the sensory element of the regulator measures the value of the control parameter, and in accordance with this resets the control unit. In control the sensory element of the regulator does not measure the parameter which they wish to regulate, but another one connected with it. In accordance with this, measurement is produced and the control unit is reset. Direct control in comparison with indirect ensures greater accuracy of control.

Speed control of GTD is carried out most frequently by direct means, i.e., by speed regulators. In some TRD speed regulation is accomplished by indirect means, i.e., by a fuel flowmeter. Direct control of gas temperature in front of the turbine entails considerable difficulties owing to the high values of temperatures. It is difficult to make a regulator low-inertial and reliable in work. There appear also difficulties from nonuniformity and instability of the temperature field of gases in front of the turbine. At the same time the temperature of gases in front of the turbine is connected with other parameters of engine operation, with which there is usually carried out its indirect control. These parameters include total pressure and temperature of air at compressor inlet, engine speed, and so forth.

Control of basic TRD parameters is carried out by change of flow rate of fuel and area of passage section of exhaust nozzle. With increase of fuel feed to engine there is an increase in the temperature of gases in front of the turbine and the head used in the turbine. Torque on the turbine shaft and engine speed also increase. With decrease of fuel feed the temperature of gases in front of the turbine and the engine speed decrease.

With increase of passage section of exhaust nozzle the pressure drop in the turbine increases, which leads to an increase of torque on its shaft and the engine speed. With decrease of passage section of nozzle the pressure drop in the turbine and the engine speed decrease.

In TRD with variable exhaust nozzle (see Fig. 1.3) speed control and control of temperature of gases in front of the turbine can be executed separately: the change of flow rate of fuel regulates the speed, and change of passage section of exhaust nozzle regulates the temperature of working gases in front of the turbine.

Regulation of temperature of gases in front of the turbine can be carried out by indirect means, for instance, according to total pressure of air at compressor inlet, which is measured by the sensory element of the regulator.

In accordance with this, measurement is carried out by resetting the control unit of the exhaust nozzle (for instance, the central body, i.e., bullet 2, in Fig. 1.3), whereupon the pressure drop in the turbine changes, which leads in turn to change of torque and, consequently, change of engine speed. Then the speed control unit enters operation, which, trying to maintain constant speed, changes in the appropriate way the fuel feed to the combustion chambers of the engine. This accomplishes regulation of temperature of working gases in front of the turbine at constant speed.

Regulation by change of passage section of exhaust nozzle is usually not very effective and therefore the majority of TRD, not having afterburners, are constructed with fixed exhaust nozzles. The change of flow rate of fuel regulates the engine speed. And since temperature of gases in front of turbine depends on flow rate of fuel, it in this case is also connected with the speed.

For TRD with afterburner located behind the turbine (see Fig. 1.4), there is the problem of ensuring burning of fuel afterburner with preservation of constant speed and temperature of gases in front of the turbine. This becomes possible only in case of application of a variable exhaust nozzle, whose passage section is increased during work under forced conditions. As the control unit of

the exhaust nozzle there can be applied folding doors 2 (see Fig. 1.4).

Control of basic TVD parameters is carried out by change of propeller pitch and flow rate of fuel. With increase of propeller pitch the moment of resistance to its rotation is increased, which leads to decrease of engine speed. Conversely, with decrease of propeller pitch the moment of resistance decreases, and engine speed increases.

With increase of fuel feed to engine the temperature of gases in front of the turbine, torque, and engine speed are increased. With decrease of fuel feed the temperature of gases in front of the turbine, torque, and speed decrease.

On single-shaft TVD (see Fig. 1.10) speed control is usually carried out by change of propeller pitch, and control of torque (temperature of gases in front of turbine) by change of flow rate of fuel. Thus it is possible to carry out separate control of speed and torque (temperature of gases in front of turbine).

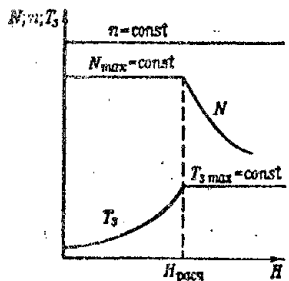


Fig. 16.3. Altitude curve of a TVD.

Figure 16.3 gives the altitude curve of a TVD, whose power from ground to rated altitude is kept constant, and then drops. TVD with such an altitude curve are called high-altitude turboprop engines. They are controlled separately according to speed and temperature of gases in front of turbine.

By change of propeller pitch the engine speed  $n$  at all altitudes is maintained constant. At the same time by changing the flow rate of fuel the temperature of working gases in front of the turbine  $T_3$  increases ground to rated altitude in such a manner that with decrease of mass flow rate of air through engine maintains constant torque, and consequently also constant engine power. At rated altitude the temperature  $T_3$  reaches its maximum permissible value and at higher altitudes maintains it constant. Torque, and consequently also power at altitudes higher than rated, drop.

## 16.2. Speed Control Units

Depending upon kind of connection between the sensor element of the regulator and the regulating unit we distinguish static (direct and indirect action), astatic, and isodromic. These types of regulators are considered below in the example of speed control units.

Static control unit of direct action. Figure 16.4 depicts the diagram of a static speed control unit of direct action. The sensor element of the regulator is a centrifugal tachometer, consisting of weights 1 and spring 2. Weights

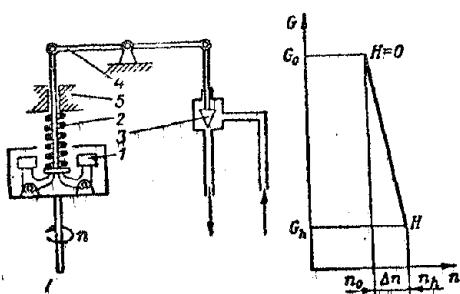


Fig. 16.4. Static control unit of direct action.

obtain rotation from engine with speed  $n$ , and appearing during rotation the centrifugal forces of the weights are balanced by the elasticity of the spring. Thus each speed corresponds to its position of the weights,

The regulating element is fuel bullet 3. Fuel moves from pump to bullet, and then to engine in the direction shown by the arrow. Upon movement of bullet 3 the fuel feed to the engine will be changed. Non-holonomic constraint between weights 1 and fuel bullet 3 is executed by rigid lever 4, which transfers the fuel bullet by the energy of weights 1 and spring 2.

Under steady (equilibrium) conditions, when engine load is kept constant, the control unit weights maintain the fuel bullet in constant position, preserving constant the flow rate of fuel, and consequently also the engine speed.

With change of conditions of flight (altitude and speed of flight) load of engine will change and in the absence of regulator its rating would change. The speed control unit will try to maintain the engine rating constant. If, for instance, the engine speed begins to increase, under action of increasing centrifugal force the weights 1 of the regulator, surmounting the elasticity of spring 2, will part and through lever 4 will transfer bullet 3 to decrease of fuel feed. If, however, the engine speed begins to decrease, the centrifugal force weights 1 will also decrease. Then spring 2, surmounting the resistance of weights, through lever 4 will transfer the fuel bullet 3 to increase of fuel feed.

Thus, decreasing or increasing fuel feed, the regulator try to restore the disturbed engine speed and maintains it on a constant level.

Static control unit of direct action does not ensure exact control. Furthermore, it possesses lowered sensitivity to change of the control parameter.

Inaccuracy of control, peculiar to the static regulator, is explained by the presence of a rigid non-holonomic constraint (lever 4) of the regulating member with the sensor element, at which each position of the regulating member (bullet 3) corresponds to its value of the control parameter (speed). The latter leads to static error of control.

Thus, for instance, in case of rise to altitude  $H$  for maintaining the engine speed  $n_0$  constant it is required to decrease the flow rate of fuel. But since fuel bullet 3 is rigidly joined by lever 4 with weights 1, shift of it to smaller fuel feed is possible only with a certain increase of speed. Thus, as a result of engine control we obtain a decrease of the flow rate of fuel from  $G_0$  to  $G_h$  with a simultaneous increase of speed from  $n_0$  to  $n_h$ . Static error of control in this instance will be equal to:

$$\Delta n = n_h - n_0.$$

Static error of control is proportional to the change of engine load; therefore sometimes the static regulator is called proportional. Figure 16.4 gives a graph of the change of engine speed with increase of flight altitude from  $H = 0$  to  $H$  as a result of its regulation by a static regulator.

Lowered sensitivity to change of the control parameter, peculiar to a regulator of direct action, is explained by the fact that resetting of its regulating member of it is carried out by the energy of the sensor element. Weights 1 and spring 2 (see Fig. 16.4) must overcome the known resistance on the bullet 3, which can be considerable.

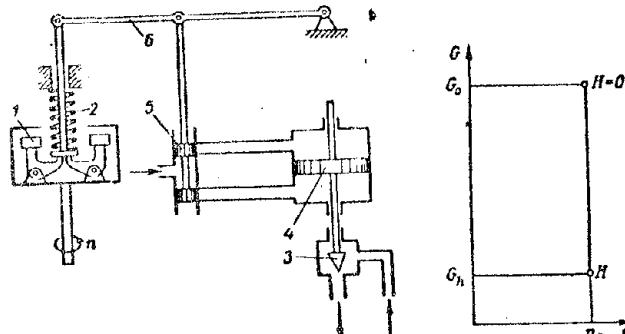


Fig. 16.5. Astatic control unit of indirect action.

Adjustment of regulator for maintaining a specified engine speed is carried out by shift of clutch 5. This changes the tension of spring 2. With increase of its tension the engine speed will increase, and with its decrease the speed will decrease.

Static control units of direct action find application when it is not required to have high accuracy of control and necessary force for resetting the regulating member is not so great. An example of them are the fuel flowmeters (see § 3 of this chapter).

Astatic control unit. Figure 16.5 depicts the diagram of an astatic speed control unit. Its sensor element consists of weights 1 and spring 2, and the regulating member is fuel bullet 3.

The astatic control unit is a regulator of indirect action and reset of fuel bullet is carried out by a slave mechanism (servo-mechanism) which consists of servo-piston 4 and valve 5. The servo-piston is directly connected with fuel

bullet 3 and moves under the action of the working fluid (oil or fuel) which is supplied to it from a pump. Valve 5 is connected through lever 6 with the sensor element and controls feed of the working fluid to the servo-piston cavities and drain from them.

In Fig. 16.5 the regulator is shown in equilibrium state, when valve 5 is in neutral position, covering the servo-piston channels. This position corresponds to steady (equilibrium) conditions, when engine load is kept constant. In this instance the fuel bullet is maintained in fixed position, preserving thereby constant a flow rate of fuel, and consequently also constant engine speed.

Upon change of load the speed control unit will also maintain constant engine rating. If, for instance, the engine speed starts to increase, the sensor element will displace valve 5 upwards, connecting the lower servo-piston cavity with drain, and the upper with feed of the working fluid. The servo-piston will then shift downwards, simultaneously resetting the fuel bullet to decrease of fuel feed to engine,

If, however, the engine speed starts to decrease, the sensor element shifts valve 5 downwards, connecting the upper servo-piston cavity with drain, and the lower with feed of working fluid. The servo-piston is then moved upwards, simultaneously resetting the fuel bullet to increase of fuel feed to engine.

Thus, decreasing or increasing fuel feed, the regulator each time restores the disturbed engine speed. Moreover, at the end of the process of control the weights 1 always arrive at initial equilibrium position, at which valve 5 will occupy its neutral position.

The astatic regulator exactly maintains the specified value of the control parameter (speed) and does not have the control error that is peculiar to the static regulator.

Figure 16.5 gives the graph  $G = f(n)$  of engine control by an astatic control unit with rise to an altitude, from which it follows that the engine speed is kept constant. Since resetting of the regulating member of a regulator of indirect action is produced by the servo-piston from an external source of energy (from a pump with the help of working fluid), the astatic regulator possesses high sensitivity to change of the control parameter.

A deficiency of the astatic regulator is its instability, owing to which the process of control is accompanied by oscillations of engine speed near the specified value. This is explained by the fact that shift of the servo-piston

is not controlled from the valve, i.e., there are no additional stabilizing devices. Therefore the astatic regulator finds application in control objects possessing considerable reserve of natural stability (see 16.4 of this chapter). Figure 11.26 showed the diagram of an astatic speed control unit controlling the propeller [VISH] (BIII). The propeller is a stable control object and the dynamics of its control proceeds satisfactorily.

Static control unit of indirect action. Figure 16.6 depicts the diagram of a static control unit of indirect action. In distinction from the astatic unit the motion of servo-piston 4 is controlled by the reverse rigid constraint between servo-piston 4 and control valve 5, made in the form of lever 6.

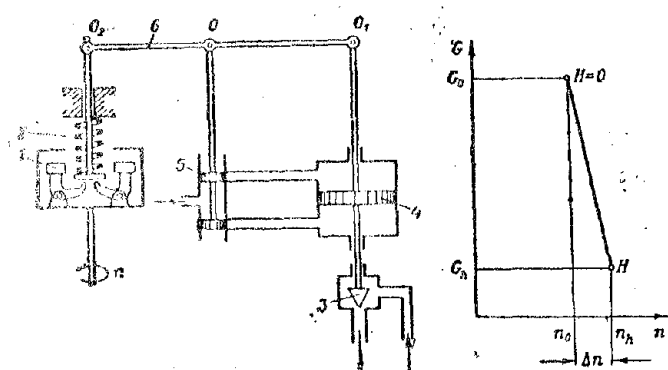


Fig. 16.6. Static control unit of indirect action. 1—weights, 2—spring, 3—fuel bullet, 4—servo-piston, 5—valve, 6—lever.

Upon deviation of speed from equilibrium conditions to some direction the sensor element in the first moment of time turns lever 6 with respect to axis  $O_1$  and displaces control valve 5 from its neutral position. After that the motion of servo-piston 4 begins, which resets bullet 3 to increase or decrease of fuel feed to the engine. Simultaneously with this the servo-piston will turn lever 6 with respect to axis  $O_2$ , attempting thereby to return valve 5 to neutral position.

The reverse rigid constraint (lever 6) stabilizes the process of control, giving the system stability. Dynamics of control then proceeds more favorably in the astatic regulator, without considerable oscillations of speed near the specified value.

At that same time owing to the reverse rigid constraint, each position of fuel bullet 3 will correspond to a definite position of weights 1. Therefore a static control unit of indirect action has static error of control (see graph  $\delta = r(n)$  in Fig. 16.6).

Isodromic control unit. Figure 16.7 depicts the diagram of an isodromic speed control unit. In distinction from static the control unit of indirect action with reverse rigid constraint the isodromic unit has flexible (isodromic) constraints. The word isodromic means that the control unit exactly maintains the specified engine speed.

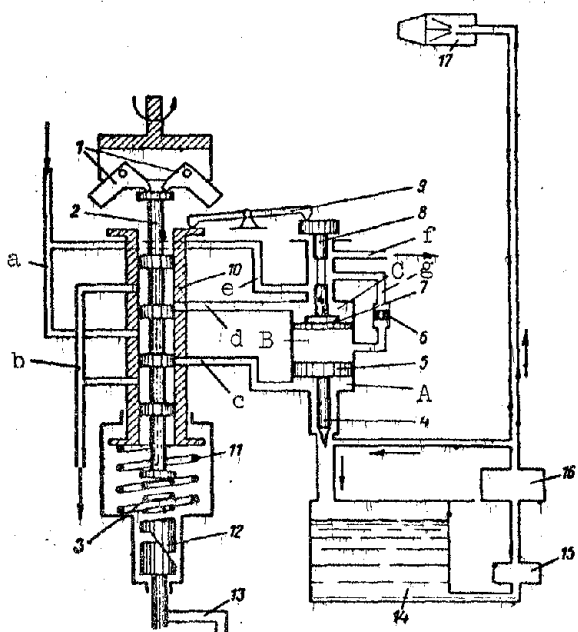


Fig. 16.7. Isodromic control unit,

The sensor element of the regulator consists of weights 1 and spring 3. The control element is valve 2, and the working member is servo-piston 5. The latter is directly connected with the regulating member, i.e., the bypass fuel bullet 4.

Isodromic constraint consists of isodrome piston 7 with valve 8, isodrome lever 9, movable case 10 with spring 11, and jet 6.

The diagram also shows fuel tank 14, booster fuel pump 15, main fuel pump 16, and fuel burners 17.

Control of engine speed is carried out by resetting bullet 4. This changes the flow rate of fuel by bypassing its excess quantity back into fuel tank 14. Adjustment of the speed control unit to a specified speed is produced with the help of cam mechanism 12 by turning lever 13, which changes the tension of spring 3.

Under steady (equilibrium) engine operating conditions the centrifugal force of weights 1 is balanced by the tensile stress of spring 3. Then movable case 10 with control valve 2 and isodrome piston 7 with its valve 8 are in equilibrium (neutral) position, at which the channels of supply and drain of oil (or fuel) from cavities A, B and C of the cylinder are covered.

Isodromic (flexible) constraint is carried out with the help of interpiston oil pad B formed between servo-piston 5 and isodrome piston 7. Depending on the position of the isodrome valve, its boring through channel g connects the interpiston pad B either with the drain through channel f, or with the supply of oil under pressure through channel e.

Fixed jet 6 limits the rate of change of volume of pad B. With neutral position of the isodrome valve the interpiston pad is closed and under these conditions the control unit operates as a static unit with rigid constraint.

With an arbitrary increase of engine speed (for instance with elevation) under the action of weights 1 valve 2 will shift downwards. Then channel a, feeding oil under pressure, will be connected with channel c, and channel d with mixed channel b. Then servo-piston 5 and isodrome piston 7 under the action

of increasing oil pressure in cavity A will start to shift upwards, the passage section of bypass bullet 4 will be increased, and the fuel entering the engine will decrease. Owing to this, the engine speed will start to decrease and valve 2 under the action of spring 3 will start to shift upwards.

During its motion upwards the isodrome piston 7 through lever 9, overcoming the elasticity of spring 11, will transfer the movable case 10 downwards, and isodrome valve 8 will connect channel g with mixed channel f. Because of this the oil from cavity B through jet 6 will start to slowly flow out and its volume will start to decrease. Since drain of oil from cavity B through the small hole of jet 6 requires a specified time, the interpiston pad B at the first moment of time acts as a rigid constraint.

However in the following moment of time, owing to the decrease of volume in interpiston cavity B isodrome piston 7 at first will delay its motion upwards, and then under the action of spring 11 will start to shift downwards, returning to initial neutral position. Simultaneously, movable case 10 will also begin to move upwards to its original position.

Since the motion of servo-piston 5 upwards for decrease of the flow rate of fuel will still continue and consequently, the engine speed will continue to decrease, valve 2 under the action of spring 3 will follow the case, also moving upwards to its initial neutral position.

At the end of the process of control the isodrome valve 8, case 10, and valve 2 arrive in the initial neutral position. Servo-piston 5 will then occupy the position at which the flow rate of fuel will ensure the initial engine speed.

In reality the process of isodromic control is more complicated, since the joint motion of pistons 5 and 7 and change of volume of interpiston pad B occurs simultaneously. On the other hand, during motion of case 10 the passage sections of its ports will be changed according to a different law than with a fixed case. This will evoke some additional wearing out of the regulator.

Nonetheless, for the isodromic control unit it remains characteristic that at the initial moment of control it is similar in its dynamic characteristics to the static control unit, and at the end of control the static error of control is removed and the engine speed is restored with high accuracy to the initial value. This follows from the fact that equilibrium conditions correspond to neutral positions of valve 2 and 8, which are always kept constant, and their position does not depend on initial adjustment of regulator to a specified speed.

With decrease of engine speed (for instance with decrease of altitude of flight) the process of control can be presented in a similar account, but at the end of the process of control the servo-piston 5, and bypass bullet 4 with it will shift downwards, which will increase fuel feed to engine, and valve 2, case 10 and isodrome valve 8 will arrive at its initial position.

The isodromic control unit combines the advantages of static and astatic units, i.e., it has a satisfactory flow of dynamic characteristics (stability in the process of control) and ensures exact control of specified engine speed.

### 16.3. Flow Control Units

The control parameter of fuel flowmeters is usually the pressure drop of fuel of the throttle valve or pressure of fuel in front of the throttle valve. At fixed position of throttle valve (with its constant passage section) the flow control units maintain a constant flow rate of fuel.

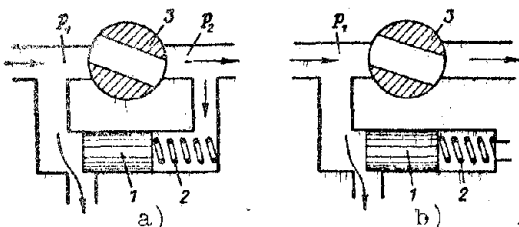


Fig. 16.8. Diagrams of simple flow control units.

Figure 16.8 depicts diagrams of simple flow control units. In diagram a) valve 1 is of the differential type. Spring 2 balances the difference of fuel pressures  $p_1 - p_2$  in front of and behind the throttle valve 3. Maintaining the specified

difference of pressures  $p_1 - p_2$  with bypass of fuel, valve 1 regulates the flow rate of fuel. Valve 1 operates only in the covered position of throttle valve 3, when in the valve there is created sufficient a pressure drop, overcoming the elasticity of spring 2. In diagram b) spring 2 of valve 1 balances the pressure of fuel  $p_1$  in front of the throttle valve 3. By maintaining the specified pressure of fuel  $p_1$  with fuel bypass, valve 1 regulates the flow rate of fuel; it operates in the covered position of throttle valve 3, when pressure  $p_1$  in front of the throttle valve attains a sufficient magnitude in order to surmount the elasticity of spring 2 and to open the drain. Adjustment of control units to a specified value of the control parameter is produced by change of tension of spring 2.

Both control units are of direct action. Valves of control units are simultaneously the sensor elements and regulating members. Their control object is the flow of fuel into the fuel lines.

Upon change of the control parameter the valves change their position and area of passage section of bypass orifice. Since shift of valves is in proportion

to the change of the control parameter, these control units are static.

Fuel flowmeters are usually applied jointly with speed control meters for guarantee of stable engine running at lowered ratings. They can be of direct and indirect action. The fuel flowmeter is sometimes applied as the main unit, indirectly regulating the engine speed, and also temperature of gases in front of its turbine at basic ratings. For this they are additionally equipped with a barostat, which, upon reacting to the change of conditions of flight (altitude and speed of flight), corrects the fuel flow in the appropriate way. The diagram of this control unit is shown in Fig. 16.12.

The flow control unit of turboprop engine regulates the flow by proceeding from the condition of maintaining the specified engine torque (temperature of gases in front of turbine).

#### 16.4. Natural Stability of GTD

An engine is naturally stable, if it can operate at the given rating stably without a regulator. Natural stability is an important property of GTD and determines the application of the particular control system.

Let us consider natural stability of a GTD in the example of a TRD with fixed exhaust nozzle. Figure 16.9 depicts; curve of moment of resistance of compressor  $M_k$  and grid of curves of turbine torque  $M_\tau$  depending upon speed. These curves are called the static characteristics of the compressor and turbine. Character of flow of curves  $M_\tau$  of engine depends on the law of fuel feed (on the characteristics of the fuel pump). In this case every curve  $M_\tau$  is obtained with the change of fuel feed in proportion to the engine speed (at fixed position of regulating unit). In this case with increase of speed, torque  $M_\tau$  of the turbine increases. Points a and b of intersection of curves  $M_k$  and  $M_\tau$  correspond to equilibrium operating conditions of the engine, at which  $M_\tau = M_k$ . Each position of the regulating unit of the pump will correspond to its points a and b. Thus the engine speed, i.e., its rating, can be changed by changing the position of the regulating unit of the pump.

In the region of points b curve  $M_k$  is steeper than curve  $M_\tau$  and therefore the engine can independently without a regulator, maintain constant speed  $n_0$ ; in this case it possesses the property of natural stability or self-balancing.

In practice, when  $n > n_0$  we obtain  $M_\tau < M_k$ , and when  $n < n_0$  we have  $M_\tau > M_k$ . Therefore, an arbitrary deviation of speed towards an increase will be prevented by the excess of moment of resistance of compressor  $M_k$  and a decreasing deviation

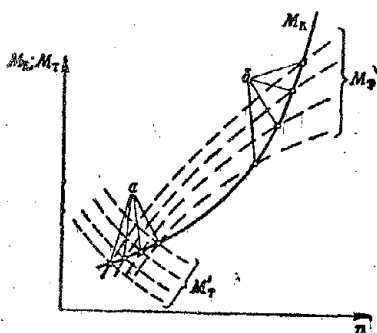


Fig. 16.9. Static characteristics of compressor and turbine.

of speed will be prevented by the excess of torque of turbine  $M_t$ . The sharper the difference in flow of curves  $M_r$  and  $M_{r1}$  in the region of points b, the greater the natural stability of the engine.

In the region of points a, corresponding to low ratings, curves  $M_t$  are steeper than curve  $M_r$ . In this case the engine will be unstable and without a regulator it is not in a state to maintain constant speed.

Actually, when  $n > n_a$  we obtain  $M_t > M_r$ , and when  $n < n_a$  we have  $M_t < M_r$ . Therefore, with an insignificant arbitrary deviation of engine speed in the direction of an increase there will appear an excess of turbine torque  $M_t$ , owing to which the engine speed will continuously begin to increase, until it reaches the speed  $n_a$ . With an insignificant arbitrary deviation of engine speed in the direction of a decrease there will appear an excess of moment of resistance of compressor  $M_r$ , owing to which the engine will decrease its speed and stop. As was already noted, the character of flow of the curve turbine torque  $M_t$  depends on the law of fuel feed. Thus, by regulating fuel feed it is possible to ensure stability of engine operation even at low ratings.

Thus, for instance, if for ratings in the region of points a the regulator always maintains the flow rate of fuel constant (independent of speed), then turbine torque  $M_t'$  with increase of speed will decrease (see curves  $M_t'$ ). This occurs because with increase of speed the flow rate of air through compressor is increased and at constant flow rate of fuel the temperature of working gases decreases. Engine operation at ratings corresponding to points a in this case will possess stability.

Thus, the static characteristics of GTD at constant flow rate of fuel, from the point of view of stability of the working process, are more favorable.

This analysis of natural stability of a TRD in equal measure can also be referred to TVD, if one were to take the propeller blade angle to be constant.

#### 16.5. GTD Control Systems

The control systems for various engine ratings are presented different requirements. Thus, for instance, from the condition of reliability for maximum rating there is required a high accuracy of maintaining constant speed; cruise

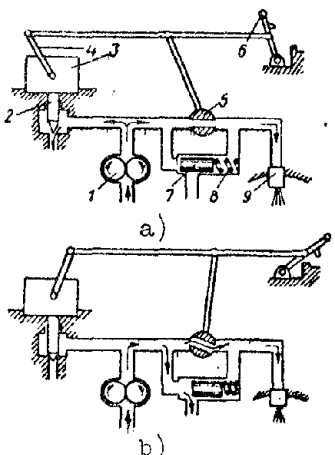


Fig. 16.10. Fundamental diagram of a separate TRD control.

speed control unit, and at lowered ratings (in the region of speeds below 0.5 to 0.7 nominal) with the help of fuel flowmeters.

Figure 16.10 depicts the fundamental diagram of a separate TRD control system with fixed-area exhaust nozzle and without afterburner (simple TRD diagram) which consists of a gear fuel pump of high pressure 1, throttle valve 5, isodromic speed control unit 3 with adjuster 4, bypass fuel bullet 2, control lever 6, flow control unit 7 with spring 8 and fuel burner 9. The diagram conditionally shows only one burner. Diagram a shows the operation of the control system at basic ratings, and diagram b at lowered ratings.

Fuel pump of the gear type of high pressure has at all ratings excess delivery. Pump is the control object. Control is carried out with bypass of excess quantity of fuel from pressure side to suction side: in the control of basic ratings by bypass bullet 2, and in the control of lowered ratings by valve 7.

Speed (rating) is assigned by pilot by setting control lever 6 in the specified position. The position of the control lever determines the passage section of the throttle valve 5 and adjustment of regulator 3 to the desired speed. The latter is attained with the help of adjuster 4 by changing the tension of the spring of the centrifugal weights of the control unit.

During operation at maximum and basic cruise ratings, valve 7 of the flow control unit under the action of spring 8 is in the off position. Automatic control of engine speed at these ratings is carried out by the isodromic control unit 3 which controls fuel bullet 2. When it moves it changes the passage section for bypass of fuel, i.e., fuel feed to burners 9.

ratings are usually connected with a specified speed, and for idling the speed is increased with increase of altitude of flight.

In the preceding paragraph it was shown that TRD as a control object at lowered ratings is naturally unstable. In order to satisfy the conditions of exact support of speed at basic ratings and stable work at lowered ratings we frequently see the application of a separate TRD control system: at basic ratings (in the region of speeds higher than 0.5 to 0.7 nominal) control is carried out with the help of an isodromic

In the region of lowered ratings when the engine is an unstable control object, the flow control unit goes into operation. During operation at lowered ratings the control lever 6 is in the position shown in diagram b. The isodromic speed control unit 3 by the action of adjuster 4 is turned off from operation and bypass bullet 2 closes the drain channel. Since the passage section of the throttle valve 5 securely covered, the pressure drop of fuel will increase. Owing to this, valve 7 of the flow control unit, surmounting the elasticity of spring 8, is displaced to the right and opens the drain for excess fuel to the suction side of the pump.

Regulating bypass of fuel in accordance with the position of throttle valve 5, the flow control unit maintains the pressure drop of fuel of the throttle valve 5 constant.

In TRD we sometimes find the application of a simpler control system, consisting of a flow control unit with a barostat and regulator (governor) of maximum speed.

The control system should ensure support of the assigned engine rating at permissible thermal and dynamic intensity. Therefore besides the basic speed governors and flow control units, GTD also have a number other automatic devices ensuring stable and safe engine operation. They include: automatic pick-up devices, automatic of altitude-speed correctors, various stabilizing devices, automatic propeller power reduction of TVD, governors of maximum (limiting) speed, system of automatic engine control during starting, and so forth.

For TRD with afterburners and two-shaft TRD there appear additional problems of control, which are not considered here. TVD control is considered below in the example of a fundamental diagram.

#### TRD Control System with Isodromic Speed Control Unit and Flow Control Unit

Figure 16.11 shows the diagram of supply and control of a TRD, which consists of the main fuel pump, automatic fuel distributor, and working burners.

The fuel pump of the plunger type includes an engine speed governor, fuel flowmeter, and throttle valve. Fuel moves to pump from aircraft tanks by a booster pump under a pressure of the order of  $2 \text{ kg/cm}^2$  through channels 34 and 38. Swash plate 35 changes the movement of plungers 4. Movement of plate is limited by stop 2.

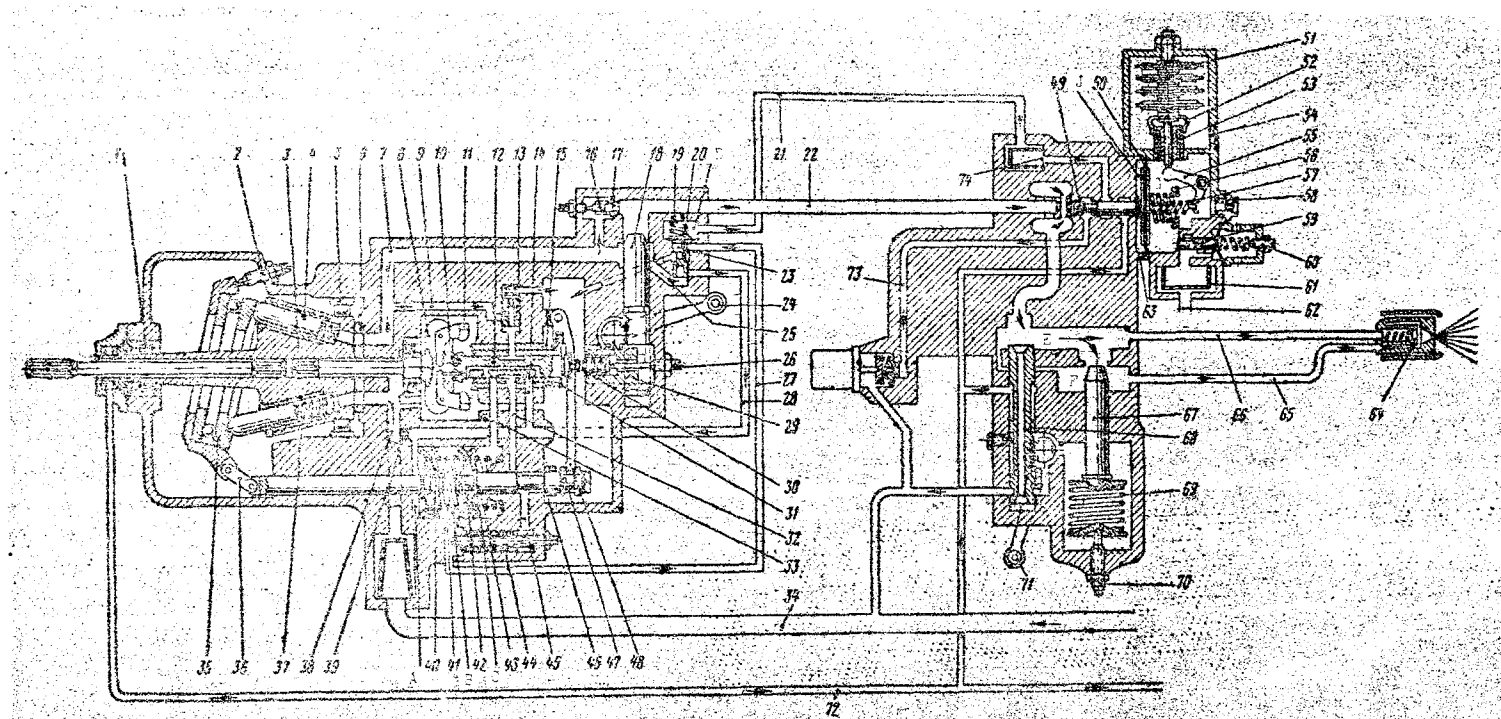


Fig. 16.11. Diagram of supply and control of a TRD with an isodromic speed control unit and fuel flowmeter. 1 and 5 - rotor bearings, 2 - regulating screw, 3 - rotor, 4 - plunger, 6 - distribution valve, 7 - pressure channel of pump, 8 - guide, 9 - channels, 10 - weight pins, 11 - weights, 12 - valve, 13 - cock, 14 - channel, 15 - spring, 16 - bullet, 17 - idling jet, 18 - throttle valve bullet, 19 - jet, 20 - spring, 21 - channel, 22 - channel, 23 - valve, 24 - control lever, 25 - channel, 26 - support screw, 27 and 28 - channels, 29 - toothed bar, 30 - spring, 31 - case, 32 - channel, 33 - channel, 34 - fuel supply channel, 35 - swash plate, 36 - link, 37 - spring, 38 - suction channel of pump, 39 - jet, 40 - servo-piston, 41 and 43 - spring, 42 - isodrome piston, 44 - throttling pack, 45 - channel, 46 - channel, 47 - isodrome valve, 48 - constraint lever, 49 - valve of automatic pick-up device, 50 - diaphragm, 51 - aneroid, 52 - bracket, 53 - channel, 54 - hole, 55 - lever, 56 and 57 - spring, 58 - jet, 59 - regulating bullet, 60 - regulating screw, 61 - filter, 62 - channel, 63 - hole, 64 - working burner, 65 - main line, 66 - auxiliary line, 67 - fuel distributor bullet, 68 - shutoff cock, 69 - spring, 70 - regulating screw, 71 - control lever of shutoff cock, 72 - drain tube, 73 and 74 - channels.

Automatic fuel distributor switches on shutoff valve and automatic pick-up. The diagram shows one two-channel working burner 64. Fuel moves to it from fuel distributor through main 65 and auxiliary 66 channels.

Servo-piston 40 is the working element. It is under the action of the difference of fuel pressure in cavities A and B, tension of spring 41 and force of tightening of spring 37 in the area of swash plate 35 connected to piston rod by link 36. With change of engine ratings the servo-piston 40, under the action of control units, changes its position and fixes the swash plate in the position at which the pump delivery corresponds to the specified engine rating.

The speed control unit is of the isodromic type. It differs from a similar unit, shown in Fig. 16.7, by the fact that its servo-piston 40 is not united with the bypass fuel bullet, but with swash plate 35 of the plunger pump. The working fluid here is the fuel.

The sensor of the regulator consists of centrifugal weights 11 and spring 30. Centrifugal weights 11 are fixed on guide 8, which through a slit connection obtains rotation from rotor 3 of the pump, revolving on two bearings 1 and 5. Through pins 10 the weights rest on control valve 12 and set it into rotation. Through valve 12 on weights 11 there is transmitted the force of spring 30, which balances the centrifugal forces of the weights. Rotation of control valve 12 promotes decrease of its friction during longitudinal shifts, which increases sensitivity of the regulator.

The control elements of regulator include control valve 12, moveable case 31, and isodrome piston 42 with valve 47. Isodrome piston 42 is placed in a common cylinder with the servo-piston and is under action of springs 41 and 43 and the difference of forces of fuel pressure in cavities B and C. Through lever 48 there is carried out isodromic constraint of isodrome piston 42 with movable case 31. The case by spring 15 is pressed to constraint lever 48.

Fuel moves from pressure side of pump through channel 9 and valve 13 to middle bore of control valve 12. From here the fuel through channel 32 passes also to isodrome valve 47. Valve 13 maintains the pressure of the fuel proceeding to the control system constant.

Control valve 12 carries out supply and drain of fuel of cavities A and B through channels 14 and 33. Cavity A of the servo-piston through jet 39 is also connected with the suction side of the pump. Isodrome valve 47 carries out supply

and drain of fuel from interpiston cavity B through throttling pack 44. The pack consists of a set of washers with holes and plays the role of a jet.

Operation of speed control unit. At any steady engine rating the centrifugal force of weights 11 is balanced by the compression force of spring 30. Movable case 31 with control valve 12 and isodrome piston 42 with its valve 47 are in equilibrium (neutral) position, at which channels 33 and 14 are covered by valve 12, and channels 32 and 46 by valve 47.

With an arbitrary increase of engine speed (for instance, with increase of altitude of flight) under the action of increasing centrifugal force of weights 11, valve 12 is displaced from neutral position to the right. Fuel proceeds through channel 14 to cavity A, and through channel 33 it will be drained from cavity B. Servo-piston 40 and isodrome piston 42 will then move together to the right, decreasing the fuel supply by the pump.

By means of constraint lever 48 movable case 31 will also be displaced to the right following valve 12, lagging behind the latter in its motion. In the next instant when with the decrease of fuel supply by the pump the engine speed will start to decrease, valve 12 under the action of spring 30 will start to move back to the left towards 31, until it covers its ports.

With the displacement of isodrome valve 47 from neutral position of the right there will begin drain of fuel from interpiston cavity B through channels 45 and 46. This will lead at first to deceleration of motion of the isodrome piston to the right, and then to its shift back to the left to the initial neutral position. Case 31 through constraint lever 48 will then shift also to the initial position, and following it, valve 12 also arrives at the initial neutral position.

The process of control is then finished. As a result, servo-piston 40 will be displaced to the right for decreased fuel feed and the engine speed will be restored.

With an arbitrary decrease of the engine speed (for instance, with decrease of altitude of flight) the centrifugal forces of weights 11 decrease and valve 12 under the action of spring 30 will be displaced to the left from neutral position. The fuel through channel 33 will then enter cavity C, and through channel 14 - it will drain from cavity A. Servo-piston 40 and isodrome piston 42 will begin to shift jointly to the left towards increase fuel feed by pump.

Owing to the constraint, by means of lever 48 case 31 begins to be displaced behind valve 12 to the left, lagging in motion behind the latter.

In the following moment of time, when with increase of fuel supply by pump the engine speed begins to increase, valve 12 under the action of increasing centrifugal forces of weights 11 starts to move to the right toward case 31, until its ports are uncovered.

Upon displacement of isodrome valve 47 from neutral position to the left, the fuel starts to proceed through channels 32 and 45 to interpiston cavity B. Owing to this the isodrome piston at first will delay its motion to the left, and then will start to shift back to the right to its initial neutral position. Case 31 through constraint lever 48 will then shift also to the initial position, and following it, valve 12 will arrive at the initial neutral position.

This terminates the process of control, and as a result the servo-piston will be displaced to the left towards increased fuel feed. Engine speed will be restored.

Described process of isodromic control in reality will not take place in such strict sequence as described, since the mechanism of isodromic control has three degrees of freedom, and in the process of control there always is possible overcontrol, i.e., temporary change of speed to a larger degree than required. However, the final result of the process of control always will be that the servo-piston will change its position, and all remaining elements of the regulator will arrive at the initial position.

Throttle valve is mounted on pressure line of pump. It consists of a profiled bullet 18 united with control lever 24 and idling jet 17.

Throttle valve is interlocked with adjusting mechanism of the speed control unit. Control lever 24 with the help of a gear and two toothed rods changes simultaneously the position of the bullet of throttle valve 18 and tightening of spring 30 of the regulator. Beginning of operation of the speed control unit is regulated by thrust screw 26.

During idling the throttle valve is covered and fuel feed to burners is carried out through idling jet 17 equipped with bullet 16 for adjustment,

Flow control unit maintains constant difference of pressures of fuel in front of and behind throttle valve 18. It operates at lowered ratings and is a static regulator of indirect action. Its sensor and control element simultaneously is valve 23 (differential valve).

From below through channel 25 to valve 23 fuel is brought in from pressure channel 7 located before the throttle valve, and from above it, to cavity D through jet 19 proceeds the fuel from channel 22 located behind the throttle valve. Valve 23 during operation is under the action of the difference of fuel pressures in front of and behind the throttle valve, and also the force of spring 20. Pressure drop in the throttle valve 18 is regulated by tightening spring 20. The working member of the flow control unit is servo-piston 40. With the help of channels 27 and 28 valve 23 carries out control of the servo-piston. At a steady engine rating the pump delivery is regulated in such a way that the pressure drop in the throttle valve is kept constant.

Operation of flow control unit. With increase of pressure drop in the throttle valve, valve 23 is displaced upwards. Owing to this, through channel 28 to cavity A of servo-piston 40 there starts to proceed fuel under pressure, and cavity B through channel 27 will be connected with the drain. The servo-piston will then be displaced to the right towards decrease of pump delivery until the specified pressure drop in the throttle valve is restored.

With decrease of pressure drop in the throttle valve, valve 23 under the action of spring 20 will be displaced downwards and will cover channels 27 and 28. Owing to this, to cavity B of the servo-piston, through channel 32, constraint valve 47, channel 45, and throttle pack 44 there will start to proceed fuel under pressure (when speed control unit is off the isodrome valve is in the extreme left position, connecting channels 32 and 45), and from cavity A through jet 39 drainage will occur. The servo-piston will be displaced to the left towards increase of pump delivery until the specified pressure drop in the throttle valve is restored.

At a steady rating, valve 23 will be displaced upwards in order to ensure constant position of servo-piston 40.

Entry into operation of speed control unit corresponds the position of the throttle valve at which its pressure drop is less than that which the flow control unit is adjusted to. In this case the valve under the action of the spring will cross to the extreme lower position and will be automatically turned off from operation.

Fuel distributor serves for distribution of fuel through channels of two-channel burners. It consists of profiled bullet 67, spring 69, regulating screw 70, and two fuel chambers E and F.

From the pump, passing throttle valve 18, fuel through channel 22 moves to chamber E, and from there directly passes to auxiliary line 66 of working burners 64. Main line 65 receives fuel through chamber F. At low fuel pressures bullet 67 under the action of spring 69 will close the passage to fuel to the main line and all fuel from the pump will move to burners through the auxiliary line. At fuel pressure over 10-20 kg/cm<sup>2</sup> the profiled bullet 67 will contract and fuel will start to proceed to working burners 64 through both main lines. The beginning of opening of the bullet is controlled by screw 70.

Shutoff cock serves for ceasing of fuel feed to working burners when engine has stopped.

Shutoff cock constitutes valve 68 united with control lever 71 with the help of a gear and toothed rod. Upon shift of valve upwards the shutoff cock covers the hole through which the fuel enters the distributor, thereby stopping fuel feed to working burners. In this case the fuel, proceeding from pump through central channel of valve 68, is drawn to the suction line of the pump. Remaining in the collectors, the fuel through a hole in the housing and bores on the valve is drained through system of drainage into the atmosphere. This accelerates stop of engine. Shutoff cock is opened when starting the engine and is closed when it has stopped.

Automatic pick-up regulates fuel feed during acceleration of engine, protecting the latter from excessive increase of temperature of gases in front of the turbine.

Automatic pick-up has valve 49, to which by spring 56 is pressed diaphragm 50. The diaphragm forms two chambers. Chamber J is connected with the atmosphere by hole 63. Chamber G through channel 62, filter 61, and regulating bullet 59 is connected with the engine compressor, and through jet 58 with the atmosphere. During work of engine, valve 49 in the area of the diaphragm is loaded by excess air pressure in chamber G and pressure of spring 56, and from the opposite side by the pressure of fuel in its face.

At steady ratings the force from diaphragm 50 exceeds the force of the fuel and pick-up device does not operate. During acceleration of engine (during pick-up) valve 49 under the action of quickly increasing fuel pressure is displaced to the right and connects, through channels 21, 74, and 73 chamber D of the flow control unit with suction line 34 of the pump. This causes displacement of valve 23 of the regulator upwards and shift servo-piston 40 of the pump

towards decrease of fuel feed. With acceleration of engine the air pressure behind the compressor will increase. Air pressure on diaphragm 50 of chamber G will also increase. This will lead to shift of valve 49 to the left. Due to this the pressure in chamber D of the flow control unit will start to increase and valve 23 of the flow control unit, being displaced downwards, will transfer servo-piston 40 to the position of large flow, i.e., in proportion to the increase of air pressure behind the compressor.

Automatic pick-up is regulated by screw 60 and jet 58.

Since with increase of altitude of flight the flow of air through the engine decreases, fuel feed during acceleration should also decrease. This altitude correction is carried out by aneroid 51. The aneroid chamber is connected through hole 54 with the atmosphere. With increase of altitude of flight the aneroid will be expand, and through the rod acting on lever 55 and spring 57 it will unload valve 49 in the area of diaphragm 50.

In expanding, the aneroid simultaneously transfers bracket 52. Channels 53 consecutively will be opened and pressure in chamber G will decrease. Owing to this, valve 49 during altitude pick-up is opened earlier and remains open for a long time, ensuring thereby smaller fuel feed to burners.

#### System of TRD Control with A Flow Control Unit and Speed Governor

Figure 16.12 depicts the diagram of a plunger fuel pump with a flow control unit and speed governor,

Control of engine is carried out with the help of a throttle valve, attached to the pressure line of the pump in front of the working burners.

Pump is of the plunger type. Fuel feed is changed by swash plate 4 connected by link 2 with servo-piston 1. Cavities a and b of the servo-piston are connected to the pressure channel. From the left side the servo-piston receives the total pressure of fuel, and from the right side, in view of the throttling action of jet 19 and bypass of fuel through bypass valve 20 and 10, there is established lowered pressure. Bypass valve 20 controls the flow control unit, and bypass valve 10 controls the speed control unit.

Servo-piston 1 during work is under the action of the difference of fuel pressures in cavities a and b, the force of the spring, and the force from swash plate 4.

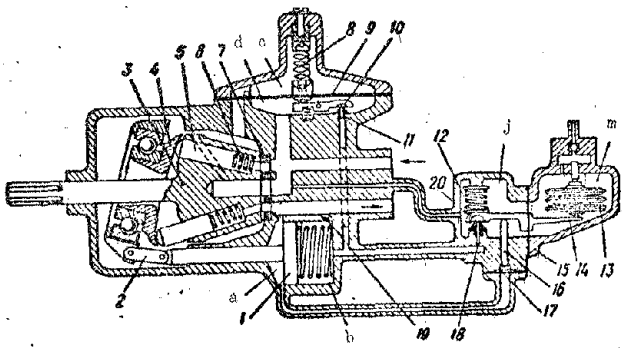


Fig. 16.12. Control diagram of a TRD with fuel flowmeter and speed governor.  
 1 - servo-piston, 2 - link, 3 - rotor,  
 4 - swash plate, 5 - plunger, 6 - spring,  
 7 - valve, 8 - spring, 9 - diaphragm,  
 10 - cock, 11 - jet, 12 - cock spring,  
 13 - aneroid, 14 - lever, 15 - reinforced  
 lining, 16 - rod, 17 - diaphragm of rod,  
 18, 19 - jets, 20 - cock.

under the pressure of fuel passed by the pump, and thus meters the pressure of fuel at the pump outlet. Barostat consists of aneroid 13 placed in chamber M. The chamber is connected to the compressor inlet. Barostat measures total pressure of air at compressor inlet.

Differential lever 14 is attached to elastic diaphragm 15, dividing cavity J (valve) and M (aneroid) of control unit housing. Diaphragm is the axis of oscillation of the lever. On one side the lever is under the action of spring 12, and on the other it is under the action of pressure gauge 17 through rod 16 and aneroid 13. Differential lever 14 is connected with valve 20 of fuel bypass from cavity b of the servo-piston.

Adjustment of regulator is produced with the help of a regulating screw by change of tension of spring 12.

Work of the flow control unit occurs in the following way. If pressure of fuel at the pump outlet for some reason is increased, its flow to the engine will be increased and engine speed will be increased. Under the action of increased fuel pressure diaphragm 17 will deflect upwards and, acting on lever 14 through rod 16, will increase fuel drain through bypass valve 20 from cavity b of the servo-piston. Owing to this the servo-piston will be displaced to the right and will reset swash plate 4 of pump to smaller delivery. The engine speed will then be restored.

If pressure of fuel (and consequently its flow rate) from some reason decreases, the engine speed will also decrease. Owing to the decrease of pressure, diaphragm

Fuel flowmeter serves as the main regulator and indirectly regulates the engine speed. The flow control unit is static, of indirect action, with a barostat. In Fig. 16.13 it is shown separately.

The regulator consists of a fuel pressure gauge 17, barostat with aneroid 13, and differential lever 14 with bypass valve 20. The fuel pressure gauge 17 is the diaphragm type and is located in the area of the channel

under the pressure of fuel passed by the pump, and thus meters the pressure of fuel at the pump outlet. Barostat consists of aneroid 13 placed in chamber M.

The chamber is connected to the compressor inlet. Barostat measures total

pressure of air at compressor inlet.

Differential lever 14 is attached to elastic diaphragm 15, dividing cavity

J (valve) and M (aneroid) of control unit housing. Diaphragm is the axis of

oscillation of the lever. On one side the lever is under the action of spring

12, and on the other it is under the action of pressure gauge 17 through rod 16

and aneroid 13. Differential lever 14 is connected with valve 20 of fuel bypass

from cavity b of the servo-piston.

Adjustment of regulator is produced with the help of a regulating screw by

change of tension of spring 12.

Work of the flow control unit occurs in the following way. If pressure of

fuel at the pump outlet for some reason is increased, its flow to the engine will

be increased and engine speed will be increased. Under the action of increased

fuel pressure diaphragm 17 will deflect upwards and, acting on lever 14 through

rod 16, will increase fuel drain through bypass valve 20 from cavity b of the

servo-piston. Owing to this the servo-piston will be displaced to the right

and will reset swash plate 4 of pump to smaller delivery. The engine speed will

then be restored.

If pressure of fuel (and consequently its flow rate) from some reason decreases,

the engine speed will also decrease. Owing to the decrease of pressure, diaphragm

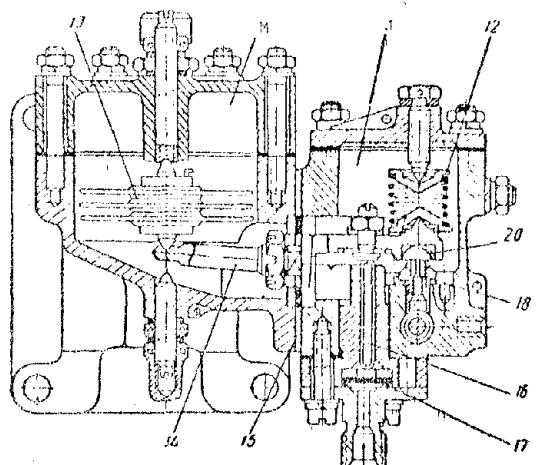


Fig. 16.13. Barostatic regulator  
(for designation of parts see Fig.  
16.12).

17 under the action of the force of elasticity of spring 12 will deflect downwards and lever 14 will decrease the output section of bypass valve 20. Pressure in cavity b of the servo-piston will be increased. Owing to this the servo-piston under the action of the spring will be displaced to the left and will transfer swash plate 4 of the pump to large delivery. The engine speed will then be restored.

Thus at constant external conditions

the flow control unit maintains constant engine rating. Change of engine rating is produced by the pilot by transposition of throttle valve 14 (see Fig. 15.4). Together with this the pressure of fuel at the pump outlet will also change. Then the flow control unit will begin operation and will establish pump delivery in accordance with the necessary flow rate of fuel.

With the change of altitude and speed of flight the mass flow rate of air through the compressor will also change. During constant flow rate of fuel this would lead to considerable change of temperature of working gases and engine speed. Correction of flow rate of fuel in accordance with altitude and speed of flight is automatically produced by the barostat. Aneroid of barostat 13 is under the action of total pressure of air at compressor inlet. Therefore, for instance, with decrease of compressor inlet pressure (upon rise to an altitude or with decrease of speed of flight) aneroid 13 will expand, and through lever 14 will increase the opening of bypass valve 20. This will lead to an increase of fuel drain from cavity b of the servo-piston and to displacement of the servo-piston to the right towards decrease of fuel feed to engine. With increase of compressor inlet pressure (with decrease of altitude of flight or with increase of speed of flight) there will occur a corresponding increase of fuel feed to engine.

Fuel flowmeter is static, since the change of position of its regulating element (swash plate) is connected with a corresponding change of the control parameter (fuel pressure). The flow control unit possesses a static control error.

Speed governor is static, of indirect action, and limits maximum speed  $n_{max}$

of TRD. Its sensor element is an tachometer of hydraulic type which constitutes elastic diaphragm 9 secured by a cover in the pump housing. Elasticity of diaphragm 9 is regulated by tension of spring 8 with the help of a regulating screw.

Diaphragm forms two chambers c and d filled by fuel. Lower chamber d, connected with suction channel of pump, houses bypass valve 10 with level control from diaphragm 9. Through bypass valve 10 there can occur bypass of fuel from cavity b of servo-piston 1. Upper chamber c is connected with cavity rotor.

Between plungers 5 of rotor 3 there are slanted drillings, connecting the suction channel of the pump through the central hose in distributive valve 7 with cavity of rotor. During rotation of rotor in these drillings the fuel is under the action of centrifugal forces, owing to which in the cavity of the rotor and in cavity c there will be established heightened pressure proportional to the rotor speed squared. Under the action of heightened pressure in cavity c diaphragm 9 will deflect and upon achievement of maximum engine speed will open bypass valve 10, through which there will occur bypass of fuel from cavity b of the servo-piston to cavity d. Owing to this, servo-piston 1, shifting to the right, will transfer swash plate 4 to the position of smaller pump delivery, at which the engine speed will be limited by the value of  $n_{max}$ .

Adjustment of regulator to the specified value of  $n_{max}$  is produced by the regulating screw by changing the tension of spring 8. At ratings below than maximum speed, valve 10 is closed by the force of elasticity of its spring and the speed control unit does not operate.

#### Fundamental Control Diagram of a Single-Shaft TVD

Figure 10.14 depicts a simplified fundamental control diagram a single-shaft TVD having two control systems: a speed control system and an engine torque control system (temperature of gases in front of turbine).

Speed control is direct and is produced with the help of an astatic speed control unit of indirect action. Its sensor element, consisting of weights 1 and spring 2, is connected with valve 4. The control object of is the propeller, and the controller unit is its blades 8. The propeller has hydraulic control. Its working fluid is oil. The servo-mechanism consists of servo-piston 6 with valve 9. The servo-piston is the working element, and the valve is the control element. with the help of lever 5 the regulator is adjusted for maintaining the

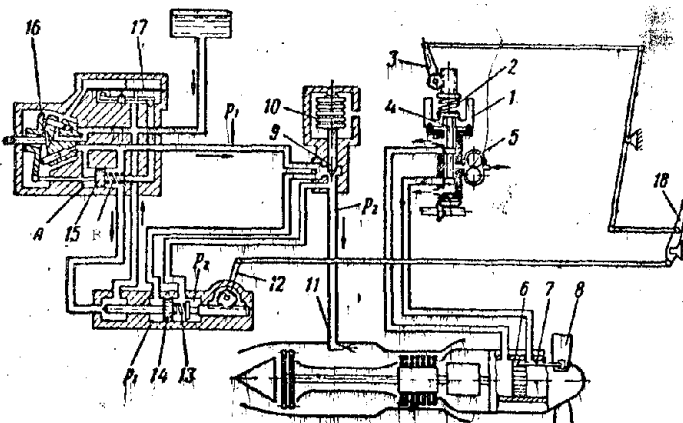


Fig. 16.14. Fundamental control diagram of a single-shaft TVD. 1 - weights, 2 - spring, 3 - adjustment lever, 4 - valve, 5 - pump, 6 - propeller servo-piston, 7 - bar, 8 - blades, 9 - fuel bullet, 10 - aneroid, 11 - working burner, 12 - adjustment lever, 13 - spring, 14 - valve, 15 - servo-piston of pump, 16 - swash plate, 17 - speed governor, 18 - control lever.

is restored. Thus, with an arbitrary increase of engine speed the blades 8 will be transposed to a higher pitch, and with a decrease, to a lower pitch. Since the moment of resistance of the propeller changes, the engine speed will also change. After restoration of primary speed, weights 1 will occupy their initial position, and valve 4 will arrive at the neutral position, covering the access of oil from pump 5 to servo-piston 6 of the propeller.

In contemporary TVD most frequently the speed control unit maintains the engine speed constant at all rating on the ground and in flight. Change of engine power is carried out by change of its torque.

Torque control is produced indirectly with the help of a fuel flowmeter of indirect action. With change of flow rate of fuel the temperature of gases in front of the turbine, and consequently, engine torque will also change.

The object of control is a fuel pump of the plunger type with variable delivery, and the controlling element is swash plate 16 of the pump. The sensor element of the regulator is valve 14 which simultaneously executes the function of the control element of the servo-mechanism. Servo-piston 15 is the working element of the servo-mechanism.

Fuel from the pump to working burners 11 moves through fuel bullet 9; its flow rate is determined by the difference of pressures  $p_1 - p_2$  and area of passage section of bullet 9. Specified pressure drop of fuel  $p_1 - p_2$  for bullet 9 is supported by valve 14, and area of passage section of bullet is regulated by aneroid 10 of the barostat.

specified engine speed.

Upon deviation of speed from the specified value the sensor element removes valve 4 from neutral position. Oil from pump 5 under high pressure enters one of the working cavities of servo-piston 6 while its other cavity is connected with the drain. Servo-piston 6 moves, and through bars 7 changes the angle of setting of propeller blades 8 so that the engine speed

Valve 14 is of the differential type. On one side it is influenced by the pressure of fuel at the pump outlet  $p_1$ , and on other side by the pressure of fuel behind fuel bullet 9  $p_2$ . The resultant force of pressure of fuel is balanced in valve 14 by the force of spring 13. Valve 14 measures the magnitude of pressure drop of fuel in bullet 9 and controls the drain of fuel from cavity B of servo-piston 15. Owing to this, servo-piston 15 through swash plate 16 maintains in the pump such a flow rate of fuel at which pressure drop of fuel  $p_1 - p_2$  in fuel bullet 9 with constant adjustment of regulator is maintained constant. If, for instance, pressure drop in fuel bullet 9 increases and flow rate of fuel increases, valve 14 will shift to the right and will increase the drain of fuel from cavity B of servo-piston 15. The latter, moving to the right, decreases the pump delivery in such a way that pressure drop of fuel in bullet 9 is restored. At the same time the flow rate of fuel will also be restored. With decrease of pressure drop of fuel in fuel bullet 9 and consequently, flow rate of fuel, the process of control will go in the opposite direction. Change of engine rating is carried out by turning lever 12. This will change the tension of spring 13 and thereby change the adjustment of the regulator to the particular flow rate of fuel.

Fuel bullet 9 is controlled by the barostat. Aneroid 10 of the barostat is under the action of total pressure of air at the compressor inlet and it corrects the flow rate of fuel with change of operating conditions (altitude or speed of flight) by changing the area of passage section of bullet 9. When air pressure at compressor inlet decreases (for instance, with rise to altitude), the aneroid will expand and will transfer fuel bullet 9 to decrease of flow rate of fuel. With increase of air pressure the fuel bullet in the appropriate way will increase the flow rate of fuel. By correcting of the flow rate of fuel upon a change of the conditions of flight, the temperature of working gases in front of the turbine will be restricted to the permissible limits.

Levers 3 and 12 for adjustment of speed control units and flow control units can be connected together by control lever 18. This can establish a definite connection between the change of engine speed and torque.

Fuel pump is also equipped by speed governor 17 of the diaphragm type. Its action was described above. The speed governor is usually adjusted to speeds somewhat higher the maximum speeds, which are obtained for the engine by control of the variable pitch propeller VISH.

## CHAPTER XVII

### GTD STARTING UNITS

#### 17.1, General Information

Gas-turbine engines [GTD] (ГТД) are started by a special low-capacity starting engine, the starter. The starter transmits to the engine during such a speed of rotation at which the compressor ensures a sufficient flow rate of air and pressure drop for turbine performance.

Figure 17.1 gives approximate curves of turbine capacity  $N_t$ , the power necessary for rotation of [TRD] (TPД) rotor  $N_k$  depending upon engine speed from beginning of starting to idling  $n_{n.r.}$ . The same graph shows the curve of change of temperature of gases in front of the turbine  $T_3$ ;  $T_h$  is ambient temperature, and  $T_{3 \text{ max}}$  is maximum permissible temperature of gases in front of the turbine. In the beginning the engine is disengaged from the starter. At engine speed  $n_1$  the supply of priming fuel to the combustion chambers is turned on. Owing to this the temperature of gases will increase to  $T_{3 \text{ max}}$  and turbine capacity  $N_t$  will increase. For guarantee of faster starting the temperature of gases in front of the turbine is maintained on the maximum permissible level  $T_{3 \text{ max}}$ . Up to speed  $n_2$  the capacity  $N_t$  is less than  $N_k$ ; therefore the engine continues to be disengaged by the starter.

Excess power in the turbine appears at speeds greater than  $n_2$ , at which the engine can work independently. However, in order to ensure reliable starting, the starter continues for a certain time to "accompany" the engine rotor in its rotation and is disconnected only upon achievement of speed  $n_3$ , when the turbine has sufficient surplus of power and the engine cannot die out. After this the

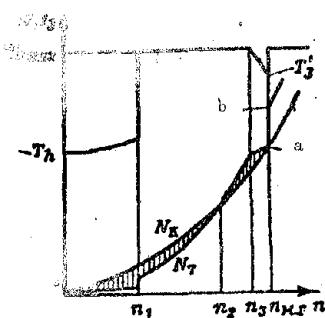


Fig. 17.1. Process of engine starting.

engine is independently brought to idle conditions  $n_{M.P.}$ . In order to ensure operation during idling, i.e., to fulfill condition  $N_r = N_k$ , fuel feed is somewhat decreased and therefore temperature of gases in front of the turbine also correspondingly will decrease to the value of  $T_3'$ ; curves of  $N_r$  and  $N_k$  will intersect at point a. Further shift of engine to operating conditions does not cause any difficulties. For this, fuel feed is increased and temperature of gases in front of the turbine is increased, for instance to the value of  $T_3 \text{ max}$ . In accordance with this the turbine capacity will increase to the value at point b. Then, by means of excess power, the will start to increase the speed.

Required power of starters depends first of all on the type of GTD, its output power and on the required time of starting. Thus, for instance, when starting a TRD the starter disengages only its rotor, and when starting a [TVD] (TRD), also the propeller. For facilitation of starting the latter is set in the position of minimum thrust. In two-shaft (two-rotor) GTD the starter only disengages one shaft (rotor), and therefore its required power is smaller, etc. For engines with high thrust (power) a more powerful starter correspondingly is required.

The power proceeding for acceleration of engine rotation can be expressed in the following way:

$$N_s = \frac{1}{75} J \omega \theta,$$

where  $J$  is the mass moment of inertia of revolving parts of the engine, applied to its rotor;

$\omega$  is the angular velocity of rotation of rotor;

$\theta = \frac{d\omega}{dt}$  is angular acceleration.

Since angular acceleration is reciprocal to the time of starting, with a decrease of the latter the required power  $N_s$  will increase. Figure 17.2 shows the dependence of required starter power on the time of starting a TRD with thrust 2270 kg and 4200 kg. With time of starting 20 sec, the required power of starters is 60 and 180 hp respectively, and with time of starting 3 sec, it is 400 and 1200 hp.

The starting system contains:

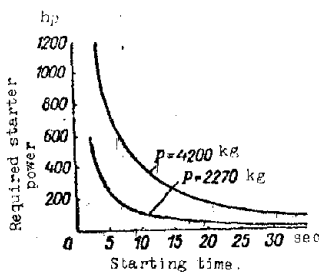


Fig. 17.2. Dependence of required power of starter on time of starting a TRD with thrust 2270 and 4200 kg.

- a) starting engine (starter) which ensures spin-up of rotor of main engine to specified speeds;
- b) priming fuel system, ensuring supply of priming fuel to combustion chambers;
- c) electrical units, ensuring ignition of priming fuel;
- d) automatic devices, controlling the process of starting.

Starting systems are self-contained and nonself-contained. In the first case the source of energy for feeding the starter (for instance, storage batteries for electric starter) is on the aircraft and starting of the engine does not depend on airport conditions. In the second case the energy for starting is ensured by airport starters,

### 17.2. Types of Starters

At present, GTD uses electric and turbo-starters. The latter can be compressor and compressorless.

Electric starters are dc quadripole electric motors of series or mixed excitation, and short duty cycle. The speed of electric starters is usually about 3000 rpm. Engine rotor receives rotation through a reduction gear with ratchet wheel engaging mechanism.

Figure 17.3 shows the ratchet wheel engaging mechanism of the starter of the TRD [VK-1] (BK-1), which consists of bevel gear 1, driven bushing 2, three pawls 3 sitting on axes 4, spring 6, and stop 5. Gear 1 has ratchet teeth, which are coupled with the three pawls. Gear 1 is linked to the pinion gear of the starter, and driven bushing 2 is united with the rotor of the main engine.

In the beginning of starting, upon engagement of the starter, gear 1, revolving counterclockwise, through pawls 3 and driven bushing 2 transmits rotation to engine motor. At the end of starting the starter is disconnected and driven bushing 2, obtaining rotation in the same direction from the engine rotor, starts to overtake gear 1. Pawls 3, under the action of centrifugal forces of their weights, surmount the elasticity of springs 6 and emerge from engagement with ratchet teeth of gear 1. Stop 5 limits turn of pawls.

Electric starter is usually fed from two storage batteries with voltage 24 V. In the beginning of starting the starter operates with parallel connected batteries, and then for increasing the power of the starter they are connected

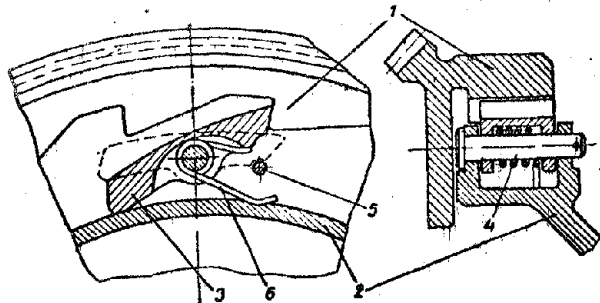


Fig. 17.3. Design of ratchet wheel engaging mechanism of the starter of the TRD VK-1.

in series. The basic deficiency of electric starters is their high consumption of electric power for each engine starting, which requires large and bulky batteries. This limits the power of electric starters, which reaches 30 hp.

Starter-generators are electrical machines that unite the starter and generator in one unit. Starter-generators have two consecutively operating windings, i.e., series or mixed and shunt.

In starting conditions the starter-generator operates as a series or compound dc electric motor is fed from storage batteries. By analogy with the common electric starter in engine operating conditions it allows a 100% brief overload. After starting the engine the series winding of the starter-generator automatically is disconnected and the shunt winding is connected. Owing to this the unit starts to operate at the rating of a shunt generator and passes current to the aircraft

power-supply network.

In accordance with operating conditions the drive of the starter-generator has bilateral action with different transmission ratios. Figure 17.4 shows the diagram of a starter-generator drive, which consists of gears  $z_1$ ,  $z_2$ ,  $z_3$ ,  $z_4$  and two clutches, i.e., ratchet clutch 2 and free-wheeling roller clutch 4. Engagement and disengagement of these clutches is produced automatically and is connected only with the direction of rotation of transmission. During work at a certain

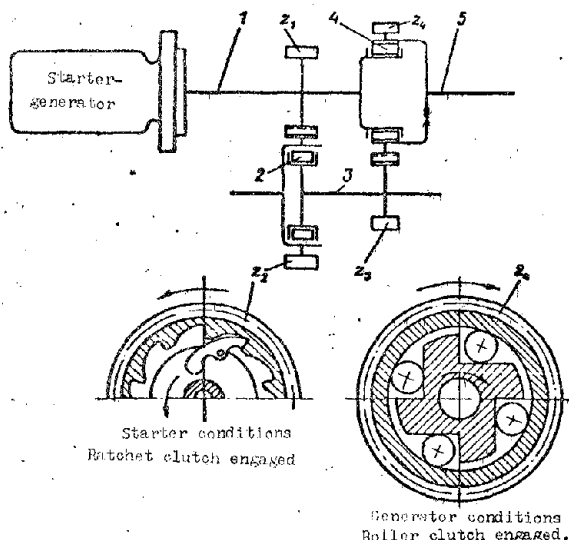


Fig. 17.4. Diagram of starter-generator drive.

rating only one clutch is engaged; the other is disengaged. Thus, during operating in starter conditions, the starter transmits rotation to engine shaft 5 through gears  $z_1$ ,  $z_2$ ,  $z_3$ , and  $z_4$ , where the transmission of rotation from gear  $z_2$  to roller 3 is carried out through ratchet clutch 2. After starting the engine begins to overtake the starter with respect to speed. Owing to this, ratchet clutch 2 automatically is disconnected, and free-wheeling roller clutch 4 is connected and

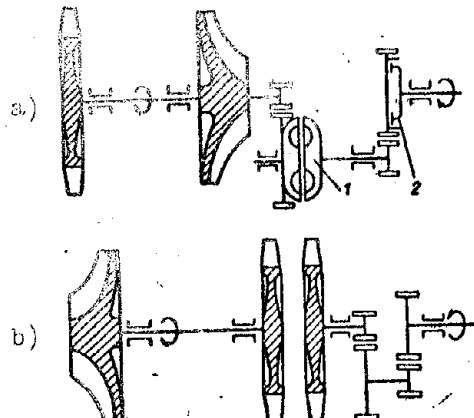


Fig. 17.5. Diagrams of a turbo-starter.

rotation from engine shaft 5 to shaft 1 of the starter-generator is transmitted directly through free-wheeling clutch 4. In this case the starter-generator changes to generator operating conditions.

The advantage of the starter-generator over the usual electric starter consists in the unification of the starter and generator in one unit, which decreases weight and simplifies the engine drive system.

Compressor turbo-starters are low-capacity GTD with centrifugal compressor, designed for brief work. Figure 17.5 depicts two kinematic diagrams of compressor turbo-starters. In diagram a the turbo-starter transmits excess power of turbine for engine spin-up through a two-stage reduction gear which houses hydraulic clutch 1 and ratchet clutch 2. The hydraulic clutch ensures constancy of transmitted moment and decreases dynamic loads in transmission at the moment of coupling.

In diagram b the turbo-starter has a two-shaft, two-stage turbine. The first stage revolves the compressor, and the second, through the reduction gear, spins up the engine. The two-shaft system allows us to somewhat decrease the speed of the second turbine stage and correspondingly to decrease the transmission ratio of the reduction gear. Initial starting moment in this instance is greater.

Compressor turbo-starters are able to ensure large power with relatively small dimensions and weight. One of their shortcomings is the complexity of construction and increased starting time, in which the starting the starter itself is turned on.

Compressorless turbo-starters consist of a turbine and mechanism (reduction gear) for transmission of rotation to the engine rotor. Some of them also have combustion chambers or steam-gas generators. Compressorless turbo-starters, depending upon form of working body used for the turbine, are broken down into:

- 1) air turbo-starters, the working substance of which is compressed air supplied from cylinders or from a separate compressor installation;
- 2) fuel-air turbo-starters, which differ from the preceding by the fact that air is preliminarily fed to the combustion chamber, where by means of

burning the fuel, its temperature is increased;

3) steam-gas turbo-starters, whose working substance can be:

a) a mixture of combustion products of kerosene or gasoline and steam;

b) vapor-gas, obtained from decomposition of hydrogen peroxide;

c) reaction products of special fuels;

4) cartridge turbo-starters, whose working substances are powder gases.

Compressorless turbo-starters can ensure high power with small dimensions and weight.

Type of starter is selected depending on its dimensions and weight, and also the convenience in utilization.

### 17.3. Igniters

Ignition of fuel mixture during engine starting is produced by a special ignition device. In Fig. 17.6 is shown ignition device, consisting of a starting burner and spark plug 6, united in one body 8.

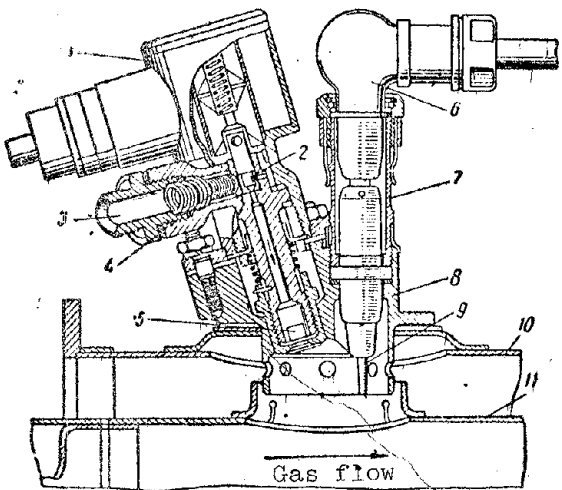


Fig. 17.6. Ignition device. 1 - solenoid, 2 - needle valve, 3 - feed pipe of starting fuel, 4 - strainer, 5 - atomizer, 6 - spark plug, 7 - plug body, 8 - igniter case, 9 - central plug electrode, 10 - housing of combustion chamber, 11 - flame tube.

(from aircraft network) in the solenoid there is created a magnetic field, and the core, surmounting the elasticity of the spring, shifts upwards and opens the valve 2 for passage of fuel to the burner. Upon stopping the current supply to the solenoid the needle valve, under the action of its spring, is closed and ceases access of fuel to burner.

Ignition plug is a current discharger and serves for ignition of fuel proceeding from starting burner during starting of GTD. Figure 17.6 shows a

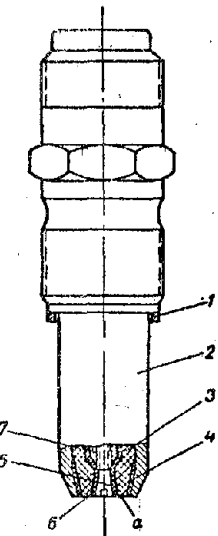


Fig. 17.7.  
Electric ignition plug. 1 - seal,  
2 - body, 3 - ceramic  
insulator, 4 - lateral  
electrode, 5 - screw,  
6 - central  
electrode, 7 -  
nut.

spark plug of high tension. It consists of body 7, inside of which there is a ceramic core with central electrode 9. Lateral electrodes, united in a group, are on the body 8 of the igniter.

During engine starting the pulse current of high tension (more than 10,000 V) moves to the plug from the ignition induction coil. Owing to this, between the central electrode 9 and body 8 there will form an electric spark which ignites the fuel.

Work of ignition device. Starting system of engine has a starting pump with independent electric drive. During engine starting it is actuated and starts to pass fuel to the starting burners of the igniters. Simultaneously with this the current is fed to the solenoid valve of the burner and to the electric ignition plug. Fuel leaving the starting burner is ignited from the electric ignition plug and the forming flame jet then ignites the main fuel proceeding through the working burner to the combustion chamber. After 30 sec of operation, by means of a time relay the supply of current stops and the starting system is turned off.

In the TRD VK-1 the igniters are mounted on two combustion chamber. Transmission of flame to the other seven chambers is carried out through connecting pipes (see Fig. 9.10).

Electric discharge ignition plugs. Along with high-tension plugs, which operate at a voltage of more than 10,000 V, lately the ignitions devices of GTD have electric ignition plugs with surface discharge (Fig. 17.7). For their operation these plugs require a voltage of order of 3000 to 4000 V and are low-voltage plugs.

The core of the plug consists of a ceramic insulator 3 in the central channel of which with the help of screw 5 and nut 7 there is attached a central electrode 6. Lateral electrode 4 carries out contact with the mass through body 2. Ceramic insulator 3 presses the lateral electrode into the body. Hermetic sealing is carried out with the help of thermocement. The material of both the central, and also the lateral electrodes is subjected to electro-erosion during work of the plug, i.e., destruction and atomization by electric spark.

The operating band  $\alpha$  of insulator 3 between central 6 and lateral 4 electrodes is covered by a layer of electrode material and its surface becomes a semiconductor in this manner. Breakdown voltage of the plug is equal to 1200 to 1500 v.

#### 17.4. Ignition Coil

The ignition induction serves for conversion of current of low voltage, proceeding from the aircraft network, into current of higher voltage, which is supplied to the ignition plug. Depending upon type of plug the coils are high-voltage and low-voltage.

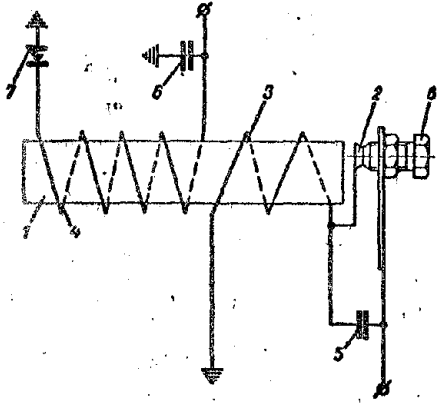


Fig. 17.8. Diagram of induction coil.

Figure 17.8 depicts a diagram of an induction coil, which consists of core 1, breaker 2, primary winding 3, secondary winding 4, condensers 5 and 6, and selenium rectifier 7.

Primary winding by one of its ends through breaker 2 is connected with the aircraft network, having a voltage from 26 to 28 V, and the other is connected with the mass. Upon inclusion of ignition, through the primary winding there starts to flow a current, which, growing in magnitude, creates around the winding a magnetic field. The armature of breaker 2 is attracted to core 1 and breaks the circuit of the primary winding. In the secondary winding there appears a current with voltage in the high-voltage coil no less than 10,000 V, and in the low-voltage coil, no less than 3000 V. This current moves to the ignition plug.

Condenser 5 is connected parallel to the contacts of breaker 2. It promotes fast change of the magnetic flux in the core (guiding of the large electromotive force in the secondary winding).

Selenium rectifier 7 is connected in the circuit of the secondary winding. It cuts off the reverse currents. Condenser 6 in the secondary circuit increases the capacity component of discharge.

Current intensity in the primary circuit is regulated by screw 8 of the breaker. Decrease of current intensity is carried out by turning adjustment screw 8 and increase by unscrewing it.

S E C O N D   P A R T

AIRCRAFT PISTON ENGINES



## C H A P T E R XVIII

### KINEMATICS AND DYNAMICS OF THE CRANKGEAR

Aircraft piston engines are four-cycle high-speed. Before the Second World War aircraft engines had liquid and air cooling of cylinders. The main advantage of first was their relative simplicity of design and convenience of operation. With the appearance of jet engines the application of piston engines was reduced. Air-cooled piston engines are still being used in civil aviation.

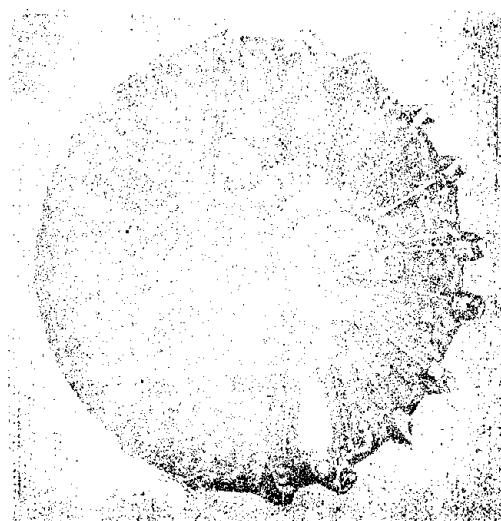


Fig. 18.1. Single-row 9-cylinder radial engine Al-14R.

Air cooling of cylinders in flight is ensured usually by the counter flow of air. Helicopters have low speed of flight and can hover motionlessly in the air. Therefore, the engines which are installed on them are equipped with special fans. The fans ensure supply of air for cooling of cylinders.

For best cooling the cylinders of air-cooled engines are arranged in the form of a star (radial engines). Radial engines are single-row (one star) and double-row (two star). The rear row of cylinders of the double-row

star is arranged with respect to the front row, which forms a checkerboard location of cylinders that ensures uniform cooling of all engine cylinders (see Fig. 23.2).

For uniform alternating of work of cylinders their number in a row is odd (most frequently 7 or 9). As an example Figures 18.1 and 18.2 show the overall

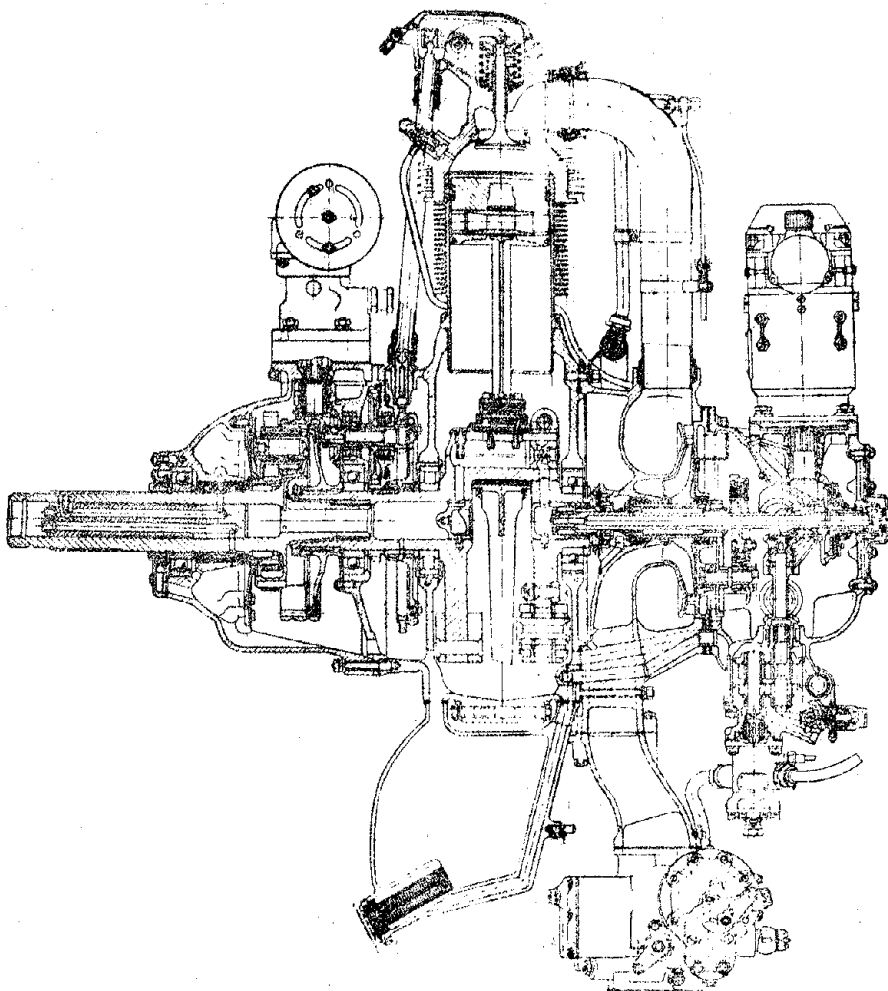


Fig. 18.2. Cross section of AI-14-R radial engine.

view and cross section of the single-row nine-cylinder radial engine [AI-14R] (AM-14P), and Fig. 18.3 shows a cross section of the two-row 14-cylinder radial engine [ASh-82T] (AM-82T). Each row of the latter has seven cylinder a piece.

For increase of power and guarantee of elevation aircraft piston engines have pressure feed. For this purpose there are usually low-pressure supercharger compressors fo the centrifugal type. The supercharger is placed in the rear part of the engine (see Figure 18.2 and 18.3). Centrifugal supercharger has a high speed (20,000 to 30,000 rpm); therefore it is driven from the engine crankshaft by a two-stage gear transmission.

Propellers are selected proceeding from engine power and aerodynamic properties of the aircraft. Optimum propeller speed, corresponding to its maximum performance, in piston engines is usually from 1000 to 1600 rpm with engine speed from 2000 to 2600 rpm. For lowering the propeller speed on piston engines, just as on [TVD] (TBI), there is a reduction gear that is a sun-and-planet

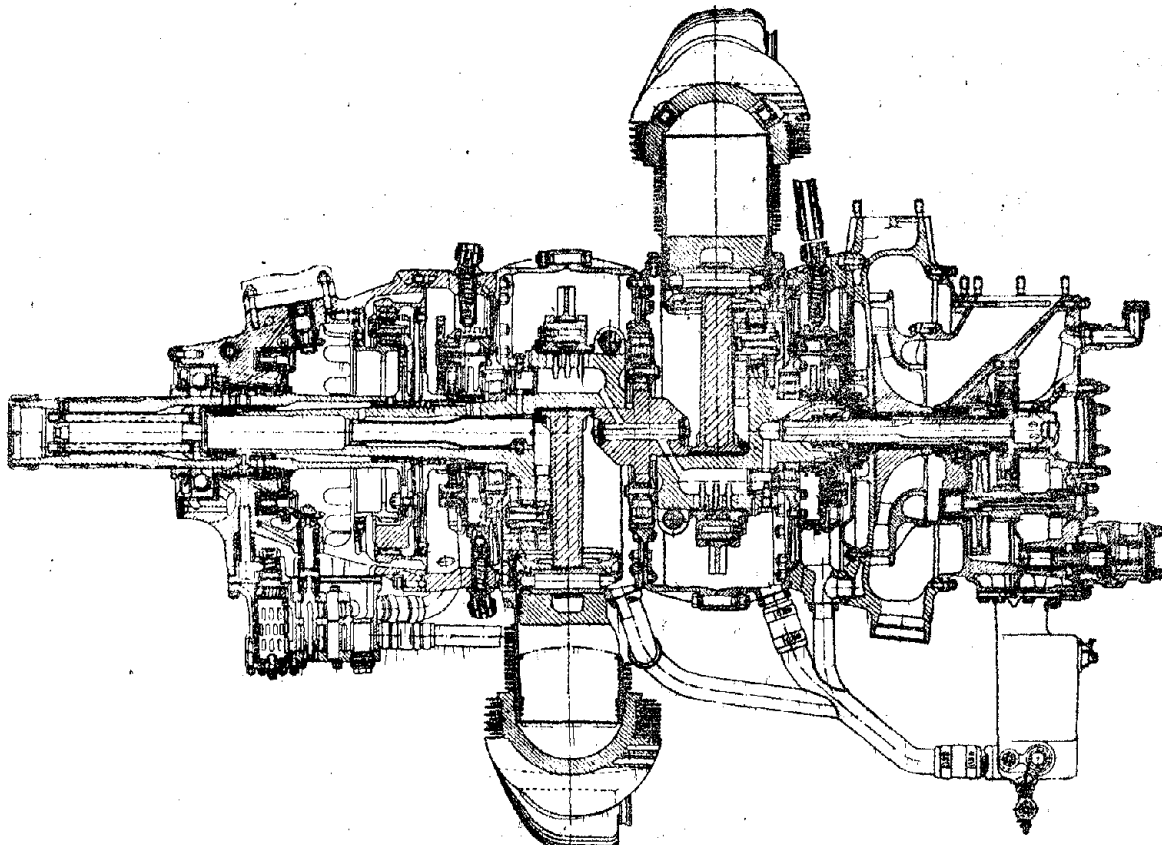


Fig. 18.3. Cross section of ASh-82T two-row radial engine.

gear transmission,

The reduction gear is placed in the front part of the engine and has an output shaft for setting the variable pitch propeller [VISH] (BIII) (see Figures 18.2 and 18.3). Low-capacity engines are frequently made without reduction gears.

The rotor speed of helicopters is about 150 to 300 rpm. In this case the rotor drive transmission has a reduction gear that ensure a transmission ratio from 0.05 to 0.15. Figure 18.4 gives the diagram of the transmission of a single-rotor helicopter; the transmission ensures rotation from piston engine 1 to the main and control rotors. Basic elements of the transmission are the rotor reduction gear 7, gear transmission (reduction gear) of control rotor 11, central transmission 4, clutch 3, free wheel clutch 6, and transmission shafts 5 and 9. The rotor reduction gear 7 is made out in the form of a two-stage sun-and-planet gear transmission and transmission to the control rotor is carried out through two pairs of bevel gears 10 and 11. Central transmission 4 also consists of a pair of bevel gears. The bevel gears ensure transmission of rotation at an angle.

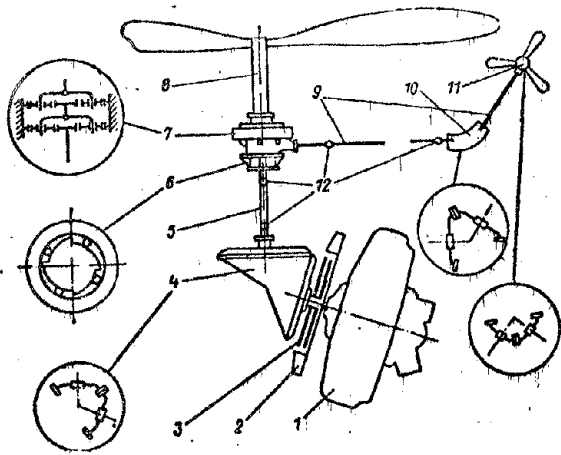


Fig. 18.4. Diagram of the transmission of a single-rotor helicopter. 1 - engine, 2 - fan, 3 - clutch, 4 - central transmission, 5 and 9 - transmission shafts, 6 - free wheel clutch, 7 - rotor reduction gear, 8 - main rotor shaft, 10 - bevel gear, 11 - control rotor reduction gear, 12 - cardan joint.

Clutch 3 engages and disengages the engine from the transmission. This is ensures easy starting of engine and landing of helicopter with engine turned off. Upon engagement of engine the clutches also ensure smooth spin-up of rotor. Free wheel clutch 6 engages drive shaft 5 with rotor 8 only in one direction of rotation and automatically disengages the rotor from the engine in case of engine failure during flight. In this case the rotor passes into conditions of self-rotation and the helicopter slowly glides in for a landing.

#### 18.1. Kinematics of a Normal Crankgear

The crankgear converts the reciprocating motion of the piston into rotation of the engine shaft. Angular velocity of rotation of the latter is:

$$\omega = \frac{\pi n}{30},$$

where  $n$  is the shaft rpm rate.

Piston path from top dead-center (Fig. 18.5).

$$s = L + R - (R \cos \alpha + L \cos \beta),$$

where  $L$  is the length of the gear;

$R$  is the radius of the crank;

$\alpha$  is the angle of rotation of the crank;

$\beta$  is the angle of deviation of the gear.

Angle of deviation of the gear  $\beta$  depends on the angle of rotation of the crank  $\alpha$  (see Fig. 18.5)

$$\sin \beta = \frac{R}{L} \sin \alpha = \lambda \sin \alpha,$$

where  $\lambda = \frac{R}{L}$  is the ratio of radius of crank to length of gear. For aircraft engines  $\lambda = \frac{1}{3,8} \rightarrow \frac{1}{4}$ ,

The expression for piston path contains  $\cos \beta$ , which can be expressed in the following way:

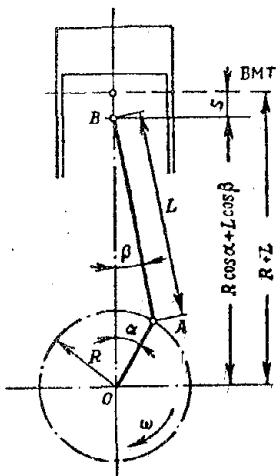


Fig. 18.5. Diagram of a crankgear.

we obtain

$$\cos \beta = 1 - \frac{\lambda^2}{4} + \frac{\lambda^2}{4} \cos 2\alpha.$$

After substitution of the obtained expression for  $\cos \beta$ , and taking into account that  $L=R/\lambda$ , we obtain the formula of the piston path in final form:

$$s = R \left[ \left( 1 + \frac{\lambda}{4} \right) - \left( \cos \alpha + \frac{\lambda}{4} \cos 2\alpha \right) \right]. \quad (18.1)$$

Speed of piston is

$$v = \frac{ds}{dt} = R\omega \left( \sin \alpha + \frac{\lambda}{2} \sin 2\alpha \right), \quad (18.2)$$

Acceleration of piston:

$$f = \frac{dv}{dt} = R\omega^2 \left( \cos \alpha + \frac{\lambda}{2} \cos 2\alpha \right), \quad (18.3)$$

Upon differentiating formulas (18.1 and 18.2) we obtain the term  $d\alpha/dt$ , which is the angular velocity of rotation of the crank;

$$\frac{d\alpha}{dt} = \omega.$$

Figure 18.6 shows graphs of the path, speed, and acceleration of the piston for  $\lambda = 1/4$ .

The normal crankgear system has central joint of gear with crank, at which the crank head of the gear is a bearing for the gear neck of the crankshaft.

One crank of aircraft engines usually receives stress from several cylinders. It is very complicated to design a central joint of several gears with one gear neck of the crankshaft. Therefore engines usually have an attachable joint of gears, in which one is the main gear L and several attachable gears l (Fig. 18.7).

$$\begin{aligned} \cos \beta &= \sqrt{1 - \sin^2 \beta} = \sqrt{1 - \lambda^2 \sin^2 \alpha} \approx \sqrt{1 - \lambda^2 \sin^2 \alpha + \frac{\lambda^4}{4} \sin^4 \alpha} = \\ &= \sqrt{\left( 1 - \frac{\lambda^2}{2} \sin^2 \alpha \right)^2} = 1 - \frac{\lambda^2}{2} \sin^2 \alpha. \end{aligned}$$

Introduced by us, term  $\frac{\lambda^4}{4} \sin^4 \alpha$  supplements the expression under the radical of the perfect square. Value of term  $\frac{\lambda^4}{4} \sin^4 \alpha$  is determined by coefficient  $\lambda^4/4$ , which for  $\lambda=1/4$  is only 0.001.

Considering

$$\sin^2 \alpha = \frac{1 - \cos 2\alpha}{2},$$

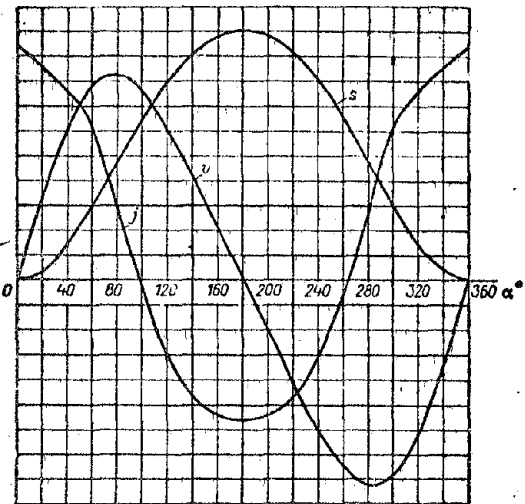


Fig. 18.6. Path, speed, and acceleration of piston depending upon angle of rotation of crank.

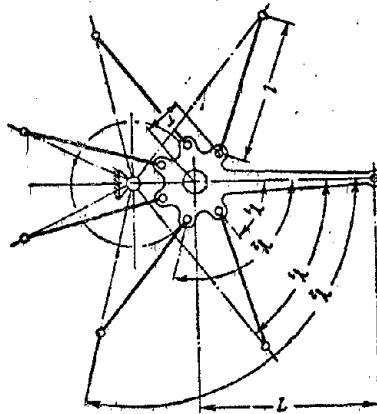


Fig. 18.7. Diagram of attachable gear joint.

The main gear has an extended crank head with a bearing and is directly connected with the gear neck of the crankshaft, which forms the normal crank mechanism (with central joint). Attachable gears by their lower heads with the help of pins are hinged to the crank head of the main gear. Normal crank mechanism is triple-hinged, and the one with attachable gears is four-hinged. This leads to a certain distinction in the kinematics of pistons with the main and attachable gears.

Usually in radial engines the angle of location of the pins on the crank head of the main gear is equal to the angle of breakdown of cylinders  $\gamma$  (see Fig. 18.7), and the length of attachable gears  $l$ , from the conditions of interchangeability, is identical. By means of various radii  $r$  of location of lower heads of attachable gears on the crank head of the main gear there is ensured an identical compression ratio for all cylinders.

Consideration of kinematics of attachable gears exceeds the bounds of this textbook. Subsequently we will use an approximate calculation, disregarding the peculiarity of kinematics of attachable gears and considering conditionally all gears to be central.

#### 18.2. Forces of Inertia of a Crankgear

There are two simple motions of the crank mechanism: the reciprocating motion of the piston along the cylinder axis and rotation of the shaft.

The rod connecting the piston with the crank, performs a complex motion. In the dynamic calculation of the crank mechanism the mass of the connecting rod is

carried on its upper (piston) and lower (crank) heads. These two carried masses are considered to be concentrated on the axes of the piston pin and the gear neck of the crankshaft and accomplishing correspondingly reciprocating motion and rotation. The dynamic equivalence of the system of carried masses of the connecting rod with its real system is ensured by the conditions:

- 1) the sum of carried masses should be equal to the mass of the connecting rod.
- 2) the common center of gravity of the carried masses should coincide with the center of gravity of the connecting rod.

In attachable connecting rods the mass applied to the piston head  $m_{np,u}$  and the mass applied to the crank head  $m_{np,k}$  are found from the following expressions (Fig. 18.8a):

$$\left. \begin{aligned} m_{np,u} &= m_{np} \frac{b}{l} \\ m_{np,k} &= m_{np} \frac{a}{l}, \end{aligned} \right\} \quad (18.4)$$

and

where  $m_{np} = m_{np,u} + m_{np,k}$  is the mass of the attachable connecting rod;

$a$  and  $b$  is the distance from piston and crank heads of connecting rod to its center of gravity;

$l=a+b$  is the length of the attachable connecting rod.

With an unknown position of center of gravity of the connecting rod, it is found on a drawing by means of calculation. With a ready-made connecting rod its center of gravity is found either by means of weighing on specially equipped balances, or by means of rocking.

Mass  $m_{np,k}$  is applied to the main connecting rod and is considered to be concentrated in the pins of the attachable connecting rods (see Fig. 18.8b). Mass of the main connecting rod  $m_r$  together with masses  $m_{np,k}$  form the system of "reduced connecting rod" with mass:

$$m'_r = m_r + \sum m_{np,k}$$

Separate masses, entering the system of the reduced main connecting rod, according to the rules of decomposition of forces into parallel components, are carried on piston and crank heads of the main connecting rod. For an example we will consider the carrying of masses of the reduced main connecting rod with one attachable connecting rod. In this case the mass applied to the piston head  $m'_{ru}$ , and the mass applied to the crank head  $m'_{rk}$ , are found from the expressions (Fig. 18.9):

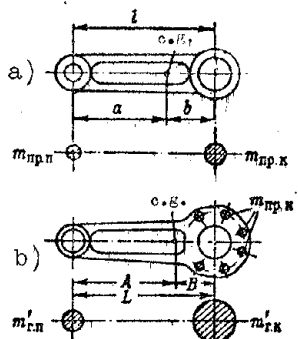


Fig. 18.8. Diagram of carrying of masses of connecting rods.

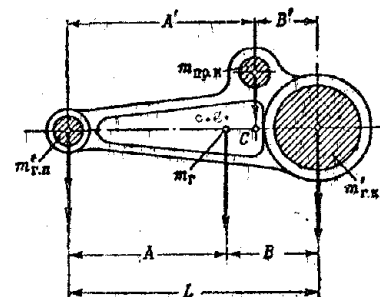


Fig. 18.9. Diagram of carrying of masses of reduced main connecting rod with one attachable connecting rod.

and

$$\left. \begin{aligned} m'_{r,n} &= m_r \frac{B}{L} + m_{np,k} \frac{B'}{L} \\ m'_{r,k} &= m_r \frac{A}{L} + m_{np,k} \frac{A'}{L} \end{aligned} \right\} \quad (18.5)$$

here A and B is the distance of the center of gravity of the main connecting rod from the piston and crank heads;

A' and B' is the distance from point C — projection of axis of pin of attachable connecting rod on axis of main connecting rod — to the piston and connecting rod heads;

$L = A + B$  is the length of the main connecting rod.

In the case of a main connecting rod with several attachable connecting rods (see Fig. 18.8b) expressions (18.5) will take on the following form:

$$m'_{r,n} = m_r \frac{B}{L} + \sum m_{np,k} \frac{B'}{L}$$

and

$$m'_{r,k} = m_r \frac{A}{L} + \sum m_{np,k} \frac{A'}{L}.$$

Since usually attachable connecting rods are identical, these expressions can be reduced to the form:

$$\left. \begin{aligned} m'_{r,n} &= \frac{m_r B + m_{np,k} \sum B'}{L} \\ m'_{r,k} &= \frac{m_r A + m_{np,k} \sum A'}{L} \end{aligned} \right\} \quad (18.6)$$

The forward moving masses [PDM] (ПДМ) of the crankgear include: mass of piston unit  $m_{np}$  and mass of connecting rod, applied to piston head  $m'_{r,n}$  (in the case of a main connecting rod) or  $m_{np,n}$  (in the case of an attachable connecting rod):

$$m_{pdn} = m_{np} + m'_{r,n}$$

or

$$m_{pdn} = m_{np} + m_{np,n}$$

The piston unit contains the piston, piston rings, and piston pin with plugs or locks,

Force of inertia of PDM is

$$P_j = m_{\text{PDM}} j \quad (18.7)$$

where  $j$  is acceleration of PDM during their reciprocating motion.

Force  $P_j$  is variable and depends on angle of rotation of crank  $\alpha$ . Period of its change is  $360^\circ$ . Direction of force  $P_j$  is opposite acceleration  $j$  (see Fig. 18.6), At top dead-center it is directed towards the head of the cylinder, and at bottom dead-centers, towards the crank. Fig. 18.12 depicts the curve of  $P_j = f(\alpha)$ .

The rotating masses [VDM] (BIM) of the crankgear include the mass of the main connecting rod, applied to the crank  $m'_{\text{cr}}$ , and mass of the elbow  $m_k$ , forming the crank,

Centrifugal force of inertia of revolving masses of the connecting rod will be

$$C = -m'_{\text{cr}} R \omega^2 \quad (18.8)$$

Centrifugal force of elbow

$$C_k = -m_k r_s \omega^2,$$

where  $r_s$  is the radius of location of center of gravity  $s$  of the crank.

For convenience the mass of the elbow with the center of gravity at radius  $r_s$  is usually replaced by mass  $m'_k$ , applied to the radius of crank  $R$  (Fig. 18.10).

From the condition of dynamic equivalence

$$C_k = -m_k r_s \omega^2 = -m'_k R \omega^2,$$

whence the reduced mass of the elbow

$$m'_k = m_k \frac{r_s}{R}.$$

Thus, the rotating mass of the crank mechanism will be

$$m_{\text{BIM}} = m'_{\text{cr}} + m'_k$$

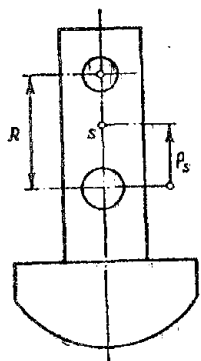


Fig. 18.10  
Reduction  
of mass of  
crank to  
radius  $R$ .

and centrifugal force of VDM is

$$C_{\text{BIM}} = -m_{\text{BIM}} R \omega^2. \quad (18.9)$$

Centrifugal force of VDM is directed along the radius of the crank,

### 18.3. Forces of Gas Pressure

Pressure of gases acting on the piston may be determined by a simplified theoretical indicator diagram (Fig. 18.11). For its construction we should know the pressure of pressure feed  $p_a$ , average indicated pressure  $p_i$  and compression ratio  $\epsilon$ . Pressure in cylinder in the beginning of compression is

$$p_a = (0.9 \div 0.95) p_a$$

Pressure of gases in the course of compression varies according to polytropic law:

$$p = p_a \left( \frac{V_a}{V} \right)^{1.35}; \quad (18.10)$$

where  $V$  and  $V_a$  are the current and total volumes of the cylinder.

Pressure at the end of the compression cycle is

$$p_e = p_a \epsilon^{1.35}. \quad (18.11)$$

Theoretical flash pressure is determined from the following expression:

$$p'_e = 0.91 p_e + A p_i, \quad (18.12)$$

where coefficient  $A$  is taken from the following data:

$\epsilon$	5	5.5	6	6.5	7	7.5
$A$	0.314	0.338	0.360	0.383	0.405	0.425

Pressure of gases in the expansion cycle varies according to polytropic law:

$$p = p_b \left( \frac{V_a}{V} \right)^{1.24}. \quad (18.13)$$

where  $p_b$  is the pressure at the end of the expansion cycle, which is found with the following formula:

$$p_b = \frac{p'_e}{\epsilon^{1.24}}. \quad (18.14)$$

Obtained peak of maximum flash pressure on the indicator diagram is cut off to the magnitude

$$p_z = 0.85 p'_e.$$

Inlet and outlet cycles occur at low pressures of gases and therefore they are not constructed on the diagram.

The theoretical indicator diagram gives the change of pressure of gases in the cylinder depending upon their volume in the cycles of compression and expansion.

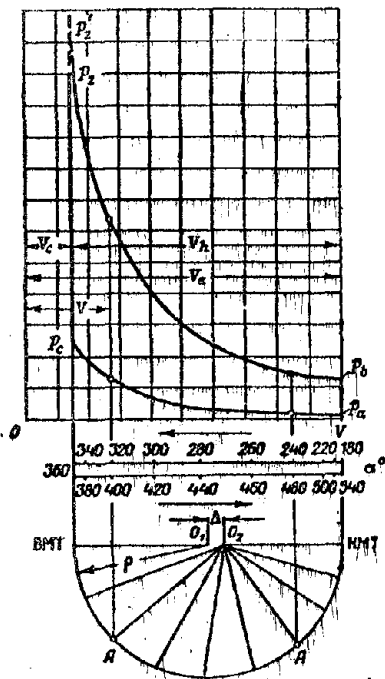


Fig. 18.11. Theoretical indicator diagram.

For every angle  $\alpha$  of turn of the crank by formula (18.1) one can determine the piston path  $S$ , and then by formula (18.15) the volume of gases  $V$ . This will allow us to construct under the indicator diagram a scale of angles of turn of the crankshaft (see Fig. 18.11).

The same can be done by graphic method. For this, under the indicator diagram we draw a semicircle with radius  $\rho$ , equal to half of segment  $V_h$ , and with center at point  $O_1$ . On diameter of semicircle we plot point  $O_2$ , displaced in the direction of bottom dead-center by the magnitude

$$\Delta = \frac{\lambda L}{2}$$

where  $\lambda = \frac{R}{L}$  is the relation of radius of crank  $R$  to length of connecting rod  $L$ .

Then from point  $O_2$  every other  $20^\circ$  we draw lines intersecting the semicircle in points  $A$ . Projections of points  $A$  on the axis of abscissas form the scale of angles of rotation of crankshaft in the compression and expansion cycles (see Fig. 18.11).

Fig. 18.12. Change of total force  $P_\Sigma$  depending upon angle of rotation of crank,

The indicator diagram with scale of angles of rotation of crank gives the change of absolute pressure  $p$  in the cylinder depending upon angle of rotation of crank. Force of pressure of gases on piston will be:

$$P_r = (p - p_h) F_n \quad (18.16)$$

where  $p$  is the absolute pressure of gases in cylinder;

$p_h$  is the external atmospheric pressure acting on the piston in the area of the crankcase;

$F_u$  is the area of the piston.

Calculations are made every other  $20^\circ$  turn of the crank and according to the obtained data the curve of  $P_r = f(\alpha)$  (Fig. 18.12) is constructed.

#### 18.4. Total Forces from One Cylinder

The connecting rod is influenced by the force of gases and force of inertia of PDM. These forces are periodically changed. In a four-cycle engine the period of change of force of gases is  $720^\circ$ , and the force of inertia is  $360^\circ$  with respect to angle of rotation of crank.

Algebraic sum of these forces gives the total force (see Fig. 18.12):

$$P_z = P_r + P_j \quad (18.17)$$

Force  $P_z$ , acting on the connecting rod, is decomposed according to the rules of mechanics into two components: into force  $N$  of lateral pressure of piston on wall of cylinder and force  $K$  acting along the axis of connecting rod (Fig. 18.13). These forces are equal to

$$N = P_z \operatorname{tg} \beta, \quad (18.18)$$

$$K = P_z \frac{1}{\cos \beta}. \quad (18.19)$$

Force  $N$  causes friction of piston against cylinder and creates disturbance of engine. Force  $K$  is transmitted through connecting rod to crank and in turn

is decomposed into two components: into tangential force  $T$  and normal force  $Z$ ; these forces are equal to:

$$T = K \sin(\alpha + \beta) = P_z \frac{\sin(\alpha + \beta)}{\cos \beta}; \quad (18.20)$$

$$Z = K \cos(\alpha + \beta) = P_z \frac{\cos(\alpha + \beta)}{\cos \beta}. \quad (18.21)$$

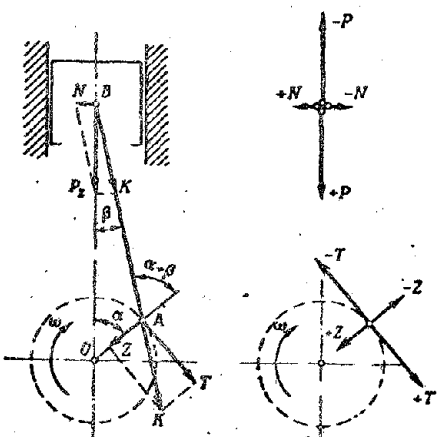


Fig. 18.13. Decomposition of forces, acting on crankgear.

Forces  $T$  and  $Z$  are variable in magnitude and direction and depend on angle of rotation of crank. Force  $T$  is directed on a tangent to the circumference of rotation of the crank and creates its torque. Positive force  $T$  is directed towards rotation of the crank, and negative against the rotation.

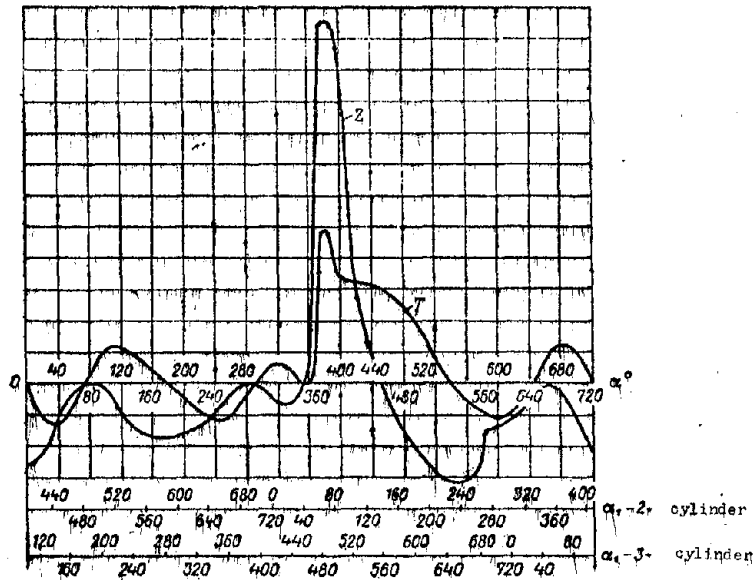


Fig. 18,14. Change of tangential  $T$  and normal  $Z$  forces depending on crank rotation angle.

Force  $Z$  is directed along the crank. Positive force compresses the crank, and negative stretches it (see Fig. 18,13). Figure 18,14 shows the change of forces  $T$  and  $Z$  depending upon angle  $\alpha$  of crank rotation.

#### 18,5. Firing Sequence

Firing order of an engine usually is determined by the firing sequence. Aircraft piston engines are of the four-cycle type in which firing in the cylinders occurs every two rotations of the crankshaft.

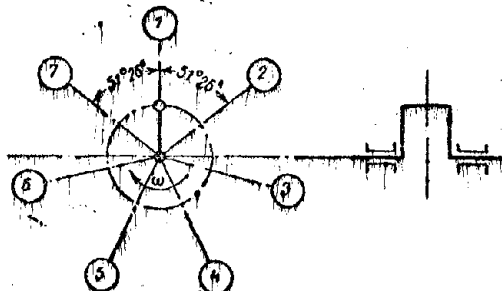


Fig. 18,15. Firing sequence of a single-row seven-cylinder engine.

For obtaining the most uniform torque and consequently, smaller loads on the crankshaft, firing in the engine cylinders of motor must be alternated in identical angles of rotation of crankshaft  $720/i$ , where  $i$  is the number of engine cylinders.

Uniform alternating of firing is ensured

by appropriate location of engine cylinders and selection of their number, and also by selection of angle of breakdown of elbows in the case of a double-elbow shaft. In a single-row radial engine the work of all cylinders is transmitted to one elbow (crank), and in a two-row radial engine to two elbows.

In the radial location of engine cylinders uniform alternating of firing is obtained with firing sequence in one cylinder in the direction of rotation of the shaft. This is possible only with an odd number of cylinders. Therefore

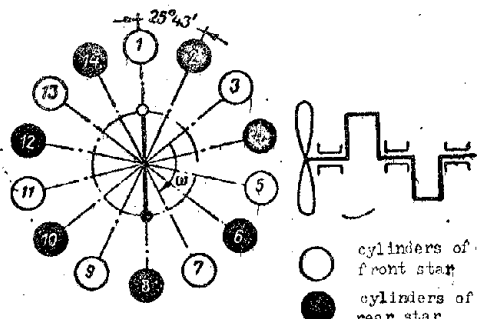


Fig. 18.16. Firing sequence of a two-row 14-cylinder radial engine.

radial engines usually have odd number of cylinders in a row. In conformity with this, for instance, the firing sequence of a single-row 7-cylinder radial engine (Fig. 18.15) will be: 1 - 3 - 5 - 7 - 2 - 4 - 6 - 1.

In two-row radial engines the elbows (cranks) have breakdown  $180^\circ$  and firing occurs first in the front, then in the rear star. For instance, the firing sequence of a 14-cylinder engine will be (Fig. 18.16), 1 - 10 - 5 - 14 - 9 - 4 - 13 - 8 - 3 - 12 - 7 - 2 - 11 - 6 - 1.

#### 18.6. Summation of Crank Forces T and Z

To one crank of aircraft engines there usually is transmitted work from several cylinders. From each cylinder through the connecting rod on the crank there act tangential T and normal Z forces. Forces T and Z of each cylinder are expressed by curves depicted in Fig. 18.14, in which  $\alpha$  is the angle of rotation of the crank with respect to the axis of its cylinder.

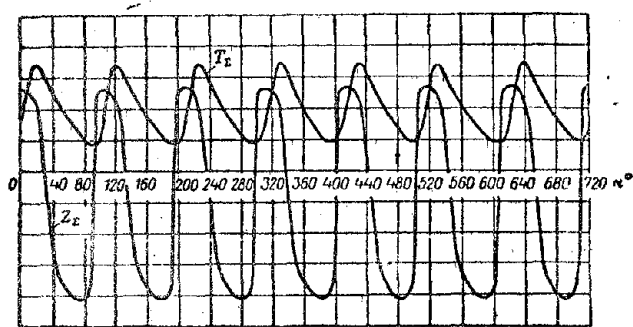


Fig. 18.17. Change of forces T and Z depending upon angle of rotation of crank.

In the summation of forces T and Z of all cylinders, acting simultaneously on one crank, curves  $T = f(\alpha)$  and  $Z = f(\alpha)$  for each cylinder must be reduced to angle  $\alpha_1$ , i.e., rotation of crank with respect to the axis of the main cylinder (having the main connecting rod). The latter, with respect to firing sequence, is

considered to be the first. If angle of rotation of crank with respect to the axis of the k-th cylinder is  $\alpha_k$ , to it will correspond the angle of rotation with respect to the axis of the first (main) cylinder

$$\alpha_1 = \alpha_k + (n-1) \frac{720}{l_{sp}},$$

where n is an ordinal number characterizing the place occupied by the k-th cylinder with respect to firing sequence in star;

$l_{sp}$  is the number of cylinders in the star.

With the help of this formula it is possible curves  $T = f(\alpha)$  and  $Z = f(\alpha)$  to construct for each cylinder its scale of angles of revolution of the crank with respect to the main cylinder. Figure 18.14 shows the scales for the 2nd and 3rd cylinders of a seven-cylinder radial engine.

Using these scales, one can determine simultaneous values of forces  $T$  and  $Z$  in all engine cylinders for every angle  $\alpha_1$ . Total forces  $T_{\Sigma}$  and  $Z_{\Sigma}$ , acting on the crank from all cylinders, will be equal to:

$$T_{\Sigma} = \sum_{i=1}^{i_{\Sigma}} T_i \text{ and } Z_{\Sigma} = \sum_{i=1}^{i_{\Sigma}} Z_i.$$

Forces  $T_{\Sigma}$  and  $Z_{\Sigma}$  are variable having period, with respect to angle of rotation of crank, equal to  $\frac{720}{i_{\Sigma}}$ . Figure 18.17 depicts curves of forces  $T_{\Sigma}$  and  $Z_{\Sigma}$  for a seven-cylinder radial engine.

#### 18.7. Force Acting on the Connecting Rod Journal of an Angular Shaft

The connecting rod journal of a crankshaft during operation is loaded by total tangential force  $T_{\Sigma}$ , total normal force  $Z_{\Sigma}$ , and centrifugal force of revolving masses of connecting rod  $C$ . Forces  $Z_{\Sigma}$  and  $C$  act on the crank. Adding them algebraically, we obtain:

$$Z_s = Z_{\Sigma} + C.$$

Forces  $T_{\Sigma}$  and  $Z_s$  are mutually perpendicular and their resultant will be equal to:

$$U = \sqrt{T_{\Sigma}^2 + Z_s^2}, \quad (18.22)$$

This force has a periodic character and depends on the angle of rotation of the crank  $\alpha$ . Force  $U$  is transmitted to the connecting rod journal of the shaft through the connecting rod bearing, i.e., the connecting rod bearing is loaded by the reaction from force  $U$ .

#### 18.8. Torque

Torque acting on one crank of a radial engine is equal to

$$M_{kp} = T_{\Sigma} R, \quad (18.23)$$

where  $R$  is the radius of the crank. Like forces  $T_{\Sigma}$ , torque with respect to angle of rotation of crank is variable.

Torque from each crank of a two-row radial engine is expressed by formula (18.23). In the summation of torques from both cranks one should consider relative shift of firing sequences in the front and rear stars of the cylinders.

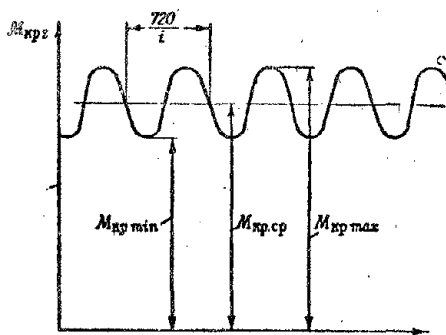


Fig. 18.18. Change of total engine torque with respect to angle of rotation of crankshaft.

The shift is equal, with respect to angle of rotation of crank, to  $720/i$ , where  $i=2l_{\text{cy}}$  is the number of engine cylinders.

Figure 18.18 depicts the curve of engine torque. Period of change of torque with respect to angle of rotation of crankshaft is  $720/i$ .

The mean ordinate of the curve  $M_{kp} = f(\alpha)$  gives the mean value of engine torque  $M_{kp, \text{cp}}$ . In a correct calculation the value of  $M_{kp, \text{cp}}$  should coincide with its value obtained by the formula

$$M_{kp, \text{cp}} = 71620 \frac{N_i}{n},$$

where  $N_i$  is the indicated horsepower of the engine;

$n$  is the rpm rate of the crankshaft.

#### 18.9. Disturbing Moment

Figure 18.19 depicts the forces applied in points A and B of a crankgear.

Forces  $T$  and  $Z$ , applied at point A, can be transferred to point O, i.e., the center of rotation of the crank. The appearing pair of forces  $T$  and  $T'$  form the torque of the crank  $M_{kp}$ . The remaining forces  $T$  and  $Z$  can be added according to the rule of the parallelogram and force  $K$  can be obtained. Extending it then to the vertical and horizontal axis, we obtain the forces  $P_{\Sigma}$  and  $N$ .

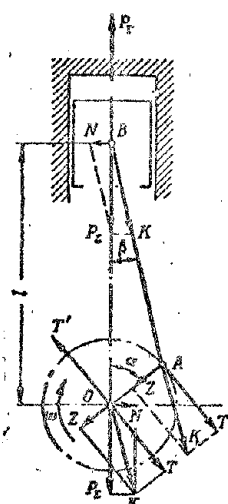


Fig. 18.19.  
Determination  
of disturbing  
moment.

Force  $P_{\Sigma}$  is expressed by formula (18.17) and is the sum of forces of gases  $P_F$  and forces of inertia of PDM<sup>1</sup>  $P_j$ .

Force  $P_F$ , applied to point O, is balanced in the engine system by the same force  $P_T$  acting on the head of the cylinder (see Fig. 18.19). Force  $P_j$ , applied to point O, the center of rotation of the crank, remains free. It is directed along the axis of the cylinder. Its balancing is considered in Chapter XIX.

Forces  $N$  are applied to the wall of the cylinder and in the center of rotation of the crank. They are expressed by formula (18.18) and form a disturbing pair of engine forces with the arm

<sup>1</sup>Forward - moving masses.

$$l = R \cos \alpha + L \cos \beta = R \left( \cos \alpha + \frac{1}{\lambda} \cos \beta \right).$$

Disturbing moment from forces  $N$  is directed opposite the direction of torque. Therefore it is taken with the minus sign:

$$\begin{aligned} M_{\text{on}} &= -Nl = -P_1 \operatorname{tg} \beta R \times \\ &\times \left( \cos \alpha + \frac{1}{\lambda} \cos \beta \right) = -P_1 R \frac{\sin(\alpha + \beta)}{\cos \beta}. \end{aligned}$$

Comparing the obtained expression with expression (18.20), we obtain:

$$M_{\text{on}} = -TR = -M_{\text{kp}},$$

i.e., disturbing moment is equal in magnitude to torque, but is directed opposite the latter. In multi-cylinder engines, from each cylinder there appear disturbing moments, which in the engine are summarized.

Test of engines is frequently produced on balance stands. For determination of engine power they measure its disturbing moment and speed.

## C H A P T E R XIX

### BALANCING OF PISTON ENGINES

#### 19.1. General Information

An engine is balanced if the forces of inertia of its forward-moving and revolving masses are balanced. Forces of pressure of gases in piston engines are balanced (see Chapter XVIII, 18.9). Forces of inertia of [VDM<sup>1</sup>] (ВДМ) [PDM<sup>2</sup>] (ПДМ) and their moments in a system of radial engines are balanced with the help of counterpoises.

In Chapter XVIII the centrifugal force of VDM is expressed by formula (18.9), and force of inertia of PDM by formula (18.7). In these formulas forces  $C_{\text{ВДМ}}$  and  $P_j$  have negative sign. However, in the investigation of engine balancing it is more convenient to reverse the signs of these forces and to consider these forces to be positive if they are directed from the axis of the shaft. We shall take centrifugal force of VDM by formula (18.9):

$$C_{\text{ВДМ}} = m_{\text{ВДМ}} R \omega^2 \quad (19.1)$$

and force of inertia of PDM by formula (18.7):

$$P_j = m_{\text{ПДМ}} i = m_{\text{ПДМ}} R \omega^2 (\cos \alpha + \lambda \cos 2\alpha). \quad (19.2)$$

The last expression can be presented in the form:

$$P_j = P_1 + P_2,$$

where  $P_1$  is a force of inertia of the 1st order,

<sup>1</sup>Revolving masses.

<sup>2</sup>Forward - moving masses.

$$P_1 = m_{\text{DM}} R \omega^2 \cos \alpha \quad (19.3)$$

and  $P_2$  is a force of inertia of the 2nd order,

$$P_2 = \lambda m_{\text{DM}} R \omega^2 \cos 2\alpha. \quad (19.4)$$

Centrifugal force of VDM is constant in magnitude, but variable in direction. Balancing of VDM was considered in Chapter VI. Forces of inertia of PDM of the 1st and 2nd orders are variable both in magnitude, and also in direction. Period of change of force of inertia of the 1st order  $P_1$  corresponds to one revolution of the crank, and period of change of force of inertia of the 2nd order  $P_2$  corresponds to half a revolution of the crank. In connection with this, their balancing is considered separately. In the crankshaft system the forces  $P_1$  and  $P_2$  are directed toward the axes of their cylinders. Magnitude of amplitude force of inertia of the 2nd order is less than that of the 1st order and composes 25-28% of it.

#### 19.2. Balancing of Single-row Radial Engines

During engine operation the forward moving masses of each cylinder experience forces of inertia of the 1st and 2nd order, which vary periodically with respect to angle of rotation of crank. They are directed toward the axes of their cylinders. These forces are transferred to the crankshaft and, geometrically summarizing, lead to resultant forces of the 1st and 2nd order.

Figure 19.1 shows the geometric summation of forces of inertia of PDM of the 1st order in a five-cylinder radial engine for current angle of rotation of crank. In a similar manner it is possible to perform summation of the forces of inertia of the 2nd order. As a result of such summation we may be convinced that the resultant forces of inertia of PDM of the 1st and 2nd order of radial engines are equal to:

$$P_{21} = \frac{1}{2} i_{\text{ss}} m_{\text{DM}} R \omega^2; \quad (19.5)$$

$$P_{22} = i_{\text{ss}} \lambda \frac{r}{l} m_{\text{DM}} R \omega^2, \quad (19.6)$$

where  $m_{\text{DM}}$  is the PDM of one cylinder;

$R$  is the radius of the crank;

$i_{\text{ss}}$  is the number of cylinders in a row;

$\omega$  is the angular velocity of rotation of the shaft;

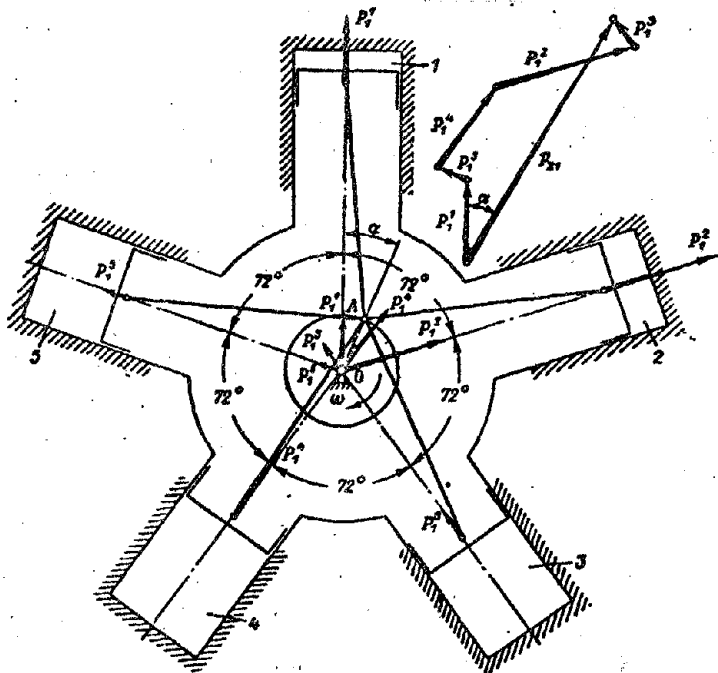


Fig. 19.1. Determination of resultant forces of inertia of PDM of a radial engine.

$\lambda$  is the relation of radius of crank  $R$  to length of main connecting rod  $L$ ;

$r$  is the radius of location of pins of attachable connecting rods on crank head of main connecting rod (see Fig. 18.3);

$l$  is the length of the attachable connecting rods (see Fig. 18.3).

The resultant forces of inertia of PDM of the 1st and 2nd order in a system of radial engines are constant in magnitude and variable in direction. They are revolving vectors of forces.

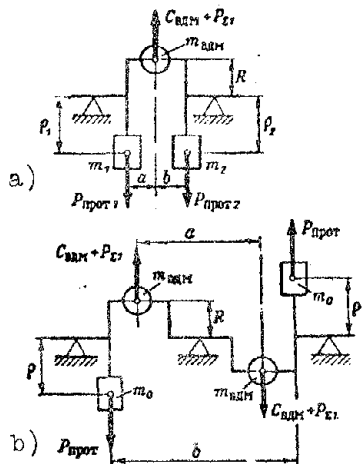


Fig. 19.2. Balancing diagram of inertia forces of VDM and 1st order of PDM of radial engines.

With the help of constructions (see Fig. 19.1) it is possible also to be convinced that the vector of resultant force of inertia of the 1st order  $P_{\Sigma 1}$  coincides with the direction of rotation of the crank revolving together with it at the same angular velocity  $\omega$  and in the same direction as the crank.

Therefore in single-row radial engines the force  $P_{\Sigma 1}$  is balanced jointly with centrifugal force of VDM  $C_{BDM}$  by common counterpoises. For this purpose, on the extent of the sides of the shaft two counterpoises are mounted. Condition of balancing of these forces will be (Fig. 19.2a)

$$C_{\text{VDM}} + P_{z1} = P_{\text{uprot1}} + P_{\text{uprot2}}$$

or

$$\left( m_{\text{vdm}} + \frac{1}{2} i_{\text{so}} m_{\text{vdm}} \right) R = m_1 p_1 + m_2 p_2. \quad (19.7)$$

Condition of balancing of moments can be presented in the following form:

$$P_{\text{uprot1}} a = P_{\text{uprot2}} b$$

or

$$m_1 p_1 a = m_2 p_2 b, \quad (19.8)$$

where  $m_1$  and  $m_2$  are the masses of the counterpoises;

$p_1$  and  $p_2$  are the radii of location of centers of gravity of the counterpoises;

$a$  and  $b$  is the distance from middle plane of elbow to counterpoises.

With the help of geometric summation (see Fig. 19.1) one can be certain that the vector of resultant force of inertia of PDM of the 2nd order  $P_{\Sigma 2}$  revolves with angular velocity  $2\omega$  of rotation of the crank.

At angle of revolution of crank with respect to the main cylinder (with main connecting rod)  $\alpha = 0$  the vector of force  $P_{\Sigma 2}$  with the crank composes angle  $180^\circ$ , and with revolution of crank at angle  $\alpha = 180^\circ$  it coincides with it. In single-row radial engines force  $P_{\Sigma 2}$  usually remains unbalanced.

### 19.3. Balancing of Two-Row Radial Engines

The angular shaft of two-row radial engines has two elbows with angle of breakdown  $180^\circ$ . Centrifugal forces of VDM  $C_{\text{VDM}}$  and resultant forces of inertia of the 1st order of PDM  $P_{\Sigma 1}$  are directed along their elbows. Forces in both elbows are equal and form a pair of forces with moment (see Fig. 19.2b):

$$M_1 = (C_{\text{VDM}} + P_{z1}) a,$$

where  $a$  is the arm of the pair.

This moment is balanced by counterpoises attached along the extreme sides of the shaft.

Condition of balancing is the following:

$$m_0 \rho b = \left( m_{\text{vdm}} + \frac{1}{2} i_{\text{so}} m_{\text{vdm}} \right) R a, \quad (19.9)$$

where  $a$  and  $b$  are the arms of pairs of forces;

$m_0$  is the mass of each counterpoise;

$\rho$  is the radius of location of centers of gravity of counterpoises.

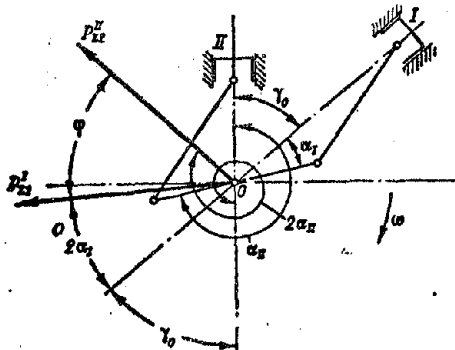


Fig. 19.3. Diagram of resultant forces of inertia of PDM of the 2nd order of a two-row radial engine.

Resultant forces of inertia of PDM of the 2nd order  $P_{Σ2}$  in elbows of the shaft also are equal. Figure 19.3 depicts the position of vectors of forces  $P_{Σ2}^I$  of the front and  $P_{Σ2}^{II}$  rear stars. Axes of main cylinders (with main connecting rods) of front I and rear II stars have angle of breakdown  $γ_0$ .

Upon revolution of elbow of front star at angle  $α_I$ , and elbow of rear star correspondingly at angle

$$α_{II} = 180 + α_I + γ_0$$

the vectors of forces  $P_{Σ2}^I$  and  $P_{Σ2}^{II}$  will revolve from their initial positions at angles  $2α_I$  and  $2α_{II}$ . The angle between vectors of forces  $P_{Σ2}^I$  and  $P_{Σ2}^{II}$  (taking into account expression  $α_{II}$ )

$$φ = 2α_{II} - 360 - γ_0 - 2α_I = γ_0. \quad (19.10)$$

Thus the angle between vectors of forces  $P_{Σ2}^I$  and  $P_{Σ2}^{II}$  is equal to the angle of breakdown between the main cylinders. Sometimes the angle of breakdown of the main cylinders is  $γ_0 = 180^\circ$ . In this case the forces of inertia of the 2nd order of PDM of the front and rear stars are located in one plane and form a rotating pair of forces with moment

$$M_2 = P_{Σ2}a. \quad (19.11)$$

Forces of inertia of the 2nd order or PDM of powerful engines attain large values and therefore they frequently are balanced with the help of two balancing counterpoises.

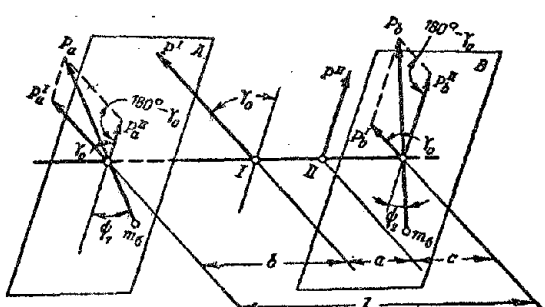


Fig. 19.4. Balancing of forces of inertia of the 2nd order of a two-row radial engine.

Figure 19.4 shows the balancing of forces  $P_a^I = P_b^I = P_{Σ2}$ . These forces are located in planes passing through points I and II perpendicular to the shaft, and form between themselves angle  $γ_0$ . Let us take two planes A and B, which contain balancing counterpoises that balance these forces.

Let us expand these forces into parallel forces applied to the shaft in planes A and B. Their components will be equal to:

$$P_a' = P^I \frac{a+c}{l} \text{ and } P_b' = P^I \frac{b}{l},$$

$$P_a'' = P^{II} \frac{c}{l} \text{ and } P_b'' = P^{II} \frac{b+a}{l}.$$

Thus it is possible to replace forces  $P^I$  and  $P^{II}$  by an equivalent force system applied to the shaft in planes A and B. Let us take  $b = c$ ; then

$$P'_a = P''_b \quad \text{and} \quad P'_b = P''_a.$$

In this case the resultant forces in planes A and B will equal to

$$P_a = P_b = \sqrt{(P'_a)^2 + (P''_a)^2 - 2P'_a P''_a \cos(180 - \gamma_0)}. \quad (19.12)$$

Resultant forces  $P_a$  and  $P_b$  are balanced with the help of counterpoises located in planes A and B and revolving with angular velocity  $2\omega$ :

$$m_\sigma \rho (2\omega)^2 = P_a = P_b,$$

where  $m_\sigma$  is the mass of a counterpoise;

$\rho$  is the radius of location of center of gravity of a counterpoise.

The mass of the balancing counterpoises will then be equal to:

$$m_\sigma = \frac{\rho P_a}{4\omega^2}. \quad (19.13)$$

Angles of location of counterpoises are found with the theorem of sines:

$$\sin \psi_1 = \frac{P'_a}{P_a} \sin(180 - \gamma_0)$$

$$\sin \psi_2 = \frac{P'_b}{P_b} \sin(180 - \gamma_0).$$

#### 19.4. Pendulum Counterpoises Dampers of Twisting Vibrations

Figure 19.5 shows an elastic shaft, on one end of which there is a solid disk, and the other end is rigidly fixed. If the shaft is twisted at angle  $\varphi_A$ , and then let go, the system begins to vibrate. These vibrations are called twisting, since they are accompanied by twisting of the shaft. These vibrations are also called natural or free, since the system, removed initially from the state of rest, further accomplishes its vibrations freely without the influence of external forces and only due to the elasticity of the shaft and inertia of mass of the disk.

Angular deviation of the disk during natural vibrations of the system is expressed by harmonic law with formula (8.1):

$$\varphi = \varphi_A \sin(pt + \beta_0),$$

where  $\varphi_A$  is the amplitude of vibrations, i.e., the largest angle of deviation of the disk from its central position;

$p$  is the angular frequency;

$t$  is the time

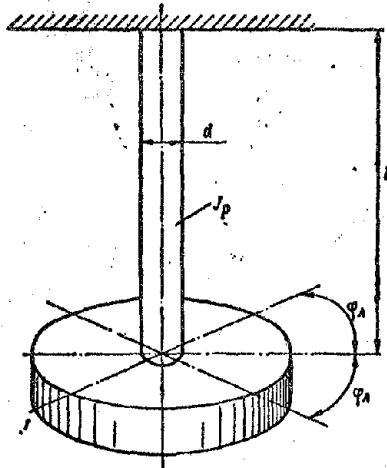


Fig. 19.5. Torsional vibrations of a shaft with one disk.

$\beta_0$  is the initial phase.

Period of natural vibrations of the shaft is equal to:

$$T = \frac{2\pi}{p},$$

number of natural vibrations of shaft per minute will be equal to:

$$n_e = \frac{60}{T} = \frac{30p}{\pi}.$$

Hence the angular frequency of natural vibrations of the shaft is equal to:

$$p = \frac{\pi n_e}{30}. \quad (19.14)$$

Crankshaft with reduction gear and propeller form an elastic multimass system having natural frequency of torsional vibrations.

During work of engine the crankshaft is loaded by torque which is variable in magnitude and depends on angle of rotation of crank (see Fig. 18.18). Expression of torque can be represented in the form of a sum:

$$M_{kp} = M_{cp} + M_{var},$$

where  $M_{cp}$  is the mean constant torque,

$M_{var}$  is the variable part of torque.

Under the action of moment  $M_{var}$  the crankshaft will twist at a larger, and then at a smaller magnitude, i.e., the shaft will experience forced torsional vibrations. In radial engines the variable part of torque can be represented in the form of the sum of two harmonic moments:

$$M_{var} = M_1 \sin(\Omega_1 t + \beta_1) + M_2 \sin(\Omega_2 t + \beta_2), \quad (19.15)$$

where  $M_1$  and  $M_2$  are the peak volumes of harmonic moments;

$\Omega_1$  and  $\Omega_2$  are the angular frequencies of harmonic moments;

$t$  is the time;

$\beta_1$  and  $\beta_2$  are the initial phases.

Angular frequencies of harmonic moments are expressed in the following manner:

$$\Omega_1 = \frac{1}{2} l_{ss} \omega \text{ and } \Omega_2 = l_{ss} \omega,$$

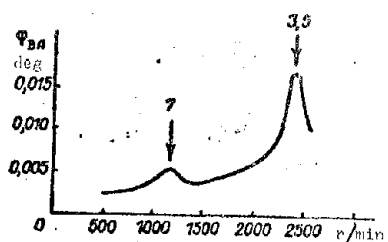


Fig. 19.6. Change of amplitude of vibrations of the crankshaft of a 14-cylinder radial engine depending on its speed.

Hence the order of harmonic moments of radial engines will be correspondingly equal to:

$$q_1 = \frac{\Omega_1}{\omega} = \frac{1}{2} i_{3B} \text{ and } q_2 = \frac{\Omega_2}{\omega} = i_{3B}.$$

For the [ASh-82T] (AM-82T) engine, having  $i_{3B} = 7$ , we obtain harmonic moments  $q_1 = 3\frac{1}{2}$  and  $q_2 = 7$  orders.

Critical (resonance) engine speed is characterized by the fact that angular frequency  $\Omega_1 = q_1 \omega$  or  $\Omega_2 = q_2 \omega$  of one of the harmonic moments becomes equal to the angular frequency  $p$  of natural vibrations of the shaft:

$$\Omega = p. \quad (19.17)$$

But

$$\Omega = q\omega = q \frac{\pi n}{30}, \quad (19.18)$$

where  $n$  is the rpm rate of the crankshaft.

Putting in formula (19.17) expressions (19.18) and (19.14), we find critical (resonance) engine speed:

$$n_{cp} = \frac{n_c}{q}. \quad (19.19)$$

Figure 19.6 shows the amplitudes of vibrations of the crankshaft of the radial engine ASh-82T in radians depending upon speed. Since in the ASh-82T engine the number of natural vibrations of the shaft per minute

$n_c = 8340$  vib/min, we obtain two resonance conditions:

$n_{cp1} = 1160$  r/min from a 7th order harmonic and

$n_{cp2} = 2320$  r/min from  $3\frac{1}{2}$  order harmonic.

For removal of resonance shaft vibrations radial engines usually have attenuators of torsional vibrations (dampers) in the form of counterpoises with a pendulum suspension (Fig. 19.7). The pendulum (bifilar) suspension is placed in two points with the help of two pins, inserted freely in corresponding holes,

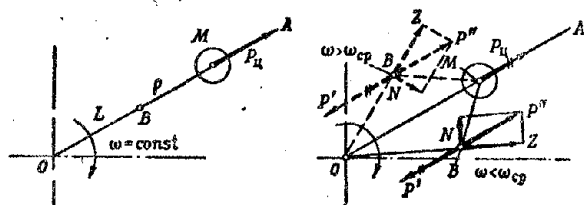
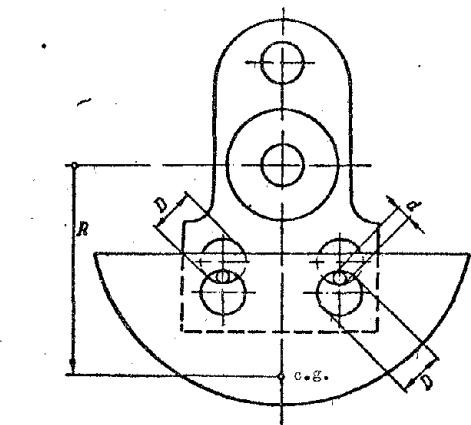


Fig. 19.7. Counterpoise with bifilar suspension.

and arm  $p$  are arranged on one straight line.

Upon the appearance of torsional vibrations, rod L, revolving with variable angular velocity, starts to vibrate with respect to its central position OA. If we were to transfer centrifugal force  $P_H$  to point B of the suspension of the pendulum, upon deflection of rod L from its central position we would obtain force  $P''$  and moment from pair of forces  $P_H$  and  $P'$ . Expanding force  $P''$ , we obtain tangential force N, which will counteract the vibrations of rod L, and normal force Z, which will stretch the rod.

Moment from pair of forces  $P_H$  and  $P'$  causes vibrations of the pendulum with respect to rod L. Angular frequency of vibrations of a pendulum with bifilar suspension is expressed by the following formula:

$$\omega_n = \omega \sqrt{\frac{R}{\delta} - 1}, \quad (19.20)$$

where  $\omega$  is the angular velocity of rotation of the crankshaft;

$R$  is the radius of location of center of gravity of pendulum with respect to the axis of rotation of the crankshaft;

$\delta = D - d$  is the pin clearance in the holes;

D and d are diameters of holes and pin.

Force N will counteract the vibrations of rod L only when the pendulum vibrates in time to the rod vibrations, i.e., under the condition of adjustment of the pendulum counterpoise:

along the sides of the crankshaft and at the counterpoise. The counterpoises are the ones which serve for engine balancing.

Principle of action of the pendulum counterpoise as a damper of vibrations is based on the following. Let us imagine a rod L (extension of side of crankshaft), revolving around a center O (see Fig. 19.7). At point B it has a hinged pendulum M with arm  $p$ , in which during rotation there appears centrifugal force  $P_H$ . In case of uniform rotation ( $\omega = \text{const}$ ) rod L

$$\rho_{st} = \Omega. \quad (19.21)$$

Putting in formula (19.21) expressions (19.20) and (19.18), we find the value pin clearance  $\delta$  ensuring adjustment of pendulum to harmonic  $q$  of the order

$$\delta = \frac{K}{q^2 + 1}. \quad (19.22)$$

From expression (19.22) it follows that a pendulum counterpoise can be adjusted only to a harmonic of one order. Adjustment of a pendulum does not depend on speed. The higher the order of the harmonic, the less should be the clearance for suspension of the pendulum.

## C H A P T E R   XX

### CRANKSHAFTS

#### 20.1. General Information

To the crankshaft is transmitted the work of gases from the engine cylinders. In turn, through corresponding transmissions the shaft rotates the propeller, and also the mechanisms of gas distribution and assemblies attached to the engine.

Single-row engines have a single throw shaft, and two-row have a double-throw shaft with breakdown of throws at angle  $180^{\circ}$ . For balancing of the system, counterpoises are placed on the shafts.

For supports of shafts of radial engines they apply antifriction bearings. Bearings of connecting rods are usually sliding; crank heads of connecting rods are not detachable (see Chapter XXI). For decrease of wear the connecting rod necks of shafts are cemented or nitrated; for jointing with the connecting rods crankshafts are made detachable.

Crankshafts carry considerable dynamic loads in operation. They are made from the best structural steels. For the purpose of lightening, the crankshafts are made hollow. Internal cavities are used for feed of lubricant to connecting rod bearings.

#### 20.2. Design of Crankshafts

Figure 20.1 shows the double-throw shaft of the two-row radial engine [ASh-82T] (AM-82T). Throws are located with breakdown at angle  $180^{\circ}$ .

Shaft journals. Three short main necks are located on one axis of the shaft on both sides of each throw. The shaft neck rests in the engine crankcase

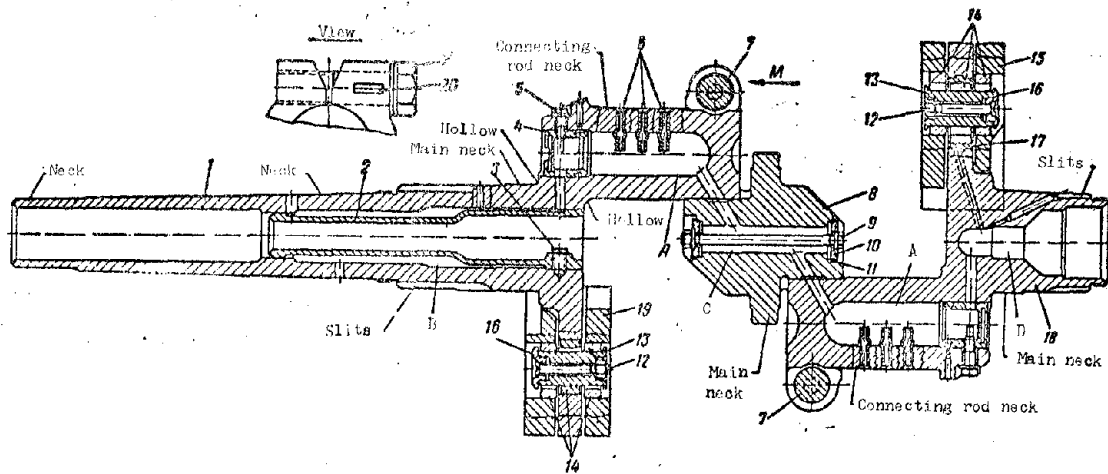


Fig. 20.1. Crankshaft of the ASH-82T engine. 1, 8 and 18 - front, central, and rear of shaft, 2 - pipe, 3 - bolt, 4 - stopper, 5 - bolt, 6 - tubes for lubrication, 7 - tie bolt of web, 9 - bolt, 10 - plugs, 11 - lining, 12 - bolt, 13 - counterpoise pins, 14 - counterpoise sleeves, 15 and 19 - rear and front counterpoises, 16 - washer, 17 - bronze sleeve, 20 - splint pin.

on roller bearings. The central main shaft neck in diameter is larger than the extreme ones. Connecting rod necks are usually somewhat smaller in diameter (by 15-20%), and significantly longer than the main necks. Decrease of neck diameter is dictated by the tendency to obtain a smaller magnitude of [VDM] ( $\Delta M$ ) of the crankgear, and increase of their length ensures a larger support surface for the sliding bearings of the connecting rods.

Connecting rod and main necks have internal bores forming cavities for oil. Cavities A of the connecting rod necks are stopped by plugs 4, and cavity B of the central main neck, by plugs 10. Plugs 4 are pressed and additionally secured by bolts 5. Under plugs 10 there are linings 11. Plugs are tightened by bolt 9.

Webs connect the main and connecting rod necks. They have prismatic form. For assembly of shaft with connecting rods there are sockets along the middle webs. The shaft thus consists of three parts: front 1, central 8, and rear 18. Connections of parts of shaft are of the terminal type. They are tightened by bolts 7.

Nose and butt of shaft. On the elongated nose of the shaft there are two necks for installation of the propeller shaft (see Figures 18.3 and 25.1). On involute slits of the nose and butt the drive gears are attached.

Nose and butt are hollow. Inside the nose, with the help of bolt 3 there is attached pipe 2, forming a annular oil cavity B.

Counterpoises. Along the extreme webs of the shaft with the help of bifilar

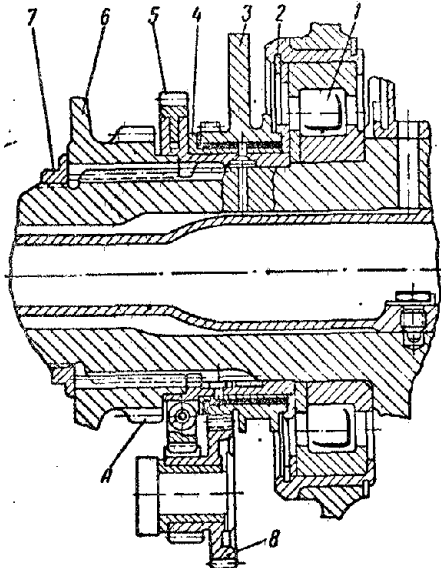


Fig. 20.2. Front support of the crankshaft of the ASh-82T engine.

is adjusted to a 7th order harmonic, and the rear one to a  $3\frac{1}{2}$  order harmonic.

Besides these main counterpoises, the nose and butt of the shaft has counterpoises of 2nd order (Fig. 20.2).

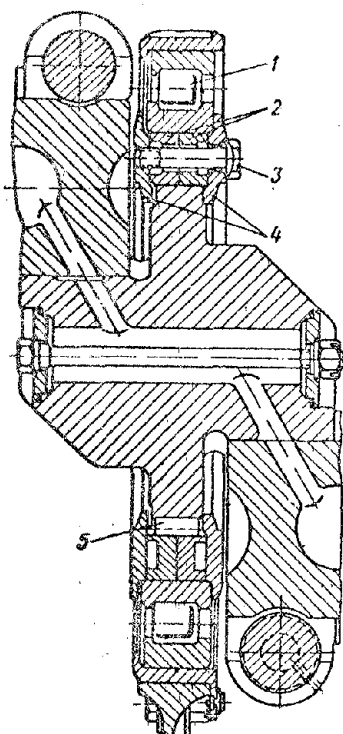


Fig. 20.3. Central support of the crankshaft of the ASh-82T engine.

suspensions (see Fig. 19.7) there are attached pendulum counterpoises 15 and 19 (see Fig. 20.1), having the form of segments. In holes under pins 13 of the counterpoises and on the front part of the shaft there are pressed steel sleeves 14. In the rear part of the shaft for decrease of wear, into this hole there is pressed a bronze sleeve 17, and steel sleeve 14 is of the floating type. For limitation of axial shafts of pins 13 on one end they have a bead, and to the other end with the help of bolt 12 there is attached washer 16. Pins 13 and sleeves 14 are cemented. Front counterpoise

Front support unit of shaft is shown in Fig. 20.2.  
Roller bearing 1 by its internal ring is mounted on the front main neck of the shaft, and by its external ring, with the help of spring ring 2 it is fixed in the seat of the crankcase. Furthermore, on involute slits of the nose of the shaft there are placed and are secured, with help of nut 7, elastic gear 5 and gear 6 of the propeller reduction gear.

On the hub of gear 5 there is pressed bearing sleeve 4, which contains a freely fixed counterpoise of the 2nd order 3. Through intermediate gear transmission 8, attached to the crankcase, the counterpoise obtains rotation from gear 5 with doubled angular velocity of crankshaft. The second such counterpoise is mounted on the shaft butt.

On the hub of gear 6 there is a gear ring A of transmission to the mechanism of front gas distribution. Axial fixation of shaft in crankcase is carried out by roller bearing 1.

The central shaft support unit is shown in Fig. 20.3. Central roller bearing 1 has a diameter significantly larger than the neck. This ensures the possibility to carry it during assembly through the central webs of the shaft. Between the internal ring of the bearing and main neck on cotter 5 there is a split insert 2 having longitudinal and cross sections. The bearing is secured with the help of two split rings 4 tightened by bolts 3.

Lubrication. Feed of lubricant to connecting rod bearings is carried out through internal cavities of shaft, which are connected by drillings in the webs. Oil moves to crankshaft through cavities B of the nose and D of the butt (see Fig. 20.1). During rotation of shaft, under the action of centrifugal forces, heavy particles of dirt, shavings, sand, and so forth contained in the oil, accumulate in cavities A on a large radius of rotation. Oil for lubrication of connecting rod bearings is ejected with the help of tubes 6 on a smaller radius of rotation, i.e., from the zone of clean oil.

Through axial drillings of bolts 5 and additional drillings of extreme webs the oil from cavity A also moves for lubricant of pistons, cylinder face, and support roller bearings. They are lubricated by spraying. For feed of lubricant to pins of rear counterpoise, and also to bearings of counterpoises of 2nd order, the shaft has drillings.

### 20.3. Strength Calculation

In a crankshaft the connecting rod, main necks and webs are calculated for strength. Calculation is usually conducted according to the method of calculation of a split beam. For this the throw will mentally be cut by two planes 1-1 and 2-2, passing through the middles of adjacent main necks of the shaft and will be considered as a beam on two supports, located in the planes of sections 1-1 and 2-2 (Fig. 20.4). The effect of the cut-off section of the shaft is considered as the torque  $M_3$  from the rear throw (if there is one) and reactive moment  $M_R$  from the front side. Figure 20.4 shows loads acting on the front throw of a two-row radial engine and the reaction of the supports.

Here  $Z_X$  and  $T_Y$  are normal and tangential forces;

$C' = C + C_m$  is the centrifugal force of revolving masses of connecting rod C and connecting rod neck of shaft  $C_m$ ;

$P_{m \text{ and }} P_{n \text{ pot}}$  are centrifugal forces of webs and counterpoise;

$M_3 \text{ and } M_R$  is the moment in the area of the rear throw and reactive moment of the reduction gear;

$Z'$  and  $T'$  are reactions of the supports.

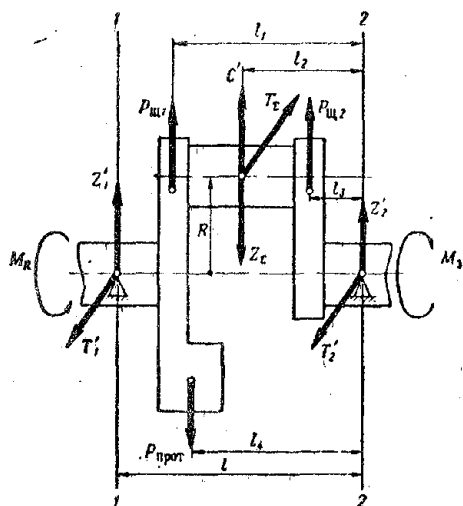


Fig. 20.4. Forces and moment acting on engine shaft throw.

to the middle of the connecting rod neck. Reactions of supports are determined separately: in plane of crank  $Z'$  and in the plane perpendicular it  $T'$ . Thus in the front main neck of the crankshaft (see Fig. 20.4) the support reactions are equal to:

$$\left. \begin{aligned} Z'_1 &= \frac{(Z_b - C')l_2 + P_{\text{spor}}l_4 - P_{\text{w1}}l_1 - P_{\text{w2}}l_3}{l}, \\ T'_1 &= \frac{T_z l_2}{l}. \end{aligned} \right\} \quad (20.2)$$

Connecting rod neck operates during bending and torsion. The highest bending moment appears on the middle section of the neck. For calculation we take the section around the oil hole, in the zone of which there appears a concentration of stresses. Through the center of the connecting rod neck in the calculating section we draw the axis of coordinates  $y-y$  and  $z-z$ ; axis  $y-y$  in the direction of action of force  $T_z$ , and axis  $z-z$  in the throw plane.

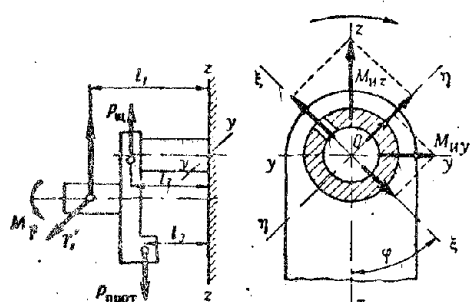


Fig. 20.5. Calculating diagram of connecting rod neck of engine shaft.

The moments acting clockwise, are taken to be positive. We plot the vectors of bending moments  $M_{ny}$  and  $M_{nz}$  according to a rule earlier adopted by us

Values loads  $Z_\Sigma$ ,  $T_\Sigma$ ,  $C$  and  $M_S$  are taken from dynamic calculation of the engine taking into account their direction.

Reactive moment in the area of the reduction gear is equal to:

$$M_R = M_s + T_z R. \quad (20.1)$$

Centrifugal forces from connecting rod neck  $C_{\text{III}}$  and webs  $P_{\text{III}}$  are found by calculation according to the gerometric dimensions of the shaft, and the centrifugal force of counter-poise  $P_{\text{spor}}$  is found from the condition of engine balancing. Forces  $Z_\Sigma$ ,  $T_\Sigma$ , and  $C'$  are applied

separately: in plane of crank  $Z'$  and in the plane perpendicular it  $T'$ . Thus in the front main neck of the crankshaft (see Fig. 20.4) the support reactions are equal to:

$$\left. \begin{aligned} Z'_1 &= \frac{(Z_b - C')l_2 + P_{\text{spor}}l_4 - P_{\text{w1}}l_1 - P_{\text{w2}}l_3}{l}, \\ T'_1 &= \frac{T_z l_2}{l}. \end{aligned} \right\} \quad (20.2)$$

For the calculating diagram according to Fig. 20.5 the bending moments in the calculating section will be:

with respect to axis  $y-y$

$$M_{ny} = Z'_1 l_1 + P_{\text{w1}} l_2 - P_{\text{spor}} l_3$$

and with respect to axis  $z-z$

$$M_{nz} = T'_1 l_1.$$

(see Chapter II, 2.6). The oil hole in the calculating section of the neck is located at angle  $\varphi$  to axis z-z. We shall draw auxiliary axes of coordinates  $\xi-\xi$  and  $\eta-\eta$ , where by axis  $\xi-\xi$  will be directed towards the oil hole. Bending moment acting in the plane of the oil hole  $M_\eta$ , is found as the sum of projections vectors  $M_{\eta y}$  and  $M_{\eta z}$ , on axis  $\eta-\eta$

$$M_\eta = M_{\eta y} \cos \varphi + M_{\eta z} \sin \varphi. \quad (20.3)$$

Twisting moment of neck is equal to (see Fig. 20.4):

$$M_{ckp} = M_p - T_i R. \quad (20.4)$$

Bending moment  $M_\eta$  and twisting moment  $M_{ckp}$  are variable and depend on the angle of rotation of the throw. Therefore calculation of the connecting rod neck is conducted for fatigue according to the outer limits of  $M_\eta$  max and  $M_\eta$  min;  $M_{ckp}$  max and  $M_{ckp}$  min, which are found within the limits of the cycle of their change. Then we determine the maximum and minimum values of stresses due to bending and torsion:

$$\left. \begin{aligned} \sigma_u \text{ max} &= \frac{M_{\eta \text{ max}}}{W_u}; & \sigma_u \text{ min} &= \frac{M_{\eta \text{ min}}}{W_u}; \\ \tau_{\text{max}} &= \frac{M_{ckp \text{ max}}}{W_{kp}}; & \tau_{\text{min}} &= \frac{M_{ckp \text{ min}}}{W_{kp}}, \end{aligned} \right\} \quad (20.5)$$

where  $W_u$  and  $W_{kp}$  are the moments of resistance to bend and torsion and are determined by formulas (7.25) and (7.20).

Amplitude of stresses and average bending stresses and torsion are found according to the following formulas:

$$\left. \begin{aligned} \sigma_a &= \frac{\sigma_u \text{ max} - \sigma_u \text{ min}}{2}; & \tau_a &= \frac{\tau_{\text{max}} - \tau_{\text{min}}}{2}; \\ \sigma_{cp} &= \frac{\sigma_u \text{ max} + \sigma_u \text{ min}}{2}; & \tau_{cp} &= \frac{\tau_{\text{max}} + \tau_{\text{min}}}{2}. \end{aligned} \right\} \quad (20.6)$$

Safety factors in bending and twisting

$$n_a = \frac{\sigma_{-1}}{\alpha_a \sigma_a + \varphi_a \sigma_{cp}}; \quad n_t = \frac{\tau_{-1}}{\alpha_t \tau_a + \varphi_t \tau_{cp}}, \quad (20.7)$$

where  $\sigma_{-1}$  and  $\tau_{-1}$  are fatigue limits for material of the shaft due to bending and torsion in a symmetric cycle;

$\alpha_a$  and  $\alpha_t$  are effective coefficients of concentration of stresses at the oil holes during bending and torsion;

$\varphi_a$  and  $\varphi_t$  are coefficients of reduction to symmetric cycle during bending and torsion.

For steel to be used in the manufacture of shafts, it is possible to take

$$\sigma_{-1} = 5500 \text{ kp/cm}^2; \quad \tau_{-1} = 3000 \text{ kp/cm}^2.$$

With the existing relations of diameter of the oil hole to the diameter of the connecting rod neck, crankshafts of aircraft engines it is possible to take

$$\alpha_0 = \alpha_1 = 2.5.$$

Taking into account the character of loads during calculation of the crankshaft we take

$$\varphi_0 = 0.2 \text{ and } \varphi_1 = 0.05.$$

Total safety factor is round by the formula

$$n = \frac{n_0 n_1}{\sqrt{n_0^2 + n_1^2}}. \quad (20.8)$$

Safety factor of connecting rod neck of radial engines is  $n \geq 2.5$ .

Main necks usually do not have oil holes and therefore are free from concentration of stresses. Calculation for torsion is conducted according to maximum twisting moment  $M_{kp\ max}$ .

For first main neck

$$M_{kp\ max} = M_{kp\ max} - M_H,$$

where  $M_{kp\ max}$  is maximum torque on engine shaft;

$M_H$  is the torque proceeding to the supercharger drive.

Maximum stress of torsion is:

$$\tau_{max} = \frac{M_{kp\ max}}{W_{kp}}, \quad (20.9)$$

where  $W_{kp}$  is the moment of resistance to torsion (see formula (7.20)). In aircraft engine  $\tau_{max} \leq 1200 \text{ kg/cm}^2$ .

Webs of crankshaft operate during bending, tension (compression), and torsion. Their calculating section is the hollow (place of transition from web to neck), where there appears a concentration of stresses. We shall draw the

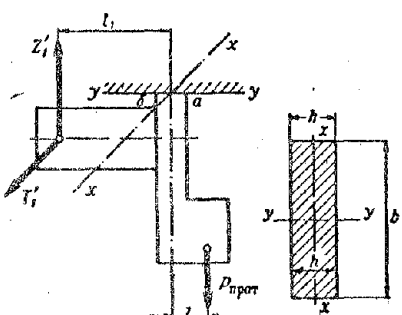


Fig. 20.6. Calculating diagram of an engine shaft web.

axes of coordinates x-x and y-y through the center of the calculating section of the web (Fig. 20.6).

For the calculating diagram the bending moment with respect to axis x-x will be equal to:

$$M_{xx} = Z' l_1 + P_{kper} l_2.$$

Signs of moments of forces are selected by taking into account the direction of their action.

Moment of resistance to bending of the web with respect to axis x-x

$$W_u = \frac{bh^3}{6},$$

where b and h are the width and thickness of the web (see Fig. 20.6).

Bending stress:

$$\sigma_u = \frac{M_{u,x}}{W_u}. \quad (20.10)$$

Tensile (compressive) force of the web is equal to:

$$Q = -Z_1 + P_{\text{up or down}}$$

Tensile forces are taken with the plus sign, and compressive with the minus.

Tensile (compressive) stress:

$$\sigma_p = \frac{Q}{F}. \quad (20.11)$$

where  $F = bh$  is the area of the web section in  $\text{cm}^2$ .

Total normal stresses in dangerous points a and b are:

$$\sigma_t = \sigma_u + \sigma_p. \quad (20.12)$$

In the summation of stresses their signs are considered. Tensile stresses are taken to be positive, and compressive stresses, negative.

The moment twisting the web is equal to:

$$M_{\text{exp}} = T' l_1$$

and torsional stress

$$\tau = \frac{M_{\text{exp}}}{W_{\text{kp}}}. \quad (20.13)$$

Here  $W_{\text{kp}}$  is the moment of resistance to torsion of the web

$$W_{\text{kp}} = kbh^2,$$

where coefficient k is taken depending upon the relation  $b/h$ :

$b/h$	1	1.5	2	3	4
$k$	0,208	0,231	0,246	0,267	0,282

Bending moment  $M_{u,x}$ , force Q and twisting moment  $M_{\text{exp}}$  are variable and depend on angle of rotation of the throw. Therefore the calculation of the web is conducted for fatigue according to the outer limits of  $M_{u,x \max}$  and  $M_{u,x \min}$ ,

$Q_{\max}$ ,  $Q_{\min}$ ;  $M_{\text{exp} \max}$  and  $M_{\text{exp} \min}$ , which are found within the limits of the cycle of their changes. Determining maximum and minimum stresses by formulas (20.5),

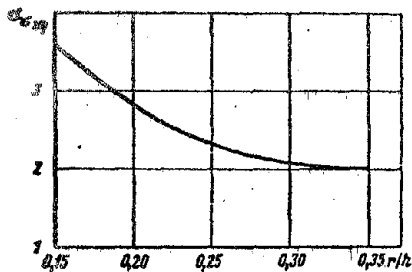


Fig. 20.7. Dependence of coefficient of effective concentration of stresses in the hollow of a crank-shaft on the relation of the radius of the hollow to thickness of web.

we find the amplitudes of stresses and average stresses by formulas (20.6) and safety factors by formulas (20.7 and 20.8).

Effective stress concentration factors during bending are found on the graph in Fig. 20.7 depending upon the relation of the radius of the hollow  $r$  to the thickness of web  $h$ , and during torsion  $\alpha_t = 2$ .

Safety factor of webs of aircraft engines is  $n \geq 2.5$ .

Terminal connection (Fig. 20.8) is calculated for twisting moment

$$M_{ckp\ max} = T'_{max} R.$$

Moment of friction in terminal connection is equal to:

$$M_{tp} = Fd = \mu Qd = 2\mu h P,$$

where  $F$  is the frictional force;

$\mu = 0.1 \div 0.15$  is the coefficient of friction in terminal connection;

$Q = P \frac{2h}{d}$  is the compression force of the neck;

$d$  is the diameter of the neck;

$h$  is the bolt gab;

$P$  is the compression force of the bolt.

Reliability of terminal connection is ensured by the following condition:

$$M_{tp} = k M_{ckp\ max},$$

where  $k = 3$  to  $4$  is the safety factor of tightening.

Hence the necessary compression force of the bolt is equal to:

$$P = \frac{k T'_{max} R}{2\mu h}. \quad (20.14)$$

Tensile stress of bolts is usually

$$\sigma_p = (0.5 \div 0.7) \sigma_y,$$

where  $\sigma_y$  is the yield point of the bolt material.

Tightening force of the bolt is checked by the magnitude of its elongation:

$$\Delta l = \frac{P l}{E_f},$$

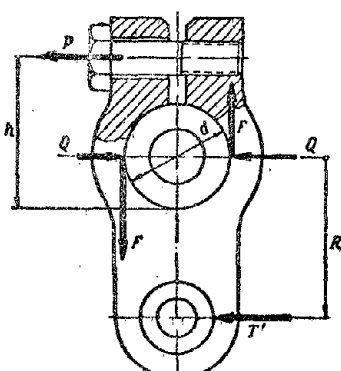


Fig. 20.8. Calculation of terminal connection of web.

where  $l$  is the length of the bolt;

$E$  is the elastic modulus of the bolt material;

$f$  is the area of cross section of the bolt.

#### 20.4. Material and Methods of Increasing the Strength of Crankshafts

Crankshafts during operation carry large dynamic loads. Therefore they are made from the best structural steels of brands [40KhNMA] (40XHMA) [18KhNVA] (18XHBA). Their billets are forged. For increasing the strength of the shaft fiber, configurations are arranged around it.

For increasing the fatigue strength of a crankshaft they frequently subject it to cleaning by shot peening and polishing. Oil holes of necks and transition hollows from webs to necks are a source of local concentration of stresses. Therefore the edges of holes are rounded off and thoroughly polished. Hollows are made with possibly larger radii and also thoroughly polished. Holes and hollows are frequently nitrated or cemented. Sometimes they apply local riveting of them with the help of rolling by roller or ball.

Neck of shafts, subjected to wear during work, are nitrated or cemented, and then thoroughly processed.

## C H A P T E R   XXI

### CONNECTING RODS

#### 21.1. General Information

Connecting rods connect the pistons with the crankshaft. In order to ensure transmission of work from several cylinders to one throw, the connecting rods are made with an attachable joint that has one main and several attachable connecting rods (see Fig. 18.7). The main connecting rod by its crank head is joined with the connecting rod neck of the shaft, and the attachable connecting rods by their crank heads are joined with the crank head of the main connecting rod.

For the purpose of obtaining small revolving masses the connecting rod bearings are chiefly sliding. During operation they carry considerable loads and therefore they are filled with plumbous bronze. The latter possesses high durability and good antifriction qualities.

Due to the large number of attachable connecting rods, the crank heads of the main connecting rods are usually whole, and not detachable.

During work the connecting rods are under the action of considerable dynamic loads. They are made from the best structural steels.

#### 21.2. Design of Connecting Rods

Figure 21.1 shows the main 5 and attachable 7 connecting rods of the radial engine [ASh-82T] (AM-82T). Connecting rods have piston and crank heads connected by a rod.

Piston heads serve for connection with piston. Into their holes are pressed bronze sleeves 6. For best running in they are leadened. The gap between the piston pin and sleeve is usually from 0.04 to 0.07 mm.

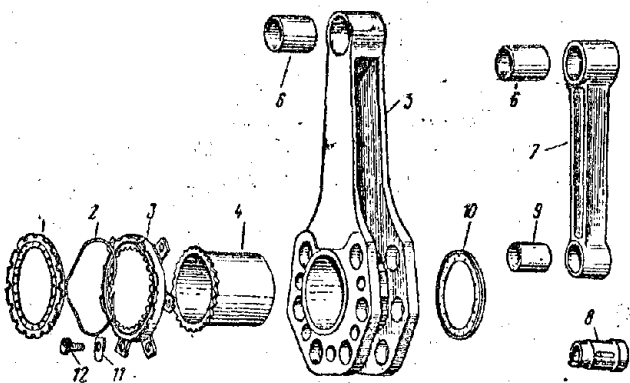


Fig. 21.1. Connecting rods of radial engine ASh-82T. 1 and 10 - sealing rings of main connecting rod sleeve, 2 - spring, 3 - retainer of main connecting rod sleeve and pins of attachable connecting rods, 4 - sleeve of crank head of main connecting rod, 5 - main connecting rod, 6 - sleeve of piston head of main and attachable connecting rods, 7 - attachable connecting rod, 8 - pin of attachable connecting rod, 9 - sleeve of crank head of attachable connecting rod, 11 - plate retainer, 12 - retainer bolt.

two webs with holes under pins. Crank heads of attachable connecting rods are similar to the piston heads. In their holes are pressed bronze sleeves 9. Pins of attachable connecting rods 8 have three necks. By their extreme necks the pins are pressed into the holes of the webs of the main connecting rod, and by their central necks are joined with the attachable connecting rods.

Fixing of bearing sleeve 4 and pins 8 is carried out by retainer 3 (see Figures 21.1 and 21.2b). The retainer has internal slits and six lugs (per number of attachable connecting rods). The retainer is mounted on the connecting rod by bolts 12 which are screwed into holes of pins 8. Sleeve 4 is fixed by slits, and pins 8 by lugs. Bolts 12 are locked by plate retainers 11.

For guarantee of best conditions of lubrication of the connecting rod bearing there are face seals in the form of steel rings 1 and 10. Sealing ring 1 has a centering bead and flanges in the form of slits. By the centering bead the ring is fixed in retainer 3, and its flanges enter the face grooves of the retainer. Between retainer 3 and sealing ring 1 there is released wave spring 2, pressing the ring to the web of the crankshaft. The working surface of ring 1 is flooded by plumbous bronze. Ring 10 seals the bearing on the other side. By its face bead the ring 10 sits on the cylindrical flange of the crank head of the main connecting

Crank heads. Into the crank head of the main connecting rod there is pressed a steel bearing sleeve 4, filled with plumbous bronze. Its working surface is reamed like a hyperbola (Fig. 21.2a). This ensures more uniform loading on the length of the bearing during bending of the connecting rod neck under a load. For best running in, the working surface of the bearing sleeve is leadened. The gap between the connecting rod neck and bearing is from 0.08 to 0.12 mm.

For connection of six attachable connecting rods the crank head has

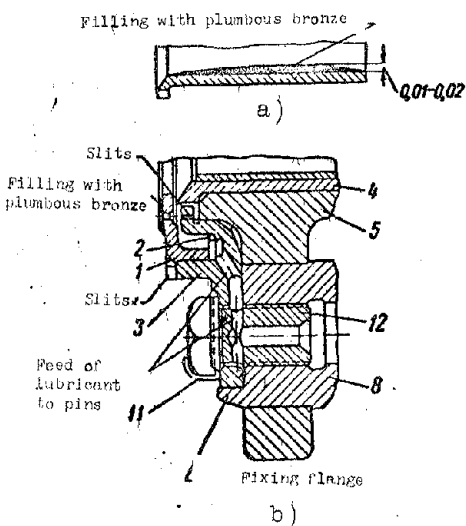


Fig. 21.2. Elements of main connecting rod of the ASh-82T engine. a) sleeve of crank head; b) retainer of main connecting rod. See Fig. 21.1 for designations.

of bar with head. For this purpose the bar is carried out with broadening of racks towards the crank head.

Lubrication of connecting rods. To connecting rod bearing the lubricant is brought in from the connecting rod neck of the shaft. For lubrication of crank heads of attachable connecting rods, oil from the cavity formed by ring 1 through drillings in retainer 3 and bolt 12 enters the cavity of pins 8. From there, through pin drillings the oil proceeds to the head. Piston heads of connecting rods are lubricated by spraying.

### 21.3. Strength Calculation

For connecting rods we calculate the bar, connecting rod bearing, and piston head.

Calculation of bar of connecting rod. Bar of connecting rod experiences variable compression and extension in work from the forces of pressure of gases and forces of inertia of [PDM] ( $\text{НМ}^2$ )<sup>1</sup>. The compressive force causes longitudinal bending of the bar. The latter is considered in two planes: in the plane of motion of the connecting rod and in the plane perpendicular to its motion. In the

<sup>1</sup>Forward-moving masses.

rod. Working surface of ring is coated with silver. For feed of oil to rings 1 and 10 there are drillings.

Bars of connecting rods during operation are subjected to longitudinal bending from forces of gases and extension from centrifugal forces of inertia. In order to obtain sufficient rigidity of connecting rod with small weight, sections of bars are made double-T. Racks of attachable connecting rods 7 are located perpendicular to plane of motion of connecting rod, which is expedient for increasing strength. Racks of main connecting rods 5 are located in plane of motion of connecting rod. They pass directly into the webs of the crank head, ensuring rigid connection

of bar with head. For this purpose the bar is carried out with broadening of racks towards the crank head.

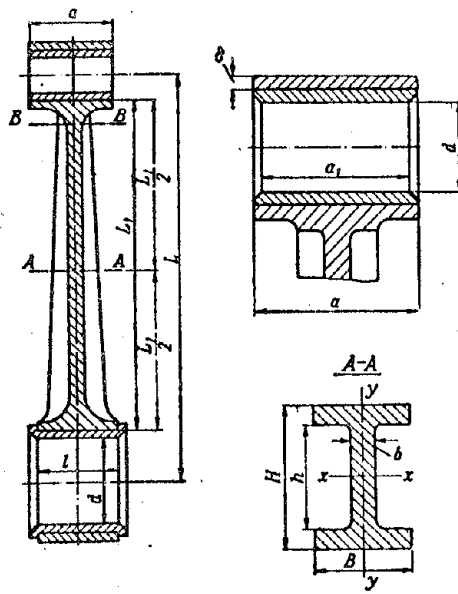


Fig. 21.3. Calculation of connecting rod strength.

plane of motion the connecting rod is considered to be hinged on length  $L$ , and in the plane perpendicular to motion, it is considered as a bar with fixed ends on length  $L_1$  (Fig. 21.3).

Maximums of compressive and tensile forces in the cycle of change of loads will be obtained at positions of crank in [VMT] (BMT):<sup>1</sup> in the beginning of expansion and at the end of release. For an average calculating section A-A of the bar the maximum compressive force by formula (18.17) is equal to:

$$P_z = P_{r \max} - m_{\text{ПДМ}} R \omega^2 (1 + \lambda), \quad (21.1)$$

and maximum tensile force is equal to:

$$P_j = m_{\text{ПДМ}} R \omega^2 (1 + \lambda). \quad (21.2)$$

where  $P_{r \max}$  is the maximum force of pressure of gases on the piston;

$P_j$  is the force of inertia of PDM of the crankgear;

$m_{\text{ПДМ}}$  are the PDM of the crankgear;

$\omega$  is the angular velocity of rotation of the crankshaft;

$R$  is the radius of the crank;

$$\lambda = \frac{R}{L}, \text{ where } L \text{ is the length of the connecting rod.}$$

Total compressive stresses and longitudinal bending are determined according to the following formulas:

in the plane of motion of the connecting rod

$$\sigma_{cz} = \left(1 + 0,000526 \frac{L^2 F}{J_x}\right) \frac{P_z}{F} \quad (21.3)$$

and in the plane, perpendicular to the motion of the connecting rod

$$\sigma_{cy} = \left(1 + 0,000526 \frac{L^2 F}{4J_y}\right) \frac{P_z}{F}, \quad (21.4)$$

where  $F$  is the area of section A-A;

$J_x$  and  $J_y$  are moments of inertia of section A-A with respect to axes x-x and y-y (see Fig. 21.3):

<sup>1</sup>Top dead-center.

and

$$\left. \begin{aligned} J_x &= \frac{BH^3 - (B-b)b^3}{12} \\ J_y &= \frac{(H-b)B^3 - hb^3}{12} \end{aligned} \right\} \quad (21.5)$$

Tensile stress will be equal to:

$$\sigma_p = \frac{P_f}{F}. \quad (21.6)$$

Calculation of connecting rod bar is produced for fatigue strength. Amplitude of stresses and average stress will be equal to:

and

$$\left. \begin{aligned} \sigma_a &= \frac{\sigma_c + \sigma_p}{2} \\ \sigma_{cp} &= \frac{\sigma_c - \sigma_p}{2} \end{aligned} \right\} \quad (21.7)$$

Safety factor of bar is determined by the following formula:

$$n = \frac{\sigma_1}{\sigma_a + \varphi_0 \sigma_{cp}}, \quad (21.8)$$

where  $\sigma_1$  is the fatigue strength in the symmetric cycle of extension and compression;  $\varphi_0$  is the coefficient of reduction to symmetric cycle and is equal to 0.16.

For the bar of connecting rods of aircraft engines  $n = 1.4$  to 3.

Connecting rod bearing is calculated on average specific pressure from force  $U_{cp}$  loading the bearing (see Chapter XVIII, 18.7). It is equal to:

$$k_{cp} = \frac{U_{cp}}{dl}, \quad (21.9)$$

where  $d$  and  $l$  is the diameter and support length of connecting rod neck. For aircraft engines  $k_{cp} = 150$  to  $200$  kg/cm<sup>2</sup>.

Piston head of connecting rod is calculated under tension, and its sleeve under specific pressure.

Maximum tensile force of piston head is equal to:

$$P_{jnop} = m_{nop} R \omega^2 (1 + \lambda), \quad (21.10)$$

where  $m_{nop}$  is the mass of the piston set.

Tensile stress of head is determined by the following formula,

$$\sigma_p = \frac{P_{jnop}}{2ab}, \quad (21.11)$$

where  $a$  and  $b$  are the width and thickness of the head.

For aircraft engines  $\sigma_p = 500$  to  $800$  kg/cm<sup>2</sup>. Specific pressure on sleeve is

determined by the formula;

$$k = \frac{P_{r\max}}{a_1 d}, \quad (21.12)$$

where  $a_1$  is the support length of the sleeve and  $d$  is the diameter of the piston pin.

For aircraft engines  $k = 700$  to  $1200 \text{ kg/cm}^2$ .

#### 21.4. Materials and Methods of Increasing the Strength of Connecting Rods

Connecting rods during work are subjected to large dynamic loads, variable in magnitude and direction. Therefore they are made from the best constructional steels [40KhNMA] (40XHMA) and [18KhNVA] (18XHBA). Blanks of connecting rods are stamped.

For increasing the fatigue strength, the stressed parts of connecting rods are thoroughly processed and polish. In certain engines the connecting rods for the same purpose are subjected to surface riveting by means of shot peening.

Inserts of connecting rods are made from low-carbon steel 20. They are flooded with plumbous bronze [BrS30] (BpC30), having good antifriction properties and sustaining high specific loads on the order of 250 to  $300 \text{ kg/cm}^2$ . For guarantee of best running in, the working surface of the bearing is lead coated. Thickness of layer of coating is from 0.005 to 0.01 mm.

Sleeves for piston heads of connecting rods and crank heads of attachable connecting rods are made from bronze and for best running in are frequently lead coated.

## C H A P T E R   XXII

### PISTONS

#### 22.1. General Information

The piston perceives pressure of gases, and through the connecting rod it rotates the crankshaft. Piston also ensures airtightness of cylinder, not allowing leakage of gases from one side into the engine crankcase, and from the other side, penetration of an excess quantity of oil from the crankcase to the combustion chamber,

During work the piston is subjected to the action of high temperatures and pressures. Its heating is nonuniform. The piston has the highest temperature in the central part of the bottom and opposite the outlet valve, where its temperature reaches 300 to 350°C. Overheating of piston causes the deposit of scale on it, scorching of the piston rings, premature firing of the working mixture, burnout of piston and, finally, jamming of it into the cylinder.

The main part of the heat is removed from the piston into the wall of the cylinder through the piston rings and its lateral surface. A smaller part of the heat is transmitted by the internal surfaces of the piston to the air and oil contained in the crankcase. During its motion the piston is also subjected to considerable inertial loads, and its lateral surface, to wear. Pistons are made from heat-resisting aluminum alloys having high coefficient of thermal conduction, good antifriction qualities, and small specific gravity.

#### 22.2. Piston Design

Figure 22.1 shows the piston of the [ASh-82T] (AIII-82T) engine with the components making up its unit.

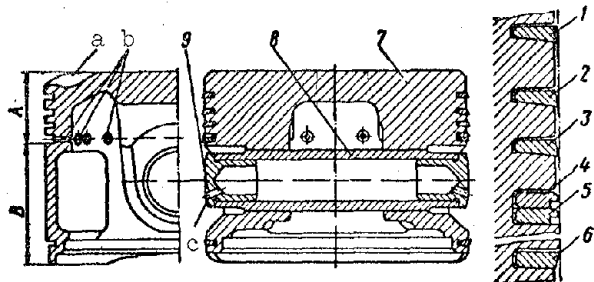


Fig. 22.1. Piston unit of the ASh-82T engine. 1-6 — piston rings, 7 — piston, 8 — piston pin, 9 — plug.

Piston has a bottom, lateral wall, and two cams with holes for the piston pin. The piston of the ASh-82T has a flat bottom with two local recesses a, which prevent the possibility of its striking against the valves in case of jamming of the latter in the position of full opening. Thickness of the bottom is determined from conditions of strength

and heat transfer. Bottom directly passes into cams and is smoothly linked with the side wall.

Lateral wall of piston is divided into two bands. Upper part A, adjacent to bottom, is the sealing band. It contains grooves for the piston rings. Lower part B, the so-called skirt of the piston, is the carrier band by which the piston leans on the wall of the cylinder and heads under its own motion to the cylinder.

Form of lateral surface of piston is made according to a special profile: height with small conicity, and cross section of slightly oval form. Conicity considers the nonuniform heating of the piston with respect to height, and the oval shape takes into account the deformation of the cylinder and piston under the action of the force of lateral pressure  $N$  (see Fig. 18.18). Conicity of the piston is made with decrease of diameter in the direction of the bottom. In the sealing band, which is more heated, conicity is greater than in the carrier band. The oval form of section is obtained by decreasing the piston diameter along the axis of the piston pin by approximately 0.1 mm. Height of the piston of aircraft engines is usually from 60 to 70% of its diameter.

Piston gaps. Gaps between piston and cylinder of a running (hot) engine are less than for a nonoperating (cold) one. This is explained by the different heating and different coefficients of linear expansion of the aluminum piston and steel cylinder. Small gaps of piston lead to its wedging in the cylinder, and large gaps impair the sealing. Magnitude of piston gap in cold state per 100 mm of its diameter is:

for upper band (at the bottom) — 0.7 to 0.95,

for lower band (at the skirt) — 0.5 to 0.6.

### 22.3. Piston Rings

Piston rings serve for sealing the piston in the cylinder. Rings have a notch called the retainer (Fig. 22.2). Due to their elasticity the rings are

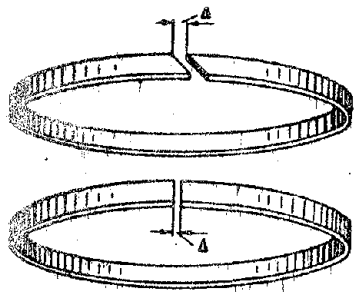


Fig. 22.2. Form of ring.

attached to the cylinder face and thereby ensure airtightness. Uniform attachment of rings on the circumference to the cylinder face characterizes their quality.

Piston rings operate in conditions of heightened temperatures and medium-dry friction. They are usually made from antifriction cast iron.

Piston rings are divided into two groups: gas-sealing (gas) and oil-sealing (oil).

Gas rings prevent breakthrough of working gases from combustion chamber into crankcase. They are arranged in the upper grooves (at the bottom) of the piston usually in a quantity of two-three a piece. Gas rings are rectangular a or trapezoidal b (Fig. 22.3). Trapezoidal rings are less inclined to burn out. Angle of cone of trapezoid generatrix is usually  $7^{\circ}30'$ .

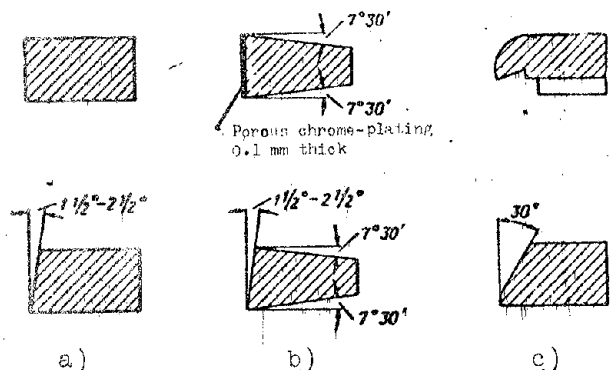


Fig. 22.3. Sections of rings.

First gas ring operates in difficult temperature conditions; therefore it is sometimes made from steel with porous chrome-plating of the working surface with thickness of chrome 0.1 mm. For best heat transfer to wall of cylinder its working surface is made cylindrical.

In other gas rings, on the working surface there is usually a bevel (cone) with angle 1.5-2.5°.

This facilitates running in of the rings to the cylinder face. Conical rings are placed on the piston with smaller diameter toward the bottom of the piston, which promotes less penetration of oil into combustion chamber.

Pump action of rings. Penetration of oil into combustion chamber occurs mainly due to the pump action of the rings (Fig. 22.4).

During motion of piston downwards the ring is pressed to the upper face of the groove, and the oil cleaned from the walls of the cylinder fills the gaps in

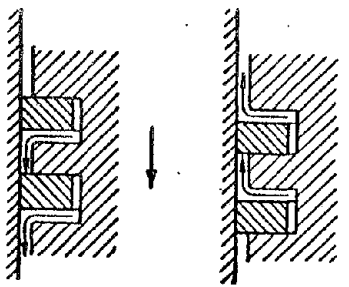


Fig. 22.4. Diagram of pump action of rings.

the piston groove. Upon change of direction of motion of the piston the ring is pressed to the lower face of the groove and presses part of the oil upwards.

Oil rings prevent penetration of excess quantity of oil from crankcase into combustion chamber. During motion of piston to [NMT] (HMT)<sup>1</sup> they remove surplus of oil from the cylinder face, and at the same time ensure required lubrication of the piston. Oil rings are

arranged in lower grooves of piston in a quantity from 2 to 4 a piece. In cross section they have the form of a scraper, and sometimes they are beveled at an angle of  $30^{\circ}$  (see Fig. 22.3c). On the face surface of rings under the scraper there frequently are grooves for passage of oil cleaned from the cylinder face to the drillings in grooves of the piston. Through these drillings the oil drains into the crankcase.

Dimensions of rings are usually made within these limits: height from 2 to 2.5 mm, and width  $(\frac{1}{25} \text{ to } \frac{1}{30})D$ , where D is the diameter of the cylinder.

Retainer of ring is straight or slanting (see Fig. 22.2). Dimension of retainer in free state of ring is usually  $\Delta = (0.1 \text{ to } 0.15)D$ , where D is the diameter of the cylinder. For free temperature expansion of rings in working state the gap in their retainer is established depending upon their operating temperature.

for oil rings  $\Delta = (0.005 \text{ to } 0.008)D$  and for gas rings  $\Delta = (0.008 \text{ to } 0.011)D$ .

Face gaps of rings. In piston grooves the rings have a free setting. Gas rings are in the zone of high temperatures, at which the oil cokes and burns easily. To eliminate grabbing of the rings in the piston grooves, their face gaps are established depending upon operating temperature.

For the ASh-82T the face gaps of piston rings are:

for first gas ring 0.16 to 0.2 mm,

for the 2nd and 3rd gas rings 0.08 to 0.12 mm,

for the oil rings 0.04 to 0.08 mm.

<sup>1</sup>Bottom dead-center.

For best sealing the ring retainers on the piston during assembly are placed on circumference relative to one another at an angle of 100 to 180°.

Location of piston rings of the ASh-82T engine. On the lateral surface of the piston of the ASh-82T (see Fig. 22.1) there are five grooves for the rings. In the first three grooves there are trapezoidal gas rings 1, 2, and 3. The first gas ring is made of steel. The fourth groove is made wider than the rest and has 12 radial drillings b in the body of the piston for drain of oil into the crankcase. In this groove there are two oil rings 4 and 5 with scrapers that clean the oil from the cylinder face during motion of piston to bottom dead-center. On the face surface of these rings under the scrapers there are bypass grooves. Through them, and then through the drillings in the piston body the excess oil is removed to the crankcase. In the fifth groove there is a conical oil ring 6 fitted with large diameter in the direction of the bottom of the piston. This ring cleans the oil during motion of the piston to top dead-center. Such location of oil rings promotes the formation of an oil film at the piston skirt during reciprocating motion of the piston and decreases its friction against the cylinder face.

#### 22.4. Piston Pins

Piston pin 8 (see Fig. 22.1) serves for connection of piston with connection of piston with connecting rod. Pins are made of hollow steel with floating (mobile) setting in the connecting rod and piston. Floating setting of pin ensures its more uniform wear. Gap of pin in cams of piston in cold state is from 0 to 0.02 mm. The large expansion of the piston in work increases this gap.

For providing axial shift of pin they use pluts 9 (see Fig. 22.1) or spring locks. Aluminum or bronze plugs are inserted in the pin hole; during axial shift of pin they can touch the cylinder face, not scratching it. For free outlet of air from cavity of pin the plugs have drillings c. Support ends of plugs are spherical. Steel spring locks are insert in grooves drilled in the holes of the piston cams.

#### 22.5. Strength Calculation

Piston. Lateral surface and cams of piston are calculated under specific pressure. Lateral surface of piston is loaded by force of lateral pressure  $N_{max}$

[see formula (18.18)]. Specific pressure on lateral surface of piston is equal to:

$$k = \frac{N_{\max}}{Dl}, \quad (22.1)$$

where D is the diameter of the piston;

l is the length of support surface of the piston (height of piston after subtracting grooves and faces).

For pistons of aircraft engines  $k = 9$  to  $19 \text{ kg/cm}^2$ .

Piston cams are calculated for force of pressure of gases  $P_{r\max}$ , which is determined by formula (18.16).

Specific pressure on support surface of cams (Fig. 22.5) is:

$$k = \frac{P_{r\max}}{2da_1}, \quad (22.2)$$

where d is the diameter of cam hole;

$a_1$  is the length of cam support surface;

For piston cams of aircraft engines  $k = 500$  to  $700 \text{ kg/cm}^2$ .

Piston ring is calculated for bending and for specific pressure on wall of cylinder. Bending stress of  $\sigma_u$  and specific pressure p are found the formulas

$$\left. \begin{aligned} \sigma_u &= E \left( \frac{s}{D} \right)^2 \\ p &= \frac{E}{3} \left( \frac{s}{D} \right)^4 \end{aligned} \right\} \quad (22.3)$$

and

where E is the elastic modulus of ring material;

s is the thickness of ring with respect to radius;

D is the diameter of the piston.

For rings of aircraft engines:

$$\begin{aligned} \frac{s}{D} &= \frac{1}{25} \text{ to } \frac{1}{30}, \\ p &= 0.5 \text{ to } 1 \text{ kg/cm}^2, \\ \sigma_u &= 900 \text{ to } 1350 \text{ kg/cm}^2. \end{aligned}$$

The piston pin is calculated for bending from the force of pressure of gases  $P_{r\max}$ . This force is considered to be uniformly distributed on the length of the piston cams and sleeve of the connecting rod according to the diagram in Fig. 22.5.

Maximum bending moment for the center of the pin will be:

$$M_{u\max} = \frac{P_{r\max}}{4} \left( L^{\frac{1}{2}} - \frac{a}{2} \right), \quad (22.4)$$

where L is the distance between middles of supports of piston cams;

a is the support length of the connecting rod sleeve.

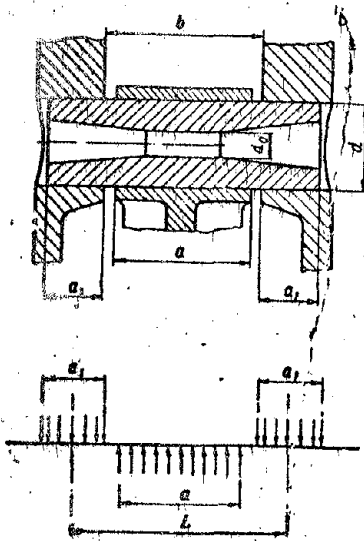


Fig. 22.5. Calculation of piston pin.

Bending stress is equal to:

$$\sigma_b = \frac{M_{b \max}}{W_b} \quad (22.5)$$

where  $W_b$  is the moment of resistance to bending [see formula (7.25)].

For the piston pins of aircraft engines  $\sigma_b = 3000$  to  $5000 \text{ kg/cm}^2$ .

#### 22.6. Materials

Pistons are made from heat-resisting aluminum alloy AK4, possessing high thermal conductivities, small specific gravity, and good antifriction qualities. Their billets are stamped.

Piston rings are manufactured from perlitic cast iron of brands [PChI] (РЧИ), [KhN] (ХН), or more heat-resistant brands [KhM] (ХМ) and [KhNV] (ХНВ), possessing good antifriction qualities.

First gas ring, operating in especially difficult temperature conditions, is frequently made of steel. For guarantee of good antifriction qualities its working surface is subjected to porous chrome-plating. The pores of the chrome-plated surface during work hold the oil, necessary for lubrication of the ring.

Piston pins are made of steel [12Kh2N4A] (12Х2Н4А). For decrease of wear their surface is cemented,

## C H A P T E R   XXIII

### CYLINDERS

#### 23.1. General Information

In cylinders of piston engines there occurs combustion of fuel and conversion of the liberated heat into mechanical work for moving the pistons. Cylinders are under the action of high temperatures and pressures of gases.

In order to ensure normal temperature conditions, the external side of cylinders have cooling ribs, with the help of which during flight of the aircraft the cylinders are cooled by the incident flow of air. Radial location of engine cylinders ensures uniform approach of air coolant to them.

#### 23.2. Design of Cylinders

Figure 23.1 shows an air-cooled cylinder of the radial engine [ASh-82] (AM-82), which consists of a steel case and aluminum head.

Case. The internal surface of the case which the piston moves through is the working surface and is called the cylinder face. For decreasing wear the cylinder face is nitrated and cleaned by fine grinding (honing). The external side of the cases have 27 annular ribs for cooling. Their height is 14 mm and interval 3.8 mm. There is also an engine flange with holes under the pins for mounting the cylinder to the crankcase.

Head of cylinder forms the combustion chamber. It is cast from a heat-resistant aluminum alloy possessing high thermal conduction, and is cleaned from the internal side. On the head with breakdown at an angle of 75° there are located two valve boxes with guide sleeves for valves of intake and exhaust. From its internal side concentrically to the guide sleeves are pressed the seats of the

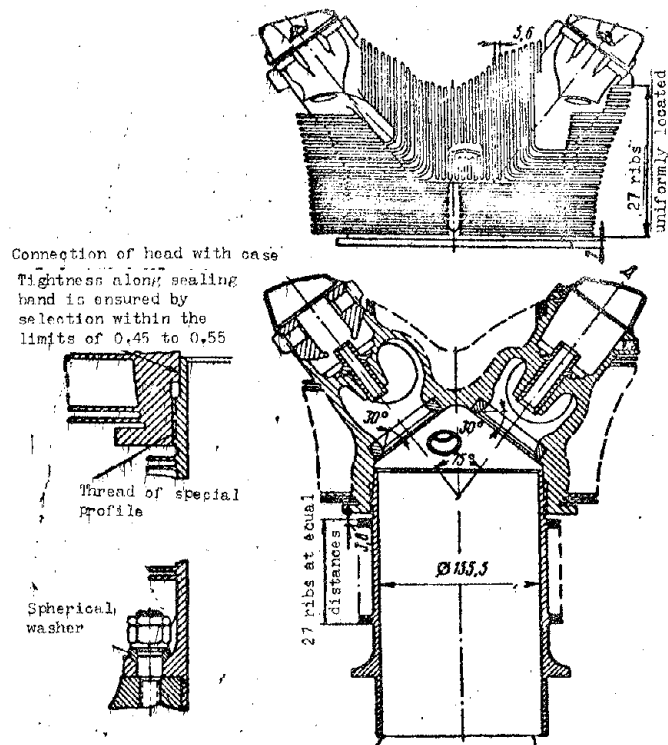


Fig. 23.1. Cylinder of the ASh-82 engine.

valves. Valve boxes form channels for passage into cylinder of a fresh charge (through inlet box) and outlet of exhaust gases (through outlet box). Furthermore, on the head there are three thread holes with sleeves for the installation of two plugs and a fuel spray nozzle. Figure 23.1 shows one of them.

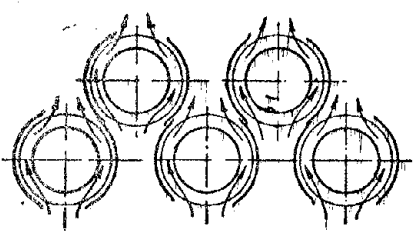


Fig. 23.2. Installation of deflectors on cylinders of a two-row radial engine.

From external side of heads there are ribs for cooling up to 40 to 60 mm high with an interval from 5 to 6 mm. On lateral surface of head the ribs are located horizontally, and in the breakdown between valve boxes, vertically. This ensures a good flow around the ribs by the air coolant. For more uniform distribution of temperature on the head the height of the ribs of the outlet valve box (hotter) is greater than that of the inlet valve box (colder). Surface of head ribbing, which is hotter, is significantly larger than the case.

Connection of head with case is done with the help of a thread having a special profile, and a sealing band. Airtightness of connection is ensured by

tightness along band from 0.45 to 0.55 mm. The thread also has a tightness of the order of 0.3 mm. For facilitating of the insertion the case into head, the latter is heated to 280 to 300°C.

Deflectors. For best cooling, deflectors are placed around the ribbed part of the cylinders. They are directing shields, made from sheet material. They form channels with the ribs (Fig. 23.2), through which the air coolant heads to the rear side of the cylinders, ensuring their uniform cooling.

### 23.3. Strength Calculation

During operation the cylinders are under the action of the pressure of gases.

Case of cylinder is calculated by formula (9.1) for extension in a cross section between the ribs under the action of maximum force of pressure of gases  $P_{r \max}$  [see formula (18.16)].

For cases of cylinders of aircraft engines  $\sigma_p \leq 1100 \text{ kg/cm}^2$ .

Flange of cylinder is calculated for bending from force  $P_{r \max}$  by formula (10.2). For cylinder flanges of aircraft engines  $\sigma_u \leq 1200 \text{ kg/cm}^2$ .

Pins for attaching cylinders to crankcase are calculated for extension from the force of preliminary tightening:

$$\sigma = \frac{kP_{r \max}}{if}, \quad (23.1)$$

where  $k = 2$  to 4 is the tightening coefficient;

$i$  is the number of pins;

$f$  is the area of the calculating section of the pin.

For pins of aircraft engines  $\sigma \leq 4000 \text{ kg/cm}^2$ .

### 23.4. Materials

Cases of cylinders are made from steel [38KhMYuA] (38ХМЮА). For decrease of wear the cylinder face is nitrated and thoroughly processed. Heads of cylinders are usually cast from heat-resisting aluminum alloy [AL5] (АЛ5), possessing high thermal conduction and small specific gravity.

Valve seats are subjected to gas corrosion; therefore, they are frequently made from heat-resistant valve steels [EI69] (ЕИ69). Seats of low-capacity engines are made from bronze.

Valve guides are made from bronze [BrAZhMts] (БрАЗhМц) or special antifriction

cast iron. Cast-iron guides are frequently used for exhaust valves, operating in conditions of high temperatures with poor lubrication.

## C H A P T E R XXIV

### GAS DISTRIBUTION

#### 24.1. General Information

The mechanism of gas distribution ensures periodic admission of fresh charge into cylinders and ejection from them of exhaust gases into the atmosphere. Aircraft engines usually have valve gas distribution. Each cylinder of radial engines has two valves, i.e., one intake and the other exhaust.

Size of passage sections of valves is determined by throat diameter  $d$ , elevation height  $h$  of valve, and angle  $\alpha$  of fitting bevel (Fig. 24.1). Diameter

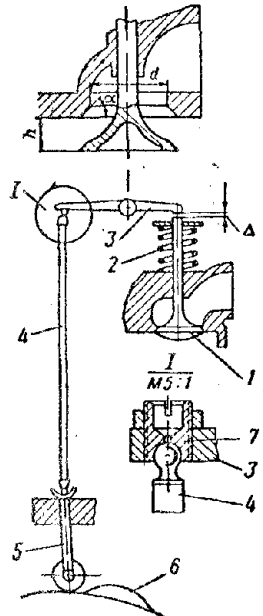


Fig. 24.1. Diagram of mechanism of gas distribution of an engine.

of throat is limited by dimensions and form of combustion chamber. Frequently the diameter of the inlet valve 5-10% greater than the outlet. With the best filling the engine power increases somewhat. Height of elevation of valve is limited by growth of inertial loads in valve mechanism and is  $h = (0.17 \text{ to } 0.3)d$ . Angle  $\alpha$  with respect to fitting bevel is usually  $30^\circ$  or  $45^\circ$ . Passage section of valve at  $\alpha = 30^\circ$  is somewhat greater than at  $\alpha = 45^\circ$ .

Phase (duration) of opening of valves is usually from  $240$  to  $270^\circ$  with respect to angle of rotation of crankshaft. By the progress of the piston the valves are opened before the dead centers (with a lead), and are closed after the dead centers (with delay). Phases of gas distribution of aircraft engines are:

inlet - beginning 20 to  $40^{\circ}$  before [VMT] (BMT)<sup>1</sup>  
end 50 to  $70^{\circ}$  after [NMT] (HMT)<sup>2</sup>

exhaust - beginning 50 to  $70^{\circ}$  before NMT  
end 20 to  $40^{\circ}$  after VMT

At the end of exhaust and in the beginning of intake, the outlet and inlet valves are simultaneously in opened state, forming the so-called covering of valves, which is from  $30$  to  $80^{\circ}$  with respect to angle of rotation of crankshaft. This improves filling of cylinders by fresh charge.

Opening and shutting of valves of radial engines is carried out by a cam washer with the help of an intermediate mechanism. The cam washer is placed in crankcase, forming the so-called lower gas distribution. Figure 24.1 shows a diagram of the mechanism of gas distribution of a radial engine, which consists of valve 1 with spring 2, double-arm lever 3, bar 4, pusher 5 with roller and cam washer 6. The washer, through a corresponding gear transmission, is driven from the crankshaft. The valve, in closed state under the action of the spring, lightly fits into the cylinder seat. During rotation of washer 6 its cams run on the roller of the pusher and move it. The pusher in turn acts on the bar, which, leaning with its upper end at the left arm of the lever, turns it with respect to the axis. The right arm of the lever is pressed to the valve and, surmounting the elasticity of the spring, it opens it. After passage of the cam the spring closes the valve, putting it in the seat.

In order to ensure tight fitting of valve in seat, between lever 3 and valve 1 at closed position of the latter, with the help of regulating screw 7 an assembly gap  $\Delta$  is established (see Fig. 24.1). In working state the cylinders expand in axial direction to a larger degree than bar 4; therefore during operation of engine, gap  $\Delta$  is increased.

Speed of rotation and number of cams of cam washer depends on number of cylinders in a row and on the direction of rotation of it with respect to the crankshaft. Let us consider the case of rotation of the cam washer opposite the rotation of the crankshaft (Fig. 24.2). With number  $k$  of similar cams their angle of breakdown on the cam washer is  $\delta = \frac{2\pi}{k}$ . Angle of breakdown of cylinders is

<sup>1</sup>VMT = top dead-center,

<sup>2</sup>NMT = bottom dead-center,

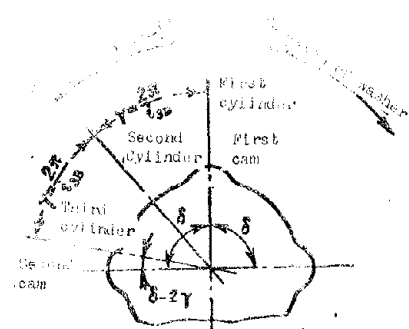


Fig. 24.2. Determination of number of cams of a washer.

$\gamma = \frac{\pi}{i_{SB}}$ , where  $i_{SB}$  is the number of cylinders in a row. In Fig. 24.2 the first cam coincides with the axis of the first cylinder. In order to ensure firing order (see Chapter XVIII, 18.5), upon turn of crank at angle  $2\gamma$  the cam washer should turn at angle  $\delta - 2\gamma$ . Then the second cam will be combined with the axis of the third cylinder. The transmission ratio of drive to the cam washer will be equal to:

$$\frac{n_k}{n} = \frac{\delta - 2\gamma}{2\gamma}, \quad (a)$$

where  $n_k$  and  $n$  are the speed of the cam washer and crankshaft.

Cycle of work of four-cycle-engines is accomplished every two turns of the crankshaft. Therefore with turn of crankshaft at angle  $4\pi$  from initial position (Fig. 24.2) the cam washer should turn at angle  $\delta$  so that the second cam is combined with the axis of the first cylinder. The transmission ratio of drive to the cam washer will be equal to:

$$\frac{n_k}{n} = \frac{\delta}{4\pi}. \quad (b)$$

Equating expressions (a) and (b), we obtain

$$\frac{\delta - 2\gamma}{2\gamma} = \frac{\delta}{4\pi}.$$

Whence the angle between cams will be equal to

$$\frac{\delta}{2\gamma} = \frac{4\pi}{4\pi - 2\gamma} = \frac{4\pi}{i_{SB} - 1}. \quad (24.1)$$

Number of cams will be equal to

$$k = \frac{2\pi}{\delta} = \frac{i_{SB} - 1}{2}. \quad (24.2)$$

Transmission ratio of drive to washer will be equal to

$$\frac{n_k}{n} = \frac{1}{i_{SB} - 1}. \quad (24.3)$$

In case of rotation of cam washer in the same direction as the crankshaft

$$\frac{n_k}{n} = \frac{4\pi}{i_{SB} + 1}; \quad k = \frac{i_{SB} + 1}{2} \quad \text{and} \quad \frac{n_k}{n} = \frac{1}{i_{SB} + 1}.$$

In this case, location of cams of inlet and outlet on cam washer should ensure

correct flow of processes of inlet and outlet of engine cylinders.

Operating conditions. Valves operate in conditions of high temperatures and pressures. Outlet valves in the process of exhaust directly are washed by hot exhaust gases and separate parts of their heads are heated to 700°C. This can cause warping, overheating, and burnout of valves. Therefore the outlet valves of powerful engine usually have internal cooling of heads.

Inlet valves work in more favorable conditions. In the process of suction they are washed by a fresh charge of mixture and separate parts of their heads are heated not more than 400 to 450°C. Therefore they usually do not require internal cooling.

Valve springs and other links of the mechanism of gas distribution work in conditions of large variable loads.

#### 24.2. Design of Gas Distribution Mechanism

valves. In accordance with different operating temperature conditions, the outlet and inlet valves are different in design. Figure 24.3 shows the valves of outlet 1 and inlet 2 of the [ASh-82] (AM-82) engine. The outlet valve is hollow, with an extended head,

Its internal is filled approximately by 50% in volume with metallic sodium. In the hole of the valve rod is pressed a plug 3 and from above a plate 4 is welded from instrument steels. During operation the sodium melts and moves during the motion of the valve under the action of forces of inertia. Sodium transmits heat from the head to the rod, cooling the head. From the rod, the heat through a guide sleeve passes to the head of the cylinder. Application of sodium as a heat carrier is explained by its small specific gravity, low melting temperature, and high boiling point,

The inlet valve is solid without internal cooling. Its head has a tulip-like shape. This ensures smooth form of channel in throat, and consequently also smaller hydraulic resistances to passage of mixture into cylinder.

In order to ensure the best fitting (airtightness), the fitting bevels of valves during assembly are thoroughly ground to the seats. Sometimes the bevel angle of the valve is made 0,5-1° less than the bevel angle of the seat. The initial width of the bevel decreases, which promotes faster running in the valves during operation.

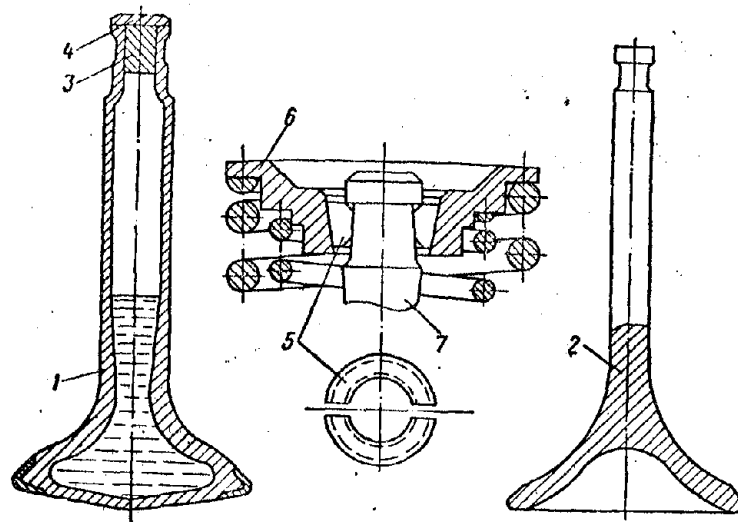


Fig. 24.3. Valves of the ASH-82 engine. 1 - outlet valve, 2 - inlet valve, 3 - plug, 4 - support plate, 5 - clamps, 6 - plate, 7 - valve stem.

In the process of engine operation there frequently is observed warping of valves seats that are pressed into the head of the cylinder. This leads to loose fitting of the valve and, as a result to burning of its bevel. More frequently this defect is encountered in outlet valves and therefore their bevels are fused by heat-resistant alloys of the Nichrome type. This protects them from burnout.

In the [ASH-82T] (AII-82T) engine for decrease of warping the seats of the outlet valves are floating (Fig. 24.4). Seat 4 on the outside has an annular flange, which during assembly enters the bore of two semirings 3. Semirings are pressed into the head of the cylinder, and the seat has a floating fit. Owing to this, when there are deformations of the cylinder head, warping of the seat is eliminated.

Valve stems for decrease of wear are processed to a high degree of purity and frequently are nitrated. Face of stem perceives the load of the lever. For decrease of wear of outlet valves, a tip of high hardness is welded to the end of the stem.

Valve springs are made from round wire with number of working turns from 4 to 8. For increase of fatigue strength they are shot-peened or polished. Each valve has two or three springs. This increases the reliability of the valve mechanism. Direction of spiraling of springs is made different so that in case of breaking one of their turns it does not fall between the turns of another.

Valve retainers. Tension of valve springs is carried out by plates 6, which

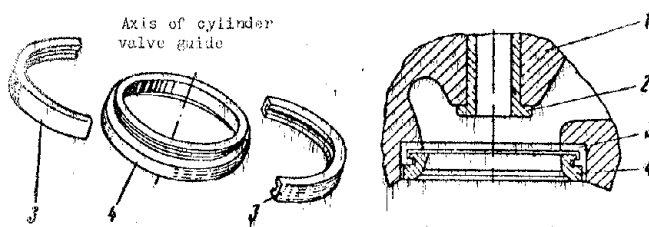


Fig. 24.4. Floating valve seat, 1 - head of cylinder, 2 - guide sleeve of valve, 3 - semiring, 4 - valve seat.

are attached to valve stem 7 with the help of retainers (see Fig. 24.3). Retainer consists of split clamps 5, the external surface of which has a cone. The valve stem has an annular bore, and the spring plate 6 has a cone hole. During assembly, the springs are preliminarily compressed by the plate and collected by the clamps in the annular bore of the stem. After that, the plate is liberated and it sits under the action of the springs with its cone hole on the clamps. Pressing them, the plate is secured to the valve stem,

Mechanism of gas distribution, Figure 24.5 shows the mechanism of gas distribution of the radial engine ASh-82. The valve is held in closed state under the action of springs, and it is driven by cam washer 4, through pusher 8, bar 9, and double-arm lever 10.

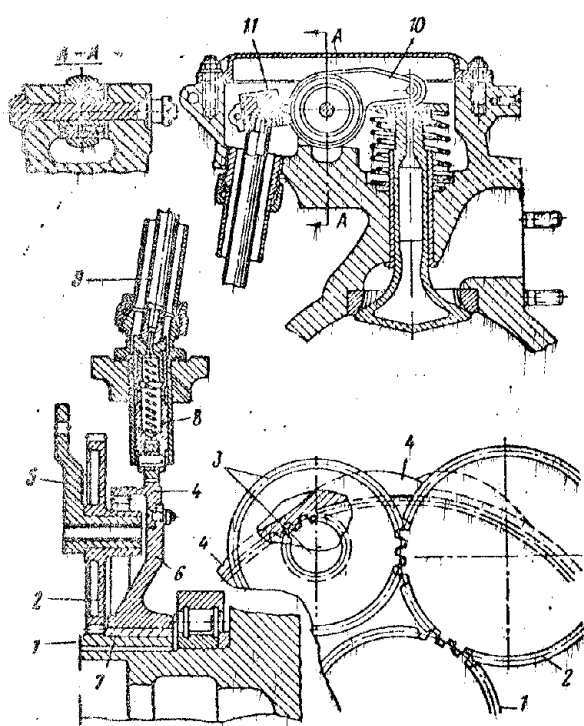


Fig. 24.5. Gas-distribution mechanism of the ASh-82 engine, 1 - pinion gear, 2 - intermediate gear, 3 - double gear, 4 - cam washer, 5 - bracket, 6 - disk of cam washer, 7 - bronze sleeve, 8 - pusher, 9 - bar, 10 - lever, 11 - regulating screw.

Cam washer 4 is made in the form of a steel ring, mounted with the help of bolts on aluminum disk 6. On external surface of rings there are two annular tracks, each of which has four cams a piece, located uniformly on the circumference. Cam washer services the work of one row of engine cylinders.

Cams of front track control the inlet, and rear track, the outlet valves. For decrease of wear cams and tracks are carbonized. The internal side of the steel ring has inner coupling teeth for driving the washer. In the central hole of disk 6 there is pressed a bronze bearing sleeve 7, with the help of which the cam washer freely sits on the hub of

gear 1, attached to the neck of the crankshaft.

Drive of the cam washer is carried out from the crankshaft through a gear transmission consisting of cylindrical gears 1, 2 and 3; gear 3 has two rims. Intermediate gears 2 and 3 sit on axes of bracket 5 attached to engine crankcase. Gear 1 is linked with intermediate gear 2, which in turn is linked with the large rim of gear 3, and the latter to its small rim, i.e., with the teeth of the cam washer. The cam washer revolves in the direction of rotation of the crankshaft; transmission ratio of drive is equal to 1/8.

Pushers 8 are made of steel and are hollow. They are placed on the circumference of the crankcase in bronze guide sleeves. The internal end of the pushers have rollers that roll the cam washer and upon passing the cams they move pusher. So that the pusher does not turn, the guide sleeves have slots for the rollers. On the external end of the pusher with free fitting is placed the tip, having a spherical socket for the bar. The spring, inserted in the cavity of the pusher, selects the gap in the mechanism of gas distribution.

Bars 9 are steel and hollow. From both ends, into them are pressed steel spherical tips. Bars are placed inside housings, which protect the mechanism from dust.

Double-arm levers (rocker arms) 10 are steel. They sit in bearings on shafts attached to the valve box of the cylinder. In the lever side of the valve there are rollers, through which the force is transmitted to the valve. On the lever side of the bar there are thread holes, into which the regulating screws 11 are screwed with the spherical support surface under the bar. The regulating screw establish the thermal gap  $\Delta$  for the valves (see Fig. 24.1). The wall of thread hole of the lever is split; locking of regulating screw 11 is carries out by a tie bolt (see Fig. 24.5).

#### 24.3. Materials

Valves are manufactured from special heat-resisting steel. For the outlet valves steel [EI69] (5M69) is applied. Inlet valves are made from less-alloyed steels [EI72] (5M72) or [EI107] (5M107). Bevels of outlet valves are fused by heat-resistant alloy of the Nichrome type. To the end of the stem is welded a tip of steel [Kh12M] (X12M). For decrease of wear, valve stems are frequently nitrated. Valve springs are made from wire steels [50KhFA] (50ХФА), and split

retainers from bronze [BrAZhN10-4-4] (BpAZh10-4-4).

Cam washer is made from case-hardened steels [13N5A] (13H5A) or [12Kh2N4A] (12X2H4A). Its working surface is case-hardened; it has hardness HRC > 58. Pushers are made of steel [12KhN3A] (12XH3A) or [37KhN3A] (37XH3A), thrust bars of steel [30KhGSA] (30XPCA), and rocker arms from steel [40KhNMA] (40XHMA).

## C H A P T E R   XXV

### REDUCTION GEARS AND SUPERCHARGERS

#### 25.1. Reduction Gears

The speed of piston engines is 2000-2600 rpm. At such speeds the propeller has low performance. For increase of propeller performance, its drive (as in TVD (TBD)) is carried out through a reduction gear with transmission ration 0.7-0.8. The exceptions are low-capacity engines, which for the purpose of simplification of design sometimes do not have reduction gears.

Radial engines have coaxial, planet-type reduction gears that ensure uniform approach of air coolant to all cylinders of the cluster and small dimensions of reduction gear.

As an example, Fig. 25.1 shows the planet reduction gear of the [ASh-82T] (AM-82T) with transmission ration  $i_p = 0.574$ . The drive gear is carried out in the form of the toothed rim of inner coupling 14 mounted on slits of disk 19. The disk sits with its hub on slits of the nose of crankshaft 22 and is mounted on it by nut 21.

The stationary gear is carried out in the form of the toothed rim of outer coupling 12 mounted on slits of support ring 11. The ring is mounted in the crankcase of the reduction gear with the help of pins. Axial retention of driving toothed rim 14 on disk 19 and stationary toothed rim 12 on support ring 11 is carried out by segment plates 10 and 16 which enter the notches of slits of the toothed rims and are mounted on the disk and support ring by screws. Free slit connections with disk 19 and support ring 11 allow the toothed rims during work to adjust themselves on the teeth of satellites, ensuring thereby equal distribution of load on the teeth. Teeth and slits of rims are nitrated.

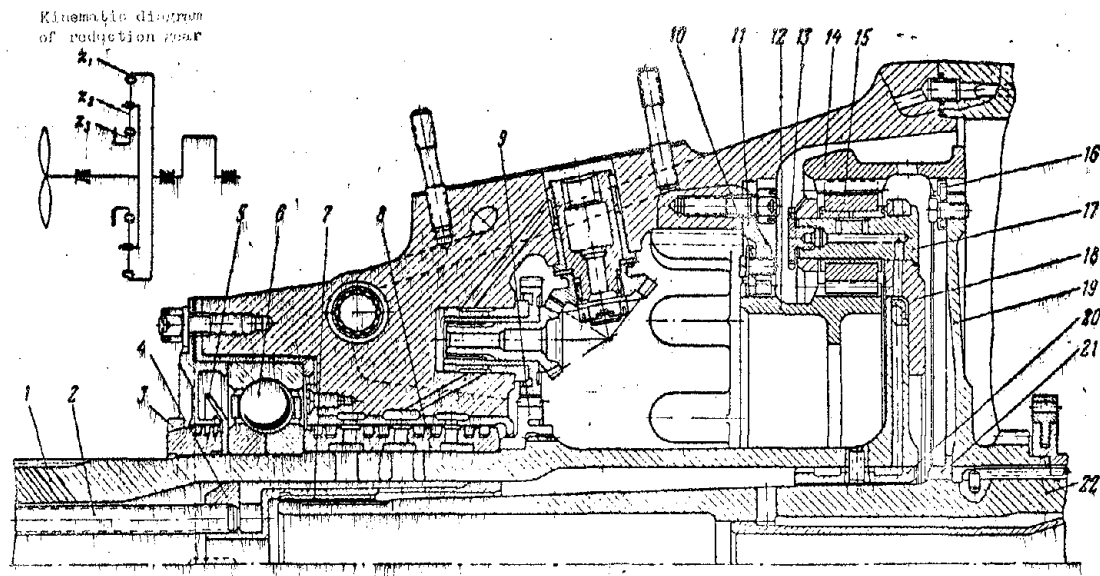


Fig. 25.1. Reduction gear of the ASh-82T engine. 1 - propeller shaft, 2 - VISH oil-feed tubes, 3 - nut, 4 - plug, 5 - oil-deflector ring, 6 - radial-support ball bearing, 7 - sliding bearing sleeve, 8 - oil-sealer, 9 - accessory drive gear, 10 - segment plate, 11 - support ring, 12 - toothed rim of stationary gear, 13 - plug, 14 - toothed rim of pinion gear, 15 - satellites, 16 - segment plate, 17 - axis of satellite, 18 - satellite-holder, 19 - disk of pinion gear, 20 - sliding bearing sleeve, 21 - nut, 22 - crankshaft.

Satellites 15 in a quantity of 12 have bearing bronze sleeves, with the help of which they are fixed on axes 17 in satellite-holder 18.

Axes of satellites are pressed into satellite-holder until they rest in the bead and are secured by plugs 13 which are locked by plate retainers. Satellite-holder is carried out in the form of a solid rim with 12 apertures for satellites and is fastened by bolts to the flange of propeller shaft 1.

Propeller shaft 1 is hollow. In its openings are placed plug 4 and two bearing sleeves 7 and 20. With the help of the sleeves the propeller shaft is fixed on the nose of crankshaft 22. On the propeller shaft there are cylindrical accessory drive gear 9, oil-sealer 8, and radial-support ballbearing 6 with oil-deflector ring 5. All these components are secured by nut 3. On the front end of the propeller shaft there are slits and threads for installation and fastening of the propeller hub.

The variable-pitch propeller VISH is bilateral. Propeller control is hydraulic and is carried out by a speed governor. Supply and drain of oil to the propeller occurs through channels in the body of the reduction gear through oil-sealer 8 of the shaft and through two tubes 2. Oil, proceeding for lubrication of

the reduction gear, moves inside the propeller shaft, lubricates two sliding bearings 7 and 20, and through drillings in the shaft flange and in satellite-holder 18 enters the cavities of axes of satellites 17 for lubrication of bearing sleeves of the satellites. From the internal cavity of the propeller shaft the oil through a drilling in the nose of crankshaft 22 passes also for lubrication of the front connecting rod neck. Teeth of the reduction gear and ball bearing 6 are lubricated by spraying.

### 25.2. Superchargers

For increase of power and guarantee of height aircraft piston engines have pressure feed. For this purpose there usually are centrifugal low-pressure superchargers (compressors), which are simple in design, have small dimensions and small weight.

Superchargers can have drive from the engine crankshaft in the form of a gear transmission or drive from a gas turbine operating on the exhaust gases of the piston engine. In the first case the supercharger is included in the piston engine, and in the second it forms a separate unit of pressure feed, i.e., a turbocompressor. In the past, turbocompressors were used on high-altitude piston engines. In contemporary piston engines, having small height, we find predominant application of superchargers with mechanical drive from the crankshaft, which are well composed in the engine system.

The rotor wheel of the supercharger has 20,000-30,000 rpm. Therefore its drive from the crankshaft is carried out usually through a two-stage gear transmission with transmission ratio 8-15. With respect to number of speeds the drives are one-speed and two-speed. Engines with height up to 2000 m usually have one-speed drive. For high altitudes two-speed drives are used, which essentially improve the altitude performance of the engines.

As an example, Fig. 25.2 shows the supercharger of the ASh-82T. Rotor wheel 4 of the supercharger is a semi-enclosed type with 22 blades. A revolving guide is carried out simultaneously with the wheel. The body of the supercharger consists of two parts: front 6 and rear 7. Rear part of body forms the gearbox and entrance to the supercharger. Vaned diffuser 5 has 9 vanes and is braced to the rear part of the body. At the diffuser outlet the bodies form an annular collection with 14 discharge branches 14. Through these branches the air passes into the

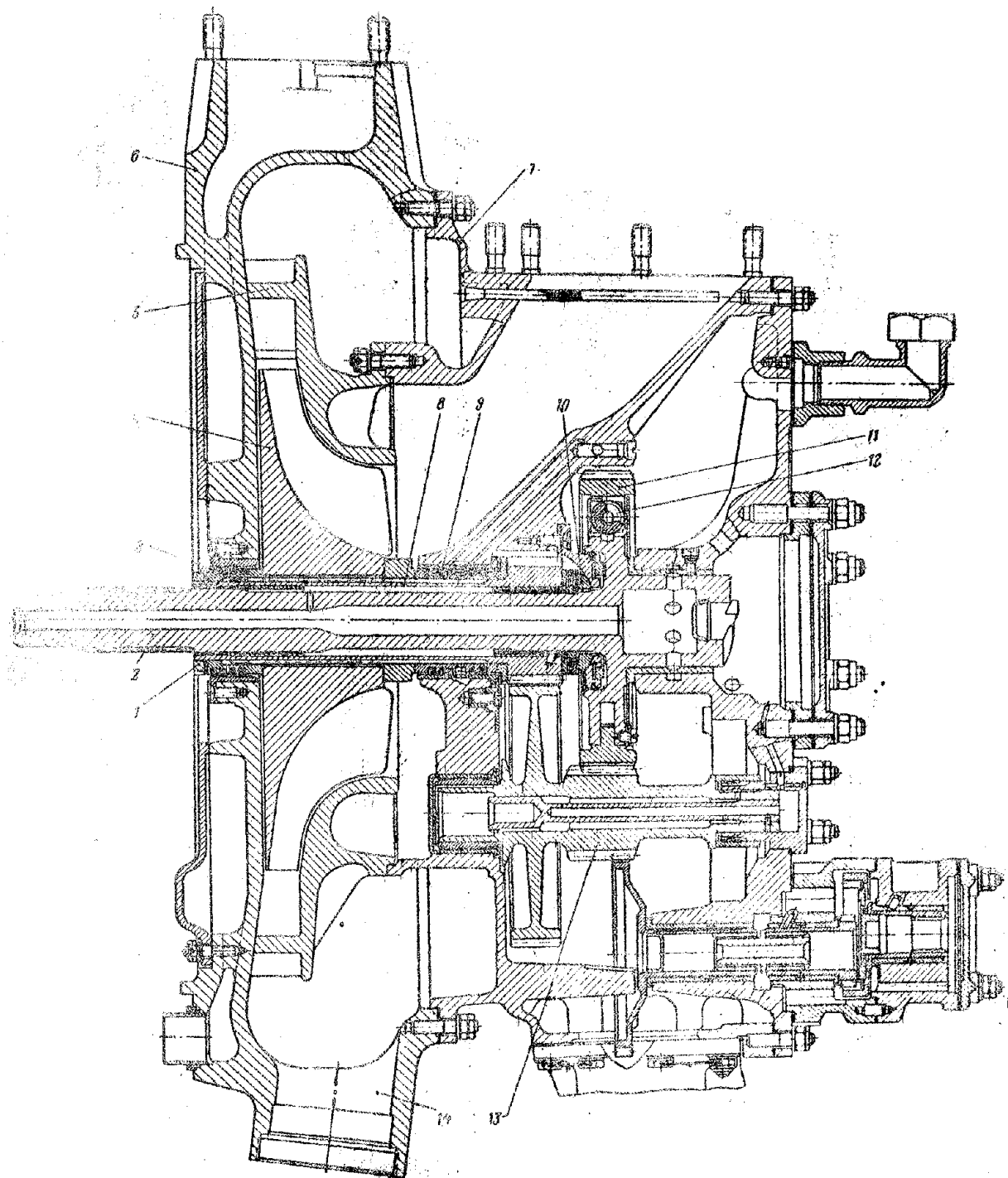


Fig. 21.2. Supercharger of the ASH-62T engine. 1 - nut, 2 - supercharger drive shaft, 3 - annular seal, 4 - supercharger rotor wheel, 5 - vaned diffuser, 6 - front supercharger housing, 7 - rear supercharger housing, 8 - rotor wheel shaft, 9 - annular seal, 10 - ball pivot, 11 - supercharger drive shaft pinion gear, 12 - gear springs, 13 - supercharger drive layshafts, 14 - discharge branch.

engine. In Fig. 3.7 the rotor wheel and diffuser of the supercharger are shown separately.

With help of slits, rotor wheel 4 is mounted on shaft 8. Shaft of supercharger 8 is hollow, and is carried out simultaneously with the drive gear. On both sides of the rotor wheel the shaft has annular seals 3 and 9, protecting from penetration of oil into the supercharger from the gear box and crankcase of the engine. The rotor wheel and annular seals are secured to the shaft by nut 1. Into the hole of shaft 8 there are pressed two bronze bearing sleeves, with the help of which it is freely mounted on drive shaft 2. For perception of axial stresses from the rotor wheel, shaft 8 has a thrust ball pivot 10.

Drive to supercharger is one-speed, two-stage with transmission ration  $i = 7.27$ . It consists of drive shaft 2 with pinion gear 11, layshaft 13 with two gears and supercharger shaft 8 carried out simultaneously with the driven gear.

On the front end of drive shaft 2 there are slits, with the help of which it is driven from the engine crankshaft. Pinion gear 11 is in the form of a toothed rim. Transmission of torque from drive shaft 2 to pinion gear 11 is carried out with the help of springs 12, forming an elastic spring coupling in the system of shaft and gear.

Upon change of engine speed the springs of the elastic coupling under the action of the appearing inertial loads are deformed and angular accelerations of the rotor wheel decrease. This lowers the inertial load on the drive.

### 25.3. Materials

For reduction gears they usually apply case-hardened steel [12Kh2N4A] (12X2H4A) or [18KhNVA] (18XIIIBA) and nitrated steel [38KhMYuA] (38XM0A). In conformity with this the gear teeth are case-hardened or nitrated. The propeller shaft and satellite-holder are made of steel [40KhNMA] (40XIIIMA). The rotor wheel of the supercharger is manufactured from light aluminum alloys [D1] (Д1), [AK1] (АК1), AK6, or from magnesium alloy [MA2] (МА2).

Body of supercharger and diffuser are cast from magnesium alloy [ML4] (МЛ4) or aluminum alloy [Al4] (АЛ4). Shafts and drive gear of supercharger are made of steel 12Kh2N4A.

## C H A P T E R   XXVI

### CRANKCASES, ACCESSORY DRIVES, AND LUBRICATION SYSTEM OF PISTON ENGINES

#### 26.1. Engine Crankcases

The crankcase is the main power body of the engine. On it are the cylinders and assemblies ensuring operation of the engine and aircraft. Inside the crankcase are the crank drive, the reduction gear with propeller shaft, the gas distribution mechanism, and accessory drives. The crankcase is also reservoir for the oil flowing from the bearings and other parts of the engine. By means of the crankcase the engine is mounted to the aircraft frame. During operation of the engine the crankcase perceives considerable loads from the cylinders, crankshaft, and propeller shaft, propeller thrust is transmitted through the crankcase to the frame of the aircraft.

For guarantee of engine assembly the crankcases are sectional with disassembly in planes perpendicular to the engine axis. Figure 26.1 shows the crankcase of the two-row radial engine [ASh-82T] (AM-82T) in dismantled form. Crankcase consists of front 2, center 3, and rear 4 of the main crankcase, nose 1, front half 5, and rear half 6 of the body of the supercharger, and rear cover 7.

In the main crankcase, consisting of three parts 2, 3 and 4, the crankshaft is mounted on bearing supports. On the outside there are flanges for attaching the cylinders. On the front 2 and rear 4 of the main crankcase there are sockets with flanges for the installation of the pushers of the gas distributers.

In the nose of crankcase 1 there is placed the reduction gear. On the outside there are flanges for attaching the speed governor and other assemblies.



Fig. 26.1. Crankcase of two-row radial engine ASh-82T.

Front half 5 of the body of the supercharger has discharge branches for feed of mixture to cylinders. Rear half 6 of the body of the supercharger forms an inlet duct. Inside there are drives to the supercharger and to other assemblies. On the front side of the supercharger body there is a vanned diffuser, and on the rear, rear cover 7. On the rear half of the supercharger body 6 and on rear cover 7 there are flanges for attachment of assemblies.

Separate parts of the crankcase are fastened together with the help of bolts and pins; parts of the main crankcase 2, 3, and 4 are fastened together with fitted bolts on crosspieces between sockets for the cylinders.

## 26.2. Accessory Drives

For guarantee of engine operation and servicing of the aircraft the engine has various accessories. The engine accessories include the fuel and oil pumps, magneto, variable-pitch propeller control unit, tachometers, starter, and so forth; the aircraft accessories include the generator, hydraulic pump, air pump of high pressure, and so forth.

Accessories of radial engines are arranged on the body of the reduction gear and on the accessory box, which is formed by the rear body of the supercharger and cover. In the first case the assemblies are driven from the propeller shaft, and in the second, from the crankshaft shank.

Accessories are driven by gear transmissions, ensuring the necessary speed for normal operation of accessories.

### 26.3. Lubrication of Piston Engines

Lubrication of engines decreases friction and heat transfer from rubbing surfaces. Oil is also used as a working fluid in the variable-pitch propeller control system.

Sliding bearings are lubricated by forced feed of oil under pressure to them. Pistons and cylinders, piston pins, gears, antifriction bearings, and other components are lubricated usually by spraying. For lubrication of the valve mechanism of radial engines they sometimes use a consistent lubricant. For lubrication of piston engines they usually apply mineral oils [MD-22] (МД-22) or [MS-20] (МС-20).

The lubrication system of piston engines, just as [GTD] (ГТД), is circulatory under a pressure of 4 to 8 kg/cm<sup>2</sup> and is carried out on the "dry crankcase" example. Oil, by means of pumps, circulates in a closed circle: oil tank — engine — radiator — oil tank. Specific circulatory expenditure of oil (pumping) is from 1.5 to 3 kg/hp-hr. Absolute expenditure of oil is from 5 to 20 g/hp-hr.

### 26.4. Materials

Separate parts of crankcases are cast from aluminum alloys [AL4] (АЛ4) and AL5 or from magnesium alloy [ML4] (МЛ4). Central parts of the crankcase, carrying the cylinders, are frequently made by stamping from aluminum alloys AK5 and AK6 or from steel [40KhNMA] (40ХНМА).

Gears and shafts of accessory drives are manufactured from the materials indicated in 12.3 of Chapter XII.

## C H A P T E R   XXVII

### IGNITION SYSTEM OF PISTON ENGINES

#### 27. 1. General Information

The ignition system ensures combustion of the working mixture in the engine cylinders. They usually apply a double system of ignition, with which combustion in the cylinders is produced simultaneously in two points from two independent sources of ignition. This ensures reliability of engine operation, and also improvement of burning conditions of the working mixture.

The ignition system includes the spark plugs, two magnetos, shielded wires with reinforcement, a switch, and a starting device.

#### 27.2. Ignition Plugs

A plug is a discharger of current, between the central and lateral electrodes of which during ignition there jumps a spark. The gap between the electrodes is called the spark gap, and voltage at which the electric discharge occurs is the breakdown voltage. The spark gap of a plug is from 0.3 to 0.4 mm, and breakdown voltage is 10,000 to 12,000 v. Aircraft plugs usually have ceramic insulation. For decrease of radio interference the plugs are shielded.

Figure 27.1 shows a [SD-19S] (СД-49С) plug, which consists of a core and body. The base of the core is ceramic insulator 5, in the central part of which on thermocement 17 is attached central electrode 18. On the electrode are: current-conducting element 11, lining 10 and ohmic resistor 9. The resistor is attached in the core with the help of spring 8 and contact head 6, mounted on thermocement 7. Resistor 9 decreases of erosion of electrodes.

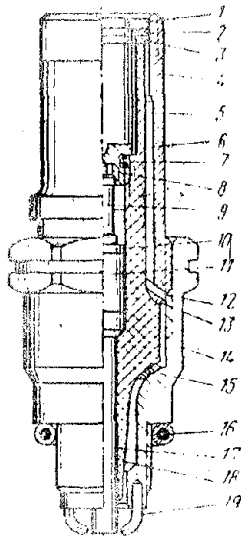


Fig. 27.1. Cross section of SD-49S plug. 1 - shield ring, 2 and 3 - linings, 4 - shield, 5 - ceramic insulator, 6 - contact head, 7 and 17 - thermocement, 8 - spring, 9 - ohmic resistor, 10 - lining, 11 - current-carrying element, 12 - spring ring, 13 - washer, 14 - body, 15 and 16 - sealing rings, 18 - central electrode, 19 - lateral electrodes.

Steel body 14 on the screwed part has an external thread and two lateral electrodes 19, soldered by copper. Steel shield 4 shields the current-carrying parts of the plug. It is screwed into the body on the thread and secures the core in it. For sealing between the body and core there is a copper ring 15, and between the core and shield there is a soft brass washer 13 and steel spring ring 12. In the upper part between the core and shield there are two paronite linings 2 and 3, and steel ring 1. Copper ring 16 serves for sealing after screwing the plug into the cylinder.

During operation the plugs are subjected to the action of high temperatures and pressures. Thermal intensity of plug is determined by its thermal conduction and external cooling. In accordance with this, there are hot, medium, and cold plugs. For guarantee of normal heat balance of plugs, they are matched to the engine in accordance with their thermal characteristics. Operation life of plugs is restricted by burning of electrodes and scale formation on them.

### 27.3. Aircraft Magnetos

A magneto is a high-voltage generator. It contains an ac magnetolectric generator, transformer, breaker and distributor.

With respect to principle of arrangement of magnetic system, aircraft magnetos occur in two types: with permanent magnet in rotor, i.e., rotor type, and with fixed permanent magnet, i.e., commutator type. Soviet aircraft magnetos are chiefly of the rotor type, quadripole, i.e., with the formation of four sparks in each revolution of the rotor (four-spark). Magnetos are made with fixed sparking, i.e., with sparking unregulated in the process of operation, and with an automatic advance angle of ignition device.

A diagram of a four-spark magneto of the rotor type with automatic ignition advance device is shown in Fig. 27.2. Rotor of magneto 16 consists of a permanent magnet with four pole terminals 15 located relative to one another at an angle of

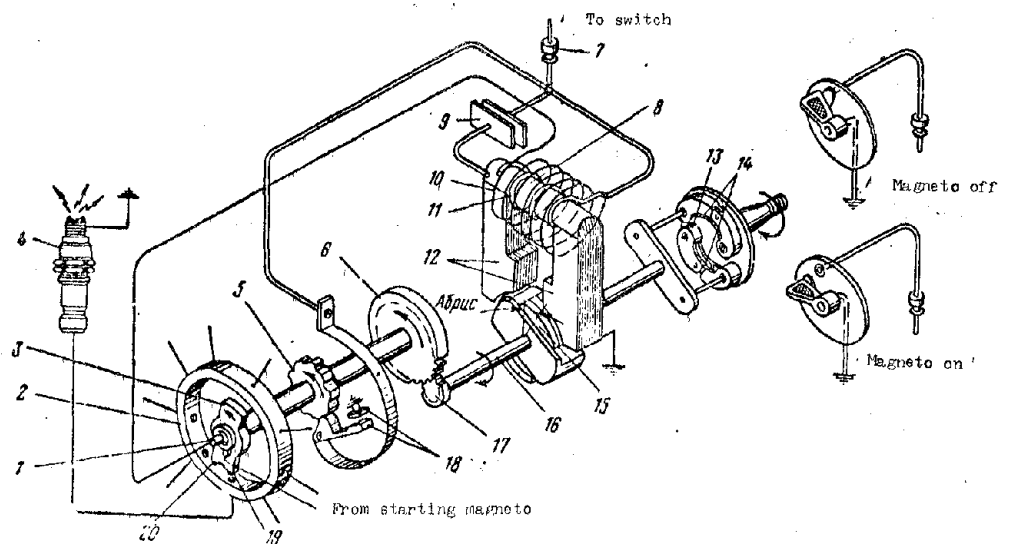


Fig. 27.2. Diagram of four-spark magneto of rotor type with automatic ignition advance device. 1 - central distributor electrode, 2 - distributive block, 3 - runner, 4 - plug, 5 - cam washer, 6 and 17 - gears, 7 - terminal, 8 - core of transformer, 9 - capacitor, 10 and 11 - secondary and primary windings, 12 - pole pieces, 13 - weights of automatic device, 14 - plate springs, 15 - permanent magnet, 16 - magneto rotor, 18 - contacts of breaker, 19 and 20 - working and starting electrodes.

$90^\circ$ . Two pole pieces 12 and core of transformer 8 form a magnetic circuit and are united in a mass. On the core of transformer 8 are wound the primary 11 and secondary 10 windings.

Primary winding 11 consists of 150 to 200 turns of copper wire with diameter 0.8 to 1.1 mm. One of its ends is soldered to core 8, and the other is connected through a lever spring to slide contact 18 of the breaker.

Breaker consists of contacts 18 and cam washer 5. The fixed contact of the breaker is united in the mass. Under the action of the spring, contact 18 is closed. Cam washer 5 has cams, the number of which is equal to the number of engine cylinders. Cam washer sits on the shaft and through a pair of gears 17 and 6 obtains rotation from rotor 16. The breaker is connected in parallel to capacitor 9.

Secondary winding 10 consists of 9000 to 13,000 turns of copper wire having diameter 0.06 to 0.07 mm. One end of it is united with the end of the primary winding, proceeding to contact 18, and the other is connected with central electrode 1 of the distributor.

Distribution consists of distributive block 2 and runner 3 with two electrodes, i.e., operating 19 and starting 20. Runner sits on the shaft of washer 5, revolving from rotor 16. Distributive block 2 has contacts (with respect to number of cylinders), each of which is united by wires with central electrodes by plug 4.

The ignition system is turned on and off by a switch. Figure 27.2 shows the on and off positions of the switch. Upon turning off the ignition system the primary circuit is closed by the switch to the mass.

Work of magneto. High voltage in the magneto appears during change of magnetic flux in the core of transformer 8. In positions of rotor a and c (Fig. 27.3) the magnetic flux the rotor is closed through the core of transformer 8, and in positions of rotor b and d, called neutral, through pole pieces 12. Upon rotation of rotor 16, in the core of the transformer there appears a basic periodic magnetic flux. Intersecting the turns of the windings, the magnetic flux each time induces 18 electromotive force (EMF) in them. With closed contacts 18 through the primary winding there will go a current of low voltage, forming in turn in the core of the transformer an electromagnetic flux with direction reverse to basic.

These two magnetic fluxes in core 8 are integrated, inducing emf in the secondary winding. However, the EMF is insufficient for sparking. Increase of EMF in the secondary winding is attained by breaking the primary circuit with breaker 5 at the moment of peak current in it. Peak magnetic flux in the core of the transformer is then sharply changed in magnitude and, intersecting the secondary winding with great speed, excites EMF in it on the order of 10,000 to 20,000 v. The obtained EMF ensures sparking of the plug.

The angle between the neutral position of the rotor (position b and d in Fig. 27.3) and its position at the moment of opening of the primary circuit, which is called the outline, is regulated in the magneto by the angular displacement of contacts 18 of cam washer 5 (see Fig. 27.2). Capacitor 9 increases the intensity of the discharge on the electrodes of the plug and decreases sparking of contacts 18 of the breaker.

An automatic ignition advance device of centrifugal type changes the advance angle of ignition depending upon engine speed. This attains an increase of engine efficiency at intermediate operating conditions.

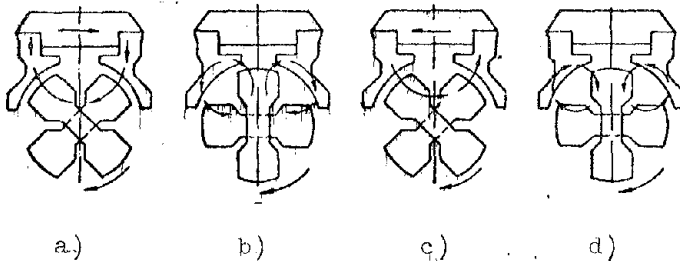


Fig. 27.3. Diagram of work of magneto.

The device consists of two centrifugal weights 13 (see Fig. 27.2), connecting the driving roller with rotor 16. Each weight consists of two parts united together by a hinged axis. Their relative position during

work is ensured by calibrated plate spring 14. The driving parts of the weights sit on two axes of the base of the device, rigidly united with the driving roller, and the driven parts are on two axes of rotor 16.

Upon rotation of the rotor the weights 13 are under the action of centrifugal forces and the forces of elasticity of plate springs 14. To each rotor speed there will correspond its position of weights. Thus, with increase of speed, weights 13, under the action of increasing centrifugal forces, surmounting the elasticity of springs 14, will be opened, revolving around their axes, and will turn with respect to the rotation (advance) of rotor 16 relative to the driving roller, and consequently also to the crankshaft. Owing to this, the advance angle of ignition is increased. With decrease of speed the advance angle of ignition will decrease.

Transmission ratio in the drive to the magneto depends on the number of cylinders  $i$  of the engine. For a four-cycle engine with four-spark magnetos  $k = i/8$ . Transmission ratio  $k_1$  of gears 17 and 6 (see Fig. 27.2) of transmission to the breaker and distributor is  $k_1 = 4/i$ . Thus the transmission ratio from the crankshaft to the breaker and distributor is equal to 0.5.

#### 27.4. Shielding of the Ignition System

During work of the magneto, around the conductors and assemblies of ignition there appears a variable magnetic flux which causes radio interference and disturbs the normal work of radio equipment. For decrease of radio interference the ignition system in all its current-carrying parts is shielded, i.e., it is placed in special metal housings made from nonmagnetic materials, which are connected with the engine mass. For shielding they usually apply aluminum and less often copper, possessing low ohmic resistance.

275. Starting Ignition

The operating magneto ensures sparking of the plugs at engine speeds above 80 to 100 rpm, and therefore engine starting is accomplished with the help of a starting induction coil or by means of a starting vibrator connected to the transformer of the working magneto. On low capacity engines they frequently apply use a special starting magneto with manual drive. In the case of application of an induction coil or a starting magneto, a current of high voltage is brought in from them directly to the starting electrode of the distributor of the working magneto.

#### Literature

1. Aircraft engines, edited by M. A. Levin and G. V. Senichkin, Mashgiz, 1951.
2. Aircraft piston engines, edited by I. Sh. Neyman, Oborongiz, 1950.
3. M. M. Maslennikov and M. S. Rapiort. Aircraft piston engines, Oborongiz, 1951.
4. R. D. Beyzel'man and B. V. Tsipikin. Antifriction bearings, Mashgiz, 1951.
5. V. A. Bodner, Automation of aircraft engines, Oborongiz, 1956.
6. I. P. Bratukhin. Design and construction of helicopters, Oborongiz, 1955.
7. V. M. Darevskiy and B. D. Kartashkin. Method of calculation for strength and stability of bodies of turbojet engines, Oborongiz, 1956.
8. G. S. Zhiritskiy, Aircraft gas turbines, Oborongiz, 1950.
9. G. S. Zhiritskiy, Design and calculation for strength of components of gas turbines, State Power Engineering Publishing House, 1955.
10. L. A. Zalmanzon and B. A. Cherkasov. Regulation of GTD and PVRD, Oborongiz, 1956.
11. V. N. Kudryavtsev. Gear transmissions, Mashgiz, 1958.
12. V. N. Kudryavtsev. Planetary transmissions, Mashgiz, 1959.
13. I. I. Kulagin. Theory of aircraft engines, Oborongiz, 1958.
14. G. A. Kuz'min and V. M. Demidovich. Investigation of the work of high-speed roller bearings of GTD during supply of large quantities of oil, Proceedings of KAI, No. XXXIII and XXXIV, 1958.
15. G. A. Kuz'min. Concerning the question of influence of the mass of a rotor shaft on its critical speed, Proceedings of KAI, No. XXXIV, 1958.
16. G. A. Kuz'min. Concerning the problem of deflections of sections in the plane of rotation of moving blades of axial-flow compressors and turbines, Proceedings of KAI, No. 60, 1961.

17. G. A. Kuz'min. Transmission ratios and efficiency of differential reduction gears of TVD, Proceedings of KAI, No. XXXIII and XXXIV, 1958.
18. G. A. Kuz'min. Calculation on strength of disks of turbomachines in an elastic state, Proceedings of KAI, No. 55, 1960.
19. A. V. Shtoda et al. Design of aircraft gas-turbine engines, Military Publishing House, 1961.
20. V. I. Polikovskiy. Aircraft power plants. Oborongiz, 1952.
21. S. D. Ponomarev et al. Fundamentals of contemporary methods of strength calculation in machine building, Mashgiz, 1950-1958.
22. G. S. Skubachovskiy. Aircraft gas-turbine engines, Oborongiz, 1955.
23. G. Yu. Stepanov. Fundamentals of the theory of vaned machines, combined and gas-turbine engines, Mashgiz, 1958.
24. B. S. Stechkin and P. K. Kazandzhan, et al. Theory of jet engines, Oborongiz, 1956 and 1958.
25. S. P. Timoshenko. Plates and shells, State Technical Press, 1948.
26. S. P. Timoshenko. Vibration theory in engineering, State Scientific and Technical Press, 1959.
27. S. P. Timoshenko. Stability of elastic systems, State Technical Press, 1946.
28. I. T. Shvets and Ye. P. Dyban. Air cooling of rotors of gas turbines, Publishing House of Kiev University, 1959.